Trinity College Dublin
Coláiste na Tríonóide, Baile Átha Cliath
The University of Dublin

An investigation into the use of ion-exchange resins as a formulation approach for modified-release oral liquid preparations

A thesis submitted for the degree of

Dodoctor of Philosophy

at the

School of Pharmacy and Pharmaceutical Sciences

Trinity College Dublin, The University of Dublin

Ireland

by

Karl Smyth

BSc. (Pharm), MPharm, P.Grad.Cert. (Statistics), M.P.S.I.

under the direction and supervision of

Professor Anne Marie Healy

B.Sc. (Pharm), Ph.D., M.P.S.I, F.T.C.D.

March 2022

Declaration

I declare that this thesis has not been submitted as an exercise for a degree at this or any other university. A small proportion of the work presented in this thesis was carried out by others and is duly acknowledged where relevant. I declare that all other work is entirely my own.

I agree to deposit this thesis in the University's open access institutional repository or allow the library to do so on my behalf, subject to Irish Copyright Legislation and Trinity College Library conditions of use and acknowledgement. This thesis is subject to a "stay" according to the terms in Calendar Part III, Section 1.102.

I do not consent to the examiner retaining a copy of the thesis beyond the examining period, should they so wish (EU GDPR May 2018).

Karl Smyth

Contents

Acknowledgements

Firstly, I'd like to begin this section by pointing out that there was a time during the PhD, when I feared that the acknowledgements would be the most substantial aspect of the thesis. Thankfully, things took an upturn, and I managed to get the show on the road, which without doubt, would not have been possible without the help of many others. On a more serious note, I would like to offer my sincere thanks to my supervisor Professor Anne Marie Healy for her help and scientific guidance throughout the course of my time in the lab. I cannot emphasise enough how grateful and appreciative I am for being provided with the chance to be part of her research group where I developed both academically and personally. On a more personal level, I'd like to express my sincere gratitude to her for always being available to discuss issues that may have been affecting me. Undoubtedly, her kindness and willingness to listen, made my PhD experience smoother, and I am eternally grateful to her for this support. I would also like to thank my co-supervisors in Xeolas Pharmaceuticals, Damian, Dennis and Maurice, who part-funded my project, were available for advice and listened to my presentations over an occasionally, unreliable/muffled phone line. I am also very thankful to the Irish Research Council for providing the funding which enabled this research to be conducted.

I'd like to thank all members of the original postgrad crew who showed me the ropes both inside and outside the lab; Alan, David, Eavan, Emer, James, Jeremiah, Johannes, Kate, Mike, Ricardo and Svenja. In particular, a special thanks to David. The second group of researchers I'd like to thank are my peers who I shared the lab with during the second half of my PhD. Although, the pandemic has robbed us of the opportunity to properly bond over "a few social drinks", I still consider you all good friends; Alex, Edana, Eva, Juljia, Klaudia, Lena, Maria, Marina, Monika and ShiZhe.

I also consider myself very fortunate to have had the benefit of sharing the lab with several post-docs who took an interest in my project, from which we developed both a strong personal and professional relationship; Loli, Peter, Stefano, Valerio and Zelalem. Also, thank you to the other post docs that I have shared the lab with over the years; Anita, Atif, Dinesh, Jay, Kieran, Lillian and Pei (May).

My journey also encompassed significant engagement with the technical staff on both a personal and lab basis. In particular, I'd like to thank Brian, Conan and David who were always there to lend a hand. Secondly, I'd like to thank them for their sense of humour, which made our engagements extremely pleasant. Also, a huge thanks to Elizabeth on the administration side of things and Mick at the Lincoln Place Entrance who I befriended during the COVID times.

I'd like to thank all my friends who have continued to persevere with me despite my prolonged absence at the many social events you continued to invite me to. From this point on, I can assure you

that my non-attendance will be firmly confined to the past. A special mention to my good friend Daryl. Thanks for all of your encouragement, positivity and friendship.

Lastly, I would like to thank my family for their unwavering support, my parents (Ann and Brendan) and my sister Jacqueline. The submission of this thesis would certainly not have been possible without your tireless support, especially my mother who has always been there for me when I most needed her. Finally, I'd like to take the opportunity to show my gratitude to my parents for the opportunities that you have provided me with.

Publications and presentations

Public presentations

- Ion Exchange Resins: Drug Delivery and Therapeutic Applications. Trinity College Dublin's School of Pharmacy and Pharmaceutical Science's Seminar Series, October 2018, Dublin, Ireland

- The use of ion-exchange technology in the development of an age-appropriate oral liquid formulation. All Ireland Schools of Pharmacy annual conference, April 2019, Dublin, Ireland.

Abbreviations and symbols

^Exo	Exothermic direction
^Endo	Endothermic direction
2θ	2 theta (diffraction angle)
2-F	2-Fluid
α_2	Alpha two
ANOVA	Analysis of variance
API	Active pharmaceutical ingredient
arb. units	Arbitrary units
ATR-FTIR	Attenuated total reflectance fourier transform infrared spectroscopy
AUC	Area under the concentration-time curve
CAN	Acetonitrile
BET	Brunauer, Emmett, Teller
BJH	Barrett, Joyner and Halenda
BP	British Pharmacopoeia
CCDC	Cambridge Crystallographic Data Centre
CI	Confidence interval
CPP	Critical process parameters
CPM	Counts per minute
Cm	Centimeter
C_{max}	Maximum concentration
CQAs	Critical quality attributes
CR	Controlled-release
D	Diffusion coefficient of the drug
DAE	Drug association efficiency
DBS	Dibutyl sebacate
DDS	Drug delivery system
DI	Deionised
DoE	Design of Experiment
DRC	Drug-resin complex
DSC	Differential scanning calorimetry
DVS	Dynamic vapour sorption
dw/dt	Dissolution rate
EC	Ethylcellulose
EDX	Energy-dispersive X-ray
EMA	European Medicines Agency
EP	European pharmacopoeia
ER	Extended-release
E.U.	European Union
EtOH	Ethanol
FBG	Fluidised bed granulation
FDA	Food and Drug Administration
Ffc	Flow function correlation
G	Gram
GIT	Gastrointestinal tract
GSK	GlaxoKlineSmith
H	Hydrogen
H Bonding	Hydrogen bonding

HCl	Hydrochloride
HME	Hot melt extrusion
HPLC	High performance liquid chromatography
HPMC	Hydroxypropyl methylcellulose
ICH	International Council for Harmonisation of Technical Requirements for Pharmaceuticals for Human Use
IEC	Ion-exchange capacity
IER	Ion-exchange resin
IPA	Isopropyl alcohol
IR	Immediate-release
IVIVC	In vitro in vivo correlation
J/g	Joules per gram
K	Kelvin
KCl	Potassium chloride
LA	Long-acting
Log P	Log_{10}(Partition coefficient of a compound between the aqueous and lipophilic phase)
M	Molar
MeOH	Methanol
mg	Milligram
MFT	Minimum film temperature
Min	Minute
mL	Milliliter
mm	Millimeter
mm s^{-1}	Millimeters per second
MR	Modified-release
MTDSC	Modulated temperature differential scanning calorimetry
MTZ	Metronidazole
MTZ BZT	Metronidazole benzoate
MW	Molecular weight
mW	Milliwatts
Na	Sodium
NaCl	Sodium chloride
NaOH	Sodium hydroxide
NIR	Near-infrared
Nl	Normliter
Nm	Nanometer
OROS	Osmotic controlled release oral delivery system
P/Po	Partial pressure
PAT	Process analytical technology
PCA	Principal component analysis
PD	Pharmacodynamics
PDCO	Paediatric Committee
PEG	Polyethylene glycol
pH	Antilog of hydrogen ion concentration in moles per liter
PIPs	Paediatric Investigative Plans
PK	Pharmacokinetics

PKa	Antilog of acid dissociation constant
PLS	Partial least squares
PRODAS	Programmable oral drug absorption system
PSA	Particle size analysis
PSD	Particle size distribution
PTFE	Polytetrafluoroethylene
PVA	Polyvinyl acetate
PVP	Polyvinyl pyrrolidone
PXRD	Powder X-ray diffraction
PR	Prolonged release
QbD	Quality by Design
R&D	Research and development
R^2	Correlation coefficient
RH	Relative humidity
RPM	Rotations per minute
SD	Spray-dried
SE	Specific energy
SEM	Scanning electron microscopy
SLS	Sodium lauryl sulfate
SODAS	Spherical oral drug absorption system
SR	Sustained-release
SSA	Specific surface area
STEP	Safety and Toxicity of Excipients for Paediatrics
T_g	Glass transition temperature
TCT	Triacetin
TEC	Triethyl citrate
TGA	Thermogravimetric analysis
T_m	Melting temperature (onset)
T_{max}	Time at which C_{max} is obtained
TR	Timed-release
TZD HCl	Tizanidine Hydrochloride
µL	Microliter
µm	Micrometer
U.K.	United Kingdom
U.S.	United States
USP	United States Pharmacopoeia
UV	Ultraviolet
WG	Wet granulation
WHO	World Health Organisation

Summary

This thesis focuses on the use of ion-exchange resins (IERs) to modify the release profile of an active pharmaceutical ingredient (API) that would help address an unmet clinical need in the population if formulated as an oral liquid. Contrasting levels of success were achieved using two APIs from which therapeutic benefit could be potentially derived if the incorporation of a "strongly" acidic IER was successful in enabling a slowing of the API release kinetics, as well as affording a degree of liquid stability for drug-resin complexes (DRCs) held in suspension in a liquid vehicle.

Based on the combination of low drug loading and rapid release of drug in deionised water (DI H_20), it was surmised that drug-resin complexes (DRCs) were not successfully formulated using metronidazole (MTZ) and the "strong" IER, Amberlite™ IRP69 (powdered IER form). In contrast, tizanidine hydrochloride (TZD HCl) proved to be an excellent API candidate for IER complexation based on a combination of high drug loadings (the maximum being approximately 50% w/w), and low levels of drug release in DI H_2O, which were both strong signs of a successful ion-exchange reaction occurring. Loading of the drug onto the resin in all cases was found to produce amorphous systems and the shifting of peaks representative of the API's functional groups implicated in the ion-exchange reaction in the FTIR spectra supported the assertation that ionic interactions had occurred. A series of experiments were performed which utilised techniques ranging from milling (ball and cryo) to spray-drying with a view to producing amorphous API and unequivocally identify the glass transition temperature of the raw material. Ultimately, cryo-milling proved successful in API amorphisation, which aided in the characterisation of the DRC systems.

By identifying TZD HCl as a suitable option for use with IERs, the exploration of alternative resin types aside from the powdered form became a topic of interest. The gel/bead-type resins (Amberlite™ IR120 were also effective complexation agents, as evidenced by the drug loading (16.0-33.8% w/w depending on the D:R ratio in the loading media) achieved. This was noticeably lower than the loadings achieved with the powdered resin form and can be accounted for on the basis of resin structure which limits the quantity of drug that can be loaded onto nonporous bead form resins.

Loading studies were also undertaken using "weakly" acidic resins. The findings of these trials were consistent with the expectation that the loading process involving a "weak" resin, such as Amberlite™ IRP64, and an ionisable API requires more care (than those employing a "strong" resin such as Amberlite™ IRP69), owing to the more selective dissociation tendency of the resin relative to the "strong" resin, the dissociation properties of which are virtually independent of pH. Varying drug loading values were attained depending on the pH of the loading medium and it was found that pH values that favoured the dissociation of the resin produced higher drug loadings.

Although these findings were of interest, their significance was far outweighed by the initial explorations into another alternative resin, Amberlite™ IRP88, a subset of the "weakly" acidic resins that differed from the IRP64 grade on the basis of the counterion (potassium in the case of IRP88, rather than hydrogen) attached to the fixed functional group. The addition of this resin type to the TZD HCl drug solution produced a distinct yellow colour quickly followed by noticeable drug precipitation that was not evident in any of the drug-resin complexation trials performed up to that point. It was hypothesised that by adding the resin possessing the potassium ion as the counterion attached to the fixed functional groups, the free base of TZD was formed, which dramatically reduced the chances of binding to the resin due to the compound not being protonated. Furthermore, the precipitation is likely caused by the far lower aqueous solubility that the free base possesses relative to the hydrochloride salt form. A combination of solid-state analyses, including FTIR analysis, and pH measurements supported this hypothesis which pointed to the API-resin incompatibility.

Despite all DRCs exhibiting rapid release behaviour in acidic medium and some resistance to drug leaching in an aqueous medium, the complexes formed using the Amberlite™ IRP64 grade displayed a suppressed rate of drug release in pH 6.8 buffer medium, which is typical of DRCs formed using "weak" resins. The release profiles of the IRP88 based-system were in stark contrast and depicted rapid release in all dissolution media tested, exemplifying the unsuitability of this resin type.

A further set of experiments utilising an alternative approach (spray-drying) relative to the more traditional batch method of complexation were successful, indicated by the drug loading figures attained (ranging from 6.2-48.8% w/w, depending on the drug-resin ratio in the drug loading media) and the drug release behaviour observed. However, solid-state analyses highlighted several downsides associated with the process such as the presence of sodium chloride and uncomplexed TZD HCl in the spray-dried product. This can be overcome by smart resin selection or the incorporation of a post-manufacturing washing step, however this lessens the appeal of the process. In general, irrespective of the ionic composition of the dissolution medium, the extent of incomplete drug release was greater with the spray-dried systems relative to the batch-produced systems.

The development of an assay procedure involving the commonly known drug displacement method formed a major component of one of the chapters of the thesis, aimed at investigating the factors that influence the drug loading and physiochemical properties of the DRCs. The results show that the drug-resin equilibrium, a distinguishing feature of ion-exchange based drug delivery system is heavily reliant on the concentration of the complex in the elution medium, with the various other factors explored showing little influence on the results obtained.

A consistent feature of DRCs formed using the “strong” resin in either of its physical forms (powder - Amberlite™ IRP69 or bead - Amberlite™ IR120) was the rapid release of drug in ionic media which necessitated the application of a rate-controlling polymer on the DRC to achieve a sustained-release profile. After ruling out the possibility of using a granulation process as part of the formulation approach to achieve the desired release profile, a sustained-release formulation of TZD HCl was successfully formulated using Wurster coating of bead-type DRCs after extensive manipulation of a variety of factors such as polymer type, polymer concentration and plasticiser inclusion. Systems that closely met the pre-requisites of the study, namely a sustained-release profile over 24 hours, were chosen for subsequent stability studies performed at 25 °C/60% RH and 25 °C/<10% RH. The solid-state characteristics were shown to remain unchanged and the chemical stability was maintained over the 3 month study. Aside from their excellent stability properties, the studies showed that the release profiles of the coated microparticles were impacted by the harsher stability conditions, a finding that was not observed at dry conditions, illustrating the systems’ susceptibility to moisture. The liquid stability studies which examined the drug leaching tendency and the impact of suspending the coated DRC material in an aqueous medium indicated that the formulations require further development work. The deterioration in dissolution performance of the aged samples is evident by the marked difference in release kinetics observed for stored suspensions, presumed to be caused by the polymer coating layer becoming compromised during storage in the aqueous environment.

The work conducted and presented in this thesis highlighted that the selection of suitable APIs for use with IERs is dependent on a variety of factors that relate to both components. Despite the setbacks encountered during the trials that explored spray-drying as a method to produce DRCs, the process was successful, demonstrated by the drug loading, drug release and solid-state studies. Based on the results from the studies in the thesis, a sustained-release formulation of TZD HCl produced using the Wurster process demonstrated an appreciable difference in release behaviour relative to the uncoated systems. Stability conditions, at which the “dry” microparticles were physically and chemically stable were identified, but the stability of the liquid suspension formulation indicated that further optimisation of the system is required to develop a stable sustained-release oral liquid with a reproducible release profile. A flow chart diagram shown in figure 1 indicates the series of sequential steps performed in this thesis. The purpose of which is to aid the reader in understanding the different strands of work reported in the thesis.

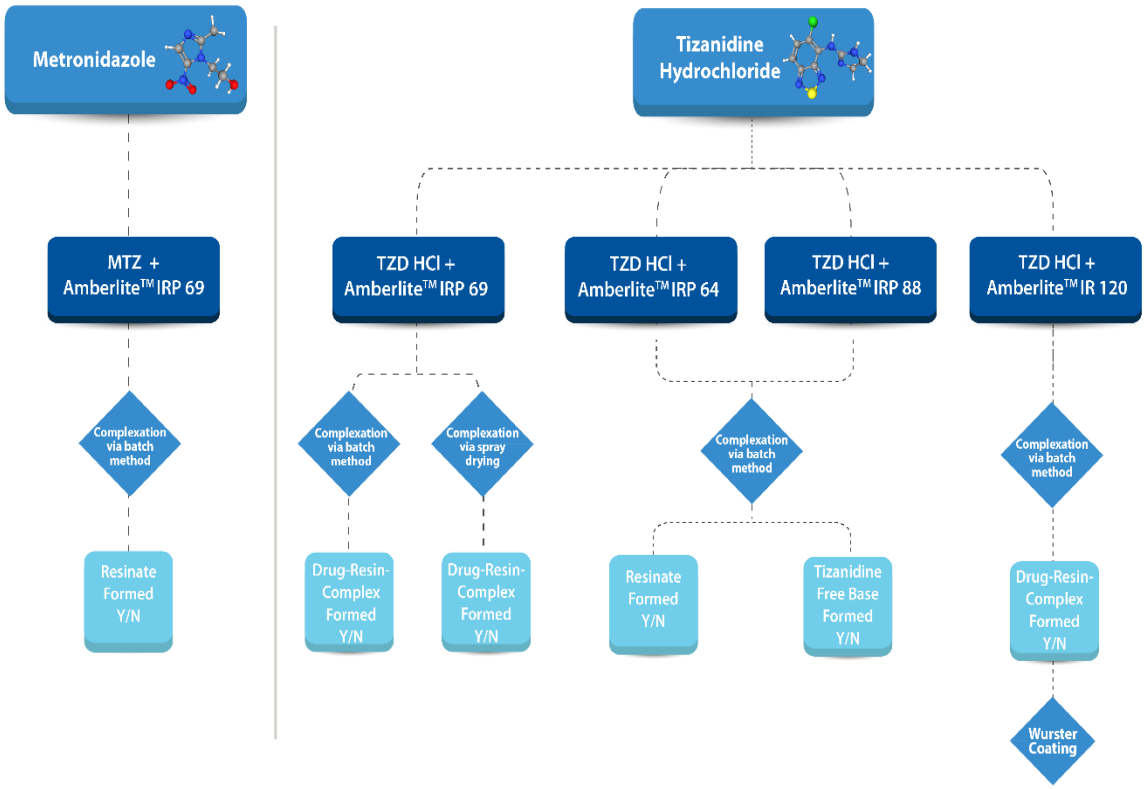

Figure 1. Flow chart outlining the progress through the different stages of the experimental work performed as part of this thesis. More detailed flow charts are presented at the start of each results chapter (Chapters 3, 4 and 5).

Origin and Scope

Over many decades, ion-exchange resins (IERs) have been an invaluable tool available to formulation scientists to help overcome specific challenges posed by a diverse range of active pharmaceutical ingredients (APIs). With respect to the pharmaceutical sector, their use has evolved from their more traditional role, which is to modulate the drug release properties of APIs, to providing enhanced stability to particular drugs. The overarching aim of the work was to develop age-appropriate formulations for two APIs which have been reported to be effective in the paediatric population, predominantly as a solid dosage form and/or "off label" use, but for which there is currently no suitable licensed formulation available. The envisaged benefits of such a formulation would not be limited to just the paediatric cohort, instead having the potential to address the unmet needs of many patient groups, depending on the specific API studied. Investigating the capability of IERs to modulate drug release is a primary focus of the thesis, as, at the outset of the project, the utilisation of IERs was envisaged to be a realistic strategy to achieve a liquid formulation with the desired release profile and stability. Linked to the established reputation that resins have for modulating drug release, is their potential usefulness as taste-masking agents, which typically requires the use of resins with different functional groups to that of the "strong" resins. A further objective of the thesis was to explore the impact of complexation using "weakly" acidic resins on the selected API to elucidate information regarding the API's propensity to interact via ion-exchange.

Irrespective of the type of resin studied, of which there are many types, ranging from "weak" to "strong" or acidic to basic, a limited number of methods to load a drug onto a resin have been reported. Within the realm of developing pharmaceutical formulations, the batch method predominates and will be the method employed for the vast majority of loading studies undertaken in the work of this thesis. Spray-drying represents an alternative but underexplored method of drug resin complex (DRC) production, with scarce evidence of its utility reported to date. However, studies in this thesis will employ this technique, which is more suited to large scale pharmaceutical processing compared to more established methods used to form the complexes.

The versatility of IERs is exemplified by their suitability for incorporation, as DRCs, into formulations that can be administered via a variety of routes of administration, as well as the capability of certain resins to be used as therapeutic agents themselves to alleviate electrolyte imbalances within the body. Despite the burgeoning use of these insoluble polyelectrolyte systems as part of a range of different drug-delivery strategies, the predominant application has remained as a drug carrier for sustained-release applications. One downside of their use is the limited sustained-release effect afforded by the resin alone, which necessitates the application of a rate-controlling membrane to enhance the

modulation of drug release. This is typically achieved using a range of coating techniques, the most well-known being the Wurster coating process, a method routinely used in industry, that is utilised as part of this work. However, this technique is more routinely used to coat material in batch sizes that greatly exceed those possible in the current work, in light of the limited quantity of API and resin available. Therefore, the Wurster process presents a challenge to coat the smaller batch sizes of DRCs and, to the best of the author's knowledge, this work is one of the first forays into coating DRCs at such small-scale.

IERs have intriguing physicochemical properties which enable the complexes formed to have unique stability and drug release properties. This thesis explores many of the factors known to affect the equilibrium nature of drug loading/release, but which are typically investigated using model drugs rather than one that has been selected to address an unmet therapeutic need. Therefore, this aspect of the work serves to complement the ultimate intention of the project which is to develop a stable oral sustained-release liquid formulation. One of the major benefits afforded by IERs is their recognised ability to produce stable sustained-release oral liquid formulations and this approach remains one of few established methods of formulating such preparations that are devoid of drug leaching into the liquid vehicle. This benefit provided the most compelling argument for using IERs in this thesis and will be explored extensively.

The overall aim of this thesis was to explore the potential of IERs to modify the release of APIs by forming complexes that displayed acceptable stability in an oral liquid formulation.

The scope of this thesis was to:

1. Investigate the feasibility of complexing two APIs to "strong" IERs that differed in physical form (i.e. powdered and bead form).
2. Identify the factors that influence drug loading values achieved as part of an evaluation of the complexation process on the drug's solid-state and drug release properties.
3. Explore the compatibility of "weak" resins with the most promising API candidate and evaluate the resultant product's physiochemical properties and drug release performance.
4. Investigate the viability of spray-drying as a technique to produce drug-resin complexes (DRCs), utilising the QbD paradigm.
5. Evaluate the suitability of resin material to form granules to facilitate the later application of a rate-controlling polymer.
6. Evaluate the suitability of the Wurster process for coating drug-loaded complexes and investigate the impact of different polymers, their concentration in the coating solution

/dispersion and the inclusion of additives on the process itself as well as the properties of the coated complexes.

7. Establish the physical and chemical stability of selected “dry” DRC microparticles.
8. Suspend selected DRC samples in an aqueous medium (vehicle) and evaluate drug release performance and drug leaching tendency.

Chapter 1:

Introduction

1.1 Oral drug delivery

1.1.1 An overview of oral drug delivery

Oral drug delivery remains the favoured route of administration for small molecule active pharmaceutical ingredients (APIs) from both the patients' and pharmaceutical industry's perspective, reflected by the fact that more than 55% of medicines on the market are oral medicinal products (1). Low manufacturing costs, established manufacturing processes, ease of product handling and high throughput, have all been cited as advantages that solid dosage form development offers over alternatives (2). The myriad of factors such as physicochemical, physiological and formulation, that act in unison, to influence the drug absorption process, renders the task of designing an oral dosage form a challenging one (3,4). Many pharmaceutical companies specialise in the use of novel oral drug delivery systems (DDSs), that can be used for drugs that are traditionally deemed unsuitable for oral delivery (5).

Oral liquids such as solutions, suspensions, syrups, and emulsions are the preferred vehicles for API administration to patient populations such as children and the elderly. Liquids provide maximal dosing flexibility, and it is possible to use a single formulation over a wide age range (including neonates). However, many drugs have foul taste characteristics and the bitterness, for example, of many APIs is more pronounced in the liquid form, and necessitates the use of taste-masking techniques (6). Hence, taste-masking is very important when addressing patient compliance challenges, and the Paediatric Investigation Plans (PIPs) commissioned by the European Union (E.U.) specifically state that studies relating to taste-masking, along with compatibility with administration systems and common foods and drinks must be undertaken (7). Factors to consider, when designing liquid dosage forms include the volume of the dose used, which must be acceptable to the patient, and the dosing device must be fit for purpose (8).

1.1.2 Age-appropriate formulations

1.1.2.1 Overview of the need for age-appropriate formulations

Many different populations have specific needs with respect to the administration of medicines, and a "one size fits all" approach is grossly inadequate (9). Two particular patient populations that differ from the standard patient for which pharmaceutical products are typically designed are the paediatric and geriatric cohorts (10). The term "special populations" was created to encapsulate those patient groups that are more vulnerable than an average healthy adult. It affords regulators the chance to introduce regulation that minimises risk to these groups (9).

The added complexity that these special populations pose to clinical trial designs, has given rise to many companies omitting these populations. Instead, they rely on extrapolation from the healthy adult population. Many studies have highlighted the reasons why this is an inappropriate practice for populations that are in a higher risk bracket for receiving sub-optimal pharmacotherapy. Physiological and anatomical differences that impact drug handling and pharmacokinetics are prime factors placing these populations in this risk category (9). The development of innovative drug delivery platforms aimed specifically at addressing the needs of these special populations is a focus of many research teams. Age-appropriate medicines ensure that the dose is suitable for patients, and facilitates patient compliance (11).

The development of an age-appropriate formulation is a challenging task due to the broad range of pharmaceutical and clinical aspects that must be considered to ensure the quality, safety, and efficacy of the final product (12). The paediatric and geriatric cohorts of the population may prefer oral liquid formulations over solid dosage forms due to the ease of swallowing. Children younger than five years old are generally unable to safely swallow solid capsules and tablets larger than 10 mm (13). Liquids are considered favourable due to the dosage flexibility they afford and ease of administration. They are also particularly suited to enteral tube administration (14). Over the last decade, there has been much discussion centred around dosage devices for oral liquids, such as an oral syringe or measuring cup, used to administer small volumes of medicine, so that the risk of unacceptable dose variability is minimised (15,16). Liquid dosage forms are not without their disadvantages, such as the need for a preservative, and the taste of API being more pronounced than in solid dosage forms. This has prompted many innovative solid dosage forms to be developed, such as mini-tablets and dose sip technologies, specifically targeted to the needs of vulnerable paediatric and geriatric patients (12).

After the correct medicine has been prescribed, adherence/compliance are two critical factors in achieving the anticipated therapeutic benefit. On average, when compared to non-adherent patients, those who adhere to treatment are three times more likely to experience positive health outcomes (17). Adherence rates with children are reported to be as low as 11%, due primarily to palatability/taste, as well as swallowability and dose flexibility issues. Such poor adherence to a drug treatment regimen can significantly compromise therapeutic efficacy (10). A comprehensive review of paediatric medicines highlighted the lack of available evidence on the acceptability of oral paediatric medicines. Acceptability can be defined as the overall ability of the patient and caregiver to use a medicinal product as intended (18). It is a vital issue to be considered, and it is likely to influence the patient's adherence. Palatability remains the most investigated area of acceptability, but a defined standard of what is and is not acceptable for children is still absent despite it being of paramount importance (19).

1.1.2.2 A focus on the paediatric patient cohort

Paediatric patients pose a variety of challenges, as illustrated in Figure 1.1, when it comes to designing medicines. Examples of such challenges include the heterogeneity of the patient population, in terms of weight and stage of physiological development (20). One categorisation, shown in Table 1.1 is based on age, physiological and pharmacokinetic (PK) development. It divides the cohort as follows: preterm infants, newborns, infants, children and adolescents (21).

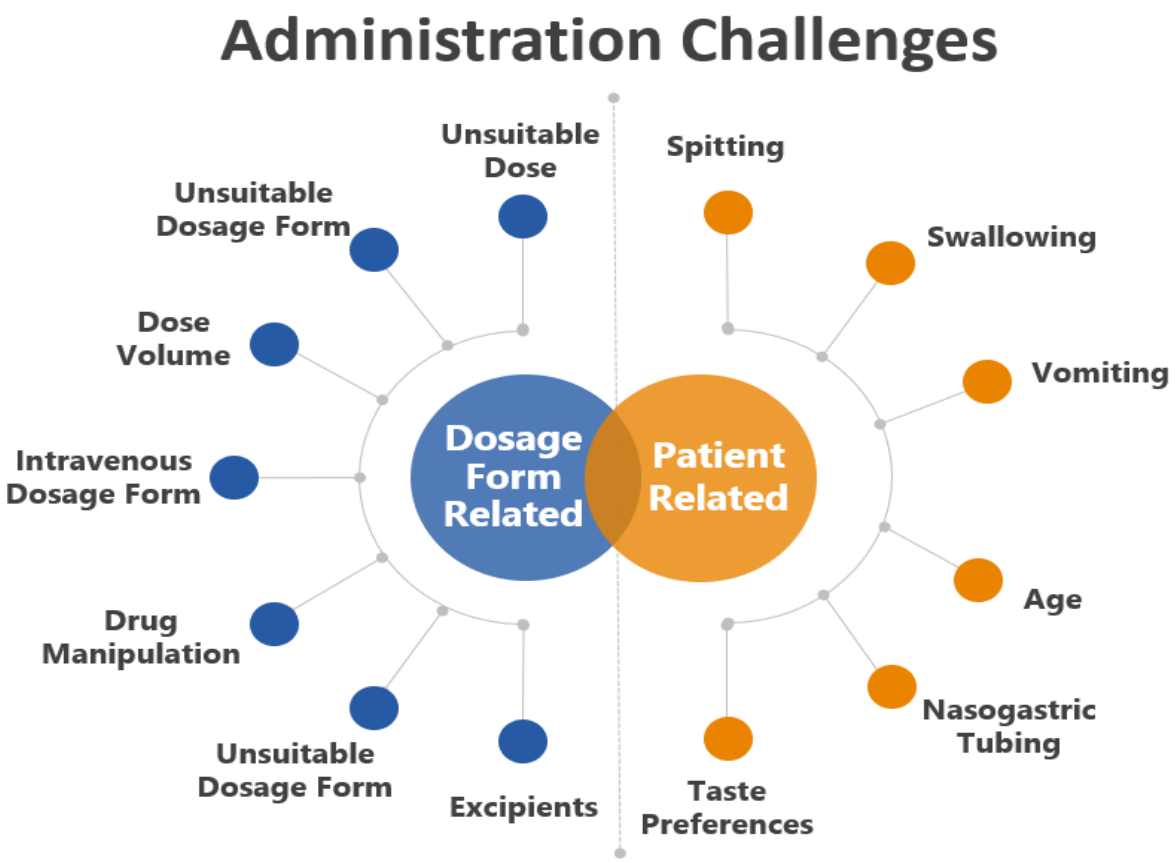

Figure 1.1. Identified administration challenges of oral medication at paediatric hospital wards divided into dosage form and patient-related challenges (adapted from reference 22).

Table 1.1. Age categorisation of children according to current E.U. guidelines and opinions (adapted from reference 23).

Category	Age
Preterm newborn infants	-
Term newborn infants	0-1 month
Infants and toddlers	1 month-2 years
Children	2-12 years
Adolescents	12-18 years

There are also ethical concerns regarding experimentation on children, which limits the PK data that is generated (11), and companies also deem the financial return from paediatric investment programs to be less lucrative (24). These issues pose a significant barrier to the development of paediatric medicines, thus manifesting in the use of unsuitable medicines and doses that fail to consider the real possibility of PK and pharmacodynamic (PD) differences between adults and children (11). One of the consequences of this oversight is the lack of suitable formulations in terms of dose and tolerability (8). This dilemma pertaining to the ethics of testing in children has been questioned in recent times. Grimsrud et al. argue that the original idea of protecting paediatrics from clinical trials, does not entail complete exclusion from trials, instead, it is intended to prevent unnecessary testing. They assert that these patients are entitled to safe and efficacious medicines, which can be achieved, through well-planned trials, using the necessary expertise, improved methodology, new modelling techniques and cutting edge analytical technology (9,25).

Paediatric dose adjustments are usually based on achieving PK or PD profiles equivalent to those achieved in adult populations (26). Compared to adults, paediatric patients differ in their biological, pharmacological and physiological attributes, and cannot be treated from a formulation scientist's point of view as just "small adults" (21). This is due to the stark differences between the two subsets of the population (27). Striking differences in the metabolism pathways in children can result in unexpected PK drug profiles, with altered clinical efficacy. The PK and PD profile of a drug varies widely depending on the developmental stage of a child, necessitating dose flexibility to suit the dosing requirements across all age groups (28). There may even be a need for more than one paediatric formulation, from birth to adulthood, due to the changes in the metabolic capacity, as the child matures, which poses an array of challenges to formulators (29).

At present, there is a tendency for "off-label" use of established adult medicines in children resulting in increased adverse events and decreased efficacy in the target population (30). These medicines are

known as “off-label”, as they have not been specially approved for use in children. The dose is often based on body weight, but this is fundamentally flawed in many cases, as this approach ignores important PK and PD nuances in this patient cohort (31). Healthcare professionals and parents or caregivers are often required to manipulate an adult medicine to obtain an appropriate dose for a child, for example, by splitting a tablet to provide a smaller dose or, in more complex cases, preparing a suspension from a crushed tablet (32). Such manipulations increase the variability in the product performance by inaccurate measurement, and there may be issues with stability or errors in instruction for manipulation (33). To illustrate the frequency of the use of these medicines, it has been reported that around 90% of babies in neonatal intensive care, 70% of patients in paediatric intensive care, and almost 70% of children in European hospitals, receive at least one unlicensed or “off-label” medicine during a hospital stay (34). In the case of infants and neonates, choking is one of the primary fears when unlicensed solid dosage forms are administered, meaning liquid dosage forms are desired. Suitable licensed liquid dosage forms for paediatrics are lacking, when it comes to many of the drugs that are used to manage common paediatric conditions, examples being phenytoin, spironolactone and hydrochlorothiazide, which are commonly formulated as extemporaneously prepared liquids. These extemporaneous products are not ideal, as taste is a common complaint, long-term stability is not assured and doubts surround the facilities used to prepare them (31).

Excipients are needed in drug formulations to improve drug solubility, taste-mask APIs and ensure stability (22). However, the safety of excipients in the paediatric population has to be thoroughly assessed, due to the immaturity of enzymes, particularly in neonates. The safety data for many excipients is limited in this context. Examples of established excipients in the field of formulation development that are prohibited from use in formulations to be given to children include sodium benzoate and benzyl alcohol (10). Strict thresholds are in place for ethanol as a co-solvent, and a question mark surrounds the use of the parabens and propylene glycol. Most worryingly, several studies have reported that paediatric patients are being exposed to levels of excipients above the permitted threshold with “off label” medicine usage (35,36). Concerns around the use of excipients led to the establishment of the Safety and Toxicity of Excipients for Paediatrics (STEP) database (12).

The lack of authorised medicines and the consequent off-label use is a significant problem in the paediatric population due to difficulties associated with conducting clinical trials, the relatively low patient numbers and the small size of the market (11). In neonates, the situation is particularly challenging due to the vulnerability of newborns and even lower patient numbers (37). Within the European Union (EU), since 2007, there have been significant efforts made to remove technical and regulatory issues and to incentivise companies to develop paediatric formulations (38). To help address the lack of suitable medicines for children, the E.U. introduced new legislation (known as

Paediatric Regulation), following in the footsteps of the U.S., who had recognised the problem a decade earlier. Since its inception, this legislation has governed the development and authorisation of all paediatric medicines and has three main objectives; more medicines for children, better product information and more paediatric research (39). Stemming from the introduction of this legislation, for all new medicinal products in development, pharmaceutical companies are obliged to provide a paediatric investigation plan (PIP) (once the pharmacokinetic studies have been completed in adults) and guidelines have been published to help advance the research. These changes pertain to any new drug, drug form, route of administration or new indication that companies are investigating. It requires them to conduct similar research in the paediatric population (40). Due to well-founded reservations about the applicability of adult bioavailability to children, Purohit suggests that an approach using advanced quantitative methods, in tandem with intelligent well thought out PK sampling, could yield greater amounts of biopharmaceutical data (11). Since the implementation of the Paediatric Regulation, from 2007 until 2015, 238 new medicines for use in children and 39 new pharmaceutical forms appropriate for children were authorised in Europe. The plans for this paediatric development, known as PIPs, are subject to agreement by the EMA and its Paediatric Committee (PDCO). A PIP can be defined as "a development plan aimed at ensuring that the necessary data are obtained to support the authorisation of a medicine for children, through studies in children" (41). The chronic lack of vital safety and efficacy information is a major hindrance to the quality of care received by paediatric patients, but the aforementioned measures have helped improve the situation. The percentage of clinical trials that have included children as subjects increased from 8.3% in 2007 to 12.4% in 2016 (12).

1.1.3 Modified-release (MR) drug formulations

1.1.3.1 Rationale for MR

Immediate-release (IR) formulations are designed to dissolve or release API without any delay so that the API can be absorbed by the body. They are intended to be used when a rapid onset of action is desired. In certain instances, formulations of this type are not subject to PK bioequivalence testing, due to their Biopharmaceutics Classification System (BCS) class (42). The FDA defines an IR formulation as one which "allows the drug to dissolve in the gastrointestinal contents, with no intention of delaying or prolonging the dissolution or absorption of the drug". The dissolution behaviour of IR formulations can be classed as either rapidly dissolving or very rapidly dissolving, which has implications for biowaiver applications (43). The EMA state that "in the case of a solid dosage form, the dissolution profile of the active substance depends on the intrinsic properties of the API" (44). Being able to fully disintegrate and dissolve, within 10 minutes of being exposed to the GIT contents is critical when a rapid therapeutic onset is required (45). The usefulness of IR forms is negated, when drugs exhibit

site-specific absorption, are chemically unstable in the GIT, and are capable of binding to the contents of the gut (1,46).

Modified-release (MR) is an umbrella term used to describe the formulations that deviate from IR formulations (47). They afford an additional temporal and spatial control of drug release, not offered by conventional dosage forms (48,49). A MR formulation, is a type of dosage form, that maintains the plasma level of drug at a steady-state, within the therapeutic range, over an extended timeframe, by mitigating the "peak-valley" fluctuations (50,51). Such a formulation design limits adverse effects associated with peak plasma concentration, as shown in Figure 1.2, and is particularly beneficial when long-term therapy is required (52,53). MR is desirable when specific PK profiles need to be achieved, site-specific drug delivery is the aim, or reducing the dose burden is the goal (54). By virtue of this formulation design, control is shifted from the patient and prescriber to the DDS, which avoids the fluctuating plasma profiles associated with conventional IR dosage forms (55). Drug release characteristics are chosen to accomplish therapeutic or convenience objectives, which ultimately increase the likelihood of better therapeutic outcomes for the patient (48). In essence, it optimises pharmacotherapy, and possibly improves the cost-effectiveness of drug therapy, whilst being based on a well-defined clinical need (50). Some of the most well-known MR products that generated substantial revenue for pharmaceutical companies are Effexor ER® (venlafaxine), Adderall XR® (dextroamphetamine and levoamphetamine) and Concerta® (methylphenidate) (56).

There is a lack of harmony amongst the different terms used for different MR forms, stemming from the advances made in the ever-evolving drug delivery community (5). Delayed (DR), sustained (SR), controlled (CR), long-acting (LA), extended (ER), timed (TR) and prolonged-release (PR) are examples of terms, that reflect the heterogeneity that exists. In particular, the terms MR and CR are used interchangeably throughout the literature (57). Aulton suggests a description that factors in the limitations of most MR dosage forms. He defines an MR Dosage form as a "system in which a portion of the drug is released immediately to achieve the desired therapeutic response promptly. The remaining dose of the drug is then released slowly, thereby resulting in a therapeutic drug concentration which is prolonged but not maintained constant" (55). Certain drugs have properties that render them unsuitable for MR. Examples being an extremely short or long biological half-life, potent drugs with narrow therapeutic indices, and those that exhibit slow dissolution (55). Warfarin is a classic example of a drug that would derive no clinical benefit from a MR formulation, as its pharmacological effect is not solely dependent on the plasma concentration (55).

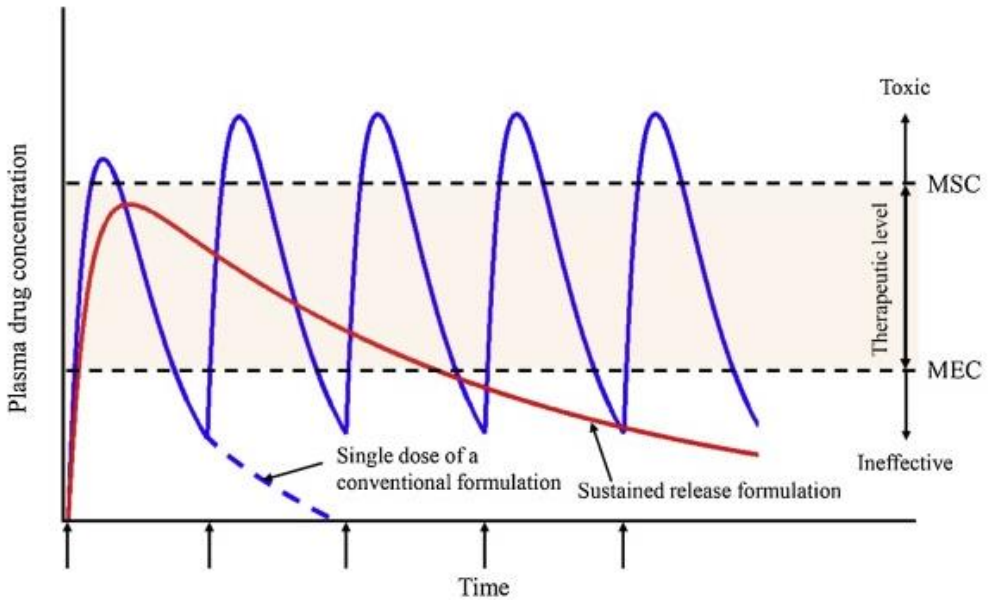

Figure 1.2. Plasma drug concentration-time profiles of conventional and SR formulations (58).

MR formulations are subject to many different conditions as they traverse the GIT (59). This journey in comparison to an IR formulation is far more complex, which is reflected by the *in vivo* behaviour (60). It has been described as a discontinuous process, whereby, the formulation experiences different types of luminal fluid, combined with different degrees and types of pressure and force in the gut (54). If a drug is being evaluated as a potentially suitable candidate for any formulation approach, sufficient solubility and permeability, taking into account the intended dose, has to be ensured. This is a more complex task for MR formulations, as the entirety of the GIT, and the associated formulation hurdles have to be considered (47).

1.1.3.2 Historical perspective

Pharmaceutical companies are constantly striving to develop novel MR systems, and any new drug product brought to the market will have an associated proprietary formulation strategy (48). This represents a shift in how MR technology is utilised by companies. Historically, this tactic was used to extend the life cycle of a patented product, but companies have started to realise the value of developing this type of drug delivery platform technology from the outset. Nowadays, companies are considering these approaches in early development plans. In Park's review on controlled drug delivery systems (DDS), drug delivery is split into three generations, shown in Table 1.2. The 1st generation covered the 1950 to 1980 period, the 2nd generation spans the 1980 to 2010 period, and the 3rd period is from 2010 onwards. He classifies the 1st generation as the golden age, illustrated by the sheer number of products that reached the marketplace during that period. A comparative slowdown in

productivity occurred during the 2nd generation, which Park argues must be explored, so the reasons for these failings can be established and prevent the 3rd generation from suffering the same fate (61).

Table 1.2. History of drug delivery technology from 1950 to the present, and the technology for the future (adapted from reference 46).

1950-1980	1980-2010	2010-2040
1st Generation	2nd Generation	3rd Generation
Basics of controlled-release	Smart delivery systems	Modulated delivery systems
Oral delivery • Twice-a-day, once-a-day	Zero-order release • First-order vs zero-order	Poorly soluble drug delivery • Non-toxic excipients
Transdermal delivery • Twice-a-day, once-a-day	Peptide and protein delivery • Long-term depot using biodegradable polymers • Pulmonary delivery	Peptide and protein delivery • Delivery for >6 months • Control of release kinetics • Non-invasive delivery
Drug release mechanism • Dissolution • Diffusion • Osmosis • Ion-exchange	Smart polymers and hydrogels • Environment-sensitive • Self-regulated release (Working only *in vitro*)	Smart polymers and hydrogels • Signal specificity and sensitivity • Fast response kinetics (Working *in vivo*)
	Nanoparticles • Tumour-targeted delivery • Gene delivery	Targeted drug delivery • Non-toxic to non-target cells • Overcoming blood-brain barrier
Successful control of physiochemical properties of delivery systems	Inability to overcome biological barriers	Need to overcome both physiochemical and biological barriers

The first truly effective MR product was the “Spansule”, introduced in the 1950s, and developed by Smith, Kline and French Laboratories. This technology, which utilised a sugar pellet that was subsequently coated using an API followed by the application of a waxy layer, enabled the delivery of dextroamphetamine sulfate over a 12 hour time period for the first time, and propelled MR technology to the forefront of formulators minds (62). The 1st generation focused on establishing and understanding distinct MR mechanisms, and the rapid development of clinically useful medicines greatly enhanced the capability of pharmaceutical companies to target certain therapeutic areas. The main challenges that formulators faced were site-dependent absorption and short transit times in the GIT. Oral formulations that only had to be administered once or twice daily, formed the bulk of the DDS developed during this period, and the *in vitro in vivo correlation (IVIVC)* of these formulations is quite well understood (63). However, the infancy of MR products is not immune to criticism. Several

commentators point out that the explosion in the area led to the release of MR products in the U.S. without any sound scientific rationale (64,65).

The lackluster success of 2nd generation DDS, which are more complex, has been ascribed to the formidable biological barrier that is the human GIT, and the inability of DDS to surmount this challenge. The *IVIVC* is harder to attain, due to drug release *in vivo* not solely relying on formulation properties (56). The fascination with zero-order release led to large resources being dedicated to optimising this technology, to achieve and maintain constant steady-state concentration in the plasma. Unfortunately for the pioneers of these technologies, researchers came to realise that zero-order release was not even necessary to develop clinically beneficial SR systems for oral delivery (63).

3rd generation DDSs are dominated by nanotechnology-based approaches, which, Park argues, is a contributing factor to the stalemate that exists (63). Park asserts that the root cause of this plateau centres around the sheer number of clinical trials that have failed. The author attributes this to a lack of translation from small animal models, such as the mouse, to humans. He suggests that a more critical evaluation of the research be conducted, to ensure that the data is conclusive, and has not been misinterpreted for fear of failure (61). In an excellent review by Yun et al., they follow suit in their criticism of the lack of diverse thinking within the drug delivery field. They express reservations about repeating the same approaches that have been used before and instead advocate more varied thinking using "trial and error methodology" which will accelerate the drug development process (56). A proliferation of new DDS is needed to overcome both the physiochemical shortcomings of APIs and the challenges presented by the mucosal barrier. An emerging type of MR is in the area of bioresponsive release. These systems are triggered by a biological stimulus, such as endogenous substance concentration, insulin being a prime example (66).

1.1.3.3 Categories of modified-release (MR)

1.1.3.3.1 Mechanisms of MR

The advancement of drug delivery technology over the last number of decades has resulted in several hundred MR products coming to market (67). This proliferation is largely a function of the sheer number of combinations of novel and established excipients that are possible (49). In contrast, the number of different types of MR mechanisms has not drastically risen, which can be partly ascribed to the marked success of products reliant on the established mechanisms of release. The different types of MR mechanisms can be split into physical and chemical. Physical methods include those based on dissolution-controlled, diffusion-controlled, osmotic pressure and ion-exchange mechanisms (Figure 1.3). These mechanisms can operate independently, together or consecutively.

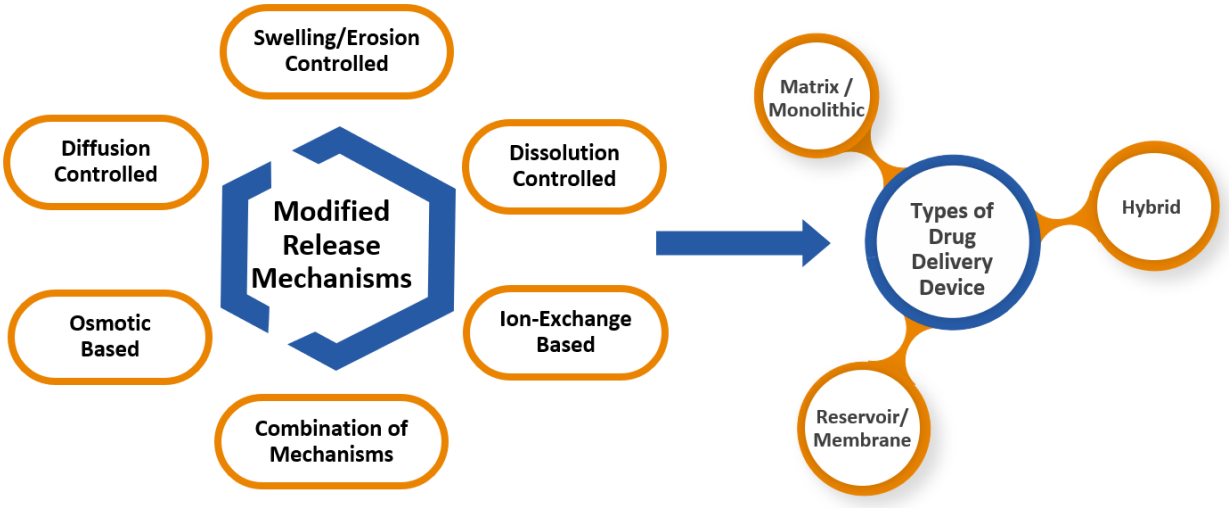

Figure 1.3. Schematic diagram showing the different types of MR mechanisms and types of drug delivery device used as part of MR dosage forms.

In dissolution-controlled drug release system, the membrane surrounding a drug core (reservoir), dissolves. The ability of a polymer to dissolve in an aqueous medium is fundamental to this mechanism. Synthetic polymers such as polyvinylpyrrolidone (PVP) and polyethylene glycol (PEG) are suitable materials for this approach. A second type of DDS that has been developed, and utilises the dissolution-mediated release mechanism, is known as a matrix device. Here, the drug is uniformly distributed in the polymer matrix. In the case of a hydrophilic matrix, for the drug to be released, dissolution of the polymer matrix is required, resulting in the matrix decreasing in size (68).

Diffusion-controlled dosage forms utilise a different mechanism that requires the drug to diffuse through a polymer membrane or a matrix. In the case of a reservoir system, the rate of diffusion follows Fick's law. With diffusion-controlled monolithic (matrix) systems, the drug release rate decreases with the square root of time, due to the drug present in the centre of the matrix having to travel a longer distance compared to the drug located at the surface (69). Examples of polymers that can be used if this drug release mechanism is desired include ethylcellulose (EC), polyvinyl acetate (PVA) and various types of polymethacrylates (55).

Polymers that are capable of swelling in an aqueous medium offer another option to control drug release, the most well-known being hydroxypropylmethylcellulose (HPMC). Many of the MR mechanisms work in tandem within the same dosage form, whether that be a matrix or reservoir system. The swelling and erosion mechanisms are prime examples of release mechanisms that are typically employed alongside one another, illustrated in Figure 1.4. Semisynthetic and synthetic hydrophilic polymers, capable of swelling with gel-like properties, have been integral to the advancement of dosage form development that relies on these two mechanisms to control drug

release (70). The drug is available from hydrophilic matrices (such as HPMC) following the dissolution of the polymeric matrix or swelling of the matrix, after which the swollen state is dissolved (68). The mechanism works by the polymer swelling upon contact, with an aqueous environment, resulting in a formation of a viscous gel layer, which expands and is highly resistant to water penetration for a relatively short duration of time. Over time, the bulk medium reduces the polymer concentration at the matrix tablet surface which impacts the structural integrity of the polymer (71). This event is characterised by the disentanglement concentration, after which the material at the surface is eroded resulting in the exposure of a new area, which subsequently becomes hydrated and swells followed by the erosion of the outermost material. The thickness of the gel layer is controlled by the balance between the swelling frontier of the tablet core, and the erosion front at the gel surface. At the same time, drug diffusion is occurring, which itself is hindered by the formation of the gel (49). Therefore, drug release is mediated through a combination of drug diffusion through the fibril network and disintegration of the matrix (72). Drug diffusion can only occur through the gel-like layer formed, and zero-order release can be approached, if the swelling and erosion fronts meet. Release modifiers are typically included to achieve the intended release profile of the drug. In addition, gel modifiers are used to adjust the gel layer's diffusional characteristics and influence gel formation. This gel-like layer is not a true gel, as it dissolves. Instead, viscous matrix or pseudogel are more apt terms, which capture the series of processes that form the gel-like layer. The high degree of viscosity results from the entanglement of adjacent polymeric chains, that create gaps, through which the drug can diffuse. These spaces are not fixed, as the structure is dynamic (55).

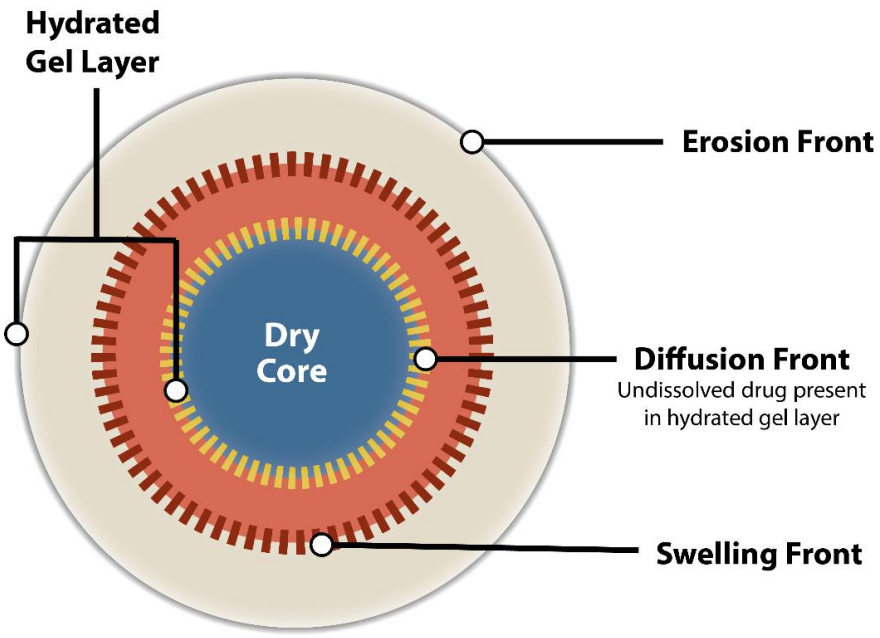

Figure 1.4. Schematic diagram showing the fronts resulting from the swelling/erosion mechanisms responsible for drug release from the system (adapted from reference 73).

Dissolution and diffusion mechanisms are the most prominent in terms of their commercial applicability. However, osmotic-based formulations experienced a period in which they proved popular, starting in the 1970s. Alza pioneered the elementary osmotic pump design (OROS®), which yielded products such as Procardia (nifedipine) XL®, Lyrinel® XL (oxybutynin) and Concerta® (methylphenidate) (74). The original design encompasses an osmotic drug core, which has a semipermeable membrane containing a laser-drilled single orifice, through which the drug is delivered. GI fluid penetrates the semi-permeable membrane which dissolves the drug, creating an additional osmotic influx of fluids, which leads to a build-up of hydrostatic pressure, forcing the drug out of the core through the orifice (68). The original design confers constant release for up to 24 hours, independent of pH, as the GI fluid influx remains constant, and the drug core is saturated. Once the drug concentration within the reservoir drops, the drug release rate will also decrease. The OROS® technique has since evolved to include more sophisticated designs, such as the push-pull design, controlled porosity osmotic pump and OROS® for liquid formulations (75). However, the number of products based on the OROS® mechanism, pale in comparison to the number of products developed using diffusion and dissolution-controlled mechanisms.

Lastly, the ion-exchange mechanism offers its own unique advantages, but more often than not, requires the addition of a rate-modifying polymer, which generally operates via a diffusion-controlled mechanism (56). This category will be discussed in more detail in a later section.

1.1.3.3.2 Types of drug delivery device

Another classification for oral MR dosage forms is based on the device from which drugs are released. For the purpose of this thesis, they will be split into matrix, reservoir and hybrid (49).

1.1.3.3.2.1 Matrix systems

A matrix system, sometimes known as a monolithic system, contains the drug dispersed throughout the excipient forming the matrix. Depending on the concentration of the drug in the polymer matrix, the monolithic dosage form is either known as a monolithic solution (if the saturation solubility is not exceeded), or a monolithic dispersion if the dosage form is manufactured in such a way, that that the drug concentration is greater than the saturation solubility in the excipient (76). These monolithic systems can be produced using either a hydrophilic or hydrophobic matrix-forming excipient, and are typically easier and less costly to manufacture compared to reservoir systems (77).

Hydrophobic/insoluble polymer matrices operate via a different principle to that discussed above. The drug particles dispersed throughout the insoluble matrix are dissolved by the aqueous medium that enters the dosage form. The release is normally proportional to the square root of time. Similar to hydrophilic matrices, water-soluble channel agents enable the entry of water into the dosage form,

and their dissolution paves the tortuous way that the dissolved drug traverses to diffuse to the surroundings of the dosage form. These channelling agents can also double up as solubilising agents, which are used to improve the dissolution of the drug and improve the overall effectiveness of the dosage form (55).

1.1.3.3.2.2 Reservoir systems

Reservoir systems consist of a core that is encapsulated by a membrane. Drug release from these systems typically occurs via osmotic pumping, dissolution or diffusion. The majority of DDS in this category function via drug diffusion. The driving force for this process is the drug concentration gradient. As long as drug saturation is present, constant drug release occurs. Once the internal drug concentration is no longer saturated, resulting in a decreased concentration gradient, the drug release will decrease accordingly. The thickness of the coating and the dissolution rate of the polymer are the main determinants of drug release (49). The membrane/barrier should not erode or swell, as is the case with hydrophilic matrices. Once the coating level dissolves, the entirety of the drug is available, which has proven to have safety implications, and nowadays this approach is not often used (76).

1.1.3.3.2.3 Hybrid systems

As the name would suggest, hybrid systems are comprised of a combination of the two aforementioned systems. A multi-unit dosage form encompassing the two dosage form designs, mentioned above, is the Toprol-XL® product (metoprolol). In this instance, coated pellets are dispersed throughout a tablet matrix (49). Hybrid systems are particularly suited to chronotherapeutic dosage forms, which aim to release API in a manner that mimics the circadian rhythm of the body (78). Examples of products include Covera-HS® which contains verapamil, and InnoPran XL® which contains propranolol.

1.2 Formulation approaches used in this work

1.2.1 Ion-exchange resins (IERs)

1.2.1.1 History of IERs

Since the 1930s, the application of synthetic IERs, has enjoyed a rich history in many different fields, ranging from the food industry to the agricultural sector to chemical engineering (79). They are perhaps best known for their application, as part of water treatment processes such as demineralisation and softening. Prior to the use of synthetic IERs, natural and synthetic siliceous materials, called zeolites, were used as ion-exchangers to purify water (80). Other uses include acting as a catalyst in chemical reactions, and the purification of APIs (81). It wasn't until the 1950s that IERs were used within the pharmaceutical field. Since then, they have proven their worth as functional

excipients, in the form of taste-masking agents, and release modifiers (82–84). An additional, and often forgotten application of IERs, is their use as therapeutic agents (85). Cholestyramine resin USP is approved by the FDA as a bile acid sequestrant, and Kayexalate® powder (sodium polystyrene sulfonate) can be used as an adjuvant in the treatment of hyperkalemia (86,87).

Many patents have been granted to pharmaceuticals companies who utilise these polyelectrolytes to achieve specific therapeutic objectives. Pioneers of the IER approach to address varying formulation challenges include: Burke, Irwin, Sprockel and Motycka (88–92). Their long-lasting contribution to the field of IERs is evident by the frequency at which their work is referenced by others in the field, and in this thesis. More recently, the authors Jeong and Park have played a significant role in furthering the understanding of drug-resinate behaviour. Through a series of innovative applications of the technology, the approach has experienced an upsurge in popularity, resulting in formulations suitable for virtually all routes of administration, apart from parenteral (93).

1.2.1.2 Categories of IER

IERs are water-insoluble, crosslinked polymers such as divinylbenzene, containing salt-forming groups in repeating positions on the polymer chains (94). Relevant properties from a drug product development perspective include their high ion-exchange capacity, physiochemical stability, and their insolubility in any solvent. The latter makes them a favourable option for the MR and taste-masking of drugs (79). The resin matrix is responsible for the physical properties of the resin, and can play a role in the drug loading achieved, depending on the properties of the loaded drug (95).

IERs can be categorised into either cation exchangers or anion exchangers (Figure 1.5), which can be further distinguished as either “strong” or “weak” exchangers (96). “Strong” resins are generally used for MR purposes (97), whereas “weak” resins can be used for taste-masking purposes (98,99). The terms “strong” and “weak” do not refer to the physical strength of the resin, instead, they are derived from the Arrhenius theory of electrolyte strength. In this context, a “strong” resin is capable of complete dissociation at any pH and irrespective of the ionic form. On the other hand, the degree to which “weak” resins dissociate is pH dependent. Examples of covalently bound ionic groups that are “strongly” and “weakly” acidic are sulfonic acid and carboxylic acid. Examples of covalently bound ionic groups attached to the matrix that are “strongly” and “weakly” basic are primary amine and quaternary ammonium groups respectively. Commercially, some of the more well-known anionic resins are Amberlite™ IR-400 (strong) and Amberlite™ IR-4B (“weak”) (95).

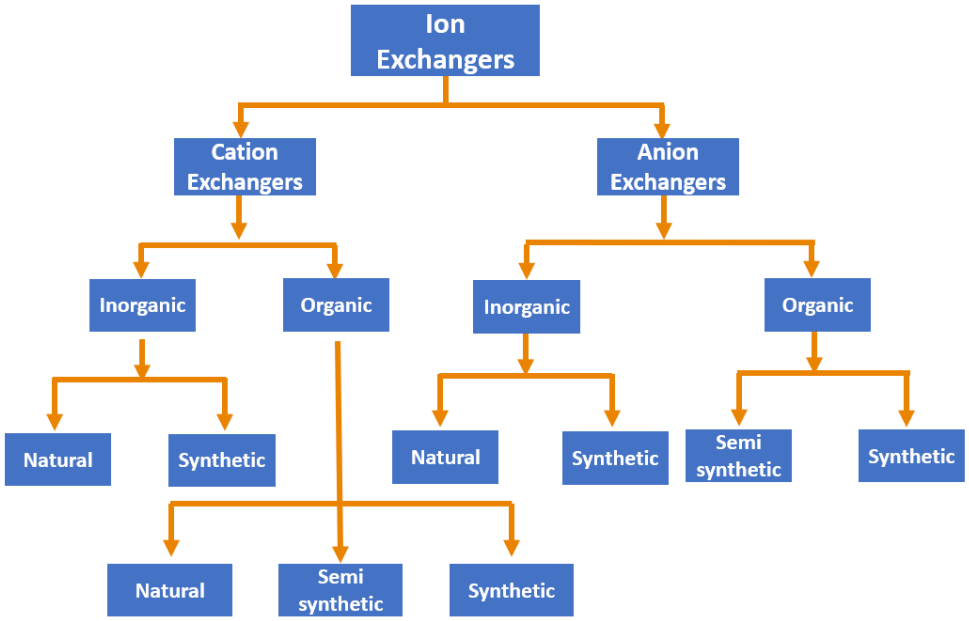

Figure 1.5. Classification of ion-exchangers (adapted from reference 89).

Resins can be manufactured into different physical forms. They are available as a powder form, which is popular in the pharmaceutical industry, or as a bead form, which is the type used for many applications in other industries. The two forms are often named “spherical” and “non-spherical”, “spherical” referring to the whole bead form, and “non-spherical” referring to the powdered form. The IER material has a highly developed structure of pores, as illustrated in Figure 1.6, which enables the concomitant trapping and release of ions. Irrespective of the resin’s form and purity, manufacturers still have to assure the safety of the product, as the resins usually constitute a large proportion of the pharmaceutical formulation. Pharmaceutical grade resins in the Amberlite™ range are indicated by the presence of P in the commercial name (95).

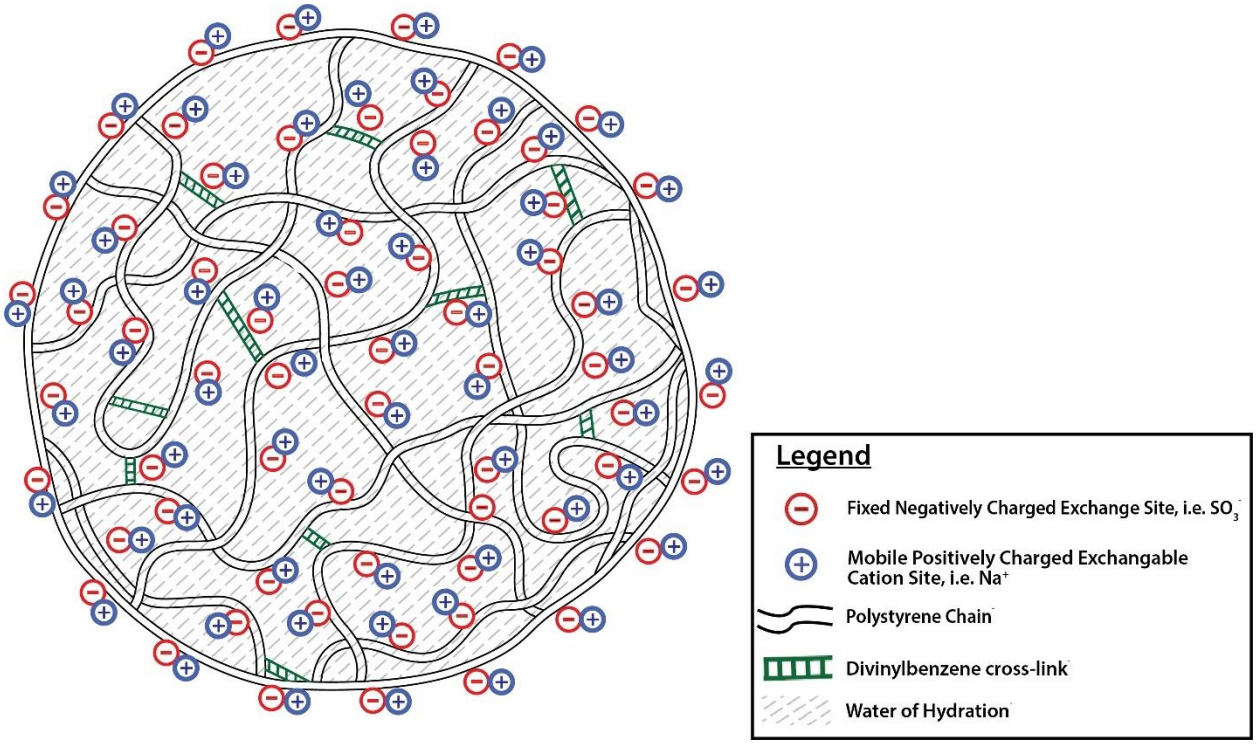

Figure 1.6. Expanded view of a polystyrene IER bead (adapted from reference 93).

One of the most prevalent acidic IER used in pharmaceutical applications is sold under the tradename Amberlite™ IRP69, which is a strongly acidic, sodium form cation exchanger (Figure 1.7). It is suitable for complexation with basic drugs that can be protonated. As it is a salt of a strong acid and base, the ability of the resin to exchange ions is virtually independent of pH. The material itself is available in a fine, free-flowing powder, and the structure consists of pores that enable the transport of ions (102). Its particle size ranges from 25-150 microns, and it is produced by milling the larger bead form, which has a particle size of 500-2000 microns (103).

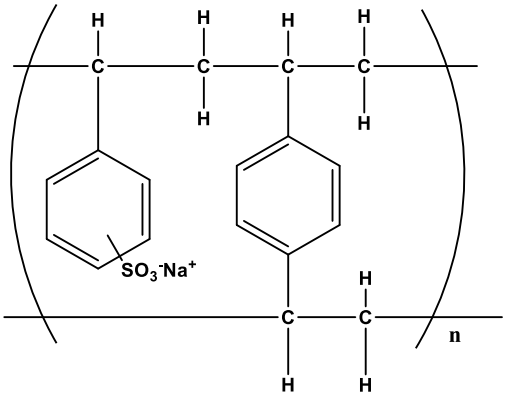

Figure 1.7. Chemical structure of Amberlite™ IRP69 (Amberlite™ IR120 has the same chemical structure but the resins differ in their physical form/particle size).

Amberlite™ IRP64, is a weakly acidic cation exchanger, derived from a porous copolymer of methacrylic and divinylbenzene, present in the hydrogen form (Figure 1.8(A)), available as a dry fine powder, and predominately used for taste-masking applications (104). Amberlite™ IRP88 is the potassium salt of a Amberlite™ IRP64 (Figure 1.8(B)) and has been used as a tablet disintegrant, due to its swelling properties (105). Although this is the grade's predominant function, as documented in many research articles and patents, its use as a taste-masking agent has also been reported in a patent lodged by GlaxoSmithKline (GSK). Moreover, there is an E.U.-approved oral suspension product containing this specific grade of resin (106).

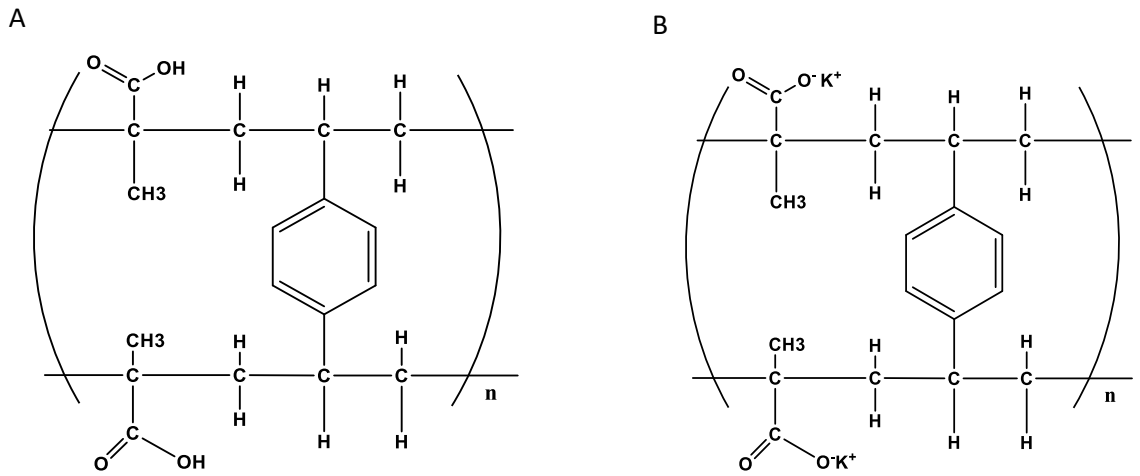

Figure 1.8. Chemical structure of Amberlite™ A) IRP64 and B) IRP88.

1.2.1.3 Ion-exchange theory

1.2.1.3.1 Overview

The critical component of IERs, are the functional groups, attached to the polymer backbone of the resin. These functional groups are responsible for the exchange of mobile ions. This is not just limited to inorganic ions but also applies to organic ions, such as drug molecules (95). The ion-exchange reaction is reversible, as shown in Figure 1.9, and the position of equilibrium is dependent on the environment. When the drug is loaded onto the resin, the complex is then referred to as the resinate, drug-resin complex (DRC) or sorbate. The ion which is present on the resin, and available for exchange, is known as the counterion, and the competition that exists between it and the drug ion, is responsible for the complexation. Upon exposure of the resinate to the luminal contents of the GIT, exchange of loaded drug can occur, with ions of the same charge, in the gastric medium (107,108).

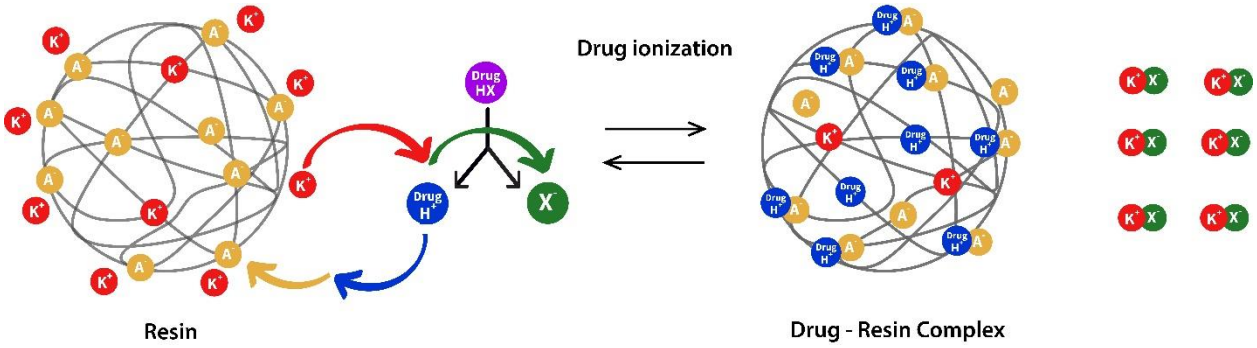

Figure 1.9. Illustration of drug release from a DRC (adapted from reference 12).

Ion-exchange can be defined as an "electrostatic interaction of ions between those in solution and on IERs, without significant change in the structure and properties of the resins". As mentioned above, the ion-exchange process is a reversible, selective and involves a stoichiometric exchange of ions with similar charges, between the IER and the external liquid phase (80). The relative affinity of a resin for specific ions can be expressed in terms of the selectivity coefficient. This parameter incorporates the ion's valence and hydrated size, along with the pH of the solution, and pKa of the drug and resin (95). The term "ion-exchange capacity" is a critical property that is the major determinant of the level of drug-loading achievable. It is measured as the "number equivalents of an ion that can be exchanged" and can be expressed with reference to the mass of the polymer (known as "Weight Capacity") or its volume (known as "Volume Capacity"). A frequently used unit for either is "milliequivalents of exchange capacity per gram of polymer." This is commonly abbreviated to mEq/g. Essentially it is the number of functional groups per unit weight or volume of the resin and is the primary factor responsible for the extent of ion-exchange that occurs between different ionic species (95). It represents the maximum drug loading that can be achieved under ideal lab conditions, and the actual loading is normally markedly lower, in the region of 25-75% (95). "Weaker" IERs such as Amberlite™ IRP64 have higher exchange capacity (10 mEq/g) relative to "strong" cation exchangers such as Amberlite™ IRP69 (4.5-5.5 mEq/g). This can be attributed to the structure of the polystyrene matrix, which has a lower propensity to swell, and the greater bulk of the ionic substituents in "strong" resins which limits the accessibility of drug ions, thus lowering the ion-exchange capacity (95).

The moisture content of resins varies drastically, depending on the product in question. The two main factors which influence the moisture content are the degree of crosslinking and the type of functional group. Lower crosslinking levels in resins lead to products with higher moisture levels. Functional groups, such as sulfonic acid and quaternary ammonium, are known to absorb large amounts of moisture, so their presence in resins will lead to products which are highly hygroscopic (101).

1.2.1.3.2 Drug-loading and drug release

Drug-loading of the drug onto the IER will be influenced by many factors of varying importance, depending on the drug and resin involved. The degree of crosslinking impacts the IERs level of porosity, as well as the swelling behaviour, and has major implications for drug loading. The inherent affinity of the drug for the IER is an often-overlooked factor that can contribute towards low loading levels being achieved. More predictable factors influencing the loading process include the concentration of drug in the loading solution, the equilibrium constant for the ion-exchange reaction, and selectivity of competing ions that may be in solution. The choice of solvent (solubility and swelling effect), the molecular size of the drug and charge density also impact adsorption capacity (108). Factors such as temperature, particle size and the extent to which the resin is swollen, have been shown to influence the kinetics of drug-resin binding (109).

The pH of the reaction medium, and the presence of competing ions, are the major determinants of the strength of the ionic interaction. The interactions between the IER and drug, although primarily chemical in nature, are also partially a result of physical adsorption. In the case of physical adsorption, no ion-exchange occurs (102). Jeong et al. introduced the concept of multiple loading stages (or steps) to optimise drug-loading. As part of their investigation into factors affecting the loading process, they found that three loading stages were required to maximise drug loading in order to overcome the equilibrium that was established between "free" drug and resin. The rationale underpinning this approach was the introduction of fresh drug solution creating a driving force towards further binding. The downside to this approach is the need for fresh drug solution at each stage, which is costly, when loading efficiency at later stages is poor (110). Despite Jeong et al.'s findings, the predominant drug loading method still involves only a single step.

The pH of the loading solution is a critical parameter that needs to be considered when using "weak" resins, as they are not dissociated across the whole pH range unlike "strong" resins (104). In other words, when "strong" resins comprise a portion of the reaction media, the pH of the loading solution is not a major factor that has to be considered which is beneficial for a number of reasons. Firstly, the pH of the drug loading solution does not have to be altered to ensure substantial drug loading and the influence of by-products from the ion-exchange reaction on the pH of the loading media does not have to be considered. In contrast, when loading the drug onto "weak" resins containing functional groups such as carboxylic acids or primary amines, it is vital that the pH of the loading medium is adjusted to ensure that the resin is ionised and capable of binding. Taking the carboxylic acid resins as an example, an optimum pH value of 6 is put forward by the manufacturers for drug-loading (104). As the pKa of carboxylic acids is approximately 4, the difference of 2 pKa units ensures the resin is predominately dissociated (101). As important as this consideration is, the ionisation state of the drug is also critical,

and a balance needs to be achieved, with respect to the loading medium pH, to ensure neither component is unionised. One advantage that “strong” resins hold over “weak” resins, is that the loading only has to be carried out at a pH that facilitates drug ionisation, in contrast to drug-binding experiments involving “weak” ion-exchangers (108).

If a basic drug is being loaded onto a cation exchanger, four combinations are possible (listed (i)-(iv) below) depending on the solid-state of the drug and resin before introducing into the liquid medium (there are four analogous combinations for an acidic drug and cationic resin).

(i) Resin (Na^+ form) + Drug (salt form)

(ii) Resin (Na^+ form) + Drug (free base form)

(iii) Resin (H^+ form) + Drug (salt form)

(iv) Resin (H^+ form) + Drug (free base form)

Reactions (i) - (iii) all have cationic by-products if binding occurs. These cationic species will compete with the drug for the resin and in turn, reduce the level of drug-loading. Reaction (iv) is the only combination that proceeds stoichiometrically and represents the best chance of achieving maximal drug loading (103).

Properties of resins, such as crosslinking, porosity and particle size, also have a prominent effect on the desorption of drug from the resin (110,111). Similar to the loading process, the selectivity of the drug for the resin, will impact the rate and extent of the release, as will the nature and concentration of electrolytes in the release medium/GIT. The hydrophobic backbone of the resin can also have an appreciable effect on drug release, due to the influence of van der Waals forces (101). These hydrophobic interactions are more substantial with backbones that have a high degree of crosslinking and, depending on the resin and its functional groups, other drug-resin interactions are a possibility that can influence drug release rates. An example is an interaction that can occur between the aromatic structure of the resin and a drug molecule that possess a transition metal element, resulting in a coordination complex forming (95,108).

Several mechanisms have been reported to be involved in the release of a drug from uncoated resinate. The model initially proposed by Boyd et al., is one of the earliest attempts to comprehensively elucidate the rate-limiting factor in the ion-exchange reaction (112). This study investigated the ion-exchange reaction from the perspective of drug loading, but the model has been extensively used to describe the drug release kinetics from resinates. Boyd et al. asserted that two separate sequential diffusion processes, particle and film diffusion, control drug release. The former

refers to the diffusion of the drug ion (red circles in Figure 1.10) through the resin particle whereas the latter pertains to the drug ion crossing the thin liquid film (represented by the dashed curved line in Figure 1.10) that surrounds the particle. Both processes are illustrated in Figure 1.10, where the ion-exchange process is graphically represented. Evident from Figure 1.10, is the drug ion moving from the bulk solution through the stagnant liquid film that envelops the particle. The porous nature of the particle affords a diffusional pathway, through which, the ion traverses and exchanges with an ionic site (green circle) deep within the resin structure (112). Jeong et al. have applied this model in several papers to investigate the drug release mechanism of coated and uncoated resinates (111). Other groups report that there are three processes involved: particle diffusion, film diffusion and chemical exchange rather than the two (particle and film diffusion) postulated by Boyd et al. (113). Reichenberg built on the rate equations that form the Boyd model by addressing its deficiencies relating to the assumptions underlying both the particle and film diffusion models. The author modified the equations and included approximations which, in effect, translated to cut-off values being assigned for the fraction of drug release (<85% and >85%) from the resinate. These modifications aided with the elucidation of the rate-limiting process and have become commonplace in the models applied over recent years (114). As a starting point, the classical Higuchi equation has been applied by several other groups interested in probing the underlying drug release mechanism of resinates (109,111).

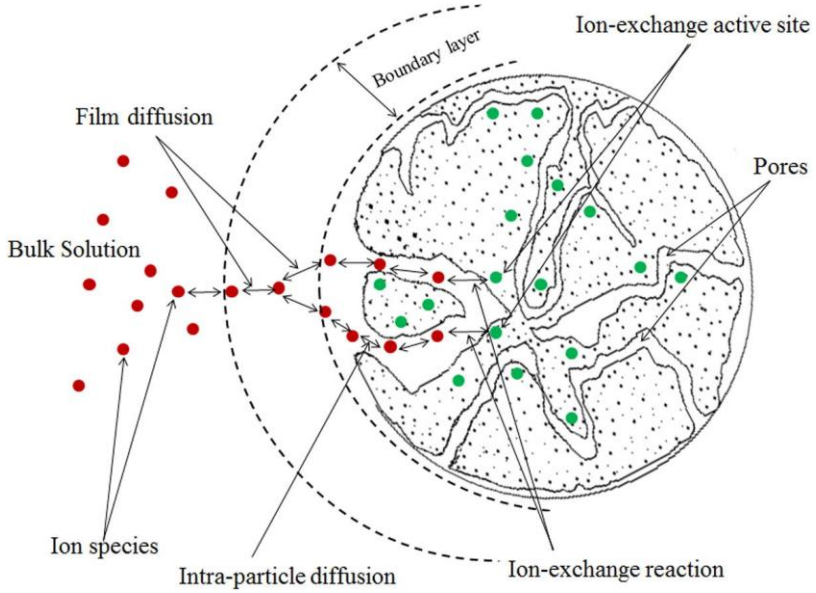

Figure 1.10. Schematic depicting the ion-exchange process (115).

1.2.1.4 Methods of complexation

Common methods of effecting complexation between suitable drugs and IERs can be broadly classified into two main categories, namely the batch method and column method (116). The vast majority of DRCs in the literature are produced via these methods. Of these two methods, the batch method

predominates, due to the simplicity of the process and the fact that it is less time-consuming. Many examples, exist in the literature, illustrating this method as an effective technique (117,118), although several novel methods have been described recently, which use granulation and hot melt extrusion (HME) to produce the desired product (119–121).

Drug loading using the batch method is accomplished by adding a known amount of resin into a drug solution and mixing until equilibrium is established. The complex formed is then subjected to filtration, washing (to remove any by-products or loosely adhered drug) and drying at either room or accelerated temperature(s) (80). In the column method, a concentrated drug solution is passed through a column, that is packed with ion-exchange particles, until the pH of effluent is equal to eluent, which indicates that the ion-exchange sites are saturated. The product is subsequently washed and dried (122). Fine powders such as the Amberlite™ IRP resins, are not as suited to the column method of loading, which is more prevalent in other fields of research and industry where resins are used. This is due to their fine particle size, which is problematic to pack in a column operation. However, Jeong et al. investigated the suitability of both methods for sorption of dextromethorphan hydrobromide monohydrate onto Dowex® 50WX2, and found higher drug-loading could be achieved with the column process, relative to the single-batch method (110).

1.2.1.5 Pharmaceutical applications and commercialisation

The use of IERs as DDS to help overcome formulation-related problems has been demonstrated in many studies, ever since Saunders and Chaudhary studied the release kinetics and complexation efficiencies of alkaloids from IERs in the 1950s (123). Their role in pharmaceutical formulations has evolved from simple excipients for tablet disintegration to modification of the rate of drug release (110). Recently, their use has diversified. Applications such as taste-masking of bitter APIs, and stabilisation of hygroscopic drugs to prevent agglomeration and deliquescence have been reported (124). Onconova Therapeutics adopted this approach as a method to improve rigosertib's solubility and stability at gastric pH values (125). IERs have also been used, as part of an intermediate coating, to reduce drug leaching, and new solvent-free methods of manufacture of DRCs, such as HME have been utilised (119,126). The vast majority of IER-based formulations are solid dosage forms, but several other dosage forms have been investigated, including iontophoretically-assisted transdermal systems, gums for buccal absorption, nasal products, and those designed for ophthalmic delivery (80). CR liquid dosage forms and orodispersable films have also been developed (117,127).

The development of MR oral liquids has been plagued by the leaching of the drug into the storage vehicle. The solubility of the drug dictates the extent to which this occurs, meaning significant drug leaching during storage can occur with water-soluble APIs, if an aqueous vehicle is used. The use of

IERs in the formulation of multi-dose liquid formulations is a promising approach, as it overcomes this limitation if a non-ionic vehicle is used. Drug release can only be initiated by the presence of ions, meaning it is one of the few feasible methods for formulating MR liquids, without the risk of premature drug release (128). IERs can offer better control over other methods for controlling drug release due to solely relying on the ionic environment, and not being susceptible to factors such as enzyme content in the release environment (129). In theory, the time it takes a displacing ion to travel into the interior of the resin, combined with the time that the drug ion has to diffuse out again, can translate into a SR effect. However, the level of control afforded by uncoated complexes, combined with the relatively short delay of drug release, is insufficient for many SR applications, due to the consistently high ion concentration in the gut (130). Therefore, there is a need for a diffusion barrier to be applied to prolong the release of the drug for the necessary duration of time. Thus, drug release can be tuned by selecting suitable cross-linked resins, in combination with an appropriate coating polymer (131).

Both aqueous and non-aqueous-based coating solutions have been demonstrated to be effective in applying diffusion-retarding polymer, by solvent evaporation, to microparticles intended to be used in liquid or solid dosage forms (90,132,133). A comparison between the two approaches (aqueous and non-aqueous solvent evaporation) for encapsulating terbutaline-loaded resinates found distinct differences in morphology and drug release behaviour between the two methods (134). Interfacial nylon polymerization was also trialled as an alternative microencapsulation technique by Torres et al., and found to be a suitable technique (135). Motycka and Nairn spray-congealed DRCs with a series of waxes, to achieve SR (91). Less popular methods of microencapsulation include the use of crosslinked chitosans, as part of a modified emulsion-solvent evaporation technique (136,137). On a large scale, the Wurster process is commonly used to coat microparticles, intended to form part of a suspension formulation (129).

Several products that utilise IERs are on the market, which indicates their potential for commercial success. Amberlite™ IRP64 enabled the development of a stable oral dosage form of cyanocobalamin. Before this, vitamin B12 formulations had been plagued by chemical instability problems (124). Most notably, this approach has proven fruitful in the development of MR oral liquids. The Pennkinetic® system, which uses complexes coated with a mixture of PEG4000 and ethylcellulose developed by the Pennwalt Corporation, is the most notable application of IERs for the preparation of MR liquid suspensions, an example being the Tussionex® drug suspension which was approved by the FDA in 1987 (102). In recent times, Tris Pharma, have developed their own LiquiXR® technology to develop ER products in liquid form through a combination of coated and uncoated complexes such as

Dyanavel® XR (amphetamine) and Karbinal® ER (carbinoxamine)(138). Neos Therapeutics is another company that heavily utilises ion-exchange technology to develop pharmaceutical formulations (139).

Seroxat® (paroxetine) oral suspension, marketed by GSK, is an example of a taste-masked product that exemplifies another application of IERs (140). Vesicare® (solifenacin) 1 mg/mL oral suspension, which is licensed for the treatment of neurogenic detrusor overactivity in paediatrics and overactive bladder in adults, is a second example of a product that avails of this taste-masking technology (106). In this instance, the use of an IER circumvents the issues of stability and palatability, that are associated with extemporaneously compounded paroxetine (95). Borodkin pioneered the use of IERs to mask the bitterness of APIs (141,142). The underlying principle governing the use of resins for the purposes of taste-masking is the DRC's insolubility at salivary pH, ensuring that an acceptable amount of drug will not be released at salivary pH (143). When the complex enters the gastric compartment, the release is initiated by an influx of competitive ions from the GIT.

Examples of other commercial success stories incorporating IER technology include the ophthalmic product Bectopic S®(betatoxol), and the nicotine replacement patch Nicorette® (144). These products utilise Amberlite™ IRP69 and Amberlite™ IRP64 respectively. Biphetamine® (amphetamine and dexamphetamine) is an example of a commercial product that has two cationic APIs bound to the same resin. Penntuss® is another example of an ion-exchange liquid formulation containing two APIs (codeine and chlorphenamine), however, it differs from Biphetamine®, as the drugs are bound separately to the same resin type, prior to being used in the same formulation. An additional interesting feature of this product is that the codeine DRC is coated with ethylcellulose (EC), whilst the chlorpheniramine DRC is left uncoated (95).

As described previously, IERs can exist in two distinct physical forms. Many of the products and systems referenced already refer to resinates formed using powdered resin. However, the bead form of the resin, can also be used for the purposes of formulation development. Raghunathan et al. were one of the first groups to report investigations into the application of a semipermeable membrane to the sulfonic acid cation exchange resin system for SR applications (145). Further studies by Burke et al. using propranolol were conducted to study the *in vitro* sorption and desorption characteristics of different resins and the authors found that only one resin was suitable for the purposes of SR (88). MR suspensions of diltiazem were later produced using "strong" cation exchangers in bead form, which were stable for four months at room temperature (117). Jeong and Park advanced the art, by preparing coated drug-loaded IER beads, which they subsequently granulated and compressed into fast-disintegrating tablets (146). A gastroretentive system containing theophylline was reported by Atyabi et al. They attribute the gastroretentive properties to the loading of bicarbonate onto the resin

beads alongside the drug, which leads to the production of carbon dioxide when chloride displaces the bicarbonate in the gut (147).

1.3 Physical processing of pharmaceutical solids

1.3.1 Spray-drying

Spray-drying is an energy-intensive unit operation, that has the potential to convert liquid feeds, such as solutions or suspensions, into a solid product (148–150). The process consists of four distinct phases (as illustrated in Figure 1.11): the atomisation of the liquid feed, contact between the liquid and drying gas, rapid evaporation of solvent causing the separation of the dried fine particles from the heated gas medium, and finally the collection of the powder. The first step occurs in the nozzle, whilst subsequent steps occur in the drying chamber, cyclone and collecting vessel respectively (151).

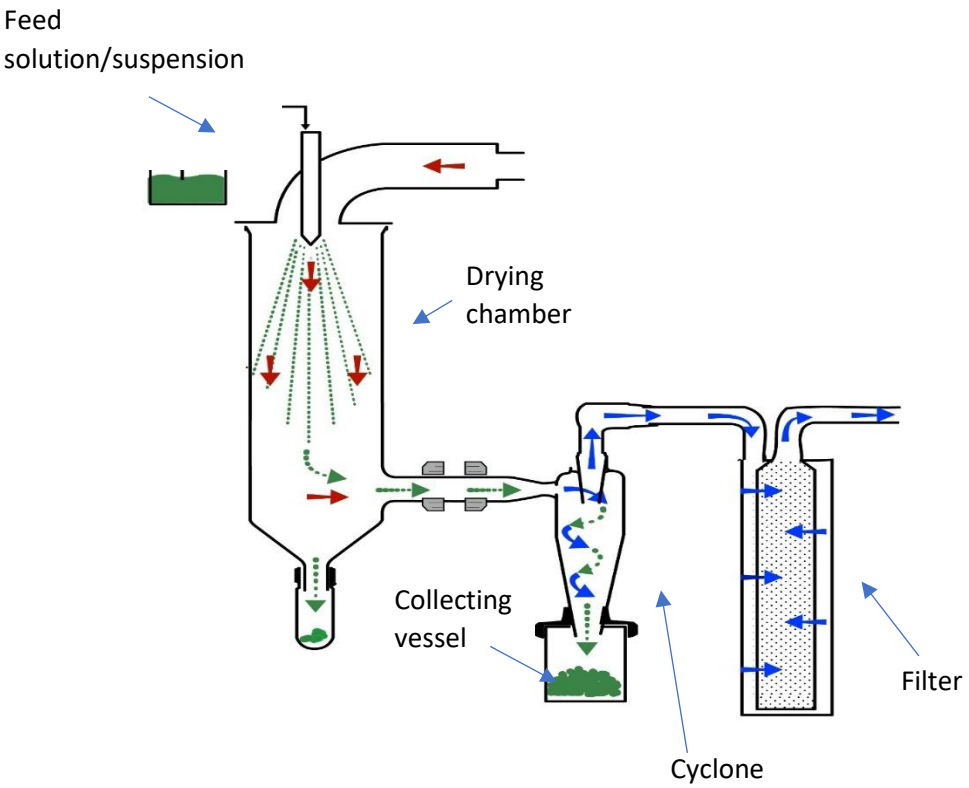

Figure 1.11. Laboratory scale spray-drying set-up (149).

Spray-drying is a complex process, due to the reliance of product quality on many formulation and process factors (151,152). It has gained the reputation of being able to produce customisable

microparticles, through particle engineering, with the desired morphology and properties (153–155). The "quality by design" (QbD) concept, which aims to develop robust pharmaceutical processes, has helped to further the understanding of the spray-drying process. It has done so through the establishment of process variable design spaces, facilitated by statistical tools such as the "design of experiment" (DoE) approach (149,151). Formulation variables are another intricate area of the process that need to be understood, to attain the desired product. Parameters of interest, also known as critical process parameters (CPPs), include but are not limited to: feed rate, inlet temperature, outlet temperature and feed composition (156). The selection of the solvent system plays a critical role in the spray-drying process (153,157). Criteria that need to be met include: no incompatibility issues, assurance of non-toxicity and ease of evaporation (158). As would be expected, with the existence of so many variables, a large degree of interdependence exists (149).

A more thorough and exhaustive list of factors, and how they are expected to affect the resulting properties of the spray-dried product, is documented in Table 1.4. Functional properties, like compressibility and density, can have a profound impact on future processability (159).

Table 1.4. Effect of spray-drying conditions on particle properties (160).

Parameter (increase)	Particle size	Particle porosity	Product moisture	Product smoothness	Powder yield
Inlet temperature	Increase	Decrease	Decrease	Decrease	Increase
Drying flow rate	Decrease	Increase	Decrease	Increase	Increase
Feed rate	Decrease	Decrease	Increase	Increase	Decrease
Humidity	Increase	Increase	Increase	Decrease	Increase
Spray nozzle diameter	Increase	Increase	Increase	Decrease	Increase
Solid content in solution/suspension	Increase	Decrease	Decrease	Decrease	Increase

In addition to the CPPs, manipulation of the spray-drying equipment can affect product quality. The vast majority of research is done at lab-scale, but larger pilot studies have been published (161). The size of the apparatus, which depends on the scale at which the product is being produced, is one of the more obvious differences compared to lab-scale. In this instance, it is vital that the droplet size distribution and evaporation profile is mimicked (151). The dimensions of the drying chamber, flow of drying gas and cyclone configuration, all can be altered, with a view to controlling the product's properties (162).

All types of atomisers rely on a force of some description to a liquid feed. This choice plays a critical role in defining the droplet size (in tandem with other process and formulation variables), and in turn, the structure of the particles produced (149). This force can be distinguished, based on the type of

energy the nozzle employs. They can be categorised as centrifugal, pressure, vibrational or kinetic (151). The two-fluid atomiser configuration, which is reliant on kinetic energy to form droplets, is commonly used in industry and at a research scale. It consists of two concentric nozzles, where the feed solution or suspension, is pumped through the inner nozzle, while the atomising gas flows through the outer nozzle (151). A variety of factors, such as the liquid's flow rate relative to the drying gas, as well as its density, surface tension and viscosity, largely dictate the droplet size produced by this type of nozzle (158). Larger droplets can deposit on the sides of the drying chamber, as they have a tendency to escape the trajectory followed by smaller particles, leading to unsatisfactory drying (151). Legako and Dunford, argue that this nozzle type, affords a lack of control over the droplet size, which has knock-on consequences, in terms of particle size distribution and nozzle clogging (163). This has led many groups to investigate ultrasonic atomisers, which use high-frequency sound waves to create smaller droplets, thus, overcoming the clogging issue reported with the two-fluid nozzle (151).

1.3.2 Spray-coating

1.3.2.1 Overview of the history and role of coating

Fluidised bed coating is a common technique used for the coating of many different materials such as pharmaceuticals and food. It is an advancement of the air suspension technique that has been successfully used to produce many different commercial products (131). In the pharmaceutical industry, it has been used to coat pellets, granules and many other different types of multiparticulates (164), spanning the encapsulation of novel biopeptides to IER complexes (131,165). Typically, coating is conducted to modify the release of the API (166,167), but is also performed to improve the organoleptic properties, as well as increase the stability of the formulation (168,169). When the coating applied is for stability purposes or to tailor the drug release, it is known as a functional coating in the context of performance. If improving the appearance of the formulation is the goal, then the coating is known as non-functional (170). It is an established process within the pharmaceutical industry to help achieve the goal of encapsulation (171,172). This process of layering and film coating has evolved over the years, and there are several examples of products containing multiple layers in the literature (164,173).

1.3.2.2 Fluidised bed coating equipment

The fluidised bed coating system can be set up in a variety of configurations such as top-spray, side-spray with a rotating disk, and bottom-spray (172). The latter is known as the Wurster process, and is best suited to coating particulates, as it has a reputation for being the most efficient, and has been specifically designed for coating (168). The Wurster equipment, shown in Figure 1.12, consists of an

expansion region, a Wurster draft tube, a distributor plate and a spray nozzle located at the centre of the distribution plate.

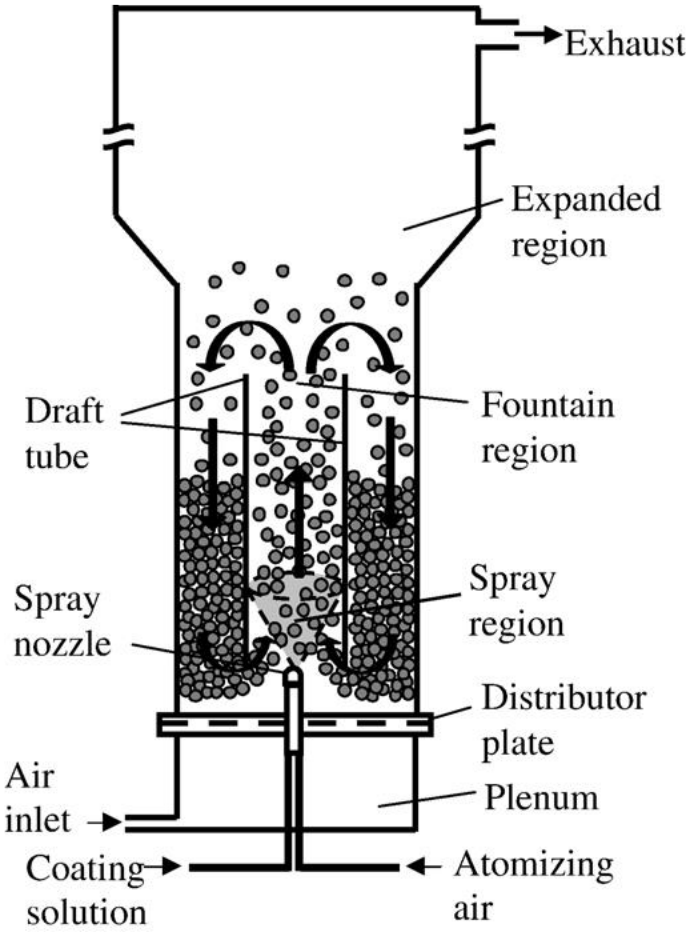

Figure 1.12. Illustration of fluidisation process in fluid bed technology (158).

1.3.2.3 Wurster coating process-The impact of process and formulation variables

During the coating process, interactions occur between the three phases (solid, liquid and gas) present in the fluidised bed, which give rise to several phenomena that occur concurrently after the initial fluidisation step, as it is a continuous cyclical process (174). The first phenomenon that occurs is the suspension of the particles in the air (fluidisation), followed by spraying of the coating solution as droplets (atomisation), with the aim of the particles and droplets colliding. If this occurs, the droplet spreads on the particle's surface (mass transfer), and ultimately adheres (drying) (168). To form a continuous film layer, the process of wetting and drying will occur several times, and the droplets will ideally coalesce prior to the heat transfer process which forms the coating later. Two crucial aspects of the coating integrity are its thickness and uniformity. The thickness of the coating relies on the number of times the particles pass through the spraying zone, and how much mass is deposited per cycle (172). The uniformity of coating is a reflection of how optimised the process parameters are and has to take into account the intraparticle and interparticle variation (169,170).

A large number of operating and design variables affect coating quality, as shown in Table 1.5 (175), however, a theory as to how combinations of these variables influence the process has not yet been fully developed. Models developed to predict coating performance for certain systems, have been found to not be applicable in many cases (176). It is a complex process, the success of which depends on the interplay between process parameters and formulation variables, meaning "trial and error" methodology is still extensively used to determine optimal coating conditions (172).

Table 1.5. List of operating variables known to affect the spray-coating process (168).

Operating variables	System design variables	Particle properties	Coating liquid variables
Drying air flow rate	Draft tube diameter	Particle size	Coating material
Atomising air flow rate	Draft height tube	Particle surface and charge	Liquid viscosity
Coating liquid flow rate	Draft tube diameter	Particle density	Liquid surface tension
Drying air inlet temperature	Distributor plate design		Liquid density
Atomising air temperature	Height of entrainment zone		Liquid concentration
Inlet air relative humidity	Nozzle distance from distributor plate		
Batch size	Nozzle tip diameter and cap opening diameter		
	Bed chamber diameter		
	Bed chamber height		

1.3.2.4 Challenges associated with the Wurster process

Disadvantages of the approach include the high cost of the process, and the tendency for agglomeration to occur. Coating particles with a fine particle size is problematic for many reasons. Fukumori et al. argue that 20 microns is the cutoff for individual particles to be coated without agglomeration (177). However, Ichikawa et al. suggest that particles within the 20-100 µm range are still likely to agglomerate. They qualify their claims, by stating that it depends on a case by case basis, but list a series of factors that they believe are responsible, such as hygroscopicity, electrostatic charging and the solubility of the particles in the spray solvent (131). More recently, it has been argued that microparticles with a size of less than 250 µm, can prove difficult to coat (178). Control of the thickness of the coating is troublesome when fine particles need to be coated. Commercially available coatings need a minimum of 10 µm to be an effective diffusion barrier, but this necessitates the use of large amounts of coating material, due to the large surface area of the particles, which leads to

longer run times. The depth of coating, together with its permeability, and the diffusion coefficient of the drug, are the main drivers of drug diffusion (131,170). Attrition of the coating is another issue, caused by particles colliding with the walls of the chamber or themselves, and has a detrimental effect on the yield, as well as providing an opportunity for agglomeration to occur (179).

1.3.2.5 Suitable polymers for modified-release (MR), proprietary coating products, and the film-formation process

Insoluble polymer coatings are usually the excipient class chosen when it comes to extending the release of orally administered drugs (180,181). Examples of such polymers include ethylcellulose (EC), polyvinyl acetate (Kollicoat® SR 30 D) and polymethacrylates (Eudragit® RS/RL). These polymers are non-toxic and have good film-forming abilities and adequate stability. Blends of these types of polymers are often utilised to achieve specific release profiles (164,182,183). This is a common occurrence for the pH-independent Eudragit® grades such as RS and RL (184,185). The purpose of this is to achieve intermediate permeability levels (186). Many studies have looked at how process parameters affect the microstructure of the films formed, which can help explain the release profile observed (182).

Companies, such as Evonik, produce ready-made organic solutions and aqueous dispersions (mean diameter of the polymeric particles is 170 nm (187)), that are especially suited to the Wurster coating process and have been used to control drug release when applied as a polymeric coating. The latter is becoming the choice of many companies for environmental reasons (188,189). Having said that, they are more challenging to work with, as based on reports in the literature (167,190), there is a higher likelihood of the release profile of systems coated using these dispersions changing over time and they can be problematic when spray-coating in a research-based setting with limited gas flow capabilities.

To understand the difference between the organic solutions and aqueous dispersions of coating polymers, the film formation process must first be considered. Film formation from organic solutions of polymers can be attributed to the evaporation of the solvent, which leads to an increase in the concentration of polymer, formation of a gel-like layer, followed by a film that is free of solvent. In the case of an aqueous dispersion, the process is more convoluted. It consists of three stages that relate to the extent of water evaporation. In stage 1, the rate of evaporation is constant as the polymeric particles are being applied. At stage 2, this rate decreases, as the distance between the polymeric particles reduces due to capillary forces. Lastly, water evaporation ceases, and the film is considered complete (191).

EC is perhaps the most extensively researched excipient that confers a SR effect (167,188). Aquacoat® ECD and Surlease® are two proprietary products that contain the polymer, and there are numerous

examples of their use in the literature (128,167,192). Nevertheless, a plasticiser is often required to overcome the issues that have been flagged during film coating trials, a consequence of the polymer's high T_g (circa 128-130 °C)and pseudolatex nature (166). Many authors argue that another class of pH-independent polymer, the methacrylate-based Eudragit® polymer, is more suitable for the spray-coating process (193). Apart from these two polymer types, which are most widely used, a third type exists, called Kollicoat® SR 30 D. It is available as an aqueous dispersion, predominantly composed of PVA (27% w/w) along with PVP and sodium lauryl sulfate (SLS) (166,194,195). In addition to its pH-independent release capabilities, the manufacturers claim that it is not necessary to incorporate a plasticiser, as the film has demonstrated adequate flexibility (166).

The design of a SR formulation using these commercial polymeric dispersions or solutions is not as straightforward as it may appear. Firstly, it may be necessary to adjust permeability, through the addition of excipients such as pore formers, but this runs the risk of disturbing the colloidal stability of the commercial dispersions (188). Secondly, an increase in the coating applied, leads to an increase in microcapsule size, which can prove problematic, if a gritty texture in the mouth for oral liquid formulations wants to be avoided (131). These issues highlight the considerations, that need to be factored in when this method is being considered as a possible manufacturing technique.

The success of the spray-coating operation relies on film formation. For this to occur, the polymeric particles in the spray, need to fuse and coalesce. The rate at which this occurs is dependent on factors such as the spray conditions, the presence of a plasticiser, and if thermal treatment is employed. Film formation is dependent on a temperature, known as the minimum film formation temperature (MFT), being reached (194). It is defined as “the temperature above which, a continuous film can be formed”, and the addition of plasticisers, aids the film formation by reducing the MFT (196). The marked effect on drug release that the plasticisers have post-curing, has been reported for multiparticulates coated with Eudragit® RS, RL, Kollicoat® SR 30 D and EC (166,192,197).

1.3.2.6 The importance of curing and plasticisers

Curing is a process that promotes the coalescence of polymeric particles and is dependent on energy (189). Curing is necessary to ensure that a continuous film has formed around the particle post-solvent evaporation. It is virtually impossible to confirm that the polymeric particles fully coalesced post-processing, so this step is generally always undertaken and needs to be optimised. This ensures a reproducible release profile during storage (194). The level of plasticiser, the inherent physicochemical properties of the drug, and curing conditions i.e. the temperature, humidity, and length of time are integral to the success of the process (192,198). Plasticisers are capable of forming secondary bonds with polymer chains thereby reducing the propensity of secondary bonding between the polymer

chains, which increase their mobility and imparts flexibility, leading to a decrease in the likelihood of rupturing. Plasticisers have enabled the use of many polymers that have excellent drug diffusion properties, yet poor film-forming properties (198). The successful incorporation of plasticiser is reflected in a decrease in T_g of the film. Their effectiveness relies on compatibility with the polymer in question (199). They are normally solvents with low volatility, and common examples include triethyl citrate, triacetin and dibutyl sebacate (199,200).

A major problem encountered during Wurster coating is the tendency of multiparticulates such as pellets and beads to aggregate. These clusters prevent uniform coating, and complete film formation around each multiparticulate to occur. Eventually, the degree of aggregation becomes too great, and fluidisation is lost, leading to a premature end to the process. A disadvantage of incorporating plasticisers in the process is the associated tackiness (201). Tack can be defined as "the force or impulse per unit area required to separate parallel two parallel surfaces initially in contact through an intervening liquid film" (202). This necessitates the use of an anti-tack agent, such as talc, to improve flowability and reduce tackiness.

1.3.3 Fluidised bed granulation (FBD)

Granulation is a type of unit operation that is characterised by particle enlargement using an agglomeration technique. Broadly speaking, the unit process can be split into two main types, dry and wet granulation. These two main categories are differentiated on the basis of the need to use a liquid as part of the agglomeration process, with the latter being subdivided into many further categories which are representative of the level of innovation in the wet granulation area (203). Fluidisation bed granulation is one such example and is a technique that has been utilised within the pharmaceutical industry for several decades to improve powder properties such as compressibility and flowability. The process comprises two main stages: spraying and drying, with the addition of a binder liquid of paramount importance during the spraying stage to cause primary particles to agglomerate and form granules (204). It is a type of wet granulation method that involves the spraying of binder fluid onto particles that are fluidised using a gas, typically nitrogen, which subsequently collide and form larger aggregates that are then rapidly dried within the fluidising chamber. A combination of capillary and viscous forces are responsible for the binding of particles (205). During the drying stage, the solvent evaporates, and more robust permanent bonds are formed. Solid bridges, that form from the binder material hardening and crystallisation of dissolved solute, determine the strength of the granule formed (204). The process possesses several advantages over multi-stage wet granulation techniques such as high shear granulation and extrusion-spheronisation, as the wetting and drying processes occur simultaneously within the same unit operation offering a point of difference relative to the aforementioned granulation techniques (206). Benefits of the process relate to reduced losses when

transferring the product and reduced processing times which is facilitated by the continuous heat and mass transfer between the fluidising air and particles (204). A list of some of the most common variables that influence granule quality attributes are shown in Table 1.6.

Table 1.6. List of operating variables known to affect the FBG process (204).

Operating variables		**Material variables**	
Apparatus variables	Process variables	Starting material	Binder solution
Design of the air distributor plate	Inlet air temperature	Particle size	Type of solvent
Nozzle position	Inlet air velocity	Particle size distribution	Type of binder
Nozzle type	Inlet air humidity	Particle shape	Binder concentration
Diameter of the nozzle tip	Inlet air volume	Moisture content	Binder content in the formulation
Shape of the product container	Fluid bed height	Cohesiveness	Binder viscosity
	Product temperature	Static charge	
	Binder liquid spray rate	Wettability	
	Nozzle atomiser air pressure	Stickiness	
	Exhaust air temperature		
	Drying time		

1.4 Quality by Design (QbD) approach to pharmaceutical processing

Over recent times, Quality by Design (QbD) methodology has become a core component of pharmaceutical development, replacing the quality by testing (QbT) philosophy which relies on ensuring the quality of the drug product by extensive testing of the final product (207). Furthermore, the QbD approach is strongly encouraged by regulators as it provides a robust framework for the design and implementation of processes that achieve a consistent level of quality and meet the pre-determined standards (208,209). A quote often associated with the QbD approach is “quality cannot be tested into products i.e. it should be built in by design”. It can be defined as a systematic, scientific, risk-based, holistic and proactive approach to pharmaceutical development that starts with predefined objectives and emphasises product and process understanding and process control (210). The QbD paradigm relies on knowledge of the design space of the process, which can be achieved using a Design of Experiments (DoE) approach that is the main statistical method used to establish relationships between the factors that influence the outputs of the process (211). When applied to a pharmaceutical process, the factors relate to both the formulation/raw material attributes as well as the process parameters, whilst the output(s) can be labelled as critical quality attributes (CQAs). This

approach requires formulation scientists to use prior knowledge of the process alongside risk management strategies to identify the input and output variables to be investigated by DoE (210). Many different types of DoE exist ranging from full factorials to screening designs (a type of fractional factorial) to response surface analysis and evidence of each type being used in the literature is aplenty (212–214).

The Taguchi method is one example of a screening experimental design that is used routinely and it is a robust design that relies on a couple of critical assumptions: the first is the absence of interactions and the second is the approximation of the additivity of the various factors studied (215). This approach is a widespread statistical technique used to effectively design experiments (212,216). It enables scientists to recognise process and formulation factors that are worth investigating further when looking to optimise the process (217,218). It is based on orthogonal arrays which facilitate efficient working, as minimal experimental runs are conducted, resulting in reduced expenditure on materials and a decreased time commitment relative to the "trial and error" approach (219). Although this specific design was not utilised by Verma et al. when optimising the production of efavirenz resinate by spray-drying, a similar method reliant on the same underlying statistical principles yielded fruitful results (220).

1.5 The active pharmaceutical ingredients (APIs) used in this work

1.5.1 Metronidazole (MTZ)

1.5.1.1 Pharmacology, chemistry and therapeutic applications

MTZ is an imidazole derivative with antibacterial and antiprotozoal activity. Specifically, MTZ has activity against anaerobic gram-negative bacilli, including the *Bacteroides fragilis* group and *Fusobacterium*. It also has activity against anaerobic gram-positive bacilli including *Clostridium* species and susceptible strains of *Eubacterium*. It can also be used as a treatment against anaerobic gram-positive cocci including *Peptococcus niger* and *Peptostreptococcus* (221). In paediatric patients, it is the first-line treatment for mild to moderate *Clostridium difficile* infection. When administered via the oral route, the drug is almost fully absorbed and the rate of absorption is rapid (222,223). MTZ is a weak base that has a pKa value of 2.6 (224), which means, in theory, that ionic interactions should occur with the acidic resin, provided MTZ is ionised (nitrogen at the 3-position highlighted by the red circle in Figure 1.13).

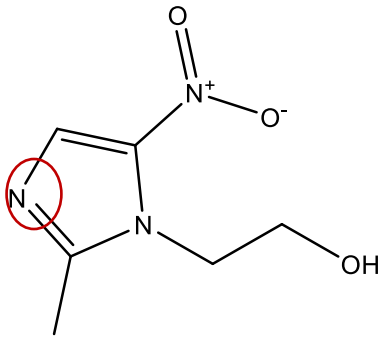

Figure 1.13. Chemical structure of MTZ.

1.5.1.2 MTZ market landscape: Past, present and future

Flagyl® which is marketed by Sanofi, is the originator product that is available in a variety of different dosage forms. As the drug is off-patent, many different generic manufacturers now produce the drug and drug products containing MTZ. MTZ is sold as a solid dosage form in 200 mg and 400 mg strengths in Ireland (225). It is also available in a parenteral form, as a solution for infusion, and as a gel or cream. In the past, the drug was available in the hydrochloride salt form, but this has been discontinued. Pfizer, as the originator, formulated a 750 mg ER tablet called Flagyl® ER, indicated for bacterial vaginosis in non-pregnant women, but this has also been discontinued (226). In 2011, orphan drug status was granted by the EMA to Formac Pharmaceuticals for the drug in a MR form, for the treatment of pouchitis (227). This formulation has not reached the marketplace yet but, based on patent literature, wet granulation is used to form granulates, which are subsequently extruded and spheronised. The resulting pellets are then dried, and coated using a fluidised bed. The aqueous coating is composed of Eudragit® L 30 D-55, talc, and a plasticiser, which permits pH-dependent release in the small intestine (228).

An oral liquid suspension product (200 mg/5 mL) is also marketed by Sanofi, but is not available in the Northern America. Interestingly, the tablet and suspension are not bioequivalent (229). The drug is known to be bitter, and has a characteristic metallic aftertaste, which can affect patient compliance. Metronidazole benzoate (MTZ BZT) is a prodrug of MTZ, that is used in the oral suspension formulation. The rationale behind the use of the MTZ BZT is the insolubility of the drug in water, which renders it tasteless (230). With the suspension formulation, MTZ BZT hydrolyses in the GIT, releasing therapeutic doses of MTZ, over a period of several hours. As far back as 1994, concerns were raised by Matthew et al., who investigated the stability of two commercially available MTZ BZT suspensions. As part of their findings, it was reported that cleavage of the ester group did not occur in the gut, meaning that it was not a ready substitute for the tablets in the treatment of GI infections (230). In a more recent study by Bempong, these findings were substantiated (231).

It is anticipated that the company Appili therapeutics will release a taste-masked liquid product (250 mg/5 mL) indicated for *Clostridium difficile* in children in the near future. A patent has been filed with the International Patent Office, and several press releases have mentioned deals with other pharmaceutical companies to market the product (232). The FDA issued orphan status in 2016 for this indication (233). A differentiating factor to the Sanofi product is the use of the free base compound in this taste-masked product. Magnesium aluminium silicate, glycerol and a blend of sweeteners and flavouring agents, confer this taste-masking effect, according to the inventors. The PK studies used as part of the patent application, show that the C_{max}, T_{max} and AUC values for the liquid suspension were not statistically different to the proprietary tablet, irrespective of the prandial state, with the exception of the C_{max} under fed conditions (lower for the suspension). These results combined with the geometric mean ratios of C_{max} and the AUC values demonstrated bioequivalence (232).

1.5.2 Tizanidine Hydrochloride (TZD HCl)

1.5.2.1 Pharmacology, chemistry and therapeutic applications

TZD HCl is an alpha-2 (α_2) adrenergic receptor agonist which acts in the central nervous system at supra-spinal and spinal levels. This effect results in inhibition of spinal polysynaptic reflex activity (234) (235). TZD HCl has no direct effect on skeletal muscle, the neuromuscular junction or on monosynaptic spinal reflexes, showing similar efficacy to that of baclofen, with a more favourable tolerability profile (236–238). In Ireland, the drug is indicated for the "treatment of spasticity associated with multiple sclerosis or with spinal cord injury or disease" (239). It is also used "off-label" for pain (240). It is recommended that patients titrate the dose to minimise the adverse effects that occur at clinically relevant doses (239).

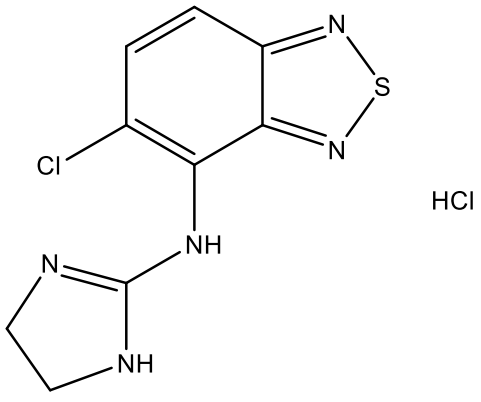

Figure 1.14. Chemical structure of TZD HCl.

1.5.3.2 Licensed formulations on the market and pharmacokinetic (PK) challenges

TZD is a BCS class one compound that is marketed as Zanaflex®, and is supplied in capsule form in a 2, 4 or 6 mg strength, and in a tablet form in a 2 or 4 mg strength (239). The capsule form of the drug is

produced using wet media milling and SODAS® technology (Nanocrystal® technology), which is a method of producing nanoparticles, developed by Elan Pharmaceuticals (241,242). Interestingly, the capsule and tablet forms are bioequivalent under fasted conditions, but not fed conditions. This has been ascribed to the pH-dependent excipients present in the capsule formulation. The T_{max} is approximately doubled in the capsule formulation, and the C_{max} is approximately two-thirds of the tablet. It is fully absorbed, although systemic absorption is low (40%), due to extensive first-pass metabolism (239). Approximately 95% of an orally administered dose is metabolised, and no active metabolites have been established (240). It also suffers from a short half-life (2.5 hours), leading to frequent administration, thus reducing patient compliance (243). The capsule formulation is a multiparticulate formulation, designed to lower the AUC and C_{max}, compared to the tablet formulation, as side effects like somnolence are a downside associated with the tablet form (244).

TZD's short half-life (2.5 hours) and indication necessitate frequent dosing throughout the day, and side effects such as orthostatic hypotension and somnolence have restricted the drug's use (245). Therefore, this makes TZD HCl a prime candidate to formulate as a MR dosage form (246). TZD HCl is highly water-soluble (20 mg/mL), so it is a challenging candidate for controlled drug delivery (247). ER micropellet capsules (6 mg and 12 mg) known as Sirdalud® MR, are marketed by Novartis in the Netherlands, Austria, and Poland. The initial adult dose recommended in the treatment of spasticity due to neurological disorders is 6 mg daily. Similar to the IR formulation, this can be titrated upwards based on clinical need, every half week or week. According to clinical experience, 12 mg is generally the optimum dose for the majority of adult patients (248).

Sun Pharma based in India, a well-known generic manufacturer, developed an ER formulation that made it to clinical trial, the PK profile of which is shown in Figure 1.15. Having said that, no evidence of it being on the market can be found (245). Based on a patent application filed in 2009, it appears to be a preparation that is composed of an intragranular phase consisting of a blend of TZD HCl, HPMC and waxy materials, and an extragranular phase containing an enteric polymer. Both of these phases constitute the "tizanidine containing composition" which is converted into a bilayer tablet by topping it with a swellable layer that is comprised of a hydrophilic swellable agent, a wicking agent and a super disintegrant. This mixture is then slugged, milled and compressed into tablets. These tablets are first coated with a polyvinyl alcohol coating, which is subsequently coated using a water-insoluble layer after which a final polyvinyl coating is applied. Lastly, a hole is then drilled into the swellable top layer (249).

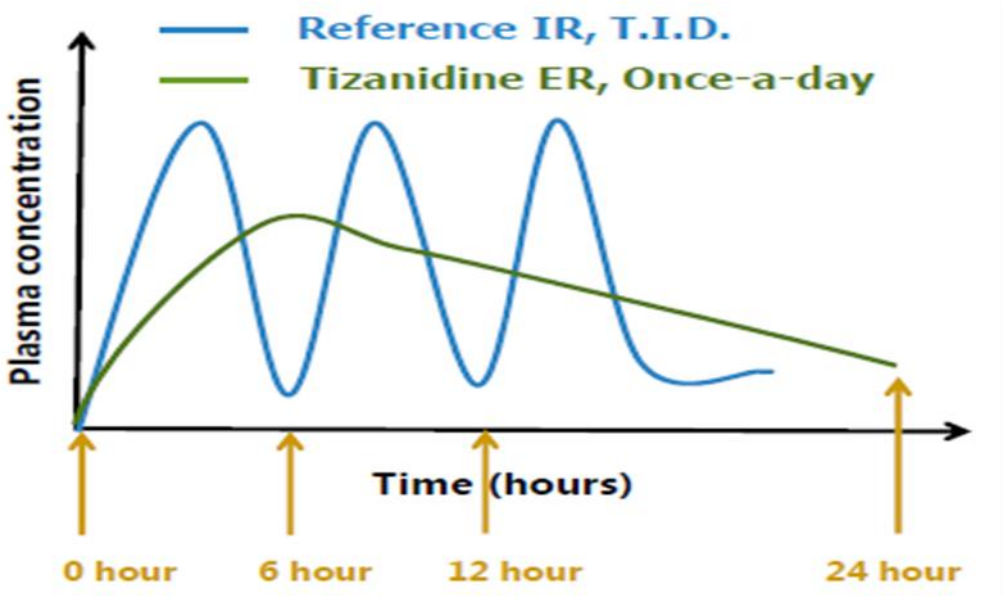

Figure 1.15. Schematic representation of comparative mean plasma TZD concentration-time profiles, illustrating Sun Pharma's proposed "once a day" TZD formulation versus the reference TZD IR formulation (245).

Although TZD HCl is not licensed for use in under 18s, its "off label" use in children is well documented (250–252) and it has been reported to be safe (253,254).

1.5.2.3 Formulation approaches used to overcome TZD HCl's PK limitations

Alternative methods of drug delivery have been studied to help overcome the drug's low oral bioavailability (255). Examples of approaches investigated, include loading it onto thiolated chitosan nanoparticles to explore the nasal delivery avenue (256), and a diverse range of transdermal delivery methods, such as drug-loaded aspasomes, microneedles and sonophoresis (257,258). Also, to overcome problems associated with oral delivery, there have been attempts recently to formulate a system that can be delivered by the buccal route (247).

1.5.2.4 The suitability of TZD HCl for the ion-exchange drug delivery approach

The pH of a 1% w/v solution is 4.4, which makes TZD HCl, an ideal candidate for ion-exchange (the compound's secondary amine is the ionisation site), considering that it is a basic compound with a pKa value of 7.46 (259). It is structurally related to the anti-hypertensive clonidine (which is between 10-50 times more potent) (260), which has been manufactured into a CR suspension using ion-exchange technology. This formulation of clonidine, known as Nexiclon® XR, released the drug over a 24 hour time period following *in vivo* administration of a single dose. The product is comprised of coated resinates suspended in an aqueous vehicle. After binding the drug to the resin, the complex is

granulated using PVP, dried and milled, to achieve a specific particle size. These uncoated granules are then coated using a Kollicoat® SR 30 D with a plasticiser, until a predetermined weight gain is achieved. These particles are then sieved and cured for a predetermined period of time. Lastly, the coated particles are suspended in an aqueous base vehicle, containing the usual excipients necessary to formulate a multi-dose liquid formulation (261).

1.5.3 Comparison of drug ionisation characteristics

The two APIs selected possess different ionisation characteristics which present scope for investigating the suitability and potential constraints of using a cation exchange resin-based formulation. Aside from the differences in the chemical structure of the APIs tested, there is a disparity in the information available relating to the dissociation behaviours. MTZ, a well-known weak base, is the most extensively studied of the two compounds, with a reported pKa of 2.6 meaning the compound is predominantly ionised at pH values below 2.6. The reported pH of a saturated solution is pH 5.8, pointing to the likely need to adjust the pH of the loading solution downwards to achieve a meaningful level of ion-exchange (224). Clear undisputed evidence can also be found in the literature in relation to TZD HCl's dissociation constant, which is 7.46. The basicity of this compound is also well-known and the pH of a TZD HCl test solution according to the British Pharmacopoeia should be between a value of 3.7 and 5, suggestive of the compound being well suited to the proposed formulation strategy (262).

Chapter 2:

Materials and Methods

2.1. Materials

Table 2.1. Material and supplier list for materials used.

Material	**Supplier**
Metronidazole (MTZ)	Sigma-Aldrich (United Kingdom)
Tizanidine hydrochloride (TZD HCl)	Kemprotec Ltd (United Kingdom)
Polacrilex resin marketed as Amberlite™ IRP64 (powder form)	Colorcon (United Kingdom)
Sodium polystyrene sulfonate USP marketed as Amberlite™ IRP69 (powder form)	Colorcon (United Kingdom)
Polacrillin potassium NF marketed as Amberlite™ IRP88 (powder form)	Colorcon (United Kingdom)
Polystyrene matrix crosslinked with 8% divinylbenzene substituted with sulphonic acid groups marketed as Amberlite™ IR120 Na (bead form)	Sigma-Aldrich (United Kingdom)
Methacrylic acid-Methylcrylate copolymer (1:1) marketed as Eudragit® L100 PO	Evonik Industries (Germany)
Methacrylic acid-Methylcrylate copolymer (1:2) marketed as Eudragit® S100 PO	Evonik Industries (Germany)
Poly(ethyl acrylate-co-methyl methacrylate-co-trimethylammonioethyl methacrylate chloride) 1:2:0.1 marketed as Eudragit® RS 12,5 solution	Evonik Industries (Germany)
Poly(ethyl acrylate-co-methyl methacrylate-co-trimethylammonioethyl methacrylate chloride) 1:2:0.2 marketed as Eudragit® RL 12,5 solution	Evonik Industries (Germany)
Poly(ethyl acrylate-co-methyl methacrylate) 2:1 marketed as Eudragit® NM 30 D dispersion	Evonik Industries (Germany)
Triethyl citrate	Sigma-Aldrich (United Kingdom)
Triacetin	Toyko Chemicals Industry (Japan)
Dibutyl sebacate	Toyko Chemicals Industry (Japan)
Poly(vinyl acetate) dispersion 30 per cent (Ph. Eur.)(27% polyvinyl acetate, 2.7% povidone and 0.3% sodium lauryl sulfate) marketed as Kollicoat® SR 30 D	BASF SE (Germany)
Phosphoric acid	Merck (Germany)
Glacial acetic acid	Sigma-Aldrich (United Kingdom)
Ethanol (96% v/v)	Corcoran Chemicals (Ireland)
Isopropyl alcohol (IPA)	Corcoran Chemicals (Ireland)
Methanol (MeOH)	Corcoran Chemicals (Ireland)
Acetone	Corcoran Chemicals (Ireland)
HPLC grade methanol (MeOH)	Fisher Scientific (Ireland)
HPLC grade acetonitrile	Fisher Scientific (Ireland)
HPLC grade water (DI H_2O)	Elix 3 connected to Synergy UV system, Millipore (United Kingdom)
Liquid nitrogen	BOC (Ireland)
Water (deionised for DVS)	Sigma-Aldrich (United Kingdom)
Hydrochloric acid (37% v/v) solution	Fischer Scientific (Ireland)
Potassium dihydrogen phosphate (KH_2PO_4)	Sigma-Aldrich (United Kingdom)
Tribasic sodium phosphate (Na_3PO_4)	Sigma-Aldrich (United Kingdom)

Citric acid monohydrate	Sigma-Aldrich (United Kingdom)
Disodium hydrogen phosphate (Na_2HPO_4)	Sigma-Aldrich (United Kingdom)
Monosodium phosphate (NaH_2PO_4)	Sigma-Aldrich (United Kingdom)
Sodium pentane sulfonate heptahydrate	Acros Organics (Belgium)
Sodium chloride	Sigma-Aldrich (United Kingdom)
Sodium hydroxide	Sigma-Aldrich (United Kingdom)
Zanaflex™ 2 mg tablets	Teva Pharma B.V. (Ireland)
Microcrystalline cellulose marketed as Avicel™ RC/CL	FMC Biopolymer (Belgium)
Hydroxypropyl methylcellulose	Sigma-Aldrich (United Kingdom)
Xanthan gum	Sigma-Aldrich (United Kingdom)

2.2. Methods

2.2.1 Unit processes

2.2.1.1 Ion-exchange resin (IER) pre-treatment

2.2.1.1.1 Purification of the resin (Amberlite™ IRP69)

A method of purification, also referred to as "activation" was used as part of this work reported by Irwin et al. (89). The "activated" resin was prepared by washing 10 g of the material with 50 mL of DI H_20 three times. The material was then washed with 50 mL of ethanol (EtOH) (96% v/v) twice and subsequently washed with 50 mL of DI H_20 twice again. 300 mL of 1 M HCl was then used to wash the material, followed by washing with HPLC grade H_2O until the eluent was pH neutral. The resin was then dried at 50 °C for 12 hours in a vacuum oven of which time a constant mass was reached.

2.2.1.1.2 Particle size reduction of the resin (Amberlite™ IRP69) using ball milling

Ball milling was performed with a PM 100 high energy planetary mill (Retsch, Germany) at room temperature. 2.5 g of material was placed in stainless steel milling jars of 50 cm^3 capacity with three stainless steel balls of diameter 20 mm, corresponding to a ball to powder mass ratio of 40:1. The speed of the solar disk was set at 400 RPM. Every 10 minutes of milling was followed by a pause period of 10 minutes to avoid overheating and this was repeated for 2 cycles.

2.2.1.1.3 Swelling the resin (Amberlite™ IRP69) before the addition of API

Pre-swelling the resin raw material was performed using TZD HCl. Varying ratios (w/w) of TZD HCl to resin were used (2:1, 1:1 or 1:2) and a single-batch method (see section 2.2.1.2) was employed. The pre-determined quantity of resin was left to sit in the 100 mL of DI H_20 for 24 hours prior to the addition of the required amount of drug to produce the desired D:R ratio.

2.2.1.2 Preparation of drug-resin complexes (DRCs) using the batch method

2.2.1.2.1 Solution stability studies of APIs in different media

Prior to loading experiments being carried out, both APIs (0.1% w/v and 0.005% w/v for MTZ and TZD HCl respectively) were dissolved in a selection of liquid media at 20 °C for varying durations of time as

specified in Table 2.2. The buffer system (HCl and KCl) used for the MTZ studies was "buffered "to pH values in the range pH 0.6- pH 3 (section 2.2.1.2.3), which covered the range of loading solution pH values. pH 6.8 phosphate buffer was prepared as per section 2.2.8.2.1. After appropriate dilutions were carried out, HPLC analysis as per the method described in section 2.2.10.1 (MTZ) and 2.2.10.2 (TZD HCl), was conducted to determine the stability of the drug in solution. All analysis was performed in triplicate.

Table 2.2. Summary of the conditions (Liquid media type, ionic strength of the liquid used to dissolve the drug, temperature of the liquid media and the time course of the experiments) used in the liquid stability studies for both APIs (MTZ and TZD HCl).

Dissolved API	Liquid media type	Ionic strength (M)	Time (h)
MTZ	pH 0.6	-	0-24
MTZ	pH 0.9	-	0-24
MTZ	pH 1.6	-	0-24
MTZ	pH 2.1	-	0-24
MTZ	pH 3.0	-	0-24
TZD HCl	NaCl	0.1-1.0	0-12
TZD HCl	HCl	0.1-1.0	0-12
TZD HCl	DI H_20	-	0-12
TZD HCl	pH 6.8 phosphate buffer	-	0-12

2.2.1.2.2 Solubility testing of APIs

The solubility of MTZ and TZD HCl were determined by placing excess solid in 25 mL glass vials that were crimped to prevent evaporation and placed in a reciprocating shaking water bath (ThermoFisher Scientific, USA) maintained at the specified temperature, in the chosen media and shaken at 50 CPM (conditions shown in Table 2.3). This was carried out for three separate vials. After 24 hours, 1 mL of the solution was filtered using a 0.45 µm Fisherbrand polytetrafluoroethylene (PTFE) hydrophilic filters (Fischer, USA) and diluted to an appropriate concentration in the PTFE mobile phase before being analysed using HPLC using the method specified in sections 2.2.10.1 (MTZ) and 2.2.10.2 (TZD HCl).

Table 2.3. Summary of the conditions (Liquid media type, ionic strength of the liquid media and temperature of the liquid media type) used in the solubility studies for both APIs (MTZ and TZD HCl).

API	Liquid media type	Ionic strength (M)	Temperature (°C)
MTZ	HCl	0.1	20
MTZ	HCl	0.1	37
MTZ	DI H_20	-	20
MTZ	DI H_20	-	37
MTZ	MeOH	-	20
TZD HCl	HCl	0.1	37
TZD HCl	DI H_20	-	37

2.2.1.2.3 Production of Metronidazole (MTZ) resinates/DRCs

The single-stage batch method was employed in an attempt to complex MTZ with Amberlite™ IRP69 using 1:1 (w/w) D:R ratios. The concentration of a pH-adjusted aqueous solution of MTZ was 0.1% w/v for screening purposes. The drug-resin suspension was kept under constant stirring at room temperature using a SM5 magnetic stirrer (Stuart Scientific, United Kingdom) at different mixing speeds (300 to 900 rpm) for a time period ranging from 6 to 24 hours. The drug resin suspension was then vacuum filtered using a V-700 vacuum pump (BÜCHI Labortechnik AG, Switzerland)) and V-850 vacuum controller (BÜCHI Labortechnik AG, Switzerland) and the solid material retained on the filter paper (Whatman®, United Kingdom) was collected. This solid material was further washed with DI H_2O to remove any unassociated MTZ, dried in the vacuum oven at 50 °C for 12 hours and then stored at room temperature for further use. Initially, a pH 'buffer' system consisting of potassium chloride (KCl) and HCl (Table 2.4) was chosen in order to produce the desired pH values covering the pH range 0.9-1.6 for the loading solution (263). A second buffer system consisting of citric acid and sodium phosphate dibasic (Table 2.5) was used to produce 0.1% w/v MTZ solutions that had pH values of 2.6 and 3 (264). Finally, 0.1% w/v MTZ solutions adjusted to a pH range covering the values 0.6 and 1.6 were prepared using 0.1 M HCl and a loading solution adjusted to pH 1.6 using 0.1 M HCl was selected for use with the "activated" resin as a comparator (1:1 w/w D:R ratio).

Table 2.4. Composition of 'buffer' systems used to achieve the required pH value (DI H_20 used to make each solution up to 200 mL where applicable).

pH value	Volume of 0.2 M HCl solution (mL)	Volume of 0.2 M KCl solution (mL)
0.6	150.0	50.0
0.9	134.0	50.0
1.6	32.4	50.0

Table 2.5. Composition of buffer systems (100 mL) used to achieve the required pH value.

pH value	Volume of 0.1 M citric acid solution (mL)	Volume of 0.2 M Na_2HPO_4 solution (mL)
2.6	89.10	10.90
3.0	79.45	20.55

The drug-resin suspension was stirred using a magnetic stirrer at room temperature for 24 hours, washed with DI H_2O to remove unassociated MTZ, dried in the vacuum oven at 50 °C for 12 hours and then stored at room temperature for further use. Investigations into the equilibration time of MTZ loading onto the resin were carried out at room temperature to establish the mixing time required for equilibration to be reached. MTZ was dissolved in a pH 1.6 buffer system (0.1 M HCl) and a 1:1 (w/w) ratio of drug to resin was used. Samples were taken at defined timepoints for 24 hours, filtered using 0.45 µm Fisherbrand polytetrafluoroethylene (PTFE) hydrophilic filters (Fisher Scientific, United Kingdom) and appropriately diluted and analysed using HPLC, as per the method described in section 2.2.10.1.

2.2.1.2.4 Production of Tizanidine HCl based resinates/DRCs

2.2.1.2.4.1 Drug loading studies involving Amberlite™ IRP64, Amberlite™ IRP69, Amberlite™ IRP88 and Amberlite™ IR120.

The batch method was used to investigate the feasibility of complexing TZD HCl to the various different resins (IRP64, IRP69, IRP88 and IR120) trialled in the work. The experimental variables (and the associated range) altered during the loading studies are listed in Table 2.6. The concentration of drug used in the experiments in the loading solutions was 0.1% w/v (1 mg/mL) for screening purposes, unless otherwise stated. The drug-resin suspension was stirred using a magnetic stirrer at room temperature for a time period ranging from 6 to 24 hours, followed by the DRCs being washed with

DI H_2O to remove unassociated TZD HCl, dried in the vacuum oven at 50 °C for 12 hours and then stored at room temperature for further use. Similar to the method described in section 2.2.1.2.3, modified batch methods (double and triple) were trialled, which involved decanting clear supernatant post-equilibration and the addition of fresh drug solution (once for the double-batch method and twice for the triple batch method). In terms of the drug loading studies, the only point of difference for the bead form (IR120) relative to the powdered forms of the resin, is the requirement to dry the bead form prior to use in the loading trials. The beads were dried in the vacuum oven at 50 °C for 12 hours, after which they were stored in a sealed glass container at room temperature. Regarding the IRP64 grade (Table 2.6), further studies using the 1:1 D:R ratio were performed by altering the pH of the loading solution (pH 5-7) and determining the impact on the drug loading. The pH was adjusted using a citric acid-Na_2HPO_4 buffer (Table 2.7).

Table 2.6. Experimental conditions used as part of the TZD HCl loading studies (batch method) using a selection of different resins (IRP64, IRP69, IRP88 and IR120).

Resin grade	D:R ratio	Temperature of loading media (°C)	Drug concentration in loading media (mg/mL)	Number of loading stages	pH-adjustment of loading media	Milling step of resin raw material used	"Activation" of resin raw material performed	Swelling of resin raw material
IRP69	3:1-1:3	20-50	1-10	1-3	-	Yes	Yes	Yes
IR120	3:1-1:3	20-40	1-10	1	-	-	-	-
IRP64	2:1-1:2	20	1	1	Yes (pH 5-7)	-	-	-
IRP88	2:1-1:2	20	1	1	-	-	-	-

Table 2.7. Composition of buffer systems (100 mL) used to achieve the required pH value.

pH value	Volume of 0.1 M citric acid solution (mL)	Volume of 0.1 M Na_2PO_4 solution (mL)
5	48.50	51.50
6	36.85	63.15
7	17.65	83.35

2.2.1.2.4.2 Equilibration studies involving Amberlite™ IRP64, Amberlite™ IRP69, Amberlite™ IRP88 and Amberlite™ IR120

Investigations into the equilibration times of the TZD HCl loading onto each specific resin during the batch process were carried out to establish the mixing time required for equilibration to be achieved. 0.1 mL of supernatant was collected at predetermined intervals during complex formation at the required temperature of the loading media, diluted with mobile phase, and then the drug amount was quantified by HPLC as per the method specified in section 2.2.10.2. Shown in Table 2.8 are the experimental variables altered for the specific systems formed using the different grades of resin.

Table 2.8. Experimental conditions used as part of the drug loading equilibration studies involving TZD HCl and a selection of different resin grades (IRP64, IRP69, IRP88 and IR120).

Resin grade	D:R ratio	pH-adjustment necessary	Milled or unmilled resin material used	Temperature of loading media adjusted (°C)	Length of time of experiment (hours)
IRP69	2:1-1:3	-	Both	Yes (20-50)	36-48
IR120	2:1-1:2	-	Unmilled	Yes (20-40)	36
IRP64	2:1-1:2	Yes (pH 5-7)	Unmilled	-	36
IRP88	1:1	-	Unmilled	-	24

2.2.1.2.4.3 pH measurements of loading media

The change in pH of the loading medium containing TZD HCl before and after the batch process for selected samples (24 hours mixing time) of drug loading was measured using a Metrohm 827 pH Lab pH-meter (Metrohm AG, Germany). The samples analysed were formed using a 1:1 (w/w) drug:resin ratio unless otherwise stated. The drug concentration remained constant at 10 mg/mL, as well as the volume of liquid (100 mL) and the temperature of the reaction was 25 °C.

2.2.1.3 Preparation of drug-resin complexes (DRCs) by spray-drying using Amberlite™ IRP69

2.2.1.3.1 Preliminary studies

As part of initial spray-drying trials, a selection of D:R ratios (w/w) (1:1, 1:1.5 and 1:2.5) and TZD HCl aqueous solutions concentrations (1 mg/mL (0.1% w/v) and 2 mg/mL (0.2% w/v)) were chosen to investigate the feasibility of the spray-drying process to produce DRCs. Prior to spray-drying, the required amount of resin was dispersed in the aqueous drug solution (500 mL) under magnetic stirring at room temperature for 24 hours. All spray-drying was carried out using a Büchi B-290 Mini Spray Dryer (BÜCHI Labortechnik AG, Switzerland) equipped with a high-efficiency cyclone configured in the open mode. A two-fluid (2-F) nozzle with a 0.7 mm nozzle tip and 1.5 mm diameter nozzle screwcap

were used. For all systems, a feed rate of approximately 9-10 mL/min, an inlet temperature of 120 °C, an aspirator setting of 100%, airflow rate of 667 Nl/hour at standard pressure and temperature conditions (p=1013.25 mbar and T=273.15 K) were used. Spray-drying yields were calculated based on the weight of powder (API and IER) collected, expressed as a percentage of the weight introduced into the feed solution, giving the yield percent by weight (% w/w). A quantity of material was taken for characterisation (DSC analysis, pXRD analysis, drug loading and dissolution testing), after which the DRCs were then further washed with DI H_2O to remove unassociated TZD HCl, dried in the vacuum oven at 50 °C for 12 hours and then stored at room temperature for further use. TZD HCl was also spray-dried as a 1 mg/mL (0.1% w/v) aqueous solution under the same process conditions as above with the exception of the inlet temperature (150 °C).

2.2.1.3.2 Design of Experiment (DoE) study design

A Taguchi L8 design (2^7) was employed (using Design-Expert software) for factor screening studies to identify the formulation and process variables that critically influence the spray-dried product. Seven factors and two levels of each factor affecting the spray-drying process were selected. All seven factors were numerical.

i Feed rate of the dispersion pump setting: 10 (3.5-4 mL/min) or 30 (9-10 mL/min)

ii Airflow rate: 667 or 1052 Nl/hour

iii Aspirator setting: 85 or 100%

iv Drug concentration in loading solution: 0.1 or 1% w/v

v Nozzle diameter: 0.7 or 2 mm

vi Drug:resin ratio (w/w): 1:1 or 1:2

vii Inlet temperature: 120 or 150 °C

A total of eight formulations were prepared. As per the DoE experimental design, TZD HCl was dissolved in water (1 mg/mL or 10 mg/mL) to form a 500 mL aqueous solution, and resin was added to the solution in one of two distinct weight ratios (1:1 or 1:2). As the liquid contents were stirred using a magnetic stirrer at room temperature, the liquid was spray-dried using a Büchi B-290 Mini Spray Dryer with a high-efficiency cyclone by altering the process parameters in the open mode configuration and a 2-F nozzle with a varying nozzle diameter, as reported above. The DRCs were then further washed with DI H_2O to remove unassociated TZD HCl, dried in the vacuum oven at 50 °C for 12 hours and then stored at room temperature for further use.

2.2.1.4 Fluidised bed granulation (FBG) using Amberlite™ IRP69

A fluidised bed system (Mini Glatt with Micro-kit, Glatt, Germany) was employed to produce granule batches with differing ratios (% w/w) of resin and binder within the fluidised bed chamber and all batch sizes of starting resin (IRP69) material were fixed at 5 g. Polyvinylpyrrolidone (PVP) was used as a binder and included among the solid contents rather than the liquid feed solution unless otherwise stated. The granulation was conducted using 12 different experimental conditions where the inlet temperature and the composition of the liquid and the solid phase were changed, as detailed in Table 2.9. The solid particles were fluidised at 20 m^3 /hour nitrogen flow rate and once stabilised, 10 mL of liquid feed solution was sprayed at 0.5 bar of pressure with a peristaltic pump setting of 0.6 (equivalent to 3-4 mL/min) using the bottom spray mode. Upon completion of spraying the liquid feed solution, the fluidised granules were further dried *in situ* in the FBG unit at a 60 °C inlet air temperature for 5 minutes. Irrespective of inlet air temperature maintained constant during the granulation step, the temperature for the drying phase was 60 °C.

Table 2.9. Experimental conditions used as part of the FBG studies.

Concentration of binder (% w/w)	Concentration of binder in liquid feed (% w/v)	Inlet air temperature (°C)
1 (PVP)	0	80
1 (PVP)	0	70
2 (PVP)	0	80
2 (PVP)	0	70
3 (PVP)	0	70
5 (PVP)	0	70
10 (PVP)	0	70
20 (PVP)	0	70
30 (PVP)	0	70
40 (PVP)	0	70
0	40% (2% w/v PVP solution)	80
40 (HPMC)	0	70

2.2.1.5 Wet granulation and spray-coating trials using Amberlite™ IRP69

1 g of Amberlite™ IRP69 was weighed out into a mortar followed by the dropwise addition of 1 mL of undiluted Kollicoat® SR 30 D and lightly mixed using a pestle until a solid wet mass was obtained. The mixture was fed through the sieve at consecutive sieve openings (1 mm, 710 µm, 500 µm, 350 µm and

149 µm) and was dried at room temperature on the benchtop overnight. The granules collected in each fraction were kept for further analysis. 5 g of drug-loaded powder was substituted into the process (using 5 mL of undiluted Kollicoat® SR 30 D) and the granules were stored for further coating trials.

3 g of granules formed using "blank" resin raw material were used in coating trials for method development. Kollicoat® SR 30 D aqueous dispersion was used as the coating agent. 10 mL of dispersion was diluted to 50 mL using acetone meaning the coating dispersion had a solid content (PVA, PVP and SLS) concentration of 6% w/v and a 1% w/v amaranth solution was included for visualisation purposes. The nitrogen flow, atomisation pressure, inlet temperature and pump rate were optimised at 25 m^3/hour, 1 bar, 80 °C and 0.6 (equivalent to 3 -3.75 mL/min) respectively. Upon completion of spraying the feed, the fluidised granules were further dried *in situ* in the FBG unit at a 60 °C inlet temperature for 5 minutes. The drug-loaded granules which were substituted into the process were hampered by fluidisation issues that could not be overcome by spraying pure solvent prior to the entry of the feed dispersion into the coating chamber.

2.2.1.6 Spray-coating using the Wurster method

A Mini-Glatt Fluidised Bed Dryer (Glatt, Germany) with a Wurster attachment was used to spray-coat all IER beads or DRCs discussed as part of this work.

2.2.1.6.1 Spray-coating of IER beads (IR120) using aqueous-based coatings

In the preliminary spray-coating studies, "blank" IER (Amberlite™ IR120) beads were used (Table 2.10). The initial runs investigated Kollicoat® SR 30 D aqueous dispersion (30% w/w polymeric content) and Eudragit® NM 30 D aqueous dispersion as potential coating agents. Depending on the run in question, acetone or water was used as a diluent prior to the feed being introduced using a single feed line to the coating chamber, unless otherwise stated. The starting batch size of the beads in each case was 5 g. The volume of the feed solution varied from 10 mL to 100 mL and the % of polymer contents in the feed dispersion varied from 0.125-2.5% w/v. Inlet temperature (60-80 °C), atomisation pressure (0.8-1 bar) and pump setting (0.6-1 corresponding to 3-8 mL/min) were investigated extensively whilst keeping the nitrogen flow constant (25 m^3/hour).

Table 2.10. List of experimental runs for the Wurster coating process using aqueous-based dispersions.

Run number	Polymer dispersion	Volume of spray solution (mL)	Concentration of solute (polymer) in the feed dispersion (% w/v)	Diluent	Ratio of dispersion to organic solvent	Inlet air temperature (°C)	Pump rate (mL/min)	Atomising setting (Bar)	Result
1	Kollicoat® SR 30 D	100	2.5	Acetone	1:5	80	3-4	0.8	Fail
2	Kollicoat® SR 30 D	50	1.25	Acetone	1:2.5	80	3-4	0.8	Pass
3	Kollicoat® SR 30 D	25	0.625	Acetone	1:1.125	80	3-4	0.8	Pass
4	Kollicoat® SR 30 D	10	3.0	n/a	n/a	60	3-4	0.8	Fail
5	Kollicoat® SR 30 D	10	3.0	n/a	n/a	80	3-4	0.8	Fail
6	Kollicoat® SR 30 D	10	3.0	n/a	n/a	80	3-4	1	Fail
7	Kollicoat® SR 30 D	10	3.0	n/a	n/a	80	6	1	Fail
8	Kollicoat® SR 30 D	15	2.0	Water	n/a	80	6	1	Fail
9	Kollicoat® SR 30 D	20	1.0	Water	n/a	80	6	1	Pass
10	Kollicoat® SR 30 D	25	0.5	Water	n/a	80	6	1	Pass
11	Kollicoat® SR 30 D	50	0.25	Water	n/a	80	6	1	Fail
12	Kollicoat® SR 30 D	100	0.125	Water	n/a	80	6	1	Fail
13	Kollicoat® SR 30 D	50	0.5	Water	n/a	80	8	1	Fail
14	Kollicoat® SR 30 D	100	0.25	Water	n/a	80	8	1	Fail
15	Eudragit® NM 30 D	20	1.0	Water	n/a	80	6	1	Pass
16	Eudragit® NM 30 D	25	0.5	Water	n/a	80	6	1	Pass

2.2.1.6.2 Spray-coating of IER beads using solvent-based coatings

2.2.1.6.2.1 pH-dependent polymers

Similar to the experiments conducted using the aqueous-based coatings, “blank” IR120 beads were used for method development. Initial coating studies used Eudragit® L100 and Eudragit® S100 dissolved in acetone at a 2.5% w/v concentration and the volume of coating solution used was 50 mL. One drop of amaranth solution was added to visualise the coating and the starting batch size of beads in each case was 5 g. The nitrogen flow rate, atomisation pressure, inlet temperature and pump setting were optimised at 25 m^3/hour, 1 bar, 60 °C and 0.6 (equivalent to 3-3.75 mL/min spray rate) respectively. Upon completion of spray-coating, the fluidised drug-loaded beads were further dried *in situ* in the instrument using a 60 °C inlet temperature for 5 minutes. In separate runs, drug-loaded

beads were substituted into the process and coated as per the aforementioned method using the optimised process and formulation factors. From this point on, coating trials were performed using 3 g of unloaded beads and this mass of starting material was loaded into the fluidised bed chamber and kept constant for the duration of the project.

Eudragit® L100 was selected as the pH-dependent coating polymer to study. Various concentrations of polymer were dissolved in IPA to produce the desired coating polymer concentrations (1-2.5% w/v) and the volume of feed solution used was 30 mL. Further studies investigated the incorporation of triacetin (TCT) which served to act as a plasticiser at a concentration of 0.37% w/v with all of the coating compositions described in Table 2.11. Drug-loaded beads were then substituted into the process and coated as per the aforementioned method using the optimised process and formulation factors. Upon completion of spray-coating, the drug-loaded beads were further dried at 60 °C inlet temperature for 5 minutes.

Table 2.11. Coating solutions used in the spray-coating trials formed during coating trials using the Eudragit® L100 grade.

Eudragit® L100 concentration in the feed solution (% w/v)	Triacetin concentration in the feed solution (% w/v)
1.00	-
1.25	-
2.50	-
2.50	0.37

2.2.1.6.2.2 pH-independent polymers

Eudragit® RL and Eudragit® RS which are the polymethacrylate-based copolymers available as organic solutions (known as Eudragit® RL 12,5 and Eudragit® RS 12,5 respectively) were used to spray-coat "blank" beads as part of the early method development process. The volume used was 30 mL and the bead batch size in each case was 3 g. In the preliminary spray-coating studies, "blank" IER (Amberlite™ IR120) beads were used before the drug-loaded beads were substituted into the process. In the case of the drug-loaded beads, it was necessary to spray 5 mL of pure IPA prior to the polymeric solution to ensure complete fluidisation and overcome static charge. The required amount of Eudragit® solution (for both grades) was diluted with IPA to a fixed volume of 30 mL to produce the required polymer concentration (0.25-8% w/v). A range of plasticisers - dibutyl sebacate (DBS), triacetin (TCT) and triethyl citrate (TEC) - were added individually to selected coating solutions. In the case of the latter, three concentrations of TEC were trialled (0.125% w/v, 0.25% w/v and 0.5% w/v). With respect

to the other two plasticisers, a single concentration of each was used (0.37% w/v) in the feed solution containing the Eudragit® RL grade (1.25 or 2.5% w/v). The nitrogen flow, atomisation pressure, inlet temperature and pump setting were optimised at 25 m^3/hour, 1 bar, 80 °C and 0.6 (equivalent to a 3-3.75 mL/min spray rate) respectively. With the exception of the atomisation pressure which was increased to 1.2 once the solid contents of the coating solution exceeded 5% w/v, all other parameters remained fixed. Upon completion of spray-coating, the drug-loaded beads were further dried *in situ* using a 60 °C inlet temperature for 5 minutes. The coating solution compositions comprising plasticiser are described in Table 2.12.

Table 2.12. Coating solutions used in the spray-coating trials formed using different concentrations of various plasticiser types and either Eudragit® RL or Eudragit® RS.

Polymer	Concentration of polymer in the feed solution (% w/v)	Plasticiser	Concentration of plasticiser in the feed solution (% w/v)
Eudragit® RL	0.50	TEC	0.125
Eudragit® RL	0.50	TEC	0.250
Eudragit® RL	0.50	TEC	0.500
Eudragit® RS	0.25	TEC	0.125
Eudragit® RS	0.25	TEC	0.250
Eudragit® RS	0.25	TEC	0.500
Eudragit® RL	1.25	DBS	0.370
Eudragit® RL	1.25	DBS	0.370
Eudragit® RL	2.50	TCT	0.370
Eudragit® RL	2.50	TCT	0.370

2.2.1.6.2.2.1 Curing conditions used for complexes coated using pH-independent polymers

To evaluate the effect of curing on drug release, selected DRCs coated with polymer feed solutions comprising 0.25% w/v Eudragit RS or 0.5% w/v Eudragit RL with and without TEC (0.125-0.5% w/v) were spread on a tray immediately post-manufacturing and placed in a Hotpack Supermatic oven (Philadelphia, PA) preequilibrated to 50 °C and held at that temperature for either 12 or 24 hours.

2.2.1.6.2.2.2 Coating studies utilising a blend of pH-independent polymers in the feed solution

Three ratios (w/w) (90:10, 75:25 and 50:50) of Eudragit® RS to RL were used by selecting the required amount of each stock solution and diluting to 30 mL using IPA. For all ratios studied, the total feed solution polymer concentration was fixed at 1% w/v. The bead batch size in each case was 3 g and

"blank" beads were used for method development prior to substituting drug-loaded beads into the process. The process parameters used were identical to those described in section 2.2.1.6.2.2.

2.2.1.7 Ball milling studies using TZD HCl

Ball milling was performed with a PM 100 high energy planetary mill (Retsch, Germany) at room temperature. 2.5 g of material was placed in stainless steel milling jars of 50 cm^3 capacity with three stainless steel balls of diameter 20 mm, corresponding to a ball to powder mass ratio of 40:1. The speed of the solar disk was set at 400 RPM. Every 30 minutes of milling was followed by a pause period of 10 minutes to avoid overheating. The effective milling time (discounting pause periods) was 20 minutes, 3 hours and 6 hours. pXRD analysis was conducted on all the samples immediately post-milling and mDSC analysis was conducted on the sample milled for 6 hours. The resistance of the milled sample to recrystallisation was assessed by pXRD at 6 hours, 12 hours and 24 hours post-storage in sealed glass vials held at room temperature. The aged sample was further analysed by mDSC after 6 hours and 12 hours over 20-120 °C firstly, followed by analysis over an extended range covering -50-130 °C. Specific details of the mDSC method are provided in section 2.2.2.2.3.

2.2.1.8 Cryo-milling studies using TZD HCl

All cryo-milling was carried out using a Cryogenic Mixer Mill CryoMill (Retsch, Germany) attached to an auto filling liquid nitrogen dewar (Retsch, Germany). A stainless steel cryo-mill chamber of 25 mL capacity filled with three stainless steel balls of 12 mm diameter were used for all cryo-milling carried out in the work of this thesis. An automatic pre-cooling step was applied before any milling was commenced. This consisted of the mill operating at a frequency of 5 Hz while liquid nitrogen circulated around the stainless-steel chamber until the cryotemperature was reached, which was automatically detected via a sensor. Depending on the milling time desired, 2 g of material was milled for the required number of cycles (ranging from 3 to 9), where each cycle consisted of a grinding phase at a frequency of 30 Hz for 10 minutes followed by an intermediate cooling phase at a frequency of 5 Hz for 2 minutes. Cryotemperature was maintained throughout milling via liquid nitrogen circulating around the milling chamber and the total effective milling time (discounting cooling phases) ranged from 30 to 90 minutes. pXRD analysis was performed after each cryo-mill run and mDSC analysis was performed for the sample milled for the longest duration (90 minutes) over a temperature range of -50-130 °C.

2.2.1.9 Melt-quench studies using TZD HCl

The crystalline raw material was melt-quenched in an aluminium weighing boat by placing on a PC-400D hot plate (Corning, United States) and heating to 125 °C until melting was evident before being quenched in liquid nitrogen. mDSC and pXRD analyses were subsequently performed.

2.2.1.10 Production of TZD free base

A 1 mg/mL aqueous solution of TZD HCl solution was adjusted to pH 9 using NaOH (4% w/v) (265) and the free base was recovered by vacuum filtration of the precipitated material using a V-700 vacuum pump (BÜCHI Labortechnik AG, Switzerland)) and V-850 vacuum controller (BÜCHI Labortechnik AG, Switzerland). The solid material retained on the filter paper (Whatman®, United Kingdom) was collected. The product was subsequently dried in a vacuum oven at 50 °C for 12 hours.

2.2.1.11 Production of physical mixtures of drug and resin

Physical mixtures of powdered resin (IRP69) and crystalline API (MTZ and TZD HCl) at specified mass ratios (w/w) were prepared by mixing with an agate pestle and mortar for comparison with the DRCs/resinates. Similarly, physical mixtures of powdered resin (IRP64 and IRP88) and crystalline API (TZD HCl) at specified mass ratios (w/w) were prepared by mixing with an agate pestle and mortar for comparison with the DRCs/resinates. Lastly, physical mixtures of bead form resin (IR120) and crystalline API (TZD HCl) at specified mass ratios (w/w) were prepared by mixing with an agate pestle and mortar for comparison with the DRCs.

2.2.2 Solid-State characterisation

2.2.2.1 Powder X-ray diffraction (pXRD)

All samples were analysed using a Miniflex II X-ray diffractometer (Rigaku, Germany) with a Ni-filtered Cu Kα radiation (1.54 A). Tube current and voltage were 15 mA and 30 kV respectively. Samples were analysed on a silicon zero background sample holder in reflection mode. Diffraction patterns were collected for 2θ ranging from 5° to 40° at a step scan rate of 0.05° per second. Rigaku Peak Integral software was used to determine peak intensity for each sample using the Sonneveld-Visser background edit procedure. The analysis was performed at least in duplicate for each sample.

2.2.2.2 Differential scanning calorimetry (DSC)/ modulated differential scanning calorimetry (mDSC)

The vast majority of (m)DSC work carried out and reported in this thesis was performed using a TA Q200 DSC (TA Instruments, United Kingdom) equipped with an RCS-90 refrigerated cooling system (TA Instruments, United Kingdom) and purged with nitrogen gas at a flow rate of 50 mL/min. The temperature was calibrated with an indium standard every three months. Standard aluminium pans with a capacity of 20 µL and 3 pinholes were used in all experiments except where otherwise stated. Universal Analysis software (TA Instruments, United Kingdom) was used to analyse data. Methodologies specific to different systems which were examined using DSC are detailed below.

2.2.2.2.1 Thermal analysis of DRC samples (TZD HCl)

Samples (1-5 mg) of starting materials, spray-dried TZD HCl, physical mixtures and DRCs (batch and spray-dried) were weighed into hermetic aluminium pans, with a capacity of 40 µL, crimped closed

and 3 pinholes inserted. A heating rate of 5 °C/min was used for analysis and samples were heated above the melting point of the crystalline API unless otherwise stated. The DSC data was analysed using Universal Analysis software (TA Instruments). Melting temperatures of drugs were determined and reported as peak temperature, and all analysis was performed at least in triplicate. The melting endotherm, where present, was determined from the total heat flow signal.

2.2.2.2.2 Determination of glass transition temperature (T_g) of TZD HCl by mDSC

Crimped aluminium hermetic pans with 3 pinholes from and a capacity of 40 µL were used in all measurements. Samples of ball milled TZD HCl, quench-cooled and cryo-milled TZD HCl (2-8 mg) were weighed out into sealed hermetic pans and then heated from 20 °C to at least 120 °C using a ramping speed of 5 °C /min while the temperature was modulated by 0.80 °C every 60 seconds. A further set of experiments, involved samples (2-8 mg) being weighed out into hermetically sealed pans and cooled to -50 °C and then heated to 130 °C using a ramping speed of 5 °C/min while the temperature was modulated by 0.80 °C every 60 seconds. The glass transition midpoint temperature was determined from the reversing heat flow signal.

In a quench-cool procedure, TZD HCl was heated in a crimped aluminium hermetically sealed pan with 3 pinholes and a capacity of 40 µL from 0 °C to 300 °C and held at this temperature for 2 minutes to allow the crystalline drug to melt. The pan was then cooled at 10 °C/min to -30 °C to form TZD HCl in the amorphous state. The pan was then reheated at 5 °C/ min to 300 °C while the temperature was modulated by 0.80 °C every 60 seconds. These analyses were carried out in triplicate for each system.

2.2.2.2.3 Thermal analysis of coated resin systems (Eudragit® NM 30 D, Kollicoat® SR 30 D, Eudragit® L100 and Eudragit® S100)

Samples of the coated DRCs prepared as per sections 2.2.1.6.1 and 2.2.1.6.2 were weighed (2-4 mg) into crimped hermetic pans with a capacity of 40 µL and 3 pinholes were inserted. Pans were first heated to 105 °C at 5 °C/min and held at that temperature for 10 min to remove residual moisture. They were then cooled to 0 °C at 5 °C/min. The temperature was then modulated by 0.80 °C every 60 seconds and the pan was reheated at 5 °C/min to 30, 160, 160 and 90 °C for the Eudragit® NM 30 D, Eudragit® L100, Eudragit® S100 systems and Kollicoat® SR 30 D systems respectively. The analysis was performed in triplicate and the glass transition onset temperature, when visible, was taken from the reversing heat flow signal in the second heating cycle.

2.2.2.2.4 Thermal analysis of coated resin systems (Eudragit® RS, Eudragit® RL and Eudragit® L100 systems)

Samples of the coated DRCs prepared as per section 2.2.1.6.2 were weighed (2-4 mg) into crimped hermetic pans with a capacity of 40 µL and 3 pinholes were inserted. Pans were first heated to 105 °C at 5 °C/min and held at that temperature for 10 min to remove residual moisture. They were then

cooled to 0 °C at 5 °C/min. The temperature was then modulated by 0.80 °C every 60 seconds and the pan was reheated at 5 °C/min to 300 °C. The analysis was performed in triplicate.

2.2.2.2.5 Determination of glass transition temperature (T_g) of DRCs systems by mDSC

Selected samples were weighed (2-4 mg) into crimped hermetically sealed aluminium pans with a capacity of 40 µL and 3 pinholes were inserted. Pans were heated from -40 °C to 300 °C at 5 °C/min and the temperature was then modulated by 0.80 °C every 60 seconds. The glass transition temperature of the systems, where present, was determined from the reversing heat flow in the first heating cycle. The glass transition temperatures were defined as the midpoint of the transition unless otherwise stated. The analysis was performed in triplicate.

2.2.2.3 Thermogravimetric analysis (TGA)

2.2.2.3.1 Evaluation of thermostability of resinates/DRCs prepared

TGA studies were conducted using a TA Q50 TGA (TA Instruments, United Kingdom) to evaluate the onset of degradation of selected DRCs/resinates produced. These samples were compared to the raw materials as well as equivalent physical mixtures of crystalline drug and resin, with the exception of the bead samples. Samples weighing between 5 and 10 mg were loaded into open aluminium pans with a capacity of 20 µL and heated using a linear heating rate of 10 °C/min from 0-350 °C unless otherwise stated. TGA data was analysed using Universal Analysis software. Calibration of the TGA Q50 was conducted every 12 weeks using nickel standards as per the equipment manual at a heating rate of 10 °C/min. Analysis was performed in duplicate.

2.2.2.3.2 Evaluation of moisture content

DRCs produced by spray-drying (section 2.2.1.3) were analysed using a TA Q50 TGA to determine the moisture/residual solvent levels. Samples weighing between 1 and 4 mg were loaded into open standard aluminium pans with a capacity of 20 µL and heated from room temperature to 150 °C at a heating rate of 10 °C/min. The mass loss over this temperature range was determined. TGA data was analysed using Universal Analysis software. Analysis was performed in duplicate.

2.2.3 Scanning electron microscopy (SEM)

The images of selected samples were captured at various magnifications using a Zeiss Supra Variable Pressure Field Emission Scanning Electron Microscope (Zeiss, Germany) equipped with a secondary electron detector at 4 kV. Powder samples were glued onto carbon tabs mounted onto aluminium pin stubs and sputter-coated with a gold/palladium mixture under vacuum prior to analysis. Initially, SEM was conducted on the raw materials, physical mixtures, DRC/resinate samples (powdered and bead form) and granules (produced using wet and fluidised bed granulation) as described above. Analysis was also performed on selected DRC samples that had been coated using the different polymer

coatings, both pre and post-dissolution. Similarly, SEM was performed on coated beads that were subject to stability testing (see section 2.2.17) over a three-month period. Lastly, SEM was performed on select samples, as part of the drug leaching studies performed (see section 2.2.9.1), when the study had been terminated at the end of a four-week period.

2.2.4 Energy-Dispersive X-ray (EDX) analysis and scanning electron microscopy (SEM)

In order to determine the elemental composition on the sample surfaces, EDX analysis was performed using a Tescan Mira Variable Pressure Field Emission Scanning Electron Microscope (Tescan, Czechia), operating at a resolution of 3 nm at 30 kV and equipped with an Oxford Inca energy-dispersive microprobe and a backscattered electron detector. Powder samples were glued onto aluminium stubs using carbon cement and coated with carbon under vacuum prior to analysis. X-ray spectra were evaluated quantitatively on the basis of the carbon peak. For qualitative EDXA, powder samples (TZD HCl, IRP69 and DRC material formed using a 1:1 w/w ratio of drug and IRP69) were utilised and an area mapped for the presence of the atom being analysed.

2.2.5 Attenuated total reflectance-fourier transform infrared spectroscopy (ATR-FTIR)

All samples were analysed using a Spectrum 1 FT-IR Spectrometer (Perkin Elmer, United States) equipped with a Universal Attenuated Total Reflectance and diamond/zinc selenide crystal accessory. Each spectrum was scanned in the range of 650-4000 cm^{-1} with a resolution of 4 cm^{-1}. Data were evaluated using Spectrum v 5.0.1. software. Four scans of each sample were taken and the reported results are presented as an average of the four scans per sample. All measurements were carried out at least in duplicate. The spectra were background corrected and the intensity of the signal normalised.

2.2.6 Raman spectroscopy

Raman spectra of the raw materials (TZD HCl, IRP69 and IR120), selected DRCs and an equivalent physical mixture (powdered system) were collected using a Raman RXN1-PhAT-785-D spectrometer (Kaiser optical systems, United States) with a PhAt system probe head (Kaiser optical systems, United States), a 150-mW laser source at 785 nm (Raman RXN1-PhAT-785-D, (Kaiser optical systems, United States)) and spectral resolution of 0.3 cm^{-1}. The measurements had an integration time of 10 seconds and one measurement was the result of five averaged scans. The distance between the probe and sample was approximately 25 cm and the spot size was 6 mm corresponding to a 28.3 mm^2 circular illumination area. The iC Raman software package (Kaiser optical systems, United States) was used for data acquisition. Baseline corrections were performed using Pearson's correction for all samples due

to the high amorphous content causing the baseline to be skewed. Furthermore, a background subtraction was carried out on the DRC samples using the iC Raman software package to help identify any unique discernible bands that can be attributed to TZD HCl due to the intense fluorescence signal associated with the resin raw material.

2.2.7 Particle size analysis

2.2.7.1 Dry dispersion mode

2.2.7.1.1 Batch-produced resinates/DRCs (MTZ)

Particle size measurements were performed by laser diffraction using a Malvern Mastersizer 2000 particle sizer (Malvern Instruments Ltd, United Kingdom) with Scirocco 2000 accessory. The dispersive air pressure used was 2.5 bars. An obscuration of between 0.5−15% was obtained using a vibration feed rate of 50%. The particle size reported is the D_{50}, the geometric median particle size of the volume distribution. The values presented are the average of at least three determinations. Mastersizer 2000 software (Version 5.61) was used for the analysis of the particle size.

2.2.7.1.2 Batch-produced DRCs (TZD HCl systems)

Measurements of particle size and particle size distributions were obtained using a Mastersizer 3000 laser diffraction particle sizer (Malvern Instruments Ltd, United Kingdom). Particles were dispersed using a Malvern Aero S accessory equipped with a micro volume sample tray using 2 bar pressure. An obscuration of between 0−15% was obtained using a vibration feed rate of 25%. Mastersizer 3000 software (Version 3.63) was used for analysis and to generate the particle size distribution data of the dry powder samples. Each result reported is the average of three determinations.

2.2.7.1.3 Spray-dried samples (IRP69)

Particle size analysis was conducted as per section 2.2.7.1.2.

2.2.7.1.4 Granules (Fluidised bed granulation and wet granulation) (IRP69)

Particle size analysis was conducted as per section 2.2.7.1.2.

2.2.7.1.5 Wurster coated beads (IR120)

Particle size analysis was conducted as per section 2.2.7.1.2.

2.2.8 Drug release studies

2.2.8.1 MTZ DRCs

50 mg samples of selected complexes formed using MTZ were tested under sink conditions using a Sotax AT-7 dissolution bath with a paddle attachment using 900 mL of either 0.1 M HCl (pH 1.2) or DI H_2O equilibrated for an hour at either 37 (± 1) ˚C or 20 (± 1) ˚C after being degassed by sonication. The paddle was rotated at 100 RPM and 5 mL aliquots of the test solution were removed at regular time

intervals for 2 hours and were replaced with fresh medium held at the same temperature. The samples were filtered through PTFE hydrophilic 0.45 µm membrane filters (Fischer, USA), appropriately diluted with mobile phase and were analysed for drug content by HPLC as per the method described in section 2.2.10.1.

2.2.8.2 TZD DRCs

2.2.8.2.1. Drug release studies (2 hours) evaluating DRCs formed using Amberlite™ IRP69 (Batch method or spray-dried)

100 mg samples (unless otherwise stated) of selected complexes formed using TZD HCl were tested under sink conditions using a Sotax AT-7 dissolution bath with a paddle attachment using 900 mL the specified media equilibrated for an hour at 37 (± 1) ˚C unless otherwise stated after being degassed by sonication. The paddle was rotated at 100 RPM and 5 mL aliquots of the test solution were removed at regular time intervals for 2 hours and were replaced with fresh medium held at the same temperature. Specific conditions for the different samples studied are listed in Table 2.13. The samples were filtered through PTFE hydrophilic 0.45 µm membrane filters (Fischer, USA), appropriately diluted with mobile phase and were analysed for drug content by HPLC as per the method described in section 2.2.10.2. pH 6.8 phosphate buffer was prepared by mixing 250 mL of $KH_2PO_4^-$ (0.2 M) and 112 mL of NaOH (0.2 M) made up to a final volume of 1000 mL with DI H_2O (266).

Table 2.13. Summary of the conditions (Drug release media type, ionic strength of the drug release media, and temperature of the drug release media) used in drug release studies for all TZD HCl-based systems evaluated over 2 hours. The "method of production" refers to the technique used to produce the DRC and "coated" refers to DRCs that were Wurster coated with either Eudragit® L100 or Eudragit® S100 as per section.2.2.1.6.2.1. "pH of loading media adjusted" refers to the pH of the drug loading solution being altered prior to resin addition and "milled/unmilled resin material used" refers to the starting resin material in the specific system of interest being subjected to a milling step.

System	Resin type	D:R ratio	Method of production	Coated/uncoated DRCs	Milled or unmilled resin material used	pH of loading media adjusted	Media type
DRC	IRP69	1:1-1:3	Batch	Uncoated	Both types	No	0.1 M HCl
DRC	IRP69	1:1-1:3	Batch	Uncoated	Both types	No	0.1 M NaCl
DRC	IRP69	1:1-1:3	Batch	Uncoated	Both types	No	pH 6.8 buffer system

DRC	IRP69	1:1-1:3	Batch	Uncoated	Both types	No	DI H_20
DRC	IRP69	2:1-1:3	Spray-dried	Uncoated	Unmilled	No	0.1 M HCl
DRC	IRP69	2:1-1:3	Spray-dried	Uncoated	Unmilled	No	0.1 M NaCl
DRC	IRP69	2:1-1:3	Spray-dried	Uncoated	Unmilled	No	pH 6.8 buffer system
DRC	IRP69	2:1-1:3	Spray-dried	Uncoated	Unmilled	No	DI H_20
PM	IRP69	55:45-45:55	-	Uncoated	Unmilled	No	0.1 M HCl
PM	IRP69	55:45-45:55	-	Uncoated	Unmilled	No	DI H_20
DRC	IRP64	2:1-1:2	Batch	Uncoated	Unmilled	No	0.1 M HCl
DRC	IRP64	2:1-1:3	Batch	Uncoated	Unmilled	No	0.1 M NaCl
DRC	IRP64	2:1-1:3	Batch	Uncoated	Unmilled	No	pH 6.8 buffer system
DRC	IRP64	2:1-1:3	Batch	Uncoated	Unmilled	No	DI H_20
DRC	IRP64	1:1	Batch	Uncoated	Unmilled	Yes (pH 5-7)	0.1 M HCl
DRC	IRP64	1:1	Batch	Uncoated	Unmilled	Yes (pH 5-7)	DI H_20
DRC	IRP88	1:1	Batch	Uncoated	Unmilled	No	0.1 M HCl
DRC	IRP88	1:1	Batch	Uncoated	Unmilled	No	0.1 M NaCl
DRC	IRP88	1:1	Batch	Uncoated	Unmilled	No	DI H_20
DRC	IR120	1:2-1:3	Batch	Uncoated	Unmilled	No	0.1 M HCl
DRC	IR120	1:2-1:3	Batch	Uncoated	Unmilled	No	DI H_20
DRC	IR120	1:2-1:3	Batch	Uncoated	Unmilled	No	pH 6.8 buffer system
DRC	IR120	1:2	Batch	Wurster coated (Eudragit® L100 or Eudragit® S100)	Unmilled	No	0.1 M HCl
DRC	IR120	1:2	Batch	Wurster coated (Eudragit® L100 or Eudragit® S100)	Unmilled	No	DI H_20

DRC	IR120	1:2	Batch	Wurster coated (Eudragit® L100 or Eudragit® S100)	Unmilled	No	pH 6.8 buffer system

2.2.8.2 Drug release studies (24 hour) evaluating the Wurster coated DRCs (IR120)

Selected coated complexes were tested under sink conditions using a Sotax AT-7 dissolution bath with a paddle attachment. As the goal of the formulation was to control the release of TZD HCl, the pH conditions were varied throughout the dissolution to mimic gastrointestinal conditions (267). The dissolution conditions used were as follows, as detailed previously by Andrews et al. (268).

• 0.1 M HCl (pH 1.2) for two hours;

• pH adjusted to 6.8 by the addition of 0.2 M trisodium phosphate Na_3PO_4 and dissolution continued for a further 2 hours;

• pH adjusted to 7.4 by the addition of drops of 2 M NaOH and dissolution continued for a further 2 hours;

• pH adjusted to 6.5 by the addition of drops of 1 M HCl and dissolution continued for 18 hours until the end.

The temperature was maintained at 37 ± 0.5 °C and a paddle stirring speed of 100 RPM was used. 5 mL aliquots were withdrawn and were replaced with fresh medium held at the same temperature at the pre-determined time intervals. Samples were filtered through PTFE hydrophilic 0.45 µm filters (Fischer, USA) and were analysed for drug content by HPLC as per the method specified in section 2.2.10.2. The dissolution study was terminated after 24 hours. All studies were conducted in triplicate.

For selected samples, the material was recovered after the drug release studies were performed and assayed as per the procedure described in section 2.2.11 for drug content.

2.2.8.3 Drug release kinetics (Korsmeyer-Peppas)

The drug release data obtained was fitted (first 60% of drug release) using the following kinetic equation using DDSolver software (China Pharmaceutical University, China) (269): Korsmeyer–Peppas (Equation 2.1):

$$Log\left(\frac{M_t}{M_\infty}\right) = logk_{kp} + nlogt \qquad \textbf{Equation 2.1}$$

where M_t/M_∞ is the fraction of drug released at time t, t, per unit area; k_{KP} is a constant that describes the structural and geometric characteristics of the drug dosage form; *n* is the release exponent which describes the drug release mechanism. The *n* has a value of 0.5, 0.45 or 0.43 when the particle shape is a thin film, a cylinder or a sphere respectively which indicates Fickian release controlled by diffusion (270). Anomalous non-Fickian transport is observed when n is between those values and 1 ($0.5 < n < 1$ for thin films, $0.45 < n < 1$ for cylinder and $0.43 < n < 1$ for spheres) (271).

2.2.8.3.4 Suspension formulation (selected Wurster coated DRCs)

Studies investigating the drug release from the reconstituted microparticle suspensions (5 mL) prepared according to section 2.2.9 performed using the method described in section 2.2.8.3.6. The dissolution performance was assessed at three different time intervals: immediately after preparation (T_0), two weeks post-preparation ($T_{2\ week}$) and four weeks post-preparation ($T_{4\ week}$).

2.2.9 Suspension formulation trials

Initial trials aimed at identifying suitable suspending agents used hydroxymethylpropylcellulose (HPMC), Avicel™ RC/CL and xanthan gum over a range of concentrations spanning 0.25-1% w/v. For the purposes of these trials, the unloaded resin was used to conserve the finite amount of drug-loaded material. TZD–resin complex microparticles (equivalent to TZD HCl 4.9 mg/5 mL) were dispersed in 5 mL DI H_2O, in which the suspending agent at a particular concentration had been dissolved. Through visual inspection, the physical properties were evaluated and xanthan gum at a 0.5% (w/v) was selected as the optimum suspending agent to suspend the beads.

2.2.9.1 Drug leaching studies

Samples encompassing both uncoated and selected coated beads were suspended in 5 mL DI H_2O containing 0.5% w/v xanthan gum and stored at room temperature for one month. At weekly intervals, 500 µL of liquid from the suspensions was taken and diluted using HPLC mobile phase before the drug quantity was determined using HPLC as per the method specified in section 2.2.10.2. Similar experiments were conducted at daily intervals for the first week using the same procedure for all five samples used in the 1-month long study.

2.2.10 High performance liquid chromatography (HPLC)

2.2.10.1 MTZ

The concentration of MTZ in solution was determined using a Waters HPLC consisting of Waters 1525 Binary HPLC Pump, Waters 717plus Autosampler and Waters 2487 photodiode dual wavelength absorbance detector). The mobile phase consisted of phosphate buffer, acetonitrile (ACN) and glacial acetic acid in the ratio of 60:40.0.1 v/v. The phosphate buffer was prepared from 10 mM potassium

dihydrogen phosphate solution. The mobile phase was vacuum filtered through a 0.45 µm PTFE membrane filter and bath sonicated for 5 minutes. Separation was performed on a Waters Symmetry® C8 column (250 mm length, diameter 4.6 mm, particle size 5 µm) with an injection volume of 20 µL and a UV detection wavelength of 271 nm. The elution was carried out isocratically at ambient temperature with a flow rate of 1 mL/min. Elution time for MTZ was 3.6 minutes (231). Breeze software was used for peak evaluation. Calibration curves were acquired biweekly (Figure 1 in Appendix 4), with freshly prepared standard solutions, while studies were ongoing. The linearity range was between 0.5 µg/mL and 200 µg/mL for MTZ with a regression coefficient of 0.999. The limit of detection for the method was 0.3 µg/mL for MTZ.

2.2.10.2 TZD HCl

By modifying methods specified in the USP monograph for TZD tablets (272), the concentration of TZD in assay media and dissolution media was determined using an Alliance HPLC with a Waters 2695 Separations module system and Waters 2996 photodiode array detector. The mobile phase consisted of 20 volumes of ACN and 80 volumes of a 3.86 g/L solution of sodium pentane sulfonate monohydrate previously adjusted to pH 3.0 with an aqueous phosphoric acid solution (88:12). The mobile phase was vacuum filtered through a 0.45 µm PTFE membrane filter and bath sonicated for 5 minutes. Separation was performed on a HypersilGold® C18 column (150 mm length, diameter 4.6 mm, particle size 3.5 µm) with an injection volume of either 10 µL or 20 µL for the assay/related substances and dissolution analysis respectively at a UV detection wavelength of 271 nm. The elution was carried out isocratically at a temperature of 50 °C with a flow rate of 1 mL/min. Elution time for TZD HCl was 7.2 minutes. Empower software was used for peak evaluation. Calibration curves were acquired once a week, with freshly prepared standard solutions, while studies were ongoing (Figure 2 in Appendix 4), The linearity range was between 0.5 µg/mL and 200 µg/mL for TZD HCl with a regression coefficient of 0.999. The limit of detection for the method was 0.149 µg/mL for TZD HCl.

2.2.11 Drug assay testing

2.2.11.1 Assay of the drug-resin complex (DRC)

To assay the amount of the drug loaded onto the resin, a drug displacement method is required using either an acidic/basic displacement fluid or salt solution. This method requires the addition of a known quantity of resin to a known volume of displacement fluid at a pre-set temperature and the system is agitated for a pre-determined period of time. The sample is then filtered after which the liquid portion is diluted using HPLC mobile phase, if necessary, and the amount of drug displaced is then quantified using HPLC. Two criteria depicted below in Equations (2.2 and 2.3) are used to assess the loading

process and have been reported by other authors in the field (118,273). The first equation requires knowledge of the initial starting quantity of drug and the amount unloaded (present in the filtrate generated from the filtration process described in section 2.2.1.2.3) and is represented as % drug association efficiency (DAE) (Equation 2.2). The second, which is more commonly reported, represents the most popular method of calculating drug loading (Equation 2.3) but requires optimisation so it can accurately reflect the system studied. Optimisation of the displacement conditions is necessary to establish a robust method for accurately estimating drug loading and the specifics for each system studied are discussed over the subsequent pages.

$$\%\ \text{Drug association efficiency} = \left(\frac{Amount\ of\ drug\ associated\ (mg)}{Amount\ of\ drug\ used\ (mg)}\right) \times 100 \qquad \textbf{Equation 2.2}$$

$$\%\ \text{Drug loading} = \left(\frac{Amount\ of\ drug\ eluted\ (mg)}{Amount\ of\ drug\ resin\ complex\ \ (mg)}\right) \times 100 \qquad \textbf{Equation 2.3}$$

2.2.11.1.1 MTZ

2.2.11.1.1.1 Drug displacement method

50 mg of each complex was accurately weighed out using a microbalance (Mettler-Toledo, United Kingdom), and added to a 1000 mL volumetric flask and made up to the mark using either MeOH or 0.1 M HCl (1000 mL). The contents of the flask were then mixed with a magnetic stirrer at 1000 RPM at room temperature for 24 hours before being filtered using PTFE filters (Fisher, USA), suitably diluted using mobile phase and analysed by HPLC (as described in section 2.2.10.1). The drug content was quantified against a calibration curve and performed in triplicate. This value formed the numerator in Equation 2.5 used to calculate the % drug loading.

2.2.11.1.1.2 Calculation of the drug content in the filtrate

Post-filtration of the drug-resin suspension, suitable dilutions of the filtrate were carried out using HPLC mobile phase, and the drug content in the filtrate was determined using HPLC in order to calculate the drug association efficiency. This value formed the numerator in Equation 2.3 used to calculate the % drug association calculation.

2.2.11.1.2 TZD HCl

2.2.11.1.2.1 Filtrate analysis

The filtrate's drug content was calculated as per section 2.2.11.1 with the exception of the HPLC method which is described in section 2.2.10.2.

2.2.11.1.2.2 Drug displacement assay

2.2.11.1.2.2.1 DRCs formed using Amberlite™ IRP69

HCl and NaCl were the acid and salt respectively used to produce the aqueous displacement fluids for studying the optimisation of the drug displacement assay for TZD HCl. The impact of ionic strength (0.1-1 M), concentration of complex (0.055 mg/mL- 0.9 mg/mL) and temperature (20-50 °C) were studied using a DoE approach. The time required to elute the drug from the resin was kept constant at 24 hours. Three multilevel factors (complex concentration - 0.056 mg/mL, 0.111 mg/mL, 0.222 mg/mL, 0.741 mg/mL, 1.0 mg/mL, displacing medium used - HCl or NaCl and molarity of displacing medium - 0.1 M, 0.5 M or 1 M) were investigated using a full factorial screening design where the single response was drug loading (% w/w at various temperatures (20 °C, 37 °C or 50 °C) and the statistical software package MODDE 12.1 (Umetrics AB, Sweden) was used to carry out the statistical analysis for all experimental designs with a confidence level of 95% ($p<0.05$).Using the experimental results, three partial least squares (PLS) models were created and used to correlate the factors with the response for each temperature. In each case, for the three models, both R^2 and Q^2 were >0.80 and complex concentration was identified as the key factor. The molarity of the displacing media seen to have a marginal effect on the response and the type of displacing media was found not to be significant. The optimised assay conditions that were identified for each displacement agent were then used to quantify the drug loading of selected samples. To confirm that this method identified appropriate elution conditions, a sample was selected to study where it was eluted using the aforementioned elution conditions followed by immediately being transferred to fresh elution medium to establish if a further quantity of drug could be detected.

2.2.11.1.2.2.2 Amberlite™ IR120

The optimisation of the assay conditions was performed according to a similar procedure as that outlined in section 2.2.11.1.2.2.1, with the only exception being that the elution temperatures studied were 20 °C and 50 °C. The optimised assay conditions that were identified for each displacement agent were then used to quantify the drug loading of selected samples. To confirm that this method identified appropriate elution conditions, a sample was selected to study where it was eluted using the aforementioned elution conditions followed by immediately being transferred to fresh elution medium to establish if a further quantity of drug could be detected.

2.2.11.1.2.2.3 Amberlite™ IRP64

The complex formed using a 1:1 D:R (w/w) ratio and produced using a drug loading solution whose pH was not adjusted using a buffer system prior to the addition of resin material was used to optimise the assay conditions. HCl and NaCl were the acid and salt respectively used to produce the aqueous displacement fluids for studying the optimisation of the drug displacement assay for TZD HCl. The

impact of ionic strength (0.1-1 M), concentration of complex (0.1 mg/mL-1 mg/mL) and temperature (20 and 37 °C) were studied. The optimised assay conditions for each displacement agent were then used to quantify drug loading of all other samples produced using Amberlite™ IRP64, as per the procedure provided in section 2.2.11.1.

2.2.11.1.2.2.4 Amberlite™ IRP88

The assay procedure of the complex formed using a 1:1 D:R (w/w) ratio was optimised in an identical manner to the method outlined in section 2.2.11.1. This was then used to assay the DRCs/resinates formed using Amberlite™ IRP88 and TZD HCl at the other two weight ratios investigated (2:1 and 1:2).

2.2.11.1.2.2.5 Wurster coated DRCs

2.2.11.1.2.2.5.1 DRCs coated using pH-independent polymers

100 mg of beads coated with either Eudragit® RS or Eudragit® RL was added to 100 mL of IPA and stirred at room temperature overnight to dissolve the coating. Subsequently, the liquid was decanted and assayed for drug content by HPLC as per section 2.2.10.2. 1000 mL of 0.1 M HCl was then added to the beads and stirred for 24 hours. HPLC analysis was conducted to determine the drug content. An identical approach was used to determine the drug content of the DRCs coated using the Eudragit® RL polymer, the blend of the two grades as well as the systems coated using feed solutions containing plasticiser.

2.2.11.1.2.2.5.2 DRCs coated using pH-dependent polymers

Assay of these materials required two calculations owing to the nature of the media used to strip the coating. 100 mg of beads coated with Eudragit® L100 were added to 100 ml of a 0.1 M NaOH solution and stirred at room temperature overnight to dissolve the coating. Subsequently, the liquid was decanted and assayed for drug content by HPLC as per the method detailed in section 2.2.10.2. 1000 mL of 0.1 M HCl was then added to the beads and stirred for 24 hours at room temperature.

HPLC analysis using the method specified in section 2.2.10.2 was conducted to determine the drug content by adding the values obtained by the stripping of the coating as well as the assay of the uncoated complex.

2.2.12 Estimation of the level of the coating obtained by Wurster coating

As a method of estimating the % weight gain after coating, the weight of 200 drug-loaded uncoated IER beads was measured using a microbalance. To calculate the % weight gain of the coated drug-loaded IER beads, the weight of 200 beads of selected coated samples was measured. The difference in weight values was then divided by the weight of the 200 uncoated drug-loaded IER beads and multiplied by 100 to estimate the % weight gain achieved.

2.2.13 Dynamic vapour sorption (DVS) studies

A DVS Advantage-1 automated gravimetric sorption analyser (Surface Measurement Systems, United Kingdom) was used to measure the vapour sorption capabilities and obtain water sorption kinetic profiles of selected formulations in addition to the raw materials. Samples were tested at 25.0 ± 0.1 °C using water as the sorbing vapour. A mass of 15–20 mg of material was placed in the sample basket and was dried to a constant mass (dm/dt <0.002 mg/min) which took between 1 and 2 hours at 0% RH. Once stable the sample was exposed to changes in RH from 10% RH to 90% RH in 10% RH increments and in reverse during the desorption process. One cycle of sorption and desorption was performed and pXRD post-DVS testing was also conducted. The analysis was performed in duplicate.

Water sorption isotherms of selected samples were calculated using the equilibrated mass (d*m*/d*t* ≤ 0.002 mg/min for 10 min) recorded at the end of each stage and expressed as a percentage of the dry sample mass. The Young–Nelson equations were used to fit experimental equilibrium sorption and desorption data of the isotherms (274).

$$M_s = A(\beta + \theta) + B\theta RH \qquad \textbf{Equation 2.4}$$

$$M_d = A(\beta + \theta) + B\theta RH_{max} \qquad \textbf{Equation 2.5}$$

Where M_s and M_d are, respectively, the mass percentage of water contents of the system at equilibrium for each %RH during sorption and desorption. *A* and *B* are constants characteristic of each system and defined by the following equations (Equations 2.6 and 2.7):

$$A = \frac{\rho_w VolM}{W_m} \qquad \textbf{Equation 2.6}$$

$$B = \frac{\rho_w VolA}{W_m} \qquad \textbf{Equation 2.7}$$

where ρ_w is the density of the water, Vol_M and Vol_A are respectively the adsorbed and absorbed water volumes and W_m is the weight of the dry material (275).

In this model, θ is the fraction of the surface covered by at least one layer of water molecules. It is defined as follows, with *E* being a constant depending on the material.

$$\theta = \frac{RH}{RH + E(1 - RH)} \qquad \textbf{Equation 2.8}$$

β is defined by the following equation:

Equation 2.9

$$\beta = -E \times \frac{RH}{E - RH(E-1)} + \frac{E^2}{E-1} \times \ln\left[\frac{E - RH(E-1)}{E}\right] - (E+1) \times \ln(1 - RH)$$

Thus, $A\,\theta$ is the mass of water in a complete adsorbed monolayer expressed as a percentage of the dry mass of the sample. $A(B + \theta)$ is the total amount of adsorbed water, and Ab is the mass of water that is adsorbed beyond the mass of the monolayer (i.e. in multilayer or cluster adsorption). B is the mass of absorbed water at 100% of RH, and, hence, $B\,\theta$ is the mass of absorbed water when the water coverage is θ for a given %RH. According to the model characteristics, from the estimated values of A, B, and E, the corresponding profiles of water adsorbed in a monolayer ($A\,\theta$), multilayers (AB) and absorbed ($B\,\theta$) were obtained (276).

2.2.14 Specific surface area analysis and pore size determination

Specific surface area for the raw materials, selected DRC samples and granules were measured using a Gemini VI analyser (Micromeritics, USA). Prior to analysis, samples were degassed under nitrogen gas, using a SmartPrep degasser (Micromeritics, USA) at 105 °C overnight, to remove residual moisture. The amounts of nitrogen gas adsorbed at the relative pressures of 0.05, 0.10, 0.15, 0.20, 0.25 and 0.30 were determined and the BET multipoint surface area was calculated. Each experiment was carried out in triplicate. The adsorption data for the relative pressures $0.35 < P/P_o < 1$ was used to calculate pore size and pore size distribution using the BJH model (277). Analyses were performed at least in duplicate for each sample.

2.2.15 Polarised light microscopy

Approximately 2-4 mg of selected samples were added to a glass slide which was then placed onto an LTS420 hot stage (Linkam, United Kingdom) of a BX53 polarised light optical microscope (Olympus, United Kingdom.) equipped with a U-POT cross polarizer and a U-AND analyser. Images were taken with an integrated Q IMAGING Fast 1394 camera (Olympus, Japan) at ×25 magnification.

2.2.16 Imaging

The morphology of selected coated and uncoated blank beads, used in the preliminary analysis, were imaged by using a 9MP 2-200 x digital microscope (Conrad Electronics, Germany) and images were processed by Image J v1.46 image analysis software (N.I.H, USA).

2.2.17 Physical stability of TZD HCl DRCs

Uncoated TZD HCl DRCs and a select number of Wurster coated DRCs, were placed on short-term stability at two relative humidity (RH) conditions (25 °C/60% RH, and 25 °C/<10% RH) for 6 months. A

suitable amount of test material was transferred to Amebis sample chambers containing a pre-prepared saturated sodium bromide salt solution for the 25 °C/60% RH condition, or phosphorous pentoxide which was used to generate the sub 10% RH condition. The sample chambers containing the test material and saturated salt solution/phosphorous pentoxide were subsequently transferred to a temperature-controlled cabinet at the specified temperature. The integrated temperature and humidity sensor within the Amebis system wirelessly transmitted and logged data regarding the environmental conditions within each test chamber to the Amebis Control Software (Amebis Ltd., Ireland) at 30-minute intervals. The Amebis system allowed for remote monitoring of both temperature and relative humidity conditions without the need to remove the chamber for data retrieval/monitoring. Samples were taken and analysed periodically by pXRD and mDSC over the course of 6 months to test for amorphous/crystalline nature. Uncoated samples and those coated using feeds containing solely Eudragit® RS and Eudragit® RL were selected for dissolution analysis (section 2.2.8.2) at months 1, 2 and 3. SEM analysis was also performed on all given samples at monthly intervals for a total of three months.

2.2.18 Chemical stability of TZD HCl DRCs

The chemical stability of TZD HCl after the DRCs being placed on stability for 3 months under the two conditions specified in section 2.2.17 was assessed by means of HPLC (quantification of the API) as per the method specified in section 2.2.10.2.

2.2.19 Statistical analysis

Statistical analysis for the Taguchi Design of Experiments (section 2.2.1.3.2) was performed using Design Expert software (version 10.0). Optimisation of the process and formulation factors was also performed using this software.

The two-sample t-test (comparison of two data sets) and one-way ANOVA followed by posthoc Tukey's test (comparison ≥ 3 sets of data) were used to test the statistical significance of the results when comparisons were made. Two-way differences were tested for statistically significant differences at a confidence level of 95% and considered different when a p value ≤ 0.05 was obtained. Version 9 of OriginPro software OriginLab, United States) and Version 9 of GraphPad Prism (GraphPad Software, USA) was used to perform the statistical analyses.

The statistical software package MODDE 12.1 (Umetrics AB, Sweden) was used to carry out the statistical analysis for all experimental designs (assay optimisation for TZD HCl) with a confidence level of 95% ($p<0.05$). The resulting models can be evaluated in terms of statistical parameters such as quality (or goodness) of fit (R^2) and quality (or goodness) of prediction (Q^2). R^2 is an indicator of how

well a regression model can be made to fit a set of data. If R^2= 1 that means a perfect fit, and R^2= 0 means no fit at all. Q^2 is used to estimate the predictive power of a model. Q^2 = 1 means perfect predictive power, Q^2= 0 means no predictive power. Mr Peter O'Connell aided in the development of these models using the MODDE software.

Chapter 3:

An investigation into the drug loading, drug release and solid-state properties of ion-exchange resin complexes formed using cation exchange resins and two different active pharmaceutical ingredients

3.1 Introduction

For many decades, ion-exchange resins (IERs) have proven to be effective solutions to numerous formulation problems that a pharmaceutical scientist may encounter. Despite these excipients having a wide variety of uses, with a rich history in pharmaceutical development, they remain underutilised and poorly understood (80). Their value has been well documented, with applications ranging from extended-release to taste-masking and their safety profiles make them suitable for use in formulations intended to be administered orally and topically (278). Aside from their impact on the dissolution behaviour of active pharmaceutical ingredients (APIs), their ability to enhance the stability of pharmaceutical formulations has also been proven (124). The structure of an IER can be best described as an insoluble polyelectrolyte that has the ability to exchange ions. This insolubility extends to all resins and is what differentiates them from other polyelectrolytes. Furthermore, within the pharmaceutical industry, the ion-exchange capability is exploited as a means to load the drug onto the resin to tailor the API's properties for a specific formulation purpose (95). This loading can be typically accomplished using one of two methods, known as the batch and column methods. The former is the preferred method of preparing drug-resin complexes (DRCs), especially when it comes to loading the drug onto finely powdered resin. It is accomplished by adding the resin to a solution of drug and stirring until equilibrium is attained, and is a well-established technique in the field (110). It is favoured over the column method due to its suitability for loading powdered resin materials, which do not lend themselves to the column process.

Fundamental to the success of the loading process is the charge compatibility between the drug and resin which enables drug loading to occur. After this prerequisite has been met, consideration of the free drug-resin equilibrium is a major focus, alongside the identification of the critical factors which influence the equilibrium state. This is of paramount importance if one is to maximise drug loading levels and has formed the basis of many research papers that have been published to date (279). Furthermore, the majority of studies in the literature have investigated the impact of complex formation on the drug release characteristics of basic compounds, which requires the use of a cation exchange resin, broadly classed as either "strong" or "weak" exchangers (80). This classification is related to the dissociation properties of the resin, which in turn impacts the performance of the DRC, particularly if the sustained-release or taste-masking of the API are the aims (82,93). Analogous to the drug loading process, knowledge of the free drug-DRC equilibrium is integral to understanding the release behaviour of API from the DRC in an ionic environment. Many of the factors known to influence the exchange reaction between the drug ions bound to the resin and the mobile ions in solution are common to those that need to be optimised with respect to the drug loading process.

Depending on the specific resin used to form the DRC, certain factors require greater consideration than others, particularly when resins with different dissociation properties are utilised (110).

Despite the well-documented history of pharmaceutical applications, excellent safety record and relatively simple method of preparation, many aspects of pharmaceutically relevant resinates remain under-investigated, in particular, the solid-state characterisation of the resins themselves and the resultant DRCs. There is also a dearth of information relating to the design of effective and reliable drug assay methods for DRCs, with little evidence of optimised assay procedures in the literature, which can make it difficult to interpret drug release testing results. A consequence of these aspects of the research being neglected is that the performance of any particular DRC is recognised, but not well understood (280).

The two APIs studied as part of this work were carefully selected, with the IER formulation approach in mind. The advantages conferred by DRC formation were envisaged to be beneficial for formulating a stable oral liquid formulation. One of the primary advantages of IERs, cited by previous authors, is their proven ability to form stable sustained-release liquids (117). The development of this type of oral liquid has been plagued by stability issues, most notably drug leaching into the liquid vehicle (281), which can be overcome through the use of an appropriate IER-based liquid formulation. The stability that is afforded by the IER based systems is related to the inherent resistance of the DRCs to drug release in an environment that contains no ions (95).

The first API studied in this chapter was metronidazole (MTZ), a well-known nitroimidazole, indicated for the treatment of anaerobic infections (282) and which is available in many different pharmaceutical forms, including a liquid formulation. Due to the API's well-documented foul taste, the marketed liquid suspension contains MTZ benzoate, rendering it tasteless due to its insolubility in aqueous media (283). The use of the ester form in the liquid product produces differences in the pharmacokinetic parameters compared to the free base form, which the manufacturer ascribes to the cleavage of the ester group in the gut after administration of the suspension formulation (224). As MTZ has desirable ionisation characteristics (pKa of 2.6) (284), that render it amenable to ion-exchange, resinate/DRC formation is worth investigating, as the approach presents an alternative method of avoiding the unpalatable taste of the free base. Moreover, the complexation of the drug and resin should not lead to the differences in C_{max} and T_{max} reported for the ester form. Furthermore, as alluded to previously, the utilisation of IERs offers scope for producing a stable prolonged-release system, which could be beneficial for certain indications of MTZ. Extended-release dosage forms of MTZ have been reported for the treatment of bacterial vaginosis and other more niche indications such as pouchitis (228,285).

The second API employed was tizanidine hydrochloride (TZD HCl), which acts as an alpha-2 adrenergic agonist, producing myotonolytic effects on skeletal muscle (244). The API suffers from several drawbacks including low bioavailability and a short half-life ($t_{1/2}$), necessitating frequent dosing (286). Similar to the other drug candidate studied, it is available as a solid dosage form. Dosage regimens of up to 36 mg daily in divided doses have been reported, which generates a significant dose burden for the patient as the product is only available in low dose strengths (2 and 4 mg) (239). This, coupled with the need for frequent dosing, stemming from the drugs short $t_{1/2}$ presents patient compliance issues, pointing to the potential benefit of a sustained-release system. Moreover, the cohort of patients that typically suffer from spasms, such as those afflicted with multiple sclerosis (MS), may derive further benefit from an oral liquid product, which has been demonstrated to confer patient compliance benefits and affords dose flexibility, due to the ability to easily titrate the dose (287,288). The compound is structurally related to clonidine hydrochloride, which has been formulated as a commercially successful product, using the same class of resin that will be used as part of this work (261). The compound's high water solubility does make it a challenging candidate to formulate as a sustained-release formulation, but the unique stability advantages afforded by the resin approach, make it an interesting prospect to explore.

The main aim of the work was to establish and subsequently evaluate the suitability of the IER-based approach to formulate liquid systems with satisfactory API loading and controlled drug release. This involves the investigation of the maximum drug loading achievable, using a series of different loading conditions. The second main objective of the work focuses on the effect that complexation imparts on the drug release characteristics across a variety of media studied. By varying the media composition, it can be quickly established if the complex forms a robust system, which in turn will confirm the feasibility of using the approach to achieve the desired release profile, as well as a stable oral liquid product. A further objective of the work is to thoroughly characterise the solid-state properties of the DRCs. This involves investigating the impact of the loading conditions on the physical form of the drug, the nature of the interactions between drug and resin and gaining visual information through the use of microscopy to further elucidate the impact of complexation on the morphology. By using a series of complementary characterisation techniques, greater insight into the loading process can be established, which serves to increase the understanding of the systems formed. A flow chart diagram shown in figure 3.1 indicates the series of sequential steps performed in this chapter. The purpose of which is to aid the reader in understanding the different strands of work reported in this chapter.

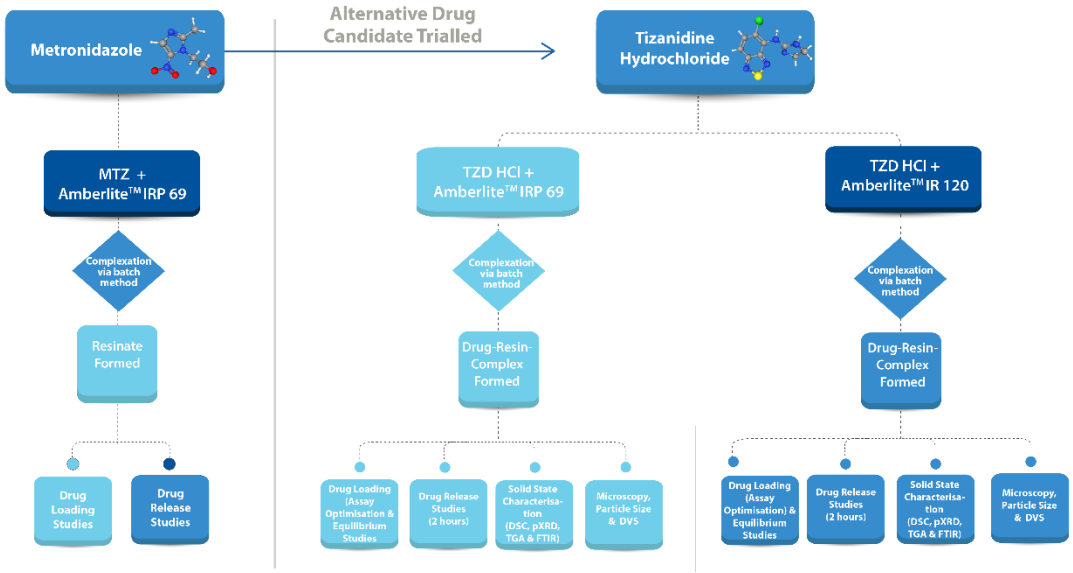

Figure 3.1. Flow chart outlining the series of sequential steps constituting the experimental progress in chapter 3.

3.2 Results and Discussion

3.2.1 Metronidazole (MTZ)

3.2.1.1 Production of resinates/drug resin complexes (DRCs) using Amberlite™ IRP69 (IRP69)

MTZ is reported to be relatively stable with little or negligible degradation in its liquid phase (289), and its hydrolysis occurs at high temperature and pH. Low pH solutions were employed for drug loading onto the IER as MTZ is a weak base, with a pKa_1 of 2.6 for the nitrogen with the lone pair of electrons in the imidazole ring (290), which is predominately ionised at very low pH values. The pH of an aqueous solution of MTZ (0.1% w/v) was found to be 6 ± 0.05, the concentration of MTZ used consistently throughout the MTZ studies, pointed to the need to adjust the pH of the loading solution using a buffer. Before the drug loading experiments were undertaken, the stability of MTZ under different pH conditions (pH 0.6-3) deemed appropriate for the drug was determined to ensure that degradation of the API would not compromise the loading studies. MTZ was found to be stable for at least 24 hours at all pH values tested (Table 1 in Appendix 1), which was sufficient for drug loading purposes and consistent with the findings of many research groups that have investigated the drug's stability at low pH (289,291). Appropriate pH values were chosen (pH 1.6 and pH 0.6) after calculations were carried out using the Henderson-Hasselbalch equation, which approximates the degree of ionisation of a compound at particular pH values depending on the acidity or basicity of the compound (292). These calculations were performed for MTZ, as a consensus exists in the literature regarding the ionisation character (pKa_1 is 2.6). By manipulating the pH of the loading solution, protonation of MTZ can be assured, which is desirable from the perspective of binding to the acidic IER. The powder yield for all complexes produced ranged from 48.75% to 56.71%, with a complete list for each sample studied available in Table 2 in Appendix 1.

The pH values selected, and the results of the loading studies are shown in Table 3.1. At a pH value of 2.6, where the drug is predicted to be 50% ionised, the level of loading achieved is approximately 13.2%. However, this level of loading achieved, as determined by the drug displacement assay, is still substantially lower than values reported in the literature for ionisable compounds (mostly weak bases) which are typically in the 35-65% range (97,111,117,131), which is surprising, considering that 50% of the drug is present in solution in the protonated state (293). One possible reason for these low loading levels is the presence of competing ions in the buffer system which have an affinity for the dissociated resin. However, as stated above, loading values still fall well below those reported by groups who also adjusted the pH using buffer systems to ensure ionisation (294). This indicates that several factors influence the selectivity of the resin for the drug, apart from the key basic requirement of ionisation.

As shown in Table 3.1, other pH values tested produced loading levels, as determined using the drug displacement method, that could not be solely explained based on % ionisation. If the pH of the

loading medium is 2 units below the pKa of an ionisable compound, then the drug should be greater than 99% ionised which, in turn, should afford it the best opportunity to bind to the resin. As can be seen in Table 3.1, the loading % value obtained at the most acidic pH tested (pH 0.6) is lower than the drug loading achieved at higher pH (1.6), which is unexpected. This finding is similar to what has been observed by a group working with ciprofloxacin in an attempt to taste mask it (295). They attributed decreased complexation at lower pH to an excess of H^+ ions in the solution, which has more binding affinity to the sulfonic acid groups of the resin and competes with the drug for binding. They reported that when the pH of the medium approaches the pKa of the drug, then optimum complexation (and hence loading) is expected to occur. An additional factor to consider is that these low pH values also lie close to the pKa of the resin, and the resin will become unionised if the pH becomes too acidic. Although these pH values do not drop below the pKa of the resin, the closer the pH is to it, the lower the proportion of ionised resin species, which in turn compromises drug binding. An intermediate pH value of 0.92 which is between the two aforementioned pH values studied was the final pH tested below the pKa. This loading medium produced systems with drug loading values that are higher ($p<0.05$) than those produced by the loading medium which was adjusted to pH 0.6 but lower ($p<0.05$) than the values determined for DRCs produced using the medium 'buffered' to pH 1.6.

As the 'buffer' used in the initial loading studies consisted of KCl and HCl, contributing two distinct competing counter ions in solution, which could hinder the potential complexation between the drug ion and the resin, it was decided to use HCl alone to adjust the pH of the loading solution. Table 3.1 shows improved drug loading results when only 0.1 M HCl was used to adjust the pH of the loading medium to pH 1.6 ($p<0.05$). This was done to order reduce the competition for resin binding sites. If the medium has many ionic species, it may decrease the electrostatic interaction between the resin and ionic drug due to shielding and a competitive binding effect (110). pH values of 2.6 (MTZ's pKa_1) and 3.0 (where the drug is expected to be predominately unionised), produced as per Table 2.5 in Chapter 2 (citrate-phosphate buffer), were tested and demonstrated reduced loading relative to pH 1.6. Another possible reason for the modest drug levels achieved with all systems tested is that the functional group of the cation-exchange resin used in this experiment is SO_3^- Na^+. As complex formation progresses, more acidic by-products can be produced. If not removed from the system, the by-products would change the pH of the reaction medium, compete with the counter ion drug moieties in the bulk solution, and affect equilibrium, and also drug loading efficiency (90). Following examination of the literature, heterogeneity exists, when it comes to the terminology used to report complexation. In this thesis, the terms used to describe the two main criteria used to determine the success of the loading process are drug association efficiency (DAE) and drug loading (Equations 2.2

and 2.3 respectively in section 2.2.11.1 in Chapter 2). Both these terms were reported by Shang et al. when investigating the ion-exchange approach for betahistine HCl (118).

Table 3.1. Comparison of the effect of different drug loading solution pH values (prior to the addition of IRP69) on the calculated drug loading (%) and drug association efficiency (DAE %) for resinates formed using "unactivated resin", a 0.1% w/v drug concentration and a 1:1 D:R ratio (w/w) unless otherwise stated. The drug loading values were determined either using the drug displacement method using 0.1 M HCl or solvent extraction using MeOH as per the procedure stated in Chapter 2, section 2.2.11.1. The three samples produced using a drug solution adjusted to pH 1.6 are distinguished based on the method used to achieve the pH value. HCl referring to dilute HCl and 'buffer' referring to the HCl-KCl 'buffer' system and citrate-phosphate buffer referring to the citrate-phosphate "buffer" system described in Tables 2.4 and 2.5.

pH of drug loading solution prior to resin addition	Drug loading (% w/w)		DAE (%)
	MeOH	0.1 M HCl	
0.6 ('buffer')	7.1 ± 0.3	7.6 ± 0.2	7.5 ± 1.6
0.9 ('buffer')	8.0 ± 0.3	8.6 + 0.5	8.3 + 1.1
1.6 (HCl)	17.4 ± 0.4	17.6 ± 0.2	22.2 ± 0.2
1.6 ('buffer')	15.0 ± 0.4	15.7 ± 0.4	15.3 ± 1.4
2.6 ("citrate-phosphate buffer")	13.3 ± 0.1	13.2 ± 0.4	13.2 ± 0.4
3 ("citrate-phosphate buffer")	8.4 ± 0.6	8.4 ± 0.3	8.4 ± 0.3
1.6 ("activated") (HCl)	22.0 ± 1.1	22.0 ± 1.1	23.4 + 0.5

There were no statistically significant differences ($p>0.05$) in the level of drug detected, when the drug loading values using both methods (drug displacement (0.1 M HCl) and solvent extraction (MeOH)) were compared. Together with the rate of loading studies, this is indicative of a weak interaction that cannot be unequivocally attributed to ion-exchange between drug and resin, which is supported by the drug release studies (sections 3.2.1.1.1). In methanol at 20 °C, the experimentally determined solubility value was 0.87 ± 0.05 mg/mL, which is supportive of the solvent being an effective extraction agent (Table 2.3).

Both the drug displacement and solvent extraction procedures demonstrated that use of the pre-treated resin ("activated") increased the drug loading achieved (to 22 ± 1.1%) when a 1:1 (w/w) D:R ratio was used, with a DAE of 23.4 + 0.5%. This sample was selected for further study, namely an investigation into the time to reach equilibrium and the impact of scale-up of batch size on drug loading and powder yield. Figure 3.2(A) illustrates that the batch size does not have a significant influence on the drug loading or powder yield over the range of values studied. The results from the study investigating drug binding kinetics are illustrated in Figure 3.2(B). The rate of loading studies indicates that the complexation was completed rapidly, and that contact time between drug species and IER does not play a major role in the interaction.

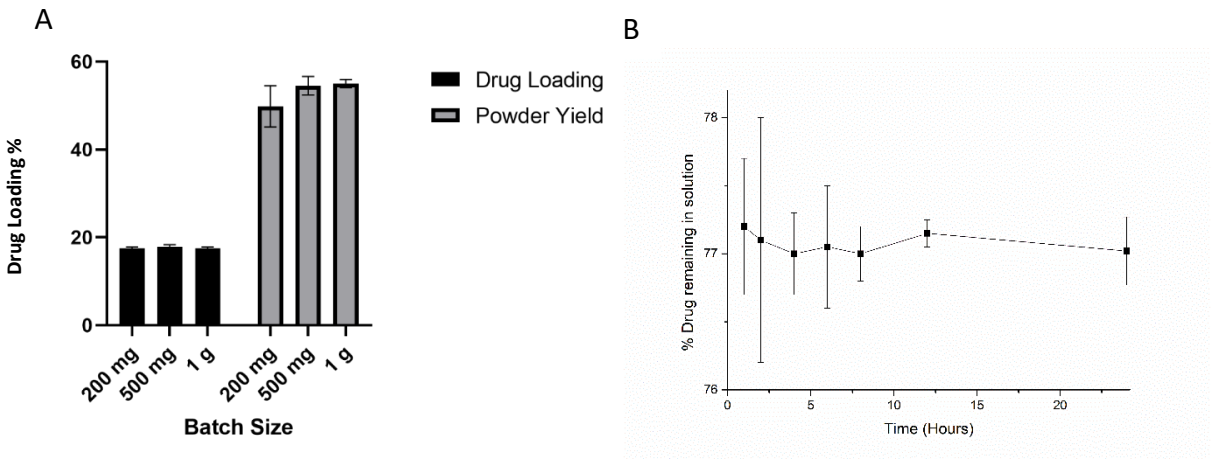

Figure 3.2. (A) Comparison of the drug loading (%) and powder yield (%) figures for the scaled-up resinates formed using a 1:1 D:R ratio (w/w) (using "activated" resin and by adjusting the pH of drug loading solution adjusted to pH 1.6 using 0.1 M HCl prior to the addition of IRP69). (B) Equilibration profile showing the loading of MTZ onto IRP69 (1:1 D:R (w/w) ratio) over 24 hours at room temperature (using "activated" resin and drug loading solution adjusted to pH 1.6 using 0.1 M HCl prior to the addition of resin).

MTZ is a drug that, in theory, should exhibit the desired ion-exchange behaviour. Many factors have been postulated as to why certain drugs do not form robust complexes with IERs. The loading of the drug depends on its molecular size, the charge intensity of both it and the resin, along with the loading conditions (110). The inherent selectivity of sulfonic acid exchange groups for the drug is another factor, as is the choice of solvent. The relatively poor drug loading levels achieved using MTZ with this class of IER, and the relatively high dose that needs to be administered to the patient, are two factors that point to the need to explore alternative methods for the production of the desired age-appropriate formulation.

3.2.1.1.1 Drug release studies (IRP69)

Figure 3.3 shows the drug release profiles of DRCs prepared using unprocessed resin and MTZ (1:1 w/w) at different loading pHs in 0.1 M HCl and DI H_2O at 37 °C. In addition, the 1:1 system formed using "activated" resin was also studied to examine the impact of pre-treating resin on drug release behaviour. Evident from the release profiles is the burst effect exhibited. All samples studied exhibit rapid release kinetics in 0.1 M HCl, characterised by 97-99% drug release after 5 minutes and essentially complete drug release after 20 minutes. With respect to the drug release behaviour in DI H_2O, the DRCs exhibit different behaviour relative to their performance in acidic media, however, the % drug release, which ranges from 62-85% still remains undesirably high. In contrast to what was observed in acidic media, marked differences in the release profiles are apparent, although all systems reach equilibrium, as signified by the levelling out of the release profiles. The % drug release from the resinate formed using "activated" resin was the lowest (65%), whereas the pH 0.6 system released 85% of the loaded drug in the aqueous environment. The two systems prepared with pH 1.6 loading solutions released approximately 77.5% of the drug in DI H_2O at equilibrium. This trend highlights a possible relationship between drug loading and drug leaching/release, as the resinate with the lowest loading had the highest leaching value in DI H_2O, whereas the resinate with the highest loading, released the lowest quantity of drug in the aqueous environment. Despite the "activated" resin exhibiting a superior performance relative to the other systems studied, the level of drug leaching (in DI H_20) detected remained unsatisfactory.

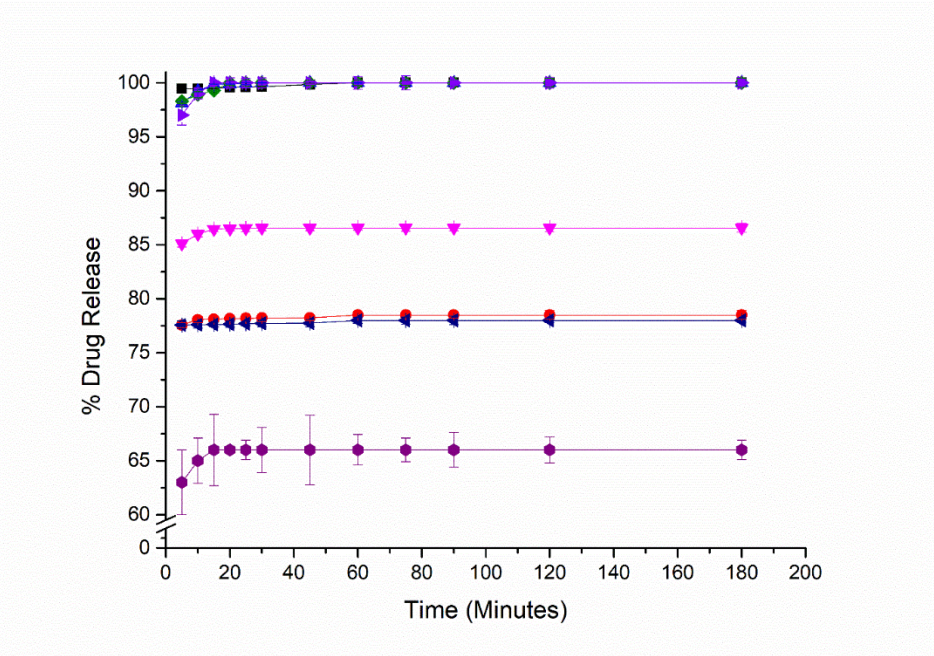

Figure 3.*3. Drug (MTZ) release studies conducted at 37 °C in either 0.1 M HCl or DI H_2O using resinates produced using a 1:1 (w/w) ratio of MTZ and IRP69 ("unactivated" unless otherwise stated) and by altering the pH of the drug loading media prior to the addition of resin as per the procedure reported in Chapter 2, section 2.2.1.2.1. Resinate (KCl and HCl-pH 1.6) in 0.1 M HCl (Black square), resinate (KCl and HCl-pH 1.6) in DI H_20 (Red circle), resinate (0.1 M HCl-pH 1.6) in 0.1 M HCl (Blue triangle), resinate (0.1 M HCl-pH 1.6) in DI H_20 (Magenta inverted triangle), resinate (pH 0.6) in 0.1 M HCl (Olive diamond), resinate (pH 0.6) in DI H_20 (Navy triangle), resinate ("activated" (pH 1.6) in 0.1 M HCl (Violet triangle) and resinate ("activated") (pH 1.6) in DI H_20 (Purple circle).*

To further elucidate the possible relationship between drug loading, drug leaching and solubility, dissolution studies were conducted at a second, lower temperature (20 °C) to help understand if the release of loosely adsorbed drug was solely a function of drug solubility (Figure 3.4). Interestingly, each system was characterised by incomplete drug release, which is a common feature of many drug release profiles reported for resinate systems. This plateau in the % drug release value can be attributed to the existence of an equilibrium between the complexed drug and free drug in solution, which prevents further drug from being released during the *in vitro* dissolution studies. Furthermore, each system exhibits markedly different dissolution behaviour in acidic media versus DI H_20, which is more typical of ion-exchange based drug delivery system. Regarding the drug release behaviour in acidic media, the rate of release is rapid prior to equilibrium being attained, with all systems achieving equilibrium after 15 minutes. The impact of the loading conditions, which was apparent in the drug loading studies, was also evident in the drug release profiles. All four DRCs released the drug at different release rates over the first 10 minutes, reflected by % drug release value at each of the first

two timepoints differing from one another ($p<0.05$). The system produced using "unactivated" resin buffered to pH 1.6 (0.1 M HCl), released the drug at the fastest rate, with 90% of the drug being eluted after 5 minutes and equilibrium being attained after 10 minutes. In contrast, the resinate produced using "activated" resin buffered to pH 1.6 using 0.1 M HCl, released drug at the slowest rate, with 73% being released after 5 minutes and equilibrium being attained after 10 minutes, albeit the % drug release at equilibrium is far lower (74% versus 92.5%). The other two systems investigated released the drug at an intermediate rate relative to the two extremes previously discussed above and achieved equilibrium at % drug release values (84% and 86%), which fall between those previously discussed. These results indicate that under the conditions studied, the system with the highest drug loading has the slowest release kinetics. By comparing the dissolution behaviour of all samples at the two temperatures studied, it is apparent that higher % drug release occurs at the elevated temperature, which can be explained on the basis of MTZ's higher solubility in DI H_2O at 37 ° C. The solubility values for the raw MTZ material in 0.1 M HCl and DI H_2O at 37 °C were determined to be 27.69 ± 1.46 mg/mL and 8.58 ± 0.035 mg/mL respectively. At 20 °C, the solubility values were 20.05 ± 1.46 mg/mL and 5.00 ± 0.09 mg/mL respectively (table 2.3). These differences in solubility values translate to differing drug release behaviours for each of the resinate samples studied, the extent to which depends on the particular sample in question, as well the temperature at which the analysis is conducted.

Pre-treatment of the resin (section 2.2.1.2.3 in Chapter 2) and altering the composition of the loading solution (section 2.2.1.2.3 in Chapter 2), to minimise the effect of competing ions did not have a dramatic effect on delaying the release of drug in DI H_20, as is evident from Figure 3.4. Three of the four systems studied did not statistically differ ($p>0.05$) in the % drug release, with the exception being pH 1.6 system. In theory, the rate of drug release from DRCs is dependent on the polymeric and ionic properties of IERs, but the ionic strength of the release/dissolution medium also plays a major role (296). The fact that the concentration of resinate in the release media is so low (50 mg/900 mL) might require the use of a lower ionic strength of HCl to slow the release rate. However, based on what has been observed thus far, this is unlikely to have much of an impact. This is because, when no suitable ions to effect ion-exchange were available in the dissolution medium, i.e. when the medium was DI H_2O, the quantity of drug released was relatively high, in the region of 63-67%, depending on the system. If ion-exchange was evident, release rates should be extremely small in DI H_2O (especially over the early timepoints), because the ionic bonds between MTZ and the resin, should be robust enough to provide a temporary release delay in DI H_20. Depending on the resin, 20% drug release has been reported in the literature when the liberation of the drug wasn't expected (297). This illustrates that leaching is not a rare phenomenon, but more so, the extent of it in this instance, is an indication that the resin and/or drug were not suitable for the intention of the formulation (298).

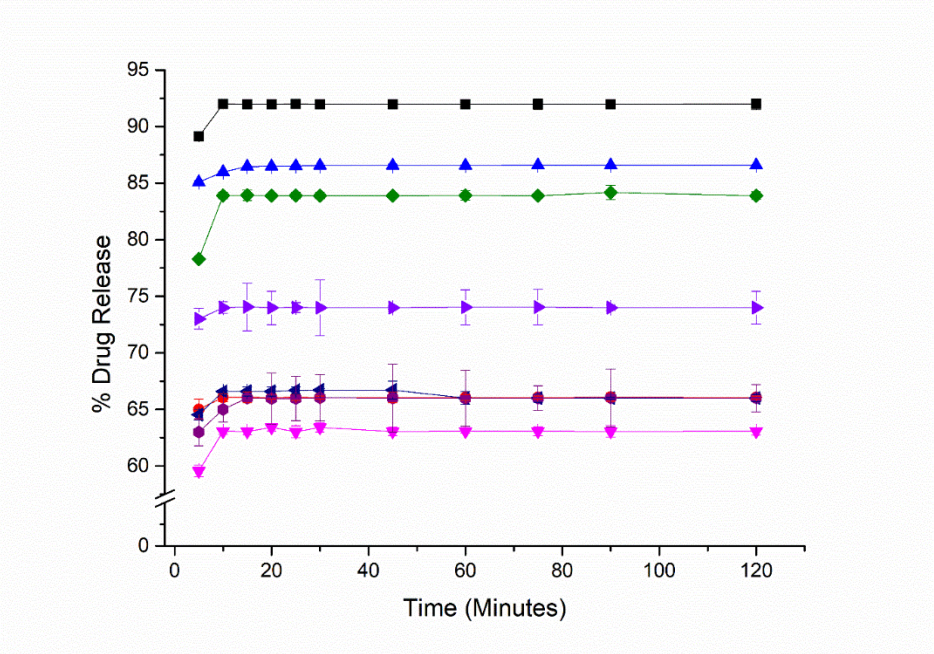

Figure 3.*4. Drug (MTZ) release studies conducted at 20 °C in either 0.1 M HCl or DI H_2O using resinates produced using a 1:1 (w/w) ratio of MTZ and IRP69 ("unactivated" unless otherwise stated) and by altering the pH of the drug loading media prior to the addition of resin as per the procedure reported in Chapter 2, section 2.2.1.2.3. Resinate (KCl and HCl-pH 1.6) in 0.1 M HCl (Black square), resinate (KCl and HCl-pH 1.6) in DI H_20 (Red circle), resinate (0.1 M HCl-pH 1.6) in 0.1 M HCl (Blue triangle), resinate (0.1 M HCl-pH 1.6) in DI H_20 (Magenta inverted triangle), resinate (pH 0.6) in 0.1 M HCl (Olive diamond), resinate (pH 0.6) in DI H_20 (Navy triangle), resinate ("activated")(pH 1.6) in 0.1 M HCl (Violet triangle) and resinate ("activated")(pH 1.6) in DI H_20 (Purple circle).*

3.2.2 Tizanidine HCl (TZD HCl)

3.2.2.1 Production of drug-resin complexes (DRCs) with Amberlite™ IRP69 (IRP69)

As stated previously, the primary aim of this work was to achieve a satisfactory level of drug loading in the DRCs. TZD HCl is a weakly basic and ionisable drug that would be expected to have an affinity for IRP69, as it has a reported pKa of 7.4 (259). Furthermore, it is a structurally related derivative of clonidine, which has a pKa of 8 and has been successfully formulated as an ion-exchange based product (261). From a structural perspective (depicted in Figure 1.14 in Chapter 1), it contains a secondary amine, which is reported to be more favourable compared to primary amines for the ion-exchange process, as it has a higher selectivity coefficient. The influence of the amine moiety has been discussed by Jeong et al. (110). Results from the TZD HCl loading studies were more in line with those typically reported in the literature. This can be attributed to the fact that the pH of a 1% w/v solution is 4.4 (the highest concentration of drug used in the studies), which is a sufficient number of pH units away from the pKa to ensure maximal ionisation. These favourable dissociation characteristics mean

that no pH adjustment of the loading solution is required, which avoids the issue of competing ions supplied by the buffer species. As illustrated in Table 3.2, a combination of high values for powder yield, drug association efficiency (DAE) and drug loading indicates that the drug-resin complex was successfully prepared using the batch process. Therefore, it can be surmised that post-addition of the resin to the drug solution, the dissolved drug, in its protonated form, exchanged with the counterion on the resin (sodium) via an ion-exchange reaction, forming the DRC. The drug loading achieved was almost 50% w/w using a 1:1 ratio (w/w). This loading figure can be attributed to the drug being ionised (approximately 99.99%) when dissolved in water and no buffering system being required. Evidence of the use of buffering systems can be found in the literature (293) and they can have a detrimental effect on drug loading due to the competition created for ionic sites on the resin through the introduction of buffering species, as witnessed with the MTZ-IRP69 system.

Furthermore, powder yields obtained for the various DRCs were far more encouraging than those obtained with MTZ, as shown in Table 3.2. These powder yields, in conjunction with the other data listed in Table 3.2, indicate that far more drug is bound to the resin than was seen with MTZ, and this is supported by lower amounts of drug being detected in the filtrate, reflected by an increase in DAE value. The influence of the batch size on the powder yield (%) values for DRC formed using a 1:1 D:R ratio (w/w) was assessed (Table 3 in Appendix 1) and it was found that statistically higher ($p<0.05$) powder yield (%) values were obtained the higher the quantity of starting materials for the majority of samples studied.

Table 3.2 illustrates the impact of the drug:resin ratio on the drug loading. When loading a drug onto an ion-exchange resin, many aspects need to be considered, aside from the drug loading value achieved. One parameter that warrants attention is the DAE, as the higher the amount of drug available, the more likely drug wastage will occur once the resin binding sites are saturated. This trade-off is illustrated nicely in Figure 3.5(A-B). These findings highlight the need to carefully examine a variety of different ratios to determine the optimal drug:resin ratio, which maximises drug loading, whilst minimising the quantity of unreacted drug that amounts to drug wastage. It is important to note that the drug displacement assay was used to calculate drug loading values. This is the favoured approach (117,131) compared to the more indirect method that compares the quantity of drug in the filtrate versus the starting quantity, which has been reported by several other groups within the field (96). In the case of TZD DRCs, the results of both types of assay corroborated one another after the optimisation of the assay method (described in Chapter 2, section 3.2.2.1.1). As shown in Figure 3.5(B), when the proportion of resin in the complex increases, the % of TZD detected in the filtrate decreases, therefore increasing the DAE. This is confirmed by the drug loading results shown in Table 3.2, which indicated that optimum complexation occurs at lower D:R

ratios. The opposite was observed for higher ratios of drug to resin, where not as much drug is retained on the resin.

Table 3.*2. Comparison of the effect of different D:R (using "unactivated" IRP69) ratios (w/w) on the calculated powder yield (%), DAE (%) and the drug loading (% w/w). The methods for calculating drug loadings (% w/w) and DAE (%) are described in Chapter 2, section 2.2.11.1.*

D:R ratio (w/w)	Powder yield (%)	DAE (%)	Drug loading on DRC (% w/w)
3:1	41.8 ± 0.8	27.6 ± 1.2	48.0 ± 0.5
2:1	55.7 ± 1.0	41.0 ± 1.0	48.2 ± 0.9
1:1	83.5 ± 1.5	89.0 ± 0.6	48.3 ± 0.9
1:2	90.0 ± 0.9	100.0 ± 0.1	24.4 ± 0.4
1:3	93.0 ± 1.2	100.0 ± 0.1	12.0 ± 0.1

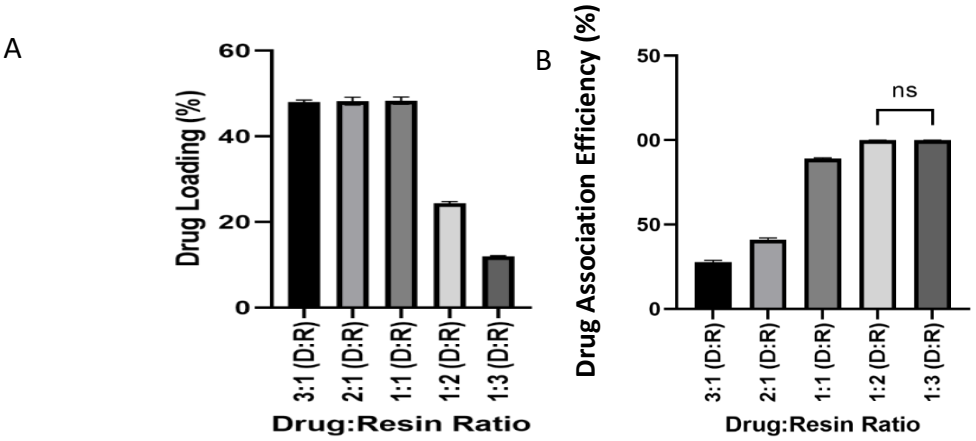

Figure 3.*5. Comparison of the effect of different D:R ratios (% w/w) (using "unactivated" IRP69) on (A) the drug loading (% w/w) of the resultant DRCs prepared and (B) the drug association efficiency (DAE) %.*

3.2.2.1.1 Optimisation of drug loading assay (IRP69)

The method for assaying the drug content of DRCs varies throughout the literature, perhaps reflective of the individual nature of the equilibrium process that characterises the complexation between drug and resin. As part of this work, initial trials used relatively concentrated suspensions of resin in 0.1 M HCl for drug displacement, similar to what has been reported by other groups within the field (117). Chickukwa et al. used more dilute solutions of acid and reported few issues in terms of accurately determining drug content (299), whereas Ichikawa et al. used a 2 M potassium chloride solution to displace the diclofenac off the resin and similarly reported little problem from a drug displacement standpoint (131). However, in the case of the TZD-IRP69 systems, a simple comparison of the drug

loading and preliminary dissolution data (discussed later), revealed that the entire quantity of drug had not been displaced off the resin using the method employed (which involved the use of lower volumes of displacement media (100 mL of 0.1 M HCl). Therefore, the starting assay method had to be amended, due to the system having a high equilibrium constant or selectivity constant, meaning the drug has a higher affinity for the resin phase over the solution phase (300). This parameter is often used to describe the distribution of ions between the two phases and is a function of the intrinsic properties of both the drug and the resin (95,279). However the value of the equilibrium constant can change depending on the conditions used to calculate the parameter, exemplified by the work of Deng et al. who found that an increase in the reaction temperature reduced the value (279). After preliminary investigations, the time selected for the assay test was fixed at 24 hours to ensure that the maximum quantity of drug had been displaced off the resin. It was found during these trials that once the exposure time approached 12 hours, the level of drug displacement only marginally increased from that timepoint onwards, indicating that the system is very close to equilibrium at the 12 hour mark. The protracted period of time required to displace the maximum quantity of drug from the resin is indicative of the strength of the interaction between the secondary amine and resin. Furthermore, analysis of the powder cake post-processing, revealed that consistent drug loading values, reflected by the narrow standard deviation (Table 3.2), could be obtained irrespective of the sampling location, indicative of acceptable content uniformity.

Optimisation of the drug loading assay conditions was performed in accordance with scarce information found in the literature and the factors that were selected to study are listed in Table 4 in Appendix 1, which formed the factorial design study conducted (Chapter 2, section 2.2.11.1.2.2.1). These factors are well known to impact the drug-resin equilibrium and were carefully selected to maximise the likelihood of successfully optimising the assay procedure. A graphical representation of the design space can be found in Appendix 1 (Figure 1). Analysis of Figure 3.6 reveals a correlation between the concentration of complex suspended in the displacement medium (HCl) and the level of drug loading detected, at all temperatures studied. The lower the concentration of complex in the medium, the higher the drug loading calculated. At lower concentrations of complex, there is an excess of competing co-ions i.e. those with the same charge as protonated TZD, which is a driving force towards drug desorption from the DRC, in the context of the equilibrium. Regarding the DRCs assayed using HCl as a displacement agent, by varying the ionic strength of the displacement medium, marginal differences in the level of drug detected are evident at 37 °C with no difference apparent at 20 °C and 50 °C. The effect of ionic strength on the determined drug loading is not as pronounced as DRC concentration. In relation to the NaCl displacement medium (Figure 3.7), the assay results follow the same trend, which can be summarised as more concentrated elution medium yielding lower drug

loadings results and the elution temperature/ionic strength of the elution medium not being major contributing factors to the quantity of drug detected. The major conclusion that can be drawn from this trial is the predominant influence that the DRC concentration in the displacement medium exerts on the calculated % drug loadings, especially when compared to the influence of ionic strength. The higher % drug loadings which were detected when the former is altered suggests that the interplay between the proportion of water in the system and the quantity of ions are linked to the ability of the resin to hydrate. This may enable ions trapped deep within the interior to be released, which may not be liberated into the displacement medium when higher ionic strengths are used, despite the overall quantity of ions in the system being similar.

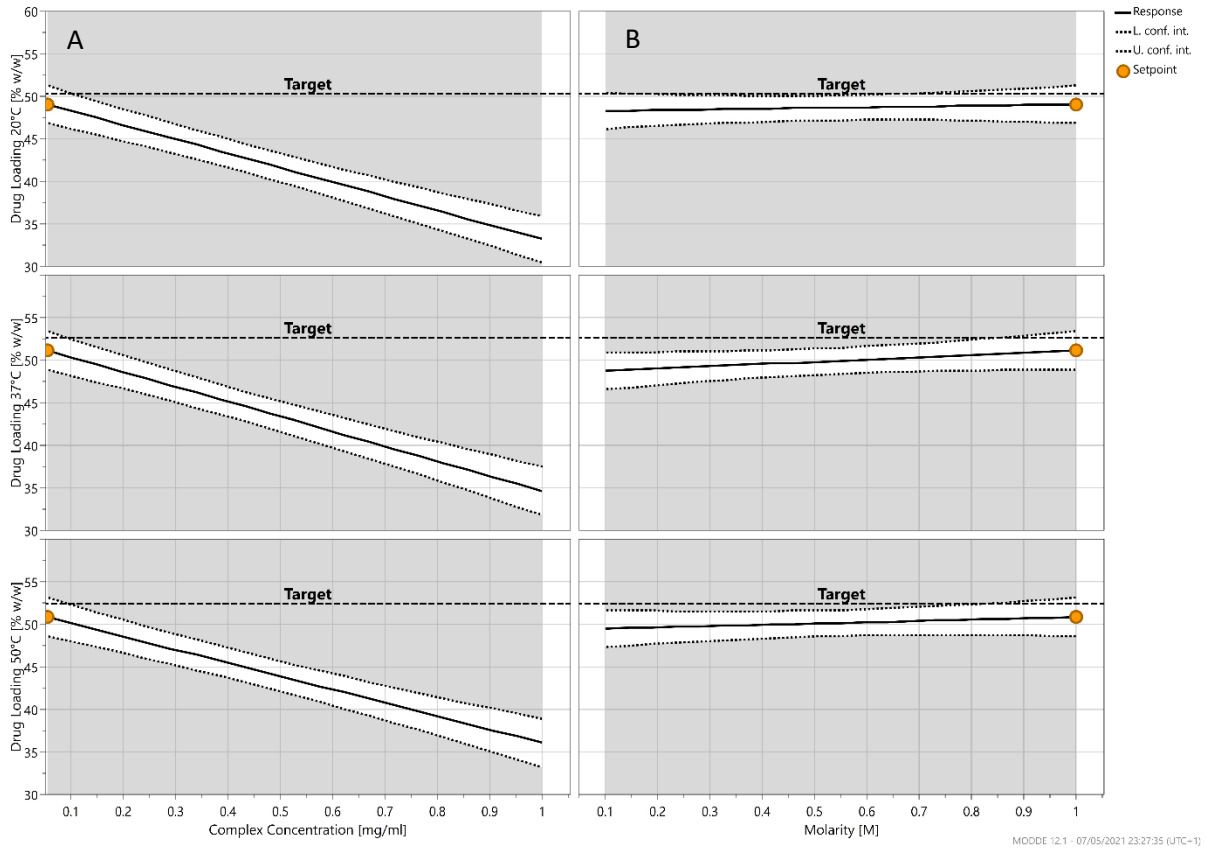

Figure 3.*6. Plot of drug loading (% w/w) versus (A) Complex concentration (IRP69) (mg/mL) and (B) Molarity (M) at 20 °C, 37 °C and 50 °C when altering the elution medium temperature (20 °C, 37 °C and 50 °C) which here comprises of HCl.*

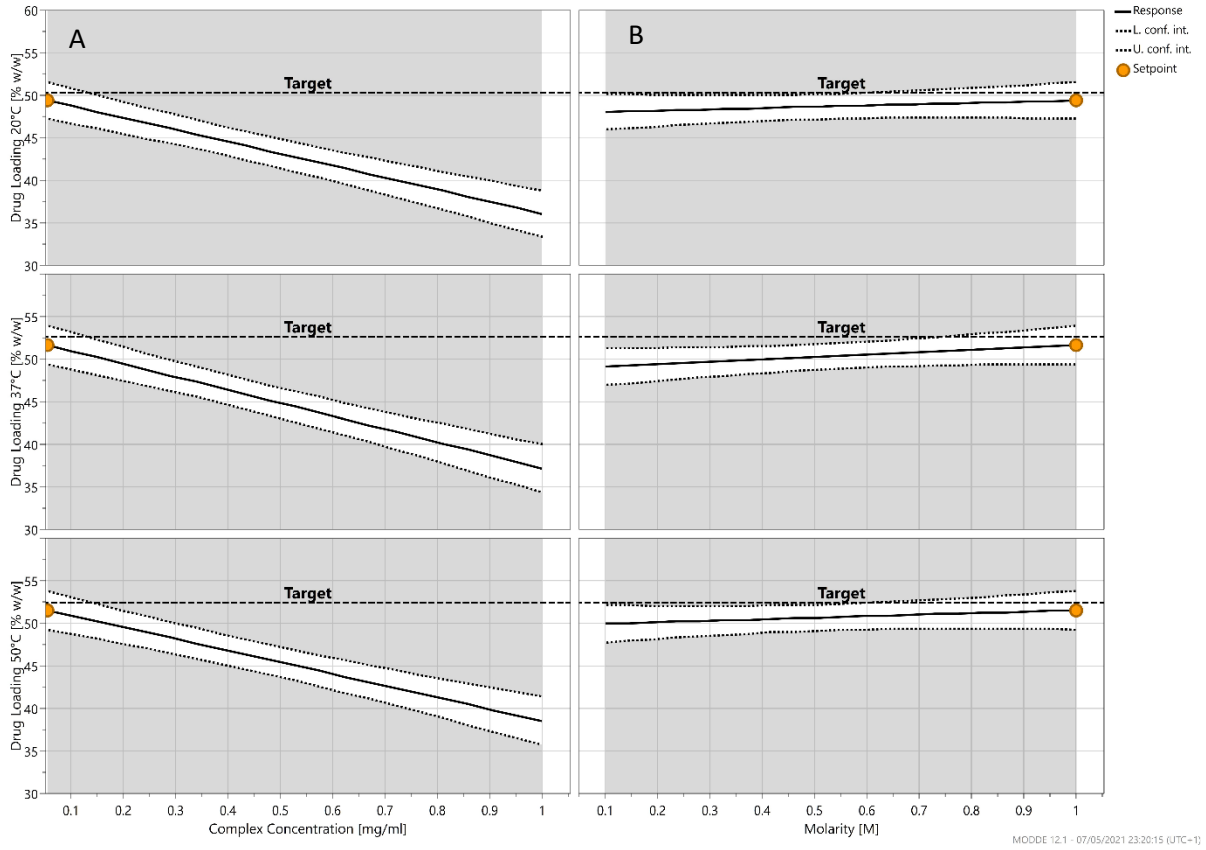

Figure 3.*7. Plot of drug loading (% w/w) versus (A) Complex (IRP69) concentration (mg/mL) and (B) Molarity (M) when altering the elution medium temperature (20 °C, 37 °C and 50 °C) which here comprises of NaCl.*

After identifying that lower DRC suspension concentrations result in an increased quantity of eluting cations per unit weight of DRC, due to a shift in the equilibrium, the optimised method was selected (0.1 M HCl, 20 °C and 100 mg/900 mL). This was subsequently used in further studies that focused on evaluating the impact of various changes to the loading process, ranging from process to formulation factors on the calculated drug loadings. As it can be difficult to elute the drug off the resin in its entirety, a sample was selected post-elution for further analysis using a sequential slurry method (Chapter 2, section 2.2.11.1.2.2.1). No drug could be detected which served to validate the method and ensure that as close to the maximum quantity of drug could be assayed using this optimised method. This approach can be used when a drug has a high affinity for the resin and requires fresh displacing medium to approach near-complete displacement (95).

3.2.2.1.2 Investigations into the factors that influence the drug loading process (IPR69)

A variety of factors dictate the quantity of drug-loaded onto the resin, several of which cannot be controlled and are unique to the specific resin and drug selected. These relate mainly to the affinity that the drug has for the resin and the selectivity that the resin has for the drug. Other factors that

are known to influence the process and can be studied are (1) the concentration of the drug in the loading solution, (2) particle size of the resin, (3) swelling of resin and (4) temperature of the loading solution.

The first factor explored was the incorporation of a pre-swelling step. On occasion, the resin can be subjected to this step prior to the introduction of a drug solution, as part of an effort to hydrate the resin before loading, which can have an impact on the loading process, as reported by the manufacturers (301). However, this measure did not result in increased drug loading ($p>0.05$) relative to the DRCs produced without a pre-swelling step (Table 3.3). A possible explanation for this observation is that the resin has sufficient time to hydrate during the standard DRC formation by the batch method. Furthermore, no statistical difference ($p>0.05$) could be observed in the assay test between the two displacement media used, providing confidence that the calculated drug loading represents the true value.

Table 3.*3. Drug loadings for DRCs prepared using pre-swollen IRP69 resin (24 hours in 100 mL DI H_2O) and different D:R ratios (w/w). Drug loadings were calculated using the drug displacement assay method described in Chapter 2, section 2.2.11.1. The drug concentration in the loading solution used in all cases was 10 mg/mL. The influence of the displacement medium composition was also assessed using 0.1 M NaCl and 0.1 M HCl as part of the drug displacement assay procedure described in Chapter 2, section 2.2.11.1.*

	Drug loading on the DRC (% w/w)	
D:R ratio (w/w)	0.1 M NaCl	0.1 M HCl
2:1	48.22 ± 0.89	47.43 ± 1.45
1:1	48.34 ± 0.91	47.45 ± 1.85
1:2	24.39 ± 0.36	24.59 ± 0.49

The influence of the concentration of drug in solution on the extent of drug loading was the next factor investigated (saturated solution concentration was previously established to be 13.42 mg/mL at 20 °C), using a range of different drug concentrations in an aqueous solution (Table 3.4). Again, no statistical difference ($p>0.05$) was found between the samples prepared, which is in agreement with the findings of Deng et al. (279). Relative to the DRCs produced using the "unactivated"material (IRP69), the difference in drug loading was statistically insignificant ($p>0.05$), as were the calculated drug loading values determined using the acidic and salt solutions. Although drug concentration had no impact on the level of drug loading achieved, a practical benefit of using the higher concentrations of the drug, is the ability to produce larger batch sizes without compromising drug loading. This is

particularly beneficial considering the time-consuming multi-step process required to produce DRCs, which includes drying to remove the majority of moisture in the systems.

Table 3.*4. Drug loadings for DRCs prepared using different concentrations of drug in the loading solution. A 1:1 D:R ratio (w/w) ("unactivated" IRP69) was used in all instances.*

Concentration of drug in the loading solution (mg/mL)	pH of drug loading solution	Drug loading on DRC (% w/w)	
		0.1 M NaCl	0.1 M HCl
1	4.90 ± 0.02	48.17 ± 0.94	49.81 ± 1.97
5	4.60 ± 0.01	48.14 ± 0.96	47.44 ± 0.94
10	4.40 ± 0.01	48.39 ± 0.81	47.54 ± 0.99

The third factor explored, related to the impact of the particle size of the resin material on the DRC drug loadings. The milling procedure employed successfully reduced ($p<0.05$) the particle size of the resin (Table 3.5). The specific surface area (SSA) values, as measured by BET analysis, are also shown and indicate that the SSA for the milled material is higher ($p<0.05$) than the unmilled material, consistent with the decrease in particle size.

Table 3.*5. Comparison of* d_{50} *and SSA values for milled and unmilled IRP69.*

Sample	d_{50} (µm)	SSA (m^2/g)
Unmilled IRP69	52.67 ± 1.05	0.29 ± 0.01
Milled IRP69	20.70 ± 1.47	0.32 ± 0.01

Three D:R (w/w) ratios 2:1, 1:1 and 1:2 were selected to study, covering a range of drug loadings. Table 3.6 shows that the extent of drug loading remained unaffected by a change in resin particle size ($p<0.05$). In contrast, the time to equilibrium did change with particle size (Figure 3.8). It is generally accepted that smaller particles with a finer particle size have a larger specific surface area, which is conducive to a faster reaction rate. Similar to the DRCs produced using unmilled resin material, the highest drug loading was obtained with the 1:1 and 2:1 ratios, which did not differ in the loading values ($p>0.05$). Predictably, the 1:2 ratio produced a DRC with a substantially lower level of drug loaded due to the dilution effect of the excess resin. Similar to the majority of the loading studies conducted thus far, the calculated values for all three ratios studied, using either displacement medium, were not statistically different from each other ($p>0.05$), nor were they were different from the DRCs produced using unmilled resin raw material ($p>0.05$).

Table 3.6. Drug loadings for DRCs prepared using milled IRP69 ("unactivated") and using the different D:R ratios (w/w). Drug loadings were calculated using the drug displacement assay method described in Chapter 2, section 2.2.11.1. The drug concentration in the loading solution used in all cases was 10 mg/mL.

	Drug loading on DRC (% w/w)	
D:R ratio (w/w)	0.1 M NaCl	0.1 M HCl
2:1	48.22 ± 0.89	48.91 ± 1.90
1:1	48.34 ± 0.91	48.87 ± 0.40
1:2	24.39 ± 0.36	24.28 ± 0.49
1:3	12.21 ± 0.43	12.4 ± 0.21

The equilibration times for selected drug resin ratios (2:1, 1:1 and 1:2 (w/w)) which covered a range of drug loadings were investigated, as shown in Figure 3.8. The impact of particle size on the equilibration rate was assessed using these same selected ratios. The 2:1 ratio requires the shortest time (10 hours) to reach equilibrium relative to the 1:1 and 1:2 ratios, which take approximately 12 hours. At all timepoints studied, the % drug remaining in solution is lower for the 1:2 system relative to the 1:1 and 2:1 ratios. Similarly, the 1:1 and 2:1 ratios exhibit different loading kinetics after the 2 hour timepoint, before which there is no statistical difference ($p>0.05$) in % drug remaining in solution, indicating that loading kinetics show a dependence on the proportion of each component (API and resin) in the system within the loading medium despite there being no statistical difference in the % drug loaded when the final product is assayed. In the case of the 2:1 ratio, the % drug remaining in solution plateaus at approximately the 60% mark, signifying that the drug is in excess relative to the resin, as all binding sites are occupied.

When the ratio of the components is altered, so that the drug is no longer in excess relative to the resin, as is the case with the 1:1 and 1:2 ratios, the % drug remaining in solution dramatically reduces to 10% and 0% respectively, signifying that this approach is much more suitable from an economic standpoint. A limited number of binding sites in the 2:1 sample is the likely reason for the high % of drug remaining in solution, whereas in the 1:1 and 1:2 samples, there is an increased availability of binding sites relative to the drug concentration, meaning that the majority of drug that is dissociated in solution has the opportunity to bind to the resin. This competition is further decreased for the binding sites in the 1:2 ratio relative to the 1:1 ratio, as the proportion of the drug in the system is increased, reflected by the faster rate of binding.

It is also apparent that the use of milled resin has a significant impact on the loading kinetics, as the majority of samples prepared using resin raw material with a reduced particle size reach equilibrium quicker relative to the systems produced using unmilled resin. This is exemplified by the 2:1 and 1:1

ratios, whereas the 1:2 systems display contrasting behaviour as they both reach equilibrium at approximately the same time (10 hours) regardless of the particle size of the starting material. In contrast, the other two systems exhibit markedly different loading kinetics, as the time to equilibrium is reduced from 10 to 3 hours for the 2:1 system and 12 to 8 hours for the 1:1 system. This can likely be attributed to the increased surface area of the milled resin (Table 3.7) which can expose potential binding sites, making them more freely accessible. As there is an excess of the drug in the 2:1 sample, the intense competition between drug ions, coupled with the increased accessibility of the binding sites appears to drive the rate of binding up. A similar phenomenon can be observed with the 1:1 system, although the effect is not as dramatic, suggestive of the lower drug concentration in solution playing a role. In the case of the 1:2 system, although statistical differences ($p<0.05$) can be seen at earlier timepoints, the abundance of binding sites remains the predominant feature that dictates drug-resin binding, so the effect of reducing particle size does not translate to a reduced time to equilibrium.

Figure 3.9 displays the effect of temperature on the loading kinetics. It is evident that the IER process can be accelerated when higher temperatures are utilised due to increased molecular motion (302). Temperature is known to have a profound effect on many complexation processes (303), and the effect of this variable is apparent in the data presented and may be attributed to the rate of diffusion being enhanced relative to ambient temperature, again reducing the time to equilibrium, as the exchange rate is increased.

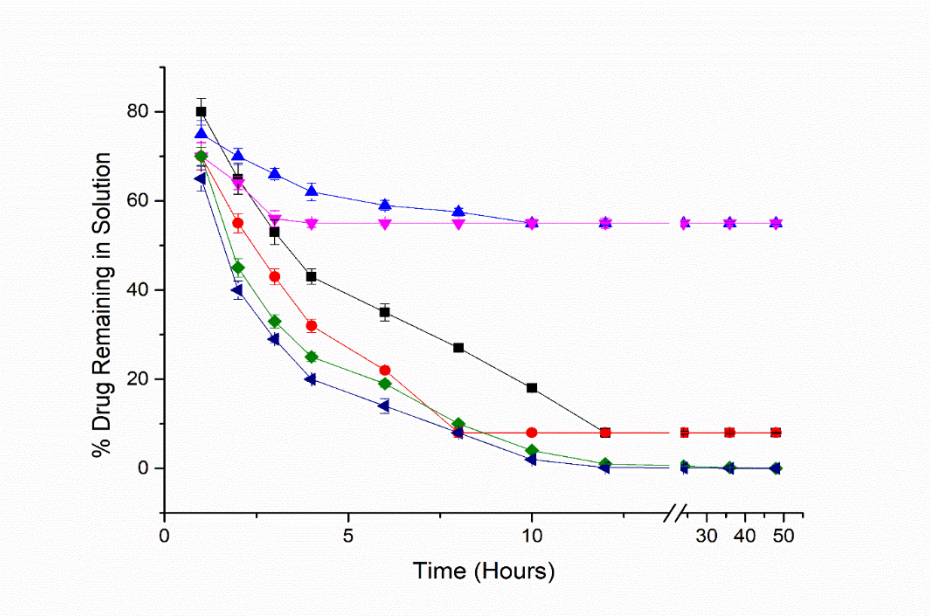

Figure 3.8. Equilibration profile showing the loading of TZD HCl onto IRP69 using different D:R ratios (w/w) (milled or unmilled "unactivated" resin) over 48 hours at a loading temperature of 20 °C). DRC (2:1)(unmilled)(Blue triangle), DRC (2:1)(milled)(Magenta inverted triangle), DRC (1:1)(unmilled)(Black square), DRC (1:1)(milled)(Red circle), DRC (1:2)(unmilled)(Olive diamond) and DRC (1:2)(milled)(Navy triangle).

Surface area results for selected systems are listed in Table 3.7. No statistical difference ($p>0.05$) in surface area values was reported for the powdered form (IRP69) between the resin raw material and drug-loaded DRC. However, an increase in surface area is evident for the milled resin raw material, consistent with the particle size data generated, which indicated that the milling operation was successful at reducing the particle size.

Table 3.7. Comparison of d_{50} and specific surface area (SSA) values for the DRCs produced using varying ratios of milled and unmilled IRP69 and different D:R (w/w) ratios using "unactivated" resin. The particle size and SSA were measured according to the methods described in sections 2.2.7.1.2 and 2.2.14 in Chapter 2 respectively.

D:R ratio (w/w)	SSA (unmilled) (m^2/g)	SSA (milled) (m^2/g)	d_{50} (unmilled) (µm)	d_{50} (milled) (µm)
2:1	0.29 ± 0.01	0.32 ± 0.01	66.33 ± 2.02	24.13 ± 0.94
1:1	0.29 ± 0.01	0.32 ± 0.01	66.56 ± 1.89	24.55 ± 0.43
1:2	0.26 ± 0.01	0.31 ± 0.01	71.10 ± 1.06	25.10 ± 0.76

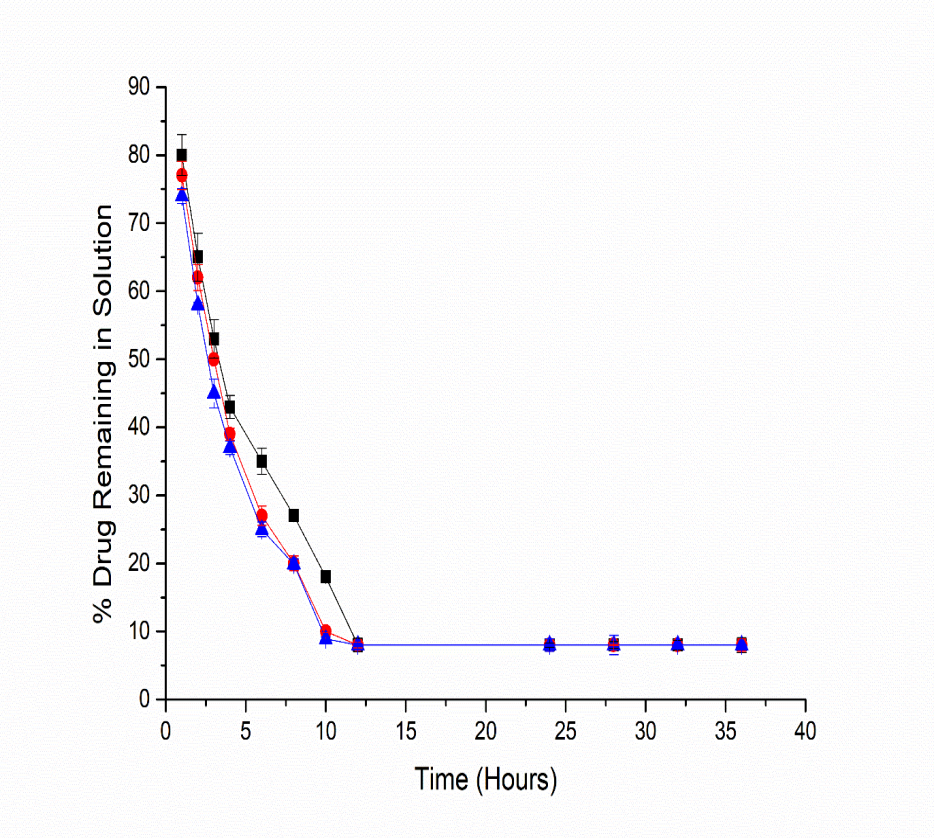

Figure 3.*9. Equilibration profile showing the loading of TZD HCl onto IRP69 (1:1 D:R (w/w) ratio) ("unactivated" resin) over 36 hours at three different loading temperatures. 20 °C (Black square), 40 °C (Red circle), and 50 °C (Blue triangle).*

When analysing the drug loading kinetics associated with IERs, the structure of the polymeric matrix is worthy of consideration. IRP69 has a reported crosslinking level of 8%, which is at the upper end of the reported crosslinking values for resins used for drug delivery purposes (110) and resins with differing degrees of crosslinking have been shown to exhibit varying influences on the kinetics of the loading process (97). The chemical structure has also been demonstrated to have a meaningful impact on the extent of drug loading. Certain drugs show slow and incomplete loading, whereas others exhibit rapid equilibration and near-complete loading efficiency. On the basis of the work initially reported by Borodkin et al., the secondary amine group in the TZD HCl structure, which is implicated in the ion-exchange reaction, is thought to be responsible for the relatively low rate of exchange (142). This is supported by the evidence presented in Pongjanyakul et al.'s paper where they rationalise their own findings through reference to the API's chemical structure, whereby the secondary amine group in the dextromethorphan shows a reduced affinity compared to the tertiary amine in propranolol, reflected by a lower selectivity coefficient for the former (109). It is generally accepted that although drugs containing secondary amine moieties have lower selectivity coefficients relative to tertiary amines,

they are more favourable compared to primary or quaternary groups, meaning that TZD HCl is still considered a favourable candidate for the IER-based formulation approach.

Table 3.8 summarises the results obtained in the preparation of the DRCs by the batch process using different contact times. From these results, it is evident that a 6 hour contact time between drug and resin is insufficient to ensure optimal loading, as equilibrium has not been reached, leading to the quantity of the drug being loaded onto the resin not being maximised. Based on the drug loading values, a contact time of 12 hours is sufficient for maximal loading to be achieved as the drug loading achieved after 24 hours is not statistically significantly different ($p>0.05$).

Table 3*.8. Drug loadings for DRCs prepared using different contact times (between drug and resin). A 1:1 D:R ratio (w/w) ("unactivated" IRP69) was used in all instances. Drug loadings were calculated using the drug displacement assay method described in Chapter 2, section 2.2.11.1. The influence of the displacement medium composition was also assessed using 0.1 M NaCl and 0.1 M HCl as part of the drug displacement assay procedure described in Chapter 2, section 2.2.11.1.*

	Drug loading (% w/w) on DRC	
Contact time	0.1 M NaCl	0.1 M HCl
6 hours	35.30 ± 0.91	35.19 ± 0.87
12 hours	48.91 ± 0.04	48.39 ± 1.35
24 hours	48.34 ± 0.53	49.81 ± 0.97

Another aspect of the loading process which was explored was the use of multiple loading steps, whereby fresh drug solution is introduced after equilibrium has initially been reached (known as the double-batch method) (detailed in section 2.2.1.2.4.1 in Chapter 2). This process was subsequently repeated (triple-batch loading) and the results are shown in Table 3.9. The drug loading levels achieved using the modified batch methods were statistically insignificantly different to those achieved using the single-stage process ($p>0.05$). However, drastically lower values for the drug association efficiency (DAE) were observed when the double-batch method was employed, which was compounded by the triple-batch step, which only served to further reduce the DAE. The logic behind the utilisation of more the one loading stage is that the by-products from the ionic interaction are removed and replaced by fresh drug solution, thus pushing the equilibrium further to the right, driving drug binding. However, this effect, reported by several groups in the literature was not observed in this work (110), thus highlighting the individuality of the ion-exchange process.

Table 3.9 also illustrates the statistically insignificant impact ($p>0.05$) of reaction temperature on the extent of drug loading which, as highlighted previously, has been shown to impact the reaction kinetics rather than the total quantity of drug bound. Tan et al. reported an increased tendency to ionise at

high temperature, which was used to explain the results they reported using hot melt extrusion as a manufacturing technology (119), but little evidence illustrating the ability of temperature to influence the resin's ionisation behaviour can be found elsewhere and the results reported in Table 3.9 do not support the assertion made by Tan et al.

Table 3.9. Drug loadings and DAE (%) for DRCs prepared using different loading temperatures and number of loading stages. A 1:1 D:R (w/w) ratio (using "unactivated" IRP69 and a 10 mg/mL concentration of drug in solution was used in all instances.

Number of loading stages	Temperature of the loading medium (°C)	DAE (%)	Drug loading on DRC (% w/w)
Single	20	8.09 ± 0.17	49.81 ± 0.97
Single	30	88.89 ± 0.21	48.17 ± 0.94
Single	40	88.91 ± 0.45	48.09 ± 0.44
Double	20	44.67 ± 0.87	48.14 ± 0.84
Triple	20	29.00 ± 0.34	48.18 ± 0.91

Similar to the resin trials conducted with MTZ, the effect of the purification/"activation" step on the resin raw material was trialled to test the effect of resin pre-treatment on the drug loading values (Table 3.10). A variety of methods have been reported in the literature, with the majority aimed at converting the ionic form of the resin (89). In this instance, the process was employed to switch the ionic form of the resin from sodium to hydrogen. This was confirmed by measuring the pH of the eluent. Once the pH of the eluent no longer increased due to the saturation of ionic sites with hydrogen, the process was complete. On this occasion, no statistical difference ($p>0.05$) is evident for the ratios studied when the "activation" step was utilised compared to the use of "unactivated" resins, pointing to the production of by-products in the reaction medium not having a major influence on the level of drug loading achievable.

After it became apparent that ion-exchange has been achieved, further emphasis was placed on understanding the possible ramifications of changing the ionic form of the resin. One benefit of undertaking this step is to control the by-product of the reaction. If the hydrogen form of the resin is used, then the by-product of the ion-exchange reaction between the resin and hydrochloride form of the drug is HCl, which is a gas and doesn't compete with the drug ion for the resin. The sodium form of the resin produces NaCl, as the by-product of the ion-exchange reaction between resin and salt form of the drug. Moreover, Conaghey et al. reported that "activation" of the resin using a pre-treatment procedure helped overcome reproducibility issues encountered during exploratory work (294). In total, when considering the binding of the drug onto the resin, four possible combinations are known, as the resin can exist in either the acid or base form, whilst the drug can be in the free

base form or soluble salt form. In this instance, the free base form is likely to present solubility issues, hence the need for the drug to be presented as the salt form.

Table 3.*10. Drug loadings for DRCs prepared using "activated" IRP69 using the different D:R ratios (w/w).*

	Drug loading on the DRC (% w/w)	
D:R ratio (w/w)	0.1 M NaCl	0.1 M HCl
3:1 ("unactivated")	48.00 ± 0.45	48.00 ± 0.50
2:1 ("unactivated")	48.22 ± 0.89	48.20 ± 0.90
1:1("unactivated")	48.34 ± 0.91	48.30 ± 0.90
1:2 ("unactivated")	24.39 ± 0.36	24.40 ± 0.40
1:3 ("unactivated")	12.00 ± 0.13	12.00 ± 0.10
3:1 ("activated")	48.12 ± 0.95	46.15 ± 1.20
2:1 ("activated")	48.01 ± 1.20	46.98 ± 1.00
1:1 ("activated")	48.14 ± 0.31	46.45 ± 0.80
1:2 ("activated")	24.99 ± 0.96	24.36 ± 0.40
1:3 ("activated")	12.30 ± 0.47	12.56 ± 0.30

3.2.2.1.3 Drug release studies (Unmilled IRP69 material)

The release profiles of the DRCs in compendial dissolution media (0.1 M HCl and pH 6.8 phosphate buffer), DI H_2O and 0.1 M NaCl are presented in Figures 3.10-3.16. Prior to analysis, the stability of the API was established in the dissolution media over a 24 hour time period (Table 5 in Appendix 1). Three distinct types of DRC were selected for testing, which differed in the quantity of drug loaded, as determined in the assay studies. Similar to the evaluation of the drug release behaviour of the MTZ-resinates, initial studies focused on the 1:1 DRC, and dissolution studies were performed in 0.1 M HCl at 37 °C. It is evident from the drug release profile (Figure 3.10), that drug is rapidly displaced from the resin after contact with the medium, with 92% of the drug being released after 5 minutes, with increasing quantities of drug being released until equilibration is reached after 25 minutes. Equilibration, characterised by a plateau in the drug release, on this occasion coincides with complete drug release. An interesting feature, that needs to be considered when evaluating drug release from DRC systems is the likelihood of the equilibrium being reached prior to complete drug release being achieved, as was the case with MTZ resinates that were evaluated in acidic media at 37 °C. This property of DRCs is dependent on a myriad of factors, related to both the dissolution medium and the intrinsic properties of API and resin, which is exemplified by the varying dissolution properties of uncoated DRCs in the literature. Furthermore, the systems studied as part of this work highlight the disparate drug release behaviour of DRCs that have different drug loadings. Interestingly, the drug release profile of the 1:1 system in pH 6.8 buffer is quite similar to that produced in 0.1 M HCl.

Approximately 85% of the drug is released from the DRC after 5 minutes which is lower ($p<0.05$) than the % drug release in acidic medium, indicating that the ions in the phosphate buffer are less efficient ion-exchangers. However, from the 10-minute timepoint onwards, there is no statistical difference ($p>0.05$) in the % drug release at any timepoint, when the release behaviour in either pH medium is compared. Furthermore, drug release proceeded to approximately complete release in both conditions.

The drug release profile of the DRC in 0.1 M NaCl (Figure 3.10) illustrates that the rate of drug release from the DRC was reduced, relative to the release rate of the drug from the DRC in the previous ionic media investigated. The primary reason for selecting a solution of NaCl to study the drug release kinetics was to serve as a comparison to the acidic medium. Following the same premise as the assay trials that also used a comparative approach, this strategy may elucidate differences in the ability of distinct counter ions in solution to displace drug ions, which could translate to a tangible difference in the drug release profile. A consequence of the release rate being curtailed is that complete release from the DRC occurred after 75 minutes, noticeably later than the time required for complete drug release in 0.1 M HCl and pH 6.8 phosphate buffer. Approximately 75% drug release is observed to be released after 5 minutes, indicative of a lower elution efficiency in this medium. The percentage of drug released at each time interval was statistically lower ($p<0.05$) in the NaCl salt solution versus the alternative ionic environments studied, until the 60 minute mark, after which the quantity of drug release did not differ significantly ($p>0.05$) relative to the pH 6.8 environment. Despite the DRC releasing the drug at a slower rate relative to the acidic environment, the system is still capable of releasing the entire quantity of drug from the complex. This may be related to the affinity that the sodium ion has for the resin, as it may not be as effective at displacing the drug ion bound relative to the hydrogen ion in the specific conditions studied, thus yielding slower desorption rates. Several studies have investigated the impact of the eluting ion and have reported varied results. Irrespective of the D:R ratio examined, the greater ability of the hydrogen ion to displace the drug ion from the resin is evident, indicating that the effect of ion type does play a role in the release kinetics.

Figure 3.10 also shows that the extent of release from the DRC in DI H_2O, which contrasted with that seen in ionic media, characterised as approximately 2% drug release occurring after 2 hours. This illustrates the formation of an ionic bond between the two components (API and IER), as opposed to physical adsorption. Although this test may seem rudimentary, many reported studies fail to include evidence of DRC dissolution behaviour in DI H_20, which is a key indicator of DRC robustness. Furthermore, the solubility of the API was determined to be 61 ± 0.29 mg/mL and 43 ± 0.9 mg/mL in 0.1 M HCl and DI H_20 respectively, consistent with that of a highly water-soluble and basic compound and broadly in agreement with the values reported in the literature (257). Although the drug displays

a lower aqueous solubility relative to its corresponding solubility in an acidic medium (0.1 M HCl), the disparity in drug release cannot be attributed to this solubility difference, and instead can be ascribed to a robust ion-exchange process.

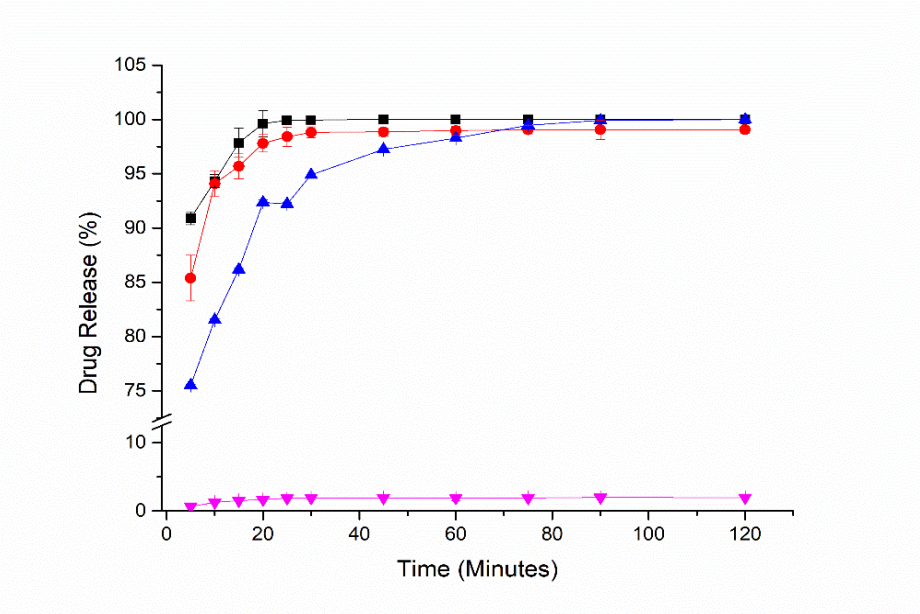

Figure 3.10. Drug (TZD HCl) release profiles in 0.1 M HCl, 0.1 M NaCl, pH 6.8 buffer and DI H_2O at 37 °C, of DRCs formed using 1:1 D:R ("unactivated" IRP69) (w/w) ratio, using the method specified in 2.2.8.2.1. DRC in DI H_2O (Magenta inverted triangle), DRC in 0.1 M NaCl (Blue triangle), DRC in pH 6.8 buffer (Red circle) and DRC in 0.1 M HCl (Black square).

The drug release behaviour from the two other DRCs studied followed a similar pattern to that of the DRC formed using a 1:1 D:R ratio (Figures 3.11-3.12). A lower quantity of the drug was loaded onto the DRCs, which are distinguished based on the ratio of drug to resin (w/w) used in the loading media. As reported in Table 3.2, the 1:2 and 1:3 ratios have drug loading values of 24.4% and 12.02% respectively.

Similar studies found in the literature report conflicting results when evaluating the influence of media composition, specifically counterions, on the release of drug from the resin. Sriwongjanya and Bodmeier reported no difference in release behaviour when several media are trialled (96), whereas Pongjanyakul et al. reported marked differences in the i*n vitro* release in different dissolution conditions (109). The results of this work, and in particular the release behaviour in 0.1 M HCl compared to pH 6.8 buffer, are in agreement with the studies that report that drug release from DRCs is independent of the solution pH.

Furthermore, the impact of ionic strength appears to play a limited role. By comparing the release rates of all three systems (1:1, 1:2 and 1:3) over the early time points in the media with identical ionic

strength (0.1 M HCl versus 0.1 M NaCl), the reduced rate of release in the salt solution indicates that other factors, such as the impact of cation type, can produce significant differences in the release profiles observed. Having said that, throughout the literature, the concentration of cations in the dissolution medium is very often the dominant influencing factor on drug release (145). Higher concentrations are expected to promote an accelerated rate of release, meaning the equilibrium between bound and unbound drug is a pivotal concern regarding release kinetics, rather than drug solubility. However, the increased rate of release in pH 6.8 buffer relative to the 0.1 M NaCl, does not support this assertion, as the concentration of cations in this buffer (140 mEq/900 mL) is reduced relative to the salt solution (229 mEq/900 mL). This reduced quantity of cations does not manifest itself in a lower drug release; instead, the opposite is observed, inferring a multitude of factors are at play. Pongjanyakul et al. argued that a pH effect could be responsible for their findings regarding the release of dextromethorphan in simulated gastric fluid (SGF) and simulated intestinal fluid (SIF), whereby the drug release is higher in SIF compared to SGF, despite the latter having a lower cation concentration. The authors argue that faster release rate in SIF could be a function of pH, as the drug is known to be less ionised at values close to its pKa (109). However, in the current work that is unlikely to be a plausible reason to support the differences observed for release in NaCl and HCl dissolution media. The phosphate buffer has a broadly similar pH value to that of 0.1 M NaCl (pH 7), and yet the drug release profiles in both the acidic medium and pH 6.8 buffer are superimposable, indicating that this is not the cause of the divergent release profile in the salt solution. Furthermore, it is generally accepted that the influence of pH is confined to DRCs formed using “weak resins” in contrast to the sulfonic acid-containing DRCs which are known as pH-independent systems (104,106,121).

Regarding the 1:2 DRC system (Figure 3.11), although the rate is slowed in 0.1 M NaCl, the DRC still reaches a similar equilibrium concentration to that achieved in pH 6.8 buffer and 0.1 M HCl, indicating that there is sufficient time for the DRC to reach equilibrium (90 minutes) and the salt solution does not negatively impact the quantity of drug released. Interestingly, alongside the longer time required to reach equilibrium, the DRC does not achieve complete drug release in any of the media tested. A maximum of 97% drug release is attained which is lower than the complete drug release accomplished using the 1:1 system ($p<0.05$), suggestive of the excess resin adversely affecting the chances of this particular system releasing the full drug loading. Regarding the drug release in DI H_2O, a large difference in the quantity of drug released compared to that observed in ionic media is noticeable, as minimal drug leaching is evident for the systems containing lower drug loads.

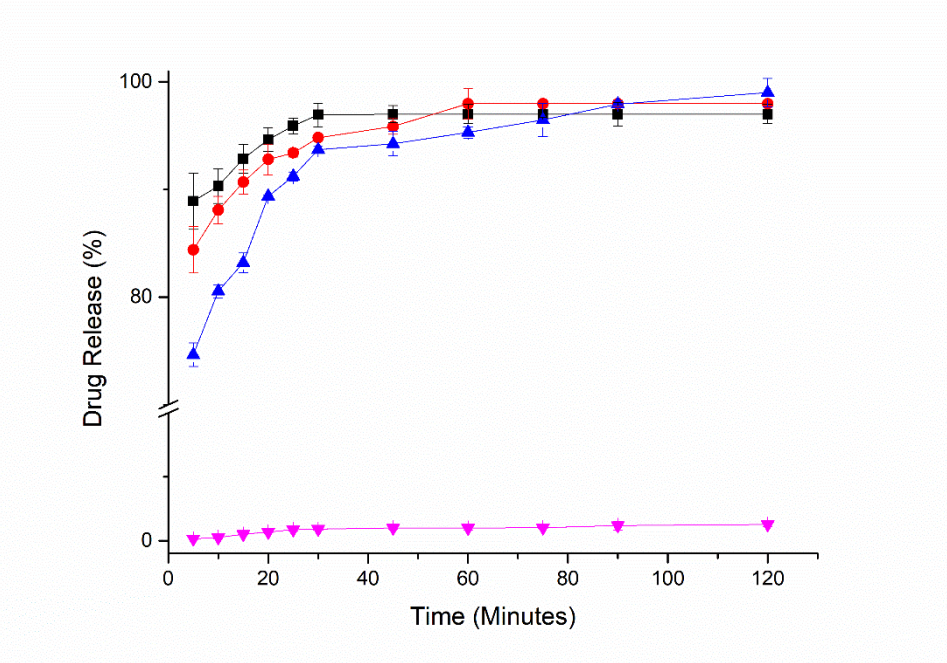

Figure 3.*11. Drug release profiles in 0.1 M HCl, 0.1 M NaCl, pH 6.8 buffer and DI H_2O at 37 °C, of DRCs formed using 1:2 D:R ("unactivated" IRP69) (w/w) ratio. DRC in DI H_2O (Magenta inverted triangle), DRC in 0.1 M NaCl (Blue triangle), DRC in pH 6.8 buffer (Red circle) and DRC in 0.1 M HCl (Black square).*

As alluded to previously, the 1:3 DRC displayed similar release behaviour to the 1:1 and 1:2 DRCs, with the release profiles depicted in Figure 3.12. No statistical difference ($p>0.05$) at any time point is evident when the DRCs' release behaviour in pH 6.8 buffer and 0.1 M HCl are evaluated. Again, the DRC displays a higher affinity for the drug ion in 0.1 M NaCl, characterised by the slower release rate. Approximately 72% of the drug is released after 5 minutes, which is substantially lower than the quantity released in 0.1 M HCl (86%) and pH 6.8 buffer (84%) at the same timepoint. Similar to the 1:2 DRC, the drug release in all media proceeds to equilibration rather than completion. This plateau in % drug release is reached after 30 minutes in 0.1 M HCl and pH 6.8 buffer and occurs after 60 minutes in 0.1 M NaCl. Akin to the 1:2 DRC having a reduced value compared to the 1:1 complex, the equilibration concentration in all media was further reduced for the 1:3 ratio. The mean value ranged from 90.45% to 92.6 % ($p<0.05$) across the media examined, except for DI H_2O, where the DRC released minimal quantities of the drug, similar to the other ratios studied. By using a higher proportion of resin relative to the drug, in this case, a 1:3 ratio, the DRC's desorption properties are markedly impacted by the excess free resin. The presence of excess unbound resin reduces the equilibrium concentration attained and the rate of drug release, relative to DRCs containing higher drug loadings. This underlines the potential for tailoring drug release behaviour using different quantities of the drug in the DRC (304). Several groups have exploited this fundamental property of resins by including "free drug" or "free resin" alongside the DRC and assessing the impact on drug release kinetics (93).

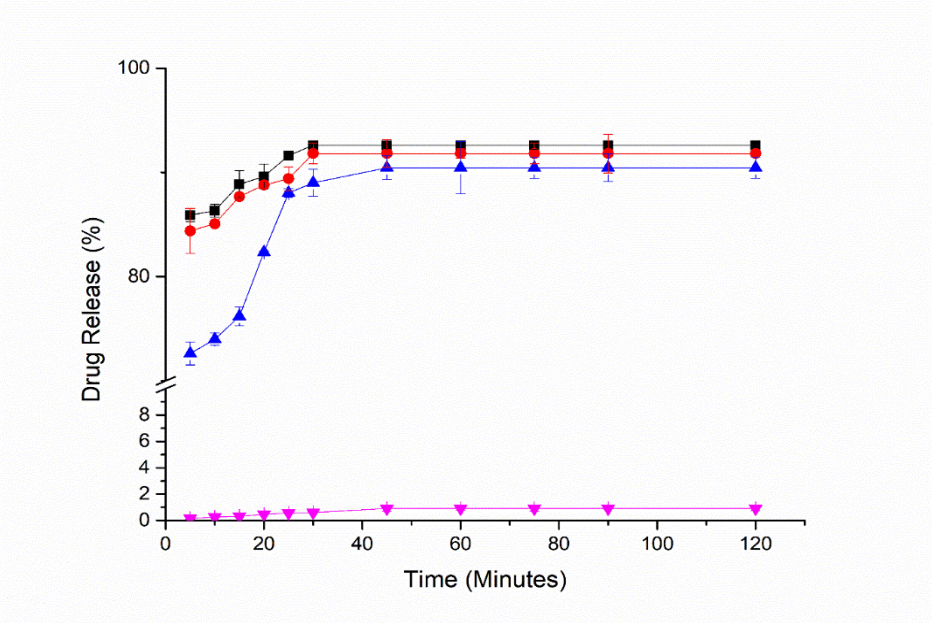

Figure 3.*12. Drug (TZD HCl) release profiles in 0.1 M HCl, 0.1 M NaCl, pH 6.8 buffer and DI H_2O at 37 °C, of DRCs formed using 1:3 D:R ("unactivated" IRP69) (w/w) ratio. DRC in DI H_2O (Magenta inverted triangle), DRC in 0.1 M NaCl (Blue triangle), DRC in pH 6.8 buffer (Red circle) and DRC in 0.1 M HCl (Black square).*

These results highlight the potential of the approach of using a non-ionic medium as the vehicle for a liquid formulation in which the DRC would be suspended when aiming to formulate a stable liquid product, due to low levels of leaching/release observed. Although ion-exchange was demonstrated, an appreciable prolongation of release was not achieved, pointing to the need for the application of a rate-controlling polymeric membrane layer to further retard release.

3.2.2.1.3.1 Drug release studies (Milled IRP69 material)

As discussed previously, resin raw material was milled to varying particle sizes to investigate the effect of the particle size on drug release from the DRCs under the same conditions that were used to study the release behaviour of DRCs formed using unprocessed resin raw material (Figures 3.13-3.15). It is evident from the drug release profile of the DRC formed using a 1:1 D:R ratio (Figure 3.13), that the drug is rapidly displaced from the resin after contact with the media, with 92% of the drug being released after 5 minutes, and increasing quantities of drug being released, until equilibration is reached. Although equilibration, characterised by a plateau in the drug release occurs after 25 minutes in 0.1 M HCl dissolution medium, the difference in % drug release between the equilibration value and the % drug release value after 5 minutes is approximately 4%, meaning that the resin exerts little sustained-release effect, as the hydrogen ion in the acidic medium is an effective displacing agent. Similar to the DRCs formed using unmilled resin, the drug release from the DRC is shown to be independent of pH, when the drug release profiles in 0.1 M HCl and pH 6.8 buffer release profiles are

compared. These drug release profiles reveal two interesting features associated with the use of milled resin material; the first being the reduced time to equilibrium in 0.1 M HCl, and the second is related to the drug release proceeding to equilibration rather than completion. The % drug release plateaus at approximately 96% for the milled samples in 0.1 M HCl and pH 6.8 phosphate buffer ($p<0.05$), whereas 100% drug release is attained with the unmilled samples. The drug release profiles in 0.1 M NaCl are also reflective of the DRCs exhibiting differing release behaviour, with the milled sample again reaching equilibration at an earlier time point compared to resinates prepared with unmilled resin material (45 minutes versus 75 minutes). Furthermore, the DRC using milled material reached equilibrium after 97% drug release rather than complete release, as was observed in the drug release profile of the unmilled samples.

Although the impact of the milled material on the extent of drug release was not anticipated, its influence on the release kinetics was more predictable. By using the milled resin material as part of the drug loading studies, the resultant DRC has a reduced particle size relative to DRCs produced using unmilled resin. Therefore, the geometry of the particle is altered, so that the path from the interior of the resin structure to the surface is reduced, meaning that less time is required for the ions to diffuse from the dissolution media into the resin's interior, exchange with the drug ion, which in turn subsequently diffuses out into the dissolution medium and is therefore detectable. Moreover, a reduced particle size increases the SSA, compared to a DRC prepared with unmilled resin, thus exposing more binding sites on the outside of the resin, which are immediately available to exchange in solution, reflected by an increased release rate of the drug from the DRC.

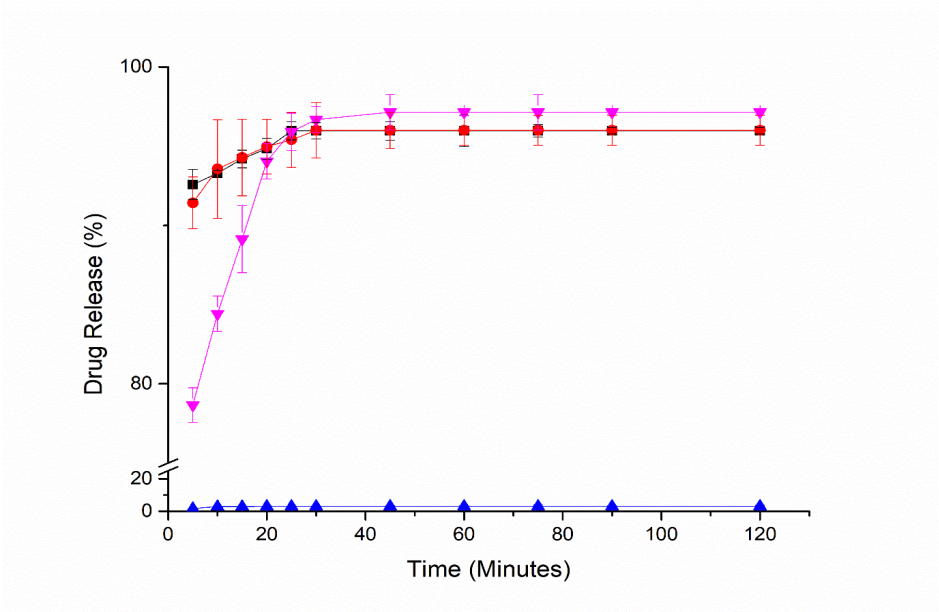

Figure 3.*13. Drug (TZD HCl) release profiles in either 0.1 M HCl, 0.1 M NaCl, pH 6.8 buffer and DI H_2O at 37 °C, of DRCs formed using 1:1 D:R ("milled IRP69") (w/w) ratio. DRC in 0.1 NaCl (Magenta inverted triangle), DRC in DI H_2O (Blue triangle), DRC in pH 6.8 buffer (Red circle) and DRC in 0.1 M HCl (Black square).*

Figures 3.13-3.15 show that the drug release behaviours in the different media studied of the DRCs prepared from milled resin follow the same general trends as those prepared from unmilled resin. More specifically, the drug release rate from the DRC is independent of the media's pH, yet it is slowed in NaCl. Again, this is a consistent feature of the release profiles of the systems investigated, irrespective of the drug loading. Another shared characteristic with the unmilled system, which is a distinguishing feature of the DRCs having lower drug loadings, is that the ion-exchange reaction proceeds to equilibration rather than completion. As shown in Figure 3.14, the 1:2 system exhibits little difference in its drug release behaviour in either pH 6.8 buffer or 0.1 M HCl, which is consistent with findings discussed to date. The drug release profiles of the system are characterised by approximately 92.2 ± 0.45% and 91.42 ± 1.3% being released after 5 minutes in 0.1 M HCl and pH 6.8 buffer respectively. The time to equilibrium differs between the media, as equilibrium is reached after 30 minutes in pH 6.8 buffer and 60 minutes in 0.1 M HCl. Another salient feature of the drug release profiles is the more moderate rate of release in 0.1 M NaCl, exemplified by approximately 84% of the drug being released after 5 minutes and equilibrium being attained after 97 ± 1.1% drug release. When compared to the DRC produced using unmilled resin, there is no difference regarding the time to equilibrium in acidic media, whereas a difference is evident in pH 6.8 buffer. At the higher pH value, the time to equilibrium is reduced for the milled sample (45 minutes) relative to the unmilled samples, which take 60 minutes to reach equilibrium.

Of all the release media studied using this particular DRC, NaCl yielded the most interesting results, due to the marked differences in drug release performance between it and the DRC prepared using unmilled resin. The effect of the utilisation of the milled resin on the time to equilibrium was substantial, reducing it from 90 to 45 minutes. Although this is reflective of the anticipated effect of using DRCs with reduced particle size relative to more coarse material, the % drug release does not differ significantly ($p>0.05$) and the % drug release at equilibrium does not differ significantly from the DRC produced using unmilled material ($p>0.05$). Therefore, the impact of a smaller particle size on DRC release behaviour in NaCl is limited to the kinetics of the release, which is in agreement with many studies in the literature (145).

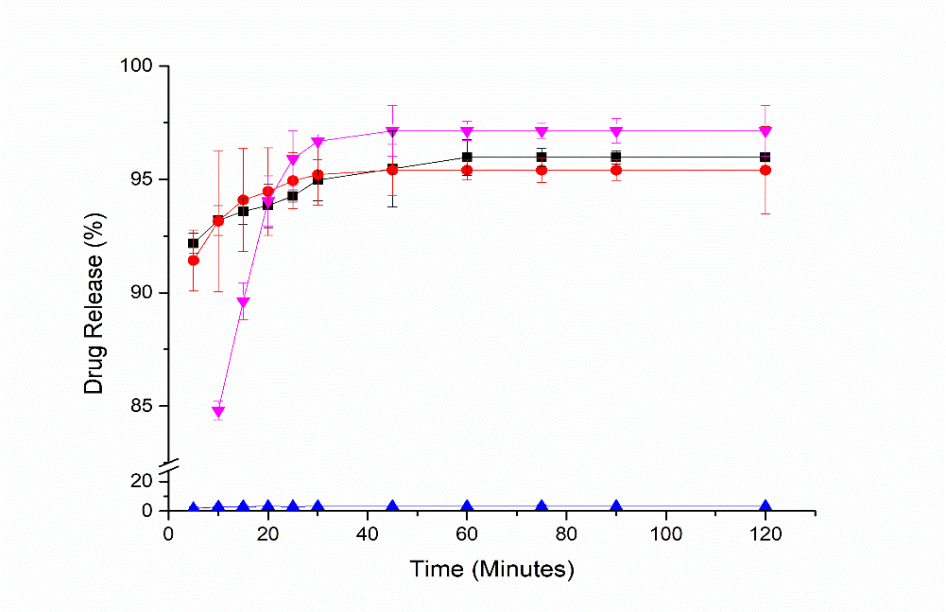

Figure 3.14. Drug release profiles in 0.1 M HCl, 0.1 M NaCl, pH 6.8 buffer and DI H_2O at 37 °C, of DRCs formed using 1:2 D:R ("milled IRP69") (w/w) ratio. DRC in 0.1 NaCl (Magenta inverted triangle), DRC in DI H_2O (Blue triangle), DRC in pH 6.8 buffer (Red circle) and DRC in 0.1 M HCl (Black square).

The DRC formed using the 1:3 D:R ratio (w/w) of the drug to resin displayed similar drug release characteristics to the DRC formed using a 1:2 D:R ratio (Figure 3.15). All release profiles are defined by incomplete release, with no statistical difference ($p>0.05$) at any time point for the samples studied in 0.1 M HCl and pH 6.8 buffer. Again, drug release in the 0.1 M NaCl is slowed relative to the other two ionic media studied, meaning the time to equilibration is extended relative to the faster-releasing systems. Relative to the DRC prepared with unmilled resin, in all three ionic media, the % drug release is higher ($p<0.05$) indicating the impact of milling on drug release kinetics may be more pronounced when DRCs with lower drug loadings are studied. The mean difference between milled and unmilled material is approximately 7% in all three types of ionic media. No discernible difference in drug release that is statistically significant ($p>0.05$) can be established in DI H_2O for milled versus unmilled rein systems.

In addition to similar % drug release values at equilibrium across the different media, compared to its unmilled DRC counterpart, this similarity extends to the % drug release after 5 minutes with no statistical differences ($p>0.05$) found when the results in each media are studied. As previously discussed, in the case of the unmilled DRC, distinct differences are evident, with respect to % drug release after 5 minutes, % drug release at equilibrium and time to equilibrium, when the release profiles of the 1:2 and 1:3 DRCs are scrutinised. However, using milled resin to form the DRCs appears to standardise the drug release behaviour of the DRCs formed using the same two D:R ratios. The impact of particle size on drug release is two-fold: smaller particles have a larger surface area, a key factor in faster drug release and also provide a shorter diffusional pathway for drug ions within the core of the resin to traverse.

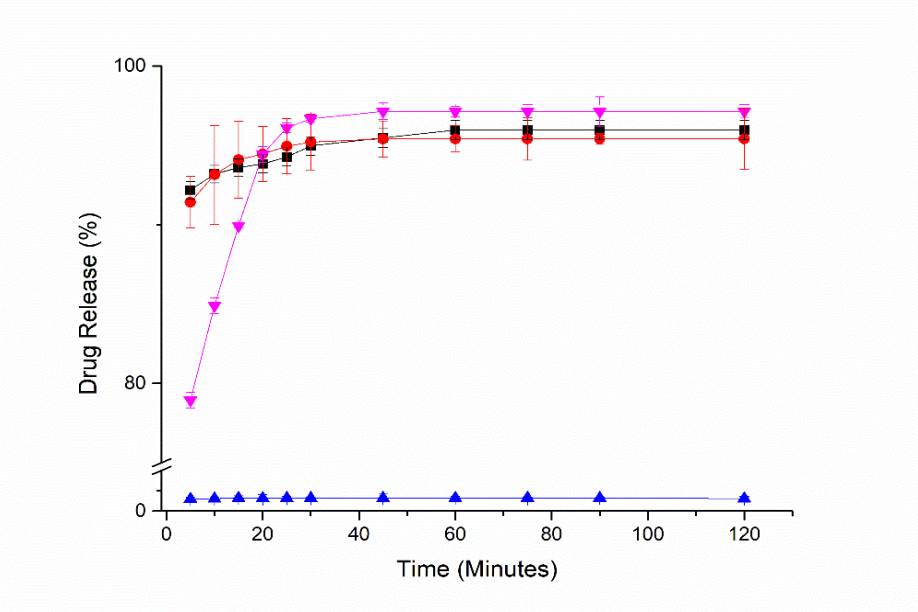

Figure 3.15. Drug release profiles in 0.1 M HCl, 0.1 M NaCl, pH 6.8 buffer and DI H_2O at 37 °C, of DRCs formed using 1:3 D:R ("milled IRP69") (w/w) ratio. DRC in 0.1 NaCl (Magenta inverted triangle), DRC in DI H_2O (Blue triangle), DRC in pH 6.8 buffer (Red circle) and DRC in 0.1 M HCl (Black square).

3.2.2.1.3.2 Drug release studies involving the alteration of the concentration of drug-resin complex (IRP69) in the drug release medium

To probe the influence of DRC concentration in the dissolution vessel on the drug release behaviour, two further concentrations of the 1:1 complex (150 mg/900 mL and 200 mg/900 mL) were studied in addition to the 100 mg/900 mL concentration. The drug release profiles in 0.1 M HCl are depicted in Figure 3.16. It is apparent from both the loading studies and the drug release studies performed up to this point, that the loading/release process is governed by an ion-exchange equilibrium. Depending on the exact intention, the equilibrium position can be altered by manipulating one or more factors. Regarding the release properties, the concentration of the complex in the dissolution medium remains an under-investigated property that can be exploited to yield more information regarding the drug

release properties. It is apparent from the drug release profiles (Figure 3.16) that the higher the concentration of complex in the dissolution medium, the longer the time needed to reach equilibrium. Furthermore, the extent of drug release i.e. the equilibrium concentration is notably reduced for the systems evaluated in the more concentrated medium, with the complete release being effectively achieved using the lowest concentration of DRC (100 mg/900 mL). At increased concentrations of the complex in the medium, the quantity of drug released at each timepoint is reduced ($p<0.05$), with the exception of the intermediate concentration tested after 5 minutes, which releases a similar amount of drug to the DRC in the most dilute condition, in the region of 89-91%. In contrast to this, the most concentrated system releases 85% of the drug after 5 minutes and reaches an equilibrium after approximately 93% of the drug has been released at the 45-minute mark. The intermediate concentration condition (150 mg/900 mL) releases the drug at a more rapid rate, reaching equilibrium after 30 minutes (96% drug release). The well-defined differences in the kinetics and extent of drug release highlight the considerable impact that the concentration of complex in the release medium can have. Moreover, the results illustrated in Figure 3.16, which clearly illustrates the existence of equilibrium, further substantiate the extensive investigation into the loading properties of the DRCs, which also requires careful consideration of the nature of the equilibrium.

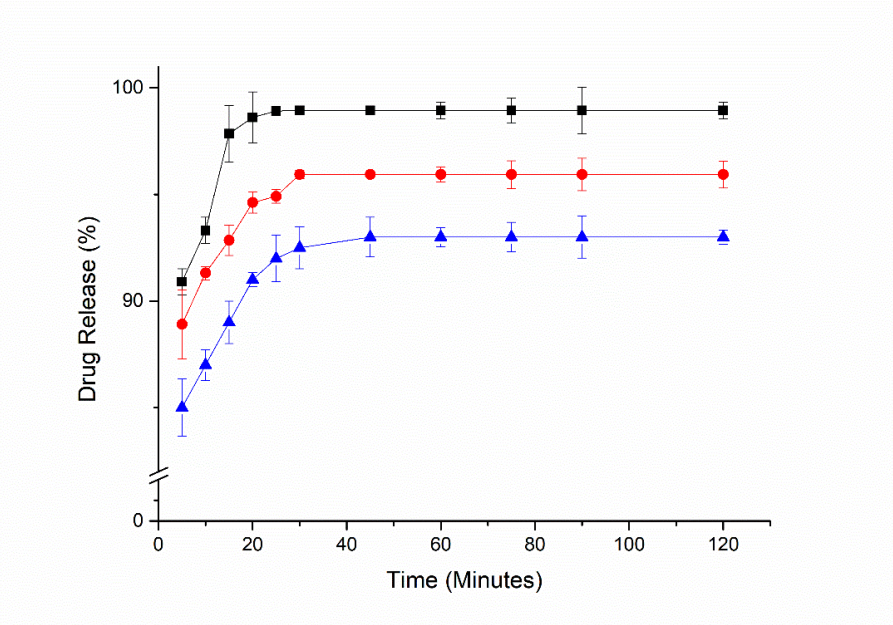

Figure 3.16. Drug release profiles of 1:1 D:R (w/w) ratio ("unactivated" IRP69) in 0.1 M HCl at 37 °C using different concentrations of complex in the drug release medium (100 mg/mL, 150 mg/mL and 200 mg/mL). 200 mg/900 mL (Blue triangle), 150 mg/900 mL (Red circle) and 100 mg/900 mL (Black square).

3.2.2.1.3.3 Drug release studies involving physical mixtures of TZD HCl and IRP69

The drug release profiles of a range of physical mixtures of drug and resin in 0.1 M HCl and DI H_2O are shown in Figures 3.17(A) and 3.17(B) respectively. Three ratios of drug to resin ranging from 45-55%

w/w drug content were selected based on the samples containing a similar quantity of drug to the level loaded onto the DRCs. It is evident from the drug release profiles, that all three physical mixtures have dissimilar drug release behaviour to that of the DRCs in both 0.1 M HCl and DI H_2O. The most defining characteristic that can be used to describe the differences observed, is the decreasing quantity of the drug being detected in the dissolution media as the study progresses. For all three physical mixtures studied in acidic media (Figure 3.17(A)), the drug release profile is characterised by an initial steady rise in % drug released. After 5 minutes, 75% of the drug is released, which is significantly lower than the quantity of drug released from the DRC system (approximately 90%). This trend continues until the 20-minute time point, beyond which the drug release behaviour deviates from this cumulative release pattern. This departure from an upward trajectory is signified by the sharp drop in % released until the 30-minute time point. Subsequently, the rate of release decreases more gradually.

Regarding the dissolution behaviour in DI H_2O (Figure 3.17(B)), the % drug release is far higher for all three physical mixture systems relative to the % drug release from the batch-produced DRC in DI H_2O. The drug release profiles of these systems follow a similar trend, as for the systems in acidic medium. The manner in which the drug is released from the system produces a profile that can consists of two distinct stages. The first stage is characterised by the cumulative drug release until the 30-minute time point, after which the % drug release begins to decrease, designated the 2^{nd} stage, and reaches a plateau after approximately 90 minutes. This fluctuating dissolution profile can be explained by considering the nature of the physical mixtures. As the samples are physical mixtures rather than complexes formed by a chemical interaction, no ion-exchange would be expected, as neither component is available in its ionised form. However, once any of the physical mixtures are introduced to either of the dissolution media, both components (API and IER) become ionised meaning the resin is capable of binding the drug. Therefore, as the drug release study proceeds, it is surmised that ion-exchange is occurring between the drug and resin, throughout the course of the experiment, thereby reducing free drug concentration, which is reflected as a reduction in the % drug release.

In essence, the drug release profiles generated by the physical mixtures are a consequence of two distinct processes occurring simultaneously, namely drug loading and drug release. Depending on which of these processes is predominant at the time of sampling, combined with the frequency of sampling, the drug release profile can differ drastically from that of a typical DRC. Irrespective of the dissolution medium, the increasing quantity of drug released in the early portion of the study can be attributed to API, which has not had the chance to bind to the resin after dissolving in the medium, meaning that it is available in solution and therefore detectable. As the study proceeds, significant complexation begins to occur between drug and resin, which manifests in a reduction of drug available

in solution, leading to lower quantities of "free drug" in solution. An interesting observation that can be made based on the results observed in both media trialled, is that the performance of the physical mixture is superior to that of the DRC, in acidic medium, for the purposes of sustained-release. However, the physical mixtures release a far higher amount of drug in DI H_20, thus negating their usefulness in light of the purposes of the project, whereby there is a need to ensure minimal drug release in a suspension vehicle but extended drug release on ingestion.

This noticeable difference in dissolution performance is broadly in agreement with the findings of Sriwongjanya and Bodmeier, who reported even starker findings. In their work, a physical mixture of drug, resin and HPMC, formed the DRC *in situ* and performed comparably to a tablet comprised of DRC and HPMC, thus negating the need for a protracted manufacturing process (96). Akkaramongkolporn et al. reported similar findings, with diphenhydramine and HPMC, indicating that this *in situ* formation can occur for a range of drugs with differing properties (305).

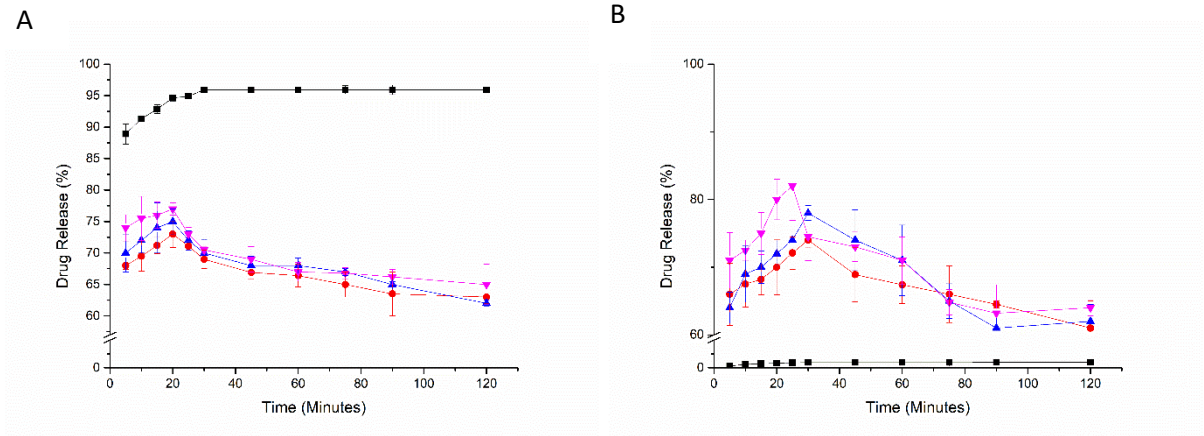

Figure 3.17. Drug release profiles in either 0.1 M HCl or DI H_2O at 37 °C, of physical mixtures (PM) prepared using varying D:R (IRP69) ratios (w/w), using the USP type 2 paddle apparatus in A) 0.1 M HCl and B) DI H_2O. PM (55:45) (Magenta inverted triangle), PM (50:50) (Blue triangle), PM (45:55) (Red circle) and DRC (1:1) (Black square). The drug release profile of the DRC prepared using a 1:1 D:R ratio (w/w) using "unactivated" IRP69 are included for comparative purposes.

3.2.2.1.4 Solid-State characterisation (IRP69)

DSC analysis was performed for pure drug, pure resin, physical mixtures and DRCs. The thermal profile of TZD HCl shows a sharp endothermic peak at approximately 291 ± 0.63 °C representative of the melting of the crystalline drug (Figure 3.18(A)). This melting event was not observed in the DRC samples, suggesting the amorphisation of the drug when loaded onto the resin. This contrasts with the physical mixtures (Figure 3.18(B)), where the melting endotherm, representative of crystalline TZD is present. These physical mixes were prepared using ratios of drug to resin (w/w) which covered the estimated drug loading, to confirm the amorphous nature of DRCs. Although a dilution effect is evident

due to the polymer matrix for each ratio, a melting endotherm is still present even for the most dilute sample studied (30% drug content). A secondary feature of the DSC traces for the DRCs, as well as the resin raw material, is the broad endothermic peak that results from the partial dehydration of the resin on heating, a common occurrence for DRC systems.

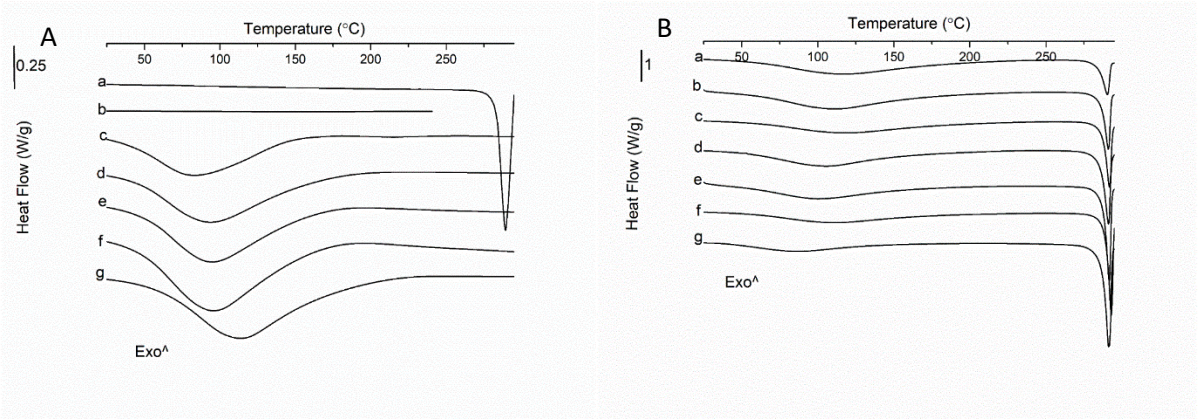

Figure 3.18. DSC thermograms of raw materials alongside DRCs produced using various ratios (w/w) of A) drug to IRP69 (w/w) ("unactivated"). a) TZD HCl raw material, b) IRP69 raw material, c) DRC (3:1), d) DRC (2:1), e) DRC (1:1), f) DRC (1:2) and g) DRC (1:3). B) physical mixtures prepared using varying ratios of drug to resin ("unactivated") (w/w). a) 30:70, b) 40:60, c) 45:55, d) 50:50, e) 55:45, f) 60:40 and g) 70:30.

The pXRD patterns of the DRCs (Figure 3.19(A)) produced using a variety of different ratios (30-70% drug content) were compared to the diffractograms of physical mixtures (Figure 3.19(B)) that were prepared to cover a narrower range of drug loadings (45-55% w/w), closer in value to the drug loading in the 1:1 DRC. The diffractograms of the DRCs are devoid of the characteristic peaks of the API. These major diffraction peaks (2θ) for TZD HCl occur at 10.5°, 12.5°, 21.67°, 25°, 27° and 32° and are in agreement with the literature (306). Instead, the DRCs are characterised by halo patterns which are indicative of their amorphous nature and thereby supportive of the DSC data. The diffractograms of the DRCs resemble that of the resin raw material, suggesting that the drug may have undergone a physical transformation upon binding to the resin, leading to its crystalline structure being lost. Contrastingly, the diffractograms of the physical mixtures of crystalline TZD HCl and resin exhibited the more intense crystalline TZD HCl peaks at 2θ values 10.5°, 12.5°, 21.67°, 25°, 27° and 32°, shown in Figure 3.19(B). Although reports of the solid-state properties of DRCs are scarce, the results obtained using the TZD HCl systems are in accordance with those reported by Akkaramongkolporn et al., which is perhaps the most in-depth study in the literature to date. A combination of DSC, pXRD and FTIR analyses enabled these researchers to conclude that the entrapment of chlorphenamine

within the resin matrix prompted a change in the molecular state of the drug from crystalline to amorphous (307).

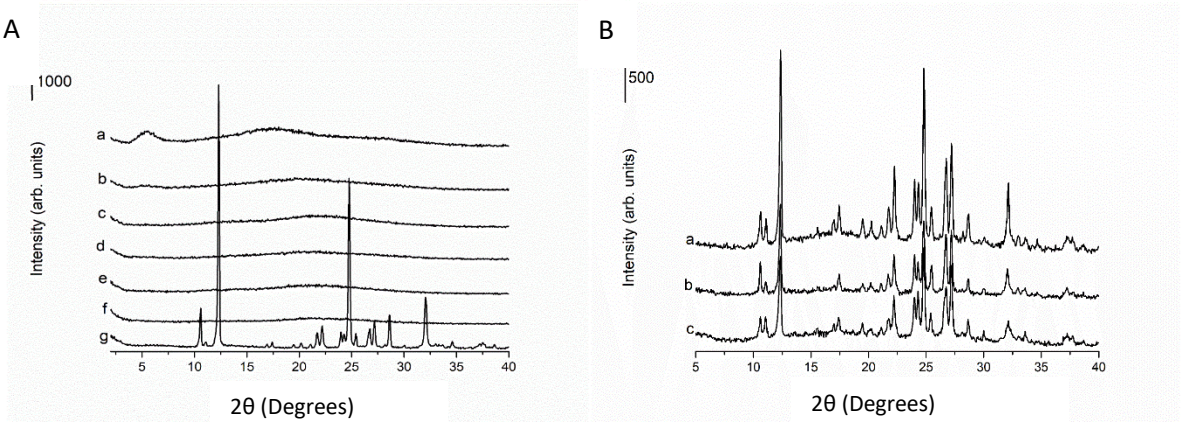

Figure 3.19. pXRD diffractograms of A) DRCs formed using varying ratios (w/w) of drug to IRP69 ("unactivated"). a) IRP69 raw material, b) DRC (3:1), c) DRC (2:1), d) DRC (1:1), e) DRC (1:2), f) DRC (1:3) and g) TZD HCl raw material. B) physical mixtures produced using varying ratios of drug to resin (w/w) ("unactivated"). a) 55:45, b) 50:50 and c) 45:55.

With respect to the DRC samples produced using altered loading conditions, melt endotherms indicative of crystalline material were not observed (Figure 3.20(A-D) and Figure 2(A-B) in Appendix 1) for any samples. The DRCs were also shown to be pXRD amorphous (Figure 3.21(A-D) and Figure 3(A-B) in Appendix 1), demonstrated by the characteristic halo pattern that is present in the diffractograms. Therefore, in the case of loading TZD HCl onto IRP69, it can be concluded that the impact of adjusting the loading solution drug concentration and the temperature of the ion-exchange reaction has little impact on the solid-state form of the DRC. Similarly, subjecting the resin to a pre-swelling step and varying the contact time between drug and resin yielded products with no evidence of residual crystallinity based on pXRD and thermal analyses. This observation is in agreement with studies that have successfully demonstrated that ion-exchange between an API and IER has occurred (118).

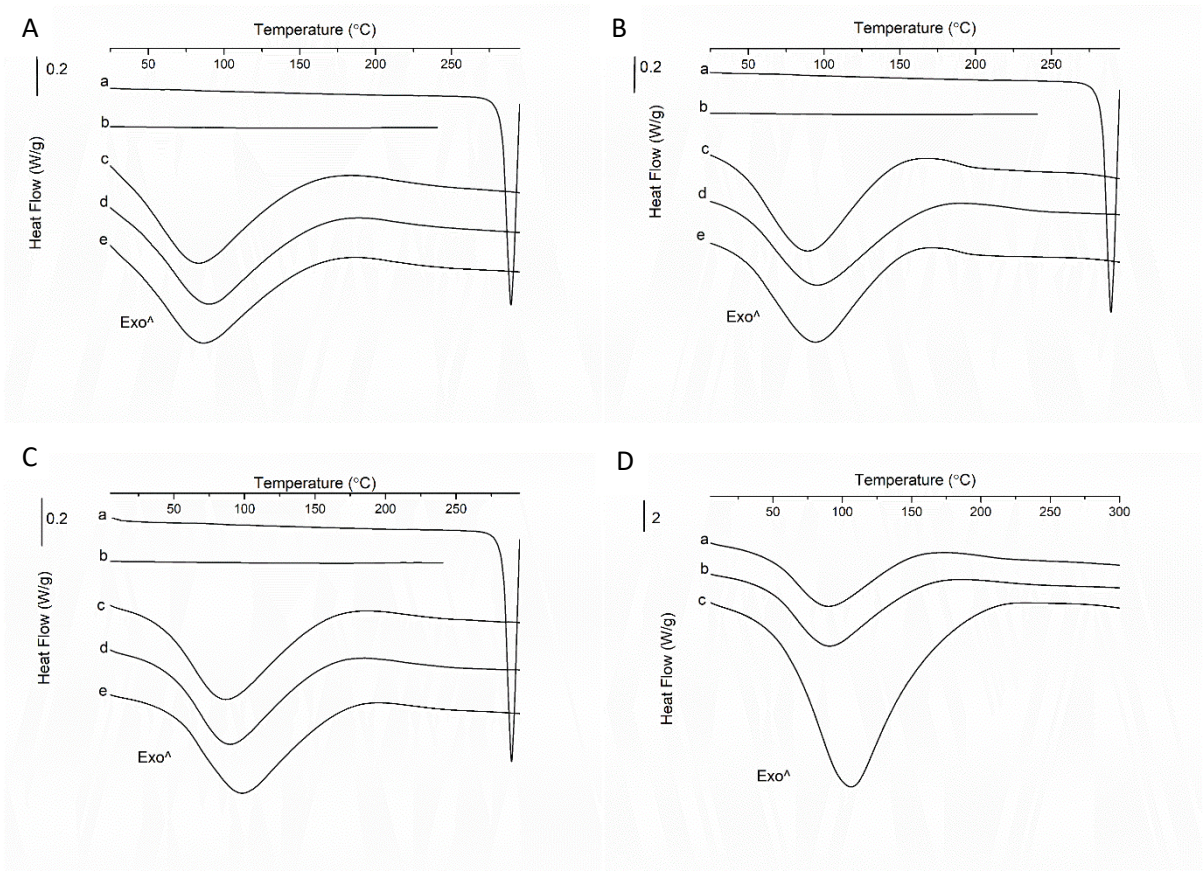

Figure 3.*20. DSC thermograms of raw materials of DRCs produced a 1:1 D:R (IRP69) (w/w) ratio using altered loading condtions (loading temperature, drug loading concentration, contact time, number of loading stages, resin pre-treatment). The DRCs were prepared by a single stage loading process at 20 °C using "unactivated resin", a 24 hour contact time and a drug loading solution concentration of 10 mg/mL unless otherwise stated. A) a) TZD HCl raw material, b) IRP69 raw material, c) DRC (1:1)(20 °C), d) DRC (1:1)(30 °C) and e) DRC (1:1)(40 °C). B) a) TZD HCl raw matieral, b) IRP69 material, c) DRC (1:1)(1 mg/mL), d) DRC (1:1)(5 mg/mL) and e) DRC (1:1)(10 mg/mL). C) a) TZD HCl raw material, b) IRP69 raw material, c) DRC (1:1)(6 hours), d) DRC (1:1)(12 hours) and e) DRC (1:1)(24 hours) and D) a) 2:1 (swollen), b) 1:1 (swollen) and c) 1:2 (swollen).*

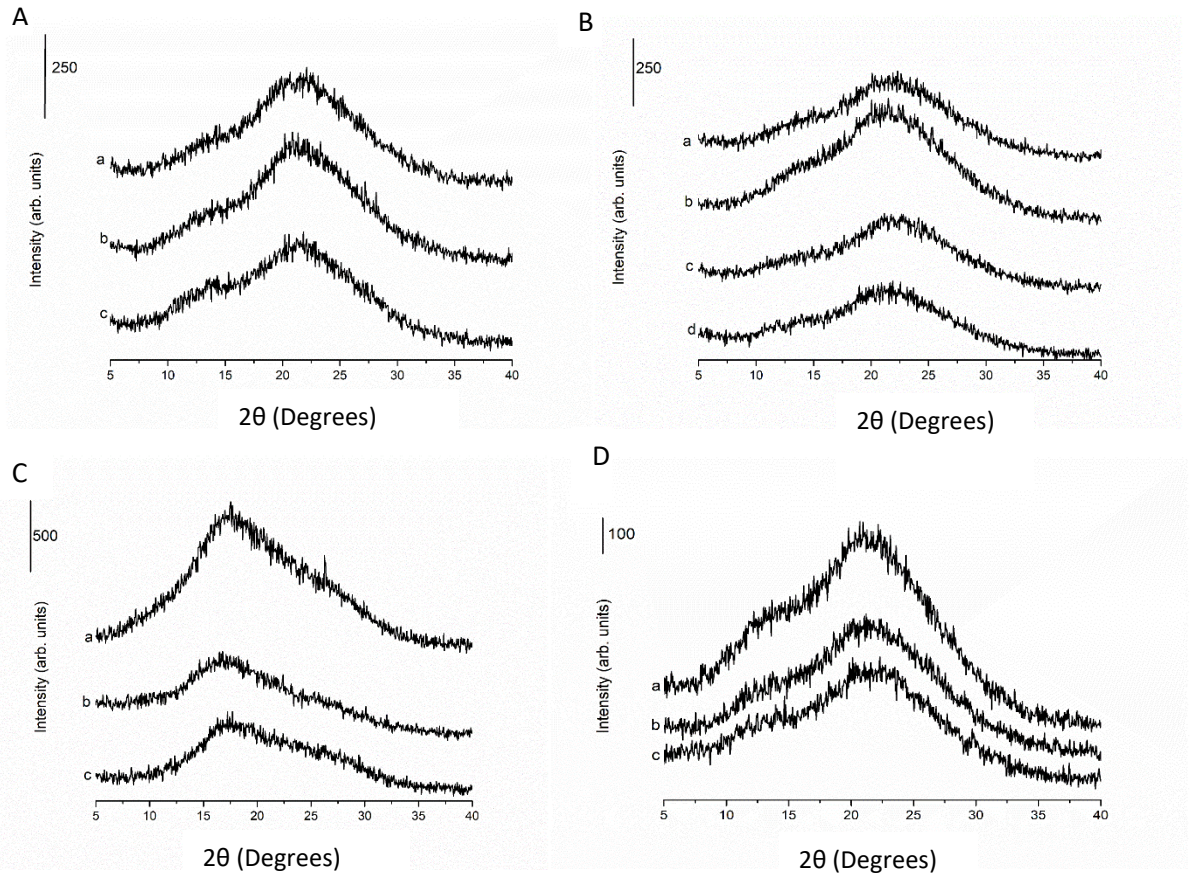

Figure 3.*21. pXRD diffractograms of DRCs produced a 1:1 D:R (IRP69) (w/w) ratio using altered loading condtions (loading temperature, drug loading concentration, contact time, number of loading stages, resin pre-treatment. The DRCs were prepared by a single stage loading process at 20 °C using "unactivated resin", 24 hour contact time and a drug loading solution concentration of 10 mg/mL unless otherwise stated. A) a) DRC (1:1) (20 °C), b) DRC (1:1)(30 °C) and c) DRC (1:1)(40 °C), B) a) DRC (1:1)(1 mg/mL)), b) DRC (1:1)(5 mg/mL), c) DRC (1:1)(10 mg/mL) and d) DRC (1:1) (double-batch) C) a) DRC (1:1)(6 hours), b) DRC (1:1)(12 hours) and c) DRC (1:1)(24 hours). D) a) DRC (2:1)(swollen), b) DRC (1:1)(swollen) and c) DRC (1:2)(swollen).*

The PLM photographs of drug-loaded resin and a physical mixture of crystalline drug and amorphous resin are shown in Figure 3.22(A-D). The DRC displayed no evidence of birefringence, in contrast to visible signs of birefringence seen in the physical mixture of crystalline drug and resin. This is suggestive of the drug losing its crystalline structure after complexation with the resin, further supporting the pXRD and DSC data. Moreover, the results are in agreement with those of Tan et al. who used the absence of birefringence exhibited by their DRC samples to support the assertion that a crystalline to amorphous transition had occurred (119).

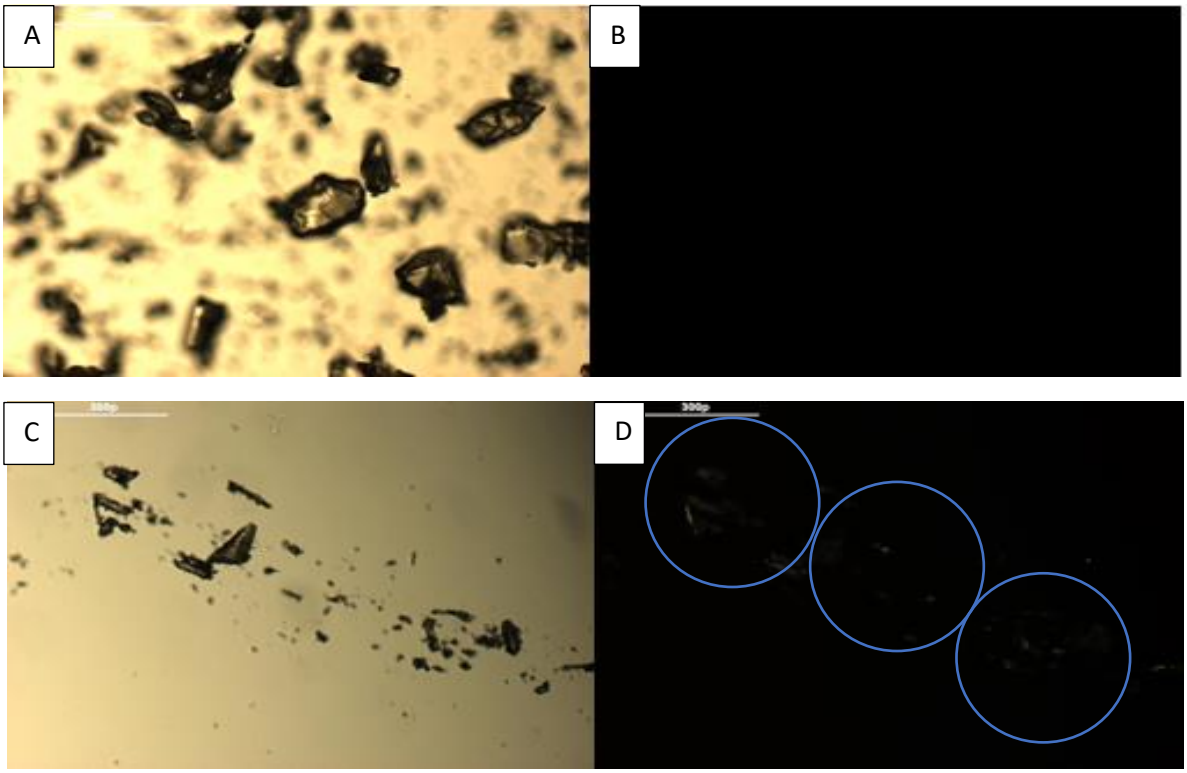

Figure 3.22. *PLM images for the DRC formed using a 1:1 (% w/w) D:R (IRP69) ratio ("unactivated") and physical mixture (PM) (1:1 w/w) of drug and resin ("unactivated"). A) DRC (non-polarised), B) DRC (polarised), C) PM (non-polarised) and D) PM (polarised). Crystalline material in D) is highlighted by blue circles.*

TGA analysis, depicted in Figure 3.23, supported the assertion that complexation has occurred between the API and resin leading to a protective effect conferred by the formation of the DRC. The onset of degradation for both components is visible in the thermogram of the physical mixture and illustrates little difference relative to each individual component, which is not surprising considering little interaction between the components is expected in the solid-state. In contrast, the onset of degradation of the API is noticeably delayed in the thermogram of the DRC relative to the physical mixture, suggestive of the API being embedded within the resin rather than being confined solely to the surface.

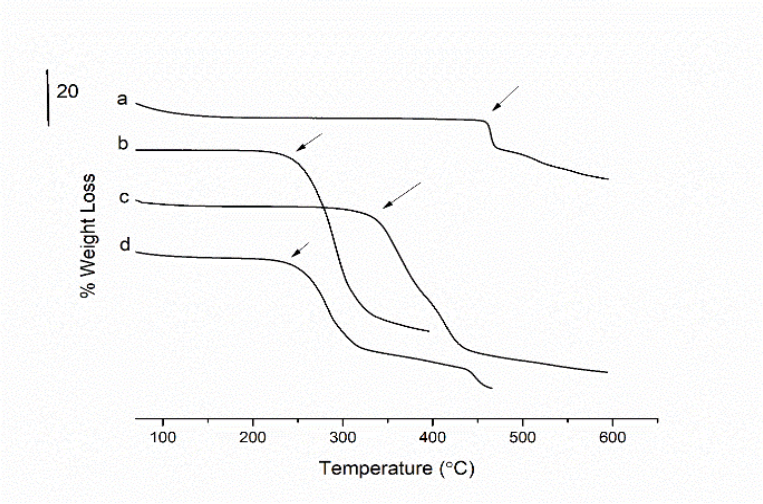

Figure 3.23. TGA thermograms of a) IRP69 raw material, b) TZD HCl raw material, c) DRC formed using 1:1 (w/w) D:R ratio ("unactivated" IRP69) and d) 1:1 (w/w) physical mixture of TZD HCl and IRP69.

3.2.2.1.5 FTIR spectroscopy (IRP69)

The infrared (IR) spectra of the drug, resin, DRC and equivalent physical mixtures are shown in Figure 3.24 The FTIR results reflected the change in the molecular surroundings of the TZD's amine group. The characteristic peaks of both components, which corresponded to those reported in the literature (119,308), can be seen in the spectrum of the physical mixture. Particularly notable is the absorption band at 3230 cm^{-1}, which is representative of the stretching vibration of the amine group of TZD, which is present in the spectra of both the physical mixture and the API. Less obvious is the peak at 1189 cm^{-1} which can be attributed to the TZD C-N stretching vibration. With respect to the DRC, the FTIR data showed some interesting features in comparison to the raw materials and physical mixture spectra. The amine absorption band of TZD is absent in the DRC sample, which is suggestive of the formation of an ionic bond between drug and resin. This assertion is supported by the difference in the N-H bending region, emphasised by the dashed red line (1603 cm^{-1})(Figure 3.24), which is less distinct, compared to the changes highlighted regarding the stretching vibration. Two distinct absorption bands are obvious at 1603 cm^{-1} and 1641 cm^{-1} in the spectra of the API and physical mixtures, whereas the spectrum of the DRC differs in this region, as a single broad band is evident. These deviations, in addition to other peak changes, such as band broadening, can be used to substantiate the formation of new chemical bonds (119). Also depicted in Figure 3.24, are the subtle differences in the region of the DRC's spectrum associated with the sulfonate stretching vibration, namely the 1150-1200 cm^{-1} band, highlighted by the deviation from the black dashed lines that goes through the centre of the absorption bands in the raw material's spectrum. Two cases of peak shifting are evident, at 1173-1162 cm^{-1} and 1036-1032 cm^{-1}. Frequently, the shift in peak value that is suggestive of interactions between the components involved in the ion-exchange reaction is often very subtle, often of the order of 5 cm^{-1} (119).

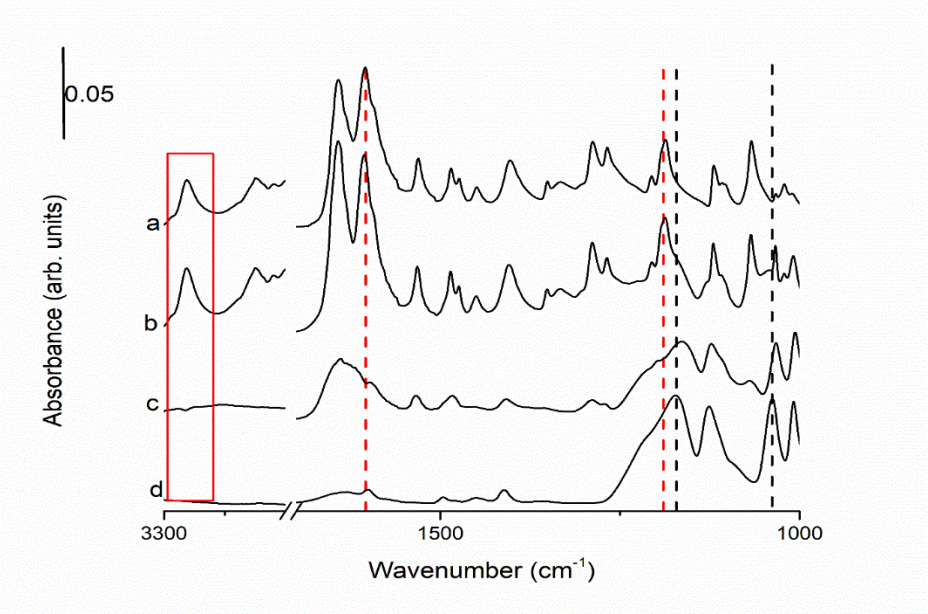

Figure 3.24. FTIR spectra of a) TZD HCl raw material, b) 1:1 (w/w) physical mixture of TZD HCl and IRP69, c) DRC formed using 1:1 (w/w) D:R ratio ("unactivated" IRP69) and d) IRP69 raw material. Red lines highlight shifts in the spectra of the DRCs relative to TZD HCl raw material whereas the black lines highlight shifts in the spectra of the DRCs relative to the IRP69 raw material.

3.2.2.1.6 SEM (IRP69)

The SEM morphology of the DRCs compared to the raw materials is illustrated in Figure 3.25(A-D). Resin raw material can be described as being irregularly shaped, showing rod-like and plate-like particles (A). The SEM micrographs of the pure drug appear as long column-like crystals, indicative of its crystalline state (B). The physical mixture of drug and resin shows the distinct appearance of crystalline material dispersed between the particles of the resin which have a largely smooth surface and the discrepancy in particle size between the two materials is apparent (C). The DRC has a decidedly different morphology compared to the physical mixture, and no obvious sign of crystalline material can be observed in the SEM images (D) meaning it is hard to discern any drug material on the surface of the irregularly shaped particles. The micrographs show that the morphology of the loaded and unloaded resin particles show little difference, which is in agreement with previous studies.

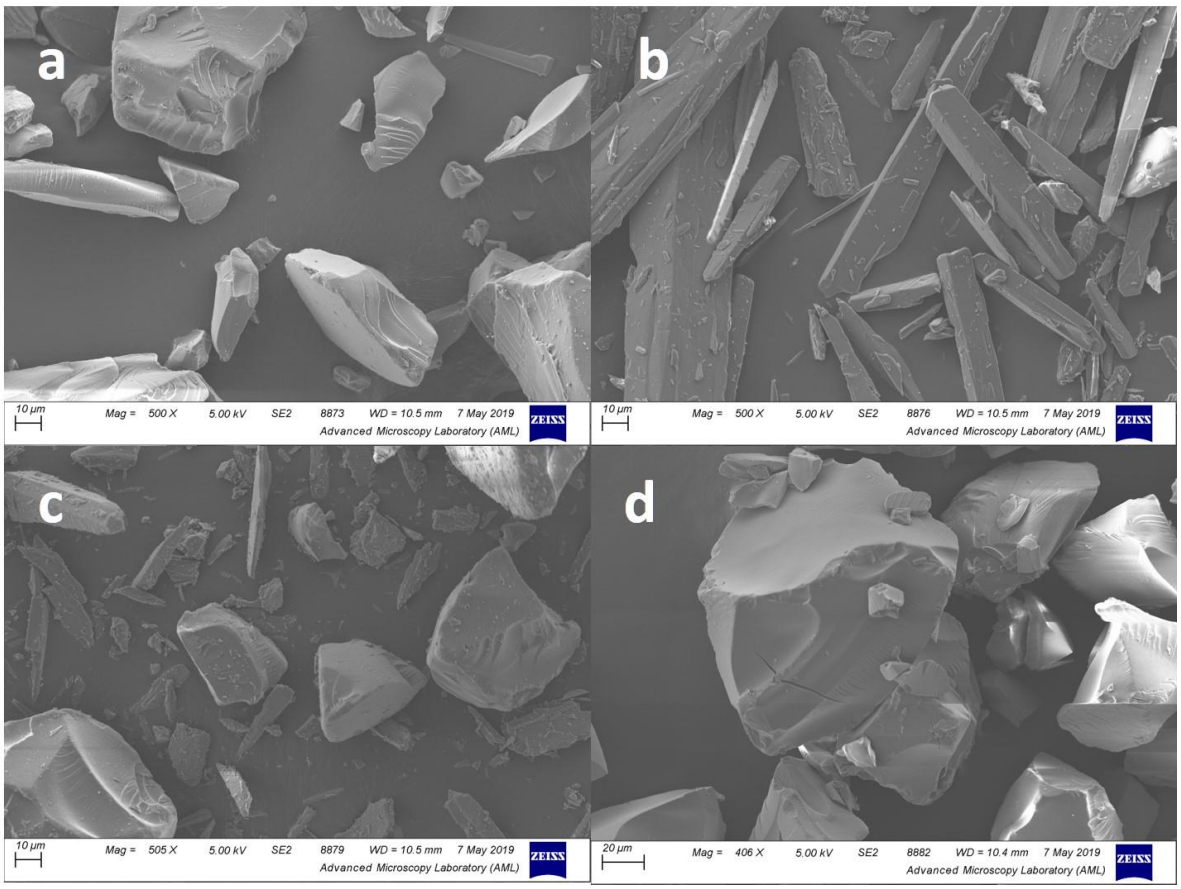

Figure 3.25. SEM images of a) IRP69 raw material, b) TZD HCl raw material, c) 1:1 (w/w) physical mixture of TZD HCl and IRP69, and d) DRC formed using 1:1 (w/w) D:R ratio ("unactivated" IRP69).

3.2.2.6.1 EDX Analysis (IRP69)

As another means to confirm drug loading, EDX analysis was undertaken on raw material, unloaded drug resin and DRC (Figures 3.26-3.28). These figures contain the quantitative and qualitative data regarding the atoms detected when a particular region of the sample was scanned. As chlorine is a unique atom to TZD and not found as part of the Amberlite™ IRP69 resin structure, EDX presented a further option to explore drug-resin binding. In this instance, the chlorine that is a substituent of one of the ring structures is of interest, as opposed to the chloride that forms the salt component (of TZD HCl). As the TZD HCl dissociates in an aqueous solution, generating protonated TZD and the salt ions (H^+ and Cl^-), the chloride ion that constitutes HCl should not be a confounding factor. Therefore, the chlorine atom can be considered an effective marker for indicating drug loading. The data presented in Figures 3.26-3.28 confirm the presence of chlorine in TZD HCl (Figure 3.26) and its absence in the resin raw material (Figure 3.27), which served as a control. Furthermore, it is evident from Figure 3.28 that chloride can be detected in the DRC.

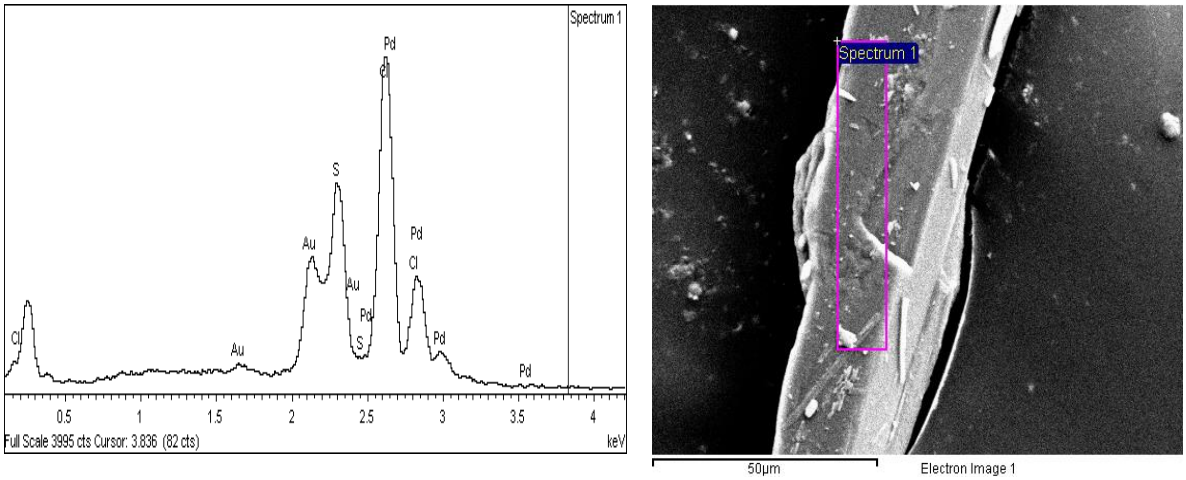

Figure 3.*26. EDX analysis of TZD HCl raw material.*

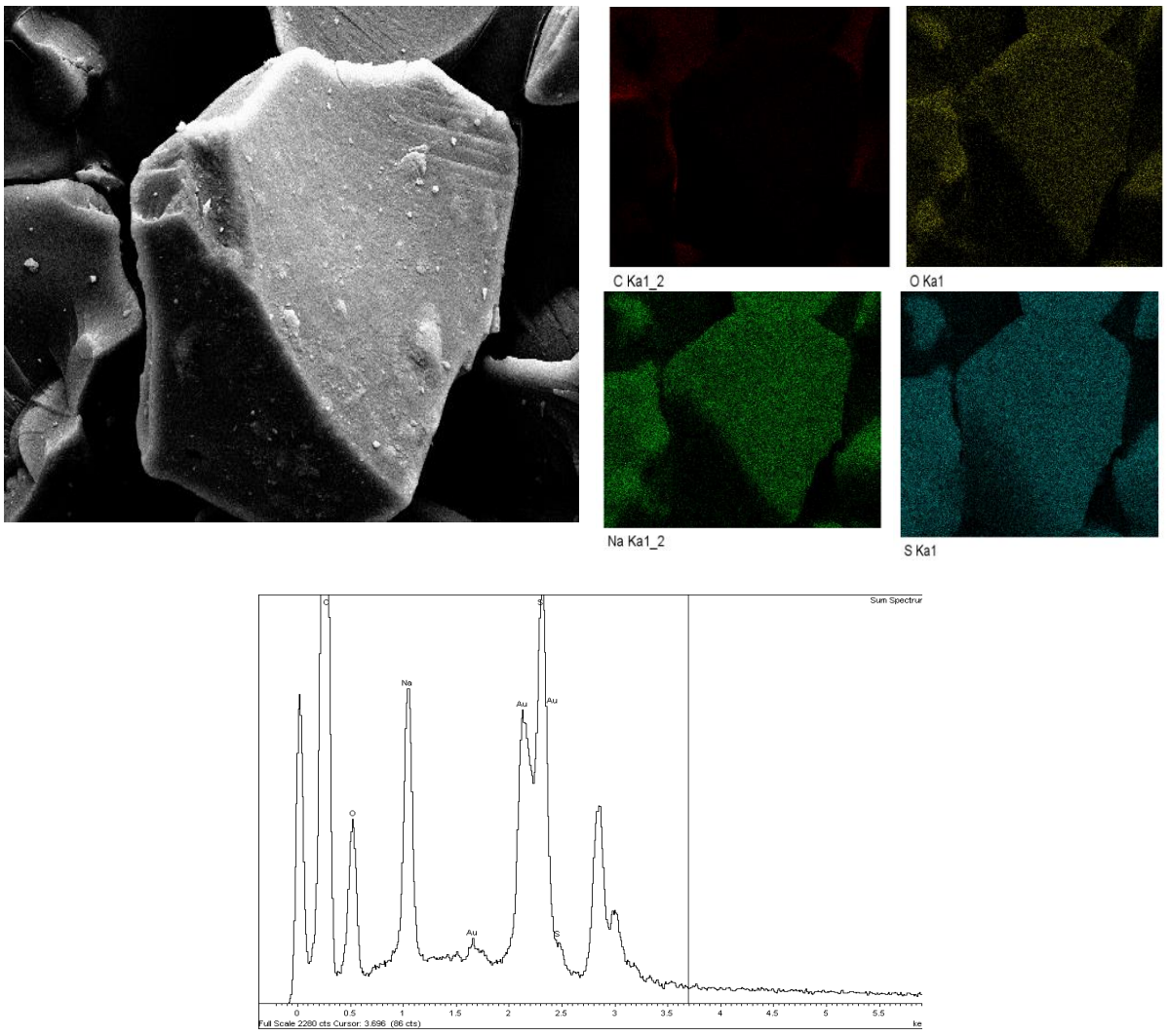

Figure 3.*27. EDX analysis of IRP69 raw material. The abundance of the specific atom within the structure is depicted by colour coverage with more coloured particles indicating a higher percentage*

of the atom in the sample. Red represents carbon, yellow represents oxygen, green represents sodium and blue represents sulfur.

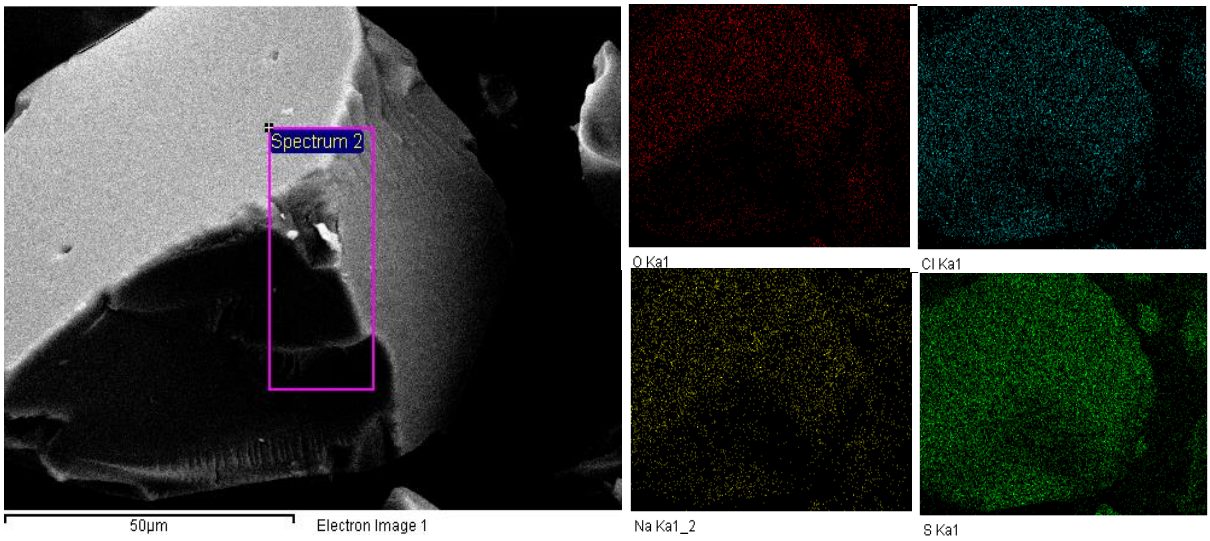

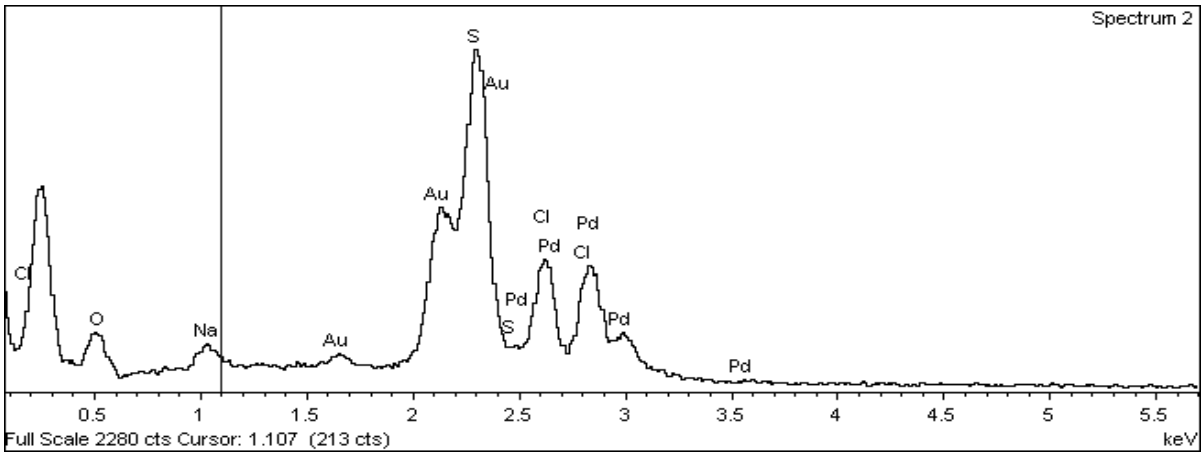

Figure 3.28. EDX analysis of DRC formed using 1:1 (w/w) D:R ratio ("unactivated" IRP69). The abundance of the specific atom within the structure is depicted by colour coverage with more coloured particles indicating a higher percentage of the atom in the sample. Red represents oxygen, yellow represents sodium, green represents sulfur and blue represents chlorine.

3.2.2.2 Production of DRCs using Amberlite™ IR120 (IR120)

As highlighted previously, Amberlite™ IR120 (IR120) is a non-pharmaceutical grade gel-type resin but it has a demonstrated history of use with APIs in a drug delivery context (88,309). As the IRP69 grade is produced by milling the larger sized IR120 grade, the latter is known as the parent resin of IRP69 (310), meaning that it is chemically similar despite the obvious difference in physical form. One

fundamental difference between it and the IRP69 grade pertains to the ion-exchange capacity (IEC), which is the theoretical number of exchangeable groups per unit volume or weight of the resin. This is a critical property that dictates the level of drug loading achievable and is lower for the bead form of the resin (IR120) in comparison to the powder form (IRP69), with a reported value of 2.28 mEq/g versus the powder's 4.3 mEq/g (111,309). This is not surprising as IR120 is a macroporous gel-type resin that has smaller pores and less surface area than the powdered resins (Table 3.11), two key attributes that contribute to the IEC. Moreover, these quoted IEC figures are ideal values and the actual value may be lower depending on the drug's individual properties.

Regarding the DRCs formed using the bead form of the resin, the surface area for the unloaded resin (raw material) does not differ statistically ($p>0.05$) from the loaded form (for the D:R ratio (1:2)) system), which is in contrast to the powdered systems (IRP69), where the DRCs have a lower surface area ($p<0.05$) relative to the resin raw material. Compared to the IRP69 grade, the spherical bead form possesses a lower ($p<0.05$) surface area, which is a consequence of the increased particle size and reduced surface irregularity compared to the IRP69 particles. Pore size values (Table 3.11) show that the pore size of the bead-type resin is reduced ($p<0.05$) relative to the powdered form. These findings are consistent with the description of the gel-type beads as microporous (as is IRP69) in nature and in agreement with literature values (311). This difference is a contributory factor to lower ion-exchange resin capacity of the bead type resin, as the drug is less likely to penetrate the interior of the resin structure, thereby rendering the functional groups in these regions less accessible. Post-loading, the pore size remains unaffected relative to those calculated for the raw materials ($p>0.05$). These calculated differences in pore size are not noticeable when the structures are examined by SEM (Figures 3.25 and 3.38). However, due to the average pore size of the pores (in the nanometer range) as determined by BET analysis, this is not surprising.

Table 3.11. Particle size (d_{50}), SSA and porosity values for DRCs formed using a 1:1 (IRP69) and 1:2 (IR120) D:R ratios (w/w) and resin raw material (IRP69 and IR120). Particle size was determined by laser diffraction as described in Chapter 2, section 2.2.7.1.2. SSA and porosity were determined as per the procedure detailed in Chapter 2, section 2.2.14. Prior to measurement, IR120 beads were dried as per the method specified in Chapter 2, section 2.2.1.2.4.1.

Sample	Particle Size (d_{50})	Specific Surface area (SSA) (m^2/g)	Pore size (nm)
IRP69 (unprocessed raw material)	52.67 ± 1.05	0.315 ± 0.010	1.97 ± 0.04
DRC 1:1 (IRP69)	66.56 ± 1.89	0.293 ± 0.020	1.99 ± 0.05
IR120 (dried)	621.67 ± 8.02	0.098 ± 0.007	1.19 ± 0.03
DRC 1:2 (IR120)	648.33 ± 5.69	0.091 ± 0.009	1.21 ± 0.03

When conducting drug loading studies, two main criteria (DAE and drug loading) which have been alluded to previously, are integral to defining the success of the loading process. Similar to what was observed with the powdered form of the resin, the DAE and drug loading values achieved were dependent on the ratio of drug to resin in the loading medium (Table 3.12). In contrast to the powdered resin, a 1:2 (w/w) D:R ratio proved to be optimal in terms of drug loading. In this instance, a higher proportion of resin relative to the drug (on a weight basis) essentially provides a higher supply of ionic sites available for binding, which translates into higher drug loading. If this optimum ratio is altered, one of the two criteria (drug loading or DAE) is negatively impacted, depending on what constituent is increased or decreased. The presence of excess drug relative to resin, as is the case with 3:1, 2:1 and 1:1 ratios (w/w), does not negatively impact the drug loading, evident from no statistical difference ($p>0.05$) between the loading values. Instead, as the D:R ratio increases, it is the DAE that decreases, which is not desirable from an economical point of view. On the flip side, the excess resin, which is present in the sample produced using a 1:3 ratio has a positive impact on the DAE. Instead, the drug loading value is reduced, as the system is essentially being diluted by increasing the number of saturated binding sites. Regarding the powder yield values, once the drug is not in excess, a value of at least 95% can be achieved which can be attributed to the relatively high drug loading coupled with the ease of collection afforded by the bead form.

Table 3.12. Drug loadings, DAEs and powder yields for DRCs prepared using altered loading conditions (concentration of the drug in the loading media and temperature of the loading media stated in the parentheses) and different D:R (IR120) ratios (w/w). The loading temperature was 20 °C and the concentration of the drug in the loading medium was 1 mg/mL unless otherwise stated. The methods for calculating drug loadings (% w/w) and DAE (%) are described in Chapter 2, section 2.2.11.1.

D:R ratio used to form DRC	Powder yield (%)	DAE (%)	Drug loading on DRC (% w/w)
3:1	7.32 ± 0.98	9.77 ± 0.29	16.12 ± 0.60
2:1	43.10 ± 1.49	14.66 ± 0.68	16.01 ± 0.22
1:1	63.82 ± 1.50	29.30 ± 1.04	16.07 ± 1.27
1:2	95.06 ± 0.38	89.00 ± 0.49	32.18 ± 1.56
1:3	99.90 ± 0.10	100.00 ± 0.03	19.09 ± 0.42
1:2 (30 °C)	94.89 ± 0.49	88.89 ± 0.49	32.08 ± 1.26
1:2 (40 °C)	95.12 ± 0.32	88.97 ± 0.39	32.05 ± 1.66
1:2 (5 mg/mL)	95.19 ± 0.49	89.45 ± 0.55	32.19 ± 1.03
1:2 (10 mg/mL)	95.09 ± 0.45	88.84 ± 0.20	32.08 ± 0.86

Considering the physical form of the resin and the level of drug loading achieved, this grade of resin was selected for further experiments with a view to prolonging the release of the API as it was particularly suited to the needs of the intended formulation strategy. Therefore, the D:R ratio of 1:2 was selected for further investigation.

The kinetics of the loading process were assessed similarly to the powdered systems (Figure 3.29). In comparison to several drug loading studies in the literature (110), the time to equilibrium was found to be relatively long (approximately 24 hours), again highlighting the individuality of the ion-exchange process. In a similar manner to what was observed with the powdered resin systems, the time to reach equilibrium increased as the proportion of resin in the system increased. These observations are in agreement with previous research by Deng et al., who assessed the thermodynamics of the binding process during the column and batch method of preparation (279). The rate of loading was relatively rapid for the bead in comparison to the powdered form of the resin, which may be a consequence of a combination of a lower ion-exchange capacity and increased particle size. The drug concentration in the starting solution (ranging from 1 mg/mL-10 mg/mL) had no appreciable effect on the extent of loading (Table 3.12). Stemming from this experimental finding, the most concentrated solution (10 mg/mL) was used for future work, discussed in Chapter 5. Intuitively, the more concentrated loading solution would translate to more efficient experimentation enabling the more rapid production of DRC material.

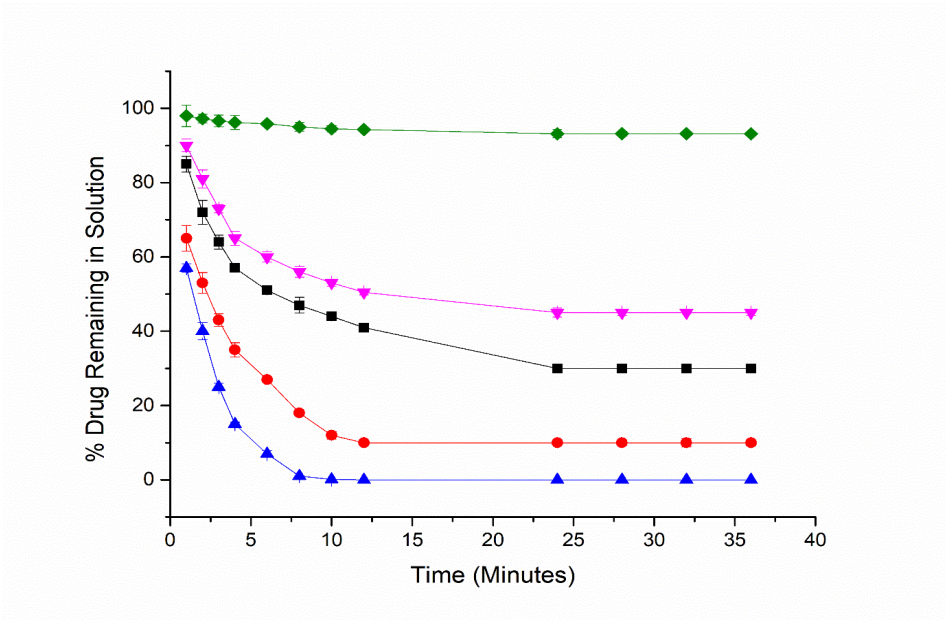

Figure 3.*29. Equilibration profile showing the loading of TZD HCl onto IR120 using different D:R ratios (w/w) over 36 hours at room temperature. 3:1 (Olive diamond), 2:1 (Magenta inverted triangle), 1:1 (Black square), 1:2 (Red circle), and 1:3 (Blue triangle).*

The effect of temperature was probed (Figure 3.30) and was shown to have little to no impact on drug loading, DAE or the loading kinetics. The temperature has been reported to impact the resin structure in a manner that renders it more accessible to drug ions through its ability to affect swelling, thus facilitating the diffusion process (119). However, the lack of demonstrated impact of an increase in temperature suggests the exchange of ions on the surface of the resin is the dominant process. From the perspective of manufacturing, the use of room temperature is convenient as no additional temperature modifications are required to ensure the process is optimised.

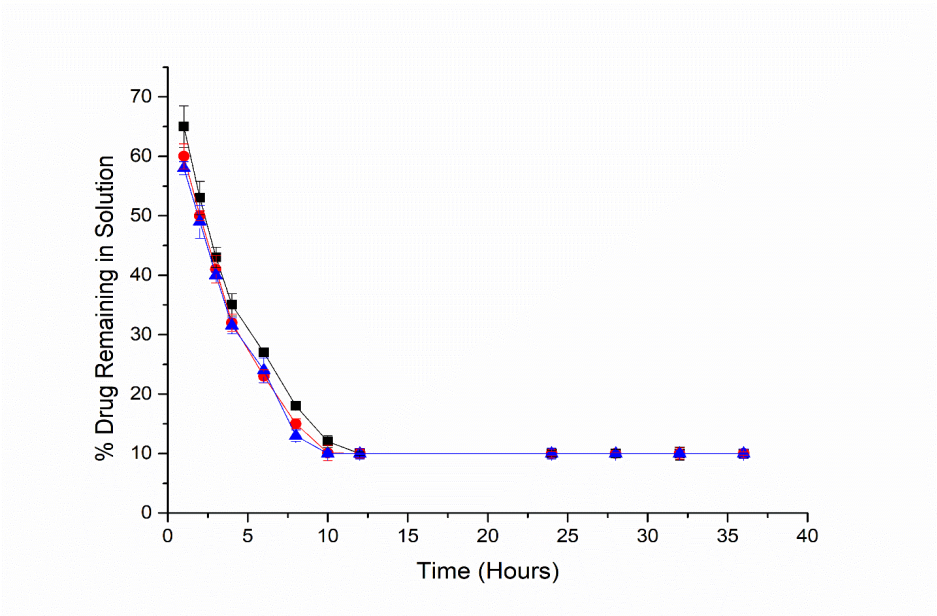

Figure 3.*30. Equilibration profile showing the loading of TZD HCl onto IR120 using a 1:2 D:R ratio (w/w) over 36 hours at various loading temperatures. 20 °C (Black square), 30 °C (Red circle), and 40 °C (Blue triangle).*

A similar optimisation of the assay procedure to that described for the IRP69-based DRCs was performed, albeit two elution temperatures were investigated rather than three. The results are listed in Table 6 in Appendix 1 and the main relationships between the variables are depicted graphically in Figures 3.31-3.32. Akin to the IRP69 findings, the complex concentration in the elution medium is the predominant influence on the calculated % drug loadings, with more concentrated systems yielding lower % drug loadings. This factor significantly outweighs the influence of the ionic strength of the medium on the determined drug loadings, in addition to the statistically insignificant effect of elution temperature. These trends are also applicable to the NaCl studies, thereby signalling that high volumes of an acidic or salt solution are sufficient to displace the maximum amount of drug from the bead-type resin. As discussed previously with the IRP69 systems, it is surmised that the effect on drug displacement of the high volume of elution medium may be two-fold. Firstly, the mean amount of ions in the medium is higher relative to a solution with a lower volume and identical ionic strength. Secondly and more interestingly, the higher volume of liquid, which consists predominantly of DI H_20 may hydrate the resin to such an extent that it facilitates the elution of ions which otherwise would remain embedded deep within the resin matrix and lead to lower calculated drug loadings.

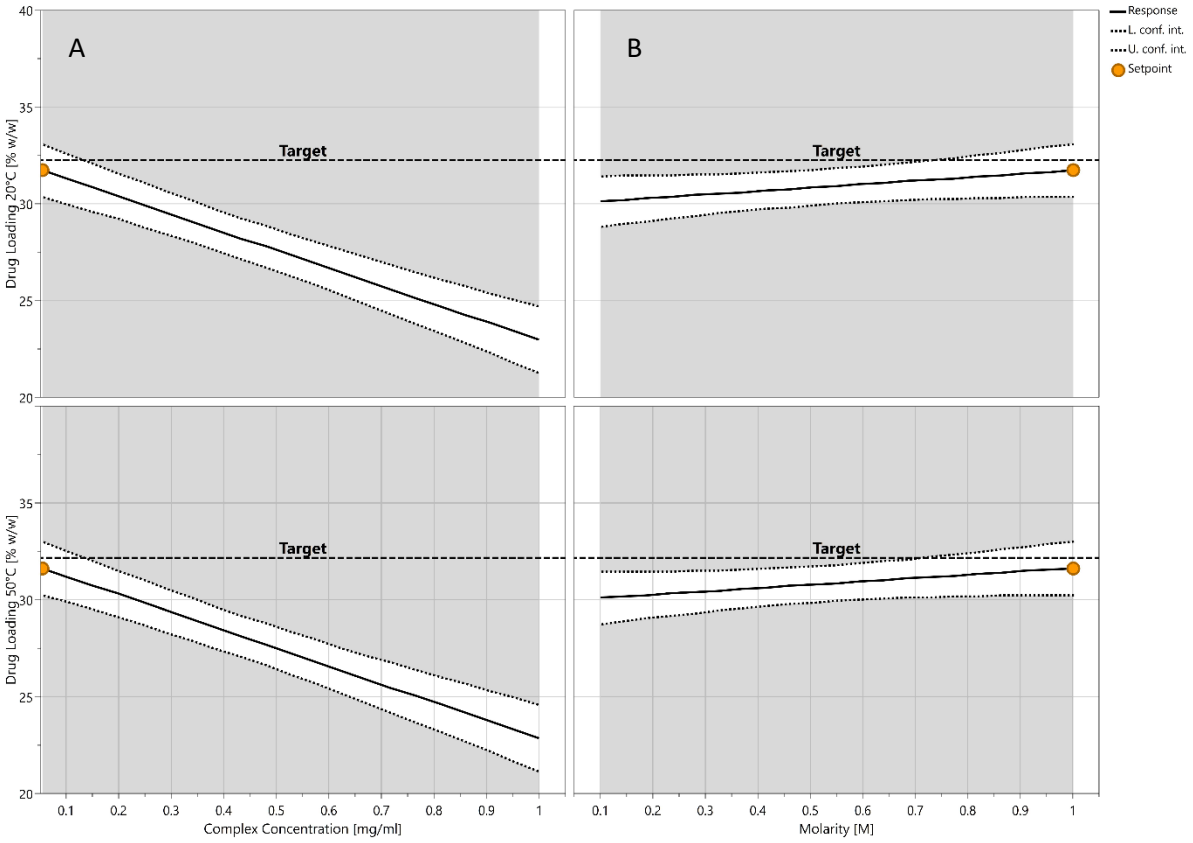

Figure 3.*31. Plot of drug loading (% w/w) versus (A) Complex (IR120) concentration (mg/mL) and (B) Molarity (M) at 20 °C and 50 °C when altering the elution medium temperature (20 °C, 37 °C and 50 °C) which comprises of HCl.*

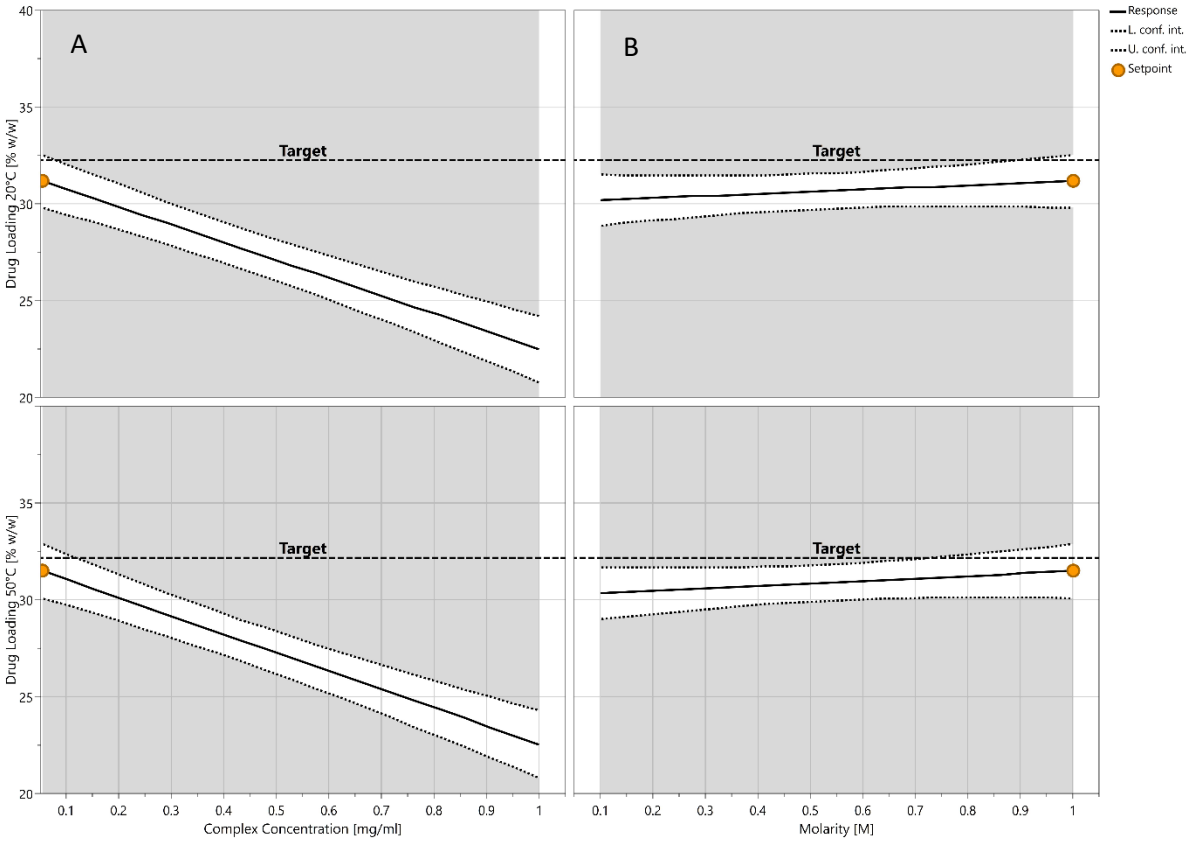

Figure 3.*32. Plot of drug loading (% w/w) versus (A) Complex (IR120) concentration (mg/mL) and (B) Molarity (M) at 20 °C and 50 °C when altering the elution medium temperature (20 °C, 37 °C and 50 °C) which here comprises of NaCl.*

3.2.2.2.1 Solid-State characterisation (IR120)

Similar to the DRCs produced using the IRP69, DSC and pXRD analyses revealed that the complexes formed using IR120 do not contain crystalline material. The diffractograms of the DRCs prepared at various D:R ratios are characterised by a halo pattern, suggestive of the drug being amorphised post-loading onto the resin (Figure 3.33). This assertion is supported by the thermal data (Figure 3.34), in which the DSC traces display no melt endotherm representative of crystalline material. The diffractograms of physical mixtures of TZD HCl and IR120 prepared (covering the lower end of the range of drug loadings (15-40%) determined for the DRCs) further support the assertion that amorphisation of the API has taken place when loaded onto the DRC, as distinct Bragg peaks are evident in the diffractograms (Figure 3.33). Analogous to the solid-state characterisation results reported for the IRP69 systems, several modifications made to the loading process, did not impact the solid form of the DRCs, as all DRCs lacked crystalline material. This is evident from the absence of Bragg peaks in the diffractograms and no visible melt endotherms in the DSC traces of all samples. More specifically, the pXRD diffractograms and DSC thermograms depicted in Figures 3.35-3.36, show that

varying temperature of the loading medium and concentration of drug in solution does not influence the solid-state of the DRC produced.

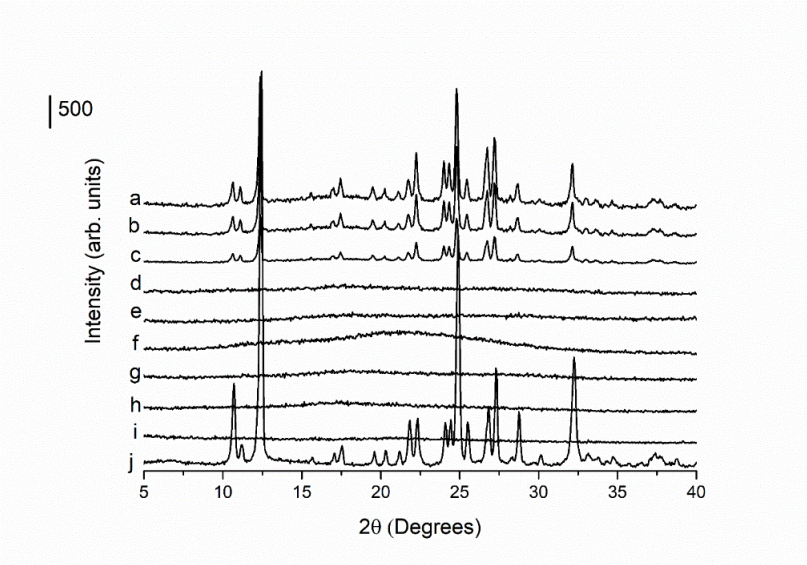

Figure 3.*33. pXRD diffractograms of raw materials, physical mixtures of drug and IR120 (PM) and DRCs formed using varying ratios (w/w) of drug to IR120. a) PM (40:60), b) PM (30:70), c) PM (15:85), d) DRC (3:1), e) DRC (2:1), f) DRC (1:1), g) DRC (1:2), h) DRC (1:3), i) IR120 raw material and j) TZD HCl raw material.*

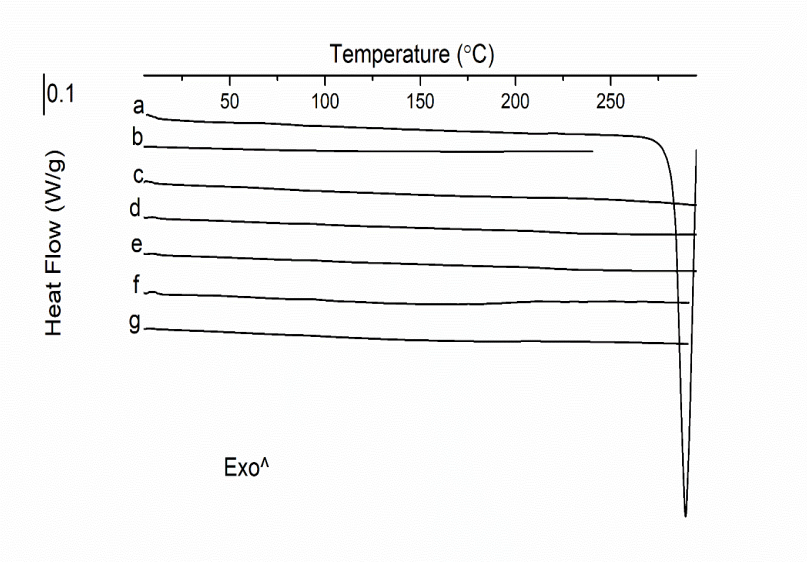

Figure 3.*34. DSC thermograms of raw materials and DRCs formed using varying ratios (w/w) of drug to IR120. a) TZD HCl raw material, b) IR120 raw material, c) DRC (3:1), d) DRC (2:1), e) DRC (1:1), f) DRC (1:2) and g) DRC (1:3).*

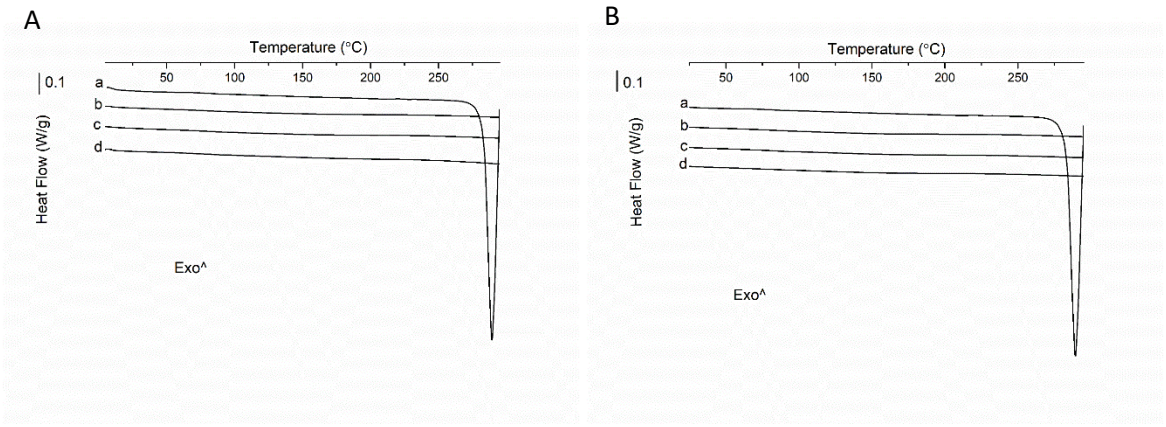

Figure 3.35. *DSC thermograms of the raw materials and DRCs produced using a 1:2 D:R (IR120) ratio (w/w) using different drug concentrations in loading solution and different loading temperatures. A loading temperature of 20 °C and a drug concentration of 1 mg/mL was used unless otherwise stated. A) a) TZD HCl raw material, b) DRC (1 mg/mL), c) DRC (5 mg/mL) d) DRC (10 mg/mL). B) a) DRC (20 °C), b) DRC (30 °C) and c) DRC (40 °C).*

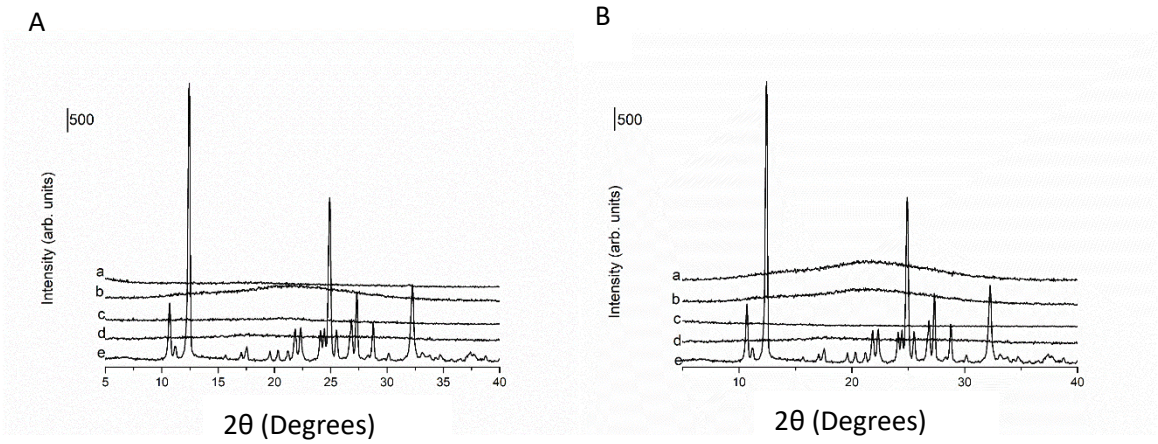

Figure 3.36. *pXRD diffractograms of the raw materials and DRCs produced using a 1:2 D:R (IR120) ratio (w/w) using different drug concentrations in loading solution and different loading temperatures. A loading temperature of 20 °C and a drug concentration of 1 mg/mL was used unless otherwise stated. A) a) DRC (1 mg/mL, b) DRC (5 mg/mL), c) DRC (10 mg/mL), d) IR120 raw material, e) TZD HCl raw material, B) a) DRC (20 °C), b) DRC (30 °C), c) DRC (40 °C), d) IR120 raw material and e) TZD HCl raw material.*

TGA analysis (Figure 3.37), supported the assertion that complexation has occurred between the API and resin. Similar to the complex formed using IRP69, the onset of drug degradation is delayed relative to the pure crystalline material. Again, it can be surmised that once the drug binds to the resin to form the DRC, the latter confers a thermal protective effect, reflected by the higher temperature needed to initiate thermal degradation.

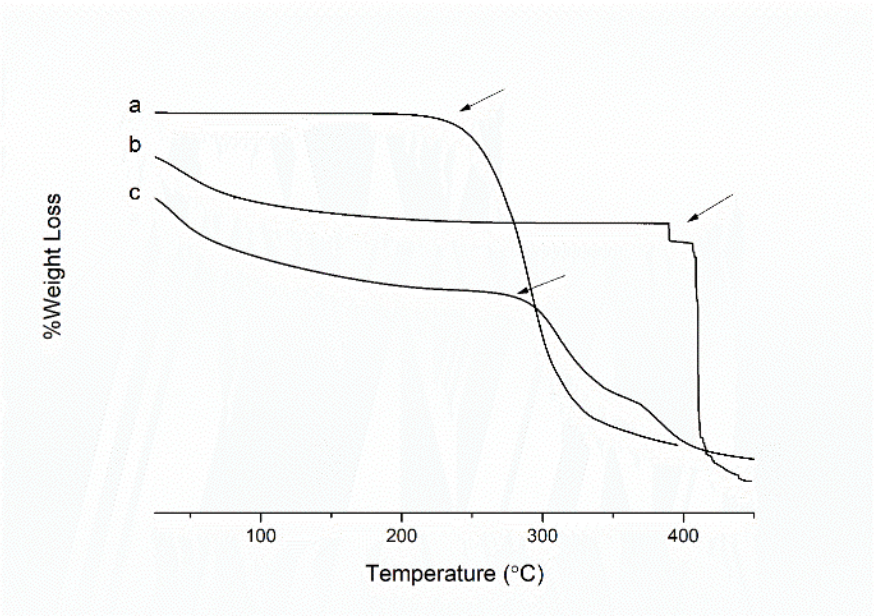

Figure 3.*37. TGA thermograms of a) TZD HCl raw material, b) IR120 raw material and c) DRC formed using a 1:1 D:R (IR120) ratio (w/w).*

In contrast to the powdered DRC, optical microscopy analysis produced inconclusive results when the bead-type DRC was examined using polarised light (Figure 5 in Appendix 1). The quality of the image produced is poor, which can be attributed to the size of the beads, which are not appropriate candidates for splitting, a potential measure that could have yielded more conclusive results. Therefore, this technique was not used to further characterise the material.

3.2.2.2.2 SEM (IR120)

Scanning electron micrographs of the drug-loaded beads are depicted in Figure 3.38. In contrast to the powdered resins, no major irregularities regarding particle shape are evident and the particles can be classed as spherical. The surface is characterised by dimples with little evidence of well-defined pores, similar to the powdered resin. Small defects in the structure are evident that may be a consequence of insufficient mechanical strength to withstand the batch process. These findings are in agreement with the literature where similar defects in DRC structures could be observed (110).

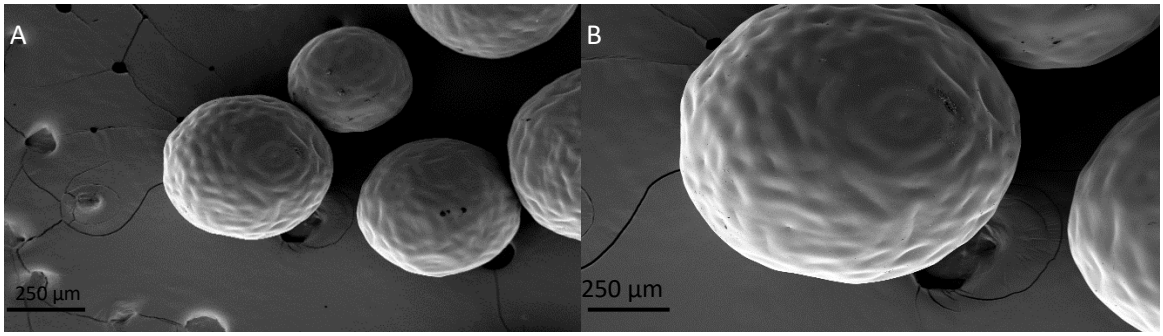

Figure 3.*38. SEM images at different magnifications of DRC formed using a 1:1 D:R (IRP69) ratio (w/w). A) x100 and B) x250.*

3.2.2.2.3 Drug release studies (IR120)

The drug release profiles of the DRCs formed using the resin in bead form are displayed in Figure 3.39. Two DRCs (1:2 and 1:3) were selected to study in 0.1 M HCl, pH 6.8 buffer and DI H_2O on the basis that they differed in their drug loadings (32.18% and 19.09%). The first DRC selected was the optimised complex, i.e. the 1:2 system, which exhibited rapid drug release upon contact with the ionic media. Similar to the dissolution behaviour of the powdered DRCs, the release profile of the system was independent of pH. Approximately 92.6 ± 0.6% and 94.4 ± 1.6% were released after 5 minutes in pH 6.8 buffer and 0.1 M HCl respectively ($p>0.05$). The time to equilibrium was approximately 60 minutes in pH 6.8 buffer, but considerably shorter in acidic medium (30 minutes), yet the DRC achieved complete drug release in both media types, indicating that there was sufficient ionic strength to displace the drug from the resin.

When comparing the drug release profiles from the bead systems to the powdered complexes, a distinct difference in the drug release behaviour of the 1:3 DRC is evident. The release of drug from the 1:3 bead system is suppressed to a large extent, conferring a sustained-release effect, typified by 13.8 ± 1.7% and 24.8 ± 1.7 % of the drug being released after 5 minutes in 0.1 M HCl and pH 6.8 buffer respectively. A consequence of this low level of drug release in the initial stages, which is followed by the tempered release of the drug, is that no clear equilibrium is reached. As mentioned previously, this equilibrium stage is characterised by the distinctive plateau, which is not present in the drug release profiles of the 1:3 DRCs, although the DRCs do start to approach complete drug release towards the end of the study.

The disparity between the drug release behaviour between the two systems studied indicates that the DRCs formed using the bead type does not follow the general trend established with the powdered DRCs. In contrast to the powdered systems, the complexes containing lower drug loadings do not reach equilibrium quicker, as well as not being able to release the entirety of the drug-loaded onto the resin. The magnitude of the difference between the two systems studied is what differentiates

this DRC formed using the bead type behaviour from what was observed previously. A possible factor contributing to the discrepancy between the DRCs formed using the bead form of the resin and the powdered form is the inherent structural differences between the two physical forms of the resin, which impacts the particle size of the DRC and drug loading achievable. These properties, in turn, can influence many other facets of the ion-exchange process and the interplay between factors is what ultimately governs the release profile of the DRC.

A second prominent feature of the drug release profiles (1:3 systems) is the noticeable difference in the drug release rate in the two ionic media studied. Comparing the drug release behaviour in 0.1 M HCl versus pH 6.8 buffer, at each time point studied, the DRC releases a lower quantity of drug in 0.1 M HCl versus pH 6.8 buffer ($p<0.05$), with the exception of the final time point studied. A plausible reason for these observations is the higher ionic strength of the pH 6.8 buffer media (140 mEq) relative to the 0.1 M HCl (98 mEq). The former contains a higher concentration of cations, the type of ion needed to effect drug release and the relationship between a higher ionic strength and an increased drug release rate is well documented. Considering the results previously discussed relating to the 1:2 ratio and the powdered DRCs, it is likely that a multitude of reasons are responsible for the release profile observed, ranging from ionic strength to ion type to drug loading level, further highlighting the unpredictable release behaviour of IER-based systems.

In line with all DRC samples studied to date, both samples released minimal drug in DI H_2O. This type of medium lacks the ions necessary to enable an ion-exchange reaction to occur, thus minimising the likelihood of drug leaching. Although the 1:3 DRC affords far greater control on the release of the drug from the DRC in ionic media, compared to the 1:2 DRC, the latter was selected for further study. Despite the system being a far less promising candidate from a sustained-release perspective, as it imparts an insufficient level of control, it does retain the ability to load a higher quantity of the drug, which is important if one wants to minimise the quantity of resin in a suspension formulation. This can be beneficial in terms of avoiding a gritty tasting sensation, linked to the particle size of the microparticles, which can adversely affect patient compliance. Lastly, it provides more scope for investigating the impact of including a rate-controlling polymer on the drug release, which is one of the primary aims of Chapter 5.

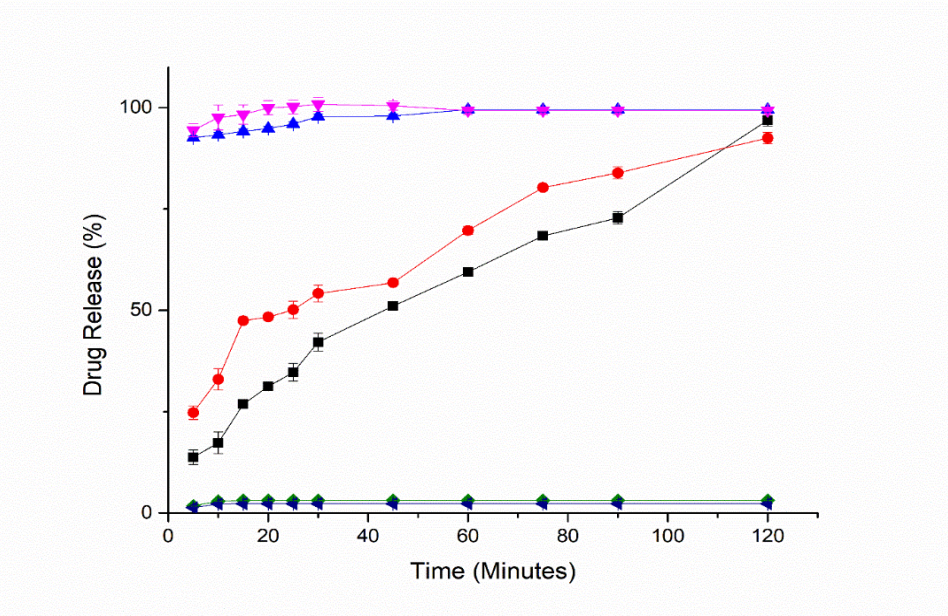

Figure 3.*39. Drug release profiles in either 0.1 M HCl or DI H_2O at 37 °C, of DRCs formed using varying D:R (IR120) (w/w) ratios. DRC (1:2) in 0.1 M HCl (Magenta inverted triangle), DRC (1:2) in pH 6.8 buffer (Blue triangle), DRC (1:2) in DI H_2O (Navy triangle), DRC (1:3) in 0.1 M HCl (Black square), DRC (1:3) in pH 6.8 buffer (Red circle) and DRC (1:3) in DI H_2O (Olive diamond).*

3.2.2.2.4 Raman spectroscopy (IRP69 and IR120)

Raman spectroscopy was employed to probe the binding of TZD to the resin, due to its known capabilities to qualitatively analyse systems formed by complexations (312). During the analysis, it became apparent that the resin, and by extension the DRCs, were not ideally suited to Raman analysis. This was due to the occurrence of luminescence in the form of fluorescence. The signal produced by fluorescence typically dwarfs that of the Raman scattering, thus making it difficult to analyse the spectra. For the purposes of qualitative analysis, background subtraction was performed, which enabled distinct drug peaks to be identified at 1530 cm^{-1}, 1410 cm^{-1} and 1350 cm^{-1} (highlighted by the red boxes) thus confirming the presence of TZD on the resin (Figure 3.40). These aforementioned peaks are more intense in the powdered DRCs relative to the bead form, perhaps reflective of the increased quantity of drug loaded onto the powdered resin.

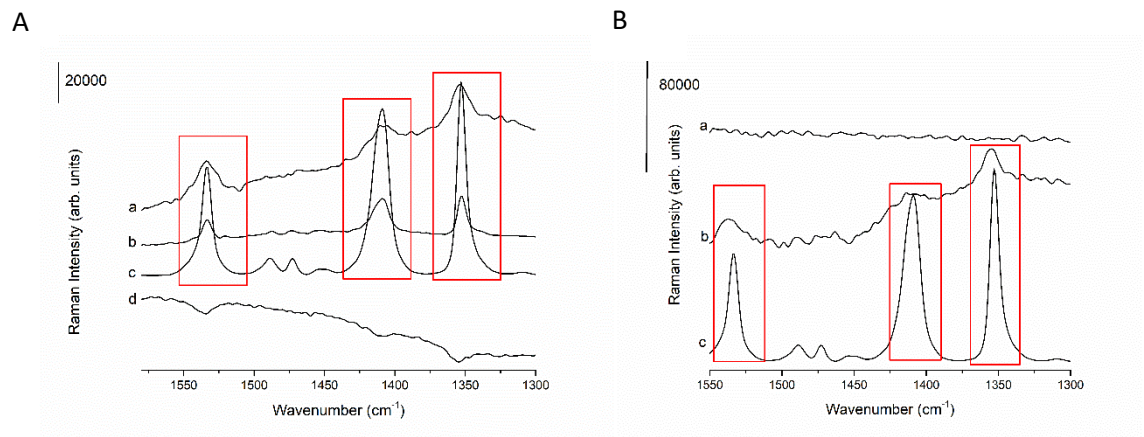

Figure 3.*40. A) Raman spectra of a) DRC formed using a 1:1 (w/w) D:R ratio ("unactivated" IRP69), b) physical mixture (1:1 w/w) of drug and resin ("unactivated" IRP69), c) TZD HCl raw material and d) IRP69 raw material. B) Raman spectra of a) IR120 raw material, b) DRC formed using a 1:2 (w/w) D:R ratio ("unactivated" IR120), and c) TZD HCl raw material.*

3.3 Conclusion

The drug-resin binding studies using the batch process produced results with a mixed level of success, depending on the particular API in question. Ultimately, the trials involving MTZ were deemed unsuccessful, based on a combination of disappointedly low drug loading figures and rapid drug release in DI water. Considering the high dose requirement of MTZ, coupled with drug loading achieved and the undesirably high drug release in DI H_2O, this formulation option was not pursued further. The complexes formed using the second drug investigated, TZD HCl, were the best performing DRCs in all aspects, including drug loading to drug release behaviour. These findings enabled extensive solid-state characterisation on a variety of complexes to be conducted and other aspects of the drug-loading process to be explored, such as the use of a sulfonic acid-containing resin in an alternative physical form (bead rather than powder). Successful complexation between the drug and the bead form of the resin was achieved and notable differences in the properties of the resultant DRCs were ascribed to the inherent differences in the resin structure. Two Design of experiments (DoE) were performed to identify the optimum parameters to develop an efficient drug displacement assay method. Based on the obtained results, the TZD HCl complexes, using either form of resin (powder or bead) were formed by robust ion-exchange interactions; however, to sustain the release of the drug for the required period, the application of a rate-controlling polymer coating is necessary.

Chapter 4:

An investigation into alternative grades of acidic ion-exchange resins (IRP64 and IRP88) and the utility of the spray-drying technique to form drug-resin complexes comprising Tizanidine Hydrochloride and IRP69

4.1 Introduction

To further explore the relationship between TZD and IERs, another class of commonly used IERs were investigated, classified as “weak” cation exchangers, which can be ascribed to their “weak” acid functionality. In contrast to the resins already studied as part of Chapter 3, the dissociation properties are dependent on the pH of the environment in which they are placed (104,106). As part of a series of loading studies, the two specific grades selected were Amberlite™ IRP64 (IRP64) and Amberlite™ IRP88 (IRP88), with both of these resins having an established reputation in the field of drug delivery (82,129,313). Their primary purpose is to serve as taste-masking agents, which will protect the drug within the salivary contents of the mouth but will release the drug rapidly upon exposure to the acidic contents of the stomach (141,314).

The two grades selected differ based on the counterion attached to the carboxylic group, which is the functional group that confers “weak” acidity. Thus, these IERs behave similar to “weak” organic acids, with solution pH dictating the degree of dissociation. On the backbone of the IRP88 grade, are potassium carboxylate groups, whereas the IRP64 grade contains carboxylic acid groups along the polymeric backbone. Both grades display good ion-exchange capacity in neutral or basic environments, which can be attributed to their pH dependence. Their ability to exchange ions below a pH value of 6, contrasts with their higher loading capabilities in higher pH environments, thereby signalling their potential to be used as taste-masking agents, as the desorption behaviour of complexed API is expected to exhibit similar pH-dependence (314). Similar to the “strong” cation exchangers investigated in Chapter 3, the solid-state properties of the “weak resins” and the associated drug-resin complexes (DRCs) have not been extensively explored which offered another avenue to pursue in this project.

The second arm of this work explored the possibility of using the spray-drying technique to formulate DRCs using Amberlite™ IRP69, which remains a relatively under investigated topic (94,220). Compared to the filtration and drying processes involved in the more conventional batch processing method, the production of DRCs using the rapid spray-drying technique requires a more systematic approach (315). This is due to the increased complexity associated with the process, rather than the “trial and error” methodology used to study the batch process for producing DRCs. Furthermore, the Quality by Design (QbD) philosophy has usurped “trial and error” methodology and has been largely incorporated into everyday thinking within the pharmaceutical industry. Through the implementation of statistical methods for the design and interpretation of experiments, critical quality attributes (CQAs) are readily identified. This forms the basis for DoE approaches and response surface methodologies, which are the main tools in scientists’ armoury that enable them to implement these QbD principles, to help establish the relationship between the factors affecting a process and the output of that process (316).

Among the limited number of studies available that report spray-drying as a feasible approach to form DRCs, Verma et al. availed of the DoE approach to design their experiments, providing precedence for the methodology reported in this work (220). For the screening studies in the current work, a Taguchi design was selected to help identify the key critical process variables, which have a significant effect on the responses of interest/critical quality attributes (CQAs) and avoid unnecessary experiments by testing combinations of pairs rather than every single possibility (317). Therefore, the DoE approach was favoured over the more traditional "trial and error" methodology and selected as the most favourable approach to pursue.

The final strand of the work in this chapter focuses on a variety of different areas emanating from the studies performed up to that point. The primary focus of this work was the investigation of the solid-state properties and moisture sorption tendencies of the API, as information is scarce regarding both aspects with respect to TZD HCl. Moreover, acquiring this information could enable further understanding of the DRCs' solid-state properties and moisture sorption tendencies, as they are not well understood and scarcely reported on. A flow chart diagram shown in figure 4.1 indicates the series of sequential steps performed in this chapter. The purpose of which is to aid the reader in understanding the different strands of work reported in this chapter.

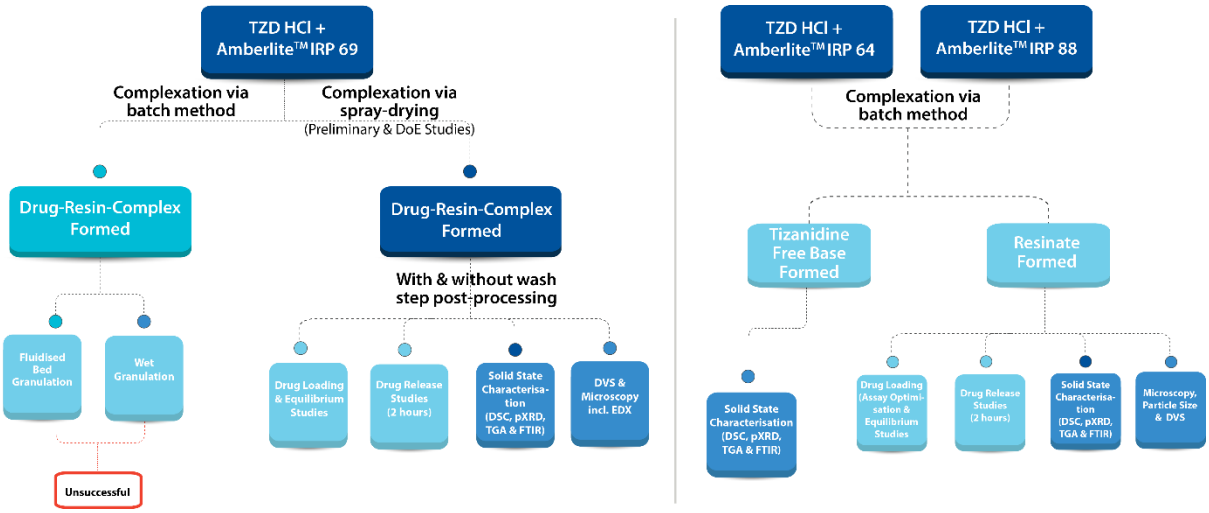

Figure 4.1. Flow chart outlining the series of sequential steps constituting the experimental progress in chapter 4.

4.2 Results and Discussion

4.2.1 Drug loading studies (IRP64 and IRP88)

The drug loading studies performed using both powdered resin grades proved to be markedly more challenging, despite these resins having reportedly larger ion-exchange capacities (approximately 10 mEq/g), compared to the "strong" resin in the powder form (IRP69) investigated previously (5 mEq/g) (Chapter 3). The impact of the ratio of drug to resin (D:R)(2:1, 1:1 and 1:2 w/w) on drug loading was explored in a comparable manner to the "strong" cation exchangers, with the drug loading results shown in Figure 4.2. More comprehensive details including the DAE and % powder yield are listed in Table 4.1. Initial trials using either grade of resin (1:1 ratio), where the loading pH was unadjusted (0.1% w/v drug concentration was used and the drug loading solution had a pH value of 4.32), produced DRCs with drug loadings that were significantly ($p<0.05$) lower than those reported in Chapter 3. This was a surprising finding, as "weak" cation exchangers are known to have higher ion-exchange capacity values, relative to their "strong" resin counterparts which is attributed to the carboxylic acid functional group providing little steric hindrance relative to more bulky ionic substituents (95). An increased loading capacity would be expected to manifest in a higher drug loading value, but on this occasion, the loading results pointed to the process requiring refinement. As is evident from Figure 4.2, DRCs formed using IRP64 displayed the highest drug loading values ($p<0.05$), when a lower D:R ratio (1:2) was used in the loading medium. Moreover, no statistical difference ($p>0.05$) in the calculated drug loadings was found when the 2:1 (D:R) ratio was compared to the 1:1 ratio. This was a surprising result considering the known higher ion-exchange capacity of "weak exchangers", pointing to the need to further investigate the interaction between drug and resin. Evident from the data presented in Table 4.1 is the detrimental impact of increasing the D:R ratio on the DAE, which inevitably translates to a reduced % powder yield too. On the basis of the % drug loading results, it is apparent that an excess of resin relative to the drug on a w/w basis, facilitates increased levels of drug binding, whether that be via ion-exchange or a physical adsorption mechanism.

In the case of the DRCs formed using IRP88, the drug loading studies indicate that a 2:1 or 1:1 (w/w) D:R ratio in the loading solution produces resinates with higher drug loadings ($p<0.05$) compared to the 1:2 ratio, with the excess resin present in the latter resulting in a reduced drug loading. No statistical difference ($p>0.05$) in drug loading was found between the 2:1 and 1:1 ratio indicative of all the ion-exchange sites being saturated. However, significant differences in the DAE were evident, as shown in Table 4.2. Considerable drug wastage is apparent when the 2:1 ratio is used, which is undesirable from a process development perspective, especially considering no statistically significant increase ($p>0.05$) in drug loading is achieved. This reduced DAE value invariably affects the powder

yield (%), which is also dramatically lowered when the 2:1 ratio is compared to the 1:1 sample. When each ratio of drug to resin was examined, a comparison of the drug loading results for the DRC produced using both grades of resin highlighted major differences in the quantity of drug loaded onto the resin for the different grades. This observation applies to the DRCs formed using the 2:1 and 1:1 ratios, with DRCs made using IRP88 resin having approximately double the drug loading compared to DRCs produced using the IRP64 grade. The 1:2 ratio was an exception, where the loadings do differ for the two resin grades ($p<0.05$), but the disparity in drug loadings is not large, underlining the need to further investigate the interaction of drug and resin using a multitude of techniques.

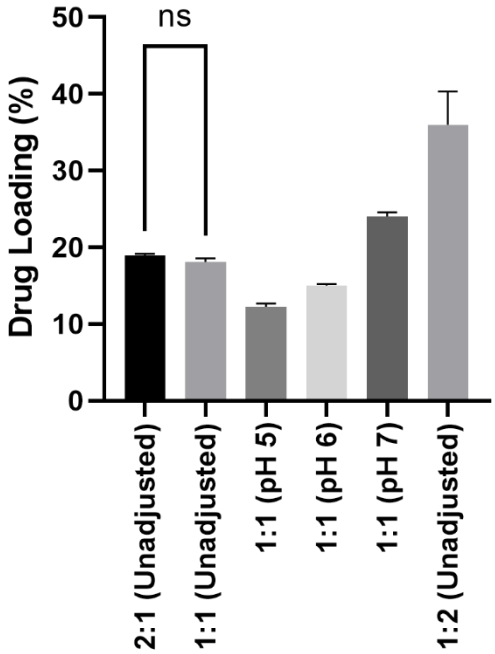

Figure 4.2. Calculated drug loadings for DRCs formed using a variety of D:R ratios (w/w) (using IRP64) with and without pH adjustment of the drug loading solution (0.1% w/v) prior to the addition of resin. ns signifies not statistically significant.

Table 4.1. Comparison of the effect of different D:R ratios (w/w) produced (using IRP64) without pH adjustment of the drug loading solution prior to the addition of resin on the powder yield (%), DAE (%) and the drug loading (% w/w). The methods for calculating the drug loading (% w/w) and DAE (%) values are described in Chapter 2, section. 2.2.11.1.

D:R ratio (IRP64)	Powder yield (%)	DAE (%)	Drug loading on the DRC (% w/w)
2:1	30.21 ± 1.38	44.10 ± 0.41	19.86 ± 0.48
1:1	80.23 ± 1.04	88.00 ± 0.56	19.29 ± 0.79
1:2	95.09 ± 0.39	97.46 ± 0.68	37.46 ± 0.43

Table 4.2. Comparison of the effect of different D:R (IRP88) ratios (w/w) produced without pH adjustment of the drug loading solution prior to the addition of resin on the powder yield (%), DAE (%) and the drug loading (% w/w).

D:R ratio (IRP88)	Powder yield (%)	DAE (%)	Drug loading on the DRC (% w/w)
2:1	47.9 ± 0.95	48.26 ± 0.31	48.34 ± 0.58
1:1	95.8 ± 0.35	96.52 ± 0.78	48.29 ± 0.39
1:2	93.4 ± 0.57	99.46 ± 0.98	35.69 ± 0.59

The assay method for the DRCs produced using IRP64 was developed in a similar methodical manner to that described in Chapter 3. As part of the experimental design, a broad range of factors were selected that are known to influence the desorption process. The assay results obtained using a selection of different assay conditions are listed in Table 4.3. Results from the NaCl studies show lower amounts ($p<0.05$) of drug detected compared to when HCl is used as the elution medium. Similar to sulfonic acid containing systems, the concentration of complex in the elution medium is a critical factor, with higher ($p<0.05$) loadings detectable, the more dilute the sample tested. This general trend is observed across all ionic strengths of the acidic and salt solutions studied, irrespective of the reaction temperature, a variable that can be manipulated to increase the level of drug displacement, which is evident in this work. This difference in the ability to displace drug is in agreement with the results reported by many groups, who all demonstrated the potential of weak carboxylic acid-based DRCs to prevent drug release at high pH values, similar to those found in the oral cavity, thus providing a potential taste-masking effect (318,319).

The disparity in elution behaviour between the NaCl and HCl elution media can be explained on the basis of pH dependence. At low pH values, the resin is in an unionised state, meaning that the drug is liberated rapidly, but at pH values approaching 6 and higher, it exists in the ionised state meaning that the integrity of the DRC is more stable. This behaviour contrasts with the strong ion-exchangers studied in Chapter 3, which produce DRCs whose loading and release characteristics are independent of pH conditions. One important thing to note is that the nature of the assay studies differs from the drug release studies presented, as they are considerably longer in duration, thus explaining the substantial quantity of drug detected. As alluded to previously, it is generally accepted that higher drug loading values are achievable using “weakly” acidic resins relative to those classed as “strongly” acidic, a consequence of the differences in the ion-exchange capacity, which is in turn dependent on the IERs structure. Interestingly, by comparing the drug loadings achieved using the powdered resins (“weak” and “strong”), evidence of lower drug loadings achieved using the “weak” resins (IRP64) is apparent for certain D:R ratios studied (1:1 and 2:1) however the drug loading calculated for the

resinate formed using the 1:2 D:R ratio is in fact higher relative to that calculated for the DRC formed using IRP69 and the same D:R ratio (37.5% w/w versus 24.4% w/w). Interestingly, the resinates formed using the IRP88 grade (using the 2:1 and 1:1 ratios) produce statistically similar ($p>0.05$) drug loadings relative to those determined for the DRCs formed using IRP69 and equivalent D:R ratios. In contrast, the drug loading achieved using the 1:2 D:R ratio is higher relative to the drug loading determined for the DRC produced using an equivalent D:R ratio (35.7% w/w versus 24.4% w/w). These results highlight the unpredictability of the drug loading process using resins with different dissociation properties, which in turn deviate largely from the dissociation properties of the API being used to complex onto the resin.

Table 4.3. Comparison of drug loading (%) values of the DRCs formed using a 1:1 D:R (w/w) ratio (using IRP64) using an unadjusted drug loading solution (0.1% w/v). These values were determined using altered loading conditions. The modification of the elution studies involved adjusting the concentration of complex in the elution medium, the molarity of the elution medium and the temperature of the elution medium. The displacement/elution medium was also varied, and the specific agent used is listed in parentheses in the "Drug loading on the DRC" columns.

			Drug loading on the DRC (% w/w)	
Concentration of complex in elution medium (mg/mL)	**Molarity of elution medium (M)**	**Temperature of elution medium (°C)**	Determined using NaCl as the displacement agent	Determined using HCl as the displacement agent
1.0	**1.0**	**20**	15.34 ± 0.08	16.54 ± 0.21
0.5	**1.0**	**20**	15.84 ± 0.10	16.88 ± 0.03
0.1	**1.0**	**20**	16.30 ± 0.25	17.14 ± 0.15
1.0	**0.5**	**20**	14.25 ± 0.15	15.22 ± 0.11
0.5	**0.5**	**20**	14.61 ± 0.10	15.56 ± 0.13
0.1	**0.5**	**20**	14.96 ± 0.13	15.96 ± 0.17
1.0	**0.1**	**20**	12.94 ± 0.12	14.94 ± 0.09
0.5	**0.1**	**20**	13.58 ± 0.03	15.48 ± 0.07
0.1	**0.1**	**20**	14.54 ± 0.43	15.94 ± 0.29
1.0	**1.0**	**37**	17.78 ± 0.09	18.88 ± 0.21
0.5	**1.0**	**37**	18.23 ± 0.04	19.23 ± 0.09
0.1	**1.0**	**37**	18.58 ± 0.16	19.51 ± 0.13
1.0	**0.5**	**37**	16.11 ± 0.15	17.01 ± 0.09
0.5	**0.5**	**37**	16.65 ± 0.33	17.75 ± 0.29
0.1	**0.5**	**37**	17.09 ± 0.08	18.19 ± 0.09
1.0	**0.1**	**37**	14.93 ± 0.21	15.43 ± 0.13
0.5	**0.1**	**37**	15.22 ± 0.13	16.12 ± 0.08
0.1	**0.1**	**37**	15.82 ± 0.08	16.46 ± 0.13

The assay method for the resinates produced using IRP88 was optimised in a similar manner to the approach described above so that many influential aspects of the drug-resin equilibrium were varied to probe the nature of the drug-resin complexation (Table 4.4). In relation to the assay studies that used NaCl as the displacement medium, several noticeable trends could be identified, which are identical to those highlighted for the IRP64 systems. Firstly, a higher ($p<0.05$) quantity of drug can be displaced when HCl is used compared to NaCl at all conditions tested. Furthermore, the influence of the ionic strength of the displacement medium, the elution medium temperature and the concentration of DRC in the displacement medium on the quantity of drug detected is apparent and can be summarised as increased ($p<0.05$) drug loadings being detected at higher temperatures, higher ionic strengths and more dilute concentrations of DRC in the elution medium.

Table 4.4. Comparison of drug loading (%) values of the DRCs formed using a 1:1 D:R (w/w) ratio (using IRP88) using an unadjusted drug loading solution (0.1% w/v). These values were determined using altered loading conditions. The modification of the elution studies involved adjusting the concentration of complex in the elution medium, the molarity of the elution medium and the temperature of the elution medium. The displacement/elution medium was also varied, and the specific agent used is listed in parentheses in the "Drug loading on the DRC" column.

			Drug loading on the DRC (% w/w)	
Concentration of complex in elution medium (mg/mL)	**Molarity of elution medium (M)**	**Temperature of elution medium (°C)**	Determined using NaCl as the displacement agent	Determined using HCl as the displacement agent
1.0	**1.0**	**20**	43.25 ± 0.43	45.29 ± 0.40
0.5	**1.0**	**20**	44.12 ± 0.31	45.87 ± 0.87
0.1	**1.0**	**20**	45.87 ± 0.12	46.26 ± 0.05
1.0	**0.5**	**20**	40.30 ± 0.39	44.13 ± 0.35
0.5	**0.5**	**20**	43.45 ± 0.38	45.10 ± 0.21
0.1	**0.5**	**20**	45.12 ± 0.49	46.08 ± 0.24
1.0	**0.1**	**20**	38.13 ± 0.25	43.13 ± 0.19
0.5	**0.1**	**20**	42.00 ± 0.49	44.30 ± 0.45
0.1	**0.1**	**20**	45.47 ± 0.14	46.12 ± 0.20
1.0	**1.0**	**37**	45.25 ± 0.21	47.25 ± 0.29
0.5	**1.0**	**37**	45.87 ± 0.43	48.27 ± 0.03
0.1	**1.0**	**37**	46.26 ± 0.05	48.50 ± 0.27
1.0	**0.5**	**37**	46.13 ± 0.15	47.13 ± 0.39
0.5	**0.5**	**37**	46.32 ± 0.37	47.32 ± 0.29
0.1	**0.5**	**37**	46.87 ± 0.09	47.85 ± 0.11
1.0	**0.1**	**37**	44.87 ± 0.44	47.13 ± 0.10
0.5	**0.1**	**37**	45.56 ± 0.23	47.87 ± 0.50
0.1	**0.1**	**37**	46.13 ± 0.04	48.00 ± 0.13

Stemming from the initial loading trials, which investigated the binding of TZD HCl to either grade of resin using a range of different D:R ratios, the results for the resinate using a 1:1 ratio of TZD HCl and IRP64 revealed lower drug loadings ($p<0.05$) relative to the resinates produced using the IRP69 grade. Considering the reportedly increased ion-exchange capacity of the "weak" resins relative to "strong resins" it is apparent from the data (lower drug loadings) that the loading process of the drug onto the "weak resins" is suboptimal indicating that the pH of the loading medium needed to be adjusted. This amendment of the loading conditions has to be done with the impact of drug dissociation in mind, as a trade-off between achieving complete dissociation of both components in solution needs to be achieved, in addition to ensuring adequate solubility of the drug at the tested pH values. As discussed previously in the case of MTZ-IRP69 DRCs/resinates (Chapter 3), a drawback of using buffer systems to adjust the pH is the introduction of the presence of competing cations, which are present in the phosphate buffer medium and provide competition for binding sites on the resin. Therefore, loading studies have to be carefully designed, when it comes to the selection of a loading pH for "weakly" acidic cation exchangers. In contrast to "strongly" acidic resins, these systems are not ionised across virtually the whole pH range. Therefore, unless due consideration is given to the pH of the loading medium, which is influenced by the drug's dissociation tendency, there is a risk that the resin could exist in its "free" acid state, meaning that the possibility of ion-exchange is limited.

For the particular resins in question, this situation would arise if the pH value is less than 4 due to their "weak" acid functionality. Relative to the IRP69 resin grade studied in Chapter 3, the drug loading calculated for the unadjusted DRC produced using a 1:1 ratio of drug and IRP64 is lower than expected, when the reported ion-exchange capacity values are compared, which are higher for IRP69 compared to IRP64, as the pH of the loading solution prior to resin addition is 4. Therefore, in the case of IRP64 grade, further loading studies were conducted at a series of higher pH values of the loading solution (greater than 5), where the resin is ionised and should be more amenable to the loading of cationic species. Loading results are illustrated in Figure 4.2. On this occasion, the loading solutions buffered to pH values of 5, 6 and 7 (Chapter 2, section 2.2.1.2.3) demonstrated reducing drug loading as the solution pH approaches the pKa of the carboxylic groups on the resin (pKa 4), which is consistent with a decreased proportion of ionic species (resin) being available. These results indicate that the higher drug loadings can be achieved using drug solutions adjusted to pH values that are favourable for resin dissociation (pH 7) relative to those that produce higher levels of drug dissociation (pH 5). This observation highlights the importance of exploiting solution pH when aiming to design an efficient and effective drug loading process.

The equilibration times for the IRP64 DRC systems are shown in Figure 4.3. The time to equilibration varied between the different systems, which illustrated nicely the challenge posed by the differing

dissociation tendencies of the drug and resin. The DRC produced using the unadjusted loading solution displayed similar loading kinetics to that of the DRC formed using the loading solution buffered to pH 5. This is not surprising, considering the pH of the unadjusted loading solution is in the region of pH 4, meaning that the buffered solution with a pH of 5 resembles it most closely for the loading solutions studied. Over the first three hours, there is no statistical difference ($p>0.05$) in the uptake of the drug from solution, but differences appear from hour four onwards, signified by the more rapid uptake of drug from the pH adjusted system. For both systems, the drug loading occurs over a relatively rapid timeframe, with a plateau being reached after 6 and 8 hours for the pH unadjusted and pH adjusted systems respectively. As for the other two systems examined, where the pH was adjusted to higher values, a larger quantity of drug is taken up at the early timepoints. At the 1 hour timepoint, the pH 6 and pH 7 systems have complexed 20% and 30% of drug available from solution respectively, with this difference closing over subsequent hours. At the 5 hour timepoint, the drug uptake from the solution buffered to pH 6 begins to level off, signified by the plateau being approached, whereas the pH 7 solution continues to be depleted of its drug content, showcased by a steep decline until the 12 hour timepoint, when equilibrium is attained.

It is evident from the varied loading kinetics that the pH of the medium plays a prominent role in the rate of drug uptake by the resin. At pH values that favour a higher proportion of drug dissociation but are not optimal for the dissociation of the "weak resin" (pH 4-6), the rate is most rapid, indicating the higher the % drug dissociation in solution, the faster the loading kinetics. At the highest pH value studied (pH 7), which is closest to the pKa of the API (7.3), the time to equilibrium is slowest, pointing to the reduced amount of drug being dissociated being a contributory factor to the slower loading kinetics. Although knowledge of the impact of altering the pH of the medium on the loading kinetics is of interest, the primary concern is the effect of this variable on the % drug loading. Regarding the loading kinetics of the DRC formed using IRP88 (Figure 1 in Appendix 2), equilibrium is reached after 24 hours, a noticeably longer length of time relative to the IRP64 systems. This may be attributed to the higher loading of the drug onto the resin and further illustrates the individuality of the loading process, with the same drug requiring different lengths of time to equilibrate depending on the properties of the resin in question.

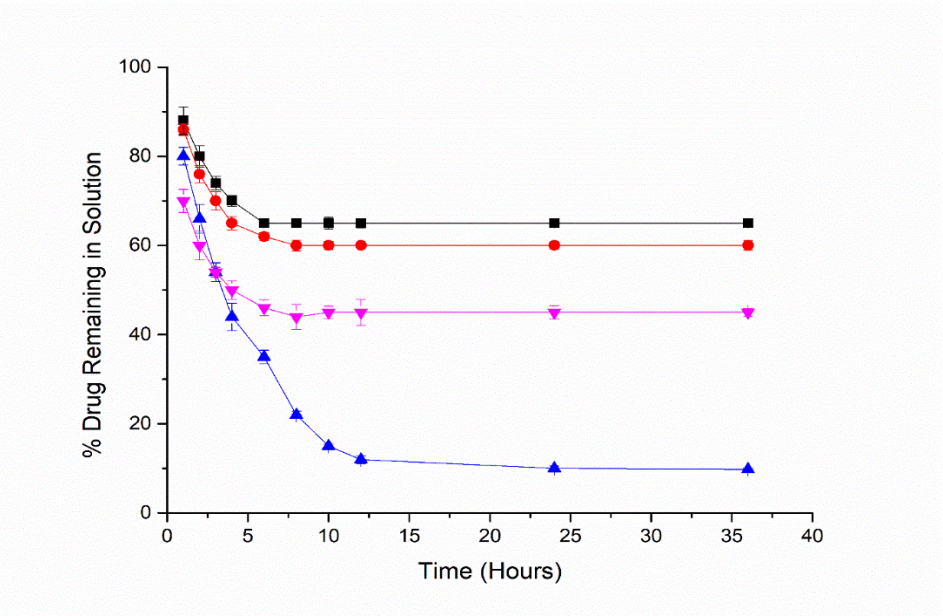

Figure 4.3. Equilibration profile showing the loading of TZD HCl onto IRP64 with a 1:1 D:R ratio (w/w) using pH adjusted and unadjusted drug loading solutions prior to resin addition over 36 hours at room temperature. Unadjusted drug solution (pH 4.32) (Black square), drug solution adjusted to pH 5 (Red circle), drug solution adjusted to pH 6 (Magenta inverted triangle) and drug solution adjusted to pH 7 (Blue triangle).

The most striking aspect of the initial loading studies was the distinct yellow colour produced after the addition of the IRP88 to the drug solution (Figure 2(A) in Appendix 2), irrespective of the D:R ratio. This was not observed following the addition of the IRP64 grade to the drug solution (Figure 2(B) in Appendix 2), which prompted several experiments aimed at investigating the cause of this colour change.

pH studies offered the most rational explanation for these observations, with the results outlined in Table 4.5. Analysis of the pH values of both resin raw materials post-addition to DI H_20 revealed marked differences, reflective of the variance in counter-ion attached to the carboxylic groups on the backbone of the resin. IRP88 gave a far higher pH value than IRP64, attributable to the dissociation of the potassium and hydrogen ions respectively. The fact that IRP64 gave a lower pH value is no surprise considering the acidic nature of the hydrogen ion. Interestingly, the pH value after 24 hours does not significantly change in the case of the IRP64 system whereas a pH unit drop of approximately 1 is observed for the IRP88 resin, suggestive of hydration being a contributory factor. Also shown in Table 4.5, are the pH values of pure drug solution (1 mg/mL) in DI H_20 measured at two timepoints after the introduction of resin (IRP88 or IRP64). The pH value of the raw material dissolved in DI H_20 is 4.32, which is consistent with the literature (272). After 24 hours (T_{24}), when complexation is expected to be completed, the pH of the loading medium that initially contained both the API and IRP64 grade is

reduced relative to the measured pH values of the liquid for the single components (IRP64 and TZD HCl), which can be attributed to the liberation of the hydrogen ion bound to the resin after the drug has been loaded. Although the difference between the T_0 and T_{24} is statistically significant ($p<0.05$), the disparity is far lower relative to that seen with the IRP88 system. For the IRP88 system post-loading, the pH values follow a similar trend to that observed with the raw material (decreased pH value at T_{24} relative to T_0). Furthermore, the pH value of the liquid to which API and IRP88 were added is far higher (pH 8.15) initially than the drug solution (but lower than for IRP88 alone), which coincides with the appearance of the yellow colour. A plausible explanation for this observation could be the production of the TZD free base as a result of the increase in pH value caused by the dissociation of the potassium ions initially bound to the resin.

An additional observation, which distinguished the samples produced using either grade of resin, related to the appearance of a precipitate during the loading studies with IRP88. This occurred after the addition of the IRP88 grade to the drug solution, evidenced by large quantities of material at the bottom of the vessel. Moreover, the filtering step that is employed post-equilibrium could be described as a protracted process, in the order of a couple of hours, whereas the resinates formed using IRP64 required just several minutes to filter the entire volume of resinate suspension These findings are in stark contrast to the drug loading studies conducted with the IRP69 grade when a change of ionic form had a negligible impact on the processability and subsequent performance of the DRC product. Solid-state analyses and dissolution studies discussed later in this chapter provided further evidence that the ion-exchange between the API and IRP88 resin was not as clearcut despite the similar levels of drug loading detected in the drug assay studies previously discussed.

Table 4.5. Comparison of pH values of aqueous media immediately after addition (T_0) and 24 hours post-addition of the resin (IRP64 or IRP88) to DI H_2O (T_{24}). Also listed is the pH value of DRC (IRP64 and IRP88) suspension in DI H_20 (immediately after the addition of resin raw material (IRP64 or IRP88) to an aqueous drug solution (T_0) and 24 hours post-addition of resin raw material (T_{24}) to an aqueous drug solution (0.1% w/v).

Concentration of drug in loading solution	Sample	pH value at T_0	pH value at T_{24}
0.1% w/v	IRP64 raw material	4.65 ± 0.03	4.58 ± 0.04
0.1% w/v	IRP88 raw material	9.71 ± 0.01	8.62 ± 0.03
0.1% w/v	TZD HCl raw material	4.32 ± 0.01	N/A
0.1% w/v	DRC (IRP64)	2.66 ± 0.03	2.44 ± 0.04
0.1% w/v	DRC (IRP88)	8.15 ± 0.04	7.11 ± 0.03

4.2.2 Solid-State characterisation (IRP64 and IRP88)

A combination of pXRD and thermal analyses were used to gain an insight into the physical form of the drug that was loaded onto either grade of resin. The pXRD diffractograms of the IRP64-based DRC (1:1) are shown in Figure 4.4, alongside the diffractograms of the crystalline raw material, the crudely formed TZD free base (Chapter 2, section 2.2.1.10) and the physical mixtures of drug and resin (IRP64) prepared (50:50, 40:60 and 15:85 w/w). The diffractogram of the DRC, which is defined by the amorphous halo pattern, resembles that of the resin raw material, indicating that both materials are pXRD amorphous. No evidence of Bragg peaks attributable to crystalline TZD HCl or TZD free base are visible in the DRC diffractogram, whereas discernible peaks in the physical mixture can still be identified. This observation indicates that the drug has been amorphised after being loaded onto the resin, similar to what was described for the DRCs formed using the sulfonic-acid containing systems (Chapter 3).

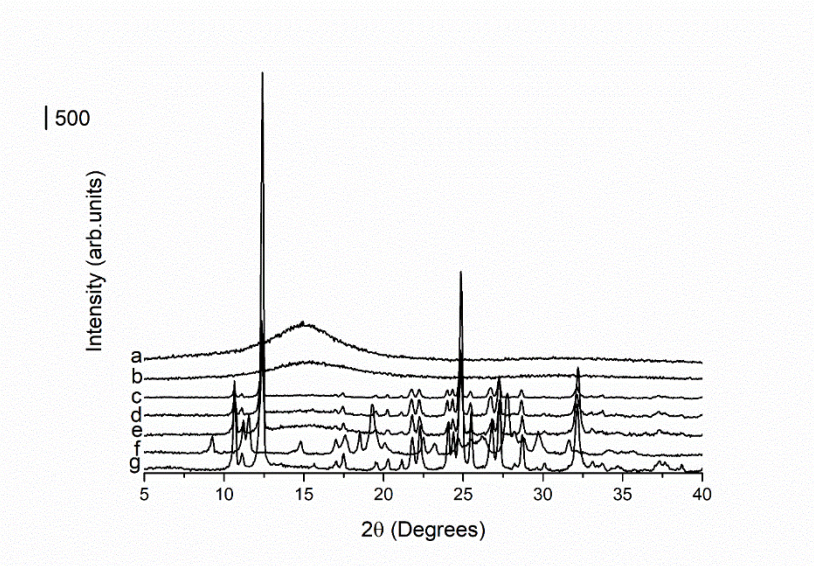

Figure 4.4. pXRD diffractograms of a) IRP64 raw material, b) DRC (formed using a 1:1 D:R ratio (w/w) and a pH unadjusted loading solution) (IRP64), c) physical mixture of TZD HCl and IRP64 (15:85 w/w), d) physical mixture of TZD HCl and IRP64 (40:60 w/w), e) physical mixture of TZD HCl and IRP64 (1:1 w/w), f) TZD free base and g) TZD HCl raw material.

Irrespective of the pH of the loading solution used to form the DRC, the diffractograms of the resultant complexes display a distinct halo pattern, reflective of the resinates' amorphous nature (Figure 4.5), with no evidence of Bragg peaks representative of the crystalline TZD HCl raw material or the TZD base.

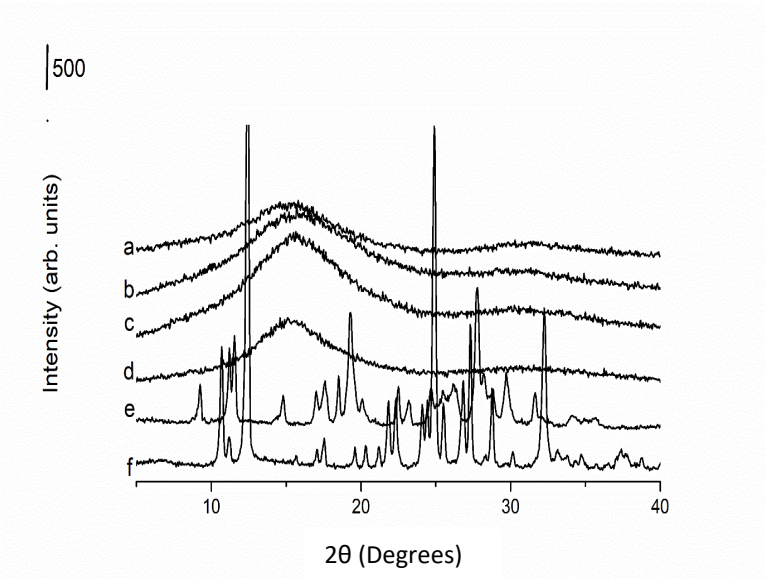

Figure 4.5. pXRD diffractograms of TZD HCl raw material, TZD free base, and DRCs formed using IRP64 and TZD HCl (1:1 D:R ratio (w/w)). The pH of the drug solutions which were adjusted as per the method described in Chapter 2, section 2.2.1.2.4.1 prior to the addition of IRP64 are listed in parentheses where applicable. a) DRC (pH 7), b) DRC (pH 6), c) DRC (pH 5), d) DRC (unadjusted pH), e) TZD free base and f) TZD HCl raw material.

Contrasting pXRD results were found for the IRP88 based DRC, as Bragg peaks are visible in the diffractogram of the 1:1 complex, highlighted by the green arrows (Figure 4.6). The peaks visible (red arrows) at 2θ values (9.28°, 11.37°, 14.91°, 18.55°, 19.33°, 22.05°, 23.05°, 26.30°and 27.73°) do not correspond to those present in the diffractograms of the TZD hydrochloride salt. Instead, these identifiable peaks correspond to those found in the diffractogram of the crudely formed base. Furthermore, a comparison of the diffractogram of the physical mixture (1:1 TZD HCl:IRP88) to that of the IRP88-based DRC reveals that the Bragg peaks found in both diffractograms do not match. When the Cambridge Crystallographic Data Centre (CCDC) website was consulted to identify the reported pXRD patterns for the known polymorphs of TZD free base and that of the salt form (Figure 3 in Appendix 2), it transpired that it was difficult to unambiguously assign the peaks 2θ values (11.37°, 14.91°, 19.33°, 26.30° and 27.73°) of the material present in the IRP88-resinate to one of the two known polymorphs, which may be attributed to the crude method of production.

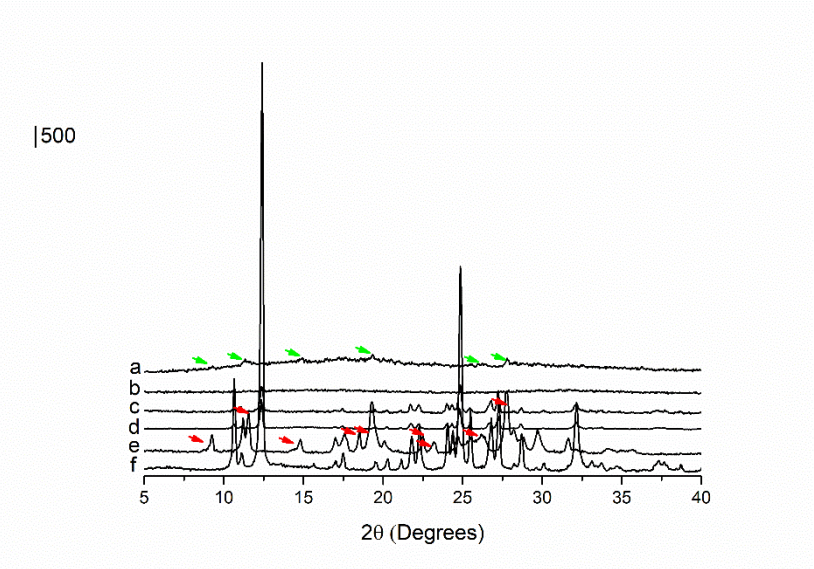

Figure 4.6. pXRD diffractograms of a) resinate formed using TZD HCl and IRP88 (1:1 D:R ratio (w/w)), (b) IRP88 raw material, c) physical mixture of TZD HCl and IRP88 (1:1 w/w), d) physical mixture of TZD HCl and IRP88 (15:85 w/w), e) TZD free base and f) TZD HCl raw material.

With respect to the IRP64-based systems, the DSC analyses supported the pXRD findings, however, the analysis did suffer from a major drawback in that the carboxylic acid-containing resins are known to degrade at temperatures above 200 °C. The DSC thermograms for the DRCs formed using IRP64 are shown in Figures 4.7 and 4.8. The complications arising from the degradation of the resin raw material are evident from the DSCs of the physical mixtures studied (Figure 4.7). Although the melting endotherm at 290 °C is evident in the thermograms of both samples, this peak is accompanied by a second earlier endotherm which is much broader and happens to coincide with the sharper melt endotherm of crudely formed TZD free base. This can be likely attributed to the degradation of the resin, based on literature reports (320). Although the resin raw material has not been heated up to the temperature that the broad endothermic event is occurring at, the onset of degradation is visible, characterised by the signal beginning to dip prior to the analysis finishing. Interestingly, the DRC has a single endotherm at 213 °C, signifying that degradation occurs at a slightly lower temperature relative to the physical mixture and no crystalline TZD HCl salt is present in the complex. One upside of this earlier onset of degradation is the ability to establish if any residual crystalline free base is present, as the 225 °C region (where the base melts) is no longer obscured. These findings for the DRC produced using a pH unadjusted drug loading solution are consistent with later thermal analysis studies performed on three other IRP64 based DRCs prepared (Figure 4.8) signifying that all drug has been converted to the amorphous form after loading onto the resin, regardless of initial starting pH of the drug solution.

The DSC thermograms pertaining to the IRP88 resin are depicted in Figure 4.8. In contrast to the unprocessed IRP64 grade, the material does not appear to be beginning to degrade prior to the analysis being stopped. Interestingly, the DSC trace for the IRP88-based DRC contains a single melt endotherm at 225 °C, representative of the crudely produced TZD free base. Furthermore, little evidence of the broad endotherm present in the thermograms of the IRP64 complexes is apparent, which supports the assertion that the IRP88 resin may not be as thermally labile as the IRP64 grade. Again, no evidence of crystalline TZD HCl can be identified, based on the lack of a melt endotherm at 290 °C. Of all the DSC studies performed using either grade of resin, the physical mixture (1:1) of TZD HCl and IRP88 produces the most intriguing result, where no obvious reason for the thermal events visible in the thermogram exists. The DSC trace is characterised by a broad endotherm that is likely the consequence of at least two thermal events that are overlapping. Moreover, the endotherm attributable to crystalline TZD HCl is absent suggestive of a solid-state interaction occurring between crystalline drug and amorphous resin during heating. Upon closer inspection of the thermogram, a small peak at 205 °C can be identified which may be the free base melting, however, it cannot be said with certainty, as this would require a solid-state reaction during the preparation of the physical mixture to have occurred or during heating in the DSC. The ambiguous nature of these results led to the TGA analysis being used to investigate if any further insight into the thermal behaviour could be ascertained.

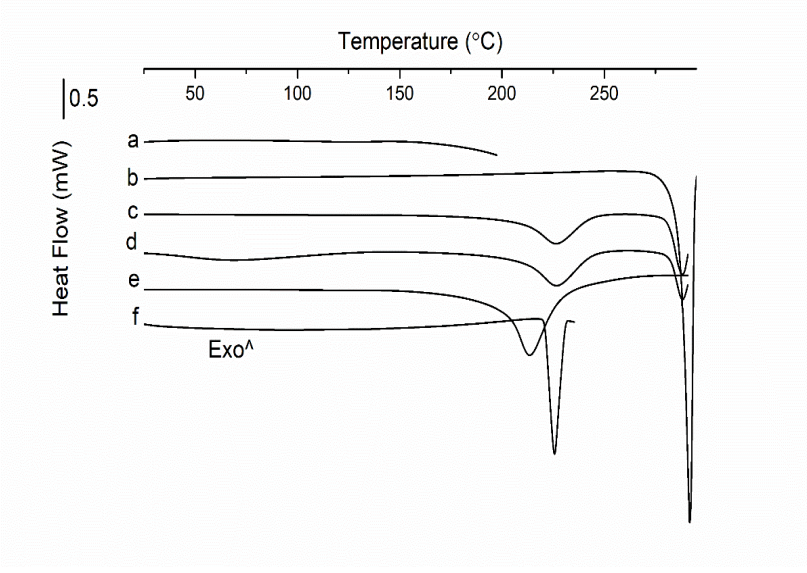

Figure 4.7. A) DSC thermograms of a) IRP64 raw material, b) TZD HCl raw material, c) physical mixture of TZD HCl and IRP64 (1:1 w/w), d) physical mixture of TZD HCl and IRP64 (40:60 w/w), e) DRC formed using IRP64 and TZD HCl (1:1 w/w) and f) TZD free base.

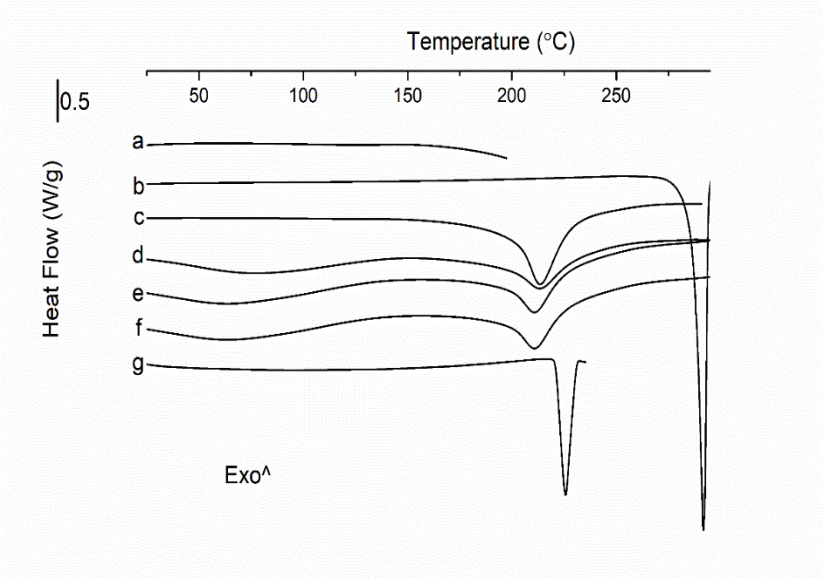

Figure 4.8. DSC thermograms of TZD HCl raw material, TZD free base, and DRCs formed using IRP64 and TZD HCl (1:1 D:R ratio (w/w)). The pH of the drug solutions which were adjusted as per the method described in Chapter 2, section 2.2.1.2.4.1 prior to the addition of IRP64 are listed in parentheses where applicable. a) IRP64 raw material, b) TZD HCl raw material, c) DRC formed using a 1:1 D:R ratio of TZD HCl and IRP64 (unadjusted), d) DRC (pH 7), e) DRC (pH 6), f) DRC (pH 5) and g) TZD free base.

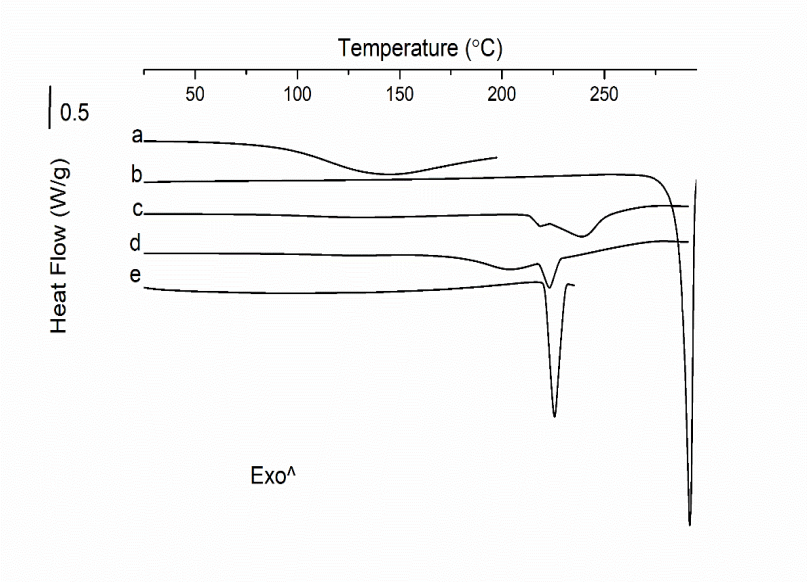

Figure 4.9. DSC thermograms of a) IRP88 raw material, b) TZD HCl raw material, c) physical mixture of TZD HCl and IRP88 (1:1 w/w), d) DRC formed using IRP88 and TZD HCl (1:1 (w/w) and e) TZD free base.

The results of the TGA analysis performed on the selected DRCs are shown in Figures 4.10(A-B). To study the thermal stability to complement the data already presented, the analysis was limited to the IRP88-based resinate and a single IRP64-based DRC. In the case of the latter, the complex produced using a loading solution unadjusted for pH was chosen, mainly because the DSC samples produced using IRP64 did not exhibit any major differences in their DSC traces. This data provided further

evidence, in addition to the DSC and pXRD analyses, that the complexation between drug and resin may not be as straightforward as the ion-exchange reaction involving the sulfonic acid-containing resin and API (Chapter 3). In the case of IRP64, the initial mass loss, discounting that attributed to residual moisture (below 100 °C), is observed at a much lower temperature relative to the sulfonic acid-containing resins, which is consistent with the DSC findings. The onset temperature of mass loss for the raw material (IRP64) occurs at approximately 210 °C, highlighted by the red arrow, with the majority of the % weight loss beginning at 360 °C, signified by the black arrow. As discussed previously in Chapter 3, TZD HCl begins to degrade prior to melting, starting at approximately 220 °C. Upon inspection of the thermogram of the complex formed using a 1:1 ratio of IRP64 and TZD HCl, subtle differences regarding the onset of weight loss are evident. With respect to the physical mixture, thermal events attributable to each component are distinguishable and can be unambiguously assigned to both TZD HCl (205 °C) and IRP64 (360 °C). Although IRP64 does exhibit a small degree of % weight loss at 210 °C in the thermal trace of the raw material, it is not possible to decipher if this is occurring in the trace of the physical mixture, as the onset of degradation of HCl salt is the predominant event at that temperature evidence by the longer duration of time over which the weight loss occurs 205-290 °C. In contrast, the thermal trace of the DRC formed using both components closely resembles that of the resin raw material. The temperature at which the initial onset of weight loss of resin occurs is evident (205 °C) whilst the majority of the mass loss occurs at an even higher temperature, in the region of 380 °C. This temperature is higher than the onset temperature (360 °C) reported for both the physical mixture and the raw material (IRP64) suggestive of interaction occurring between the two components during the drug loading process which alters their thermal behaviour.

Concerning the thermal studies involving IRP88, the raw material, which contains the potassium salt form of carboxylic acid along its backbone, demonstrates higher thermal stability relative to the IRP64 grade, which contains carboxylic acid groups. The onset temperature of degradation occurs at 355-365 °C, which is considerably higher than the value reported for the IRP64 resin.

The TGA analysis also reveals that the crudely formed TZD base begins to degrade at the lower temperature of 205 °C relative to the crystalline salt form (220 °C), which is consistent with DSC findings. Akin to the IRP64 system, the TGA trace of the DRC differs from that of the physical mixture, indicative of some type of interaction or solid-state change, as alluded to previously. In the scan of the DRC two distinct thermal events attributable to free base and resin can be identified (205 °C and 360 °C respectively). Moreover, the TGA data pertaining to the DRC is also ambiguous, with a noticeable onset of degradation occurring at approximately 205 °C and the main degradation occurring at 320 °C. Both of these events cannot be attributed to any specific component with certainty, however, it is likely that the free base form is degrading at the earlier temperature, whereas the resin begins to

degrade at 320 °C, considerably earlier than pure resin material. Taking these findings into account, together with the DSC data and pXRD studies, it is likely a proportion of drug material has not bound ionically to the resin during the loading process, or had the chance to embed within the matrix structure, thus limiting its presence to the surface. This would explain the degradation of material at lower temperatures, as the resin cannot offer any form of thermal protection.

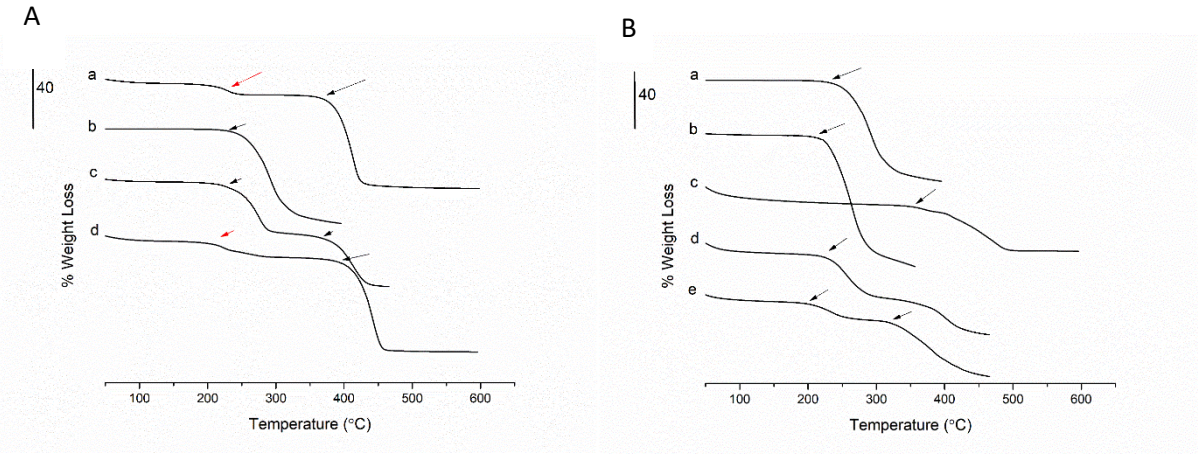

Figure 4.10. TGA analysis of A) a) IRP64 raw material, b) TZD HCl raw material, c) physical mixture of TZD HCl and IRP64 (1:1 w/w) and d) DRC formed using a 1:1 D:R (w/w) ratio of TZD HCl and IRP64 (unadjusted). B) a) TZD HCl raw material, b) TZD free base, c) IRP88 raw material, d) physical mixture of TZD HCl and IRP88 (1:1 w/w) and e) DRC formed using a 1:1 D:R (w/w) ratio of TZD HCl and IRP88.

Upon further consideration of the ion-exchange reaction between drug and resin, together with analysis of the DSC and TGA data, it was suspected that the free base of TZD was formed upon the addition of the potassium salt resin to the drug solution. This occurrence produced a characteristic yellow colour, typical of amine-containing compounds, such as TZD. This would also explain the melting endotherm observed in the DSC data that was observed at a temperature significantly below that of the salt form. Few reports of the melting temperature of the free base exist, but there are many examples in the literature of free base compounds melting at lower temperatures relative to their salt forms (321).

4.2.3 FTIR spectroscopy (IRP64 and IRP88)

Similar to the FTIR studies performed on the DRCs produced using the sulfonic acid-containing resins (Chapter 3), FTIR analysis was conducted to investigate the potential complexation between the API and polymethacrylate resins. The spectra of the DRCs formed using IRP64 are depicted in Figure 4.11. To aid with the assignment of vibrational bands unique to either component, the spectra of the salt form of API, crudely-formed TZD base, the resin raw material and a physical mixture of unprocessed API (salt) and resin are also shown in Figure 4.11. It was possible to discern differences between the DRC sample prepared using a pH unadjusted loading solution and the physical mixture on the basis of the N-H stretching vibration at 3250 cm^{-1}. As was the case with the complexes formed using the

sulfonic acid-containing resin, the absence of the peak attributed to the stretching vibration of the ionised primary amine group, is indicative of an interaction being mediated by electrostatic forces between the carboxylic groups of the resin and the aforementioned N-H group. Likewise, the DRCs produced using the pH adjusted drug loading solutions did not contain this peak that was present in the physical mixture. The physical mixture of drug and resin displays a spectrum that resembles that of the single components combined. Again, similar to many of the physical mixtures of drug and resin examined, the peaks belonging to the TZD HCl are less intense due to a dilution effect. When the resin raw material is considered, the characteristic peaks used to unequivocally identify it are related to the carboxylic acid moiety, which is implicated in the ion-exchange reaction. They are positioned at 1695 cm^{-1}, 1390 cm^{-1} and 1150 cm^{-1} which represent C=O stretching, O-H bending and C-O stretching respectively. Unexpectedly, no clear evidence of the O-H stretching vibration can be found. Having said that, the hydroxyl group is known to be very broad and sometimes barely distinguishable, as oftentimes it is obscured by moisture, making it difficult to identify specific intermolecular interactions. Furthermore, the peak attributed to the O-H bending vibration is relatively weak, indicating that the sample signal may be an issue, which would inevitably cause difficulties regarding the detection O-H stretching vibration. Fortunately, the other peaks present in the DRCs studied provide clear evidence of vibrational shifts (indicated by the broken red lines) exemplified by the bending vibrations of the N-H groups in TZD HCl shifting from 1641-1649 cm^{-1} and the peak at 1605 cm^{-1} not being discernible. A plausible reason for the absence of the second N-H peak is a shift in its position to a higher wavenumber causing a broad amalgamation between it and the other N-H peak, both of which have suppressed absorbance values. Furthermore, there is a noticeable shift in the fingerprint region, where the C-O stretching vibration shifts from 1147 cm^{-1} to 1167 cm^{-1}, indicative of this bond present in IRP64 being implicated in intermolecular bonding.

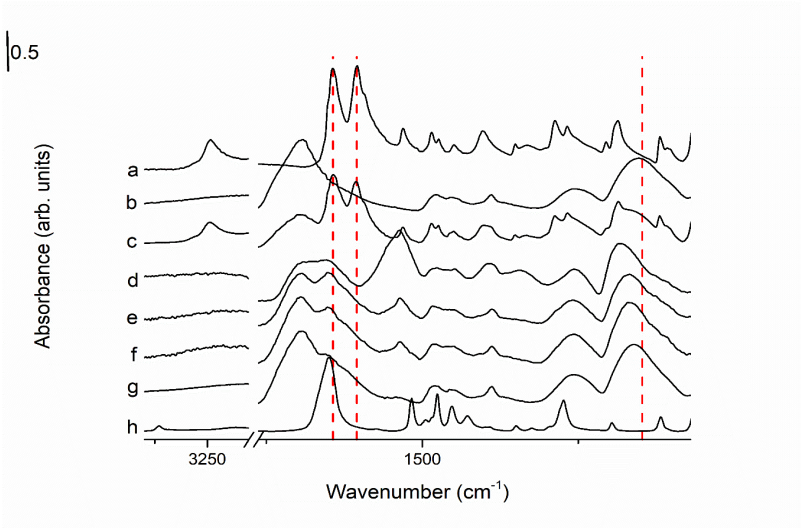

Figure 4.11. FTIR spectra of a) TZD HCl raw material, b) IRP64 raw material, c) physical mixture of TZD HCl and IRP64 (1:1 w/w), d) DRC formed using a 1:1 D:R ratio (w/w) of TZD HCl:IRP64 (drug loading solution adjusted to pH 7), e) DRC formed using a 1:1 D:R ratio (w/w) of TZD HCl:IRP64 (drug loading solution adjusted to pH 6), f) DRC formed using a 1:1 D:R ratio (w/w) of TZD HCl:IRP64 (drug loading solution adjusted to pH 5), g) DRC formed using a 1:1 D:R ratio (w/w) of TZD HCl:IRP64 (unadjusted drug loading solution) and h) TZD free base. The pH of the drug solutions which were adjusted prior to the addition of IRP64 are listed in parentheses where applicable. The red dashed lines signify the main peaks present in the raw materials (TZD HCl and IRP64 where discernible shifts in the individual spectra of the resinates are evident).

Figure 4.12 displays the spectrum of the DRC (1:1) formed using IRP88, alongside that of the raw materials, the crudely formed free base and a physical mixture of unprocessed drug and resin. Similar to the FTIR analysis of the IRP64 samples, it was possible to identify discernible differences between the DRC and the physical mixture. The resin raw material is characterised by an intense peak at approximately 1550 cm^{-1}, which is representative of the carboxylate group (119). The spectra of the physical mixture displayed several characteristic peaks that can be attributed to the individual components that constitute the system, as no interaction would be anticipated. In contrast to this, the spectrum of the DRC displays several differences to that of the physical mixture, most notably the N-H stretching and N-H bending vibrations at 3361 cm^{-1} and 1600 cm^{-1} respectively. In relation to the peak at 3361 cm^{-1}, it does not correspond to the crystalline raw material, nor is it identical to any of the peaks that characterise the resin raw material. Regarding the peak at 1600 cm^{-1}, it is absent in the spectrum of the PM, but present in the spectrum of the base, supporting the view that the base may be bound to the resin. In the case of the N-H stretching vibration band (3250 cm^{-1}) that is prominent in the spectra of the crystalline API and the physical mixture, the peak is absent in the DRC spectrum, whereas one of the bands representing the N-H bending vibration (1642 cm^{-1}) shifts to a higher wavenumber (1648 cm^{-1}), again signifying an interaction between the components. Perhaps the most interesting feature of the spectrum of the IRP88-based DRC, which differentiates it from DRCs formed

using IRP64, relates to the peak at 3361 cm^{-1}. This peak is likely representative of the unprotonated primary amine, as it is also present in the spectrum of the crudely produced base, which is suggestive of the presence of this material within the resin matrix after the loading process. Together with the DSC and pXRD data for this system, this FTIR data suggests that it is highly likely that the free base form of TZD is physically adsorbed to the resin in a substantial quantity in addition to the complexation that occurs between ionised TZD and IRP88. Furthermore, owing to the resin's large molecular weight, hydrophobicity and irregularly shaped structure where the surface contains many cavities, the physical adsorption phenomena may also be promoted (103,108,119). Tan et al. highlight this physical adsorption phenomenon as a plausible reason for their observations for certain resinates produced that contain API yet lack specific, robust intermolecular interactions (119). As discussed already, this has implications in terms of drug release behaviour, solid-state stability and processibility. To the best of the author's knowledge, this is one of the first studies showcasing the unsuitability of a particular resin for an API, outside of obvious charge incompatibilities, through a combination of pXRD, spectroscopic and thermal analyses.

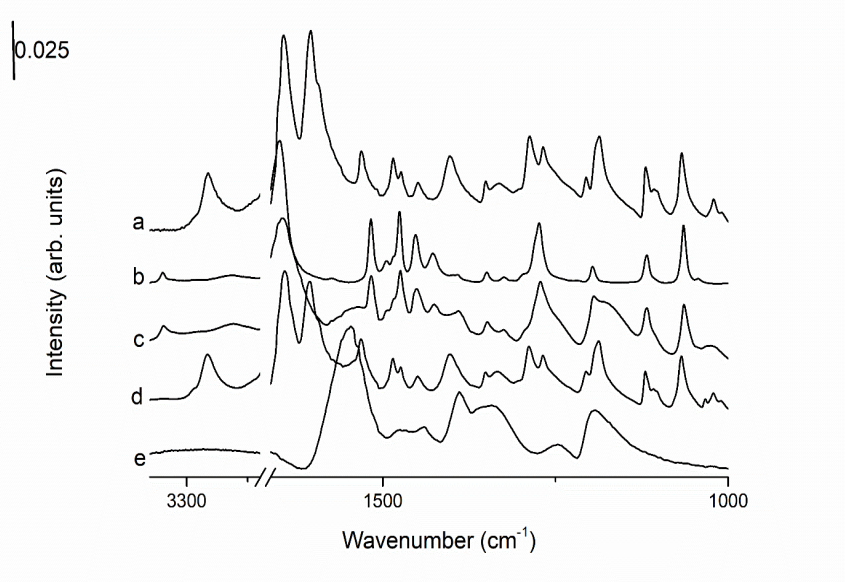

Figure 4.12. FTIR spectra of a) TZD HCl raw material, b) TZD free base, c) DRC formed using a 1:1 (w/w) TZD HCl:IRP88 ratio, d) physical mixture (1:1 w/w) of TZD HCl and IRP88 and e) IRP88 raw material.

4.2.4 Drug release studies (IRP64 and IRP88)

The drug release profiles of the IRP64-based 1:1 DRC are shown in Figure 4.13. Drug release rates were dependent on the pH of the medium, as well as the ionic composition. The high affinity of the IRP64 resin for the H^+ ion results in rapid desorption of the exchanged drug ion when exposed to the 0.1 M HCl, with close to 100% drug release achieved within 20 minutes. When the release kinetics were evaluated in alternative ionic media (0.1 M NaCl and pH 6.8 phosphate buffer), it was found that the drug released from the DRC at a slower rate, with 100% drug release achieved at 60 minutes.

Regardless of the electrolyte environment, similar drug release profiles were produced, highlighting the lack of selectivity that the DRC shows for any ion present in either of the two dissolution media studied. Although the rates of drug release in 0.1 M NaCl and pH 6.8 buffer are lower relative to the rate of drug release observed in the acidic medium, complete drug release is still achieved within 60 minutes, meaning the dissolution process would still be classed as rapid. A similar trend with the DRC produced using the "strong resin" was observed in Chapter 3, with complete release achieved after 20 minutes in 0.1 M HCl, whereas complete drug release in pH 6.8 buffer and 0.1 M NaCl was achieved after 25 and 75 minutes respectively. This dissolution behaviour is consistent with the expectation that the dissociation properties of the resinates formed using "weak" cation exchangers are pH-dependent, much like the resins used to produce them. The scientific rationale underpinning these observations is related to the polymethacrylic resin's pKa (pKa = 4) value, which renders the overwhelming majority of ionic sites undissociated at pH 1.2, in excess of 99%, which translates to a minute fraction of the drug being ionically associated to the resin at acidic pH values (pH 1.2). On the other hand, the resin's pKa (4) has been exploited at higher pH values, demonstrated by the effectiveness of polycarboxylic exchange resins at preventing drug release. This has been illustrated by many groups, including the likes of Agarwal et al. who demonstrated no chloroquinine phosphate release above pH 4, yet drug released rapidly upon exposure to acidic pH, with 100% release being achieved after 10 minutes in pH 1.2 (322). Although the results of the present work, signify that DRC formation does not have as pronounced an impact on the drug release behaviour as the results reported by Agarwal et al., it is evident that the binding of TZD onto IRP64 still has imparted some level of control on the drug release characteristics. The differences in the taste-masking ability of DRCs loaded with different APIs, reflected by their propensity to prevent drug release at pH values above pH 5, has been ascribed to the API's amine functionality. If the amine group suspected of being involved in an ion-exchange reaction is a tertiary one, as is the case with chloroquinine phosphate, it is accepted that this type of functional group is more favourable for the purposes of taste-masking, compared to other amine types, such as the secondary amine, present in TZD HCl (141).

Drug release from the DRC in DI H_2O, the final medium trialled, produces a release profile that differs significantly from those observed for ionic media at all timepoints from 20 minutes onwards. An initial burst release (23%) occurs after 5 minutes, but a plateau is reached after approximately 30 minutes. In contrast to the ionic media, this plateau occurs at 60% drug release, indicating that a level of ion-exchange has been achieved. However, this % of drug release in DI H_2O, where theoretically minimal drug release should occur, indicates that other types of interactions, outside of those classed as ionic, are responsible for the drug loadings achieved. Oftentimes, hydrophobic interactions can occur

between the drug and the resin backbone (323), which could contribute towards the loading figure determined, but do not confer the same benefits afforded by the ionically bound drug.

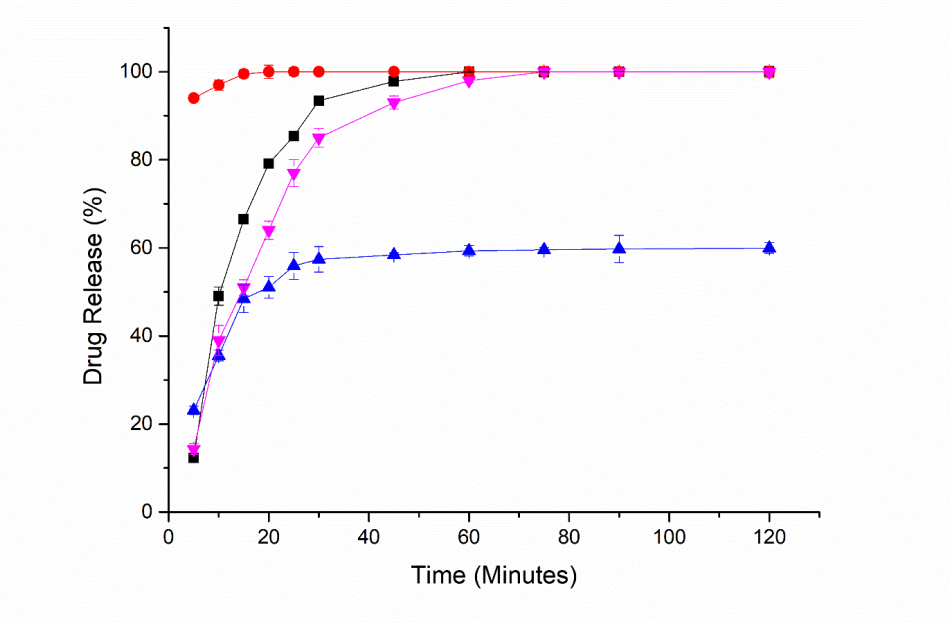

Figure 4.13. Drug release profiles in either 0.1 M HCl, 0.1 M NaCl, pH 6.8 buffer or DI H_2O at 37 °C, of DRCs formed using a 1:1 D:R (IRP64) (w/w) ratio formed using an unadjusted pH drug loading solution. DI H_2O (Blue triangle), 0.1 M NaCl (Black square), pH 6.8 (Magenta inverted triangle) and 0.1 M HCl (Red triangle).

Adjusting the pH of the loading medium to which the carboxylic acid-based resin (IRP64) was added produced differences in the release profiles of the resultant DRCs formed. On this occasion, two types of media were selected for studying the desorption properties of the DRCs. There are notable differences in the rate and extent of drug release for each sample tested in DI H_2O and 0.1 M HCl (Figure 4.14). The degree to which the dissolution behaviour differs depends on the pH adjustment made for the API loading solution. As highlighted previously, the cumulative drug release from the DRCs produced using an unadjusted loading solution is rapid, with over 90% of loaded TZD released after 5 minutes and the complete drug release occurring after 20 minutes. Similarly, rapid desorption from all three resinates produced using pH adjusted solutions is evident in the acidic medium studied. Akin to the loading studies, the desorption profile of the DRC formed using the loading medium adjusted to pH 5 is very similar to the DRC produced using unadjusted loading media, with no statistical difference ($p>0.05$) at any timepoint measured. In addition, the dissolution profiles of the other resinates produced, using the altered loading media (pH 6 and 7), display rapid desorption rates that are characteristic of the "weak" exchangers (314). 80% of the drug is released after 5 minutes from the DRC formed with drug loading solution that was adjusted to the highest pH (pH 7), and the time to reach equilibrium is the longest (60 minutes) relative to the other DRCs tested. In the case of the DRC formed using the medium adjusted to pH 6, the release rate is closely aligned with that of the

two resinates formed using the alternative loading media. Apart from the 5 minute timepoint, lower quantities of the drug are released at each timepoint ($p<0.05$) until equilibrium is approached after 45 minutes. These findings are in agreement with many similar studies that have investigated the use of resins as an option to taste mask APIs through the avoidance of a burst effect (121,314).

In contrast to the drug release behaviour in acidic media, the DRCs display more varied release rates in DI H_2O. Although the release after 120 minutes for all four systems is higher than many values reported in the literature, there is a distinct difference in dissolution performance between the two medium types (DI H_2O and ionic media), which provides assurance that some level of ion-exchange has been achieved. The drug release follows the same general trend that was highlighted in the acidic media trials. That is, the resinates produced using media with lower pH values (pH 4 (unadjusted) and pH 5) release the highest quantity of drug (60% and 70% respectively) and at the fastest rate, compared to resinates produced using solutions adjusted to higher pH values (pH 6 and pH 7). During the initial stages of the dissolution study and up until the 25 minute timepoint, the aforementioned DRCs (pH 6 and pH 7 systems) release drug at a similar rate, after which, drug release plateaus in the case of the pH 6 system and steadily increases for the pH 7 system. This results in 40% and 60% drug release after 2 hours for the resinates produced using loading solutions adjusted to pH 6 and 7 respectively. Although the extent of drug release from the DRC produced using a loading solution adjusted to pH 7 is statistically similar to the % drug release from the DRCs produced using an unadjusted loading media and one adjusted to pH 5, there is a marked difference in the rate at which drug is released from the DRCs in DI H_20. As referenced earlier the DRCs produced using loadings solutions adjusted to pH 6 and 7 display distinct release behaviour reflected in the slower release kinetics over at least the first 90 minutes in DI H_2O depending on the specific DRC. Similarly, in 0.1 M HCl, the same two DRCs (pH 6 and pH 7) exhibit the slowest release kinetics over at least the first 30 minutes depending on the specific DRC. Overall, a comparison of the dissolution profiles in both media types (0.1 M HCl and DI H_2O) of the four DRCs reveals the DRC produced using a loading solution adjusted to pH 6 as the best performing system on the basis of it leaching the least amount of drug in DI H_2O whilst retaining a rapid release rate in 0.1 M HCl. Interestingly, this DRC has neither the highest nor the lowest drug loading relative to the other three DRCs studied, which suggests that no obvious relationship between drug loading and the DRCs propensity to leach drug into DI H_20.

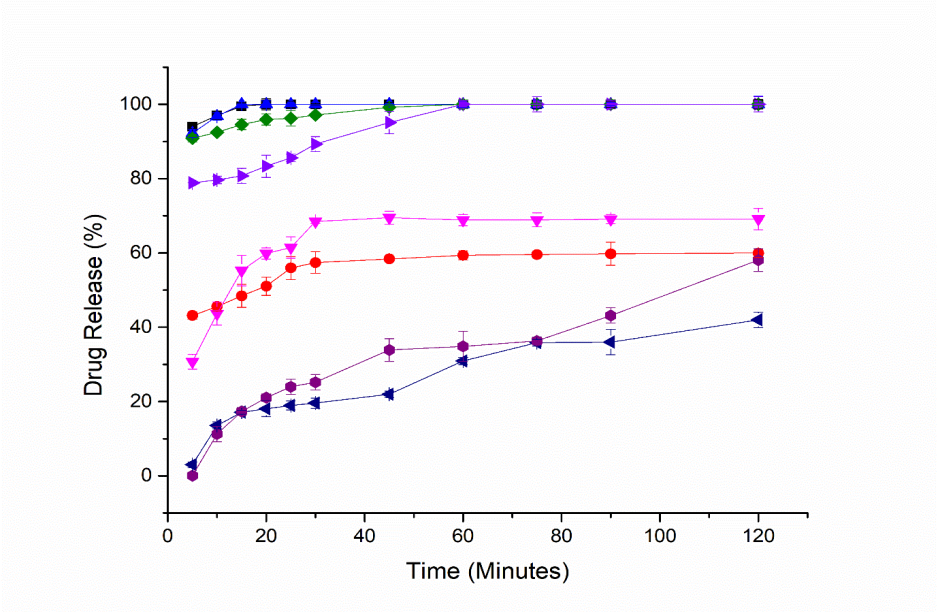

Figure 4.14. Drug release profiles in either 0.1 M HCl or DI H_2O at 37 °C, of DRCs formed using a 1:1 D:R (IRP64) (w/w) ratio (pH adjusted and pH unadjusted drug solutions). DRC (unadjusted) in 0.1 M HCl (Black square), DRC (unadjusted) in DI H_2O (Red circle), DRC (adjusted to pH 5) in 0.1 M HCl (Blue triangle), DRC (adjusted to pH 5) in DI H_2O (Inverted magenta diamond), DRC (adjusted to pH 6) in 0.1 M HCl (Olive diamond), DRC (adjusted to pH 6) in DI H_2O (Navy diamond), DRC (adjusted to pH 7) in 0.1 M HCl (Violet triangle) and DRC (adjusted to pH 7) in DI H_2O (Purple circle).

Similar to the studies described for IRP64 systems, the *in vitro* release profiles of the DRC formed using IRP88 were studied (Figure 4.15) using the paddle apparatus according to the method previously described in section 2.2.8 in Chapter 2. By comparing the resinates' performance in a selection of dissolution media that encompassed both ionic media and DI H_2O, it became apparent that the resinate did not perform as expected, even when compared to the IRP64 resinates, which themselves exhibited a limited level of control on the drug release. Similar to the IRP64 resinates, the drug is rapidly displaced off the resin at low pH, which is not surprising, considering the pH environment is unfavourable in terms of retaining the drug. Therefore, ionic bonding between components no longer occurs, leading to immediate drug release, characterised by 95% of the drug being released from the resinate within 5 minutes and complete drug release occurring after 15 minutes. This rapid release rate at low pH has been described previously and is attributed to a low percentage of the ionic sites being dissociated under acidic conditions (313). This behaviour in DI H_2O, pH 6.8 buffer and 0.1 M NaCl is suggestive of weak complexation, as the release of the drug is rapid in all three media. Similar to the initial timepoints when the IRP64 resinates were studied, a burst effect is evident, but to a larger extent, as approximately 65% of the drug is released at the 5 minute timepoint and complete release is achieved after 20 minutes. The dissolution profile shows that the systems do not exhibit any resistance to drug leaching in a medium where there are no ions to effect drug release, i.e. DI H_2O. This behaviour is typical of a drug that has been physically adsorbed onto the resin surface and has

high enough water solubility to be dissolved in the medium. The drug release profiles in pH 6.8 buffer and 0.1 M NaCl indicate that the drug is released at an intermediate rate compared to release in DI H_2O and 0.1 M HCl over the first 5 minutes, but no statistical difference ($p>0.05$) in the release profile can be detected thereafter. This combination of rapid release, approaching completion in DI H_2O, and the lack of a differential drug release behaviour in the higher pH environment, supports the assertion that the interaction between drug and resin is not strong.

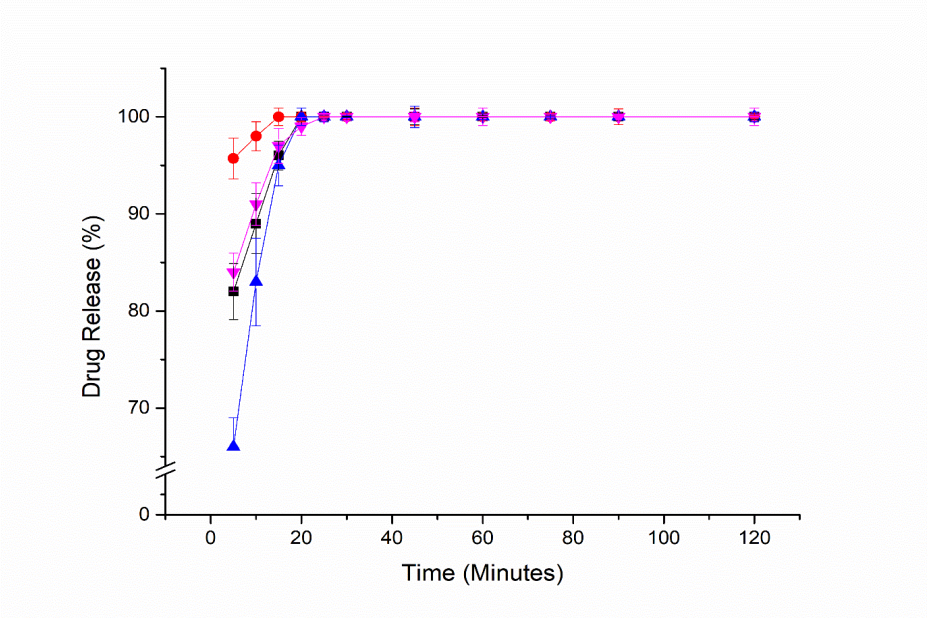

Figure 4.15. Drug release profiles in either 0.1 M HCl, 0.1 M NaCl, pH 6.8 buffer or DI H_2O at 37 °C, of resinates formed using a 1:1 D:R (IRP88) (w/w) ratio, using the USP type 2 paddle apparatus in DI H_2O (Blue triangle), 0.1 M NaCl (Black square), pH 6.8 buffer (Magenta inverted triangle) and 0.1 M HCl (Red triangle).

4.2.6 DVS analyses (IRP64 and IRP88)

Although DVS analysis is a prominent technique that has displayed its worth in assessing the sorption tendencies of many different materials, little evidence can be found of its application to IERs (324). The uptake of moisture of selected IRP64-based samples and the system formed using IRP88 (shown in Figure 5 in Appendix 2) were assessed and the water vapour sorption-desorption curves are displayed in Figure 4.16. DVS isotherms of the raw material and TZD free base are depicted in Figure 4 in Appendix 2 and show that the API sorbs far lower quantities of moisture relative to the amorphous resins. As expected, all the resins examined were hygroscopic, as they all absorbed quantities of moisture at 90% RH at 25°C which were at least 20% of their dry weight (Table 1 in Appendix 2). A closed hysteresis loop was evident in the sorption-desorption profiles of all drug-loaded samples, while the resin raw materials were unable to release all of the bound sorbed moisture, producing open hysteresis loops. The presence of hysteresis indicates that the sample is less able to release (desorb) the moisture taken in (sorbed), which may be caused by a change in the structure of the material after

the ingress of water (325). In this respect, the moisture sorption behaviour of the resinates did not vary for samples prepared by adjusting the pH of the loading solution, and all samples showed profiles dissimilar to that of raw material. The resinates produced using drug solutions adjusted to pH 5 and 6 have remarkably similar isotherms, reflective of very similar moisture sorption/desorption tendencies. The isotherm related to the system prepared with drug loading solution adjusted to pH 7 exhibits an isotherm containing a similarly shaped hysteresis, however, this sample sorbs a higher amount of moisture from the 40% RH condition onwards. As remarked earlier, the IRP64 raw material displays several contrasting features, most notably the open hysteresis and also the higher moisture uptake from the 50% RH condition onwards. As previously stated, this type of hysteresis is often associated with a change in the structure or solid-state of the starting material, however, in this instance, this is extremely unlikely as there is a general consensus amongst researchers that the raw amorphous polymer is incapable of crystallising. A more likely reason is the inability of the amorphous resin to fully expunge the high quantity of moisture sorbed throughout the bulk of the structure.

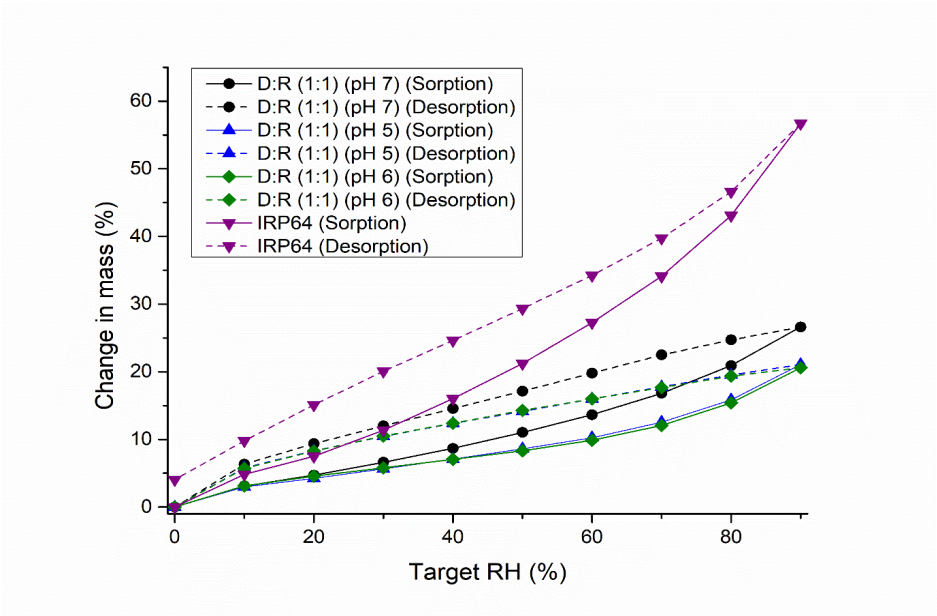

Figure 4.16. Vapour sorption and desorption isotherms of IRP64 raw material and selected IRP64 resinates (formed using a 1:1 D:R ratio (w/w)) which have been produced by altering the pH of drug loading solution prior to resin addition.

Moisture isotherms of the IRP88 raw material and the 1:1 resinate are similar to those of the IRP64 based systems (Figure 5 in Appendix 2). The raw material has the highest moisture uptake of all the samples studied, consistent with its established role as a disintegrant within tablet formulations (313). Again, the material exhibits an open hysteresis, although smaller than that displayed for the IRP64

resin. The 1:1 DRC exhibits far lower moisture uptake (approximately 20%) than the resin alone, similar to the IRP64-based DRC produced using drug solutions adjusted to pH 5 and 6.

pXRD analysis performed on the resinates formed using IRP64 (Figure 4.17) and IRP88 (Figure 6 in Appendix 2) post-DVS analysis, highlighted the stability of the DRCs upon exposure to high humidity, showing that this facet of stability is not just limited to resinates formed using sulfonic acid-containing resins. The diffractograms of the three selected resinates produced from pH 5, pH 6 or pH 7 loading solutions ranging are illustrated in Figure 4.17, with all three samples remaining pXRD amorphous.

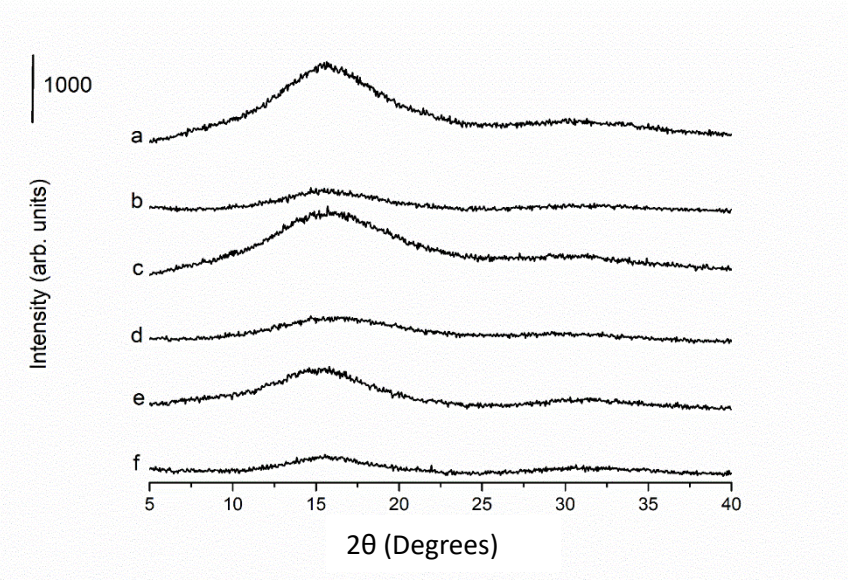

Figure 4.17. pXRD analyses (pre and post-DVS analysis) of the batch-produced resinates formed using IRP64 (1:1 (w/w) D:R ratio (w/w)) and by altering the pH of the drug loading solution prior to the addition of resin. a) pH 5 (Pre-DVS), b) pH 5 (Post-DVS) c) pH 6 (Pre-DVS), d) pH 6 (Post-DVS), e) pH 7 (Pre-DVS) and f) pH 7 (Post-DVS).

4.2.7 SEM (IRP64 and IRP88)

SEM images of TZD HCl and TZD free base are presented in Figure 4.18(A-D). There are noticeable differences in morphology and particle size of the two materials. The free base material appears as small clusters at low magnification (500x) (Figure 4.18(A)), which are still evident at much higher magnification (8000x) (Figure 4.18(B)). The higher magnification provides some insight into the shape of the individual particles which can be described as column-like, resembling that of the crystals of the salt form, albeit the particle shape is far more irregular. However, in the case of the salt form (Figure 4.18(C-D)), little evidence of particle aggregation can be found and the particles are significantly larger relative to the free base form, as is evident from the lower magnifications required to take a clear image.

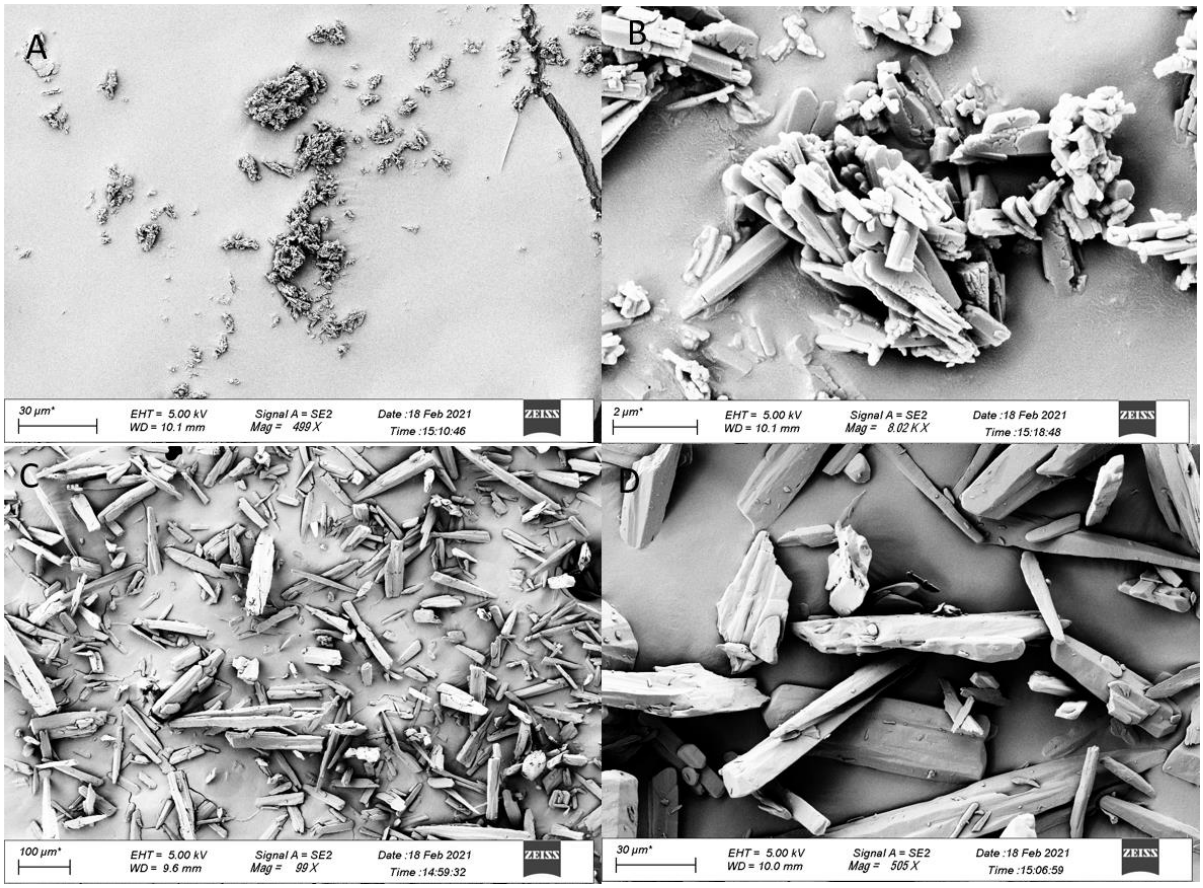

Figure 4.18. SEM images of a) TZD free base (x500), b) TZD free base (x8000), c) TZD HCl raw material (x100) and d) TZD HCl raw material (x500).

Figures 4.19-4.20 shows the SEM micrographs for a selection of DRC/resinate samples in addition to the raw materials (IRP64 and IRP88). Each resin grade exhibits distinctive characteristics that define the morphology. The IRP64 grade (Figure 4.19(A)) is more heterogenous in its appearance relative to the IRP88 grade (Figure 4.20(A)) characterised by a mixture of agglomeration between particles that have cracked surfaces as well as smoother faces. However, post-loading all resinates (IRP64-based) appear to have similar morphological characteristics, with no evidence of residual crystalline material on the surface, that might be attributable to TZD HCl or free base. Therefore, it can be inferred that the drug material has been embedded into the polymeric matrix, similar to what has been postulated by other groups investigating the binding of drug species to “weak” cation exchangers (314). Evident from images is the increase in the size of the resinates relative to the raw material, as well as the reduced prevalence of particles with a smoother surface.

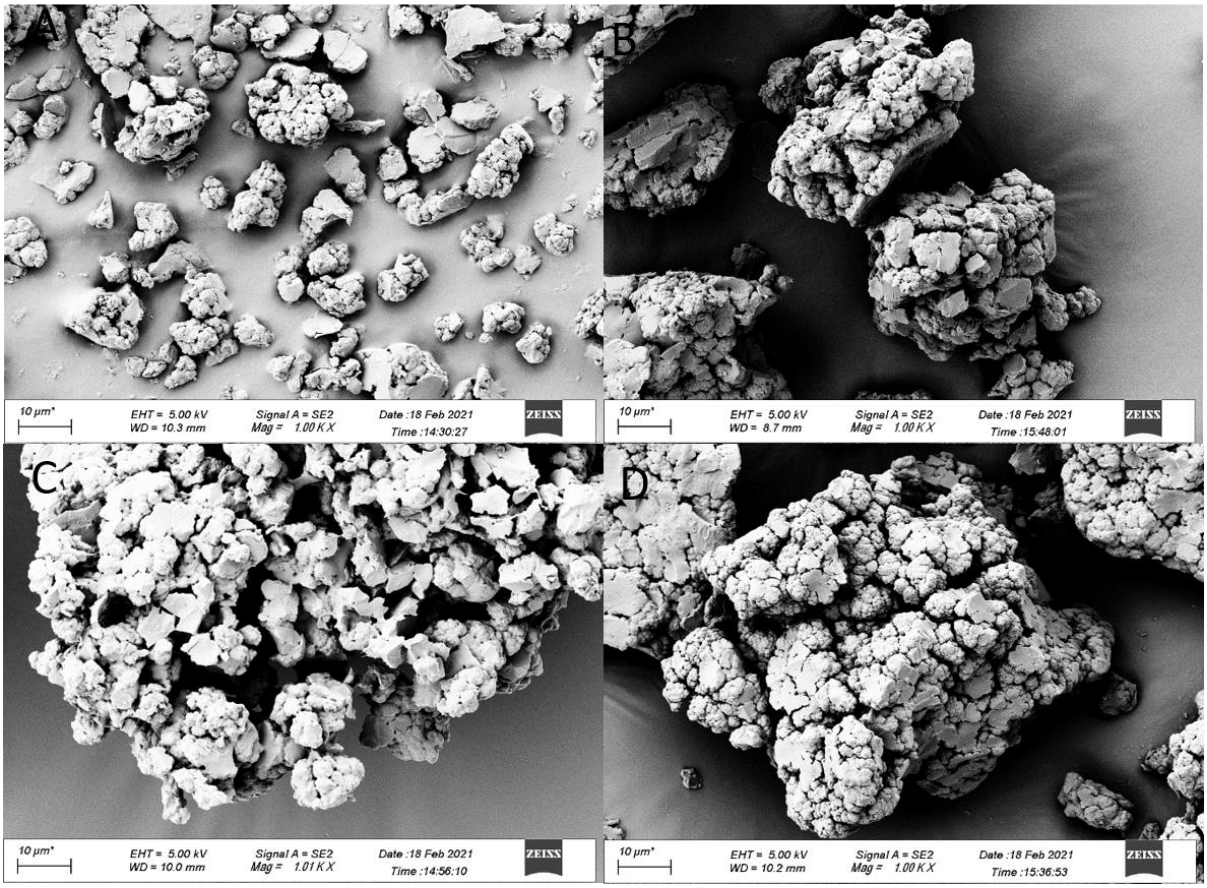

Figure 4.19. SEM images of resin raw material and DRCs formed using a 1:1 D:R (IRP64) ratio (w/w) where the pH of drug loading solution has been adjusted before the addition of resin material. a) IRP64 raw material, b) DRC (pH 5), c) DRC (pH 6) and d) DRC (pH 7).

The images presented in Figure 4.20(A-B) reveal that the morphology of the IRP88 resin grade resembles that of the IRP69 resin discussed in Chapter 3. These smoothened surfaces contrast with the IRP64 grade which has a notably roughened surface. Moreover, there is a far lower level of heterogeneity in the IRP88 raw material, with little evidence of agglomeration. Distinct jagged particles are visible in the resinate image, which are larger than their IRP64 counterparts. Regarding particle size, the impact of drug loading is to further increase the size of the complexes formed, with evidence of slight agglomeration present. However, the surfaces remain far less coarse compared to IRP64 resinates. Furthermore, the appearance of voids within the particles increase in prevalence compared to unloaded material, which is a likely consequence of the complexation occurring in water, where the resin can swell and further expand the inherent indentations within the particle. Similarly, to the observations reported for the IRP64 resinates, little evidence of clearly identifiable crystalline drug material can be found on the surface of the particle, suggestive of it being masked within the interior of the matrix.

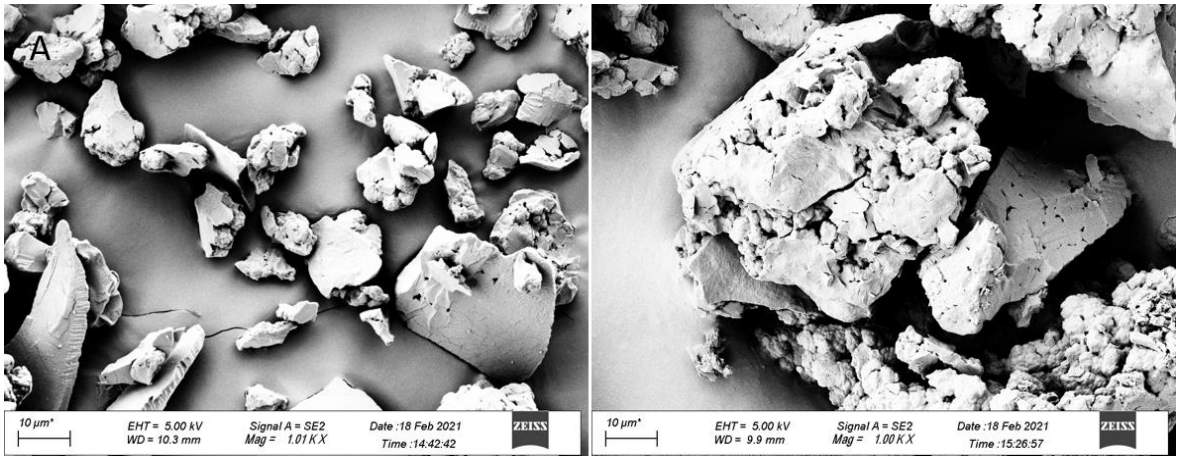

Figure 4.20. SEM images of a) IRP88 raw material and b) resinate (formed using a 1:1 (w/w) D:R (IRP88) ratio.

4.2.8 Drug loading via spray-drying (IRP69)

4.2.8.1 Initial trials (loading studies, moisture sorption studies, solid-state characterisation and drug release studies)

This method of preparation was selected on the basis of spray-drying being a rapid, single-step process that lends itself to manufacturing scale-up (326). The process also has an established reputation for producing particles with a narrow size distribution with low moisture content (154). These advantages can be realised once a firm understanding of the process parameters has been achieved, which was the first aim of this work. As alluded to in the introduction to this chapter, within the context of drug-resin complex formation, the use of spray-drying is relatively under-investigated using Amberlite™ IRP69, with this process being first reported by Kim et al., who formed a complex using donepezil and the "weak" cation exchanger Amberlite® IRP64 (94). Subsequently, Verma et al. used the technique to successfully produce DRCs containing efavirenz and the weak exchanger Tulsion-335 using a DoE approach (220).

Although the technique has been reported as a method of complex formation in the literature, several issues unique to the process were not reported, which became apparent during initial spray-drying trials and made DRC formation more challenging than initially envisaged. The first pertained to the particle size of the DRC, which necessitated adequate stirring speed and a sufficiently slow feed rate to avoid sedimentation in the feed tube of the spray dryer. The second issue, which became apparent upon spray-drying, could also be related to the size of the complex. During the drying process, the deposition of powder in the collecting vessel at the base of the drying chamber (rather than the main collection vessel at the base of the cyclone separator) was noticeable. Although substantial powder yields were achieved for the purpose of this research, this phenomenon would prove problematic on a commercial scale due to the loss of valuable product. The particle size analysis results of the four

trial samples (Figure 4.21) revealed that the particles deposited below the drying chamber were larger ($p<0.05$) than those collected in the collecting vessel. These particles were unable to pass through the spray-dryer due to their large particle size, causing them to be collected below the drying chamber. This contrasts with the particles sampled from the main collecting vessel which were of sufficient size to remain within the airflow stream, thus avoiding premature deposition in a location other than the collecting vessel.

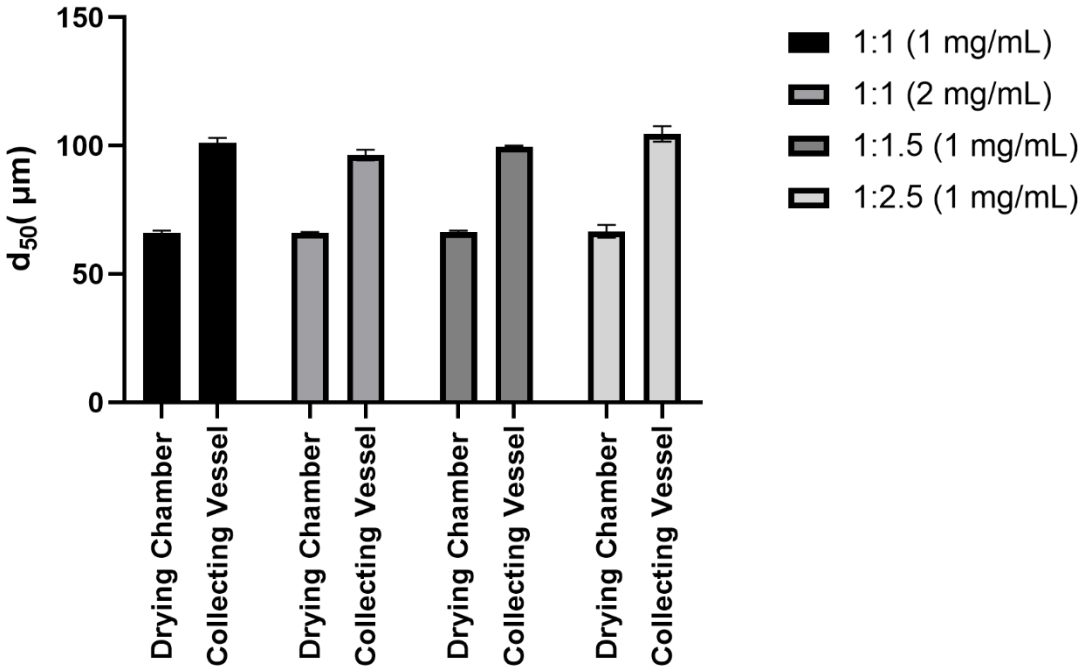

Figure 4.21. Comparison of d_{50} values of selected spray-dried DRCs formed using different D:R (IRP69) ratios (1:1, 1:1.5 and 1:2.5 (w/w)) and concentrations of drug loading solution (1 mg/mL and 2 mg/mL) that were collected from two different locations in the spray dryer (vessel below the drying chamber and the main collection vessel at the base of the cyclone separator itself).

The pXRD diffractograms of the samples collected in both locations and not subject to any further processing steps are depicted in Figure 4.22. Each diffractogram is characterised by the presence of Bragg peaks in each diffractogram, representative of TZD HCl at 11.1°(2θ), 12.3°(2θ), 17.5°(2θ), 22.3°(2θ), 24°(2θ), 24.3°(2θ), 24.8°(2θ), 26.7°(2θ) and 27.2°(2θ). However, the peak of the strongest intensity at the 32° (2θ) position, which is a consistent feature of all samples, could not be assigned to TZD HCl. This prompted consideration of the interaction between the drug and resin during the complexation stage prior to the drying process. By combining the salt form of the drug with the sodium salt form of the resin, NaCl is generated. Therefore, it was hypothesised that NaCl and uncomplexed TZD were present on the surface. This hypothesis was confirmed by a combination of DSC analysis and

further pXRD analysis. The thermograms of the spray-dried systems (unwashed) are depicted in Figure 4.24(A), and support the assertion that uncomplexed TZD HCl is present in the spray-dried product. This is signified by a melt endotherm in each DSC trace, which varies in enthalpy value depending on the location of sampling and ratio of drug to resin studied. Melting point depression is also evident, based on the melt onset values ranging from 270 °C to 280 °C being noticeably suppressed relative to the pure drug value (290 °C). These lowered values are not entirely surprising considering the presence of the high molecular weight resin in the system, which can still interact via hydrophobic interactions with APIs courtesy of its aromatic structure, thus conferring a melting point depression effect (323). The presence of NaCl in the unwashed complexes was confirmed by pXRD analysis through comparison to a standard, shown in Figure 8 in Appendix 2.

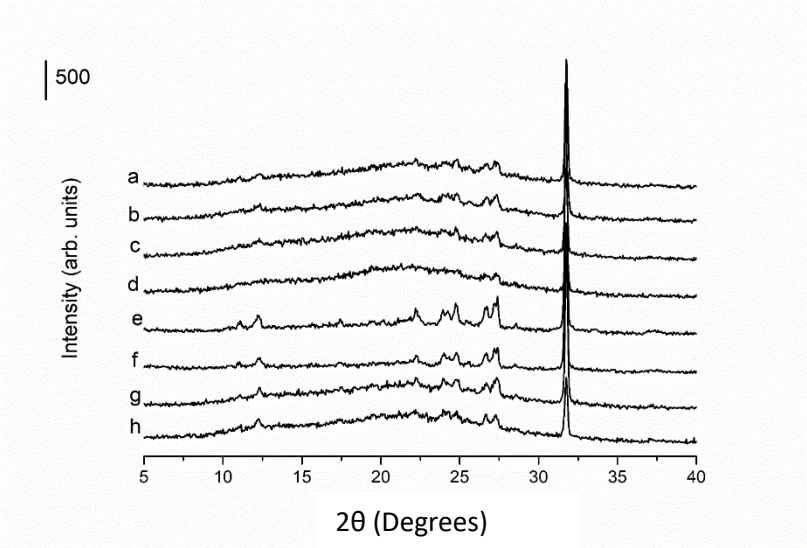

Figure 4.22. pXRD diffractograms of spray-dried DRCs produced using various D:R (IRP69) ratios (w/w) and different concentrations of drug in the loading solution, sampled from different locations (drying chamber or cyclone) within the spray dryer (stated in parentheses). It can be assumed that a 1 mg/mL drug loading concentration was used unless otherwise stated. a) 1:1.5 (drying chamber), b) 1:1.5 (collecting vessel), c) 1:2.5 (drying chamber), d) 1:2.5 (collecting vessel), e) 1:1 (drying chamber (2 mg/mL)), f) 1:1 (collecting vessel (2 mg/mL)), g) 1:1 (drying chamber) and h) 1:1 (collecting vessel). All samples were not subjected to a washing step post-processing.

The presence of the salt by-product, together with the likelihood of unreacted TZD HCl, likely present on the surface of the complex, necessitated the use of a washing step. All samples were subsequently analysed by pXRD and DSC, with the results shown in Figures 4.23(A-B) and 4.24(B) respectively. The diffractograms are devoid of Bragg peaks and characterised by the halo pattern, indicative of a lack of crystalline material, which is supported by the absence of the melting endotherm in the DSC traces. These findings provide evidence that the washing step was successful at removing any by-products.

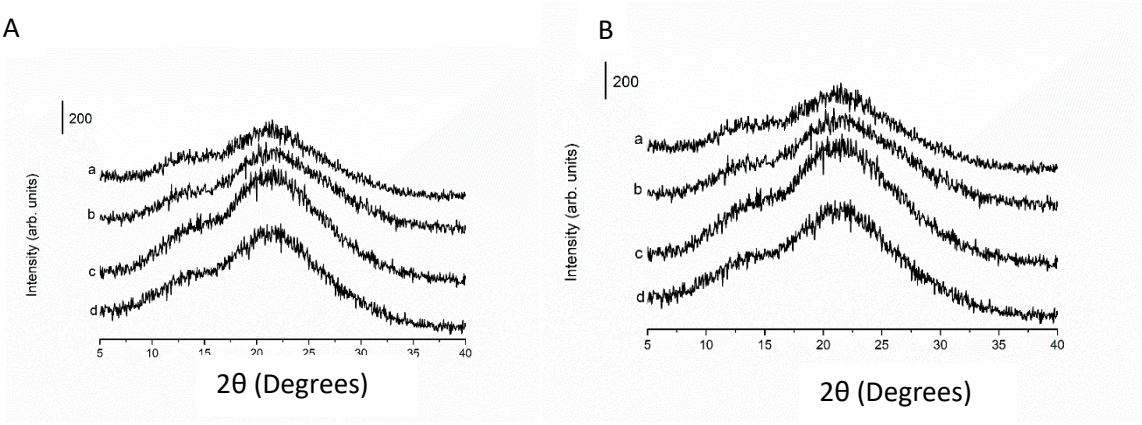

Figure 4.23. pXRD of spray-dried DRCs produced using various D:R (IRP69) ratios (w/w) and different concentrations of drug in the loading solution, sampled from different locations within the spray dryer (stated in parentheses). It can be assumed that a 1 mg/mL drug loading concentration was used unless otherwise stated. A) Drying chamber and B) Collecting vessel. a) 1:1.5, b) 1:2.5, c) 1:1 (2 mg/mL). and d) 1:1. All samples were subjected to a washing step post-processing.

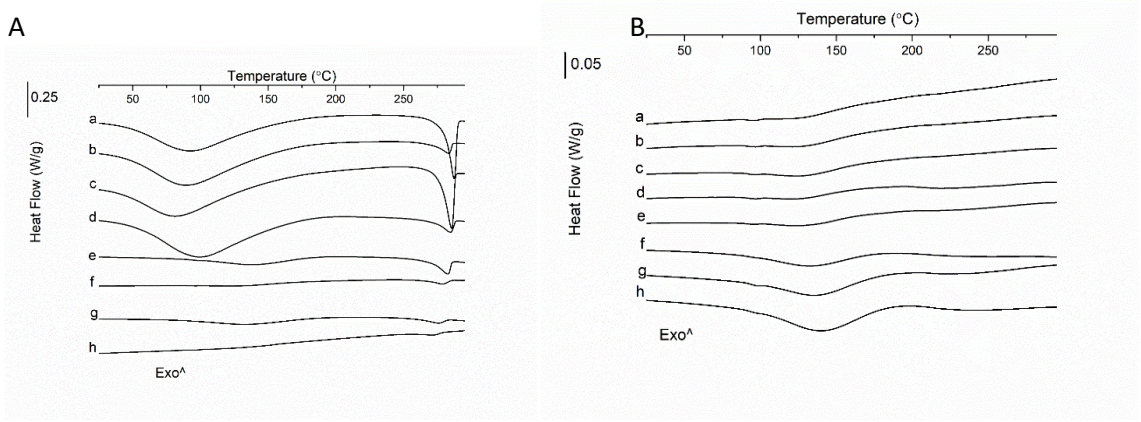

Figure 4.24. DSC thermograms of spray-dried DRCs produced using various D:R (IRP69) ratios (w/w) and different concentrations of drug in the loading solution, sampled from different locations within the spray dryer (stated in parentheses). It can be assumed that a 1 mg/mL drug loading concentration was used unless otherwise stated. Samples subject to a post-processing washing step using DI H_2O are distinguished from those which were not washed. A) spray-dried DRCs (unwashed) and B) spray-dried DRCs (washed). (a) 1:1 (drying chamber), (b) 1:1 (collecting vessel), (c) 1:1 (drying chamber (2 mg/mL)), (d) 1:1 (collecting vessel (2 mg/mL)), e) 1:1.5 (drying chamber), f) 1:1.5 (collecting vessel), g) 1:2.5 (drying chamber) and h) 1:2.5 (collecting vessel).

The calculated assay values for the spray-dried samples (both washed and unwashed) are listed in Table 4.6. When comparing equivalent systems (on a weight per weight basis), it is evident that a disparity exists between the washed and unwashed samples when the 1:1 ratios are compared. This discrepancy can be attributed to the quantity of unreacted drug which serves to inflate the drug

loading values for the unwashed samples, as it has not been removed as part of a washing step. Having said this, the increase in % drug loading is not very high but is statistically significant ($p<0.05$), and can be ascribed to the majority of the drug being taken up by the resin during the loading stage, established during the loading studies reported in Chapter 3. As stated previously, a 24 hour contact time is used to bind the drug to the resin prior to spray-drying and resultant drug association efficiency is calculated to be 89%. This means approximately 11% of the starting TZD HCl content has not bound to the resin but is still present in the medium that is subsequently spray-dried. Based on further spray-drying studies, reported later on in this chapter, when TZD HCl is spray-dried from an aqueous solution on its own, an extremely low yield is recovered, which helps to explain the marginal increase in calculated drug loadings of unwashed spray-dried product. Furthermore, no statistical difference for washed versus unwashed spray dried product is evident when the 1:1.5 or 1:2.5 ratios are examined, which can be explained by the absence of unreacted drug in the loading media, as there is a sufficient amount of resin available to bind the drug dissociated in the loading solution. Also depicted in Table 4.6, is the effect of drug concentration (1 mg/mL versus 2 mg/mL) and D:R ratio (w/w) on the drug loading alongside the powder yields (based solely on the material recovered from the collecting vessel). Akin to the batch-produced DRCs, complexes formed using higher proportions of resin relative to the drug in the loading media contained lower drug loadings and higher powder yields. The excess resin, present in the 1:1.5 and 1:2.5 samples, served as a diluent due to the 1:1 ratio proving optimal from a drug loading perspective. This dilution effect produced lower drug loadings, which is not unexpected, considering the fundamental loading process does not change compared to the batch method, in contrast to the drying mechanism. In contrast, an increased concentration of drug in the loading solution at an equivalent D:R ratio did not significantly affect the % drug loading or the powder yield (%).

Table 4.6. Comparison of the drug loadings of DRCs determined using the drug displacement assay for selected samples produced by spray-drying using different D:R (IRP69) ratios (w/w) and drug concentrations in the loading solution. It can be assumed that the concentration of the drug in the loading solution was 1 mg/mL unless otherwise stated.

		Drug loading (% w/w) on DRC	
D:R ratio	Powder yield (%)	DRCs subject to washing post-processing	DRCs not subject to washing post-processing
1:1	30.9 ± 1.14	48.10 ± 1.89	50.50 ± 0.75
1:1 (2 mg/mL)	30.0 ± 1.41	48.02 ± 0.11	50.18 ± 0.91
1:1.5	37.0 ± 0.93	36.40 ± 0.81	36.31 ± 0.75
1:2.5	59.0 ± 1.23	25.00 ± 0.40	18.04 ± 0.39

Figure 4.25 summarises the mean particle size (d_{50}) of the TZD HCl, IRP69, spray-dried DRC (1:1 and 1 mg/mL) and batch-produced DRC. From this data, it is clear that the spray-drying process results in particles with a smaller particle size relative to the batch process ($p<0.05$). The surface area analysis performed generated results that support this finding, as the specific surface area (SSA) values determined by BET analysis of the spray-dried particles (0.504 ± 0.001 m^2/g) were higher ($p<0.05$) relative to batch-produced DRC (0.29 ± 0.001 m^2/g) for an equivalent D:R ratio studied (1:1). SEM analysis (Figure 4.26) revealed a smoother surface for spray-dried materials compared to standard batch method produced material and is not unsurprising considering both drying processes are fundamentally different which is likely to account for the differences seen. A further point is that the particle size of the milled DRC, originally produced by the batch process (Figure 4.25 and Chapter 3), is still considerably lower than that of spray-dried material, highlighting the limits of the spray-drying process if smaller sized particles are desired.

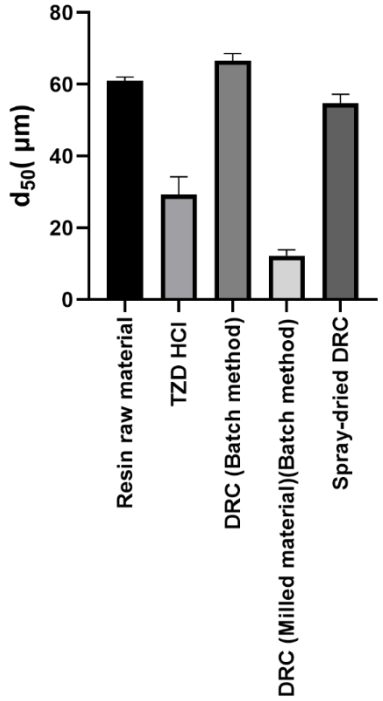

Figure 4.25. Comparison of particle size (d_{50}) of unprocessed raw materials and the DRCs (batch-produced and spray-dried) formed using a 1:1 D:R (IRP69) (w/w) ratio. The two DRCs (batch-produced) are distinguished on the basis of one using unmilled starting resin material and the other using milled starting resin material (IRP69).

Spray-drying of the system caused a distinct change in the morphology of the resultant product. Similar to the microparticles produced by the batch system, there appeared to be no evidence of residual crystalline material. However, the surface of the spray-dried material is noticeably smoother than batch-produced DRCs, resembling that of the raw resin material, less heterogeneity with regard to particle size and shape is apparent, evidenced by few visible remnants in the spray-dried images (Figure 4.26). The overall particle shape remains similar to that of the DRCs produced using the batch process, indicating that the spray-drying process did not affect that characteristic of the particles. The impact of the spray-drying process on the size of the particles is difficult to ascertain, as the bigger particles present in each image are approximately the same size, reflected by the closeness of the d_{50} values illustrated in Figure 4.25.

A B

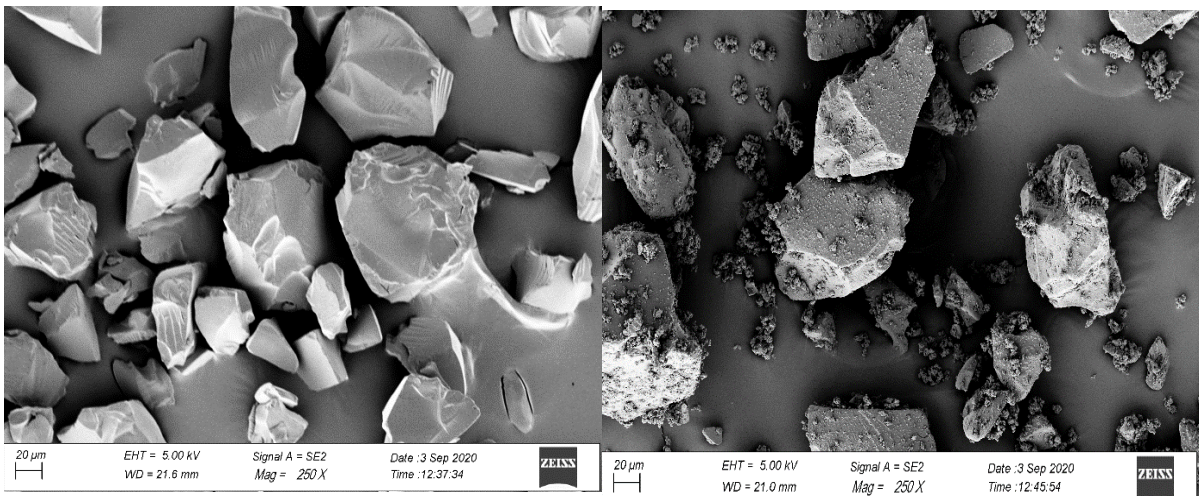

Figure 4.26. SEM images of a) spray-dried DRC and b) batch-produced DRC. The drug concentration in each loading solution (batch and spray-drying processes) was 1 mg/mL and the D:R (IRP69) ratio was 1:1 (w/w).

FTIR analysis was performed on the spray-dried DRCs (1:1 w/w ratio) produced to investigate the formation of intermolecular bonds indicative of ionic bonding (Figure 4.27). Together with the solid-state analyses using pXRD and DSC, this spectroscopic evidence can unequivocally identify the formation of a complex, in which the properties of the API are impacted (314). The spectra of the spray-dried products pre and post-washing displayed noticeable differences in the 3250 cm^{-1} region. This absorption band is representative of the stretching vibration of the amine group of the TZD HCl structure and is the functional group capable of forming the salt pair with the resin through bonding to the sulfonic acid groups along the backbone. This band is clearly visible in the spectrum of the physical mixture of drug and resin, where little interaction would be expected. In the case of the spray-dried products, the peak is present in the spectrum of the unwashed sample but is absent in the spectrum of the spray-dried sample that was subsequently washed. Considering the evidence from the DSC analysis and knowledge of the loading process, which revealed that a 1:1 ratio does not result in 100% uptake of drug from solution, the uncomplexed drug present on the surface of the resin is likely responsible for this peak. The washing step is necessary to eliminate this unreacted crystalline drug off the surface, the success of which, is confirmed by the peak's absence, thus producing a spectrum that resembles that of a DRC produced using the batch process. Similar to the batch-produced systems discussed in Chapter 3, more subtle differences are observed in the 1600 cm^{1} region of the spray-dried samples. A peak at 1603 cm^{-1} with a strong intensity, representative of the N-H bending vibration is absent or shifts to a higher wavenumber (signified by the red dashed lines in Figure 4.27) so that it merges with its neighbour located at 1640 cm^{-1} to produce a broad peak with

no clear distinction between the two aforementioned peaks. Discrepancies regarding the C-N stretching vibrations are also apparent in the spectra of the spray-dried samples (and by extension the batch-produced DRC). A peak with low intensity at 1350 cm^{-1} attributable to C-N stretching vibration of the aromatic amine is visible in the spectrum of the untreated spray-dried sample, but absent in the washed sample (signified by the red dashed lines in Figure 4.27). Similarly, the peak at 1189 cm^{-1}, representative of the C-N stretching vibration of the secondary amine group cannot be deciphered in the spectrum of the washed sample, akin to the batch-produced sample, whereas in the unwashed spray-dried sample, a trace amount is evident (signified by the red dashed lines in Figure 4.27). These events are suggestive of complexation and are consistent with findings in the literature (118). Again, similar to the initial FTIR analysis on the DRCs (Chapter 3), changes in peak position or intensity of peaks representative of sulfonic acid groups are less obvious within the complicated fingerprint region of the spectra. Subtle differences in the region of the resinates' spectra associated with the sulfonate stretching vibration, namely the 1150-1200 cm^{-1}, are highlighted by the deviation from the black dashed line that goes through the centre of the absorption bands in the resin raw material's spectrum (Figure 4.27). Two cases of peak shifting are evident, 1173-1162 cm^{-1} and 1036-1032 cm^{-1}, and are consistent with those reported by previous authors, who cite such changes as further evidence of ion-exchange (119).

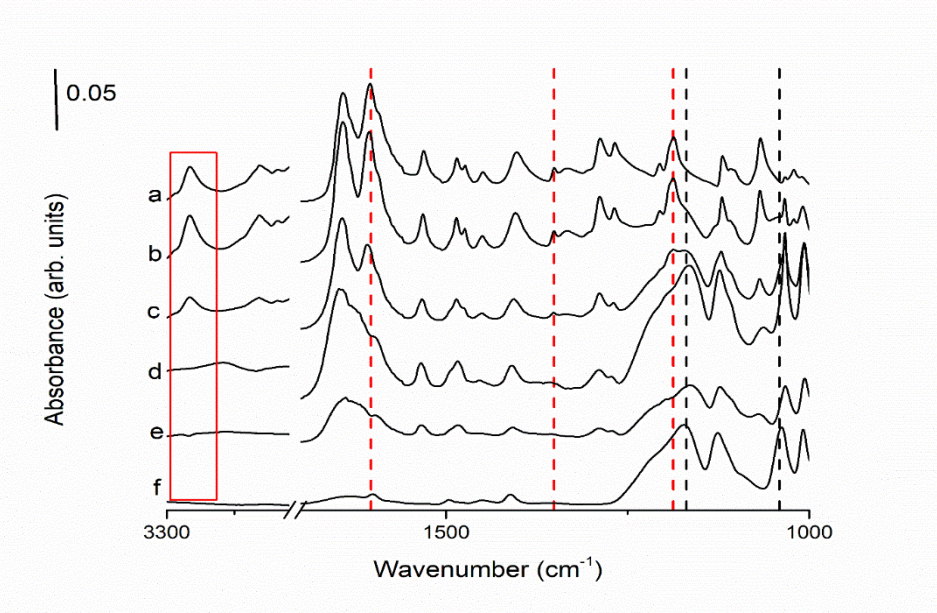

Figure 4.27. FTIR spectra of raw materials, a physical mixture of drug and IRP69, batch-produced DRC (1:1 D:R (IRP69) ratio)(1 mg/mL drug concentration) and spray-dried DRCs (1:1 D:R (IRP69) ratio)(1 mg/mL drug concentration) with and without a post-processing wash step. a) TZD HCl raw material, b) physical mixture of TZD HCl and IRP69 (1:1 w/w), c) spray-dried DRC (unwashed), d) spray-dried DRC (washed), e) DRC formed using a 1:1 D:R ratio (w/w) (batch-produced) and f) IRP69 raw material.

DVS analysis was performed to compare the moisture sorption/desorption profiles of the DRCs produced (by spray-drying and the previous batch process), the IRP69 raw material and a physical mixture of drug and resin. The isotherms display marked differences in the sorption behaviour (Figure 4.28). This is illustrated by the high moisture uptake by the resin raw material at 90% RH relative to the batch-produced DRC, physical mixture and spray-dried DRC. This is not surprising considering the well-known hygroscopicity of the resin raw material, attributed to the sulfonic acid groups (327). Although the moisture uptake from the physical mixture system is significantly lower than that of the resin material, due to the presence of crystalline API in the system, the uptake is still relatively high (25%). In contrast, the DRCs produced the most unusual behaviour with respect to the % moisture uptake at 90% RH. Regarding the batch-produced DRC, there is a gradual increase in moisture uptake across the entire RH range examined. This extent of moisture uptake is lower than the physical mixture studied (after 30% RH), which is unexpected as it is suspected that the resin contains the amorphous form of the drug, whereas the physical mixture consists of resin and crystalline drug. By loading the drug onto the resin, leading to complex formation, the ability of the resin itself to sorb moisture may be impacted, leading to lower than anticipated moisture sorption values.

Furthermore, the spray-dried system produces even more remarkable results. Again, there is a gradual increase in moisture uptake, which does not deviate from the batch-produced DRC until the 70% RH condition at which point a dramatic rise in moisture uptake occurs until 90% RH (43%). All systems studied, including the spray-dried sample, produce a hysteresis gap, indicating that the structure shows a different affinity for water after it has been exposed to an elevated humidity environment relative to the dry material. However, the hysteresis loops show different characteristics depending on the sample. Similar to the isotherms produced using the “weak resins”, the IRP69 isotherm has an open hysteresis loop, which is not the case with the physical mixture or spray-dried DRC. This phenomenon is also present in the isotherm of the batch-produced DRC. Interestingly, the physical mixture and batch-produced DRC do not have a large hysteresis relative to the raw material or spray-dried material, signifying that the method of preparation produces tangible differences in one of the main characteristics defining moisture behaviour (hysteresis). Unlike the spray-dried sample, which has the most distinctive isotherm profile examined, the batch-produced DRC has an open hysteresis loop suggestive of a change in the material upon exposure to moisture. However, pXRD analysis performed on the DRCs post-analysis confirmed that no crystallisation of API occurred (Figure 9 in Appendix 2). This is a testament to the known excellent stability properties of DRC that have been demonstrated previously (Chapter 3) for the batch-produced systems. This open hysteresis may be attributed to the difficulty the moisture faces in escaping the interior of the particle over the time course of the study. With the exception of the spray-dried material, all other samples display large

hysteresis gaps (until the final RH) that are commonly encountered with pharmaceutical formulations, characteristic of type IV and V isotherms. This can be ascribed to the bulk absorption phenomenon, the most common moisture sorption mechanism for amorphous materials, which is a slow diffusion-controlled process (328). Regarding the spray-dried system, the isotherm does partially resemble a mesoporous system based on the sudden increase in mass occurring just above the monolayer range (>0.3 p/p_0), however, the desorption behaviour does not produce the characteristic mesoporous hysteresis (type IV) (329). Interestingly, the spray-dried sample does not have an open hysteresis, which may be due to the reduced particle size of the DRC relative to the batch-produced DRC, making it easier for the moisture to be expunged from the centre of the DRC structure.

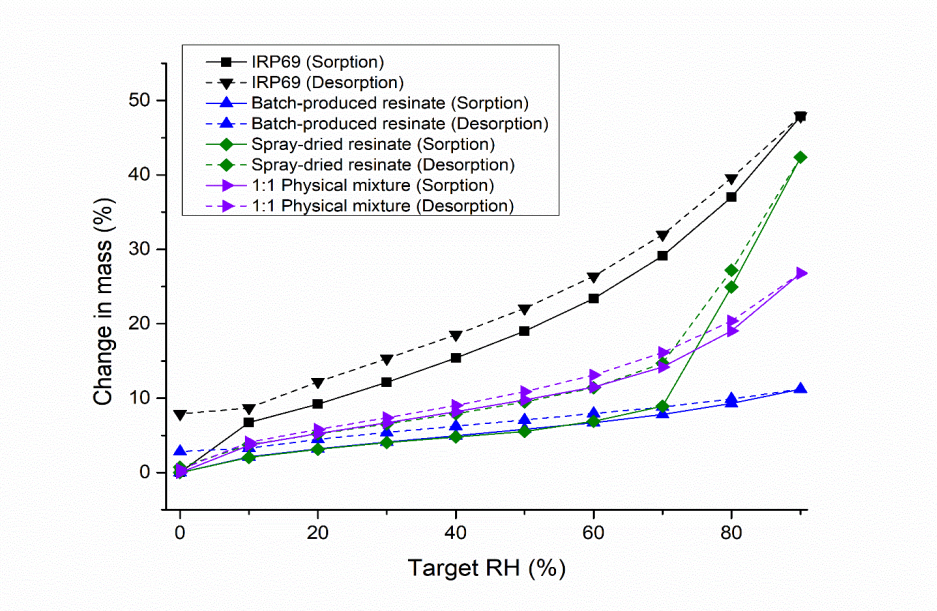

Figure 4.28. Vapour sorption and desorption isotherms of IRP69 raw material, DRCs formed using a D:R (IRP69) ratio of 1:1 (w/w) by either spray-drying or the batch-method and a physical mixture of drug and IRP69 (1:1 w/w).

Prior to the production of the DRCs by spray-drying as per the Taguchi design of experiment (DoE) study (detailed later), the drug was spray-dried from an aqueous solution to determine if any solid-state conversions could occur. Two inlet temperatures (120 °C and 150 °C) were selected to coincide with the parameters specified in the Taguchi design. As illustrated in the pXRD and DSC analysis (Figure 10(A-B) in Appendix 2), a reduction in crystallinity was observed, which was not impacted by the inlet temperature of the spray dryer. This was signified by reduced enthalpy values and peak intensities relative to the raw material in the DSC and pXRD analyses respectively. FTIR (Figure 10(C) in Appendix 2) data further supported this assertion, with the peak position and intensity of the characteristic absorption bands displaying no change relative to the unprocessed raw material.

4.2.8.2 Drug release studies (IRP69)

Drug release studies were performed using the spray-dried samples produced during the feasibility study in 0.1 M HCl (Figure 4.29), to investigate the influence of the washing step on the performance of pre and post-wash resinates. Irrespective of the sample being washed or the D:R ratio/drug concentration in the loading solution, the drug is released from the DRC rapidly, ranging from 81% drug release for the 1:2.5 D:R ratio to approximately 88% drug release for the 1:1 D:R ratio after 5 minutes. Despite the fast drug release kinetics, complete drug release is not achieved for any sample. By achieving an equilibrium concentration that results in incomplete drug release, the DRC performs similarly to many DRCs previously reported (89,109).

For each sample tested (washed versus unwashed), there is no difference ($p>0.05$) in the quantity of drug released after 5 minutes when DRCs formed using the same D:R ratio were compared. The release from the spray-dried DRCs follows a similar pattern to DRCs produced by the batch method regarding the influence of D:R ratio, with the % release at equilibrium following this order: (1:1 (1 mg/mL or 2 mg/mL))>1:1.5=1:2.5). The 1:1 ratios (1 mg/mL and 2 mg/mL), that were not washed, reach equilibrium after 20 minutes, which is quicker than their washed counterparts (45 minutes and 75 minutes respectively), whilst no statistical difference ($p>0.05$) exists in the % drug release at equilibrium for unwashed and washed material for both samples. Similarly, the DRCs produced using the 1:1.5 ratio display no statistical difference ($p>0.05$) in the % drug release at equilibrium and the non-washed samples reach equilibrium faster relative to the washed (45 minutes versus 60 minutes). Interestingly, the washed and unwashed samples of 1:2.5 system do not differ in terms of the % drug release at equilibrium and the time to equilibrium. Relative to their counterparts produced by the batch process, the washed samples take longer to reach equilibrium as the DRCs produced using the 1:1, 1:1.5 and 1:2.5 ratios take 0, 25 and 25 minutes respectively, noticeably shorter than the spray-dried samples (washed).

Regarding the release kinetics of the washed samples, no clear trend can be established, as the 1:1 ratio takes either 45 or 75 minutes to reach equilibrium depending on the concentration of the loading solution used to produce the complex. With regard to the other two ratios studied (1:1.5 and 1:2.5) the higher the proportion of resin in the complex, the quicker the time to equilibrium (25 minutes versus 60 minutes).

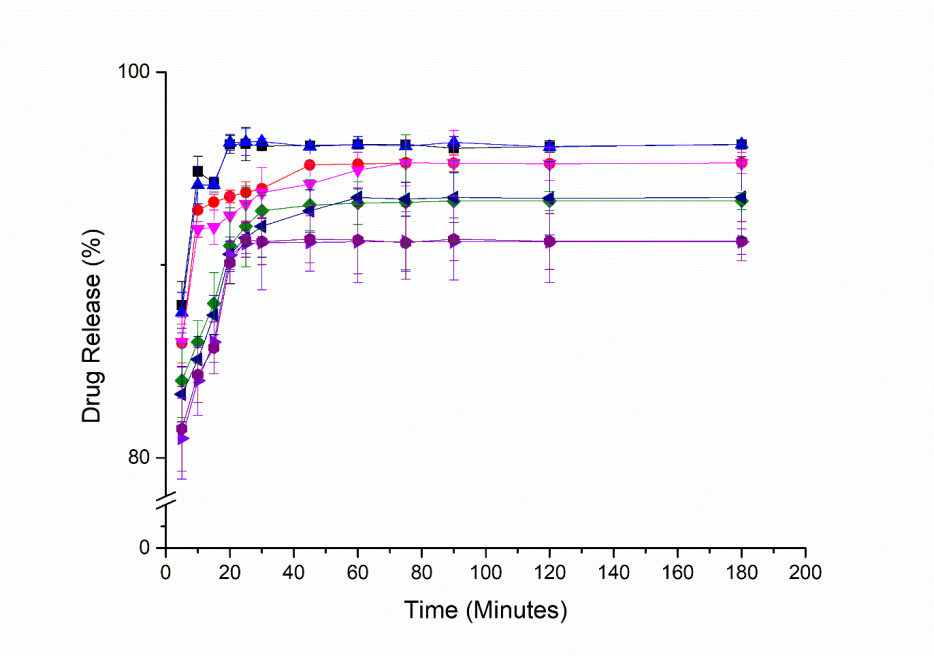

Figure 4.29. Drug release profiles in 0.1 M HCl at 37 °C of selected spray-dried DRCs produced using different D:R (IRP69) ratios (w/w) and concentration of TZD HCl in the loading medium (stated in parentheses). It can be assumed that a drug loading solution concentration of 1 mg/mL was used unless otherwise stated. Samples subject to a post-processing washing step using DI H_2O are distinguished from those which were not washed. DRC (1:1) (pre-wash) (Black square), DRC (1:1) (post-wash) (Red circle), DRC (1:1) (2 mg/mL) (pre-wash) (Blue triangle), DRC (1:1) (2 mg/mL) post-wash sample (Inverted magenta triangle), DRC (1:1.5) pre-wash sample (Olive diamond), DRC (1:1.5) post-wash sample (Navy triangle), DRC (1:2.5) pre-wash sample (Violet triangle) and DRC (1:2.5) post-wash sample (Purple circle).

The dissolution performance of the spray-dried samples (washed) was studied in an alternative ionic media (pH 6.8 buffer) alongside DI H_20 (Figure 4.30). Minimal drug release is observed in DI H_20, which would be expected if ion-exchange, as opposed to physical adsorption, is the mechanism responsible for drug loading. This finding is consistent with the expectation that DI H_20 would only elute a very limited amount of drug from the uncoated resinate. Initial drug release from all DRCs studied is rapid in pH 6.8 buffer, regardless of the D:R ratio or drug concentration in the loading medium used to produce the DRC. The % drug release after 5 minutes ranges from 88% to 90% but no statistical differences exist between all samples studied at this timepoint ($p>0.05$). All samples exhibit similar % drug release at each timepoint ($p>0.05$) which is in contrast to what was observed in the acidic environment. In 0.1 M HCl, the impact of drug loading on the release was evident when the 1:1 ratio was compared to the DRCs produced using 1:1.5 or 1:2.5. Having said that, drug release in acidic medium does share a similarity with the release in pH 6.8 buffer in that drug release from all DRCs

studied is incomplete in both media. Furthermore, the time to equilibrium follows a trend, summarised as higher drug loadings requiring the lowest amount of time to reach equilibrium. Akin to the release behaviour in acidic media, the 1:1 ratio produced using the more concentrated drug solution takes a longer time to reach equilibrium relative to the DRC formed using the 1 mg/mL solution. However, at lower drug loadings the kinetics contrast with those described in 0.1 M HCl as the 1:2.5 systems takes 75 minutes and the 1:1.5 system requires 60 minutes to reach equilibrium. These results highlight the disparity in drug release kinetics that can exist when the same sample is studied using different media compositions.

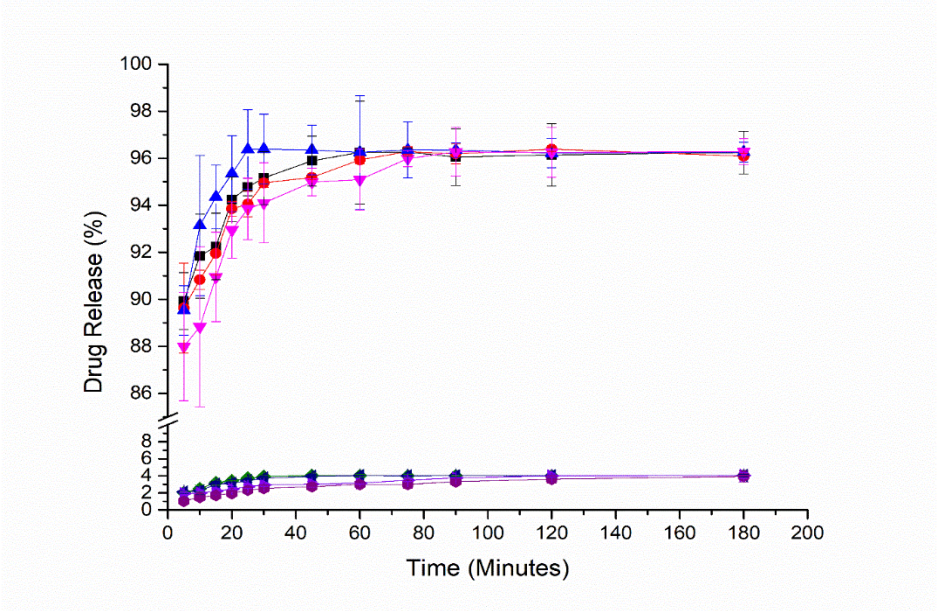

Figure 4.30. Drug release profiles in either 0.1 M HCl or DI H_2O at 37 °C of selected spray-dried DRCs (subject to a washing step post-processing) produced using different drug:IRP69 ratios (w/w) and concentration of TZD HCl in the loading medium (stated in parentheses). It can be assumed that a drug loading solution concentration of 1 mg/mL was used unless otherwise stated. DRC (1:1) in pH 6.8 (Black square), DRC (1:1)(2 mg/mL) in pH 6.8 (Red circle), DRC (1:1.5) in pH 6.8 (Blue triangle), DRC (1:2.5) in pH 6.8 (Inverted magenta triangle), DRC (1:1) in DI H_20 (Olive diamond), DRC (1:1) (2 mg/mL) in DI H_20 (Navy triangle), DRC (1:1.5) in DI H_20 (Violet triangle) and DRC (1:2.5) in DI H_20 (Purple circle).

To the best of the author's knowledge, this is the first case of evidence being presented for the impact of the processing method on the release of the drug from DRCs (Figure 4.31). The disparity in drug release behaviour extends to all three D:R ratios studied (1:1-1:2.5) when comparing batch-produced DRCs to those formed by spray-drying. The % drug release at equilibrium is lower for the spray-dried systems in all instances when DRCs with equivalent drug loadings are compared. Interestingly, for the three distinct drug loadings studied, the difference between the % drug release at equilibrium is

constant (approximately 5%). In addition, in the case of the 1:1 systems, the difference in the drug release kinetics do not reflect the reduced d_{50} value and the increased SSA (1.7-fold) for the spray-dried versus batch-produced system, which would be expected to result in faster drug release for the former. In fact, the reverse is evident, with the larger sized DRC particles with a smaller SSA reaching equilibrium faster relative to the spray-dried resinate. At the other two D:R ratios studied, the time to equilibrium is not statistically different ($p>0.05$) for the spray-dried versus batch-produced samples, but the difference in % drug release at equilibrium remains apparent. These results suggest that the choice of processing method can have a noticeable impact on the drug release characteristics that cannot be ascribed to factors such as particle size and SSA. This indicates that the equilibrium that is inevitably established once the DRC system is introduced to a liquid medium is under the influence of other factors that require further investigation.

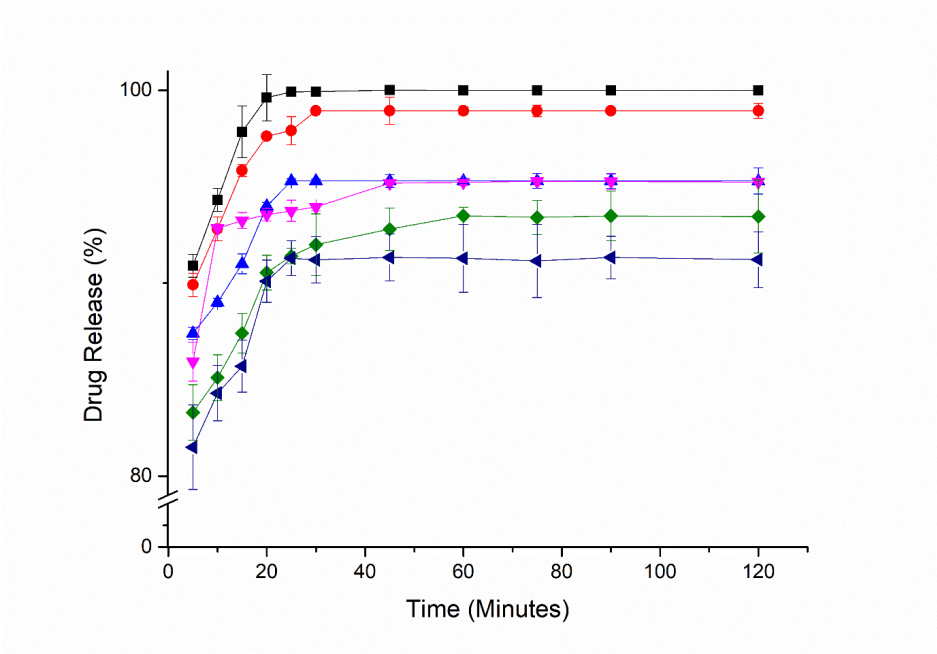

Figure 4.31. Drug release profiles in 0.1 M HCl at 37 °C of selected spray-dried and batch-produced DRCs produced using a drug loading solution concentration of 1 mg/mL and different D:IRP69 ratios (w/w) in the loading medium. 1:1 (batch-produced)(Black square), 1:1.5 (batch-produced)(Red circle), 1:2.5 (batch-produced)(Blue triangle), 1:1 (spray-dried)(Inverted magenta triangle), 1:1.5 (spray-dried)(Olive diamond) and 1:2.5 (spray-dried)(Navy triangle).

4.2.9 Design of Experiment (DoE) studies involving IRP69

4.2.9.1 Taguchi design

As part of this work, just eight spray-drying runs were conducted to investigate several independent variables at 2 levels (L8 design), which is a major positive for the Taguchi design relative to a full or fractional factorial design. In essence, a large amount of data is generated in a minimal amount of

time. The concept that underpins this statistical method is known as the sparsity effect, defined by only a few key unknown variables contributing significantly to the experimental variation observed (330). The factors chosen as part of the design were based on a combination of the findings from the preliminary studies, and the known influence of the spray-drying process parameters on the responses of interest (315,331). When adopting a Taguchi method into the experimental design, previous knowledge of the process is beneficial to take full advantage of the orthogonal arrays, which underpin the statistical method (332).

The seven factors and three responses evaluated are presented in Table 4.7. The screening studies performed to screen the most significant process/formulation variable that impacts product quality produced numerical models for each response ($p<0.05$). As shown in Table 4.7, two of the runs did not produce response values, which can be attributed to spray dryer nozzle blockage, causing the experiment to be aborted. Nozzle diameter was one of the factor variables studied and served as a point of difference compared to the work of Kim et al. who utilised the standard 0.7 mm nozzle throughout (94). Common to the two failed preliminary runs were the highest flow rate studied and the nozzle with the smaller diameter (0.7 mm), pointing to the latter being unsuitable for spray-drying the liquid feeds at high feed rates. In these instances, the large particle size in suspension was problematic, despite the use of the nozzle cleaner, pointing to the material being pumped too quickly through the system.

Table 4.7. Taguchi design matrix for the spray-dried DRCs formed using IRP69. Factor 1: concentration of drug in loading medium (mg/mL), factor 2: feed flow rate: (%), factor 3: inlet temperature (°C), factor 4: nitrogen rotameter setting (mm), factor 5: aspiration setting (%), factor 6: nozzle orifice diameter (mm) and factor 7: D:R ratio. Response 1: powder yield (% w/w), response 2: moisture content (%) and response 3: d_{50} (µm). The feed rate values refer to the flow setting on the spray dryer. 10% and 30% are equivalent to 3.5 mL/min and 9 mL/min respectively. The nitrogen flow values refer to the rotameter setting on the spray-dryer. Values of 40 and 60 mm are equivalent to 667 and 1744 Normlitres/hour, respectively. 1 and 2 refer to the part by weight of resin relative to the drug in the loading medium.

	Factor							Response		
Run	**1**	**2**	**3**	**4**	**5**	**6**	**7**	**1**	**2**	**3**
1	1	10	120	60	100	2	1	21.50	2.50	47.10
2	1	10	120	40	85	0.7	2	41.00	6.44	56.10
3	10	10	150	40	100	0.7	1	37.10	2.31	49.95
4	10	30	120	40	100	2	2	0	0	0
5	1	30	150	60	100	0.7	2	64.70	6.97	55.05
6	10	10	150	60	85	2	2	50.50	5.43	40.98
7	1	30	150	40	85	2	1	0	0	0
8	10	30	120	60	85	0.7	1	52.30	8.73	93.53

Figure 4.32(A-C) displays the most influential factor variables on the individual responses by means of Pareto charts. In all these charts, the maximal effects are illustrated in descending order, from left to right. Regarding the % powder yield, the feed rate of the liquid feed and the D:R ratio in the loading medium were the most significant factors. The D:R ratio has a negative impact on the % powder yield meaning a higher proportion of resin in the spray-dried formulation produces higher yields. This finding is consistent with that reported for the batch-produced DRCs. In contrast, the feed rate has a positive impact on the process yield, meaning that higher feed rates produce higher powder yields. This is understandable as, at higher feed rates, the feed liquid is less inclined to sediment within the feed tube, which results in a reduced yield.

The speed at which the liquid reaches the atomiser of the spray-dryer also has a significant influence on the moisture content of the DRCs produced. This factor has a positive influence on the moisture content meaning higher feed rates produce DRCs with higher moisture contents. Furthermore, it is the only factor across all three responses studied, which has a magnitude that exceeds the Bonferroni limit of the Pareto chart, which highlights its importance. In addition to the t-value limit, the Bonferroni threshold represents another type of statistically based cut-off limit which is higher than the t-value cut-off. Factors which have effects that are above the Bonferroni limit will be more significant than those that fall below it but remain above the t-value limit (333). The effect of the feed rate can be explained by alluding to the residence time within the spray-dryer, which is reduced when higher feed rates are used, which affords the product less opportunity to be dried. The second significant influence on the moisture content was the aspirator suction velocity rate which was found to have a negative effect on the moisture content. This parameter controls the rate at which the drying medium is pulled through the system (315), so reduced moisture content values for the DRCs produced when this variable is increased is an expected outcome.

With respect to the particle size, the only significant variable was the spray-dryer airflow rate which has a negative effect on d_{50} value, meaning the higher the airflow through the apparatus, the lower the particle size of the resulting resinate. The higher the value of this parameter, the larger the quantity of drying medium required to disperse the liquid droplets within the drying chamber. Again, this finding is in keeping with the consensus that exists in the literature, as more energy is provided by higher atomisation flow, which enables the liquid droplets to be broken down, thus producing smaller particles (315). Moreover, all significant factors mentioned deviate from the line in the half-normal probability plots (Figure 11 in Appendix 2), another chart used to study the effect of each factor on the response variable, further supporting the assertions made that the aforementioned factor variables are important.

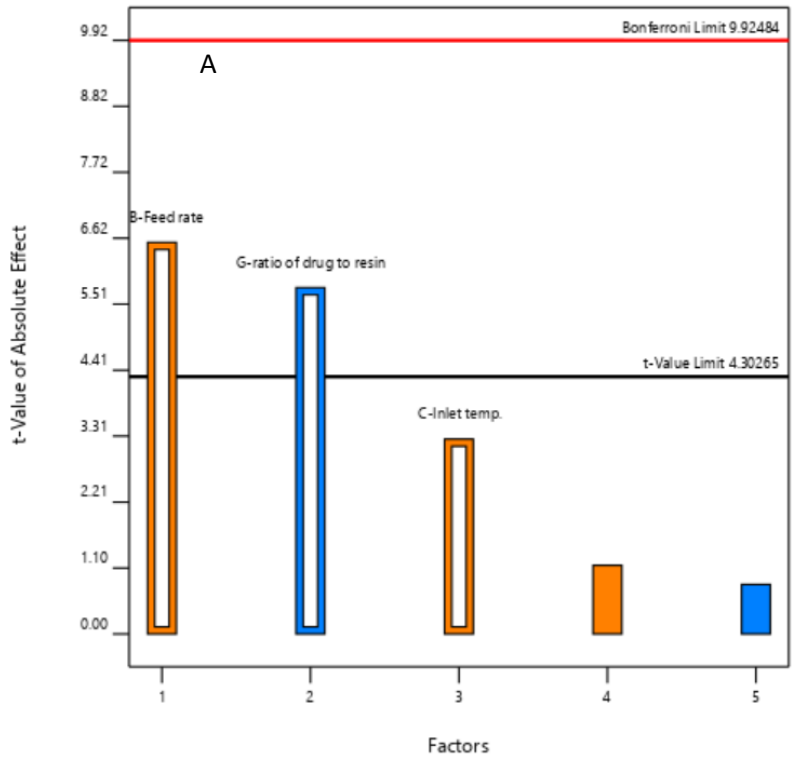
Bonferroni Limit 9.92484
A
9.92
8.82
7.72
6.62
5.51
4.41
3.31
2.21
1.10
0.00
B-Feed rate
G-ratio of drug to resin
t-Value Limit 4.30265
C-Inlet temp.
t-Value of Absolute Effect
1
2
3
4
5
Factors

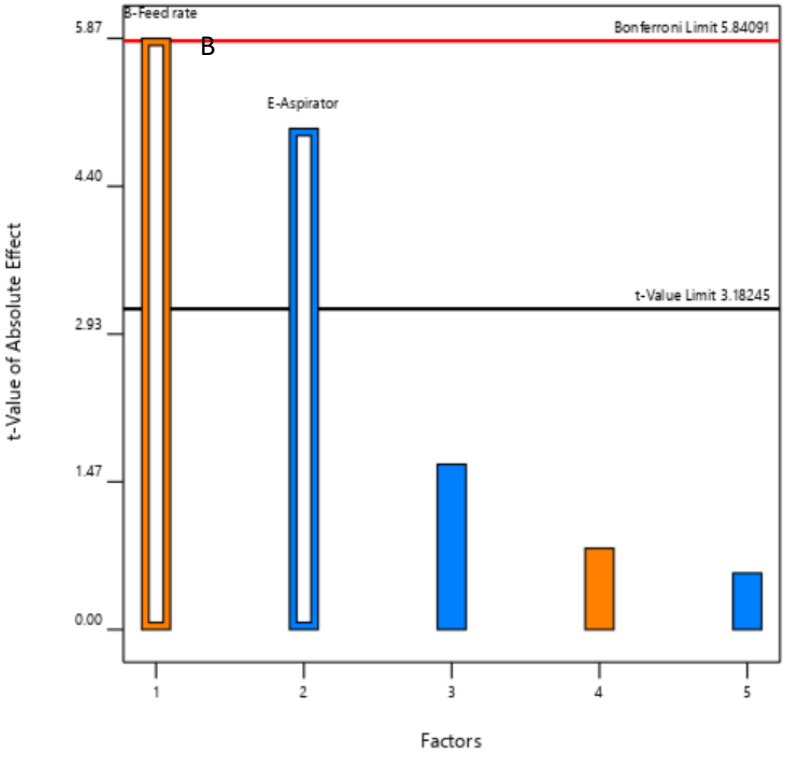
B-Feed rate
Bonferroni Limit 5.84091
B
5.87
4.40
2.93
1.47
0.00
E-Aspirator
t-Value Limit 3.18245
t-Value of Absolute Effect
1
2
3
4
5
Factors

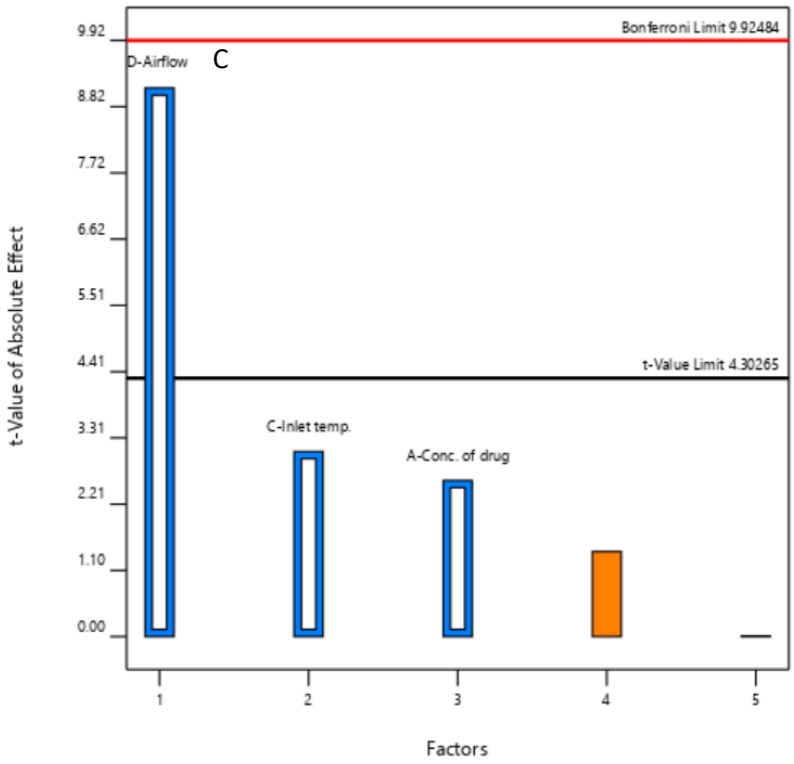

Figure 4.32. Pareto charts illustrating the influence of the factors assessed in the Taguchi design. A) powder yield (%), B) moisture content (%) and (C) particle size (d_{50}). Orange bars represent a positive effect, while blue bars represent a negative effect.

4.2.9.1.2 Solid-state characterisation (pXRD and DSC analyses)

pXRD analyses of the DRCs produced according to the Taguchi design are shown in Figure 4.33(A-B). Based on the diffractograms, it is evident that spray-dried product contain both unreacted TZD HCl and the sodium chloride by-product, similar to the preliminary studies. This assertion is supported by the DSC data, where each sample displays an endotherm in the 280-290 °C range and melting point depression is evident. This melt endotherm is representative of the unreacted crystalline drug, with the melt enthalpy lower for samples containing higher proportions of resin to the drug. Each DSC trace is also characterised by a moisture loss endotherm.

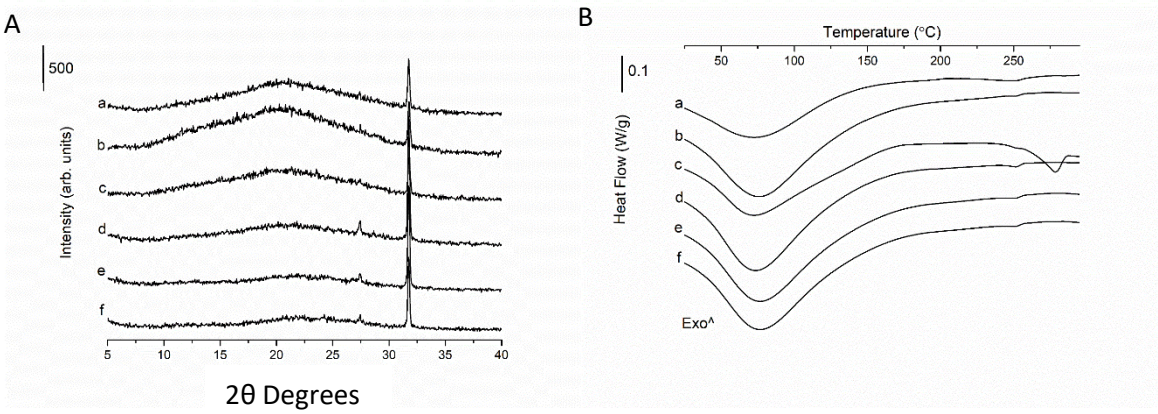

Figure 4.33. A) pXRD diffractograms and B) DSC thermograms of spray-dried DRCs(IRP69) produced according to the Taguchi design. a) Run 1, b) Run 2, c) Run 3, d) Run 5, e) Run 6 and f) Run 8.

4.2.10 Amorphisation of TZD HCl

Although TZD HCl has been used as a medicine for the last three decades, at the outset of the project, the drug's amorphisation tendency and consequently the T_g remained under-researched. An API's T_g value is a characteristic feature, knowledge of which dictates the processing methods that can be used with the API and the stability conditions that any potential formulation may have to be subjected to. These considerations largely contribute to this property's prominence in solid-state research and yet, scarce evidence relating to TZD HCl is reported in the literature. This predicament, combined with no clear and obvious T_g being detectable, meant that the main conclusion that could be drawn from the DSC analyses of the DRC samples reported in Chapter 3 was the absence of crystallinity, rather than amorphisation of the API being achieved. To address this gap in the literature, several strategies were trialled in an attempt to establish the T_g of the API. In the context of the DRC formation, Hughes, a prominent voice in the ion-exchange field, argues that the T_g of DRC provides little value, owing to remarkable stability afforded by the formation of a salt pair in tandem with the extensive crosslinking within the resin structure (280). However, in light of the high drug loadings achieved using both the powdered and bead-type resin (approximately 50% w/w and 30% w/w respectively), it was deemed an important property to determine.

A melt-quench method, which is often used in the preformulation stage to amorphise APIs was trialled to identify the T_g of TZD HCl. On this occasion, the method was unsuccessful due to the degradation observed upon melting, which hampered the chances of successfully detecting the T_g. This is borne out in the DSC data shown in Figure 12(A) in Appendix 2, where a melt endotherm is still visible in the thermogram and no T_g is visible. The second method trialled, *in situ* quenching with the DSC instrument itself, also proved unsuccessful, evidenced by the lack of a T_g and presence of crystalline material (Figure 12(B) in Appendix 2). This observation suggests that the drug is a poor glass former. Although not directly part of this series of experiments, the third method trialled, which was reported earlier in the chapter, was spray-drying. The aim of this experiment tied in with the overall objective of identifying the suitability of the spray-drying process to produce DRCs. Again, this strategy proved unsuccessful in terms of identifying a T_g, but as can be seen from the pXRD data (Figure 10(A) in Appendix 2), a reduction in crystallinity relative to the unprocessed API can be observed.

The final strategy trialled was the adoption of a milling-based approach, which is typically used for particle size reduction. Previous reports of ball milling crystalline APIs have reported difficulty in amorphising crystalline API without the presence of a polymer. However, several examples do exist in the literature (334), highlighting that this resistance to amorphisation is dependent on the individual drug in question. Ball milling at room temperature proved to be successful at reducing the crystallinity of the API, as illustrated in Figure 4.34(A-B). The greatest reduction in crystalline material was

observed when the sample was milled for the longest duration studied (6 hours), and the material appears to remain stable at least 24 hours post-processing when stored at room temperature (Figure 4.34(B). However, no discernible T_g could be detected using the mDSC analysis (Figure 4.39).

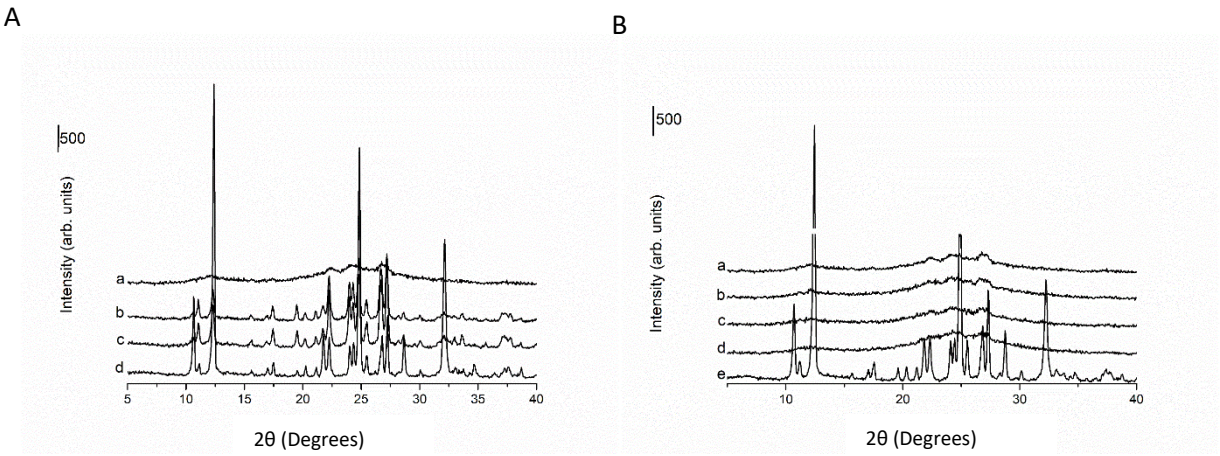

Figure 4.34. A) pXRD diffractogram of TZD HCl raw material (as received) and ball milled TZD HCl raw material for different time periods. a) 6 hours, b) 3 hours, c) 20 minutes and d) TZD HCl (as received). B) pXRD diffractogram of aged TZD raw material which had been ball milled for 6 hours. a) 24 hours post-milling, b) 12 hours post-milling, c) 6 hours post-milling, d) freshly prepared and e) TZD HCl (as received). Ball milling was performed as per the procedure reported in Chapter 2, section 2.2.1.7. Post-milling, all samples were stored at ambient conditions.

As the ball milled samples were predominately amorphous, the DVS behaviour was probed to assess the tendency of the API to recrystallise upon exposure to high humidity. As alluded to previously, the moisture sorption and stability properties of DRCs remain very much under-investigated, with only one study conducted to the best of the author's knowledge. As it was hypothesised that the drug is amorphised, when bound to an ion-exchange resin after loading, the rationale underpinning these experiments is based on assessing the physical stability of amorphous API relative to the API in the DRC when exposed to high relative humidity (RH) during the DVS analysis. Two samples, one freshly prepared (ball milled) and another aged (12 hours post-ball milling stored at ambient conditions) were analysed to investigate the propensity of the sample to recrystallise after a single sorption-desorption cycle within the DVS chamber. DVS analysis (Figure 4.35) revealed that the ball milled material (both freshly prepared and aged for 12 hours at room temperature) crystallised at the same RH within the chamber (20% RH) reflected by the marked change in mass (%) which is followed by a pronounced drop off in mass as the crystalline form has a far lower affinity for moisture relative to its amorphous counterpart (335,336). pXRD results are supportive of this assertion and are depicted in Figure 4.36 and show that the crystallinity of both samples increases after exposure to humidity in the DVS cycle. The intensity of the peaks in both samples is approximately the same, indicating that short term ageing

does not render the sample more susceptible to a subsequent decrease in amorphicity on exposure to a high humidity DVS environment.

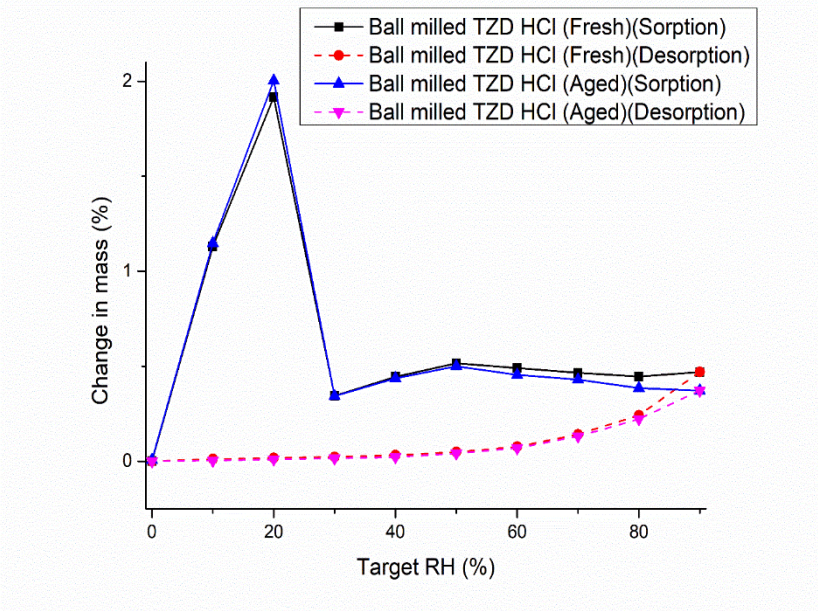

Figure 4.35. DVS sorption cycle of TZD HCl a) freshly prepared by ball milling and b) aged for 12 hours (room temperature) after ball milling. DVS and ball milling were performed as per the procedures detailed in sections 2.2.13 and 2.2.1.7 respectively in Chapter 2.

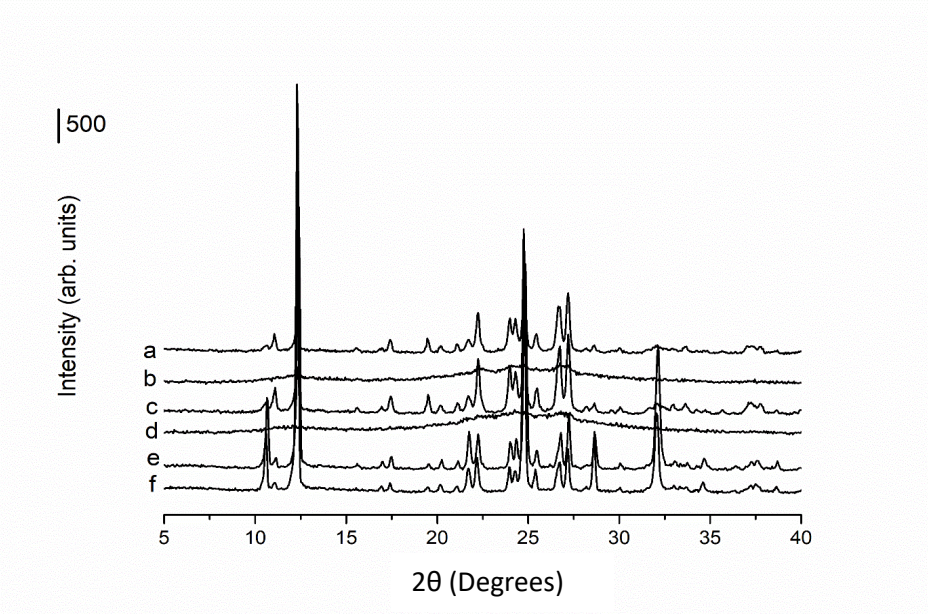

Figure 4.36. pXRD diffractograms of ball milled (aged and freshly prepared) and as received TZD HCl raw material pre and post-DVS analysis. a) aged (12 hours) ball milled sample (post-DVS), b) aged (12 hours) ball milled sample, c) freshly prepared ball milled sample (post-DVS), d) freshly prepared ball milled sample, e) TZD HCl (Post-DVS) and f) TZD HCl (as received). Ball milling and DVS analysis were performed as per the procedures reported in Chapter 2, sections 2.2.1.7. and 2.2.13 respectively.

The second milling-based approach trialled was as cryo-milling. The advantage of the approach is the low temperature of the system, which facilitates the detection of the amorphous phase by slowing the recrystallisation process (334,337). pXRD analysis (Figure 4.37) revealed that the crystallinity decreased, the longer the milling time, akin to what was observed for the samples ball milled at room temperature. Interestingly, DSC analysis (Figure 4.38) revealed a discernible T_g value, which was calculated to be -20 °C. This is surprising, as the diffractograms of the cryo-milled samples had more intense Bragg peaks than those samples milled at room temperature, yet no T_g was discernible in the thermograms of the ball milled samples. This value is unusually low, when considering the high melting temperature of the drug (290 °C), especially in light of the empirical rule (T_g=(2/3)T_m in kelvin)(338) meaning that the method routinely used in the DSC analysis did not span a large enough temperature range to detect the T_g. This oversight only became apparent after the DSC method trialled as a last resort when characterising the cryo-milled sample, revealed the glass transition. However, in the DSC analysis (Figure 4.39), encompassing the expanded temperature range which was intended to cover the expected T_g value, no discernible event attributable to a glass transition was visible in the freshly prepared (room temperature) ball milled sample or the aged material (12 hours). These observations serve to highlight the important impact that the preparation method can have on the properties of the glassy state.

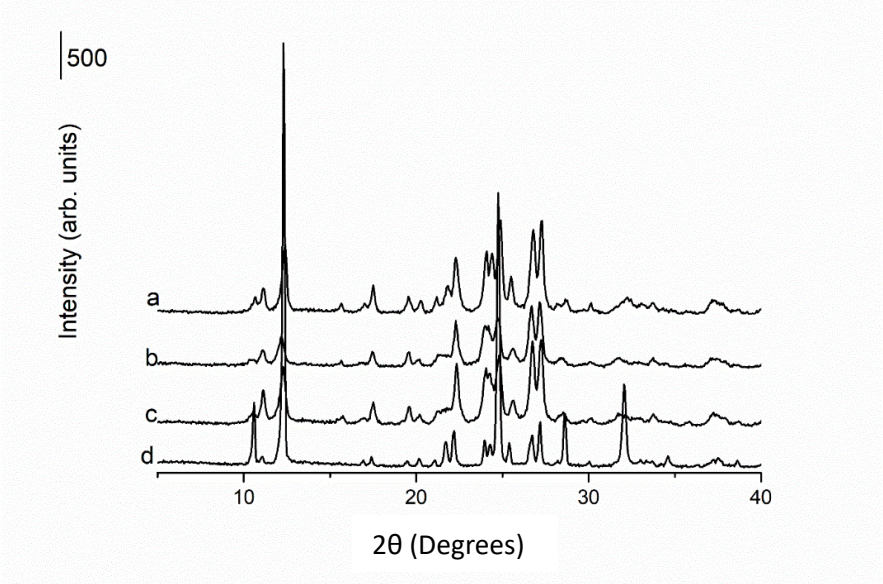

Figure 4.37. pXRD diffractograms TZD HCl cryo-milled for different durations of time and the raw material as received. a) cryo-milled TZD HCl raw material (30 minutes), b) cryo-milled TZD HCl (60 minutes), c) cryo-milled TZD HCl (90 minutes) and d) TZD HCl (as received). Cryo-milling was performed as per the procedure reported in Chapter 2, section 2.2.1.8.

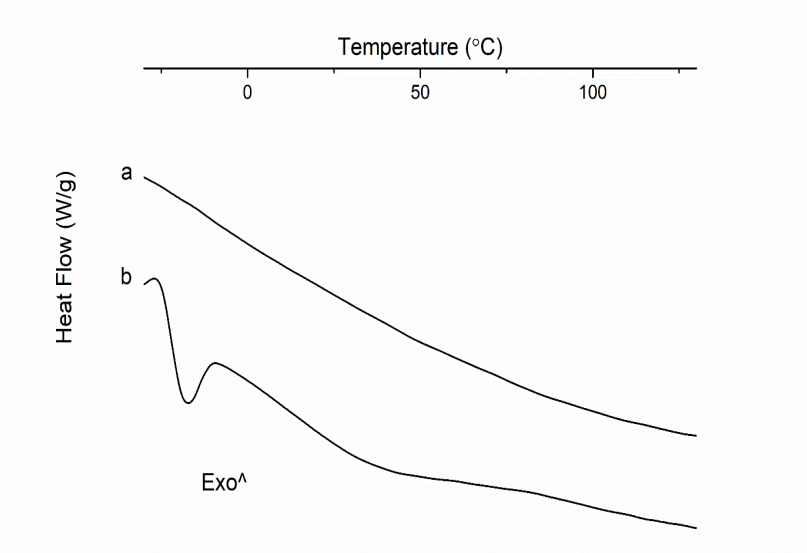

Figure 4.38. DSC thermograms of TZD HCl raw material that was either ball milled or cryo-milled for different durations of time. a) ball milled for 6 hours and b) cryo-milled for 90 minutes. Ball milling and cryo-milling were performed as per the procedures reported in Chapter 2, sections 2.2.1.7 and 2.2.1.8 respectively.

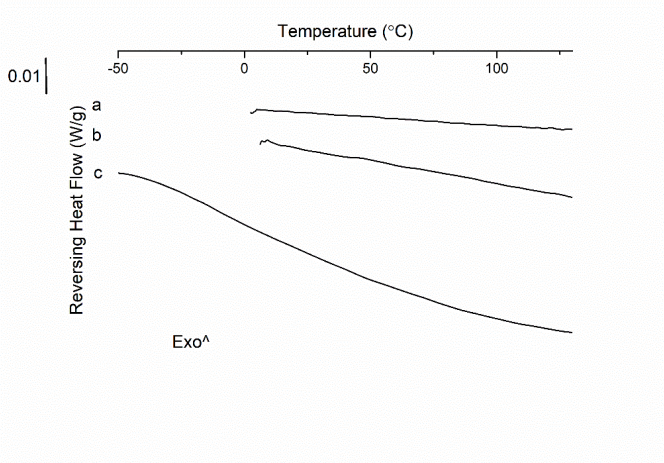

Figure 4.39. DSC thermograms of ball milled TZD HCl raw material over different temperature ranges. a) freshly prepared (ball milled) (0-130 °C temperature range), b) aged (6 hours) ball milled sample (0-130 °C temperature range) and c) aged (6 hours) ball milled sample (-50-130 °C temperature range) Ball milling were performed as per the procedure reported in Chapter 2, section 2.2.1.7.

After establishing the T_g value of the predominantly amorphous API, DSC analysis on selected DRCs ((1:1)(IRP69)) and (1:2)(IR120) was performed, using the method that was sufficient to detect the raw material's T_g value. As illustrated in Figure 4.40, a stepwise decrease in heat capacity, indicative of a glass transition, can be observed in a position broadly similar to the API's T_g for the powdered resin sample. However, no T_g could be detected for DRC formed using the bead form of the resin. A possible reason for this could be the lower level of drug-loaded onto the bead-type resin relative to the powdered sample, a consequence of the known reduction in ion-exchange capacity. To the best of the

author's knowledge, this is one of the first reports of identifying an API's T_g post-loading onto an ion-exchange resin.

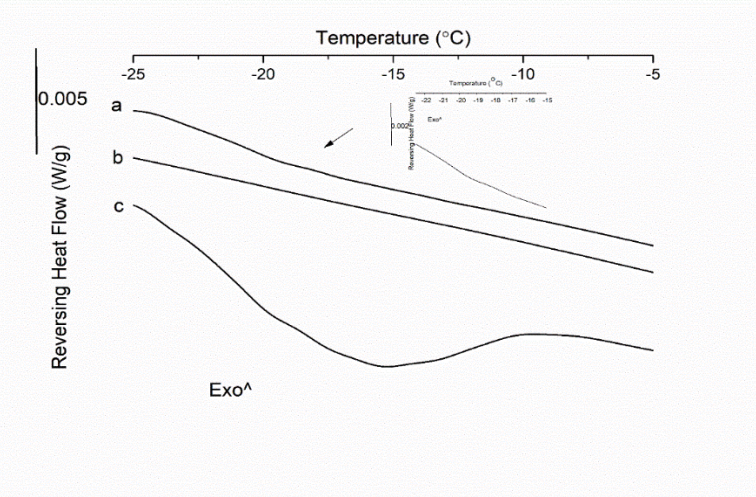

Figure 4.40. DSC thermograms of a) DRC formed using a 1:1 D:R ratio (w/w) (IRP69), b) DRC formed using a 1:2 D:R ratio (w/w) (IR120) and c) cryo-milled TZD HCl raw material (90 mins).

4.3 Conclusion

This work has demonstrated that TZD HCl is capable of binding to alternative IERs that possess functional groups which confer "weak acid" properties. A combination of drug loading studies, solid-state characterisation, and dissolution testing highlight the additional challenges and considerations that face formulators when choosing a resin whose dissociation properties are reliant on pH. All three factors (drug loading, solid-state and drug release) were shown to be impacted by the initial pH of the drug solution used as the loading medium and the type of ion bound to the fixed functional group on the resin backbone. The latter was shown to have a noticeable impact on the solid form of the drug, as the introduction of potassium ions to the loading medium was shown to lead to the formation of the free base of the API. This event compromises the ion-exchange reaction that can occur between drug and resin which results in a noticeably inferior drug release performance in the media studied.

Also illustrated in this work, was the feasibility of using the spray-drying approach to produce complexes, which presented its own unique challenges that were not experienced during the batch-processing studies. Several problems were identified during the solid-state characterisation studies that were either overcome using a series of "trial and error" methodology or rationalised through consideration of the ion-exchange reaction. In comparison to the batch-produced DRCs studied in Chapter 3, the DRCs exhibited similar dissolution behaviour in all dissolution media studied pointing to DRC formation being successful.

Investigations into the amorphisation tendency of the API, using a variety of different approaches yielded mixed results but the T_g was established at a temperature that was far lower than originally anticipated. All findings reported in this chapter highlight the need to thoroughly investigate a variety of different factors when formulating TZD HCl using an IER approach, irrespective of the method of processing or the selection of resin.

Chapter 5:

Investigation of a selection of pharmaceutical unit processes to aid with the manufacture of sustained-release ion-exchange based formulations

5.1 Introduction

In addition to being one of few reliable approaches for formulating sustained-release liquids due to their ability to circumvent drug leaching into the liquid vehicle (127), the production of drug-resin complexes (DRCs) using ion-exchange resins (IERs) has proven to be effective at altering the drug release properties of APIs, as is evident from a large number of publications in the literature (117,127,178). However, to sustain or delay the release of the drug for any appreciable length of time so that therapeutic benefit can be derived from such a formulation, a rate-controlling polymer is usually required (92). Water-insoluble polymers like ethylcellulose and certain Eudragit® grades are prime candidates for helping to achieve this goal and have an established reputation for imparting an additional level of control on the drug release from IERs (127,164,178). A diverse range of techniques have been reported for the application of a polymeric layer, depending on whether the resin material is in the bead or powder form. The latter presents challenges attributed to the powder's fine particle size and irregular shape, which is typically addressed using a granulation step (120). By granulating the material, the DRC is rendered suitable for air-suspension coating and this approach will be trialled as part of this chapter.

Regarding the bead-type resins, due to their larger particle size and more regular spherical shape, they are ideally suited to air-suspension coating processes, which can be performed in a fluidised bed apparatus (126,178). There is also an option to coat the spherical particles using techniques more suited to small-scale studies. Examples of the latter include coacervation phase separation techniques and oil-in oil (o/o) solvent evaporation procedures (127,147). One downside of many techniques reported as part of the small-scale microencapsulation studies is the lack of potential for scale-up, which is a cited advantage of the Wurster coating process which can be used in a fluidised bed apparatus. Having said that, to the best of the author's knowledge, the coating studies performed using DRCs to date use more sizeable batch sizes compared to those used as part of the current work (164,178,194). In this study, the cumbersome approach used to produce drug-loaded material limits the quantity of material that can be produced at any one time along with the finite supply of raw material means that larger batch sizes are not feasible, resulting in the weight of starting material being fixed at 3 g for the majority of coating studies.

The primary aim of this work was to investigate the feasibility of coating the drug-resin complexes (DRC) formed in Chapter 3 which encompassed both the powdered and bead-type DRCs. Depending on the physical form of the DRC, alternative methods of processing were envisaged, attributable to the unique characteristics of each resin. Once the suitability of the DRC for the process has been established, the impact of polymer type, post-coating treatment and the inclusion of excipients, such as plasticisers, will be investigated to assess their impact on the coated DRCs' drug release

performance and physicochemical properties. A further aim of this work is to evaluate the chemical and physical stability alongside the drug release performance of "dry" DRCs and when incorporated into an aqueous-based liquid medium. TZD HCl is licensed in over 20 countries in Europe as an anti-spasmodic agent with the majority of products being immediate-release solid dosage forms. In a small number of countries, a modified-release product solid oral dosage form called Sirdalud® SR is available, illustrating the therapeutic opportunity for a sustained-release product. A flow chart diagram shown in figure 5.1 indicates the series of sequential steps performed in this chapter to aid the reader in understanding the different strands of work reported.

Figure 5.1. Flow chart outlining the series of sequential steps constituting the work in chapter 5.

5.2 Results and discussion

5.2.1 Manufacturing approaches

5.2.1.1 Fluidised bed granulation (FBG) of Amberlite™ IRP69 (IRP69)

The fluidised bed granulation (FBG) approach was the first option trialled to increase the particle size of the resin/DRC to help overcome the challenges associated with the fine resin/DRC particles which, ironically, is agglomeration. The association between fine-sized particles and agglomeration tendency is well documented (131), but this issue is further compounded in the case of IERs because of their hygroscopicity which will inevitably hamper the fluidisation of the particles. As the ultimate intention is to coat the granules formed with a rate-controlling polymer, using the Wurster insert, the potential benefit of using this processing approach is two-fold, as it potentially could provide an understanding of the fluidisation characteristics in addition to its primary purpose which is to form granules. This technique is also growing in popularity (339,340), yet the novelty of the approach is retained with respect to IERs. The lack of reported literature on the application of FBG to IERs led to a substantial preliminary screening process on "blank" IRP69 resin materials (described in Chapter 2, section 2.2.1.4) with the details outlined in Table 5.1.

Table 5.1. Experimental conditions for fluidised bed granulation studies using IRP69. Choice of binder indicated in parentheses.

Concentration of binder in terms of total solid contents (% w/w) when included in solid form	Concentration of binder in terms of total solid contents (% w/w) when included in solution	Inlet air temperature (°C)
1 (PVP)	0	80
1 (PVP)	0	70
2 (PVP)	0	80
2 (PVP)	0	70
3 (PVP)	0	70
5 (PVP)	0	70
10 (PVP)	0	70
20 (PVP)	0	70
30 (PVP)	0	70
40 (PVP)	0	70
0	40 (2% w/v PVP solution)	70
40 (HPMC)	0	70

The formation of granules proved troublesome, even after a variety of binder concentrations were trialled. Polyvinylpyrrolidone (PVP) was selected as the binder of choice, due to its established reputation as an effective granulating agent (341). An adjustment of the inlet temperature during the studies using low binder concentrations rendered little change after visual inspection, pointing to the need for higher binder concentrations. As illustrated by Figure 1 in Appendix 3, particle size analysis revealed that an unusually high amount of binder was required to form granules, and inclusion of the binder amongst the solid contents in the chamber proved to be the most effective mode of binder addition compared to the inclusion of the binder in the feed solution. HPMC was trialled as an alternative binder at the highest concentration tested, but the process yielded granules with undesirable handling properties. SEM analysis, depicted in Figure 5.2 (and also Figures 2-3 in Appendix 3), revealed the successful formation of agglomerates, which are irregular in shape rather than well rounded and uniformly sized granules. This is likely a consequence of the rapid particle growth that constitutes the agglomeration process, whereby liquid bridges initially hold the wetter particles together, prior to solid bridge formation after the solvent is evaporated (342). Because of the preliminary findings, this approach for manufacturing granules was not pursued further.

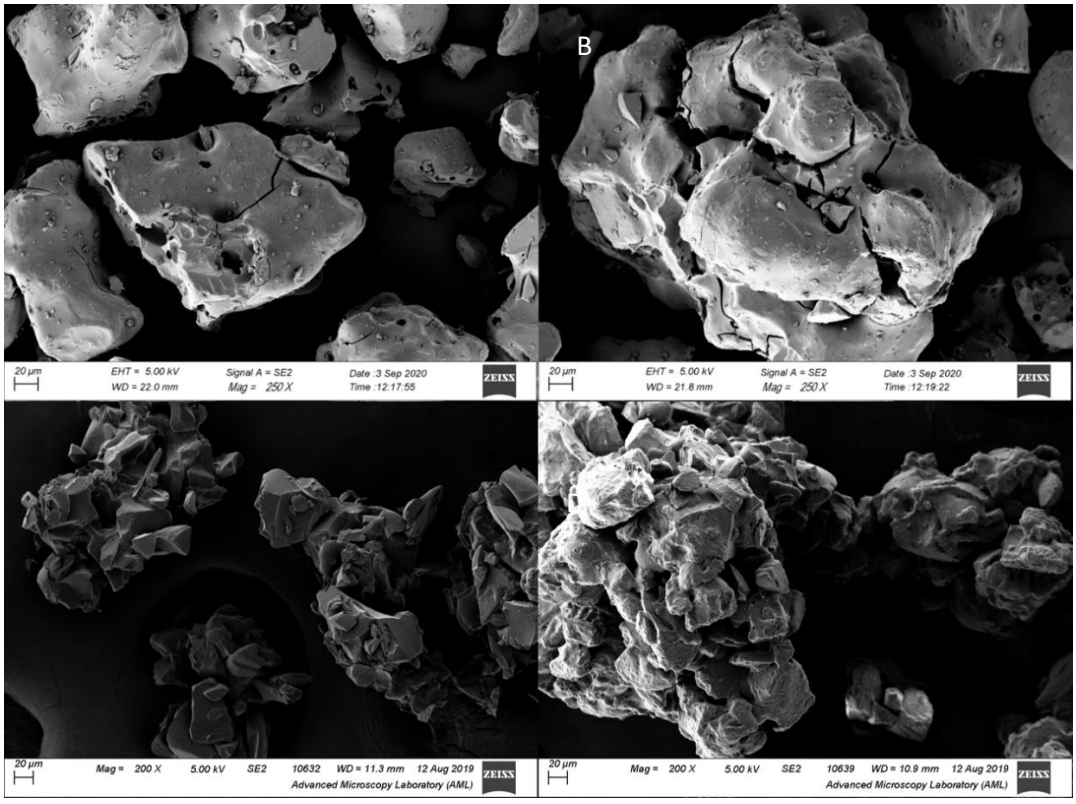

Figure 5.2. SEM images taken using two different magnifications of granules produced using FBG which were formed using "blank" IRP69 and different concentrations (w/w) of binder (PVP) (included as a part of the solid phase). A) 10% PVP (250x), B) 20% PVP (250x), C) 30% PVP (200x) and D) 40% PVP (200x).

5.2.1.2 Wet granulation of Amberlite™ IRP69 (IRP69)

A modified wet granulation method (described in Chapter 2, section 2.2.1.5) followed by sieving was trialled as an alternative option to FBG as a means of producing granules at a small-scale. This process also broadly resembles the method reported in several patents assigned to Tris Pharma which divulge the use of IRP69 in the manufacturing process of commercial products (103,138). These initial trials used blank resin due to the value of the drug-loaded DRC. Four distinct sizes of granules were produced (Figure 4 in Appendix 3) and granules with a d_{50} value of approximately 210 µm were selected for further preliminary coating trials. SEM analysis revealed the formation of distinct clusters of resin particles formed during the granulation process (Figure 5.3), with a different morphology to those formed using the FBG process. Upon coating, the morphology of the granules is characterised by a smoother surface, presumably imparted by the coating (Figure 5 in Appendix 3). However, a large variation in granule shape exists, pointing to the need for the system to be optimised.

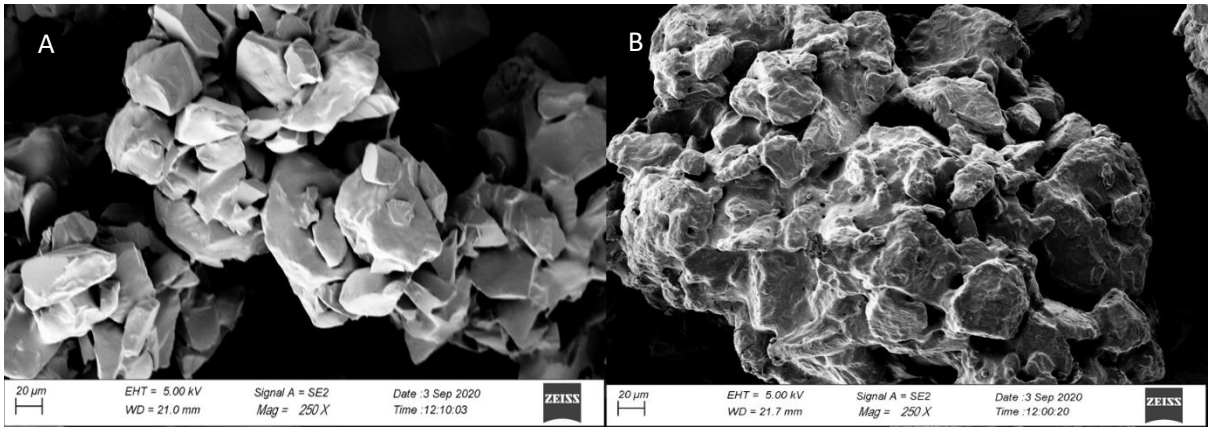

Figure 5.3. SEM images of different sized granules comprising "blank" IRP69 and Kollicoat® SR 30 D produced by the modified wet granulation method that had d_{50} values of A) 85 µm and B) 120 µm.

Initial attempts to fluidise the unloaded granules and coat them using the Wurster insert were successful (Figure 5.4). A dilute aqueous dispersion of Kollicoat™ SR 30 D containing several drops of amaranth solution to visualise the coating was used. However, once drug-loaded DRC was substituted into the process using identical process and formulation parameters, the granules were no longer suitably fluidised. This was due to the material sticking to the sides of the chamber which could not be alleviated by spraying pure solvent prior to the coating suspension, meaning that the application of a polymeric coating was not possible. Regardless of the parameters employed, this hurdle could not be overcome leading the author to seek an alternative method of formulation.

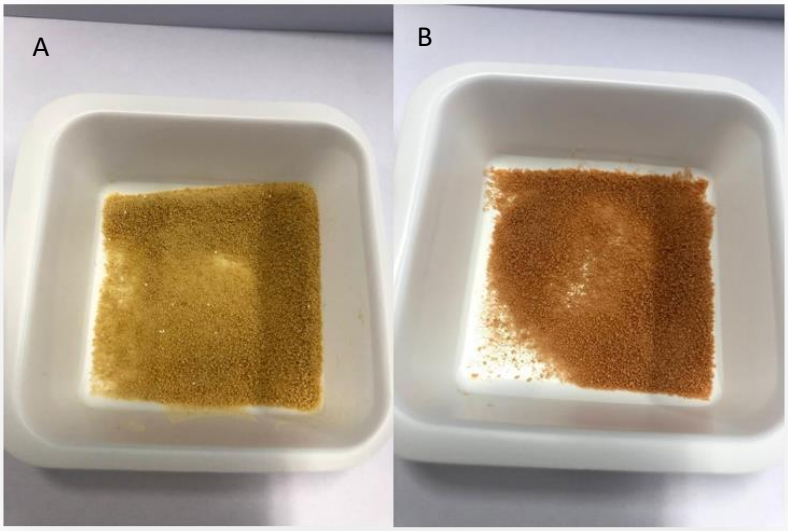

Figure 5.4. Comparison of A) Uncoated granules (comprising "blank" IRP69 and Kollicoat® SR 30 D) and B) Wurster coated granules ("blank" IRP69 and Kollicoat® SR 30 D) using Kollicoat® SR 30 D and amaranth solution. Both types of granule were formed using wet granulation.

5.2.1.3 Spray-coating of drug-loaded ion-exchange beads (IR120)

To the author's best knowledge, this work is one of the first attempts at spray-coating small batch sizes of ion-exchange beads (less than 30 g). For small-scale studies, organic phase separation methods have been the method of choice for coating DRCs. Torres et al. demonstrated aqueous solvent evaporation using cellulose acetate butyrate as an alternative (134) and an effective mechanism to coat resins, whilst emulsion-solvent evaporation in an oily phase and coacervation also proved successful (89,92,132). These methods suffer from drawbacks such as imperfections in the resulting coating, which requires large volumes of solvent to help overcome the problem and ensure adequate modulation of drug release. An added downside is the excessive size of the microparticles produced owing to the increased level of coating applied, which is not usually a factor in spray-coating, as the process ensures dense coatings can be achieved (131). Spray-drying has been reported as an effective microencapsulation technique for the encapsulation of tramadol-loaded DRCs (122), but doubts over its suitability have been cast by Raghunathan et al. who questioned the quality of the coatings applied (145). From the author's previous experience of spray-drying, the method was not considered due to issues associated with spray-drying from suspension and nozzle blockage. Therefore, Wurster coating, which is still the predominant method, although a more complicated process that requires extensive method development, is more attractive from a drug loading and manufacturability perspective, so

the decision was made to pursue it. As alluded to previously, the technique is envisaged as a more feasible method to coat the DRCs, which can be attributed to the particle size of the beads, an advantageous property relative to the finer sized powdered particles which are liable to agglomerate (178). Moreover, by coating the drug-loaded ion-exchange bead directly, it circumvents the need to form a granule that in turn has to be coated.

5.2.1.3.1 Coating trials using an aqueous-based dispersion (IR120)

Aqueous-based coating systems are the preference of the pharmaceutical industry relative to their solvent-based counterparts for the application of polymeric coatings. This is due to well documented environmental issues, concerns with respect to residual solvent content, as well as safety and economic issues (192,343). Kollicoat® SR 30 D, an aqueous dispersion consisted of 27% polyvinyl acetate, 2.7% povidone and 0.3% sodium lauryl sulfate, was selected as the initial trial polymer due to it being specifically designed for spray-coating. Many groups have used it to coat IERs (166,344). Furthermore, it is the coating polymer that is used in the Tris Pharma patents for products that have reached the marketplace (138).

The first set of experiments (described in section 2.2.1.6.1 in Chapter 2) involved spraying undiluted Kollicoat® SR 30 D onto unloaded beads ("blanks") to preserve the limited quantity of drug-loaded material until method development had been completed. It quickly became evident that the feed was too viscous, causing nozzle blockage, and was prone to sedimentation within the tube. Further trials involved diluting the feed with water, which was successful at avoiding the sedimentation and nozzle blockage issue but led to fluidisation issues that hindered the completion of a successful run (Figure 6 in Appendix 3). Preliminary trials revealed a balance that needed to be struck between sedimentation in the feed tube and agglomeration tendency, which depends on the feed rate and volume of liquid sprayed. The temperature was also shown to be critical to the performance of the manufacturing process. A final modification trialled was the use of an organic solvent, i.e. acetone, as a diluent for the Kollicoat® SR 30D feed. Adjustment of temperature, flow rate and atomisation was necessary to achieve a run devoid of fluidisation issues, nozzle clogging and sedimentation, all undesirable features of the coating process which lead to poor product quality (168). Upon further examination of the literature, it was found that several publications did not detail critical process parameters (129,166,345). Other publications that describe spray-coating and the associated process parameters are less ambiguous and use higher air or gas flows (40-45 m^3/hour)(110,111) than are available in the laboratory (30 m^3/hour) (111). This led to many experimental runs being conducted to ensure that the initial parameters selected were the reason for repeated failures, rather than any limitations imposed by the use of the lab-based equipment. Although extensive "trial and error" experiments led to a successful run illustrated by Figure 5.5(A) (and Figure 7 in Appendix 3), the addition of an organic

solvent to an aqueous dispersion was not desirable as, along with potential stability implications, the benefit of using an aqueous-based coating system would be lost.

As alluded to previously, the coating process can often be problematic when the particle size is small, as the cohesive forces between particles are inversely related to the particle diameter, leading to agglomeration (346). However, the particle size of the beads, which have a calculated d_{50} of 621.67 ± 8.02 µm should pose few problems from this perspective. It is more likely that the formation of liquid bridges between particles is due to the aqueous dispersion selected, in tandem with the process parameters selected and perhaps the hygroscopic nature of the beads. Furthermore, the residual moisture can reduce the effective T_g of the polymer leading to tackiness (347), facilitating agglomeration. In addition to the obvious detrimental impact to the quality of the product, illustrated by Figure 5.5(B), agglomeration may obstruct the airflow in a manner that adversely affects the flow patterns within the chamber that are critical to creating an even coating, free of imperfections (214).

Figure 5.5. Images of A) A successful Wurster coating run using "blank" IER beads (IR120) using Kollicoat® SR 30 D (and amaranth solution) (run 2) and B) An unsuccessful Wurster coating run using "blank" IER beads (IR120) using Kollicoat® SR 30 D (and amaranth solution) (run 1). The run numbers refer to those designated in Table 2.10 in Chapter 2.

A second aqueous-based dispersion known as Eudragit® NM 30 D was also trialled. This is a polymethacrylate-based copolymer that other research groups have used to formulate sustained-release systems (178). This polymer was trialled to confirm that aqueous dispersions of polymers were unsuitable for coating the beads, considering the limitations of the Mini-Glatt (with respect to nitrogen flow supply), and that the difficulties experienced were not confined to the polyvinyl acetate-based dispersion Eudragit® NM 30 D is similar to Kollicoat® SR 30 D, in that it is an aqueous dispersion containing a polymer that confers pH-independent release, making it an appealing option for the

purposes envisaged. Unfortunately, similar issues (Figure 6 in Appendix 3) that were prominent during the Kollicoat® SR 30 D trials were evident when an undiluted and aqueously diluted dispersion was sprayed onto blank beads. These observations confirmed the unsuitability of aqueous-based coating systems for coating ion-exchange beads, bearing in mind the limitations of the Mini-Glatt. Thermal analysis also failed to provide clear evidence of the coatings being applied to the majority of coated systems studied, further highlighting the inadequacy of the coating process (Figures 8-10 in Appendix 3).

5.2.1.3.2 Coating trials using an organic solvent-based coating solution (IR120)

Due to the failure to achieve reproducible coating and fluidisation using the aqueous dispersions, as alluded to above, solvent-based coating systems were selected as the next option to explore. Despite not being the favoured option of pharmaceutical companies, evidence in the literature does exist for their use in coating microparticles (184,348). Their incorporation into the process proved inevitable due to the hygroscopic nature of IER beads and the restrictions of the nitrogen supply to the spray-coater.

5.2.1.3.2.1 Coating studies involving pH-dependent polymers (Drug release)

To confirm that the ion-exchange beads were suitable for Wurster coating and to gain an understanding of the coating process using a solvent-based system, Eudragit® L100 (L100) and Eudragit® S100 (S100) were trialled as coating agents based on their desirable properties which make them amenable to the Wurster coating process. Both of these polymers are highly soluble in organic media leading to their extensive use in the literature (173). As they are pH-dependent polymers, which are not intended for release in the gastric environment, their predominant use is for site-specific drug delivery (Ileum and jejunum respectively) (349). Differences in their chemical structure allow for the specific pH dependent release. Both grades are anionic copolymers based on methacrylic acid and methyl methacrylic acid but they differ in the ratio of the constituents (1:1 ratio for L100 and 1:2 ratio for S100) (350). Similar to the granulation trials, “blank” resin material (bead form) was used for initial method development trials due to the scarcity of drug-loaded material. Successful coating was achieved using the two grades studied (described in Chapter 2, section 2.2.1.6.2.1) illustrating that coating (amaranth solution used for visualisation purposes) of the beads was possible despite the low batch size and the gas flow limitations (Figure 5.6).

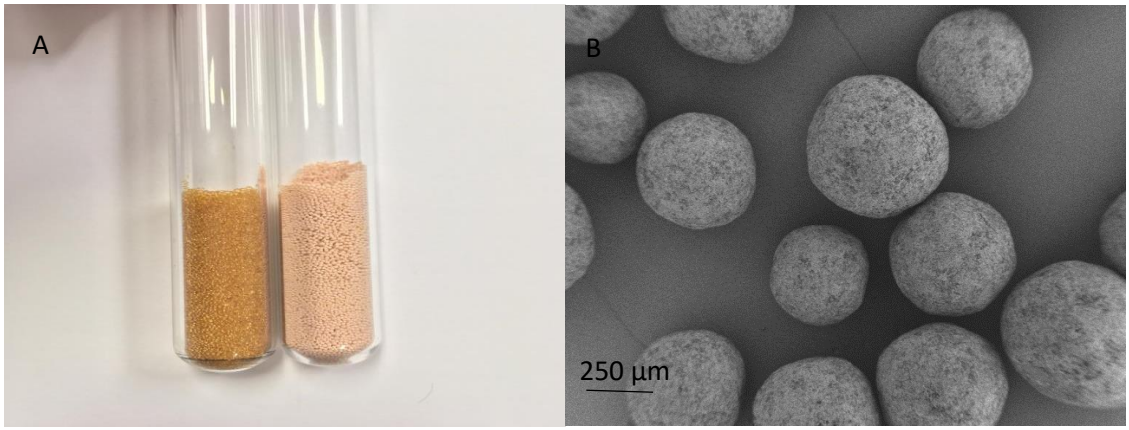

Figure 5.6. A) Side by side image comparing uncoated "blank" IER beads (IR120) (left) with Wurster coated "blank" IER (beads)(coated using a 2.5% w/v Eudragit® L100 coating solution which included several drops of amaranth solution) (right) and B) SEM image take at x50 magnification of Wurster coated "blank" IER (beads)(coated using a 2.5% w/v Eudragit® L100 coating solution which included several drops of amaranth solution).

Drug-loaded material was then substituted into the process and the coated material's release profile was evaluated over a 2-3 hour period. The USP Type 2 apparatus was selected based on it being an established method for assessing the release of DRCs. Throughout the course of the dissolution studies, no evidence of clinging or sticking to the paddle shaft could be observed and no floating was evident, indicating the suitability of the method for assessing drug release behaviour across the pH range examined. Initial drug release studies focused on the impact of the coating, intended to be pH-dependent, on the drug release profile in several different media. The effect of coating type and the level of coating applied on drug release are depicted in Figures 5.7-5.8. An additional level of control on the drug release is afforded by the introduction of a polymeric coating for all formulations assessed, as is evident from the suppression of drug release over the timeframe of the study. This is consistent with an effective coating layer being deposited on the microparticles, indicative of a successful coating process.

When considering the drug release profiles of each sample across the test conditions investigated, an evaluation of the success of the coating process could be made, based on the extent of drug release. Irrespective of the dissolution medium used, there is minimal drug release (<1%) from the S100-coated DRC (Figure 5.7) over the first 10 minutes, indicating the polymeric membrane is intact for this duration of time. The extent of drug release remains constant in DI H_20 for the remainder of the study, which contrasts with the behaviour of the coated system in ionic media. There is no statistical difference ($p>0.05$) in the quantity of drug released at each timepoint over the first 45 minutes of the study when the drug release profiles in DI H_2O and 0.1 M HCl are compared. From the 60 minute

timepoint onwards, there is a discernible difference in the quantity of drug released, characterised by higher % drug release values ($p<0.05$) in the acidic medium over time, without a plateau being reached. Although the DRC has been coated using a polymer intended for enteric coating purposes, these results likely reflect a minor breach in the integrity of the coating applied, perhaps attributable to deformities present, as the rate of drug release is relatively slow compared to the release rate in pH 6.8 buffer. These defects can facilitate polymer erosion, by providing the medium with access to the DRC, thus increasing the likelihood of swelling which can render the coating ineffective.

The release behaviour at pH 6.8, provided further evidence of the imperfection of the coating applied. The Eudragit® S100 grade is specifically designed for colonic delivery and therefore is expected to dissolve at pH values of 7 and above. As the phosphate buffer medium used in these studies had a pH value of 6.8, it was expected that little drug release would be observed if a robust coating had been applied. Having said that, the difference between the pH values of the dissolution medium and the pH which triggers drug release from a coated system (using Eudragit® S100) are very close so it is not unreasonable to expect that drug release would be observed considering the pH of the dissolution media may be liable to change over time and the trigger pH may not be exactly pH 7.0. Similar to the rationale provided for the extent of drug release seen in acidic media, an uneven fragile coating layer and the ability of the resin to swell once in contact with the medium are the two likely reasons for the level of drug release observed. The second reason can exacerbate the defects associated with the coating, and in turn, accelerate the deterioration of the polymeric layer so that its benefit is lost. As depicted in Figure 5.7, the rate of drug release increases steadily from the 15 minute onwards, approaching a plateau value of 45% drug release after 2 hours. Although this value is significantly higher ($p>0.05$) than the % drug released at the same timepoint in 0.1 M HCl (10%) and DI H_2O (1%), which signifies the coated system's greater vulnerability at higher pH values, it is likely that that the layer is not completely breached as the % drug release is still considerably lower compared to the uncoated systems reported in Chapter 3.

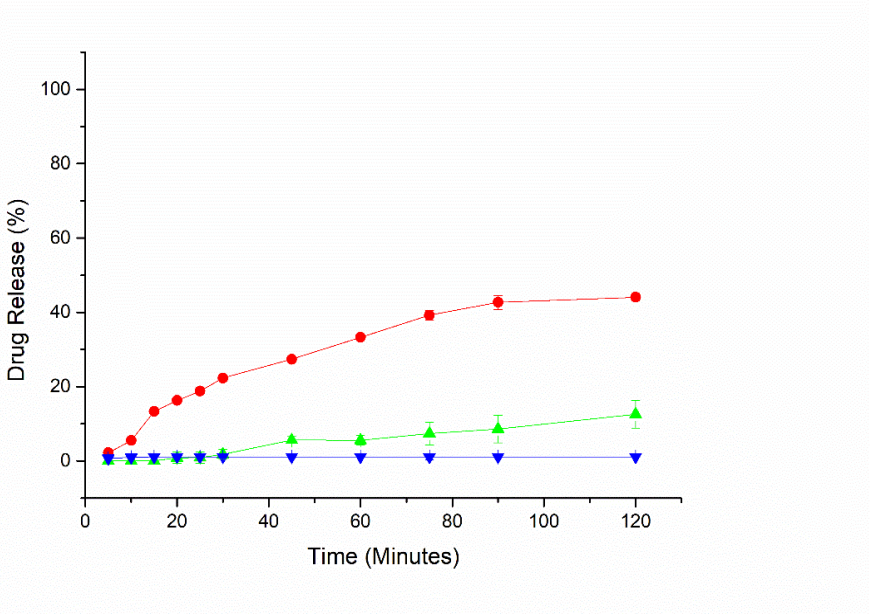

Figure 5.7. Drug release profiles in either 0.1 M HCl, pH 6.8 buffer or DI H_2O at 37 °C, of drug-loaded beads (IR120) coated with Eudragit® S100. 0.1 M HCl (Green triangle), DI H_2O (Blue inverted triangle) and pH 6.8 (Red circle). The concentration of Eudragit® S100 in the coating solution is 2.5 % w/v.

The drug release profiles of the DRC coated with the second grade of pH-dependent polymer (Eudragit® L100) used are shown in Figure 5.8. Eudragit® L100 is designed to dissolve at pH values greater than 6, thus making it a desirable option for site-specific delivery in the jejunum. Compared to the systems coated using the Eudragit® S100 polymer, there are some marked differences, most notably in pH 6.8 medium. Compared to the Eudragit® S100-coated systems, the release at pH 6.8 is rapid with a plateau being reached after 30 minutes. In excess of 90% drug release is achieved after 5 minutes. No statistical difference ($p>0.05$) can be detected over the first 10 minutes and from the 30 minute timepoint onwards. This behaviour contrasts with the more tempered drug release observed in the other media studied (0.1 M HCl and DI H_20), which share similar drug release characteristics to those observed with Eudragit® S100-coated systems. The disparity in dissolution performance of the coated system in pH 6.8 buffer and 0.1 M HCl indicates the pH-dependent properties of the film coating. The release profiles again indicate the limitations of the coating applied, as indicated by the extent of drug release, particularly in acidic pH. In contrast to the Eudragit® S100 systems, a plateau is reached after 90 minutes in 0.1 M HCl, with the % drug release levelling out at 40%, a value that is not statistically different ($p>0.05$) to that calculated for the Eudragit® S100 system in pH 6.8 buffer. Regarding the drug release in DI H_20, approximately 10% drug release is observed after 120 minutes, again indicative of coating layer that requires optimisation. The disparity between the quantity of drug leached from the coated particles in 0.1 M HCl and DI H_2O can be accounted for by considering the ability of the acidic medium to displace the drug from the resin, through the exchange of ions, once it

has come into contact with the exposed portion of the microparticle. In the case of DI H_20, this is not possible as the medium lacks the ions necessary to promote drug release.

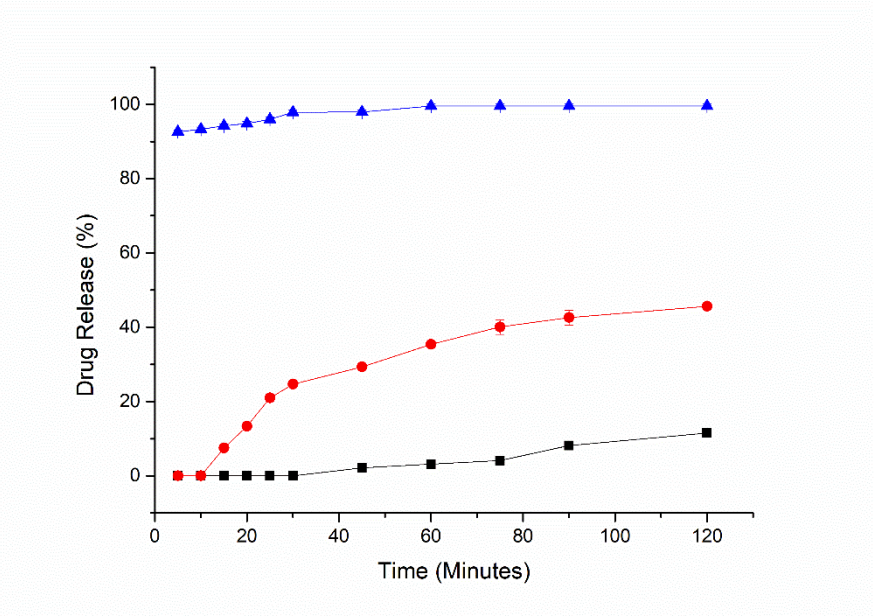

Figure 5.8. Drug release profiles in 0.1 M HCl, pH 6.8 buffer or DI H_2O at 37 °C, of drug-loaded beads (IR120) (uncoated) and Wurster coated with Eudragit® L100. DI H_2O (Black square), pH 6.8 (Blue triangle) and 0.1 M HCl (Red circle). The concentration of Eudragit® L100 in the coating solution is 2.5 % w/v.

The purpose of using distinct grades of polymer that did not differ greatly from one another aside from the specific pH at which they dissolve was to investigate if the parameters used to coat the beads using one type of polymer were transferable to another individual polymer type (at similar coating concentrations). Furthermore, these trials provided confidence in the coating process and a level of assurance that the application of an appreciable level of polymer to the beads was not a fortuitous event.

The final element of the preliminary dissolution work involved the assessment of the drug release behaviour of a 1:1 w/w mix of uncoated and coated (S100) particles. Through the inclusion of coated and uncoated complexes, drug release can be tailored to achieve specific outcomes, dependent on the API in question, the nature of the coating polymer and the chemistry of the resin (351). The drug release profiles of a 1:1 (w/w) mix of uncoated and Eudragit® S100-coated DRCs in 0.1 M HCl, pH 6.8 buffer and DI H_20 are depicted in Figure 5.9. Although the process used to apply coatings to the DRCs requires refinement, the potential of this approach was apparent from the results shown in Figure 5.9. Minimal drug release is evident in DI H_20 reflective of the robust coating imparted by the Eudragit® S100 coating and the inability of the DI H_2O to displace the drug off the resin. In contrast, appreciable

levels of drug release are achieved in both 0.1 M HCl and pH 6.8 buffer. Both the rate and extent of drug release of the blend differ from that of the individual components that constitute the blend. Relative to the uncoated DRCs in either 0.1 M HCl or pH 6.8 buffer, the rate of release is far slower. This is not unexpected as the coated beads, which comprise half of the sample, should not release the drug at either pH as the complex is protected by the enteric coating. Conversely, in pH 6.8 buffer and 0.1 M HCl, the sample comprising a mixture of uncoated and coated beads (1:1) releases a higher % of drug ($p<0.05$) relative to that observed when the coated beads are studied on their own (Figure 5.7). Again, this can be attributed to the presence of the second type of bead, which confers its own distinguishable release profile, which in this instance is uncoated and can release the drug immediately upon contact with the drug release media.

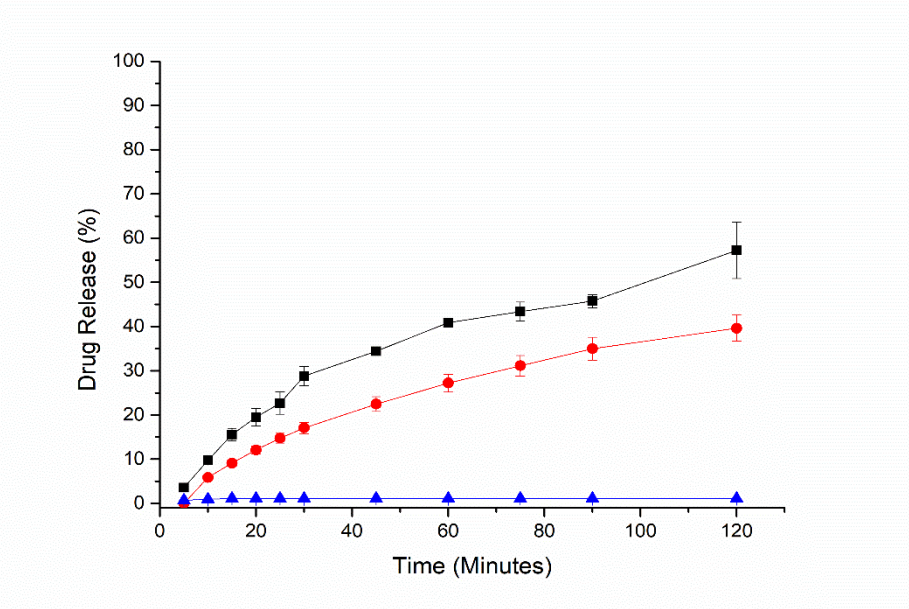

Figure 5.9. Drug release profile in 0.1 M HCl, pH 6.8 buffer or DI H_2O at 37 °C, of 1:1 (w/w) blend of uncoated drug-loaded beads (IR120) and drug-loaded beads (IR120) Wurster coated with Eudragit® S100 in pH 6.8 buffer (Black square), 0.1 M HCl (Red circle), and DI H_2O (Blue triangle).

As highlighted previously (Figures 5.7 and 5.8), surprisingly, both samples coated with either grade of polymer (1% w/v), released the drug in an anomalous manner, which prompted questions over the integrity of the polymeric coating. More specifically, the extent of drug release observed after 2 hours in an acidic medium, which happened to be lower in the case of the Eudragit® S100-coated beads relative to those coated with the Eudragit® L100 grade was unexpected. A possible reason for this could be the differing chemistry of the polymers, which can be attributed to the higher number of methacrylic acid groups in the S grade relative to the L grade, which could impact the integrity of the polymer coating once it encounters conditions such as those present in the dissolution studies (352).

However, the polymeric coating is expected to be robust enough to withstand any potential breach in the coating over a pharmaceutically relevant timeframe. An additional factor, unique to IERs, which could contribute to the challenge to effectively coat the particles is their known tendency to swell upon introduction into aqueous media, which inevitably causes many coatings to rupture. This behaviour has prompted previous authors to include a hydrophilic impregnating/solvating agent such as PEG 4000 in the coating solution to maintain the geometry of the coated polymer by controlling the swelling (129), which otherwise would change and compromise the integrity of the coating, which is a distinct possibility in this work. Although this issue has not been reported for DRCs coated specifically with Eudragit® polymers and is associated more with ethylcellulose films (145), it is still worth mentioning, considering the obvious breach in film integrity, providing a challenge to obtaining the desired controlled-release profile. Although a small amount of drug release from enteric systems in low pH environments is not entirely unusual, the quantity of drug released from the systems studied points to deficiencies in the manufacturing process.

After establishing suitable processing parameters for coating the DRC beads using either Eudragit® L100 or Eudragit® S100 at a 5 g batch size and evaluating the initial dissolution behaviour, further drug release studies were conducted alongside a combination of solid-state and particle size analysis. Several points of difference existed with respect to the previous trials involving pH-dependent polymers. The first pertained to the studies being limited to the Eudragit® L100 grade (selected over the Eudragit® S100 grade because of a lower pH value being required to effect drug release), the second referred to three concentrations of coating polymer in the coating solution (1% w/v, 1.25% w/v and 2.5% w/v) being evaluated, the third relates to the spray solvent and the fourth pertains to the duration of the drug release studies, which were extended to 24 hours. A consequence of this long experiment time is the incorporation of a pH shift during the drug release study which can impact the systems in question from two different perspectives. The first relates to the polymeric coating surrounding the particle, which in this instance is a pH-sensitive polymer designed to dissolve at pH values above 6. Subjecting the systems to a pH shift (low to high pH) enables complete dissolution of the polymeric matrix and permits the bulk of the drug to diffuse out into the dissolution medium. Secondly, the pH shift requires an additional medium to be introduced to the test which provides a fresh influx of ions that serves to shift the equilibrium to a position that favours drug release.

The extent of drug release at low pH values over the course of 120 minutes is approximately 20% for the Eudragit® L100-coated systems studied (Figure 5.10). Although this is higher than one would expect of an enterically coated particle, it indicates that the film formed around the particle is not completely compromised, as the % drug release is substantially lower relative to uncoated material. Furthermore, the DRC beads coated using the 1.75% w/v coating solution produce a near-identical

drug release profile to that of the system coated using the 1% w/v coating solution, characterised by the extent of drug release at each timepoint showing no statistical difference ($p>0.05$) from one another. Interestingly, the DRC beads coated using the 2.5% w/v coating solution, released the drug at a slower rate from the 3 hour timepoint until 10 hours post-addition to the dissolution medium, indicative of a thicker coating being applied. Moreover, the extent of drug release after 24 hours is statistically lower ($p<0.05$) than that of the DRC beads coated using more dilute coating solutions, again indicating the presence of a thicker coating layer. The results from these drug release studies, particularly at the early timepoints, indicate that the imperfect coating layer may not be the sole contributor to the premature drug release observed. The ability of DRCs to swell when exposed to liquid media, thus rupturing the coating layer, may also dictate the extent of drug release observed and partially explain why the release profiles of the different samples over the initial stages resemble one another. Lastly, APIs can diffuse through the membrane itself, a phenomenon largely under the influence of the physicochemical properties of both the API and polymer (196). However, the risk of drug migration through the polymeric membrane in this instance is low as the drug is complexed to the IER. An unintended consequence of drug release occurring from the outset is the steady drug release profile that is obtained. As stated previously, although this release profile is desirable when the goal is to produce a sustained-release system, the fact that the coating polymer is a pH-sensitive agent negates this positive, as the performance of the coated particle is inadequate at low pH.

Aside from the drug release studies, the particle size (Table 5.2) and solid-state (Figures 10-11 in Appendix 3) of the coated beads were characterised. It was found that that the beads coated using all three concentrations of L100 had d_{50} values that were larger ($p<0.05$) than the uncoated DRCs. No statistical difference ($p>0.05$) in the d_{50} values of the beads coated using the two lowest concentrations of polymer in solution were observed, which is not surprising considering the subtle difference in solid contents in the feed solution. However, the beads coated using the highest concentration of polymer (2.5% w/v in the coating solution) have a larger d_{50} value ($p<0.05$) than the other two coated systems, indicative of a thicker coating layer being applied. This is not surprising considering this coating solution contains at least double the amount of polymer relative to the other feed solutions used to coat the beads, and highlights the ability to produce thicker coating layers, as long as the difference in feed solution concentration is large enough. In addition to the particle size calculations, % weight gain calculations were also performed to support the particle size measurements and gain insight into the impact of the polymer coating. The results are included alongside the data reported for the pH-independent systems later on in this chapter to serve as a comparison and illustrate the fact that each polymer behaves differently when used as a coating

agent, exemplified by its film thickness, even if the process parameters are broadly similar and in some cases identical.

These results support the dissolution findings which showed that the systems coated using the 2.5% w/v Eudragit® L100 solution release a lower quantity of drug over time ($p<0.05$) relative to the complexes coated using 1% w/v and 1.25% w/v coating solutions. Furthermore, the complexes coated with the two lowest concentrations studied, produced release profiles that strongly resembled one another, in agreement with the particle size data. With respect to the solid-state characterisation, both pXRD and DSC analysis indicated that all three coated systems were amorphous, signified by the halo pattern in the diffractograms and absence of melt endotherms in the DSC traces of all samples studied (Figure 11(A-B) in Appendix 3).

Table 5.2. Measured d_{50} values for uncoated DRCs and Wurster coated DRCs (Eudragit® L100). The DRCs were formed using a 1:2 D:R (IR120) ratio (w/w). The concentration of Eudragit® L100 used in the coating solution is listed in parentheses where applicable.

Sample	d_{50} (µm)
Uncoated	621.67 ± 8.02
Coated (1% w/v)	710.50 ± 9.85
Coated (1.25% w/v)	720.50 ± 5.68
Coated (2.5% w/v)	765.00 ± 4.68

A final drug release study involving pH-dependent coatings examined the impact of plasticiser inclusion within the feed solution to be sprayed with a view to ascertaining if film integrity could be improved. The impact of plasticiser incorporation was briefly investigated after the initial coating studies involving pH-dependent polymers were performed on the back of the studies involving the pH-independent polymers. The role of plasticiser in the formation of coating films is well documented (192) and discussed extensively as part of the pH-independent trials. Ultimately, as depicted in Figure 5.10, the incorporation of triacetin failed to have the desired impact, as the extent of premature drug release was still approximately 20% after 120 minutes. Compared to systems coated using the same concentration of polymer (2.5% w/v) without the inclusion of plasticiser, the rate of drug release is accelerated from the 3 hour timepoint onwards until the 10 hour mark, after which no statistical difference in drug release ($p>0.05$) could be detected.

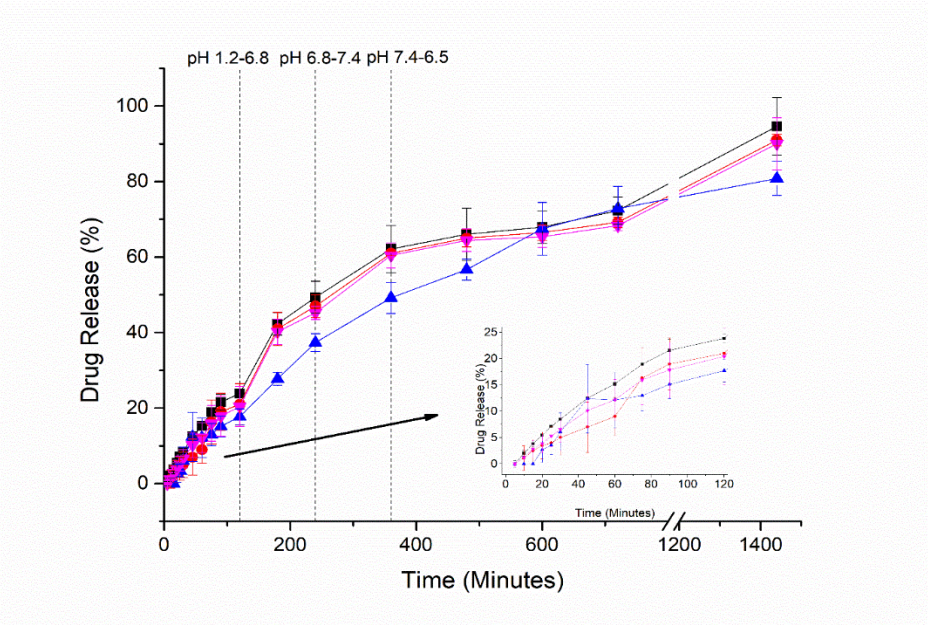

Figure 5.10. Drug release profile over 24 hours (performed using the drug release method detailed in Chapter 2, section 2.2.8.2.1.2) of drug-loaded beads (IR120) Wurster coated with different concentrations of Eudragit® L100 in the coating solution. 1% w/v (Black square), 1.75% w/v (Red circle), 2.5% w/v (Blue triangle) and 2.5% w/v plus triacetin (% w/w) (Inverted magenta triangle).

To investigate the integrity of the coating (Eudragit® L100), the material coated using the 2.5% w/v coating concentration was examined by SEM and also recovered after a 2 hour dissolution study in 0.1 M HCl, dried and examined using SEM (Figure 5.11). The impact of the coating layer is apparent on the particle morphology, as the indentations present on the surface of the uncoated bead are no longer present once the coating is applied. Once the coating is applied, the drug-loaded beads become more spherical relative to the irregular shape that the uncoated material had. Although the coated particles are not perfectly spherical, the integrity of the coating appears to be free of imperfections, signifying that the particles have been effectively coated. Post-exposure to the acidic dissolution medium, the deficiencies of the coated system become apparent and a wide disparity exists from particle to particle (Figure 5.11(C-D)). Noticeable cracks in the surface of each coated bead are prevalent, which may be caused by the swelling of the resin in the acidic medium rather than the dissolution of the polymer layer itself, as polymeric debris is visible (Figure 5.11(C)). These vulnerabilities are the likely cause of several particles having a significant portion of their surface exposed, which in turn is responsible for the level of drug leaching detected during the dissolution study. However, the vast majority of the bead surface is still coated, even for microparticles that were afflicted most by a compromised coating layer, which is reflected in the drug release profile of the coated particles.

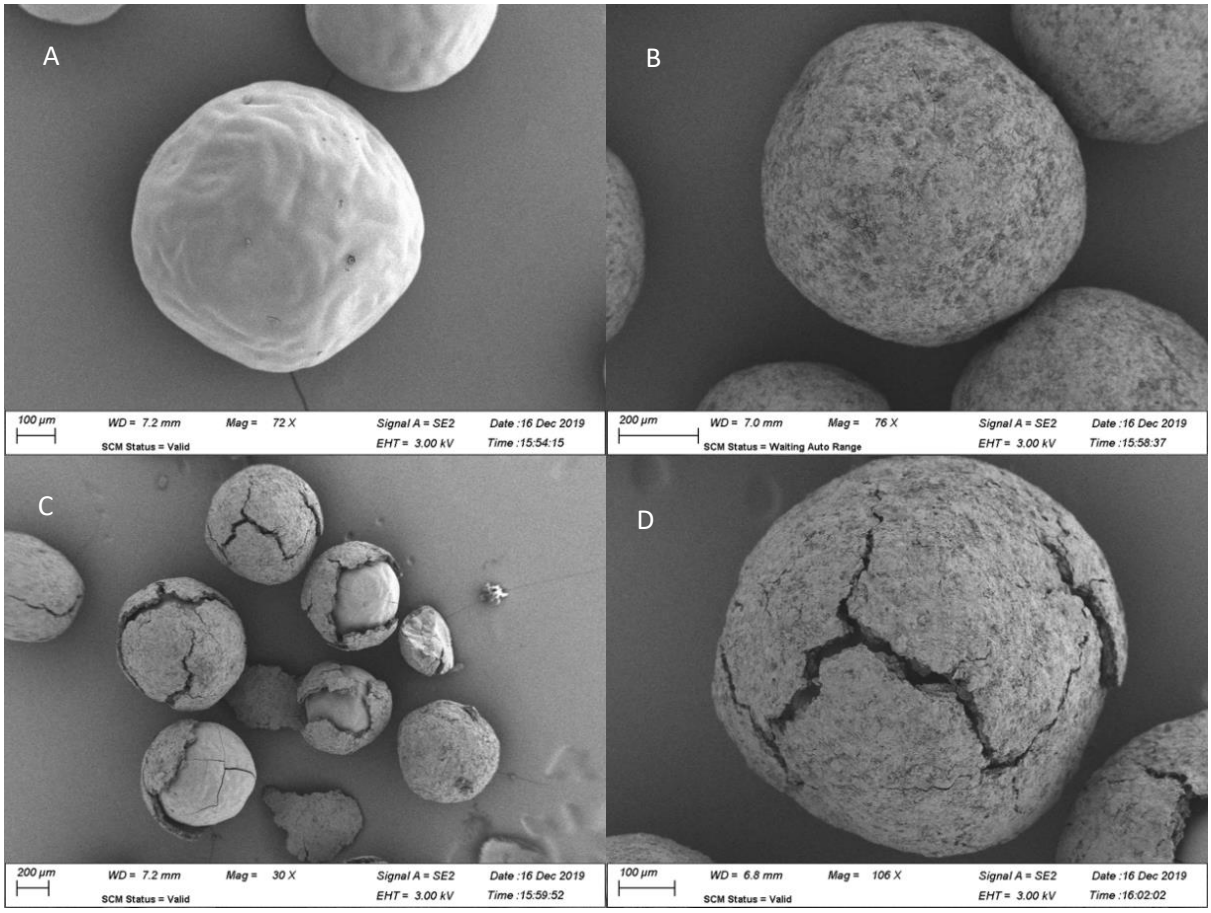

Figure 5.11. SEM images (taken at different magnifications) of Wurster coated DRCs (IR120) (coated using a 2.5% w/v Eudragit® L100 coating solution) pre and post-dissolution testing (0.1 M HCl for 2 hours). A) uncoated DRC (IR120) (x75), B) Wurster coated (L100) DRC (pre-dissolution) (x75), C) Wurster coated DRC (Eudragit® L100) (post-dissolution) (x30) and D) Wurster coated DRC (post-dissolution) (x100).

5.2.1.3.2.2 Coating studies involving pH-independent polymers

Following the coating trials using the Eudragit® range of pH-dependent polymers, the emphasis of the spray-coating work switched to the use of pH-independent polymers. The rationale underpinning this decision was two-fold, the primary reason being the unsatisfactory dissolution performance of the enteric coated DRCs and the second relating to pH-independent polymers being more suited to sustained-release dosage forms. Again, the Eudragit® brand was used, as these polymethacrylate-based copolymers, are traditionally an integral component of sustained-release drug delivery systems (178,185,353). Eudragit® RS 12,5 and Eudragit® RL 12,5 were selected for the development of a sustained-release system due to their well-established use in the drug delivery field (183,354) and availability as ready-made solutions. Furthermore, both grades of polymer have proven effective at retarding the release of DRCs (127,133). Both grades insoluble at physiological pH and capable of swelling, with Eudragit® RL films being more permeable than Eudragit® RS films due to the higher

proportion of quaternary ammonium groups in the Eudragit® RL type (8.8-12%) versus the Eudragit® RS type (4.5-6.8%)(355).

By virtue of "trial and error", a design space for the process using the Eudragit® RS grade was established as detailed in Chapter 2, section 2.2.1.6.2.2, in which fluidisation remained steady throughout the whole run and no evidence of agglomeration was found. To confirm that coating was achieved, images were taken comparing uncoated beads with several coated bead samples comprising "blank" material (Figure 5.12). The images indicate that coating was achieved and the polymer was not lost entirely to the filters, signified by the obvious change in the appearance of the coated beads relative to their uncoated counterparts, characterised by their shape and colour.

This same design space was found to be applicable in the case of the Eudragit® RL, with the formulations and operating conditions of the Mini-Glatt listed in Chapter 2, section 2.2.1.6.2.2. It was necessary to dilute the polymer concentration in the spray solution using IPA, as the viscosity of feed, coupled with the small batch size of each trial (3 g), necessitates relatively low quantities of polymer be sprayed onto the beads. This is unusual as this type of process, even at the research scale, usually uses a batch size of at least 30 g. Starting from a 0.25% w/v polymer content in the feed solution, a series of increasing polymer concentrations were investigated for their effect on the fluidisation of blank beads and the agglomeration tendency. Beads could be successfully fluidised up to and including 8% w/v for both grades of polymer (Eudragit® RS and Eudragit® RL). After 5% w/v, the spray-coating conditions needed to be amended to avoid agglomeration of the beads. This necessitated an increase of the atomisation pressure, which would be expected to decrease droplet size, thus reducing the probability of agglomeration (356). After establishing suitable values for the critical process parameters that enabled successful coating runs devoid of fluidisation or nozzle blockage to be achieved, particle size analysis was performed on the "blank" Eudragit® RS coated beads. The results, depicted in Figure 12 in Appendix 3, revealed an increase in particle size relative to the uncoated beads ("blank"/unloaded) once the concentration of polymer in solution reaches 2.5% w/v. Below this, no statistical difference ($p>0.05$) was evident. In addition, many of the samples coated using coating solutions above 2.5% do not differ significantly from one another, a likely consequence of a large portion of the polymer being lost to the filters when more concentrated coating solutions are used.

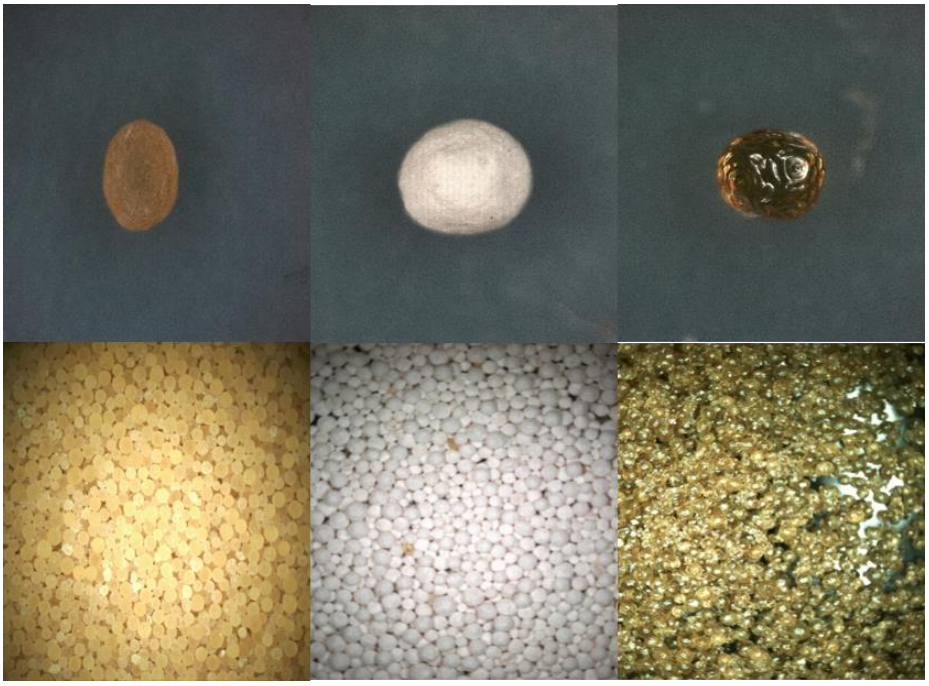

Figure 5.12. Digital microscope images of A) "Blank" resin (IR120) Wurster coated using Eudragit® RL (2.5% w/v coating solution concentration), B) "Blank" resin (IR120) Wurster coated using Eudragit® L100 (2.5% w/v coating solution concentration) and C) uncoated DRC.

After successful coating of microparticles was achieved with the surrogate runs, the drug-loaded resin was substituted into the process, and the DRC beads were coated using a series of different polymer concentrations (0.25-7.5% w/v) that were largely within the range established during the method development stage, with the exception of the lower concentrations, which were anticipated to produce little trouble by way of agglomeration based on the findings up to that point. One minor issue experienced with the drug-loaded beads, which did not occur when studying the unloaded beads, was poor fluidisation in the initial stages of the process. This was solved by spraying pure solvent into the chamber, which had the desired effect of overcoming the particle adhesion to the walls of the chamber. Electrostatic charging is the most probable cause of this phenomenon, leading to defects in coating quality due to non-homogeneity, which have also been reported by Ichikawa et al. in their work (131).

Particle size analysis was performed on the products of all successful runs, and the d_{50} values for coated drug-loaded beads are listed in Table 5.3. The coated particles produced using the most dilute coating solutions are larger (d_{50} = 633.67 ± 2.29 µm and 634.33 ± 2.11 µm, for Eudragit® RS- and Eudragit® RL coated systems respectively) than the uncoated complexes (621.67 ± 8.02 µm), signifying that layers of polymer have been deposited on the complex. Furthermore, the results demonstrate a trend of increasing particle size as the concentration of the polymer solution increases. There is a

plateau at higher coating solution concentrations (2.5% w/v onwards) for both polymer types that can be attributed to more polymer being retained on the filters as the concentration of polymer in solution increases. At equivalent concentrations of polymer in solution, the median particle size of the coated DRCs using either the Eudragit® RS or Eudragit® RL grade do not differ significantly from one another ($p>0.05$). This applies to all concentrations studied and is not unexpected considering the similarities between the Eudragit® RS and Eudragit® RL grades. In general, these results are in agreement with those of previous authors who reported similar findings relating to the polymer concentration and microcapsule size (117,134). They also provide some evidence that coating has been successful, the degree to which will be assessed using further techniques such as SEM, in addition to dissolution testing.

Table 5.3. Comparison of d_{50} values for Wurster coated DRCs (IR120) using a range of coating concentrations and the Eudragit® RS and Eudragit® RL grades.

	d_{50} (μm)	
Concentration (% w/v) of polymer in coating solution	Eudragit® RS	Eudragit® RL
0.25	633.67 ± 2.29	634.33 ± 2.11
0.50	639.33 ± 3.21	642.33 ± 5.52
0.75	656.09 ± 3.61	654.42 ± 5.08
1.00	664.67 ± 5.51	660.67 ± 5.10
1.25	675.33 ± 3.02	674.33 ± 6.21
2.50	685.67 ± 6.24	687.33 ± 4.57
3.75	686.67 ± 6.92	682.56 ± 4.58
5.00	688.67 ± 9.60	688.38 ± 4.64
7.50	686.67 ± 7.51	688.67 ± 3.21

Due to the small batch size, the assessment of the level of coating achieved relied on a comparison between the weight of uncoated beads versus that of coated beads. This was necessary as the normal method which relies on the reported weight gain of the batch post-processing was not appropriate at the lab scale (117). Electrostatic forces coupled with the beads' size and flow properties mean that handling of the beads is problematic especially when transferring from the coating chamber to a vessel for post-processing analysis. Furthermore, some beads are inevitably lost due to the attritional nature of the process. These losses are normally inconsequential if the batch size is large, but they become important when small batch sizes are being trialled, as is the case in this work. These losses

compromise the accuracy of the % weight increase assessment based on a comparison of the entire batch pre and post-coating and an alternative method had to be selected. The method chosen relied on determining the weight of a sub-lot of coated beads and comparing that value to the weight of an equivalent number of uncoated beads, with the results shown in Table 5.4. The calculated weight gain values, which range from 6-12.65%, follow a similar trend to that reported for the particle size analysis. At each concentration of coating polymer studied, no difference ($p>0.05$) in % weight gain was found when the two polymer grades studied were compared. As the % of coating polymer in solution increases from 0.25 to 2.5% w/v, the calculated % weight gain also increases and the weight gain values at each concentration are statistically different ($p<0.05$) from one another. This relationship between % coating polymer and calculated % weight gain no longer applies once the concentration of polymer in the feed solution exceeds 2.5% w/v, as is evident from the % weight gain values not differing from one another over the 2.5 to 7.5% w/v polymer concentration range. Interestingly, the % weight gain values for the systems coated using Eudragit® L100 produced higher % weight gain values (Table 5.4), spanning 31-36%, reflective of a thicker coat being applied and consistent with the increased d_{50} values obtained for these systems relative to those coated using the pH-independent Eudragit® grades.

Table 5.4. Comparison of calculated % weight gain values for Wurster coated DRCs (IR120) using a range of coating concentrations using the Eudragit® RS, Eudragit® RL and Eudragit® L100 grades.

		% weight gain	
Polymer	Concentration (% w/v) of polymer in coating solution	Eudragit® RL	Eudragit® RS
RS or RL	0.25	6.04 ± 0.30	6.10 ± 0.12
RS or RL	0.50	6.71 ± 0.23	6.55 ± 0.31
RS or RL	0.75	8.03 ± 0.30	7.92 ± 0.19
RS or RL	1.00	8.70 ± 0.21	8.42 ± 0.36
RS or RL	1.25	10.10 ± 0.15	9.96 ± 0.93
RS or RL	2.50	12.00 ± 0.69	12.34 ± 0.37
RS or RL	3.75	12.31 ± 0.43	12.17 ± 0.91
RS or RL	5.00	12.13 ± 0.67	12.63 ± 0.56
RS or RL	7.50	12.65 ± 0.88	12.85 ± 0.97
		% weight gain	
Eudragit® L100	1.00	31.09 ± 0.68	
Eudragit® L100	1.25	31.60 ± 0.74	
Eudragit® L100	2.50	35.90 ± 0.42	

5.2.2 Drug release studies (Wurster coated IR120 beads)

Prior to dissolution studies being performed using the coated DRC beads, the release profile of Zanaflex® (TZD) 2 mg tablets in 0.1 M HCl was assessed for comparative purposes (Figure 13 in Appendix 3) using a modified (2 tablets instead of 1) dissolution method (Section 2.2.8.2 in Chapter 2) based on that reported in the USP (272). This adaption was necessary, as the HPLC method was not sensitive enough to detect the low concentration of drug from the tablets at early time points. This study revealed that the drug release kinetics in 0.1 M HCl can be described as rapid, with 100% being released after 30 minutes. This observation coupled with the drug's short half-life in the body (2.5 hours) highlights the potential for a modified-release product that may be achieved using a combination of ion-exchange and coating technologies.

As noted in Chapter 3, the TZD effectively released abruptly from the uncoated DRCs, meaning these systems could not satisfy the requirements of sustained-release formulation, thereby requiring the application of a rate-controlling barrier. With this objective in mind, a selection of coated complexes were produced, as described above, using the different coating polymer concentrations and polymer types and their release characteristics were assessed (Figures 5.13-5.14). Relative to the uncoated DRCs, all coated DRCs displayed altered drug release behaviour, which showed a strong dependence on the coat to core ratio. As the batch size of the starting material (drug-loaded beads) remained constant throughout the spray-coating trials, the coat to core ratio was altered by increasing the concentration of coating material in the feed solution to thoroughly investigate the potential of altering the polymer coating concentration to modify the drug release kinetics.

Initial dissolution studies focused on the complexes coated using Eudragit® RS (Figure 5.13) and it is apparent from the drug release profiles that the release rate from the coated DRCs is highly dependent on the level of coating applied, with a more sustained-release pattern being achieved when more concentrated coating solutions are used, a finding consistent with that of previous authors (117). This is evidenced by the distinct difference in release profiles of samples coated using coating solutions containing a 1.25% w/v or lower polymer concentration compared to those coated using higher concentrations of polymer (2.5% w/v or higher). For the sake of clarity, the % polymer coating refers to the % of the polymer in the coating solution. Upon inspection of the drug release profiles, it is apparent that the high concentrations of the Eudragit® RS grade used as part of the coating solution produced an effective coating layer, reflected by the low level of drug released (<7%) after 24 hours. These findings are in agreement with those of Sriwongjanya and Bodmeier who found that the Eudragit® RS polymer was even more effective, relative to the data presented as part of this work, at retarding drug release using an aqueous solvent evaporation method to coat the DRC systems. In their

study, a similarly low quantity of drug release was detected over a 90 hour dissolution study for all three DRCs that were coated, highlighting the impervious nature of this type of acrylate polymer (133). Furthermore, there are many reports in the literature of incomplete drug release from coated DRCs attributable to substantial portions of the drug still being contained within the resin matrix (145,357). The impermeable nature of this polymer grade, which is well-known (358), is conferred by the low number of quaternary ammonium groups in the salt form, which produces low permeability films (359). It is this low permeability coupled with a reduced tendency to swell when exposed to aqueous media that is responsible for the low level of drug diffusion through the film, which points to the need to use lower concentrations of coating polymer in solution.

The drug release profiles of the DRC beads coated using the lower concentration range (0.25-1.25% w/v) show that the use of coating polymer concentrations in this range produced more desirable release kinetics. Predictably, an increased quantity of the drug was released over the time course of the dissolution study when the lower the coating concentration used, as part of a "trial and error" approach. When comparing the resultant release profiles, the impact of coating thickness is apparent from the 3 hour timepoint onwards, as all % drug release values were statistically different ($p<0.05$) from one another, clearly illustrating the impact of the polymeric coating. Over the initial timepoints studied (5-60 mins), the extent of suppression afforded by coatings applied using the 0.25% and 0.5% w/v polymeric concentrations did not differ significantly ($p>0.05$) however, the rate of release was significantly higher relative to that seen with the complexes coated using the 0.75-1.25% w/v concentrations. Furthermore, the complexes coated using feed solutions containing 0.25% w/v and 0.5% w/v concentrations of polymer were the only two systems that released a high enough proportion of drug so that it could be detected from the 5 minute timepoint onwards. This contrasts to the complexes coated using 0.75% w/v, 1% w/v and 1.25% w/v polymer concentrations, which release a detectable quantity of drug only after 15, 20 and 30 minutes respectively. Figure 5.13 also shows that, in general, the % drug release from systems at the timepoints tested is reduced ($p<0.05$), the higher the polymer concentration in the coating solution. The only exception being the systems coated using 1% w/v and 1.25% w/v, from which there is no statistical difference ($p>0.05$), suggestive of the coating process requiring improvement. In general, the drug release profiles illustrate the fine balance between prevention of the burst release and complete suppression of drug release that must be achieved to formulate a sustained-release formulation using water-insoluble polymers, in particular low permeability grades. Together with the % weight gain calculations, the dissolution data suggests that the release rate decreases as the amount of polymer applied to the complex increases. This relationship can be attributed to a thicker coat being applied which provides an increased level

of resistance to the diffusion of drug ions, commonly referred to as an increased diffusional path length (188). The drug release profile of complex coated using 0.25% w/v satisfied the requirements of the formulation, as a sustained-release pattern was maintained over a 24 hour time period and complete release was very nearly achieved, meaning it was selected for further study.

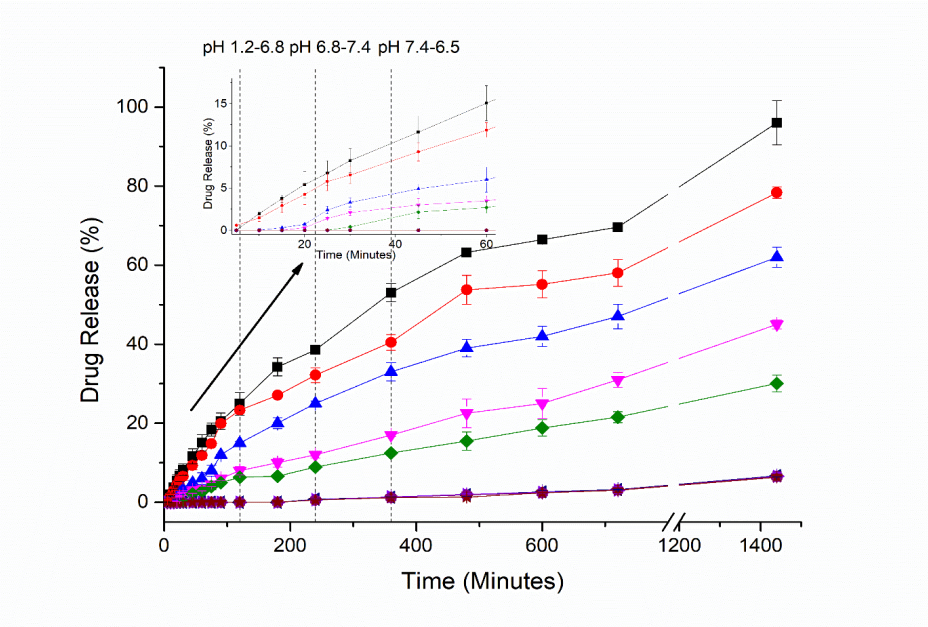

Figure 5.13. Drug release profile over 24 hours (performed using the drug release method detailed in Chapter 2, section 2.2.8.2.2) of drug-loaded beads (IR120) Wurster coated with different concentration of Eudragit® RS in the coating solution. 0.25% w/v (Black square), 0.5% w/v (Red circle), 0.75% w/v (Blue triangle), 1% w/v (Inverted magenta triangle), 1.25% w/v (Olive diamond), 2.5% w/v (Navy triangle), 3.75% w/v (Violet triangle), 5% w/v (Purple circle) and 7.5% w/v (Wine star).

One finding from the drug release studies performed using the complexes coated with the Eudragit® RS grade was the need to try an alternative water-insoluble derivative of the acrylate polymers in the form of Eudragit® RL. A higher concentration of quaternary ammonium groups in the chloride salt form in this grade renders it highly permeable and amenable to swelling (360). Therefore, the systems coated using this grade of polymer would be expected to release at a faster rate relative to the systems coated using the less permeable grade. Figure 5.14 shows the effect of incorporating Eudragit® RL into the coating solution, where all formulations, bar one, are characterised by incomplete drug release. In contrast to the systems coated with Eudragit® RS, the majority of which exerted an excessive sustained-release effect (<80% drug release after 24 hours), the majority of the loaded drug is released after 24 hours from complexes coated using RL (approximately 80%). Similar to the Eudragit® RS coated systems, the release rate was dependent on the level of coating applied, with more concentrated coating solutions yielding a higher suppression of drug release, resulting in incomplete release for all systems coated, with the exception of the 0.25% w/v. This correlates well with the

particle size data of the coated beads, reported in Table 5.3, which was substantiated by the alternative method of estimating coating, reported in Table 5.4.

This difference in the drug release behaviour can be ascribed to the nature of the coating polymer, with Eudragit® RL having high permeability, thus releasing the drug more rapidly in comparison to the Eudragit® RS which is the low permeability polymer. By examining the dissolution profiles of all systems presented, it is apparent that systems coated using a lower concentration of polymer in the feed solution are most suitable, akin to what was observed with the Eudragit® RS grade. Of all the systems studied, the complex coated using 0.5% w/v Eudragit® RL was selected for further study. A steady release over the course of 24 hours is achieved, with close to 100% total drug release, which was one of the main prerequisites of the work, as it could enable once-daily administration, which has the potential to improve patient compliance. Having said that, any of the complexes coated with feed solution containing a polymer concentration of 0.5-1.25% w/v, meet the primary aim of the work, defined at the outset. When the feed solution comprised of a 0.25% w/v concentration of polymer is used to coat the beads, the release from the coated DRC over 24 hours is too rapid, as complete drug release is achieved after 12 hours. Therefore, it was not considered for further analysis.

Inspection of the drug release profiles (Figure 5.15) reveals that the drug release from all 9 systems could be broadly characterised by a quick-release phase, followed by at least one or more prolonged release phases, with the magnitude of each phase being dictated by the polymeric concentration in the feed solution. As alluded to already, at progressively higher concentrations of coating polymer in solution, the release from coated systems is suppressed to a greater extent, presumably due to a thicker coating layer being applied. This is the case until a plateau in drug suppression is reached, which is achieved when a coating concentration of 3.75% w/v is used. Similar to the Eudragit® RL grade, higher concentrations of polymer in the feed solution produce coated particles that result in a large extent of incomplete drug release. Furthermore, the release profiles of the complexes coated using the three highest polymer concentrations resemble each other closely, indicative of most of the polymer beyond the 3.75% w/v concentration being lost to the filters of the machine, rather than being applied to the beads as a coating. The quick-release phase in the profiles of the complexes coated using dilute concentrations of coating polymer was generally longer to that seen relative to the profiles of the complexes coated using more concentrated coating solutions. Moreover, the shorter the time it takes for a more tempered release rate to be reached i.e. the shorter quicker release phase, the lower the total % drug release value at the end of this phase. To illustrate this point, complexes coated using feed solutions comprising 0.5% w/v and 0.75% w/v polymer concentrations, release 72% and 68% of the drug in 8 hours respectively compared to the complexes coated using feed solutions comprising 1% w/v and 1.25% w/v polymer concentrations, which release approximately

52% and 48% in 6 hours. The shape of the drug release profiles pertaining to the complexes coated using polymer concentrations ranging from 3.75-7.5% w/v is similar to those produced by coating complexes using 1-1.25% w/v polymeric concentrations in the feed solution. The anomaly is the release profile of the complex coated using the 2.5% w/v polymer concentration, which displays a comparably higher rate of drug release relative to the other coated complexes over the time period (360-720 minutes) which was designated as the plateau phase in the % drug release. Finally, the complex coated using the 0.25% w/v samples is the complete outlier in the data set, as the rapid release phase concludes after approximately 120 minutes, which is a far shorter timeframe relative to all other samples studied, suggestive of the polymer concentration in the solution being lower than the critical concentration necessary to impart a sufficient degree of control on the drug release, which is evident for all other samples studied.

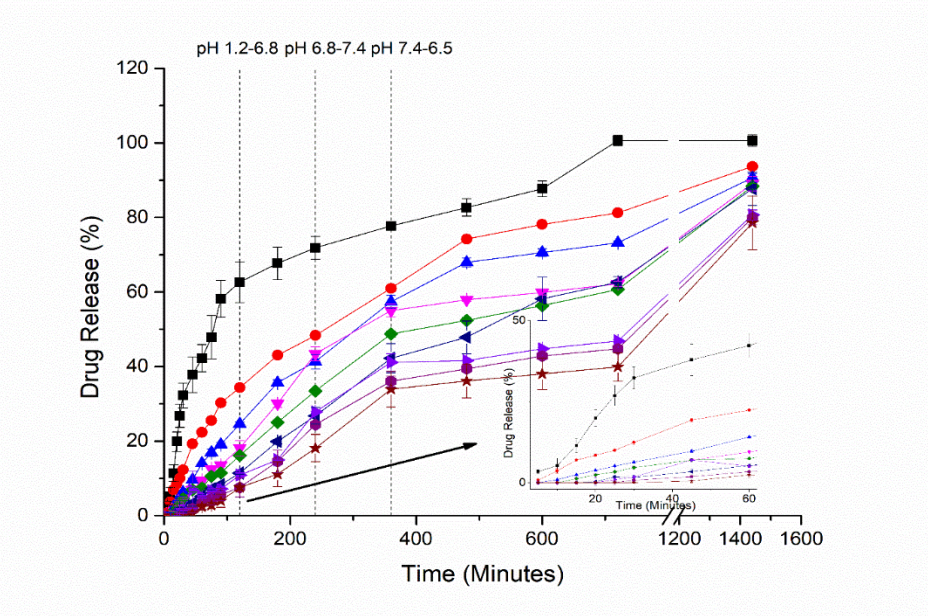

Figure 5.14. Drug release profile over 24 hours of drug-loaded beads (IR120) Wurster coated with different concentrations of Eudragit® RL in the coating solution. 0.25% w/v (Black square), 0.5% w/v (Red circle), 0.75% w/v (Blue triangle), 1% w/v (Inverted magenta triangle), 1.25% w/v (Olive diamond), 2.5% w/v (Navy triangle), 3.75% w/v (Violet triangle), 5% w/v (Purple circle) and 7.5% w/v (Wine star).

A consistent feature of the dissolution profiles of the coated complexes produced using either grade of polymer is the drug release rate remaining independent of pH. This is evident from the gradual increase in drug release over the timeframe of the study and the absence of any sudden increase in the amount released after the introduction of media to alter the overall pH. Similar studies assessing the impact of a pH shift on the drug release behaviour have been conducted in this manner, and have reported the method as suitable for characterising drug release from DRCs (361). One aspect of this

method, namely, the addition of fresh media, is beneficial for ion-exchange systems that reach ion-exchange equilibria relatively quickly in a fixed volume of the medium. This has been attributed to the assistance it provides in helping to drive further release from the DRCs upon exposure to fresh media. In the case of the TZD system, this was not of much benefit, as complete drug release from uncoated DRCs has been shown previously, however it is worth noting, particularly for uncoated DRC systems of drugs such as dextromethorphan and propranolol, for which large degrees of incomplete drug release from DRCs have been reported (145). Moreover, Pongjanyakul reported the beneficial impact of using the USP type 2 apparatus and adjusting the pH upward from 1.2 to 6.8 when attempting to attain a complete drug release profile in tandem with testing the influence of different sample volumes and sampling frequency as part of a factorial design (361). The addition of medium to increase the pH of the dissolution medium to neutral means that the total amount of cations present are higher, which again can drive the equilibrium to the right resulting in further drug release. Additionally, through the introduction of the sodium ion, which has been reported to have a higher affinity for the strong resins, another factor that may favour drug release is introduced into the equation. The role of this factor, in this particular case, is likely to be low, as little evidence could be ascertained from the assay studies as to the impact of the displacing ion on drug release. As many coated samples displayed incomplete release after 24 hours and the studies were conducted under sink conditions, the remaining solid material was recovered post-dissolution and assayed to establish if this material could be accounted for and to rule out the possibility of degradation or drug precipitation. Assay results for recovered material equated to the quantity of drug not released during the drug release study indicating that the polymeric layer is responsible for the incomplete release (Table 1 in Appendix 3).

5.2.2.1 Drug release kinetics (Wurster coated IR120 beads)

The obtained release data (first 60% of the release of the drug) was fitted to the well-known kinetic model known as the Korsmeyer-Peppas equation) to gain insight into the drug release mechanism. The values of the correlation coefficients are listed in Table 2 in Appendix 3 and reveal that several systems are fitted well using the model whilst the release behaviour of others could not be modelled accurately using the aforementioned equation

The Korsmeyer-Peppas model, also known as a power-law model, is a semi-empirical model that has been demonstrated to be particularly suited to polymeric systems, for which it was designed, and it has proven useful in cases where the release mechanism is either not known or it is thought that at least two independent drug release mechanisms are at play (270). The diffusion exponent *n* which can be ascertained from the model has been used to characterise the release mechanism which can be broadly distinguished as Fickian (*n* values up to 0.5) or non-Fickian (270,362). These mechanisms can be further distinguished as case I (Fickian), case II, anomalous case and super case II. The last three

cases can be classified as non-Fickian models, with case II representing zero-order kinetics, characterised by an *n* value of 1. Regarding case 1, the *n* value is 0.5 and diffusion is primarily responsible for the drug release rate. When the exponent values fall between 0.5 and 1, the model is classed as anomalous transport due to a combination of mechanisms (diffusion and swelling) being responsible for the drug release rate (362). Finally, when the value of the diffusion exponent *n* is greater than 1, the super case II model applies (363).

This exponent (*n*) alongside the rate constant value for each system (RL and RS coated) are listed in Table 5.5. At this stage it is important to highlight that the applicability of the model for the systems studied is limited based on consideration of the fits (Figure 14 in Appendix 3). In general, the data from the RS coated systems fits the model better relative to the RL coated systems. The inadequacy of the model is apparent for systems coated using coating concentrations of at least 2.5%. This observation applies to both grades of polymer and can be attributed predominantly to the lag time which can be observed at the early timepoints of the drug release plots. This lag period is more pronounced for systems coated using higher polymer coating concentrations. Therefore, the model offers no insight regarding the drug release mechanism for the systems coated using the higher (>2.5% w/v) coating solution concentrations. A model that factors in a lag time is therefore required to accurately model the data. Over the polymer coating concentration range 0.25-1.25% w/v, it can be seen that the exponent value varies depending on the concentration of coating polymer in the solution used to coat the DRC beads. In general, the value for the exponent increases as the coating concentration increases and at equivalent coating concentrations, the value is higher for the Eudragit® RS grade relative to the Eudragit® RL grade.

Over the aforementioned concentration range, the RS coated systems can be classified as anomalous (non-Fickian) transport as the *n* values fall between 0.563 and 0.763. The values for the Eudragit® RL coated systems span a larger range (0.33-0.648) indicating that a diverse range of mechanisms may be responsible for drug release (270). The sample coated using the 0.25% w/v concentration has the lowest value of *n* (0.333) which is representative of Fickian diffusion, a consequence of the thin film applied from the most dilute coating solution. Fickian release, a type of diffusional controlled release, which is dictated by the diffusivity property of an API, typically occurs when the T_g of the polymer is lower than the environment, providing enhanced polymer chain flexibility, enabling easier access of solvent (362). However, this is not the case in this instance as the Eudragit® RL grade has a T_g of approximately 55 °C (364) and the drug release study is performed at 37 °C. Anomalous transport, which has a cutoff for the *n* exponent of 0.85 for the spherical samples, covers the bulk of the other samples studied, and may be attributed to a combination of swelling and diffusion effects, as the polymeric chains rearrange their position and the drug continues to diffuse from the matrix into the

media resulting in both processes occurring at similar magnitudes to one another. In contrast to Fickian diffusion, this behaviour is typically observed when the T_g of the polymer is higher than the environment (362). It is important to note that the Korsmeyer-Peppas equation is only valid for the first 60% of the release of the drug from the systems studied (plots shown in figure 14 in Appendix 3). Therefore, there is a wide variation in the timeframe over which the exponent was calculated which can be attributed to the slower release kinetics from the Eudragit® RS coated systems versus equivalent Eudragit® RL coated systems. In the majority of publications where the release kinetics from DRCs are fitted using the Korsmeyer-Peppas model, the primary emphasis of the commentary is on the meaning of the exponent and the rate constant value is neglected. In his work, it is evident from the data reported in Table 5.5, that a large disparity exists with respect to the rate constant values for systems coated using equivalent coating concentrations (up to and including 1.25% w/v) of either polymer. This is not surprising when one considers the drug release profiles of the coated systems (Figures 5.13 and 5.14) which illustrate the profound influence of polymer type on the release behaviour.

Although semi-empirical mathematical models have been extensively used to elucidate the drug release mechanisms for many pharmaceutical systems, they suffer from many drawbacks with respect to IER-based systems despite evidence in the literature reporting their use in interpretating the drug release data from a kinetic perspective. This assertion can be rationalised by considering the series of processes (migration of the counter ion into the interior of the matrix and migration of the drug ion into solution) implicated in controlling the drug release from the resinate. Quantitative studies on IER-based systems have predominantly focused on attainment of equilibrium owing to the rapid diffusion of the ions, a consequence of their small size. In contrast, the ion-exchange process involving large organic ions, such as those used as part of a drug delivery strategy, are slower, meaning kinetic measurements are of interest (95). When modelling the release from the DRC it is important to consider both the diffusion of the counter ion and drug ion, as well as the dissociation of the drug ion, thus liberating the “free drug” ion. The two most well-known drug release mechanisms implicated in the release process, proposed by the eminent author Boyd, are particle (diffusion of drug within the matrix) and film diffusion (across the liquid film that envelops the particle), the former of which, predominantly controls the release of drug from the ionic complex (95,344). These processes are not considered in the well-known semi-empirical Korsmeyer-Peppas model, used in this work, thus pointing to its unsuitability to accurately model the release data, reflected in the *n* values.

As alluded to previously, a popular approach for modelling the release behaviour of the drug from DRCs, and identifying the rate-limiting process, is known as the Boyd Model, which has been subsequently modified by Reichenberg and Bhaskhar, using a series of approximations involving

Fourier transformations and integration. Although, this method and the subsequent modifications has proven useful for modelling the release of uncoated ion-exchange based systems (109,365), it is not particularly suited to coated IER systems, the subject of this work, where the influence of the polymeric membrane has to be considered. The overall release kinetics has to factor in the diffusion resistance of both the counter ion and drug within this coating layer, which is acknowledged to be the major contributing factor to the release rate, together with diffusion through the film later surrounding the particle. Despite this obvious limitation, prominent authors within the field have reported its applicability, whilst acknowledging the limitations of grouping together distinct elements of the dosage form (core and coat), thus, essentially considering it a homogenous system and limiting the model's applicability (92,117,131,344).

Jeong et al. proposed their own mechanistic model, where particle diffusion is solely considered as the rate-controlling mechanism, which the authors justify by citing the poor fits they obtained with their data, when Boyd's film diffusion model was used. The authors point to the drawbacks of the well-known model, which is ascribed to the approximations associated with each model (particle and film diffusion), especially with respect to swelling tendency and the lack of differentiating between the coating and core domains. It is this swelling tendency that forms a large basis of their own model with a view to developing one that is more useful for design purposes. The validity of the model was confirmed by the closeness in fit of the simulated data relative to the experimental data (344).

Aside from the lack of suitability of a semi-empirical method, very often the discussion in the literature centres around the meaning of the exponent rather than the rate constant. Moreover, the extent of this discussion is scarce and very often is restricted to stating the mechanism of drug release indicated by the value of the exponent, rather than any meaningful conclusions being drawn from the data. Depending on where the value falls within the arbitrary cut-off values, broad assertions can be made with respect to the predominant process governing drug release for the systems coated using polymer concentrations up to and including 1.25% w/v. Similar comments are made in this work although the limitations of this approach are illustrated by the fits depicted in figure 14 in Appendix 3. Overall, it is clear that modelling the release rate of the drug from DRCs requires further work, as no model to date has been identified as the gold standard to understand the drug release kinetics without having significant limitations. Evidence of the utility of drug release models such as the Higuchi model (mainly in a supportive capacity) can be found, showing that deeper consideration of the release process from the DRCs is required (111). Although the mechanistic model reported by Jeong et al. was reported to accurately model the experimental data, uptake by other research groups has been low.

Table 5.5. Comparison of the calculated rate constant (KKP) and exponent (n) for each Wurster coated DRC (IR120) produced using both grades of polymer (Eudragit® RS and Eudragit® RL) and a series of different polymer concentrations using the Korsmeyer-Peppas model (Equation 2.1 in Chapter 2, section 2.2.8.3.3).

	Polymer Grade			
	Eudragit® RS		Eudragit® RL	
Polymer concentration (% w/v)	KKP (h^{-1})	n	KKP (h^{-1})	n
0.25	1.712	0.563	10.421	0.333
0.50	1.404	0.564	3.493	0.471
0.75	0.760	0.618	1.835	0.555
1.00	0.223	0.703	1.238	0.600
1.25	0.193	0.763	0.852	0.648
2.50	0.001	1.212	0.493	0.724
3.75	0.002	1.222	0.416	0.729
5.00	0.001	1.243	0.261	0.791
7.50	0.001	1.295	0.152	0.842

5.2.2.2 SEM to investigate polymer integrity (Wurster coated IR120 beads)

To investigate the integrity of the applied coating layer (Eudragit® RS grade) post-exposure to the dissolution media, SEM analysis was performed and the images of select samples exposed to dissolution media for 24 hours are shown in Figure 5.15. These samples were selected on the basis of them being coated with sufficiently different concentrations of polymer to investigate if the SEM images reflect the differences observed in the release profile. Noticeable differences in the morphology after exposure to the dissolution media for 24 hours can be observed in the SEM images, which show partially coated beads with remnants of coating for the beads coated with lower concentrations of polymer and surfaces with few cracks at higher polymer concentrations. This indicates the robustness of the coating and that the mechanical properties of the coating properties employed are critical to achieving the desired drug release profile.

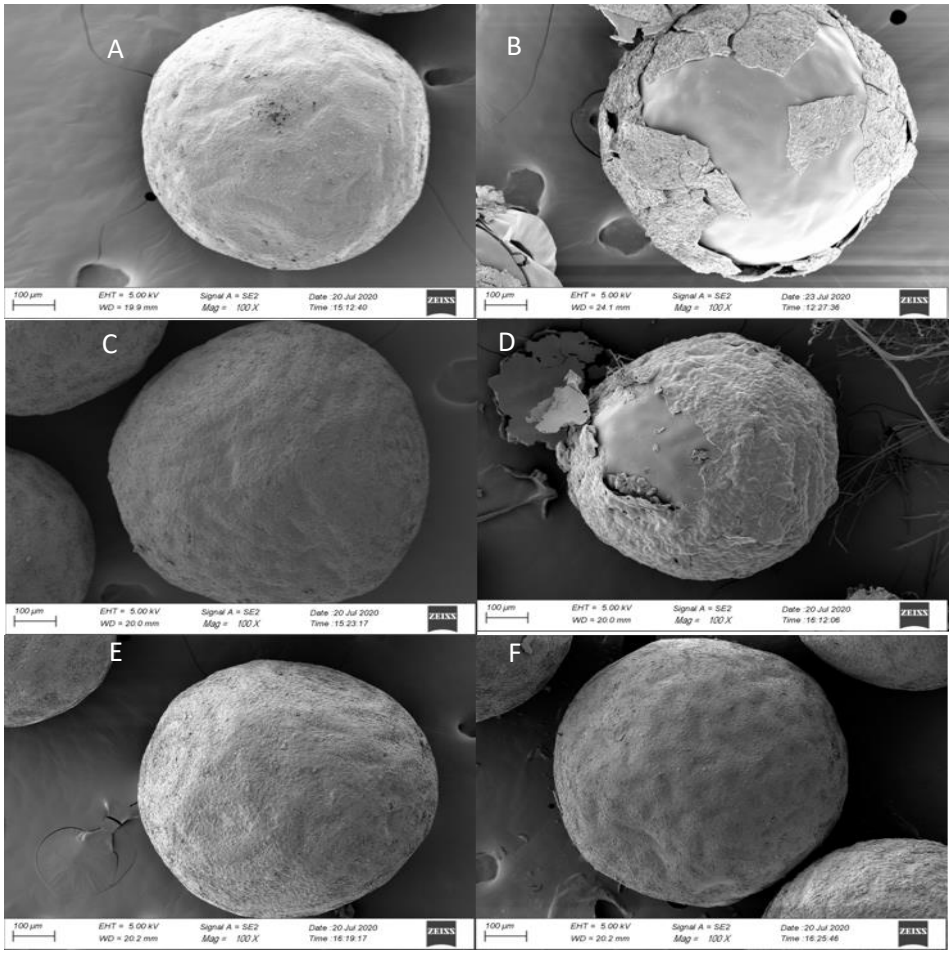

Figure 5.15. SEM images of selected Wurster coated DRCs (IR120) (pre and post-dissolution) produced using different concentrations of the Eudragit® RS grade in the coating solution. A) 0.25% w/v (pre-dissolution), B) 0.25% w/v (post-dissolution), C) 2.5% w/v (pre-dissolution), D) 2.5% w/v (post-dissolution), E) 5% w/v (pre-dissolution) and F) 5% w/v (post-dissolution). The drug release testing was performed using the drug release method detailed in Chapter 2, section 2.2.8.2.2.

A similar procedure was carried out after a 24-hour dissolution study, to investigate the appearance of the Eudragit® RL coating, with the results of SEM analyses performed on select beads post-dissolution shown in Figure 5.16. Again, the selected samples display a compromised polymeric membrane which is the result of exposure to the dissolution media. Greater disruption to the polymeric membrane is observed relative to the Eudragit® RS coated systems which was not unexpected given that the Eudragit® RL grade has a higher permeability, making the DRC more accessible to the dissolution media, which may cause swelling to occur, thus compromising the integrity of the coating. Predictably, this deterioration in membrane quality is exacerbated for the coated complexes produced using more dilute polymeric solutions compared to those produced using more concentrated feeds.

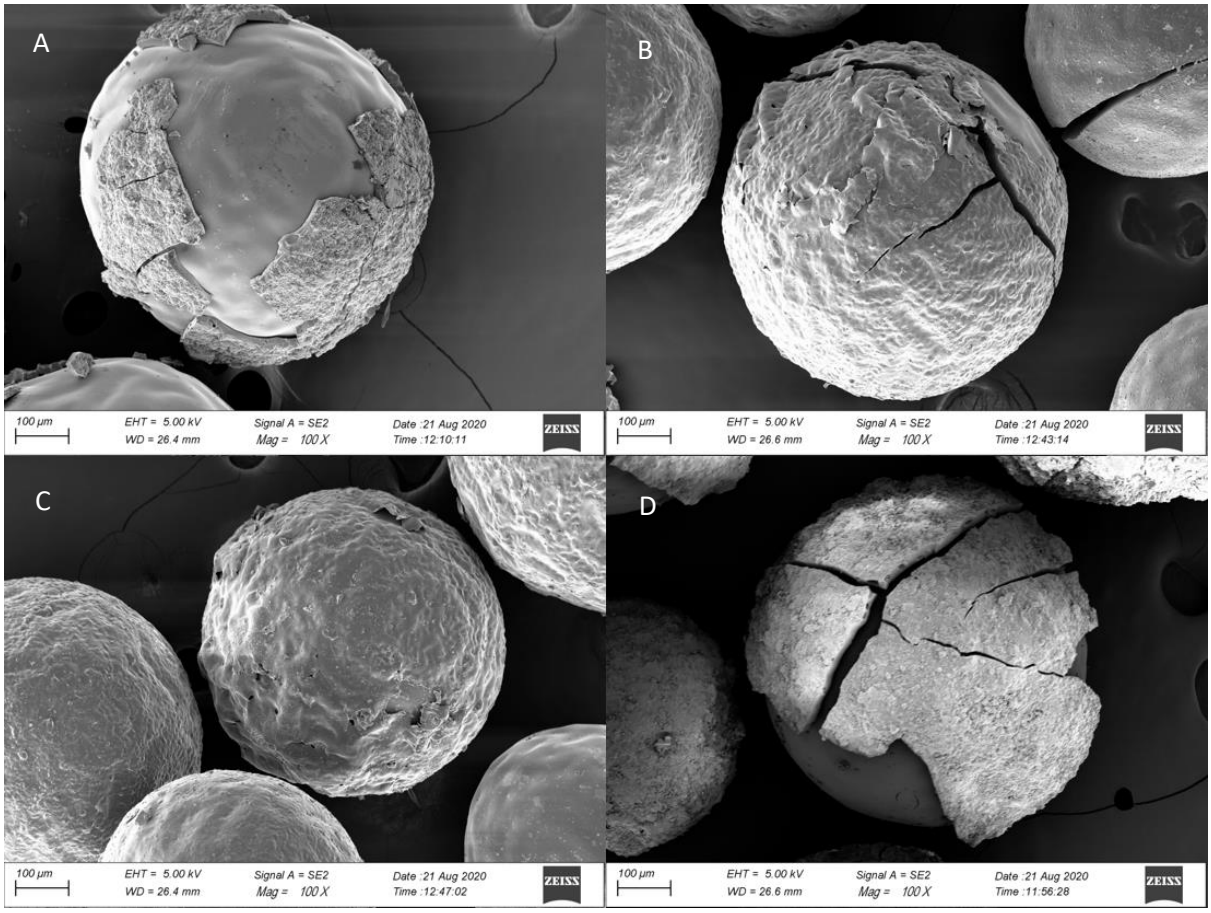

Figure 5.16. SEM images of selected Wurster coated DRCs (IR120) produced using different coating concentrations of Eudragit® RL post-dissolution (performed using the drug release method detailed in Chapter 2, section 2.2.8.2.2). A) 0.5% w/v, B) 1%, w/v, C) 2.5% w/v and D) 5%. w/v.

5.2.2.3 Investigation of polymeric blends (Eudragit® RS/ Eudragit® RL)

A final element of the spray-coating studies involved the utilisation of polymer blends that have been previously shown to be miscible with one another (185). The process parameters identified during the coating studies that utilised polymeric solutions containing a single component were then used to spray-coat drug-loaded beads using a blend of the polymeric components. Similar to the trials conducted using a single polymer in solution, all runs using the blends that were trialled produced yields in the region of 70%, with no evidence of agglomeration.

Similar to the preliminary dissolution studies that utilised a mixture of two different bead types (coated and uncoated) in the work that utilised pH-dependent polymers, a series of screening trials evaluating the dissolution performance of beads coated with a blend of the pH-independent polymer were performed. By combining different grades of polymer, the film-forming properties can be altered and varying release profiles can be attained (366). The wide variety of drug release patterns attainable using blends can help accomplish aims such as providing the required stability in certain release media

or achieving a pre-determined rate of drug release over a defined time period (367). Qu et al. previously reported the utility of using a blend of Eudragit® RS and Eudragit® RL and demonstrated the effectiveness of combining these two compatible polymers to alter the release of drug from IERs (368). As referenced previously, both grades of polymer have been demonstrated to be effective at retarding drug release and knowledge of the impact of the individual Eudragit® grade on drug release is critical to determining suitable blend ratios of Eudragit® RS to Eudragit® RL. Three ratios of Eudragit® RS to Eudragit® RL were selected to probe the possibility of customising the release profile by altering the ratio of polymers with differing degrees of polar character at a fixed concentration of total polymers content (1% w/v). The low permeability of the Eudragit® RS grade pointed to the need to use a lower quantity of it in solution relative to the more permeable Eudragit® RL grade to achieve an increased level of drug release at earlier timepoints, and the ratios selected reflected this with the exception of the 1:1 (w/w) ratio.

The release profiles of the coated complexes indicate that a sufficient degree of control can be attained by varying the polymer contents of the feed solution, as shown in Figure 5.17. Of all the systems that were coated using a blend, the complexes spray-coated using a coating solution comprising a 50:50 RS:RL (w/w) ratio, yielded the slowest release over 24 hours whilst the 10:90 (w/w) RS:RL ratio enabled the fastest release of drug from the DRC. The release profile of the 25:75 (w/w) RS:RL ratio lies approximately between that of the two extreme ratios selected, thus offering the option of tailoring the release profile further using blends of polymers and not being restricted by the use of solely one polymer. Also included in Figure 5.17 are the release profiles of the complexes coated using solutions containing 100% Eudragit® RS and 100% Eudragit® RL, which further highlight the impact of using a mixture of polymer types, as it is evident that the 10:90 (w/w) RS:RL system releases drug at a comparably lower rate relative to the 100% Eudragit® RL system and the release kinetics of the DRC coated using a 50:50 (w/w) ratio of RS:RL remains far higher relative to the 100% Eudragit® RS system. Similar to many of the systems studied to date, the effect imparted by the coating applied on the drug release becomes apparent as the dissolution study proceeds, which aids in the elucidation of the effect of subtle changes to the composition of the coating solution on the drug release profile. With respect to the 10:90 (w/w) RS:RL coating system, the release profile resembles that of the Eudragit® RL coated system, with no statistical difference ($p>0.05$) between the % drug release values until the 6 hour mark, when the influence of the Eudragit® RS component of the film coating becomes apparent, signified by the lower % drug release ($p<0.05$) at each subsequent timepoint for the duration of the dissolution study. As the proportion of Eudragit® RS in the system increases the disparity in % drug release relative to the Eudragit® RL coated system becomes more apparent and is more noticeable at earlier timepoints. However, the drug release profiles of the complexes coated with the

50:50 (w/w) and 25:75 (w/w) do converge at early timepoints, presumably due to a combination of the lower drug release, imperfect coatings applied and the risk of coating rupture which may lead to the release of the drug. Similar to the other systems, as time proceeds, the impact of polymer coating, in particular, those produced using higher quantities of the Eudragit® RS grade, on the drug release becomes evident and is reflected by statistically lower drug release ($p<0.05$) relative to one another from the 3 hour mark onwards. Despite having a high proportion of the Eudragit® RS grade in the coating, the release from the systems coated with a polymer blend is still far higher relative to the complex coated solely using the Eudragit® RS grade. This can be attributed to the presence of the highly permeable RL grade which is more amenable to swelling and the ingress of dissolution media, thus promoting the release of drug from the complex. This flexibility takes advantage of the varied rate of diffusion of the drug through the polymeric film, which differs depending on the permeability. As shown, each ratio permits the gradual release of the drug, which progressively increases until the dissolution study is ceased.

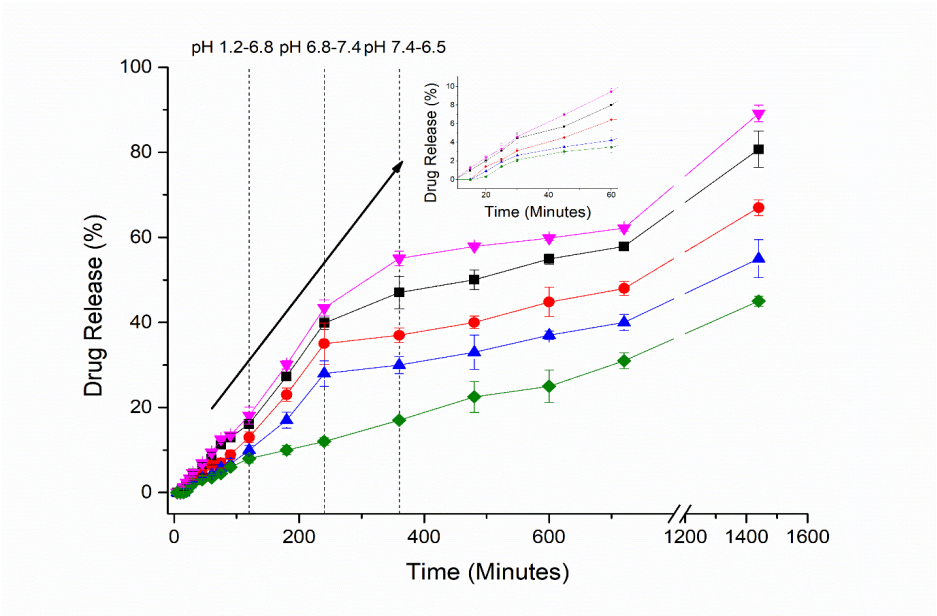

Figure 5.17. Drug release profile over 24 hours of drug-loaded beads (IR120) Wurster coated with different blends of Eudragit® RL and Eudragit® RS (w/w) in the coating solution (total polymeric content in feed solution was fixed at 1% w/v). 10:90 RS:RL (Black square), 25:75 RS:RL (Red circle), 50:50 RS:RL (Blue triangle), 100% RS (Olive diamond) and 100% RL (Inverted magenta triangle).

For the optimised systems, drug release studies were conducted in DI H_2O to ensure that systems release low quantities of drug throughout the study, as no ions are present to promote drug release. As depicted in Figure 15 in Appendix 3, the release matches the dissolution profile expected in DI H_2O for ion-exchange systems coated with a water-insoluble polymer. When compared to the uncoated

system, the quantity of drug released is further reduced (to <5% drug release over 24 hours compared to 10% for the uncoated systems) which is likely due to the polymeric layer hindering release from the DRC, as the pores and channels through which the dissolution medium can gain access are coated. The release kinetics of this small quantity of drug also differ, with the uncoated system's onset of release being much earlier compared to the coated systems, again attributable to the lack of a polymeric film surrounding the surface of the DRC. This is supported by the SEM images depicted in Figure 16 in Appendix 3 which show that the polymeric membrane remains intact post-dissolution testing in DI H_2O.

5.2.3 Assay of the drug content within the coated DRCs (IR120)

The coated drug-loaded beads that were selected for the drug release studies reported above were assayed for drug content using a modified drug displacement procedure (Chapter 2, section 2.2.11) similar to the method described by Junyasprasert and Manwiwattankul to quantify the amount of diltiazem in the microcapsules they prepared (117). A relationship between the drug content in the coated complexes and the concentration of coating polymer in solution, consistent with the report of Junyasprasert and Manwiwattankul, was apparent and can be described as lower drug loadings for the samples coated using more concentrated coating solutions. This is because the drug loading is a % by weight and with an increased level of coating applied, the % drug content decreases. For samples coated with either Eudragit® RS and Eudragit® RL, no drug was detected in the assay medium, when isopropyl alcohol (IPA) was used to strip the coating, as would be expected since the primary purpose was to remove the coating of the beads prior to the liquid being decanted and replaced with an aqueous acidic solution. Results from the assay procedure are reported in Table 5.6. These assay results were used to determine the % drug release as part of the drug release studies discussed in section 5.2.2.

For samples coated using a pH-dependent polymer, the initial enteric coating polymer layer was stripped using a solution of NaOH. Unsurprisingly, the drug was detected when the liquid was assayed as there were ions present to promote drug release. Similar to the assay of the pH-independent polymer-coated systems, the liquid containing the coating layer was decanted and an acidic aqueous solution was added to the beads to displace drug ions and assay the material displaced. Unlike the pH-independent systems, the sum of both values calculated from both liquids was taken to calculate the total drug loading values and are reported in Table 5.7. The TZD contents in all microcapsules were quantified to be in the range 24-31% w/w. The drug content of the coated beads was closely related to the ratio of coating to the core, as the higher the quantity of coating applied, the lower the drug content for a given weight of microparticles (131). This is intuitive when one considers that thicker coating layers are applied when more concentrated coating solutions are used, thus reducing the

quantity of drug material in the sample if the quantity of assayed material is kept constant. The microcapsules still retained a high drug load which was deemed suitable for the purposes of the project. This is in agreement with the findings of many groups who investigated the air suspension coating of DRCs (127).

Table 5.6. Comparison of drug loadings of Wurster coated DRCs (IR120) produced using either grade of polymer (Eudragit® RS or Eudragit® RL) and a range of different polymer concentrations. The drug loadings were determined as per the method detailed in Chapter 2, section 2.2.11.

	Drug loading on the DRC (% w/w)	
Polymer concentration (% w/v) in the coating solution	Eudragit® RS	Eudragit® RL
0.25	31.20 ± 0.45	30.90 ± 0.51
0.50	30.18 ± 0.16	30.01 ± 0.06
0.75	29.42 ± 0.56	29.21 ± 0.39
1.00	28.45 ± 0.27	28.57 ± 0.08
1.25	27.99 ± 0.13	27.89 ± 0.20
2.50	26.84 ± 0.41	26.55 ± 0.31
3.75	26.52 ± 0.45	26.32 ± 0.25
5.00	26.05 ± 0.68	26.45 ± 0.42
7.50	25.74 ± 0.73	25.64 ± 0.61

Table 5.7. Comparison of drug loadings of Wurster coated DRCs (IR120) produced using Eudragit® L100 and a range of different polymer concentrations. The drug loadings were determined as per the method detailed in Chapter 2, section 2.2.11.

Polymer concentration (% w/v) in the coating solution	**Drug loading on the DRC (% w/w)**
1.00	28.20 ± 0.28
1.25	27.90 ± 0.45
2.50	24.52 ± 0.36

5.2.4 Effect of plasticiser incorporation into the feed solution on the coating process and the properties of the resultant coated DRCs (IR120)

By evaluating the release profiles of the complexes coated using polymeric solutions comprising a single polymer as well as a blend, it became apparent that coatings with varying abilities to impact the drug release characteristics were applied using the process developed. The next strand of the project that was investigated related to the impact of additives included in the polymeric feed used to coat the DRCs. Their effect on the coating process was primarily assessed based on the ability to generate a product using a process devoid of fluidisation issues and an evaluation of the drug release characteristics. The flowability of the particles in addition to the solid-state characteristics were also studied but were of secondary concern. The primary additives used in a polymeric solution intended for particle coating using the Wurster apparatus are low molecular weight compounds known as plasticisers. These compounds are often added to improve the performance of the polymeric film coating by reducing the rigidity of the 3-D film structure and promoting polymer coalescence (270). In the experiments discussed over the subsequent paragraphs, the aim was to identify a suitable plasticiser and assess its impact on the resultant coated complexes' properties. One downside of the use of plasticisers is the associated tackiness which can often be alleviated using talc (201).

Again, "blank" resin beads were used when these studies commenced, as the emphasis was on establishing a suitable plasticiser, which was likely to entail a series of "trial and error" experiments leading to unnecessary wastage of valuable drug-loaded material. At the outset, two plasticisers were selected, dibutyl sebacate (DBS) and triacetin (TCT) to probe their influence on the polymeric coating. In addition, to their established use with IERs in the literature, these plasticisers represent hydrophilic (triacetin) and hydrophobic (dibutyl sebacate) classes. A selection of concentrations of DBS and TCT was selected and assessed for the impact on the film formation process (131). One of the main findings from the method development trials using either type of plasticiser was the need to maintain a minimum ratio between the proportion of polymer and plasticiser in the coating solution to ensure that coating runs could be completed without being plagued by irreversible agglomeration. The use of exceedingly high levels of plasticiser in the formulation creates a "sticky" coating ascribed to the lowering of the T_g of the coating film, resulting in failed runs, examples of which are illustrated in Figure 17 in Appendix 3. Despite these series of failed runs, defined by the irreversible agglomeration, which usually hinders any chance of coating, the complexes were successfully coated using coating solutions comprising Eudragit® RL and either plasticiser studied. However, drug release studies performed using these coated drug-loaded complexes revealed that the incorporation of plasticiser had a detrimental impact on the integrity of the polymeric coating as the drug was released at a faster rate relative to the release kinetics reported for samples coated with plasticiser-free polymer solution.

As discussed previously, the two coating concentrations of Eudragit® RL used to form coated complexes which were selected to study (1.25% w/v and 2.5% w/v), display distinct release profiles (Figure 5.18) at early timepoints (lower drug release from the 2.5% w/v coated system) but begin to converge from the 10 hour timepoint onwards and show no statistical difference ($p>0.05$) with respect to the % drug released (approximately 90%) after 24 hours. Regarding the plasticised coatings, the impact on the release is more unpredictable, as no statistical difference ($p>0.05$) is detectable until the 6 hour mark for the TCT-containing systems. Irrespective of the % polymer coating in the feed solution, the release is relatively rapid, with 40% release being achieved after 4 hours relative to 25% and 30% for the systems coated using plasticiser-free polymer feed concentrations of 1.25% w/v and 2.5% w/v respectively. After the 4 hour timepoint, the impact of the thicker coating for the TCT-containing systems is evident, as the drug is released at a slower rate relative to that coated using 1.25% feed concentration until the 24 hour timepoint. The dissolution behaviour of complexes coated using the solutions containing the Eudragit® RL grade and DBS also failed to produce a superior degree of control on the drug release, which would be indicative of a more robust and/or flexible film being formed. Having said that, over the first 120 minutes the plasticised sample (2.5% Eudragit® RS and DBS) does not differ significantly ($p>0.05$) from the unplasticised sample but the profiles begin to diverge from 180 minutes onwards. The release from the plasticised sample is accelerated, as is evident from the higher release ($p<0.05$) at all timepoints, thereafter producing a profile that resembles that of the complex coated using RL (2.5%) and triacetin. Regarding the 1.25% coated samples, in general, the release from the DBS-plasticised samples follows the same general trends discussed above, i.e. accelerated release. At earlier timepoints, the plasticised sample does not differ as much from the unplasticised complex relative to those coated using the higher concentration of polymer (2.5% w/v) but a marked difference becomes apparent after 90 minutes, leading to a release pattern similar to that of the system plasticised with TCT, again reflective of the plasticiser selection not being fit for purpose.

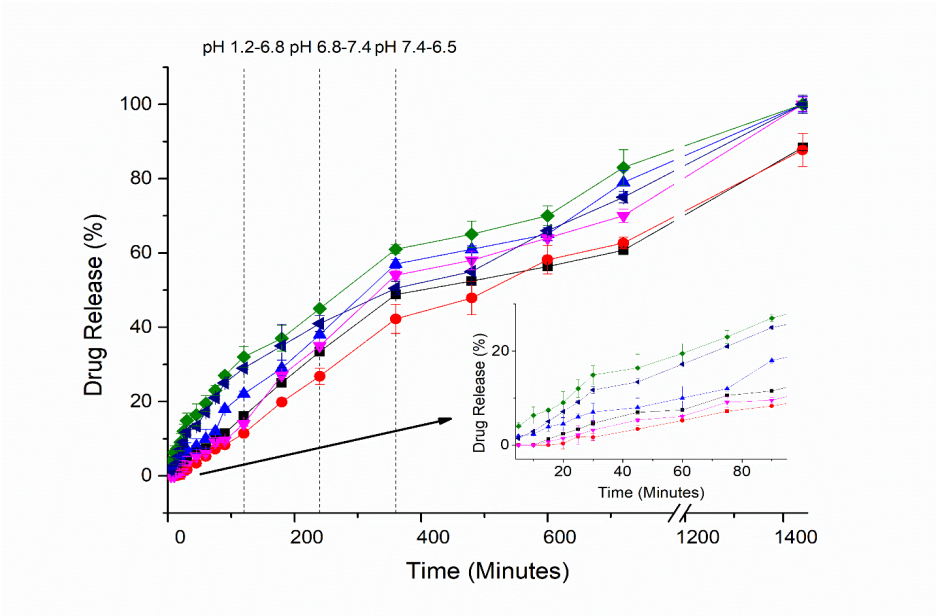

Figure 5.18. Drug release profile over 24 hours of drug-loaded beads (IR120) Wurster coated with different concentrations of Eudragit® RL in the coating solution with and without different concentrations (and types) of plasticiser (DBS or TCT). 1.25% w/v Eudragit® RL (Black square), 2.5% w/v Eudragit® RL (Red circle), 1.25% w/v Eudragit® RL and DBS (Blue triangle), 2.5% w/v Eudragit® RL and DBS (Inverted magenta triangle), 1.25% w/v Eudragit® RL and TCT (Olive diamond) and 2.5% Eudragit® RL and TCT (Navy triangle).

SEM analysis (Figure 5.19) supported the assertion that the plasticisers selected were not optimal from the perspective of forming a flexible robust film that would maintain integrity over the course of the dissolution study. This is evident from the unstructured and roughened bead surface which contradicts the main aim of plasticiser inclusion, which is to produce smooth-surfaced microcapsules. These macroscopic defects are likely to be responsible for the accelerated drug release which was evident in the dissolution studies. The discrepancy between the anticipated benefit of plasticiser inclusion and the results observed can be explained by a probable incompatibility between the drug, polymer and plasticiser. As stated previously, the two plasticisers selected cover both the hydrophilic and hydrophobic classes which differ in their ability to dictate drug release behaviour, yet a flexible robust film coating was apparently not achievable, pointing to the need to try another alternative. The hydrophilicity/hydrophobicity of the plasticiser is integral to its ability to affect the film and pore-forming capability, and the findings were contrary to reports of the use of DBS with the Eudragit® polymers (200), which could conceivably be attributed to unsuitable processing parameters coupled with the influence of the API and/or resin's physiochemical properties.

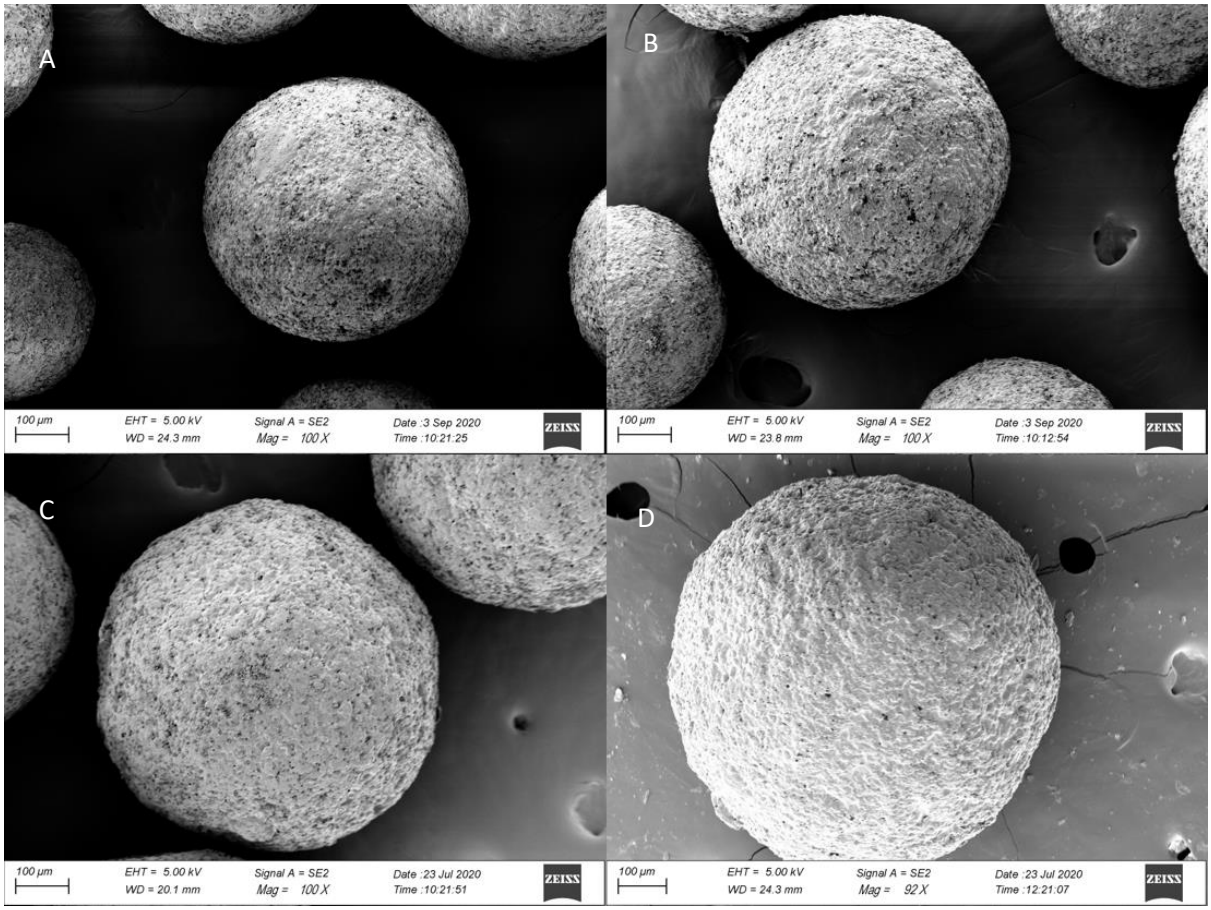

Figure 5.19. SEM images of Wurster coated DRCs (IR120) produced using a coating solution containing varying concentrations of Eudragit® RL and different plasticiser types (DBS and TCT). A) 1.25% w/v Eudragit® RL and DBS, B) 2.5% w/v Eudragit® RL and DBS, C) 1.25% w/v Eudragit® RL and TCT and D) 2.5% w/v Eudragit® RL and DBS.

Due to the unsatisfactory results obtained with the initial plasticizers evaluated, a third and final type (triethyl citrate, TEC) was trialled to study the effect of its inclusion on processibility, solid-state properties and dissolution behaviour. TEC has been used extensively in drug delivery applications across a range of techniques including hot melt extrusion and Wurster coating (192,366). Three concentrations (0.125, 0.25 and 0.5% w/v) of the plasticiser were selected to study and were added to the polymeric solutions, which comprised either 0.25% w/v Eudragit® RS or 0.5% w/v Eudragit® RL (samples previously selected for further study) and the results obtained were far more encouraging. No evidence of accelerated drug release, as was observed with TCT and DBS, could be found, suggestive of the plasticiser affording an additional level of control and being compatible with the Eudragit® grades chosen.

The impact of the curing conditions (described in Chapter 2, section 2.2.1.6.2.2.1) on the resulting release pattern was also examined, with the results of curing for two different time durations using a

selection of plasticised samples shown in Figure 5.20 (and Figures 18-21 in Appendix 3). Regarding the complexes coated using the RL grade, at the lowest concentration of plasticiser used (0.125% w/v), the curing conditions had a marginal effect on drug release (Figure 5.20). For the complexes coated using the two higher concentrations of TEC, the impact of the duration of curing had virtually no impact signified by no difference ($p>0.05$) in the % drug release at the majority of dissolution timepoints, in particular, the 24 hour mark which is the final timepoint studied. Similar to what has been reported thus far as part of this work, all systems are characterised by incomplete drug release, an observation that also applies to the complexes coated with Eudragit® RS and plasticiser. The thermal treatment used in the curing process, which necessitates the use of high temperatures, above that of the minimum film-forming temperature of the polymer, is necessary to ensure that homogenous films are formed. In theory, this negates the risk of changes in the dissolution behaviour of the coated DRCs upon storage as the heat is known to accelerate the coalescence process of polymeric particles which may be incomplete post-coating (198)

With respect to the low concentration of TEC, its presence in the coating solution appears to impart a reduced rate of drug release from the DRCs over the middle portion of the release study, rather than it being a consistent feature across all timepoints in the study and the release profiles begin to converge after 12 hours, indicating that the influence of the plasticiser on the release kinetics is limited. Relative to the unplasticised sample, a distinct slowing of the drug release is evident from the profiles of plasticised samples that are cured for either 12 or 24 hours. From the 8 hour timepoint onwards, the improved performance (retarded release) of the cured samples relative to the uncured plasticised sample becomes apparent. There is a significant difference in the drug release rate between uncured and cured plasticised coated beads, but the difference between samples cured for 12 and 24 hours is not significant, indicating that a 12 hour curing time duration is sufficient to produce beneficial film coating properties, reflected by the slowed drug release. As alluded to previously, the use of higher concentrations of TEC in tandem with a maximum curing time of 24 hours did not induce any significant change in the release profile of the coated samples when the general pattern is considered. Over the initial timepoints of the Eudragit® RL system plasticised with TEC (Figure 5.20), an accelerated release rate can be observed, which is suggestive of competing mechanisms that are occurring simultaneously, namely improved film formation and drug migration into the polymeric membrane. This rationale was provided by Yang et al. to explain the complex dissolution behaviour observed in their studies but another plausible reason could be the saturation of the coating film with hydrophilic TEC molecule within the predominantly hydrophobic film which serves to weaken it once exposed to an aqueous medium (192). Overall, the results suggest an optimum balance being achieved at lower plasticiser concentrations.

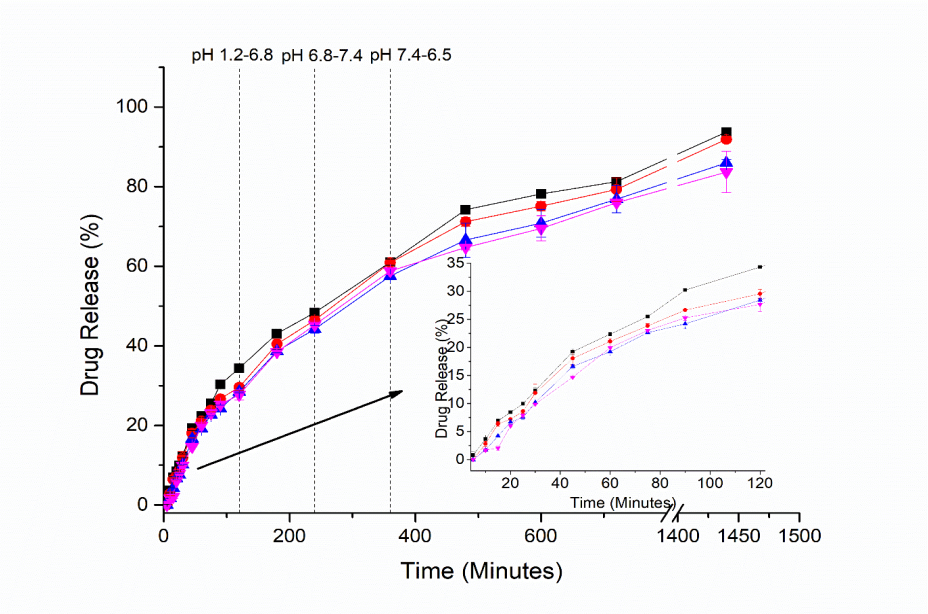

Figure 5.20. Drug release profile over 24 hours of Eudragit® RL Wurster coated beads (IR120) (0.5% w/v) and drug-loaded beads (IR120) coated with a coating solution containing Eudragit® RL (0.5% w/v) and TEC (0.125% w/v) which were then subsequently cured for 0, 12 or 24 hours. 0.5% w/v Eudragit® RL alone (Black square), Eudragit® RL and TEC (uncured)(Red circle), Eudragit® RL and TEC (12 hours cured) (Blue triangle) and Eudragit® RL and TEC (24 hours cured) (Inverted magenta triangle).

To clarify that the reduced rate of release could be attributed to the curing time and presence of plasticiser, the drug-loaded beads coated using a feed concentration containing solely Eudragit® RL were subjected to the same thermal (curing) treatment and their dissolution properties assessed (Figure 5.21). The release profile of the cured systems (12 and 24 hours) show no difference ($p>0.05$) to the uncured coated system, indicating that the film formation process is unaffected by post-processing conditions. Oftentimes, the release profile of coated microparticles during storage can be unpredictable, as both an increase and decrease in the release rate have been reported (196). This has been ascribed to differing coalescence behaviour of the polymeric particles and is more widespread with coatings applied using aqueous dispersions (369). The curing process is used as a tool to accelerate the coalescence of the polymeric particles and in most instances results in a decrease in the release rate if the film formation was incomplete prior to the input of thermal energy (198). These results support the assertion that the plasticiser has a marked impact on the drug release characteristics, similar to that reported by previous authors (194).

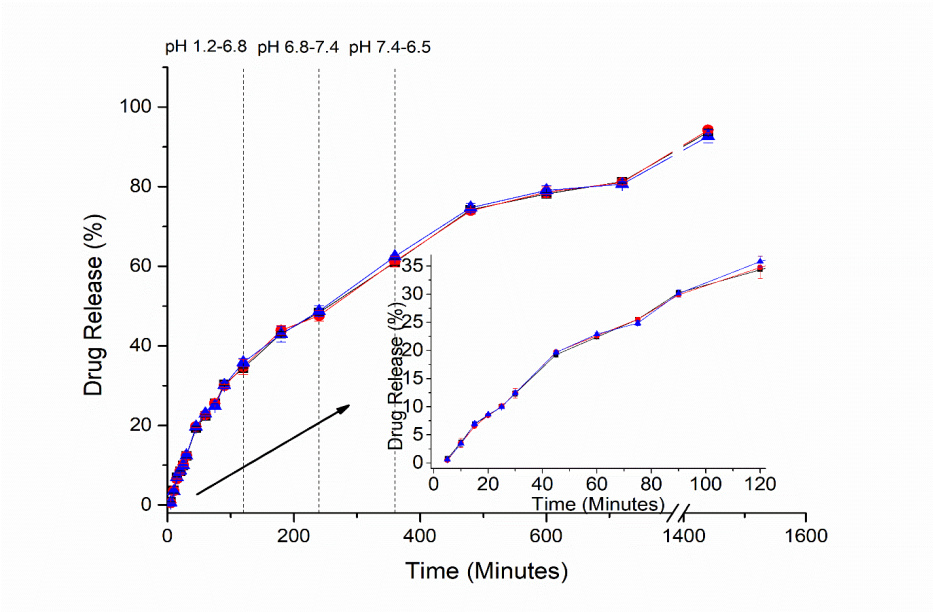

Figure 5.21. Drug release profile over 24 hours of drug-loaded beads (IR120) Wurster coated with a coating solution containing 0.5% w/v Eudragit® RL which were then subsequently subject to a curing step for 0 hours, 12 hours and 24 hours. Uncured (Black square), cured (12 hours) (Red circle) and cured (24 hours) (Blue triangle).

Identical drug release studies were performed using the other coated DRC selected for further analysis, i.e. beads coated with Eudragit® RS (0.25% w/v). Overall, the impact of plasticiser incorporation, alongside the influence of curing time on the drug release kinetics followed the same general trend revealed in the studies that used the RL coated systems plasticised using the lowest TEC concentration (0.125% w/v). The presence of plasticiser in the coating solution has a more pronounced effect relative to that observed with the unplasticised film coatings applied on the release kinetics, reflected by suppressed % drug release values at all timepoints from the 15 minute mark onwards for the duration of the dissolution study (Figure 5.22). In contrast to the RL coated systems, curing does not influence the drug release behaviour, irrespective of the duration of the step, indicating that plasticiser inclusion aids with the fusion of the polymeric particles. It can be inferred from these results that the presence of TEC within the coating solution imparts a favourable effect on the polymeric coating, which may be related to enhanced flexibility of the film, a known benefit of introducing a plasticiser to the formulation.

Again, the unplasticised coated complexes were subject to identical thermal treatment used to cure the plasticised samples to clarify whether the curing dependency pertains solely to plasticised samples (Figure 5.23). The release profiles of all three samples (uncured, cured for 12 hours and cured for 24 hours) are essentially superimposable on one another indicating that the application of thermal

energy has little impact on the film properties that influence the release kinetics. When the concentration of plasticiser in the coating solution is increased (Figures 20-21 in Appendix 3), the release patterns resemble those produced using the lowest concentration (0.125% w/v), where the incorporation of plasticiser does lead to slower release kinetics until the 24 hour timepoint at which point no statistical difference ($p>0.05$) is evident. Again, the curing step has little impact on the release kinetics as no statistical difference ($p>0.05$) can be detected at the majority of timepoints studied when the plasticised samples are compared. These findings highlight that the curing step is redundant in the case of the Eudragit® RS coatings, as its main purpose is to produce stable release profiles by ensuring complete coalescence of the polymeric particles constituting the coating. However, as no difference ($p>0.05$) was apparent between the thermally treated complexes and those that are not subject to this step, it is evident that this has already been achieved during the application of the film, thus negating the need for a curing step.

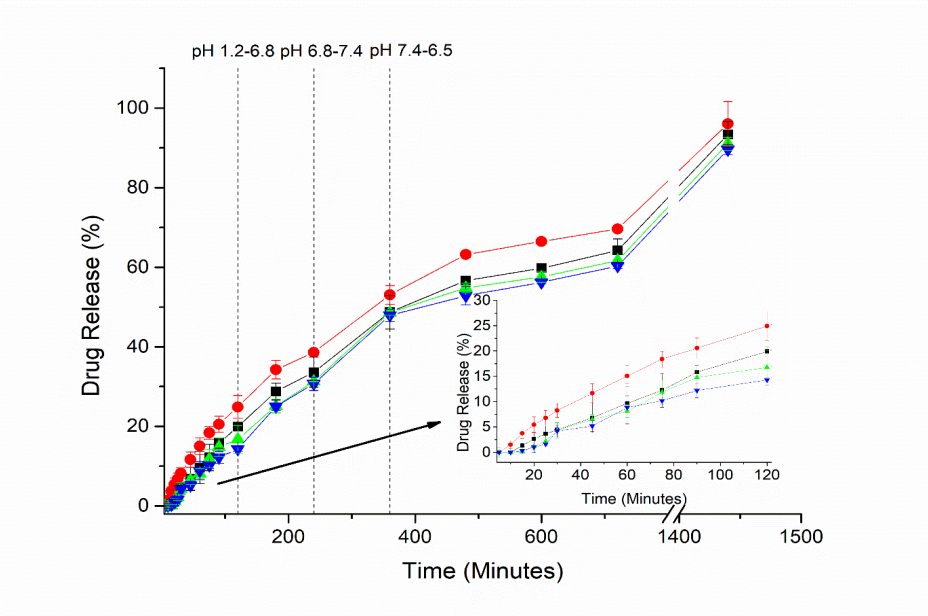

Figure 5.22. Drug release profile over 24 hours of Eudragit® RS Wurster coated beads (0.25% w/v) and drug-loaded beads (IR120) Wurster coated with using a solution containing Eudragit® RS (0.25% w/v) and TEC (0.125% w/v) which were then subsequently cured for 0, 12 or 24 hours. 0.25% w/v Eudragit® RS (Red circle), Eudragit® RS and TEC (uncured)(Black square), Eudragit® RS and TEC (12 hours cured) (Green triangle) and Eudragit® RS and TEC (24 hours cured) (Inverted blue triangle).

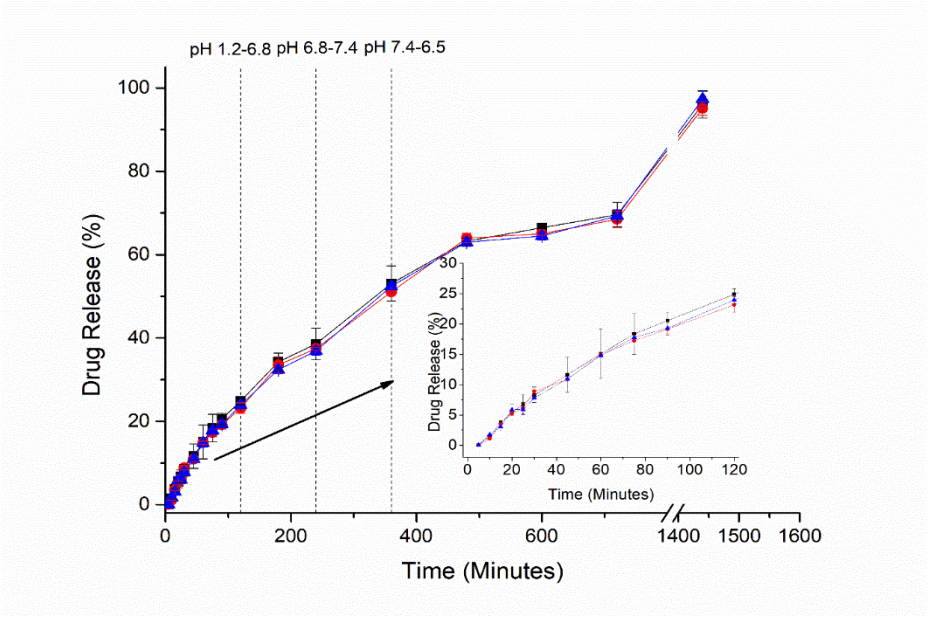

Figure 5.23. Drug release profile over 24 hours of drug-loaded beads (IR120) Wurster coated with a coating solution containing 0.25% w/v Eudragit® RS which were then subject to a curing step for 0 hours, 12 hours and 24 hours. Uncured (Black square), cured (12 hours) (Red circle) and cured (24 hours) (Blue triangle).

5.2.5 Solid-state analyses of coated DRCs (IR120)

Thermal properties of the coated beads were assessed using DSC in order to probe the physical state of the drug within the DRCs coated using the two grades of polymer that confer pH-independent release. The main purpose of assessing the coated systems using this technique was to establish if the solid-state of the drug changes after processing. Nikowitz et al. studied the impact of the Wurster coating process on the degree of crystallinity of diltiazem and reported that the coating layer facilitated drug recrystallisation. They attributed this finding to the migration of amorphous drug into the polymeric layer surrounding the drug-containing pellet (370). There have been other reports of drugs migrating to the polymeric coatings applied by Wurster coating and subsequent recrystallisation (371). The frequency of this occurrence is higher when aqueous coatings are applied and appears to be linked to the solubility of API being encapsulated. The potential impact of curing on the migration tendency has been shown by Siepmann et al. who reported an increased degree of drug accumulation near the film coating, which was accelerated by the curing process (372). The study reported this phenomenon for low T_m drugs, so it would be expected that TZD HCl would exhibit a degree of resistance due to its high melting point (167). The results depicted in Figure 5.24 suggest that the systems examined remain stable to recrystallisation post-coating as no endotherm representative of the crystalline drug is visible. This data was supported by the pXRD analysis, depicted in Figure 5.25.

All samples produce diffractograms characterised by the distinctive halo pattern, indicative of amorphous material.

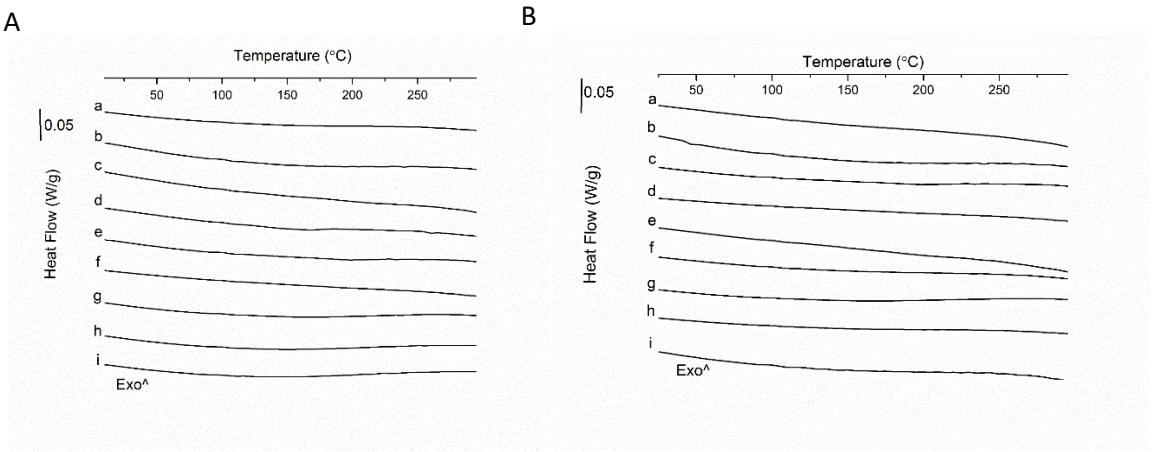

Figure 5.24. DSC thermograms of DRCs (IR120) Wurster coated using different coating concentrations of A) Eudragit® RL and B) Eudragit® RS. a) 0.25% w/v, b) 0.5% w/v, c) 0.75% w/v, d) 1 % w/v, e) 1.25% w/v, f) 2.5% w/v, g) 3.75% w/v, h) 5% w/v and i) 7.5% w/v.

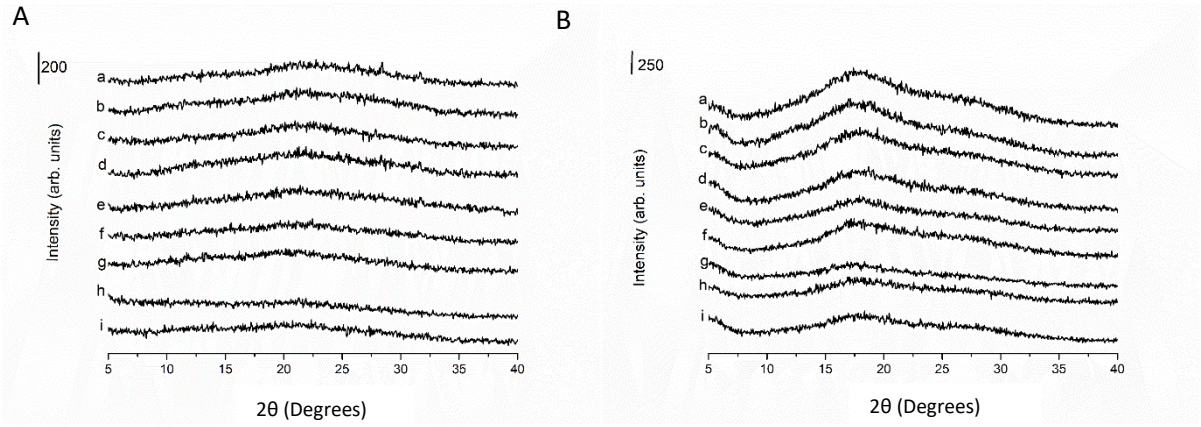

Figure 5.25. pXRD diffractograms of DRCs (IR120) Wurster coated using different coating concentrations of A) Eudragit® RL and B) Eudragit® RS. a) 0.25% w/v, b) 0.5% w/v, c) 0.75% w/v, d) 1 % w/v, e) 1.25% w/v, f) 2.5% w/v, g) 3.75% w/v, h) 5% w/v and i) 7.5% w/v.

Figures 22-23 in Appendix 3 show the pXRD patterns of all DRCs coated using a coating solution comprising of the three concentrations of TEC and either grade of Eudragit®. Irrespective of the concentration of plasticiser employed during the Wurster coating process, all samples were shown to be pXRD amorphous, as no Bragg peaks were present. This was further investigated by DSC to establish if crystallinity content below that detectable by pXRD could be observed. Similar to the non-plasticised samples, no sign of crystalline material was evident during the DSC analysis. The thermograms were characterised by the lack of any thermal event, whether that be a melt endotherm or glass transition.

The absence of a T_g that could be attributable to any coating component is possibly due to small quantities layered onto the bead. Regarding, the resin material itself, to the best of the author's knowledge, no T_g has been reported for the sulfonic acid-containing resins and the data presented in Figure suggests the materials do not undergo a glass transition in the temperature range studied. Similar findings were also observed in the thermal and pXRD analysis of the samples coated using the blend of Eudragit® RS and Eudragit® RL (Figure 24 in Appendix 3).

5.2.6 DVS analysis (Wurster coated IR120 beads)

The moisture sorption properties of selected samples were studied using DVS analysis. In addition to the bead form of the resin raw material and the uncoated DRC, DVS analysis on an additional four coated DRCs was also performed. The samples were selected in part due to their dissolution profiles characterised by a steady rate of drug release leading to close to complete drug release after 24 hours and to compare the impact of polymer type on the moisture sorption kinetics of coated complexes versus uncoated DRCs. Furthermore, the impact of plasticiser inclusion in the coating layer was also assessed. The same five complexes (uncoated and four coated DRCs) were selected for solid-state stability analysis, discussed in the subsequent section, so the DVS analysis (Figure 5.26) served to provide complementary information on the stability properties. Of all the samples studied, the resin raw material sorbs the highest quantity of moisture, 25% more than the uncoated complex which sorbs the second highest quantity of moisture of all six samples studied. This finding suggests that loading the drug onto the resin reduces the complex's ability to sorb moisture relative to the raw material, which is understandable when the ion-exchange process is considered. When the drug is loaded onto the resin, the sodium ion bound to the sulfonic acid group is replaced by the larger organic ion that is less likely to favour the sorption of moisture. Regarding the sample coated using the Eudragit® RL grade, moisture uptake is far higher when the isotherm of the complexes coated with a mixture of polymer and plasticiser is compared to that of the complex coated using only the Eudragit® RL grade. This indicates that the incorporation of this excipient promotes moisture uptake, which is not observed when the isotherm of the sample coated using a coating solution comprising Eudragit® RS and TEC is studied. Although the hysteresis associated with the latter system is far bigger relative to that seen with the sample coated solely using Eudragit® RS, the % mass change at the 90% RH condition does not differ significantly ($p>0.05$). Furthermore, when the complexes coated using the two different grades are compared to one another, it is found that at the 90% RH condition, there is no statistical difference ($p>0.05$) in the quantity of moisture sorbed. This finding suggests the vulnerability to moisture sorption of the coated film applied, particularly when an additive in the form of TEC is incorporated into the feed solution to be sprayed onto the beads. pXRD analysis (Figure 25 in Appendix 3) performed post-DVS analysis revealed that the physical form of the drug that forms

part of the coated complex does not change. On the basis of the data presented to date regarding the powdered form of the resin coupled with similar studies in the literature, it is likely that the limit of detection (LOD) of the pXRD is not masking any trace crystalline material. This was signified by the amorphous halo pattern that is the dominant feature of all diffractograms.

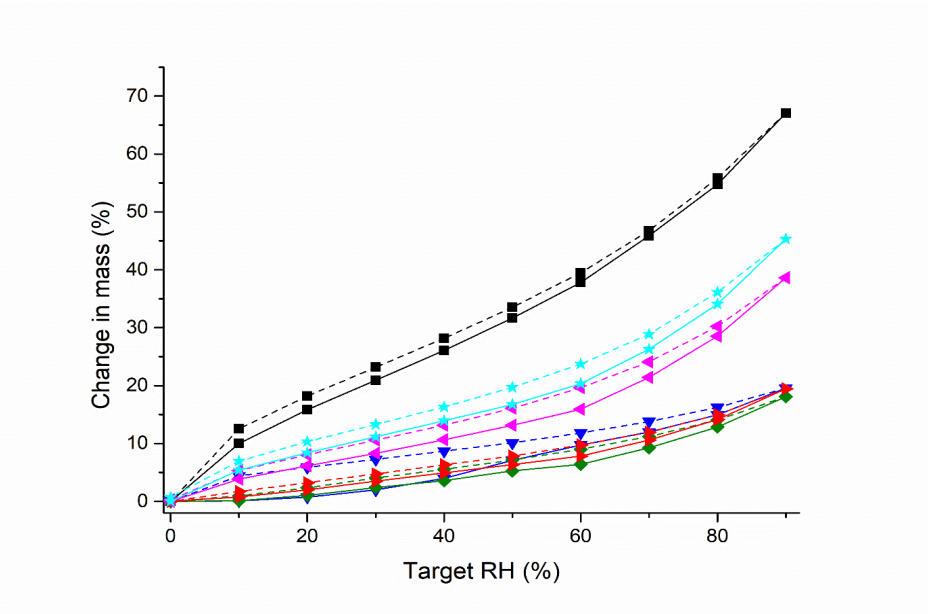

Figure 5.26. DVS kinetic plot of resin raw material (IR120), uncoated DRC and Wurster coated DRCs. IR120-sorption (Black square-continuous curve), IR120-desorption (Black square-dashed curve), uncoated DRC-sorption (Aqua star-continuous curve), uncoated DRC-desorption (Aqua star-dashed curve), coated DRC (Eudragit® RL and TEC)-sorption (Magenta triangle-continuous curve), coated DRC (Eudragit® RL and TEC)-desorption (Magenta triangle-dashed curve), coated complex DRC (Eudragit® RS and TEC)-sorption (Blue triangle-continuous curve), coated complex DRC (Eudragit® RS and TEC)-desorption (Blue triangle-dashed curve), coated complex DRC (Eudragit® RS)-sorption (Olive diamond-continuous curve), coated complex DRC (Eudragit® RS)-desorption (Olive diamond-dashed curve), coated complex DRC (Eudragit® RL)-sorption (Red triangle-continuous curve) and coated complex DRC (Eudragit® RL)-desorption (Red triangle-dashed curve).

In the case of the DRCs which are in bead form, the isotherms of water vapour uptake display closed hysteresis loops (335), indicating that the water sorption mechanism is a completely reversible process, a contrast from the open loops present in the isotherms of powdered samples. The DVS data was fitted using the Young and Nelson equation, a well-known model used to fit the sorption isotherms (274,373). Through the identification of quantitative correlations between equilibrium moisture content and the % RH using this theory, the moisture uptake can be classified into different categories, namely surface adsorption, solvent condensation and bulk absorption (374). The extent to

which the moisture uptake fits each of these individual classifications is calculated using the equations based on the Young Nelson theory.

The high correlation coefficient calculated for each sample indicates the excellent fit of the model equation (Equations 2.4 and 2.5 in section 2.2.13 in Chapter 2) to the experimental data, indicating that the Young-Nelson model is a suitable approach for the comparison of moisture uptake by the samples. The moisture distribution patterns of all samples analysed are shown in Figures 26-28 in Appendix 3. The calculated *A* and *B* parameters, which provide insight into the mechanism of water uptake are listed in Table 5.8. The differential distribution of water within the systems is evident from the data presented in Figures 26-28 in Appendix 3, and is dependent on the presence of the drug, coating polymer and inclusion of a plasticiser. Interestingly the value of the *A* parameter was three times higher relative to the *B* parameter for the resin raw material (Table 5.8), indicating that adsorption was the predominant mechanism of moisture uptake rather than absorption into the bulk which is reported to be more prevalent in amorphous systems (274). The disparity in value between the *A* and *B* parameters narrows considerably when the DRC sample is studied, perhaps reflective of the presence of drug material in the system that may have a lower propensity to sorb moisture at the surface. Regarding the coated samples, the *B* parameter remains relatively constant with the exception of the Eudragit® RS/TEC sample, which will be discussed separately. In contrast, the *A* value drops relative to the uncoated sample meaning that the bulk absorption mechanism predominates. This may be attributed to the hydrophobicity of the coating polymers, in particular the Eudragit® RS grade, which renders the systems coated solely with a water-insoluble polymer less amenable to surface adsorption. Interestingly, the presence of TEC in the coating appears to increase the *A* and *B* parameters for each system relative to that calculated for unplasticised samples, suggesting that it may promote moisture sorption. This effect is far more pronounced in the case of the Eudragit® RS system, the more hydrophobic of the two polymers studied. This finding supports the moisture sorption plot in Figure 5.26 and can be rationalised based on TEC being a hydrophilic compound itself. The E term in the Young Nelson model relates to the strength of the vapour interaction with the surface, with the resin raw material having the lowest value of all samples studied (0.187). This indicates that the loading of the drug onto the resin leads to the moisture vapour having a stronger affinity for the surface, reflected by the 2 fold increase. Furthermore, the application of a plasticised polymeric layer (Eudragit® RS or Eudragit® RL grade) further increases the value 1.5-1.66 fold relative to the E parameter of the uncoated DRC (0.405). Interestingly, the highest values for the E parameter was obtained for the DRCs coated using either grade of polymer (without TEC) relative to those obtained using the uncoated DRC (2.35-2.44) This finding is suggestive of the coating composition influencing the strength of the vapour interaction with the surface.

Table 5.8. List of estimated A, B and E (Young and Nelson parameters) and fit correlation coefficient (r^2) for selected Wurster coated DRCs, the uncoated DRC and resin raw material (IR120). The composition of the coating solution is stated in parentheses.

Sample	*E*	*A*	*B*	r^2
Resin raw material	0.187	0.0090	0.003	1.000
Uncoated DRC	0.405	0.0050	0.004	0.997
Coated DRC (0.25% w/v Eudragit® RS)	0.990	0.0010	0.005	0.996
Coated DRC (0.5%w/v Eudragit® RL)	0.953	0.0010	0.004	0.999
Coated DRC (0.25 %w/v Eudragit® RS and 0.125% w/v TEC)	0.672	0.0005	0.009	0.994
Coated DRC (0.5% w/v Eudragit® RL and 0.125% w/v TEC)	0.609	0.0030	0.005	0.997

5.2.7 Stability studies involving IR120 beads (Uncoated and Wurster coated)

Stability studies constituted the final aspect of work detailed in this chapter. The experiments performed as part of this section can be grouped into two main categories: (1) solid-state stability of "dry" DRC beads and (2) liquid stability of suspended DRC beads. A selection of samples were chosen to investigate the physical stability of the DRCs and are listed in Table 5.9.

Table 5.9. DRCs (Uncoated and Wurster coated) systems and composition of their coating solutions (where applicable) selected for stability studies.

Coating polymer (concentration (% w/v) of polymer in coating solution)	TEC concentration (% w/v)
- (Uncoated)	-
RS (0.25)	-
RS (0.25)	0.125
RL (0.50)	-
RL (0.50)	0.125

5.2.7.1 Stability of "dry" DRC (IR120) beads (Physical and chemical)

Stability studies performed on the "dry" DRC beads revealed the samples to be physically stable after 6 months at 25 °C when subjected to 60% relative humidity and sub 10% relative humidity. As illustrated in Figures 5.27-5.30 (and Figures 29-32 in Appendix 3), all five samples remain pXRD amorphous, indicated by the halo pattern, with no evidence of Bragg peaks representative of crystalline TZD HCl. The lack of variation in physical stability observed was irrespective of plasticiser

inclusion or not. Similarly, DSC analysis at each of the four timepoints for all five samples shows no evidence of crystalline material, with the instrument having a LOD of 0.2 µW (375). Stabilisation against moisture-induced crystallisation of amorphous API loaded onto the resin has been observed by previous authors (376). The only downside revealed during physical stability studies was the appearance of agglomeration after 2 months. This occurred in samples coated with Eudragit® RS and both samples containing TEC in the coating (with either Eudragit® RS or Eudragit® RL). In the case of the plasticised samples, this can be explained by an increased level of tackiness, which is one of the downsides of plasticiser incorporation. It is known that the Eudragit® polymers have a tendency to agglomerate, in the absence of anti-tacking agents, especially when a plasticiser is incorporated to aid film formation. As noted already, regarding the unplasticised samples, the Eudragit® RS exhibits an agglomeration tendency, whereas the Eudragit® RL grade does not. A possible reason for the difference which was put forward by Wesseling et al. who studied the properties of Eudragit® films comprehensively, and observed similarly increased tackiness values for Eudragit® RS films is the higher number of quaternary ammonium groups present in the Eudragit® RL grade (201).

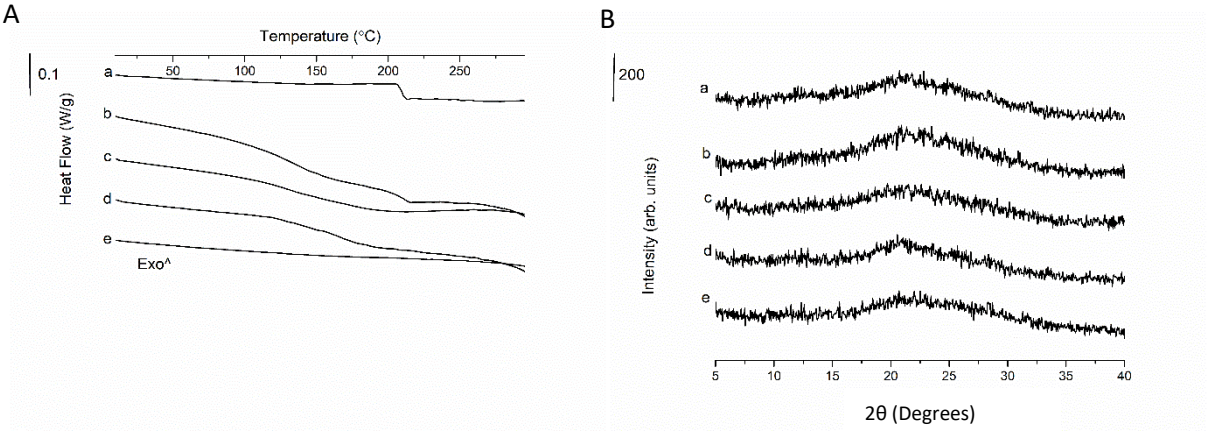

Figure 5.27. A) DSC thermograms and B) pXRD diffractograms of DRCs (IR120) stored at 25 °C and 60% RH for 1 month. The concentration of the components in the coating solution are indicated in parentheses where applicable. a) Eudragit® RS (0.25% w/v) and TEC (0.125% w/v), b) Eudragit® RL (0.5% w/v) and TEC (0.125% w/v), c) Eudragit® RS (0.125% w/v), d) Eudragit® RL (0.5% w/v) and e) uncoated DRC.

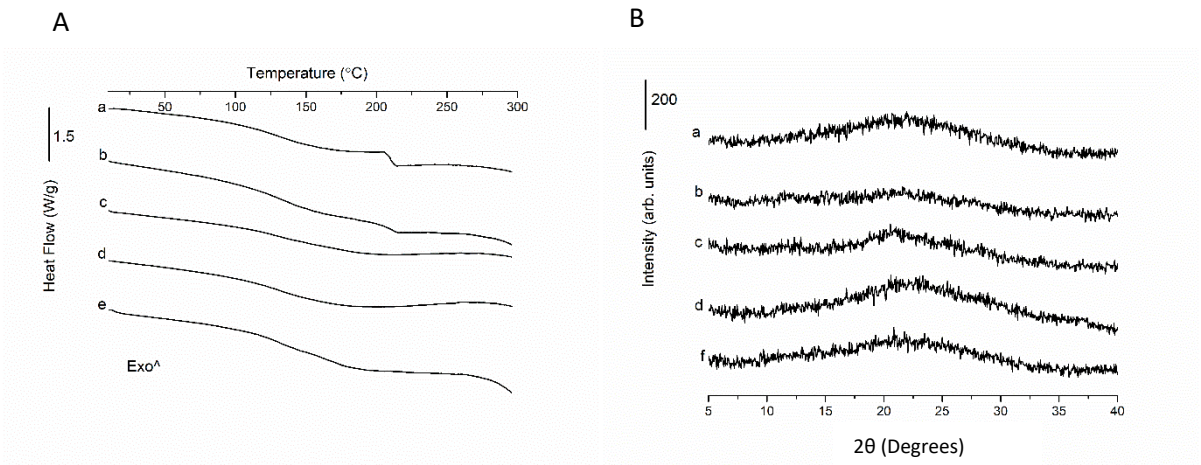

Figure 5.28. A) DSC thermograms and B) pXRD diffractograms of DRCs (IR120) stored at 25 °C and <10% RH for 1 month. The concentration of the components in the coating solution are indicated in parentheses where applicable. a) Eudragit® RS (0.25% w/v) and TEC (0.125% w/v), b) Eudragit® RL (0.5% w/v) and TEC (0.125% w/v), c) Eudragit® RS (0.25% w/v), d) Eudragit® RL (0.5% w/v) and e) uncoated DRC.

These results are consistent with those of previous authors (377), in that the binding of the drug onto the resins provided excellent physical stability over the duration of the study irrespective of whether it is subject to a dry or humid environment. As highlighted previously, the RH conditions did not exceed 60% RH so stability beyond that value at 25 °C cannot be inferred. One major advantage cited by the manufacturers that can help explain the excellent stability afforded by the resins is the ability of the drug to resist recrystallisation, as the functional groups are fixed in space. The resin itself is rendered permanently amorphous due to the level of crosslinking within the structure. After the resin interacts and binds the drug, a salt pair is formed due to the charged drug binding the functional groups on the resin backbone. The result is the DRC being an amorphous structure whereby the drug cannot crystallise as the functional groups to which they bind cannot reorder themselves as they are fixed in space (280).

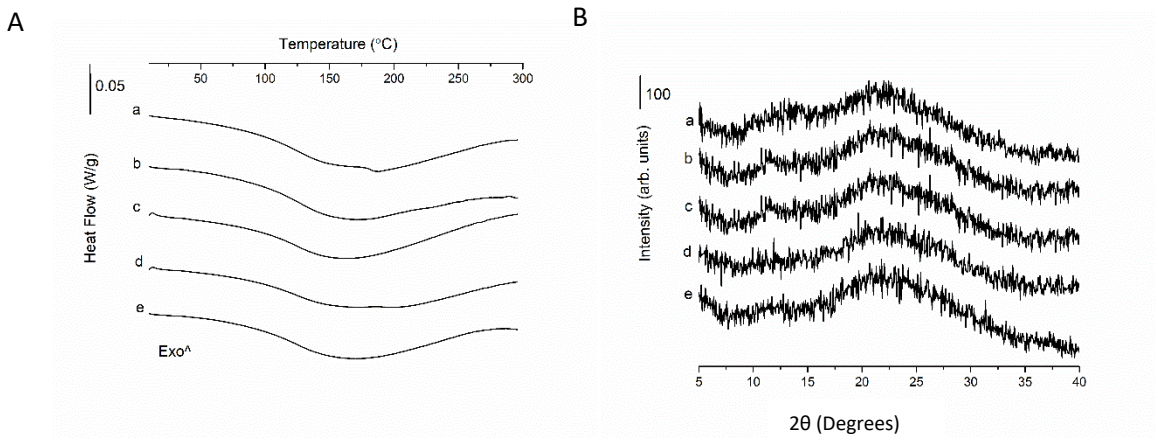

Figure 5.29. A) DSC thermograms and B) pXRD diffractograms of DRCs (IR120) stored at 25 °C and 60% RH for 6 months. The concentration of the components in the coating solution are indicated in parentheses where applicable. a) Eudragit® RS (0.25% w/v) and TEC (0.125% w/v), b) Eudragit® RL (0.5% w/v) and TEC (0.125% w/v), c) Eudragit® RS (0.25% w/v), d) Eudragit® RL (0.5% w/v) and e) uncoated DRC.

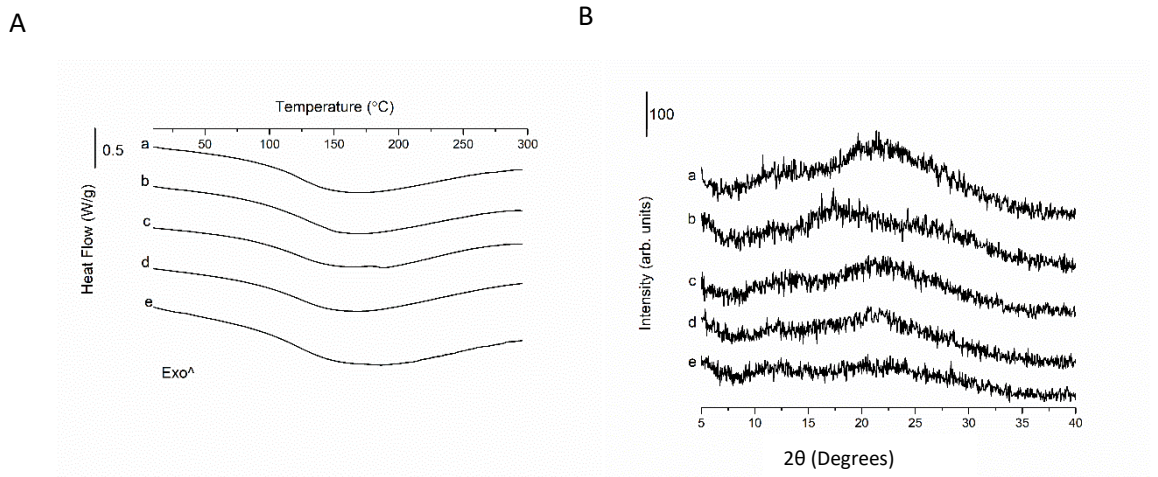

Figure 5.30. A) DSC thermograms and B) pXRD diffractograms of DRCs (IR120) stored at 25 °C and <10%. RH for 6 months. The concentration of the components in the coating solution are indicated in parentheses where applicable. a) Eudragit® RS (0.25% w/v) and TEC (0.125% w/v), b) Eudragit® RL (0.5% w/v) and TEC (0.125% w/v), c) Eudragit® RS (0.25% w/v), d) Eudragit® RL (0.5% w/v) and e) uncoated DRC.

TGA analysis was conducted to assess the uptake of moisture at each stability timepoint for both conditions (Table 5.9). This was particularly important considering the hygroscopic nature of IERs and the need for accurate quantities of DRC to be weighed for drug release testing, chemical stability assessment and DSC analysis. Unsurprisingly, a greater amount of moisture was taken up by the DRCs, irrespective of the coating applied, at the higher RH condition (60% RH) relative to the sub 10% RH

condition. Comparing the month 1 versus month 6 values for each sample stored in “dry condition” (10% RH) reveals all five samples to have higher moisture content values ($p<0.05$) after being exposed to the stability conditions for 6 months relative to 1 month. Having said that, the increase is marginal, particularly when compared to the data generated using the 25 °C/60% RH condition. In the case of the higher humidity condition, with the exception of the uncoated sample, whose moisture content increases approximately 11-fold when comparing the month 6 and month 1 values, all samples exhibit a 6-fold increase in moisture content when the 6-month and 1-month figures are compared. These findings illustrate that the application of a rate-controlling polymer affords some level of protection against moisture over the period studied.

Examination of the photomicrographs of the samples after storage at the relevant conditions reveal less drastic changes in comparison to the stark differences observable when the beads are subject to dissolution testing (Figures 5.15 and 5.16). After one month of storage (Figure 5.31) no obvious differences in appearance are detectable despite the samples being subject to contrasting conditions (25 °C/60% versus 25 °C/<10%). After 6 months of storage (Figure 5.32), the appearance of certain select bead samples (Figure 5.32(B)(a, b and c), upon close inspection, appears to deteriorate to a greater extent in the high humidity conditions relative to dryer conditions, with the majority of samples having pronounced dimples on the surface. These samples are the uncoated DRC and the DRCs coated using the Eudragit® RL grade (with and without plasticiser) which is the more permeable grade of the two pH-independent polymers studied, perhaps highlighting a susceptibility of this polymeric coating to the moisture in the environment. Furthermore, several defects on the surface become apparent. Having said that, the polymeric membrane appears to be largely intact around the entirety of the particles exposed to both stability conditions despite the coated particles’ surface losing their smoothness.

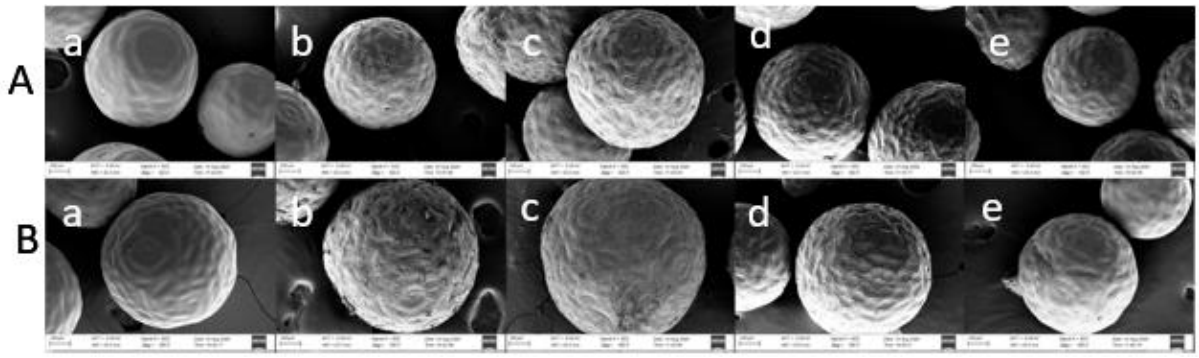

Figure 5.31. SEM images of DRCs (IR120) (See Table 5.9) stored for one month at A) 25°C/60% and B) 25°C/<10% RH. a) uncoated DRC, b) 0.5% w/v (Eudragit® RL) and 0.125% w/v (TEC), c) 0.25% w/v (Eudragit® RS) and 0.125% w/v (TEC), d) 0.5% w/v (Eudragit® RL) and e) 0.25% w/v (Eudragit® RS).

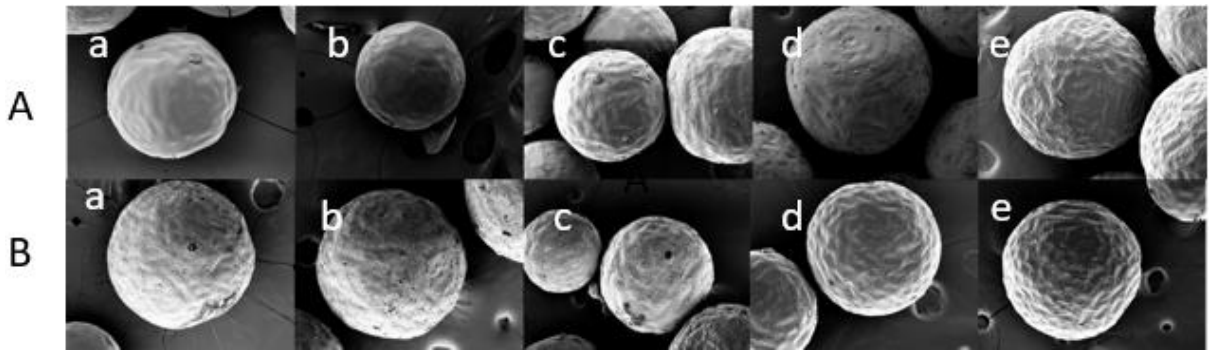

Figure 5.32. SEM images of DRCs (IR120) (See Table 5.9) stored for six months at A) 25 °C/<10% and B) 25 °C/60% RH. a) uncoated DRC, b) 0.5% w/v (Eudragit® RL), c) 0.5% w/v (Eudragit® RL) and 0.125% w/v (TEC), d) 0.25% w/v (Eudragit® RS) and 0.125% w/v (TEC) and e) 0.25% w/v (Eudragit® RS).

Table 5.9. Comparison of moisture uptake (assessed by TGA as per the method detailed in Chapter 2, section 2.2.2.3.2) of all samples (IR120) placed on stability (25 °C/<10% RH) and 25 °C/60% RH) over 6 months.

Sample	**Moisture content (w/w) after 1 month**		**Moisture content (w/w) after 2 months**		**Moisture content (w/w) after 3 months**		**Moisture content (w/w) after 6 months**	
Stability Condition	25 °C <10% RH	25 °C 60% RH	25 °C <10% RH	25 °C 60% RH	25 °C <10% RH	25 °C 60% RH	25 °C <10% RH	25 °C 60% RH
Uncoated	1.09 ± 0.19	7.59 ± 0.29	1.20 ± 0.26	10.23 ± 4.42	1.52 ± 0.11	10.40 ± 0.36	1.60 ± 0.21	11.00 ± 0.45
Coated (RS)	0.83 ± 0.11	6.83 ± 0.01	1.04 ± 0.06	7.61 ± 0.56	1.47 ± 0.21	7.80 ± 0.82	1.50 ± 0.30	8.00 ± 0.50
Coated (RL)	0.84 ± 0.10	7.27 ± 0.13	1.05 ± 0.19	7.61 ± 0.56	1.48 ± 0.24	8.00 ± 0.04	1.52 ± 0.16	8.10 ± 0.40
Coated (RS and TEC)	1.06 ± 0.10	7.40 ± 0.06	1.37 ± 0.03	7.12 ± 0.55	1.69 ± 0.01	7.50 ± 0.20	1.41 ± 0.11	8.20 ± 0.67
Coated (RL and TEC)	1.18 ± 0.11	7.47 ± 0.18	1.29 ± 0.26	7.68 ± 0.47	1.43 ± 0.30	8.30 ± 0.37	1.57 ± 0.25	8.90 ± 0.98

Although the systems investigated in these studies are "dry" DRC beads, the effect on the storage conditions on drug release is worth investigating as it can offer valuable insight into the performance of the coating after being placed on stability. Moreover, these studies can serve as a precursor to the dissolution testing involving the suspension formulation, which will subject the DRC beads to additional stress from the liquid storage medium, and help illustrate the impact of moisture on the coated DRCs. The drug release profiles of selected samples, placed on stability at both conditions for three months are depicted in Figures 5.33-5.35. To aid with the elucidation of the impact of the

stability conditions on the release behaviour, the release profiles of equivalent fresh samples are also shown in Figures 5.33-5.35. Depicted in Figure 5.33 are the release profiles of complexes subject to either 25 °C/60% RH or 25 °C/<10% RH for one month. It is evident from the profiles that the "dry" stability conditions do not impact the coating layers applied using either grade of polymer, in that their release patterns do not differ markedly from those of the unstressed complexes. The same cannot be said for the coated complexes subjected to the higher humidity conditions which exhibited an accelerated release rate relative to freshly coated complexes and those stored in dryer conditions. The Eudragit® RL coated system displays more rapid release kinetics relative to the complexes coated with the less permeable Eudragit® RS grade, which may be attributed to the Eudragit® RL polymer's higher permeability which facilitates the ingress of moisture. One consequence of the accelerated release of the drug from both systems stored at 25 °C/60% RH is that both systems achieve 100% drug release, which is not observed with the other complexes, a clear indication of the integrity of the coating being compromised.

Based on the analysis of the 2 and 3-month timepoints (Figures 5.34-5.35), the release profiles of complexes stored at 25°C/<10% RH do not deviate greatly from the unstressed microparticles and no deterioration in performance is evident. In contrast, the release rate from the coated systems exposed to elevated humidity conditions increases the longer the samples are placed on stability over the timeframe studied. This difference is not drastic but is illustrated nicely by comparing the time at which 90% of the drug is released (t_{90}). With respect to the Eudragit® RS and Eudragit® RL coated system, this value is 10 hours for both systems after being placed on stability (at 25°C/60% RH) for 3 months, whereas after 2 months it is just over 11 hours for each of the coated systems. These values flag two main issues with the stability of samples subject to elevated humidity. The first is the gradual loss of the sustained-release effect, which is likely due to the impact of moisture on the rate-controlling membrane surrounding the complex and the second is the similarity in the t_{90} values. If the coating layers applied remained perfectly intact during the course of the stability study and the impact of moisture had not been detrimental to the performance of the coated DRCs, it would be expected that the complexes coated using the different grades of Eudragit® would demonstrate noticeably different abilities to sustain the release of the drug, as reflected in the t_{90} values. This is illustrated perfectly in the case of the unstressed microparticles as there is a distinct difference in the drug release kinetics afforded by the distinction in the chemistries of the two polymer grades.

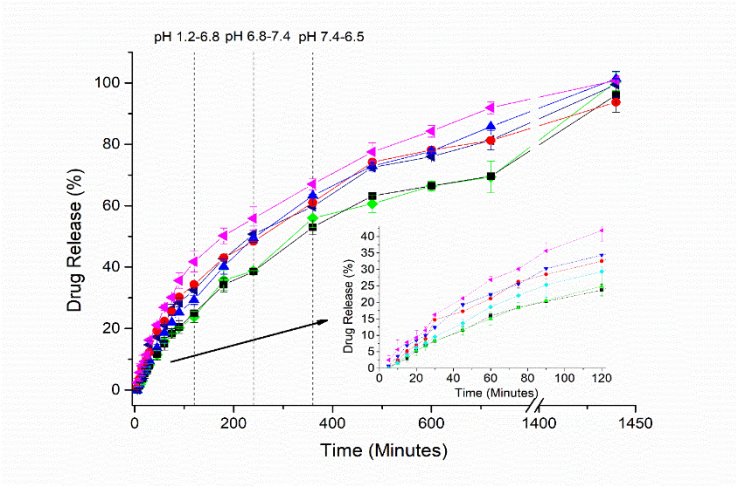

Figure 5.33. Drug release profile over 24 hours (performed using the drug release method detailed in Chapter 2, section 2.2.8.2.2) of drug-loaded beads (IR120) Wurster coated with coating solutions comprising of either Eudragit® RS (0.25% w/v) or Eudragit® RL (0.5% w/v) that are freshly prepared, stored at 25 °C/60% RH for 1 month or stored at 25 °C/<10% RH. Freshly prepared-RS coated (Black square), freshly prepared- RL coated (Red circle), RS coated stored at 25°C/60% RH (Blue triangle), RL coated stored at 25°C/60% RH (Inverted magenta triangle), RS coated stored at 25°C/<10% RH (Green diamond) and RL coated stored at 25°C/<10% RH (Navy triangle).

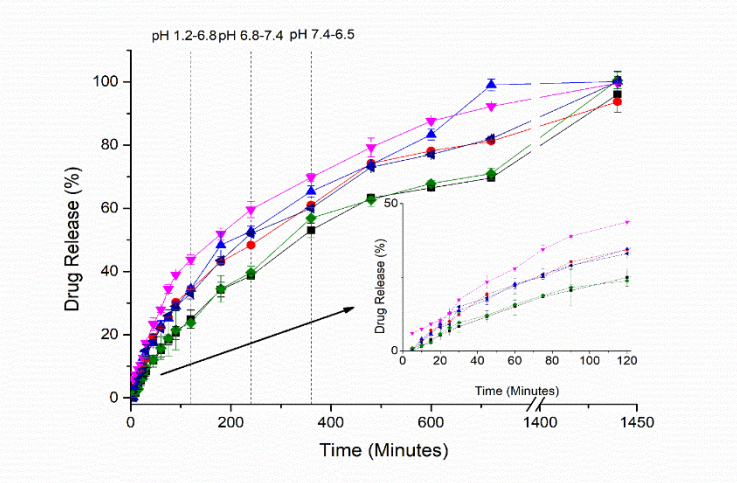

Figure 5.34. Drug release profile over 24 hours of drug-loaded beads (IR120) Wurster coated with coating solutions comprising of either Eudragit® RS (0.25% w/v) or Eudragit® RL (0.5% w/v) that are freshly prepared, stored at 25 °C/60% RH for 2 months or stored at 25 °C/<10% RH. Freshly prepared RS coated (Black square), freshly prepared RL coated (Red circle), RS coated stored at 25°C/60% RH (Blue triangle), RL coated stored at 25°C/60% RH (Inverted magenta triangle), RS coated stored at 25°C/<10% RH (Olive diamond) and RL coated stored at 25°C/<10% RH (Navy triangle).

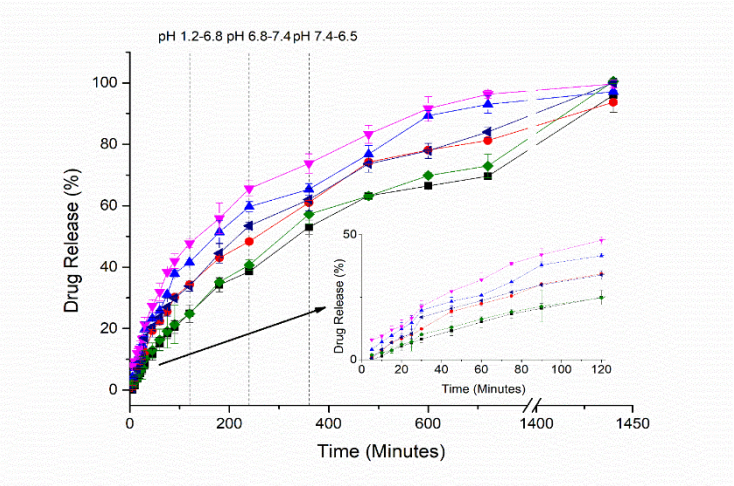

Figure 5.35. Drug release profile over 24 hours of drug-loaded beads (IR120) Wurster coated with coating solutions comprising of either Eudragit® RS (0.25% w/v) or Eudragit® RL (0.5% w/v) that are freshly prepared RS coated (Black square), freshly prepared RL coated (Red circle), RS coated stored at 25°C/60% RH (Blue triangle), RL coated stored at 25°C/60% RH (Inverted magenta triangle), RS coated stored at 25°C/<10% RH (Olive diamond) and RL coated stored at 25°C/<10% RH (Navy triangle).

Chemical stability testing was performed on the samples that were also tested for drug release after storage for 3 months at both stability conditions to ensure potency was retained throughout the course of the stability study. HPLC analysis revealed no degradation had occurred, as evidenced by the absence of any peaks which could be attributed to related substances as specified by the USP, and the HPLC assays revealed that the percentage recovery of TZD HCl was between 99.5 and 99.93% of the theoretical concentration (Table 3 in Appendix 3). Degradation peaks were not present in the chromatograms of the selected samples that were subject to stability analysis (Figure 33 in Appendix 3), thereby suggesting the DRC samples have good chemical stability at either of the conditions tested, irrespective of a coating applied as well as the type of coating.

5.2.7.2 Liquid stability of Wurster coated IR120 beads

Prior to the assessment of the drug leaching properties and drug release performance of any liquid formulations, a series of trials aimed at successfully suspending the ion-exchange beads were performed. One of the main factors that had to be considered when suspending the beads, was the need for the suspending medium to have low ionic strength, so that premature drug release is limited. Therefore, DI H_20 was selected as the liquid vehicle. The choice of suspending agent is also critical and three agents formed part of the screening trials. Furthermore, the concentration range employed in these studies is within the typical range that has been trialled in previous studies and the objective of this screening exercise was to identify the optimal concentration and agent to adequately suspend the DRC beads (297,378). As illustrated in Figure 5.36(D), xanthan gum was successful at suspending

blank beads (approximately 13.3 mg/ 5 mL) when the concentration used was greater than 0.5% w/v. Regarding the other two suspending agents selected, which were HPMC and Avicel® RC/CL, the beads were not successfully suspended using any of the concentrations trialled, characterised by the formation of a sediment which could not be redispersed upon agitation (Figure 5.36(A-C)).

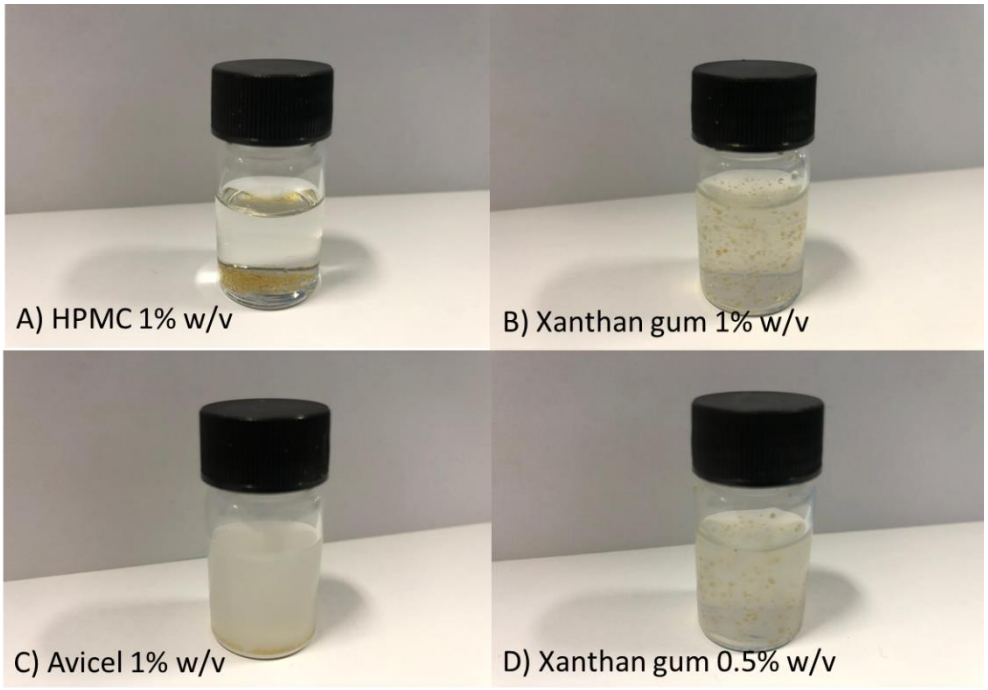

Figure 5.36. Images of a selection of failed suspension trials in DI H_2O (A-C) using a selection of suspending agents (and concentration used (% w/v)) and "blank" beads (IR120) alongside the sample where the beads (13.3 mg/mL) were adequately suspended (D).

These suspending agents have all been used to suspend ion-exchange beads with varying degrees of success, with xanthan gum having the most recognised reputation due to its pseudoplastic behaviour, which is desirable for suspension formulations (378). The lowest concentration of xanthan gum used (0.25% w/v) failed to suspend the beads adequately indicating that the medium was not viscous enough to suspend the beads. On the basis of these initial trials, the optimum xanthan gum concentration was taken to be 0.5% w/v, as the 1% w/v concentration produced a suspension with too high a viscosity, making pouring from the container in which it was stored difficult. The high viscosity of the pseudoplastic liquid means the sedimentation rate is slow, yet it can be lowered through agitation which applies shear strain, yielding redispersion of the particles. Furthermore, the use of xanthan gum achieves a second goal of the suspending process, in that an excipient is selected that does not have the same charge as the IRP69 grade in an aqueous environment, thus minimising potential interaction with the resin. Again, in light of this consideration, xanthan gum has been proven to be compatible with sulfonic acid-containing resins (297).

As discussed above, the Wurster coating process generated coated DRC beads that could still be adequately suspended using xanthan gum. This enabled the extent of drug leaching to be evaluated with the drug leaching values presented in Table 5.10. Ideally, the IER-based formulation should be devoid of drug leaching into the suspending medium during storage, whilst retaining the ability to release the API after exposure to an appropriate ionic environment encountered in the GIT. As the time course of the experiments progressed, an increased level of drug leaching was observed. However, the degree of drug leaching was still relatively low (5.5%), irrespective of the system examined.

Regarding the uncoated system, the quantity of drug leached does not differ statistically ($p>0.05$) over the 4-week study when the values after week 1 and 4 are compared. All systems studied did not differ from one another in the level of drug leaching detected after one month. Regarding the 1-week timepoint, all samples leached a similar amount of drug as the uncoated sample with the exception of the Eudragit® RS coated system which leached a lower quantity ($p<0.05$). This finding illustrates that the coating applied may be compromised, allowing some drug leaching after being suspended in an aqueous environment for one week. Although the Eudragit® RS system leaches a statistically lower quantity of drug ($p<0.05$) relative to the uncoated material, a likely consequence of the film's low water permeability, the difference is marginal, and the quantity leached does not differ statistically ($p>0.05$) from that of the other coated systems. When the weekly leaching values for each sample are compared, all coated samples display lower leaching values ($p<0.05$) after week 1 compared to week 4, indicating that the coating offers some protective effect against leaching that subsides over time.

Previous studies that have investigated the robustness of the sustained-release coating layer have reported a similar tendency of the drug to diffuse into the suspending medium over a prolonged duration of time (117,379). As with most coated microcapsules that do not falter immediately, a small level of leaching can occur which reaches a plateau and is generally a function of the drug's solubility in the suspending medium. Depending on the polymer used to encapsulate the API, the thickness of the coating, contents of the suspending medium and the properties of the API itself, the time to reach this plateau can vary, often by a matter of months. This is exemplified by comparing the drug leaching values for the coated diltiazem systems reported by Junyaprasert and Manwiwattaanakul, to the stability of the terbutaline DRCs reported by Cuna et al. The systems reported by the former reach a plateau after 90 days (approximately 2-3% leaching depending on the system) (117), whereas the leaching data for the terbutaline systems highlights the importance of the processing method on the stability and is slightly ambiguous. The authors reported less than 6% of the drug had leached over 6 months for all systems studied, but certain DRCs produced showed coating rupture after day 1 (127).

Table 5.10. Comparison of drug leaching values (% w/w) from selected suspension samples described in Chapter 2, section 2.2.9.1 (containing the required weight of microparticles to produce a TZD concentration of 4 mg/5 mL) that have been stored at room temperature over a 28-day period and assessed at weekly intervals (as per the method described in Chapter 2, section 2.2.9.1). The leaching % values are based on the amount of drug in solution as a % of assayed drug in the specific DRC (coated or uncoated IR120) tested.

Sample	Concentration of microparticles in suspension	Drug leaching value (% w/w) on day 7	Drug leaching value (% w/w) on day 14	Drug leaching value (% w/w) on day 21	Drug leaching value (% w/w) on day 28
DRC (Uncoated)	12.43 mg/ 5mL	3.86 ± 0.64	4.39 ± 0.11	4.60 ± 1.21	5.06 ± 0.79
Coated DRC (Eudragit® RL-0.5% w/v)	13.3 mg/5 mL	3.69 ± 0.91	3.96 ± 0.66	4.44 ± 0.71	5.18 ± 0.46
Coated DRC (Eudragit® RS-0.25% w/v)	12.82 mg/5 mL	2.88 ± 0.42	4.08 ± 0.23	4.16 ± 0.49	4.99 ± 0.34
Coated DRC (Eudragit® RL-0.5 % w/v and TEC-0.125% w/v)	13.2 mg/5 mL	3.64 ± 0.59	3.96 ± 0.52	4.19 ± 1.16	5.02 ± 0.14
Coated DRC (Eudragit® RS-0.25% w/v and TEC-0.125% w/v)	12.81 mg/5 mL	2.77 ± 0.75	3.48 ± 0.69	4.01 ± 0.81	4.89 ± 0.53

To further investigate the drug leaching behaviour of the systems, the liquid samples were tested daily to assess the drug leaching behaviour (Table 5.11). Premature release from the beads can be detected in all samples from day 1, albeit at very low levels for the coated samples. Regarding the uncoated sample, an increase in drug leaching is observed over time until day 4 when a plateau is reached, signified by no statistical difference ($p>0.05$) in the leached drug levels between day 4, 5 and 6. Concerning the coated systems, the drug leaching behaviours all follow a similar trend. The systems leach a higher ($p<0.05$) amount of drug on day 6 relative to day 1 but the plateau is reached after approximately 4 days, as signified by no statistical difference in the values from that timepoint on. With respect to the Eudragit® RL grade, similar to the leaching studies conducted at weekly intervals, the impact of the polymer coating appears to be negligible regarding the leaching of the drug into the medium which is suggestive of a certain level of drug leaching being unavoidable. Relative to the uncoated system, the amount leached at each timepoint studied does not differ ($p>0.05$). In contrast, the complex coated using the Eudragit® RS grade polymer demonstrates a reduced propensity to leach drug, as is evident from the lower leaching values at the majority of timepoints tested, in particular day 1 and day 6, compared to the uncoated system. This is consistent with the polymer's reduced

permeability characteristics which render it less susceptible to the release of the drug, which has been exploited for sustained-release purposes.

In contrast to the noticeable impact on drug release, the inclusion of the plasticiser in the Eudragit® RL film coating has no significant effect ($p>0.05$) on the leaching levels observed, when compared to the uncoated system. This is reflected in the leaching values which do not differ significantly ($p>0.05$) from one another. This observation is not applicable to the other grade of polymer studied. When the system coated using TEC and Eudragit® RS is studied, reduced leaching levels ($p<0.05$) are observed after day 1 relative to the uncoated system, but over time, the level of drug leaching does not differ significantly ($p>0.05$), as illustrated by the day 6 values. This indicates that incorporation of the plasticiser into the film compromises the integrity of the polymeric layer as the complex leaches an equivalent level of the drug relative to the uncoated system which does not occur if the film contains solely Eudragit® RS. This illustrates the importance of thoroughly assessing the impact of feed solution additives to the film structure as they could have a detrimental impact on product performance, thus undermining the role of the primary excipient within the formulation.

Table 5.11. Comparison of drug leaching values (% w/w) from selected suspension samples described in Chapter 2, section 2.2.9.1 (containing the required weight of microparticles to produce a TZD concentration of 4 mg/5 mL) that have been stored at room temperature over a 6-day period and assessed at daily intervals. The leaching % values are based on the amount of drug in solution as a % of assayed drug in the specific DRC (coated or uncoated IR120) tested.

Sample	Drug leaching value (% w/w) on day 1	Drug leaching value (% w/w) on day 2	Drug leaching value (% w/w) on day 3	Drug leaching value (% w/w) on day 4	Drug leaching value (% w/w) on day 5	Drug leaching value (% w/w) on day 6
DRC (Uncoated)	0.83 ± 0.03	1.34 ± 0.26	2.28 ± 0.25	3.28 ± 0.19	3.37 ± 0.13	3.82 ± 0.54
Coated DRC (Eudragit® RL-0.5% w/v)	0.59 ± 0.43	1.16 ± 0.48	2.19 ± 0.53	3.2 ± 0.97	3.42 ± 1.07	3.66 ± 0.91
Coated DRC (Eudragit® RS-0.25% w/v)	0.47 ± 0.04	1.04 ± 0.07	2.08 ± 0.38	2.18 ± 0.23	2.51 ± 0.68	2.83 ± 0.42
Coated DRC (Eudragit® RL-0.5% w/v and TEC-0.125% w/v)	0.87 ± 0.28	1.08 ± 0.24	2.21 ± 0.82	2.94 ± 0.94	3.10 ± 0.69	3.62 ± 0.59
Coated DRC (Eudragit® RS-0.25% w/v and TEC-0.125% w/v)	0.52 ± 0.16	1.11 ± 0.68	2.06 ± 0.56	2.55 ± 0.73	2.58 ± 0.02	2.71 ± 0.75

The surface morphologies of the beads which were stored in the aqueous vehicle for four weeks as part of the drug leaching study are shown in Figure 5.37. No obvious ruptures in the polymeric layer are evident on the surface of the beads despite drug leaching into the storage/suspending medium being detected for all samples. This contrasts with the DRCs analysed by SEM post-dissolution (Figure 5.16) which displayed noticeable changes in morphology represented by breaches in the polymeric layer that envelops the beads after the 24 hour study. The greater volume of the medium used in the dissolution studies may play a role in this discrepancy observed but a more likely reason is the agitation that forms part of the dissolution test that is absent in the drug leaching studies. Despite the well-known tendency of IERs to expand upon contact with aqueous environments, little evidence of this can be found after the drug leaching studies.

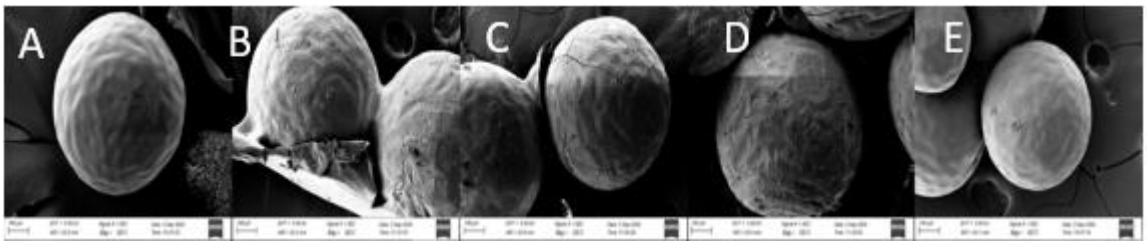

Figure 5.37. SEM images of uncoated and coated DRCs (IR120) suspended in an aqueous medium for one month as part of the drug leaching studies. The concentration of polymer coating is stated in parentheses. A) DRC coated with Eudragit® RS (0.25% w/v), B) DRC coated with Eudragit® RL (0.5% w/v), C) DRC coated with Eudragit® RS (0.25% w/v) and TEC (0.125% w/v), D) DRC coated with Eudragit® RL (0.5% w/v) and TEC (0.125% w/v) and E) uncoated DRC.

When assessing the samples at daily intervals, the coating layer alongside the nature of the polymer played a minor role in the level of drug leaching observed, as would be expected. Although the polymers are water insoluble, the increase in drug detected over time is likely to be due to an ingress of water which compromises the integrity of the polymeric coating, especially for the Eudragit® RL grade which has a greater tendency to swell and become permeable. It is worth noting that a consequence of the drug leaching phenomenon is the reduced drug content in the suspended beads and, although it has not been determined experimentally as part of this work, the likelihood is implicit based on the analysis of the leaching results. Although the leaching results are encouraging, it is evident from the drug release studies that the liquid formulation requires considerable optimisation in a number of areas. The first factor to be considered, which has been alluded to previously, is the choice of the aqueous storage vehicle which is not ideally suited to maintaining the integrity of the film coating. Secondly, the particle size of the systems is a cause for concern, as the DRC beads are of a size that is likely to provide a gritty texture mouthfeel, thus potentially reducing patient compliance. Lastly, the formulation is only at a relatively early stage of development with the need for several more excipients to be included, such as preservatives, sweetening and flavouring agents so that any potential that the prototype formulation may have can be realised. The impact that these excipients may have would have to be evaluated, as it can range from changing the intrinsic pH of the formulation to interfering with the drug-resin binding (in particular for preservative agents such as the parabens and sodium benzoate).

5.2.7.3 Drug release from constituted trial suspension formulations (IR120)

After establishing that the "dry" microparticles coated using either Eudragit® RS or Eudragit® RL were physically stable to drug recrystallisation at the conditions tested (Chapter 2, section 2.2.17) in tandem with the encouraging drug leaching studies (approximately 5% drug leaching over a one-month period

at room temperature), the drug release from constituted suspensions was evaluated. As the release profiles of the systems coated using a feed solution comprising of either 0.5% w/v Eudragit® RL or 0.25% w/v Eudragit® RS were similar (both in the "dry" form and after storage for 3 months at 25 °C/60% RH), the former was selected to study as it showed no evidence of agglomeration during the stability studies, in contrast to the RS coated system. Together with the uncoated DRC, this coated system was investigated to establish the influence of the liquid storage medium on the reproducibility of the release profile. The utilisation of IERs are a viable option for the successful formulation of sustained-release suspensions and diltiazem is one such example of a drug that has been formulated in this manner to overcome similar challenges that TZD HCl faces (117).

Interestingly, at T_0, the drug release from the uncoated DRC beads in liquid suspension is slower ($p<0.05$) over the first 15 minutes relative to the release of drug from the "dry" uncoated DRC beads which suggests that the viscosity of the suspending medium is responsible for slowing the release of the drug (Figure 5.38). Over the first 25 minutes of the study, the T_{2week} and $T_{4\ week}$ uncoated DRC suspension samples release a higher quantity of drug ($p<0.05$) relative to the "dry" uncoated DRC and the T_0 reconstituted sample. The increased rate of drug release from the aged samples over the initial stages of the dissolution study can be attributed to the presence of unbound API that has leached from the DRC into the liquid vehicle during storage. In contrast to the "dry" uncoated DRC and the T_0 reconstituted sample, the unbound API that has leached from the DRC is detectable from the outset of the dissolution study, which is illustrated by the faster drug release kinetics in the drug release profile.

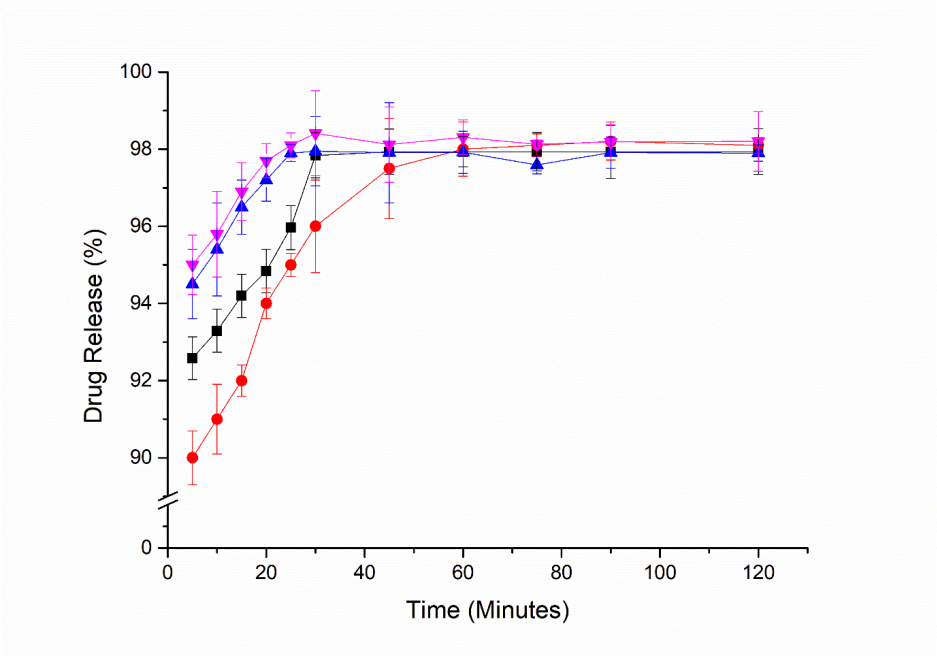

Figure 5.38. Drug release profile over 24 hours of uncoated drug-loaded beads (IR120) that are either available as "dry" DRC beads or suspended in an aqueous media for different lengths of time. "Dry" DRC beads (Black square), suspended DRC beads at T_0 (Red circle), suspended DRC beads at $T_{2\ weeks}$ (Blue triangle) and suspended DRC beads at $T_{4\ weeks}$ (Inverted magenta triangle).

As shown in Tables 5.10 and 5.11, evidence of drug leaching was observed for all coated systems stored at ambient temperature, which is reflected by a faster drug release rate from the liquid-based formulation. Based on the data presented, there appears to be an inherent tendency to leach the drug once the resin comes into contact with the medium. Regarding the coated system (0.5% w/v Eudragit® RL), as illustrated in Figure 5.39, relative to the % drug release observed from the "dry" DRC coated beads, drug release for the coated DRC bead suspension at T_0 did not differ significantly ($p>0.05$), which is not unexpected as the formulation is immediately tested after reconstitution. However, significant differences in drug release profiles are observed for the suspensions that are held for 2 or 4 weeks ($T_{2\ week}$ and $T_{4\ week}$) before release testing. Evident from Figure 5.39, is a diminished sustained-release effect that is compounded the longer the complexes are held suspended in the aqueous suspending medium. These findings can be rationalised by considering the drug leaching studies which demonstrate two main consequences of the DRCs being suspended in aqueous media. The first pertains to the drug that has leached from the DRC over the course of a two week or four week period and is present in the liquid medium and will be immediately available once the formulation is introduced to the dissolution vessel. The second is likely a consequence of the water-permeable properties of the polymer coating applied to the microparticle. The ingress of moisture may lead to the DRC swelling which in turn could potentially rupture the polymeric coating causing the sustained-

release effect to be compromised. This severely impacts the potential of the formulation reflected by the accelerated drug release behaviour. In the case of the $T_{4\ week}$ sample, complete drug release is attained after 12 hours, marked sustained-release effect relative to the marketed Zanaflex™ product. Similarly, approximately 95% of the drug is released at this timepoint when the $T_{2\ week}$ sample is examined, which illustrates the detrimental impact the aqueous environment has on the polymeric membrane surrounding the particle, particularly when the sample is aged. Similar findings have been reported by Cuna et al. with their coated DRCs which they produced using a non-aqueous coating method to apply a Eudragit® RL/RS blend. On this occasion, the coated particle was unable to maintain its initial release profile and liable to change over time, resembling the findings reported in this work (127). Overall, the results of the suspension studies point to the need for an alternative suspending medium in which the polymeric coating is not likely to dissolve.

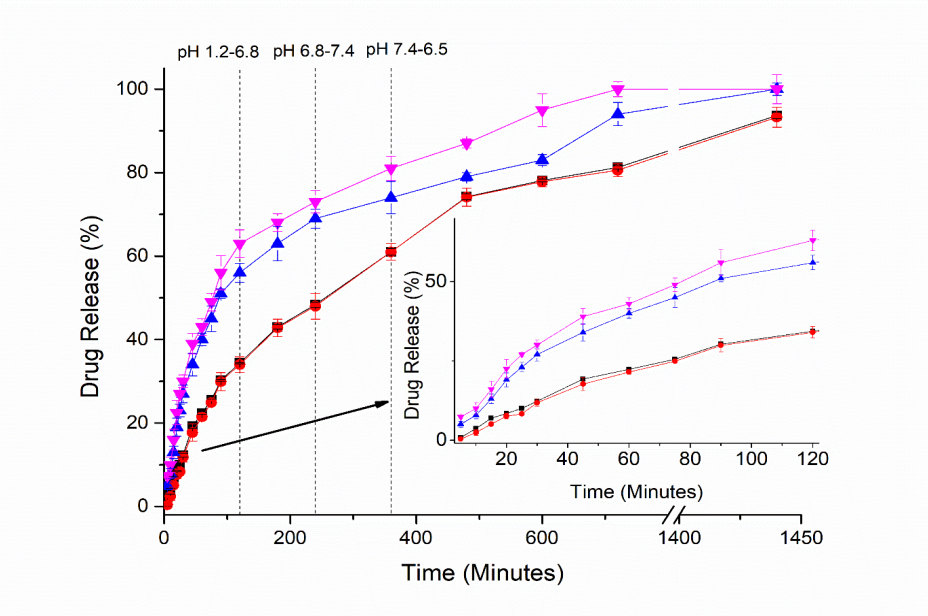

Figure 5.39. Drug release profile over 24 hours of drug-loaded beads (IR120) Wurster coated with a coating solution containing 0.5% w/v Eudragit® RL that are either presented to the dissolution medium as "dry" DRC beads or suspended in an aqueous medium for different lengths of time. "Dry" coated DRC beads (Black square), suspended coated DRC beads at T_0 (Red circle), suspended coated DRC beads at $T_{2\ weeks}$ (Blue triangle) and suspended coated DRC beads at $T_{4\ weeks}$ (Inverted magenta triangle).

5.3 Conclusion

Despite the demonstrated benefits of IERs when it comes to prolonging the release of a complexed API, the suppression of the drug release rate is API-dependent and very often a further rate-controlling polymer is required to achieve the intended release profile. A selection of approaches have been reported in the literature, several of which (granulation and Wurster coating) were trialled in this work with variable levels of success. The bead form of the resin proved to be a more suitable option relative to the powdered form for the application of a rate-controlling polymeric membrane to sustain the release of TZD HCl, with the ultimate intention to formulate a suspension-based product. This work highlighted that that aqueous-based coating dispersions were unsuitable for coating the DRCs using the Wurster process due to the detrimental impact on product quality which contrasted with the coatings applied using organic polymer solutions, exemplified by varying levels of drug release suppression depending on the grade and concentration of coating polymer. Solid-state stability analysis revealed that the selected "dry" microparticles were physically stable long-term at the conditions tested. In contrast to the dry environment, exposure of the microparticles to a liquid environment revealed stability issues characterised by low levels of drug leaching (approximately 5%) into the suspending medium over time. This was confirmed by drug release studies which were characterised by faster drug release rates from coated systems stored in an aqueous vehicle which increases on ageing yet still display a marked sustained-release effect relative to the intrinsic drug release properties of the API. The work demonstrated that despite the low levels of drug leaching into the liquid vehicle alongside the altered drug release profile due attributable to storage in a liquid environment, TZD HCl could be formulated as a sustained-release liquid product using a method traditionally more suited to large scale studies.

Chapter 6:

General Discussion

As outlined in the origin and scope section, the primary aim of this thesis was to investigate the feasibility of using IERs to modify the release profile of two different APIs formulated as a stable oral liquid formulation. Owing to the commercial aspect of the project, the two APIs investigated were selected based on the fact that a stable sustained-release oral liquid formulation of each had the potential to address unmet therapeutic needs. In Chapter 3, the three drug candidates were tested for their ability to complex with a powdered form of a sulfonic acid-containing IER with the resulting product being evaluated in terms of drug loading, drug release behaviour and characterised using conventional techniques such as FTIR, pXRD and DSC. Once an appropriate drug candidate for the IER-complexation approach was identified, a range of alternative resins were tested to investigate their impact on the properties of the API, and this formed the basis of Chapters 3 and 4. This aspect of the work involved exploring the influence of how different factors, identified from a perusal of the literature, affected the drug loading values achieved using resins that themselves exhibited different properties, thus highlighting the individuality of the loading process. Chapter 4 also involved the evaluation of the DRC performance of complexes produced by spray-drying. Initial studies utilised "trial and error" experimentation to establish the feasibility of the approach, the success of which led to the production of DRCs by spray-drying using a QbD methodology. Chapter 5 focused primarily on the manufacturing of polymer coated DRC systems, using unit processes such as granulation and Wurster coating, and an evaluation of their dissolution performance. The most promising DRC systems were selected for further studies, aimed at formulating them into an effective sustained-release system, with a subsequent evaluation of the physical and chemical stability of selected systems in a "dry" and aqueous liquid environment.

6.1 Investigating the suitability of ion-exchange resins (IERs) as a formulation strategy

As part of this work, the resin selected was a "strong" cation exchanger known as Amberlite® IRP69, which is one of the most popular resins (powder form) on the market with an established reputation for modulating the release of drugs, evident from its prominence in both the research and patent literature (109,309).

MTZ was chosen as a drug to investigate as a potential candidate to complex with a "strong" cation exchanger known as Amberlite® IRP69, which is one of the most popular resins (powder form) on the market with an established reputation for modulating the release of drugs. Clear evidence is available in the literature reporting its propensity to ionise, attributable to the compound being a weak base (289). Although many formulations of the drug are available in both the solid and liquid form, no known licensed liquid product containing the free base of the compound exists to the best of the author's knowledge. The utilisation of IER-based formulations provided a potential avenue to produce

a stable oral liquid product. The loading results obtained with MTZ were not entirely unsatisfactory and suggestive of physical adsorption being responsible, but loading still remained on the lower end of the scale with respect to typical drug loadings reported (108). These values can be still be classed as undesirable considering the high dose of MTZ which makes high drug loading a pre-requisite. These unfavourable loading results are compounded by the drug release data in either media tested. In the low pH environment (0.1 M HCl) the release profiles are characterised by a burst release of drug in which the majority of the drug-loaded is released, signifying that the complex requires the application of a rate-controlling polymer to provide a sustained-release effect. Although this is far from ideal, the drug release behaviour in DI H_20 provides clear evidence that the resinates do not perform as one would expect if robust ion-exchange bonds were responsible for complex formation. Further to this point, manipulation of the pH of the loading solution, aimed at maximising the dissociation of the drug in solution did not lead to significantly improved results. This can be attributed to the presence of competing ions that were introduced when the buffer species was used. This finding was further rationalised through reference to the findings of Rajesh et al. who found that the effect of the API solubility cannot be dismissed despite the well-known relationship between solution pH and dissociation tendency, signifying a balance between the two API properties needs to be achieved (295). Predictably, these resinates showed no dramatic improvement in performance in either DI H_2O or 0.1 M HCl, with drug solubility being the predominant factor influencing drug release rather than the formation of an ionic complex, highlighting the need to investigate an alternative API to derive the expected benefit from an IER-based approach.

Successful loading of an API onto Amberlite® IRP69 was achieved using TZD HCl which is a weakly basic drug with a reported pKa of 7.3. The ability of this API to form drug-resin complexes is perhaps unsurprising, considering the loading of clonidine HCl, a structurally related compound, onto the same resin was reported by Tris Pharma who commercialised the technology (351). A 1:1 (w/w) ratio of drug to resin was found to be optimal with respect to the two main considerations used to determine the success of the loading process: the drug association efficiency (DAE) and % drug loading. The former is important from a drug wastage standpoint, whilst the higher values of the latter are desirable in terms of minimising the final size of the dosage form. As the proportion of the drug in the loading medium increased, equivalent drug loading levels were achieved, however, the DAE was drastically reduced, corresponding to increased drug wastage. Conversely, a higher proportion of resin in the loading medium relative to the drug, produced DRCs with reduced drug loading values, attributable to the presence of unsaturated resin binding sites. Previous strategies that have been reported to be effective at increasing the level of drug loading were trialled and included pre-treatment of the resin, multiple-stage loading steps and increasing the temperature of the loading solution (110,279).

However, relative to the conventional single-stage loading method at ambient temperature, these measures produced similar drug loading results which could be a consequence of the affinity that the API and resin have for one another, reflected in the drug loading. Encouragingly, the level of drug loading (approximately 50% w/w) reported for the optimal ratio of drug to IER is at the upper end of the reported scale when it comes to achievable drug loadings, far exceeding the drug loadings achieved using MTZ. This is beneficial from the perspective of reducing the proportion of excipient in the formulation, a major goal of any formulation design.

Although solvent extraction is the typical method of choice for assaying conventional polymer-based systems, the method employed as part of this work utilised a different approach reliant on the displacement of organic drug ions off the resin into solution. A large number of studies in the literature employ this approach, known as the drug displacement method, as the primary way of determining the drug loading achieved after complexation (90,110,344). As a way of validating the drug displacement method and verifying that it was superior to a solvent extraction method, the latter was performed in a select number of experiments and provided further evidence that ion-exchange had been successful due to disparity in the quantity of drug detected using each method. This difference is not unexpected as methanol lacks the necessary ions to displace the drug from the resin, supported by no drug being detected using HPLC analysis, prompting the selection of the drug displacement assay as the method of choice for assaying drug content.

Despite its prevalence in the literature, one issue that became apparent during the initial studies investigating the assay of drug material was the need for extensive method development, something that often goes unreported in the literature. As part of the work of this thesis, the establishment of a robust assay procedure helped overcome discrepancies that were apparent when the results of initial assay experiments were compared to the dissolution data. Subsequent trials examining the effect of the ionic strength, the concentration of the complex in the assay medium and temperature on the drug-resin equilibrium revealed the concentration factor to be critical in eluting the maximum quantity of drug from the resin. Through these experiments, it became apparent that an equilibrium existed between the API and resin in an aqueous environment which could be manipulated through optimisation of the assay conditions. Similar modifications were made during the assay studies involving NaCl solutions, that acted as a comparator to the acidic solution and were shown to be as effective as the aqueous acidic solutions in displacing API from the resin, once a thorough understanding of the drug-resin equilibrium was established.

Kinetic studies revealed that the proportion of each component in the loading solution had a distinct influence on IER loading kinetics which could be further manipulated by pre-treatment of the resin.

The recognised influence of particle size reduction of the resin raw material was illustrated in this work, which can be exploited to reduce the total processing time required to produce the product.

The findings from the drug release studies performed using a selection of uncoated DRCs provided two interesting results. The first, which is the less desirable of the two, relates to the release of the API in ionic media, where the release kinetics of the API from the DRCs can be classed as rapid. The release profiles show no evidence of a sustained-release effect imparted by complexation and are characterised by a burst release, which is not an uncommon occurrence when the drug release medium is effective at displacing the bound ion. However, it does signify the need for microencapsulation using a polymeric membrane as sustaining the release of the API is the primary goal, a topic explored in Chapter 5. The second major finding from the dissolution studies pertains to the release behaviour of the DRCs in DI H_20, where minimal drug release was observed signifying that a robust ion-exchange system was formed. This contrast in drug release behaviour relative to that observed in ionic media provides assurance that ionic complexation has occurred, yet this simple assessment is often neglected in many publications that report on the dissolution properties of drug-resin complexes. According to the theory of ion-exchange, minimal drug release should be observed in DI H_2O as the medium lacks the necessary ions to promote drug release, an expectation that is borne out in the case of drug-resin complexes formed using TZD HCl and IRP69. ATR-FTIR analysis provided further evidence that an interaction between drug and resin has occurred as complexation can be inferred from comparisons of the spectra of the raw materials, optimised DRC and equivalent physical mixture. The absence of the peak attributable to TZD HCl's secondary amine group implicated in the ion-exchange reaction combined with the shifting of peaks assigned to the sulfonic acid group of the resin is indicative of an ionic interaction in the DRC (119). Relative to the majority of the literature citing differences in the FTIR spectra as evidence that supports the formation of a DRC, more conclusive data is presented here.

As part of this work, a greater emphasis is placed on the results of the thermal and pXRD characterisation analyses used in this work relative to what is described in the literature. The thermal and pXRD analyses suggest that the drug has lost its crystalline structure when bound to the resin. This cannot be attributed to machine sensitivity issues as equivalent physical mixtures of crystalline drug and resin display Bragg peaks and melt endotherms during pXRD and DSC analysis respectively. Similar to the FTIR data reported in many of the publications, the solid-state characterisation of the DRCs is limited, as the majority are focused on reporting the impact on the drug release properties rather than definitively characterising the physical form of the drug loaded onto the resin. Further experiments, involving a variety of techniques, revealed the propensity of TZD HCl to amorphise, which aided the identification of the API's T_g value that occurred at an unusually low temperature (-

20 °C). To the best of the author's knowledge, this is the first report of the API's glass transition temperature, which in turn enabled the detection of the amorphous API when the DRC was analysed.

The impact of an alternative physical form of the resin containing the same functional group (sulfonic acid) was also evaluated for its impact on the loading and release of TZD HCl, another feature of this work that has not been addressed comprehensively in the literature. The bead-type resins have a lower ion-exchange capacity (IEC) relative to the powder form, which can be ascribed to a less porous structure that limits the drug ion's access to potential ion-exchange binding sites in the interior of the bead. A similar assay method development process to that outlined for the powdered systems revealed that lower loadings (approximately 30% w/w versus approximately 50% w/w) could be achieved using the bead form of the resin (Amberlite™ IR120) compared to the equivalent powdered form (Amberlite® IRP69), consistent with a reduced IEC value. Identical factors to those reported for powdered systems exert a pronounced effect on the assay studies, most notably the concentration of complex in the assay medium. The loading studies also demonstrated that a 1:2 D:R ratio (w/w) in the loading medium was optimal as it ensured a high drug loading figure whilst also maintaining a sufficiently high DAE. This correlates well with the lower reported IEC relative to the powdered form which has a larger number of ion-exchange sites available to participate in the exchange reaction. Disparities in the loading kinetics were identified by varying the ratio of components in the loading medium in addition to adjusting the temperature of the loading medium. Both adjustments produced results that were consistent with those reported by previous authors (380).

Alongside the effect of the physical form of the same resin type on loading and release properties, the larger particle size, as determined by laser diffraction, pointed to potential advantages of the bead form from a coating perspective, a topic explored in Chapter 5. Although the beads used in these experiments were not of pharmaceutical grade, they were appropriate for the purposes of illustrating the concept of ion-exchange and investigating the feasibility of coating the beads using Wurster coating, which typically requires larger quantities of material for processing relative to those used for loading studies utilising the batch-method approach. As no pharmaceutical grade beads were available in similar sized quantities, the focus centred on the use of the Amberlite® IR120 range. The resulting DRCs, when extensively characterised displayed no discernible differences in solid-state form relative to the DRCs formed using IRP69. The dissolution data presented highlighted the feasibility of using the bead-type DRCs as an alternative to the powdered systems based on the notable disparity in drug release behaviour in ionic and deionised media. Rapid release of the drug characterises the profiles of the samples studied in ionic media, whereas the limited drug release in DI H_20 shows effective ionic complexation between the API and resin. Again, the solid-state analysis suggests the drug is molecularly dispersed within the resin matrix, as is evident from the lack of signals of crystalline

material in the pXRD and DSC data. The only difference relative to the powdered systems is the inability to detect the T_g of the amorphous TZD loaded onto the resin, a likely consequence of the reduced loading achieved.

6.2 Investigation of alternative resins and methods of production (spray-drying) to produce drug-resin complexes (DRCs)

6.2.1 The investigation of alternative resins to ionically bind to TZD HCl

Alternative powdered resins were explored in Chapter 4 with the intention of further understanding the effect that the resin structure/properties can have on the resultant DRC's performance. Similar to the void in the literature regarding comparative studies investigating the interaction of APIs with resins available in different physical forms, little evidence could be found in the literature comparing the complexation of an API with resins classed as "strong" and "weak". The loading studies revealed that the "weak" cation exchangers require more care, owing to their pH-dependent dissociation properties, to ensure both drug and resin are ionised, a prerequisite for ionic complexation. This contrasts with the "strong" resins explored in Chapter 3 which are ionised across virtually the entire pH range, which simplifies the loading procedure. Initial trials which formed a DRC using the "weak" carboxylic acid (Amberlite™ IRP64) and an unadjusted drug solution yielded disappointing drug loading results which translated to poor dissolution performance in DI H_2O, highlighting the challenge posed by the differing dissociation properties of TZD HCl and IRP64. In that instance, the pH of the loading solution was approximately 4, meaning it was unlikely that the resin was ionised to any appreciable extent. This particular resin requires the pH to be 5 and above for appreciable ionisation. When the pH of the loading solution was increased using different buffering systems, statistically significant differences in drug loading could be observed with a maximum loading value (24% w/w) obtained at pH 7. This finding illustrated that prioritisation of the resin being fully dissociated should take precedence over ensuring the API is fully dissociated.

A further finding from the loading studies pertained to the kinetics of the loading process, which revealed that altering the loading conditions greatly impacts the rate at which equilibrium is achieved, signifying that a multitude of competing and interrelated processes contribute to the overall kinetic profile produced. The primary purpose of utilising "weak" resins in commercial products is to taste-mask an API, and relies on the ability of the DRC to resist the desorption of the loaded drug at high pH values, such as those found in the mouth (118,119). However, the same DRC (TZD HCl and IRP64) exhibits contrasting behaviour at low pH due to the hydrogen ions' affinity for the functional groups attached to the polymeric backbone that contains the bound drug ion. This dichotomy is illustrated in both the drug release studies and, to a lesser extent, the loading studies, which are achieved using 0.1 M HCl and 0.1 M NaCl/pH 6.8 phosphate buffer. At low pH, the DRCs exhibit rapid release

characteristics relative to the higher pH environment, represented by a stark difference in the release kinetics (100% drug achieved after 15 minutes in 0.1 M HCl versus 60 minutes in either 0.1 M NaCl or pH 6.8 phosphate buffer), in line with many publications documenting the use of "weak" resins (313,314,319). Assay studies comparing the use of an aqueous acidic solution versus salt solution are less numerous, but this work demonstrated that the salt solution was a slightly more inefficient displacement agent relative to the acidic solution. It was interesting to note that all DRCs suffered from the drawback of undesirable high drug release (42-69%) in DI H_2O, the key measure of a DRC's effectiveness, pointing to the systems requiring extensive refinement.

The inclusion of Amberlite® IRP88 in the loading solution produced interesting results, which were apparent immediately after its addition to the drug solution, signalled by a distinct yellow colour during the batch processing method. This was unexpected as the material differed from Amberlite® IRP64 resin solely based on the nature of the counterion which is a potassium ion in IRP88, rather than a hydrogen ion. Consultation of the literature was not fruitful, with little evidence reporting drastic changes in the appearance of the loading solution and none comparing the incorporation of the IRP64 and IRP88 grades, never mind any issues associated with either one. After careful consideration of the possible options that could help explain the observations, it was hypothesised that the addition of the resin material to the drug solution was causing a change to the chemical form of the drug. This hypothesis was tested using simple pH measurements which provided evidence that this process may be causing a chemical change to TZD HCl, most likely the formation of the free base of the compound, as the pH of the loading suspension is raised to a value (pH 8.15) that could potentially generate the free base form, prior to the API having the opportunity to bind to the resin. This free base is incapable of binding to the resin as it is not protonated and also exhibits far lower solubility relative to the salt which explains the drug precipitation observed. Interestingly, despite the major issues encountered during the DRC formation process, the drug assay values revealed drastically improved drug loadings (approximately 48.3% w/w for each system) for the IRP88-based DRCs, with the exception of the 1:2 ratio, relative to the IRP64-based DRCs produced using equivalent D:R ratios. However, this does not translate to the improved dissolution performance, instead, the contrary and occurs as little evidence of an ion-exchange effect is apparent from dissolution profiles at a variety of pH values, pointing to an inferior performance relative to the IRP64-based DRCs.

In contrast to the role of the thermal and pXRD analysis in the characterisation of the sulfonic-acid containing DRCs, these techniques proved invaluable in further elucidating the interaction between TZD HCl and the "weak" resins. Using a combination of physical mixtures and crudely formed free base material, both techniques lent further weight to the assertation that the formation of the free base is occurring (in the case of the IRP88 grade) due to the presence of a significantly depressed melting

point relative to that of the crystalline melt of the hydrochloride salt. It is widely accepted that free base compounds have a lower melting point than their salt counterparts and it was found that the melting point of the crudely formed free base matched that of the residual material present in the IRP88 complex and was in agreement with the value reported for the free base material in the literature (381). The potential of resin incorporation to impact the form of the drug is an area that remains under-investigated; thus this work represented one of the first forays into the investigation of the impact of appropriate resin selection on drug stability prior to drug-resin binding.

6.2.2 The investigation of the spray-drying technique to produce TZD-IRP69 complexes

The other main focus of Chapter 4 was the examination of an alternative processing method more suited to pharmaceutical scale up than the batch loading method. At the outset of the project, spray-drying of the DRC as a method of formation has only been reported in two other publications to the best of the author's knowledge (94,220). In both of these publications, the authors extensively characterised their systems but limited information was reported regarding the suitability of the drug-resin combination for the process. The advantages of spray-drying are well documented in terms of speed, reproducibility and ability to tailor the properties of the final product by varying the process and formulation factors (382). Furthermore, the process is very much suited to scale up, which is a distinct advantage compared to the filtration and drying process that follows conventional batch processing of the DRCs. Therefore, this study differentiated itself from those performed previously, which used Tulsion™-355 and Amberlite™ IRP64, on the basis of using Amberlite™ IRP69, and the comparative aspect of the work which serves to highlight the differences between spray-dried and batch-produced DRCs.

Initial studies aimed at establishing if the process was viable and if sedimentation within the feed tube would prove problematic, due to the feed being a suspension. A second main objective of the preliminary trials was to generate a product for evaluating the dissolution behaviour in addition to physicochemical characterisation which would enable a comparison to the DRCs produced using the more traditional batch method. A reasonable powder yield (approximately 30-59%) enabled these goals to be realised and resulting DRCs exhibited differing drug release behaviours in ionic media versus DI H_2O, illustrative of an effective ion-exchange based system. However, these encouraging results were not generated without several issues that went previously unreported in the literature, such as the considerable sedimentation within the feed tube that was observed along with the appearance of powder in the vessel below the drying chamber, with the former being largely alleviated using faster feed rates.

Thermal and pXRD analyses again proved useful as part of the characterisation of the spray-dried DRCs as they highlighted the first drawback unique to the process. This related to the presence of the unreacted drug in the spray-dried product which would typically have been removed during the washing step after the filtration process that forms part of the batch method. Secondly, the pXRD diffractograms showed an intense peak that did not correspond to crystalline TZD HCl. Upon further examination of the ion-exchange reaction, it was shown to be sodium chloride (NaCl), a by-product of the reaction, which is not relevant to the batch-produced DRCs as it too would be removed as part of the washing step. On the basis of both of these findings, the effect of a washing step performed post-spray-drying was investigated, and the resulting solid-state characterisation of the washed product revealed no evidence of residual crystalline API material and NaCl. The main finding stemming from the drug release studies related to the extent of incomplete release being exacerbated in the case of the spray-dried systems, signifying that the spray-drying process does have a pronounced influence on the release process that requires further investigation.

Due to the large number of factors to be considered as part of the spray-drying process in addition to the novelty of the approach, a DoE approach was employed in an attempt to gain insight into the relevant factors that have the largest influence on the performance of a spray-dried DRC product. Although the Taguchi design is limited from the perspective of gleaning information regarding the interactions between independent valuables, it is useful for examining the effect of many different variables that otherwise would require a large number of experiments, materials and time (332). Influenced by issues flagged during preliminary studies, different nozzle sizes were employed aimed at investigating which was most appropriate for spray-drying a high concentration of suspended material. The largest nozzle size (2 mm) was found to be most suitable, as two of the runs that formed part of the Taguchi design and required the use of the nozzle with the narrowest diameter (0.7 mm) failed, signifying that the larger nozzle was a more appropriate choice. The results of the Taguchi screening study design highlighted the importance of feed rate, the ratio of drug to resin in the loading medium, aspirator setting and the atomisation airflow on the selected responses, which were powder yield, median particle size (d_{50}) and moisture content

6.3 Suitable unit processes for manufacturing sustained-release formulations comprising IERs

The work reported in Chapter 5 focused on using a series of techniques to formulate a sustained-release system containing TZD HCl. The primary aim of the work was to produce a coated DRC system with a sustained-release profile over 24 hours that had the potential to be formulated as a liquid product. The work built on the extensive studies reported in Chapter 3 that identified both Amberlite® IRP69 and Amberlite® IR120 as suitable carriers, worthy of further development work. The powdered

DRC system (Amberlite® IRP69) was initially examined as an option to achieve the intended release profile. Due to the fine particle size of the DRCs, which precluded the use of the Wurster coating process, it was decided that a granulation approach was appropriate prior to coating the particles to avoid the well-documented issues associated with coating fine particles (164). To the best of the author's knowledge, fluidised bed granulation (FBD) has not been utilised to produced granules comprising IERs, despite the technique growing in popularity over recent years. Compared to more conventional systems, IERs presented difficulties regarding granule formation until it was established that a large amount of PVP which acted as a binder was necessary to form the granules. This was found after systematic "trial and error" experimentation that encompassed a wide range of binder concentrations and varying the mode of binder inclusion. Including the binder with the solid resin contents within the fluidised bed chamber prior to the spraying of granulating liquid was a suitable approach based on the particle size measured, which showed a statistically significant increase in granule size as the PVP concentration was increased, which was verified by SEM imaging.

Due to the troublesome nature of the process and the fragile nature of the granules, an alternative method of granulation was trialled using sieve screening, similar to the wet granulation methods reported in the patent literature (103). Again, the results of particle size analysis and SEM imaging supported granule formation using "blank" resin in addition to a demonstrated improvement in flow properties relative to the resin raw material. Preliminary coating trials were performed using this granulated material but issues were encountered (sticking of the material to the walls of the chamber which could not be overcome) when granules containing drug-loaded DRC were substituted into the coating process, an issue that did not arise during the coating trials using the "blank" granules formed by wet granulation. These issues proved to be insurmountable and, due to the finite supply of drug-loaded material, prompted the investigation of alternative methods to produce an IER-based sustained-release TZD HCl formulation.

Stemming from the unsuccessful trials with the powder IER form, drug-loaded resin in the bead form (using Amberlite® IR120 resin) was selected for the development of a model formulation to keep the project progressing. As part of Chapter 3, the bead-type IER had been established as an alternative to the powdered form and it is more suited to the Wurster coating process, evident from numerous publications in the literature that utilise the technique to coat DRCs, albeit at a far larger scale (129,164,178). For smaller sized batches, solvent evaporation and emulsion coacervation are methods used to coat DRCs but these methods have their own drawbacks and were not considered as viable options to produce coated systems that had the potential to be scaled up (89,132). The area of coating microparticles at a 5 g or less scale using the Wurster coating technique remains a thoroughly underinvestigated area and this work aims to address the challenges presented by IERs and coating at

such small-scale. Initial studies using “blank” resin beads as a surrogate indicated that aqueous-based coating systems were unsuitable for coating ion-exchange beads due to a combination of sedimentation problems within the feed tube, fluidisation issues and agglomeration tendency of the beads. The latter is perhaps unsurprising in light of the hygroscopic nature of the beads. Having said that, several examples in the literature exist illustrating the effectiveness of aqueous-based dispersions for coating the bead-type resins, so a more likely reason for the issues encountered is the limitations associated with the lab-scale spray coater used and batch size used (178,345). Despite the vast majority of runs being unsuccessful, it was found, using an iterative approach, that the incorporation of the organic solvent when diluting down the contents of the aqueous dispersion prior to spray-coating produced several runs that were not considered complete failures i.e. scarce evidence of sedimentation and no evidence of agglomeration or fluidisation issues. As this defeated the purpose of using an aqueous dispersion, which is the preferred option for environmental and safety reasons, as well as possibly compromising the stability of a colloidal aqueous dispersion, this tactic was discontinued and the use of an organic solution containing the coating polymers was explored instead

Although less popular due to environmental concerns nowadays, organic solutions of polymers are still available and have a demonstrated history of success when it comes to Wurster coating (184,196). The use of pH-dependent polymers, specifically Eudragit® L100 and Eudragit® S100, as part of the coating process generated drug release data that was promising. However, there was a consistent drug release over the course of 24 hours in a dissolution medium where the pH environment was acidic initially (first 2 hours) before being increased for the remainder of the experiment (6.5-7.4). This occurrence highlighted deficiencies in the coating, or the possible rupturing of the coating in solution (due to resin swelling), as enteric coatings if complete and robust would be expected not to release the drug in acidic environments, which were the conditions used for the first two hours of dissolution studies. However, these spray-coating runs were free from any of the issues encountered during the trials that used the aqueous coating dispersions, which indicated that the choice of coating system was critical to ensuring the effective coating of the DRCs.

Of all the polymers tested as potential coating agents, the pH-independent polymers, Eudragit® RS and Eudragit® RL, produced the most encouraging results from the outset. “Blank” beads were first trialled with the Eudragit® RS grade as a means of identifying suitable processing parameters to avoid wasting valuable drug-loaded material. Dissolution studies revealed that coating solutions containing Eudragit® RS at a concentration of greater than 5% w/v coated the beads with too thick a layer of polymer so that the drug could not be detected in the dissolution media until the latter stages of the experiment. Considering that the polymer is a pH-independent one with low permeability, this finding

pointed towards the need to use lower concentrations of Eudragit® RS and/or the Eudragit® RL grade which is classed as a highly permeable polymer. Through a series of methodical experiments, the impact of lower concentrations of Eudragit® RS in the coating solution was assessed and revealed the suppression on the drug release imparted by the polymer layer could be amended by using more dilute coating solutions. Similar trial experiments as part of method development using unloaded resin were conducted to help construct a design space for both the Eudragit® RL and Eudragit® RS grades, and facilitated the avoidance of drug-loaded material being wasted.

The dissolution results performed using the samples coated with Eudragit® RL illustrated that the difference in permeability conferred by the increased level of quaternary ammonium groups drastically influenced the drug release kinetics of the coated DRCs. Higher concentrations of polymer in the coating solution were required relative to the low permeability polymer (Eudragit® RS) to achieve a similar level of release at an identical timepoint, thus highlighting the opportunity to fine-tune the release of the drug-loaded beads. Further to this point, on occasion, these polymers are used together as a blend to achieve the desired release profile for a particular formulation in question, a common tactic explored by many other research groups (186,383). This work revealed that control over the release could be achieved by altering the ratio of the components in the blend, with the higher proportion of Eudragit® RL, leading to a faster release relative to those systems coated using solutions comprising higher concentrations of the RS grade. Solid-state characterisation of all samples studied revealed the absence of crystalline API material indicating that processing conditions do not cause reversion to the crystalline state. It is important to highlight that the release profiles of DRCs coated using coating solutions comprising either Eudragit® RL (0.5% w/v) or Eudragit® RS (0.25% w/v) do resemble that of the DRCs coated using Eudragit® L100 (pH-dependent polymer), however considering the fact that the latter is supposed to afford protection against premature drug release in acidic media, a decision was made to pursue the pH-independent polymers in future studies, discussed below.

The incorporation of several different plasticisers into the process provided varied results after extensive method development and illustrated the importance of correct plasticiser selection to not compromise the integrity of an already well-performing system. Initial trials revealed a suitable ratio of dibutyl sebacate or triacetin to polymer in the feed solution which permitted the coating of beads with either grade of Eudragit® without the tendency to agglomerate. Drug release studies and examination of the surface of selected samples revealed a roughened surface which is uncharacteristic of successful plasticiser incorporation and is consistent with the increased release observed from the systems, possibly suggesting the unsuitability of the plasticisers. The incorporation of TEC into the coating solution produced results that were more in line with what is expected of plasticiser inclusion.

The drug release from the coated DRCs that included TEC appears further retarded (relative to the use of Eudragit® polymer alone), the degree to which was dependent on the concentration of plasticiser in the coating solution. The final element of this work investigated the impact of curing on the drug release and revealed that curing could further influence the rate of drug release, depending on the concentration of plasticiser used in the coating solution and the duration of curing.

Short-term stability studies were also performed as part of Chapter 5. Select samples that exhibited the target sustained-release profile over 24 hours in addition to the uncoated complex were placed on long-term stability (25 °C/60% RH and 25 °C /<10% RH) for 6 months and assessed periodically. All five samples showed no evidence of API recrystallisation at either condition studied based on DSC and pXRD analysis over the timeframe studied. Evidence in the literature of DRCs' solid-state stability is limited and generally short-term (less than one month), so these results are encouraging and highlight the excellent stability profile of the "dry" DRCs. Drug release testing performed on selected "dry" microparticles placed on stability over a three-month period revealed a deterioration in product performance for the samples exposed to the higher RH, evident from the faster release over the timeframe studied. This is common to both of the coated samples (using coating solutions comprising 0.25% w/v Eudragit® RS and 0.5% w/v Eudragit® RL) but more pronounced in the case of the DRC coated with the more water-permeable polymeric layer (Eudragit® RL) which signified that the more hydrophobic polymer confers greater protection against moisture. Furthermore, the integrity of the coating appears to be more compromised the longer the samples are placed on stability (at high RH), reflected by the lower sustained-release effect imparted by the coating. The lower control afforded by the polymeric membrane surrounding microparticles subject to the higher humidities can be partially explained by consideration of SEM analysis results which revealed that the polymeric layer appears to be still intact, however, relative to the sample stored at a lower humidity condition, there does appear to be some notable differences in microparticle appearance, most notably a roughened surface which is likely to be responsible for the differences observed in the release profile. Fortunately, the chemical stability studies performed on the samples stored for 3 months indicate that they retain their potency and are devoid of degradation products. Overall, the stability studies revealed that the coated microparticles are most suited to being stored in drier conditions, which can be ascribed to their tendency to swell at higher RH as well as the ability of their polymeric coatings to absorb moisture which may compromise their ability to modulate the release of the API.

Trials aimed at selecting a suitable suspending agent and concentration established that xanthan gum at a concentration of 0.5% w/v provided adequate suspension and was used in the subsequent drug leaching studies and dissolution trials. Despite the overall release profile of certain other (coated DRC systems (coated using pH-dependent polymers) not differing substantially from those selected (DRCs

coated using pH-independent polymers), it was decided to pursue the idea of suspending the DRCs coated using the pH-independent polymers at the selected concentrations due to concerns over the release of the API from the enteric coated systems in acidic environments. Drug leaching studies performed over the course of one month at weekly intervals revealed that the formulation was unsuitable for a multidose formulation in its current form due to the low levels of drug leaching (approximately 5%) that were detectable after one week. These observations were consistent across the three formulations tested (DRC coated with Eudragit® RS, DRC coated with Eudragit® RL and uncoated DRC). These findings prompted drug leaching studies to be performed at daily intervals from T_0, and revealed that drug that has leached into the liquid vehicle is detectable from day 1 and progressively increases over the course of the study. Drug release studies performed using the constituted suspensions (with coated DRCs held in a 0.5% w/v xanthan gum vehicle) revealed that the release profile of the coated DRCs was markedly different relative to equivalent systems in the "dry" microparticle form after 2 and 4 weeks of storage. This contrasts with the T_0 timepoint where no discernible difference is evident, which is not surprising considering the deterioration in sustained-release performance of the aged samples is attributed to the increased permeability of the polymeric layer over time during in-liquid storage which does not have the chance to occur at the T_0 timepoint. These results show that the formulation does not perform as well as certain coated DRC samples reported in the literature (117) but it is by no means the worst system either, compared to those that have been shown to rupture after one day's storage in aqueous media (127). Despite the level of sustained-release being diminished, which occurs progressively over time, the release profile is reflective of a system that still is largely surrounded by a polymeric membrane, which is supported by the SEM imagery.

6.4 Main findings of the thesis

The research constituting this thesis can be summarised as a number of key findings which are listed below.

- The successful loading of drug in appreciable levels onto an IER is heavily dependent on the properties of both the drug and resin.
- Spray-drying is an effective alternative method for the production of DRCs compared to the batch process, but requires several simple alterations to ensure no undesirable by-products are retained in the spray-dried material.
- Coating of drug-loaded complexes is necessary to achieve an appreciable level of control on the drug release from the DRCs, in line with the aims of the project.
- The incorporation of excipients ranging from polymers to plasticisers had a significant impact on the drug release and tackiness.

- Coating of IERs at a small-scale in a fluidised bed coater was possible, with high permeability pH-independent polymers, offering the best control of drug release in line with the aim of the project.
- The “dry” DRC microparticles (coated and uncoated) were physically and chemically stable systems at the conditions used (25 °C/60% RH, and 25 °C/<10% RH) over the timeframe studied (6 months).
- The sustained-release character of coated DRCs stored in an aqueous liquid vehicle became compromised over time, a likely consequence of the tendency of the API to leach into the liquid storage vehicle.

6.5 Future work

Arising from the results reported in this work are a number of future possible areas to explore which can further aid in the understanding of the API-resin interaction as well as helping to develop an age-appropriate formation. These ideas are listed below.

- Investigate the “column” method as a means to load the drug onto the resin, preferably the bead form. This method has reported to be a more time efficient method of loading relative to the batch-method but fine-sized powders do not lend themselves well to the process (95).
- Scale-up of the Wurster coating process using pharmaceutical grade approved ion-exchange beads.
- Investigate solid-state characteristics of coated DRCs that included talc among the coating suspension contents.
- Explore the use of an alternative liquid storage vehicle such as a medium-chain triglyceride to investigate if the drug leaching into the medium can be minimised and dissolution performance improved.
- Investigate the feasibility of minimising drug leaching by altering the pH of the liquid storage vehicle, in which DRCs coated using the pH-dependent polymers are suspended, with a view to reducing polymer dissolution/porosity.

Appendix 1

1.1 Metronidazole (MTZ)

Table 1. Liquid stability of MTZ over a 24 hour time period at various pH values.

Time	pH 0.6	pH 0.9	pH 1.6	pH 2.6	pH 3
0	100.09 ± 0.06	100.02 ± 0.06	100.02 ± 0.04	100.04 ± 0.08	100.02 ± 0.09
12	100.04 ± 0.01	100.02 ± 0.04	100.01 ± 0.08	100.08 ± 0.09	100.04 ± 0.09
24	100.02 ± 0.05	99.99 ± 0.09	100.06 ± 0.02	100.01 ± 0.04	100.03 ± 0.09

Table 2. Comparison of powder yields of the resinates produced using different drug loading solution pH values (prior to the addition of IRP69). The resinates were formed using "unactivated resin" and a 1:1 D:R ratio (w/w) unless otherwise stated.

Sample	Powder yield (%)
0.6	48.75 ± 0.45
0.9	49.37 ± 0.36
1.6	52.85 ± 0.29
1.6	53.81 ± 0.78
2.6	51.60 ± 0.93
3.0	49.23 ± 0.54
1.6 ("activated")	56.71 ± 0.48

1.2 Tizanidine HCl (TZD HCl)

Table 3. Comparison of the influence of the total quantity of starting raw materials (TZD HCl and IRP69) on the calculated powder yield for the DRC formed using (1:1 D:R ratio) (w/w)("unactivated" resin).

Total quantity of starting raw materials (mg)	Powder yield (%)
200	79.50 ± 1.50
500	81.06 ± 0.26
1000	82.00 ± 0.35
2000	83.00 ± 0.65
5000	83.50 ± 0.35

Table 4. Calculated drug loading (% w/w) values for the 1:1 (w/w) D:R ratio (IRP69) as part of the optimisation of the drug loading assay studies. Optimisation required the variation of the concentration of complex in the displacement medium, the displacement medium used and the temperature and ionic strength of the displacement medium.

Concentration of complex in displacement medium (mg/mL)	Displacement medium	Molarity of displacement medium (M)	Temperature of displacement medium (20 °C)	Temperature of displacement medium (37 °C)	Temperature of displacement medium (50 °C)
			Drug loading (% w/w)		
0.056	HCl	0.1	50.20 ± 1.98	50.34 ± 1.58	50.05 ± 1.78
0.111	HCl	0.1	47.28 ± 0.03	48.32 ± 0.37	49.81 ± 0.97
0.222	HCl	0.1	43.95 ± 0.08	44.25 ± 0.08	44.80 ± 0.20
0.741	HCl	0.1	34.38 ± 0.77	36.38 ± 0.53	38.38 ± 0.93
1.000	HCl	0.1	32.29 ± 1.05	33.19 ± 0.99	33.99 ± 1.77
0.056	HCl	0.5	50.20 ± 1.30	50.10 ± 1.12	50.25 ± 1.31
0.111	HCl	0.5	47.23 ± 0.76	50.40 ± 1.78	50.86 ± 1.97
0.222	HCl	0.5	44.45 ± 0.48	45.25 ± 0.58	45.80 ± 0.65
0.741	HCl	0.5	35.18 ± 0.84	36.75 ± 0.39	39.47 ± 0.97
1.000	HCl	0.5	33.79 ± 1.80	33.99 ± 0.54	34.98 ± 1.34
0.056	HCl	1.0	49.90 ± 0.30	50.08 ± 1.07	50.15 ± 0.04
0.111	HCl	1.0	48.16 ± 1.21	50.51 ± 1.47	51.00 ± 1.76
0.222	HCl	1.0	45.35 ± 0.58	45.97 ± 0.82	46.80 ± 0.97
0.741	HCl	1.0	36.58 ± 1.44	39.55 ± 1.04	40.67 ± 0.76
1.000	HCl	1.0	34.19 ± 1.05	35.49 ± 0.34	36.48 ± 1.14
0.056	NaCl	0.1	47.48 ± 0.23	48.34 ± 0.70	49.21 ± 1.00
0.111	NaCl	0.1	47.18 ± 0.53	48.26 ± 1.97	49.41 ± 1.27
0.222	NaCl	0.1	43.45 ± 0.78	44.85 ± 0.28	45.02 ± 0.29
0.741	NaCl	0.1	34.98 ± 1.77	36.98 ± 0.73	38.88 ± 0.53
1.000	NaCl	0.1	32.59 ± 1.65	33.59 ± 0.49	34.39 ± 1.30
0.056	NaCl	0.5	49.31 ± 1.34	49.98 ± 1.12	50.15 ± 1.98
0.111	NaCl	0.5	49.06 ± 1.98	50.04 ± 1.88	50.45 ± 1.78
0.222	NaCl	0.5	47.23 ± 0.76	50.10 ± 1.48	51.46 ± 0.57
0.741	NaCl	0.5	44.85 ± 0.29	45.85 ± 0.88	46.80 ± 1.65
1.000	NaCl	0.5	36.18 ± 0.44	37.65 ± 0.99	39.67 ± 1.07
0.056	NaCl	1.0	48.91 ± 1.20	51.07 ± 1.90	51.09 ± 1.96
0.111	NaCl	1.0	48.66 ± 1.51	51.11 ± 1.47	51.19 ± 2.06
0.222	NaCl	1.0	45.95 ± 1.58	46.37 ± 0.82	46.80 ± 1.16
0.741	NaCl	1.0	37.58 ± 1.04	40.00 ± 1.64	41.67 ± 0.96
1.000	NaCl	1.0	34.79 ± 1.40	34.99 ± 0.94	35.48 ± 1.04

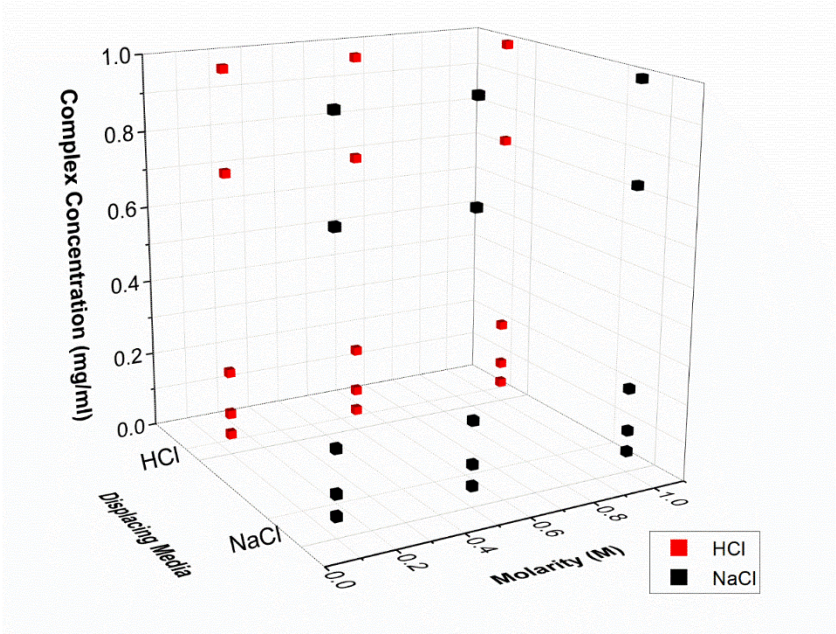

Figure 1. Design space for TZD HCl-IRP69 assay optimisation study.

Table 5. Liquid stability of TZD HCl raw material at room temperature over 24 hours in A) 0.1-1 M NaCl. B) 0.1-1 M HCl and DI H_2O

Time	DI H_2O	0.1 M HCl	pH 6.8 buffer	0.1 M NaCl	1 M HCl	0.1 M NaCl
0	100.09 ± 0.06	100.02 ± 0.06	100.05 ± 0.06	100.01 ± 0.06	100.06 ± 0.09	100.04 ± 0.11
12	99.99 ± 0.06	99.99 ± 0.06	99.99 ± 0.06	99.99 ± 0.06	99.91 ± 0.08	100.0 ± 0.03

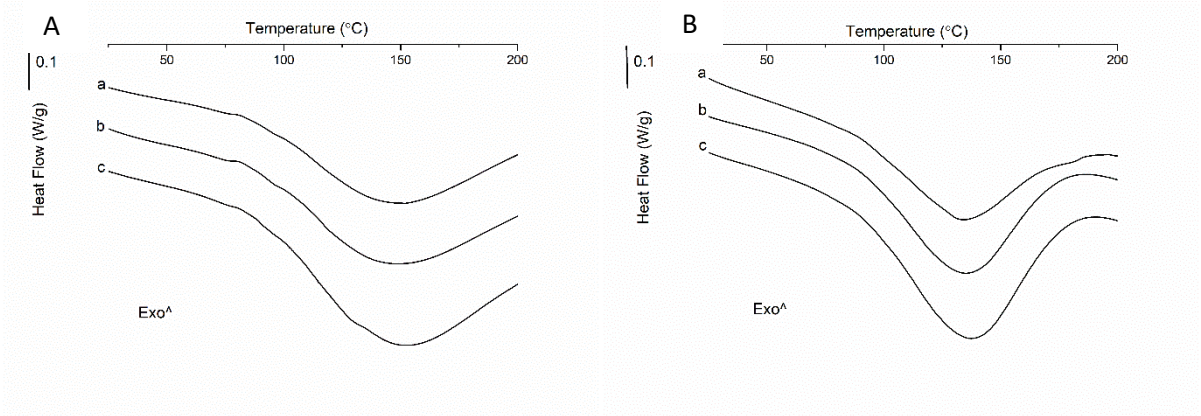

Figure 2. DSC thermograms of DRCs produced using various D:R (w/w) ratios. A) milled resin (IRP69) and B) "activated" resin (IRP69). a) 2:1, b) 1:1 and c) 1:2.

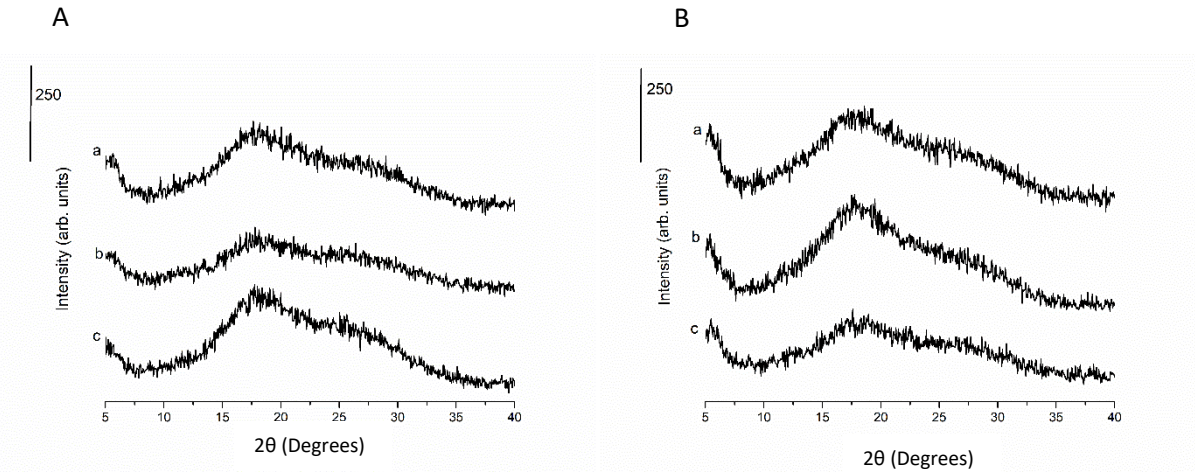

Figure 3. pXRD diffractograms of DRCs produced using various D:R (w/w) ratios. A) milled resin (IRP69) and B) "activated" resin (IRP69). a) 2:1, b) 1:1 and c) 1:2.

Table 6. Calculated drug loading values for the 1:2 ratio (w/w) (IR120) as part of the optimisation of the drug loading assay studies. Optimisation required the variation of the concentration of complex in the displacement medium, the displacement medium used and the temperature and ionic strength of the displacement medium.

Concentration of complex in displacement media (mg/mL)	Displacement media	Molarity of displacement media (M)	Temperature of displacement media (50 °C)	Temperature of displacement media (20 °C)
			Drug loading (% w/w)	
0.056	HCl	0.1	30.67 ± 1.06	30.88 ± 1.03
0.111	HCl	0.1	30.78 ± 1.56	30.08 ± 1.20
0.222	HCl	0.1	26.56 ± 0.25	26.86 ± 0.95
0.741	HCl	0.1	23.78 ± 0.69	23.98 ± 0.87
1.000	HCl	0.1	21.20 ± 1.02	21.25 ± 1.51
0.056	HCl	0.5	31.71 ± 0.98	31.11 ± 0.91
0.111	HCl	0.5	31.78 ± 1.96	31.70 ± 1.80
0.222	HCl	0.5	27.06 ± 0.65	27.21 ± 0.98
0.741	HCl	0.5	24.78 ± 1.69	24.31 ± 0.89
1.000	HCl	0.5	21.70 ± 1.52	21.75 ± 1.09
0.056	HCl	1.0	31.97 ± 1.02	31.27 ± 1.13
0.111	HCl	1.0	32.08 ± 1.56	32.10 ± 1.62
0.222	HCl	1.0	27.76 ± 1.65	27.45 ± 1.33
0.741	HCl	1.0	25.08 ± 1.39	25.22 ± 1.09
1.000	HCl	1.0	22.65 ± 1.42	22.63 ± 1.60
0.056	NaCl	0.1	30.50 ± 0.59	30.41 ± 1.70
0.111	NaCl	0.1	30.38 ± 1.26	30.80 ± 0.99
0.222	NaCl	0.1	26.96 ± 1.25	27.04 ± 1.05
0.741	NaCl	0.1	23.28 ± 1.69	23.20 ± 1.22
1.000	NaCl	0.1	21.04 ± 1.62	21.22 ± 1.08
0.056	NaCl	0.5	31.21 ± 1.46	31.08 ± 1.20
0.111	NaCl	0.5	31.48 ± 1.03	31.20 ± 1.41
0.222	NaCl	0.5	27.46 ± 1.65	27.26 ± 1.05
0.741	NaCl	0.5	24.98 ± 1.10	25.28 ± 1.31
1.000	NaCl	0.5	21.79 ± 1.22	21.89 ± 1.39
0.056	NaCl	1.0	32.29 ± 1.29	32.11 ± 1.35
0.111	NaCl	1.0	32.18 ± 0.54	32.80 ± 0.98
0.222	NaCl	1.0	27.66 ± 1.25	27.93 ± 1.29
0.741	NaCl	1.0	25.58 ± 1.90	25.72 ± 1.19
1.000	NaCl	1.0	22.95 ± 1.20	22.81 ± 1.73

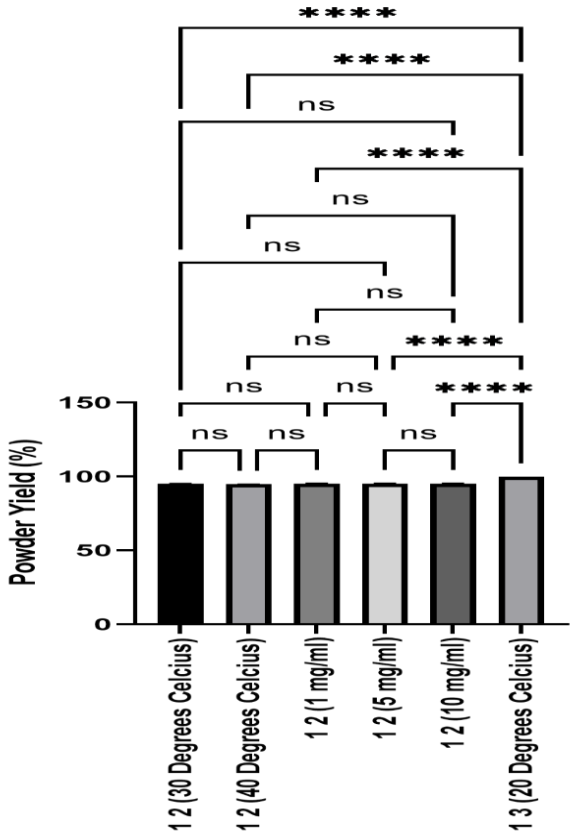

*Figure 4. Comparison of powder yield (%) values for DRCs produced using varying D:R ratios (w/w)(IR120) and using different drug concentrations and loading temperatures. The loading temperature and loading drug concentration are 20 °C and 10 mg/mL unless otherwise stated. NS signifies statistically insignificant and **** signifies statistically significant (p<0.0001).*

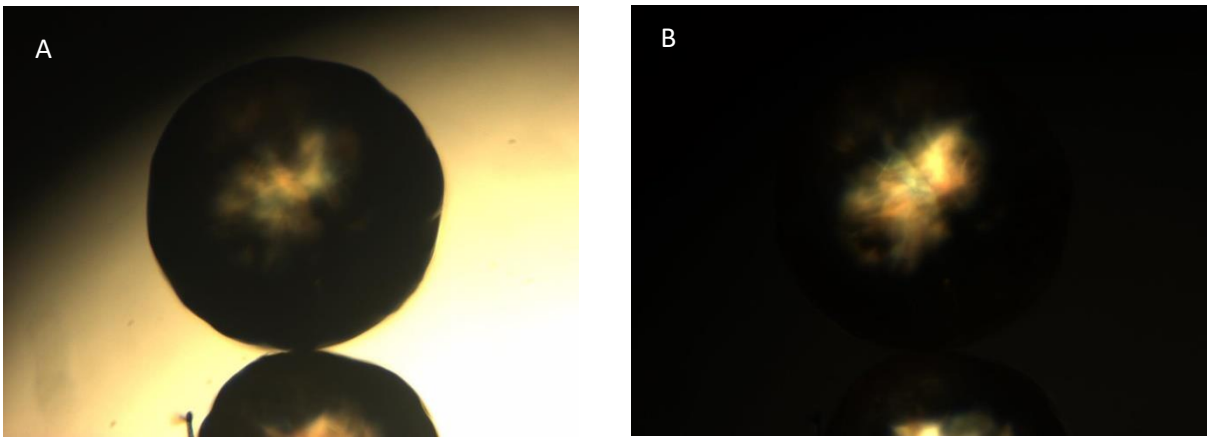

Figure 5. Optical microscope photomicrographs of DRC formed using a 1:2 D:R ratio (w/w)(IR120) using a) non-polarised light and b) polarised light.

Appendix 2

2.1 IRP64 and IRP88 studies

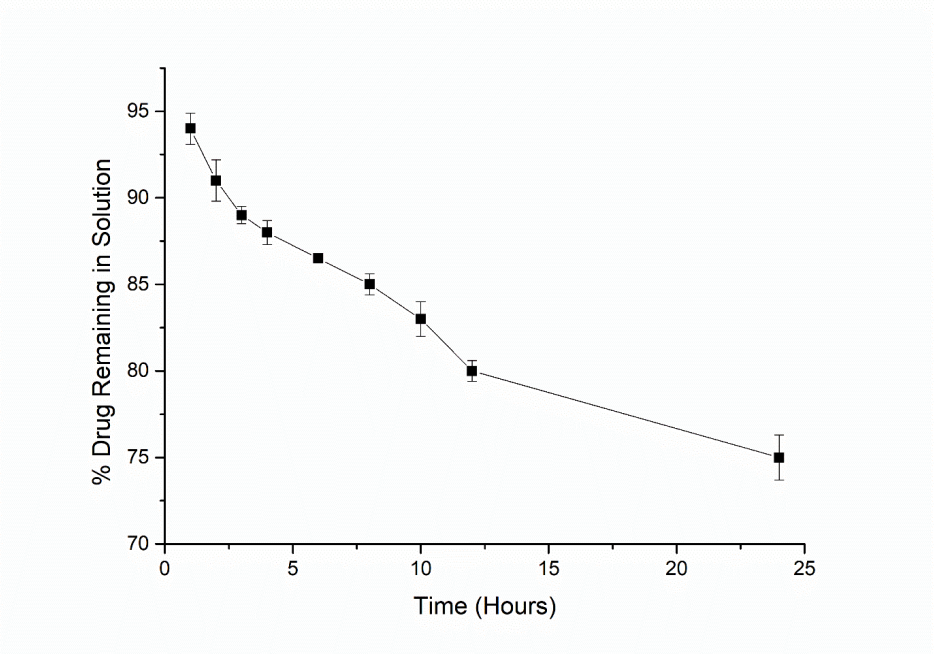

Figure 1. Equilibration profile showing the loading of TZD HCl onto IRP88 (1:1 D:R (w/w) ratio) over 24 hours at room temperature.

A B

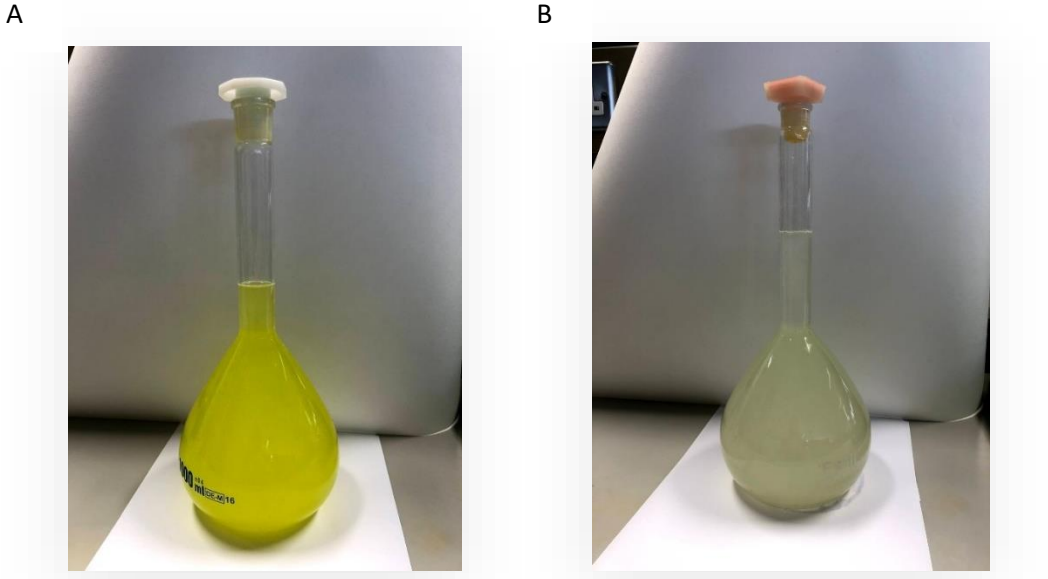

Figure 2. Image of loading medium containing A) 1:1 (w/w) D:R ratio of TZD HCl and IRP88 immediately post-addition of IRP88 and B) 1:1 (w/w) D:R ratio of TZD HCl and IRP64 immediately post-addition of IRP64.

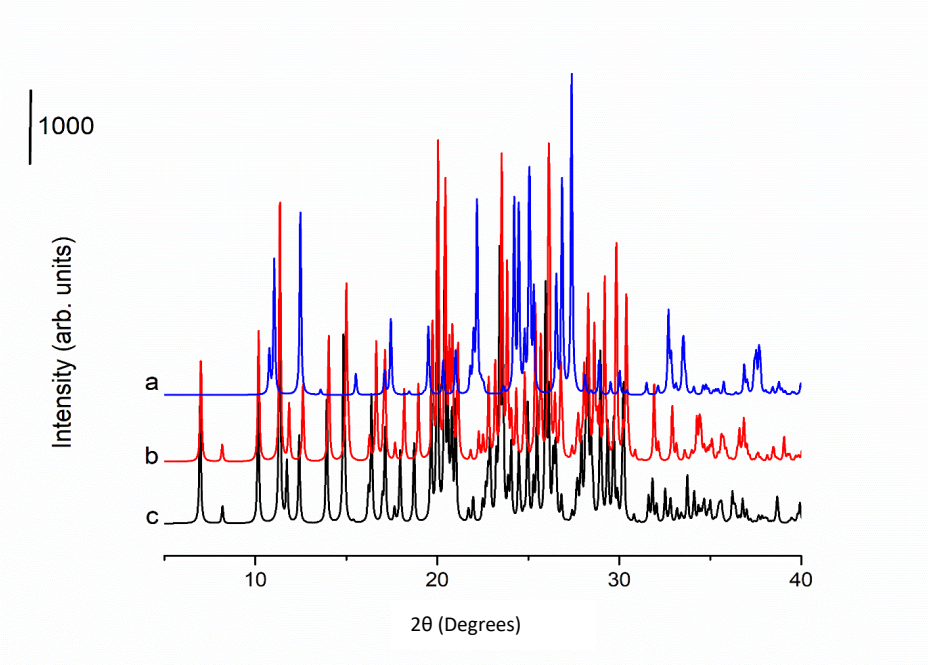

Figure 3. Calculated pXRD patterns available from the CCDC of a) TZD HCl, b) TZD Form II and c) TZD Form I.

Table 1. Comparison of equilibrium moisture uptake values of resin raw materials, TZD HCl raw material, TZD free base and the DRCs prepared using a 1:1 (w/w) D:R ratio (using either IRP64 or IRP88) at 90% RH after being subjected to stepwise increases in humidity starting at 0% RH after at 120 minute drying step as part of DVS analysis. For samples produced using a drug loading solution where the pH was adjusted prior to the addition of IRP64, the pH value of the adjusted solution is indicated in parentheses.

Sample	Moisture uptake (%) at 90% RH
IRP64	26.610
IRP88	78.990
TZD HCl	0.065
TZD Base	4.037
D:R (IRP88) 1:1	14.020
D:R (IRP64)(pH 5)	21.070
D:R (IRP64) (pH 6)	20.590
D:R (IRP64) (pH 7)	56.701

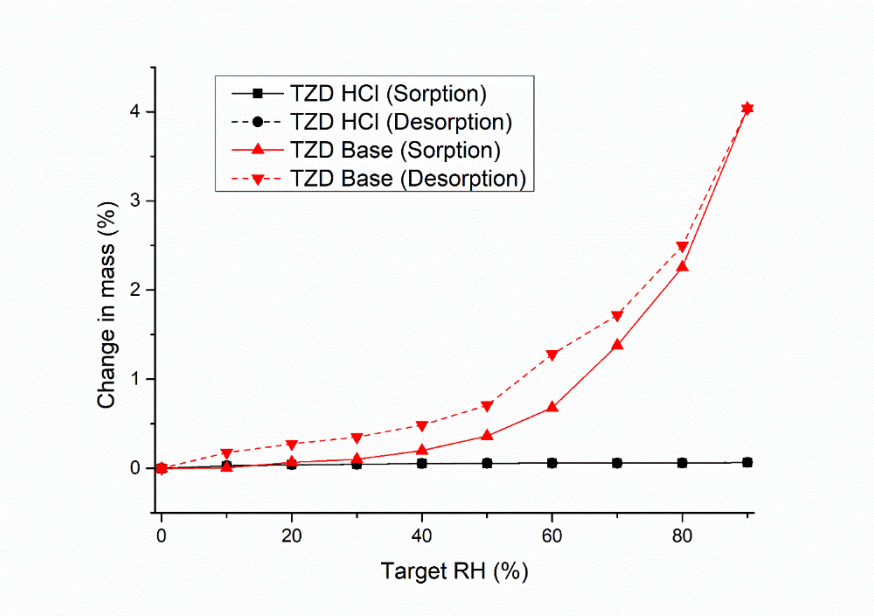

Figure 4. Vapour sorption and desorption isotherms of TZD HCl raw material and TZD free base.

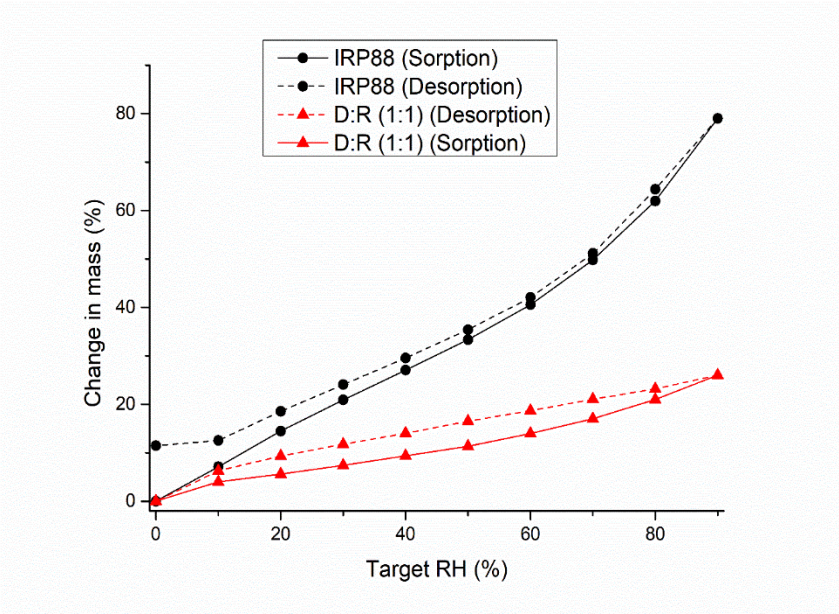

Figure 5. Vapour sorption and desorption isotherms of IRP88 raw material and resinate (formed using a 1:1 (w/w) TZD HCl:IRP88 ratio).

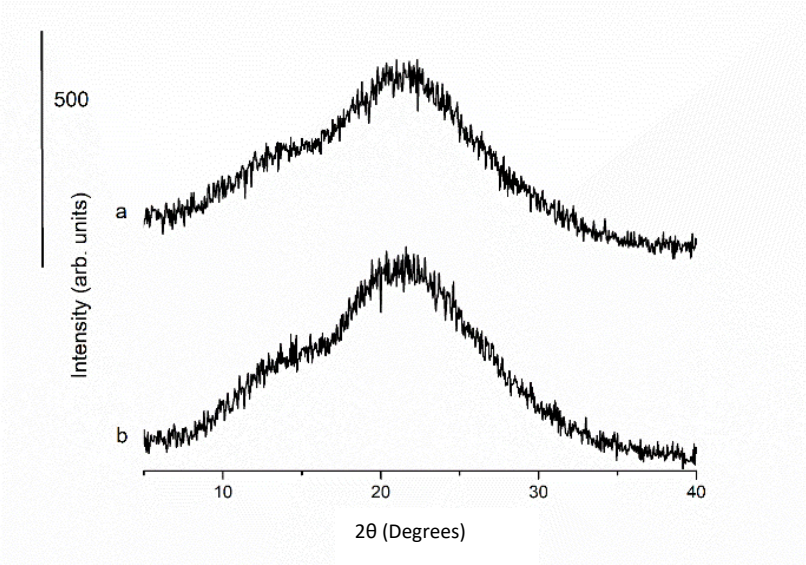

Figure 6. pXRD diffractograms of resinate formed using 1:1 (w/w) TZD HCl:IRP88 ratio. a) Pre-DVS analysis and b) Post-DVS analysis.

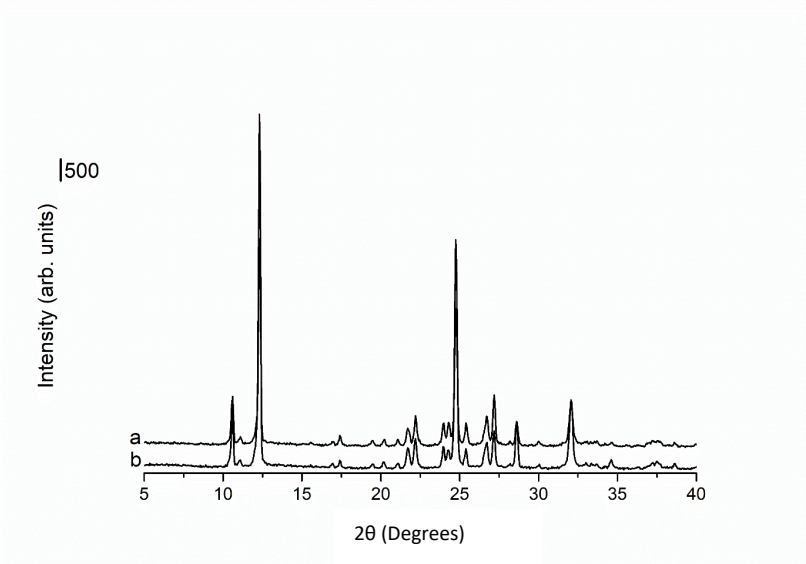

Figure 7. pXRD diffractograms of a) TZD HCl raw material (as received) and b) TZD HCl raw material (post-DVS analysis).

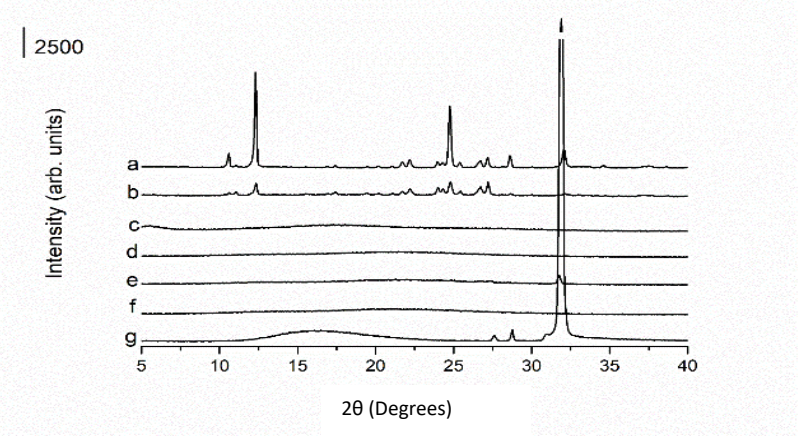

Figure 8. pXRD diffractograms of a) TZD HCl raw material, b) 1:1 (w/w) physical mixture of TZD HCl and IRP69, c) IRP69 raw material, d) spray-dried DRC (1:1 w/w D:R (IRP69) ratio) (washed post-processing), e) spray-dried DRC (1:1 w/w D:R (IRP69) ratio) (unwashed post-processing), f) batch-produced DRC (1:1 w/w D:R (IRP69) ratio) and g) NaCl raw material.

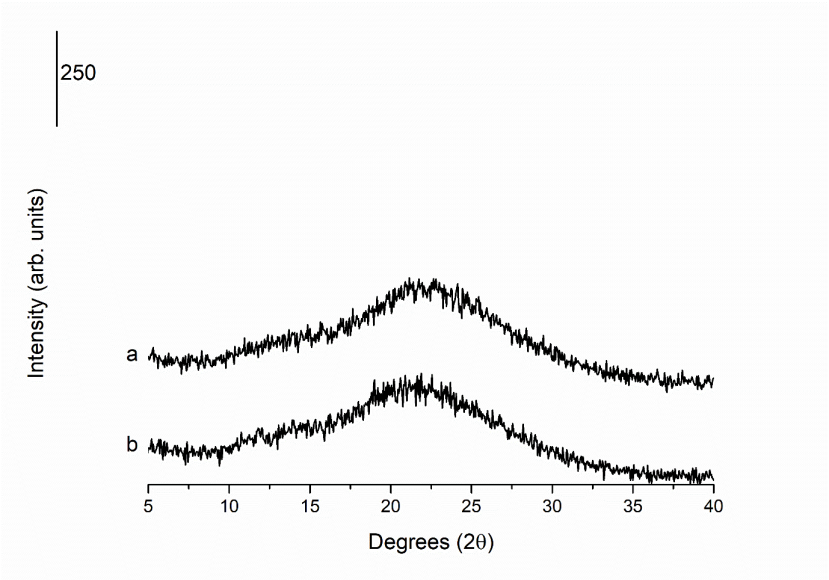

Figure 9. pXRD diffractograms of a) spray-dried DRC (1:1 w/w D:IRP69 ratio) (pre-DVS) and b) spray-dried DRC (1:1 w/w D:R ratio) (post-DVS).

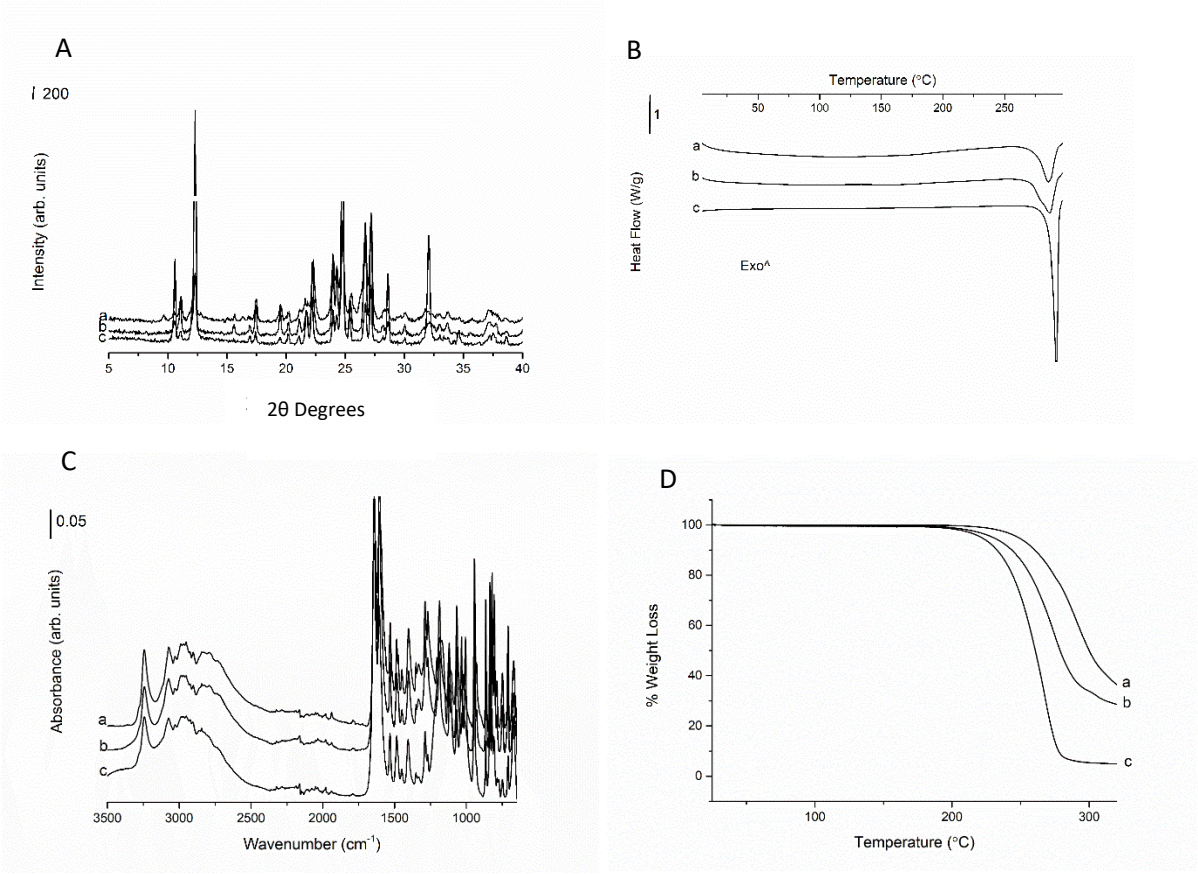

Figure 10. A) pXRD diffractogram, B) DSC thermogram and C) FTIR spectra showing a) spray-dried TZD HCl (using a 120 °C inlet temperature), b) spray-dried TZD HCl (using a 150 °C inlet temperature) and c) TZD HCl raw material (as received). D) TGA thermograms of a) TZD HCl raw material (as received), b) spray-dried TZD HCl (150 °C inlet temperature) and c) spray-dried TZD HCl (120 °C inlet temperature).

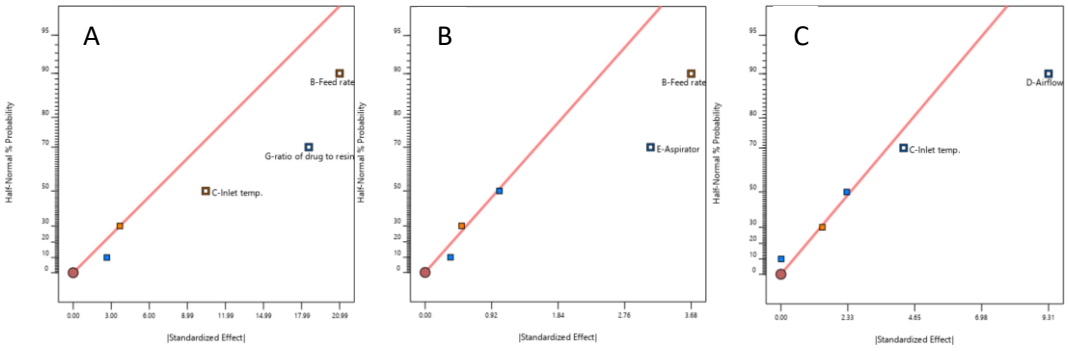

Figure 11. Half normal plots of A) powder yield (%), B) moisture content (%) and C) d_{50} (µm).

2.2 TZD HCl raw material studies

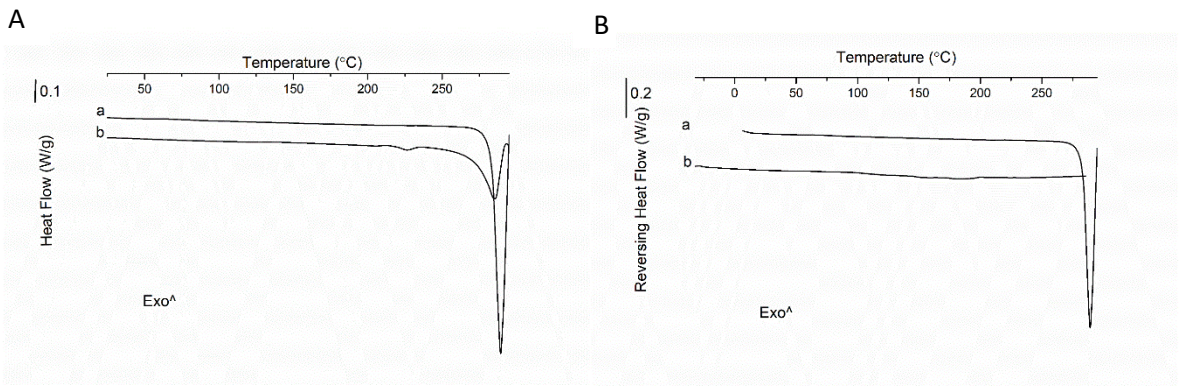

Figure 12. DSC thermograms of A) TZD HCl raw material a) as received and b) melt-quenched. B) TZD HCl raw material a) as received and b) melt-quenched in situ in the DSC instrument.

Appendix 3

3.1 Wurster coating studies

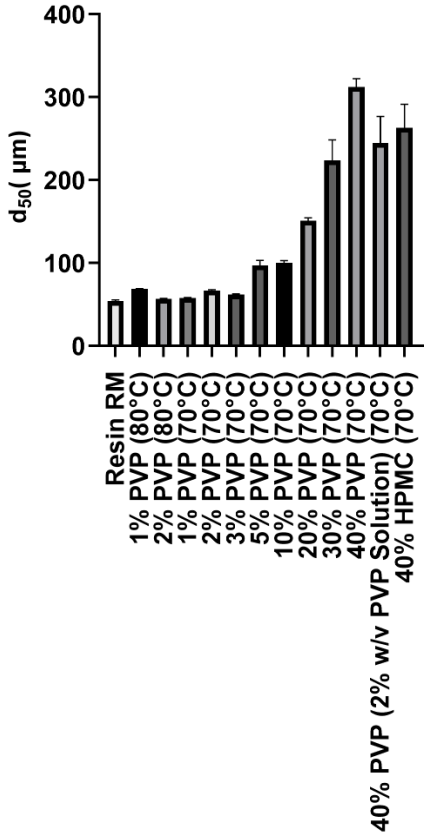

Figure 1. Comparison of the d_{50} values for IRP69 raw material and the granules formed using fluidised bed granulation and a series of different binder (PVP and HPMC) concentrations (% w/w). The binder was included in solid form unless otherwise stated.

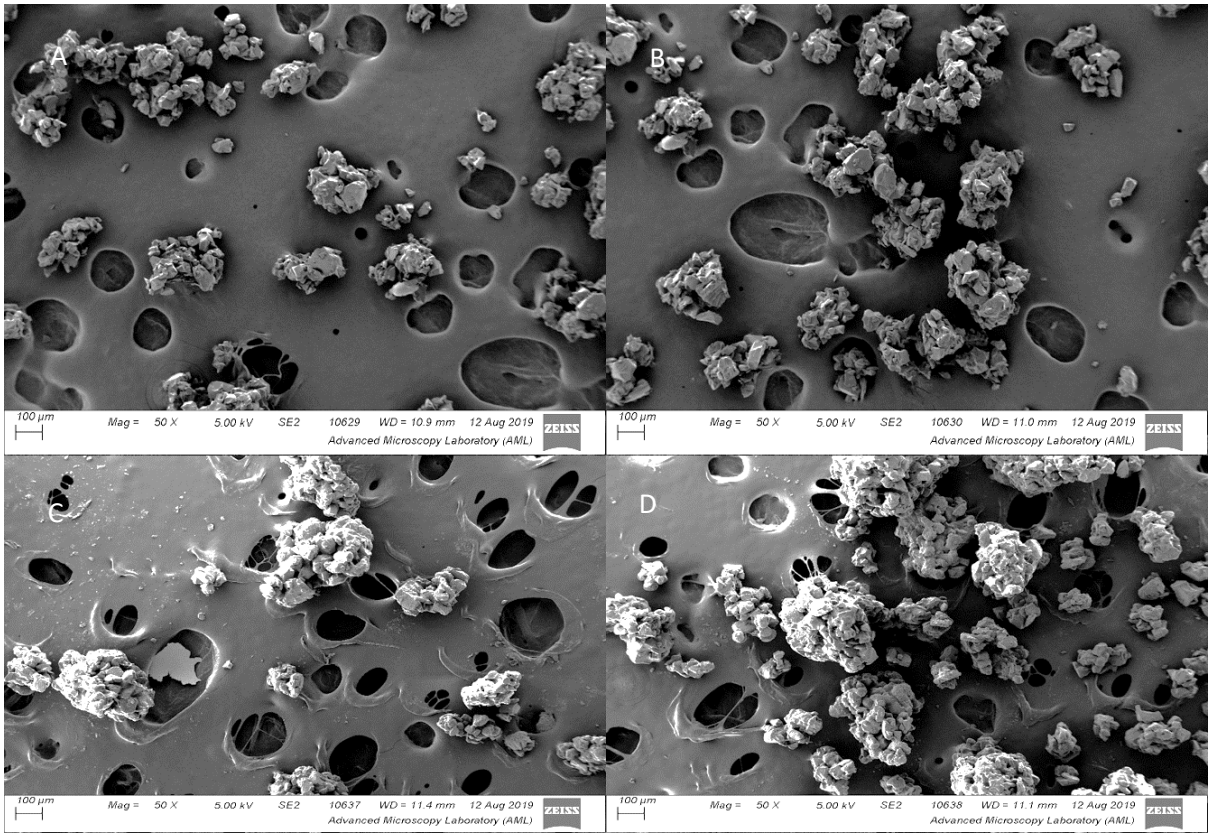

Figure 2. SEM images of granules (produced using "blank"/unloaded resin (IRP69 grade) formed by fluidised bed granulation (FBG) using different % (w/w) of PVP at lower magnifications (50x). A) 2%, B) 3%, C) 5% and D) 10%.

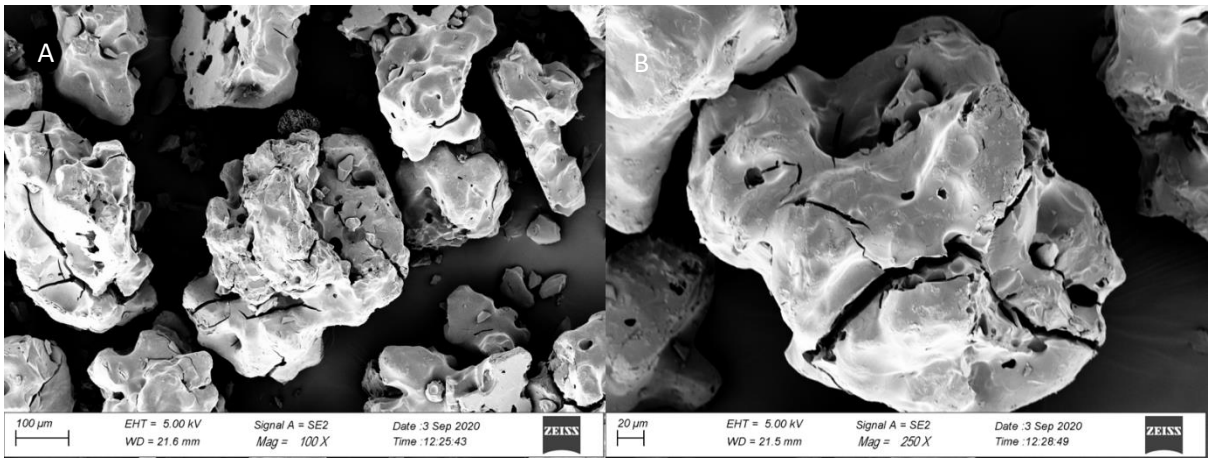

Figure 3. SEM images taken at different magnifications of granules (produced using "blank" resin (IRP69 grade) formed by FBG using HPMC as a binder. A) 100x and B) 250x.

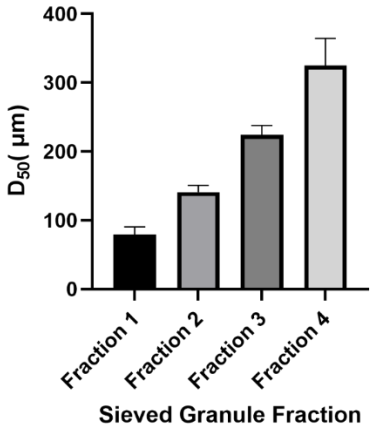

Figure 4. d_{50} values of granules ("blank" comprising IRP69 grade) produced by wet mass granulation and subsequently sieved.

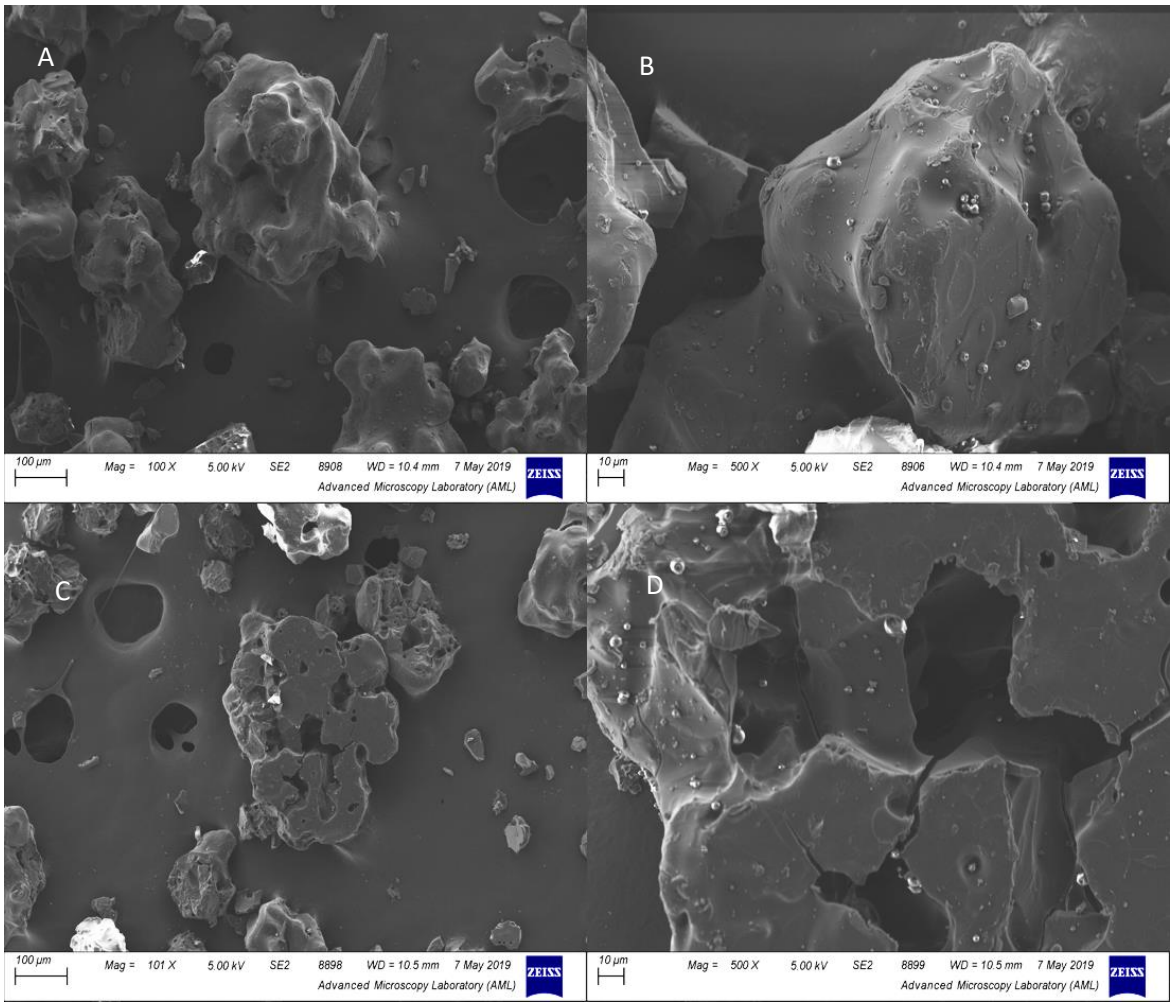

Figure 5. SEM images taken at different magnifications of granules (comprising "blank" resin (IRP69 grade) produced by FBG that have been subsequently Wurster coated using Kollicoat® SR 30 D. A) 100x, B) 500x, C) 100x and D) 500x.

Figure 6. Images of unsuccessful of Wurster coating runs (using "blank" IR120 beads) produced using Kollicoat® SR 30 D and Eudragit® NM 30 D.

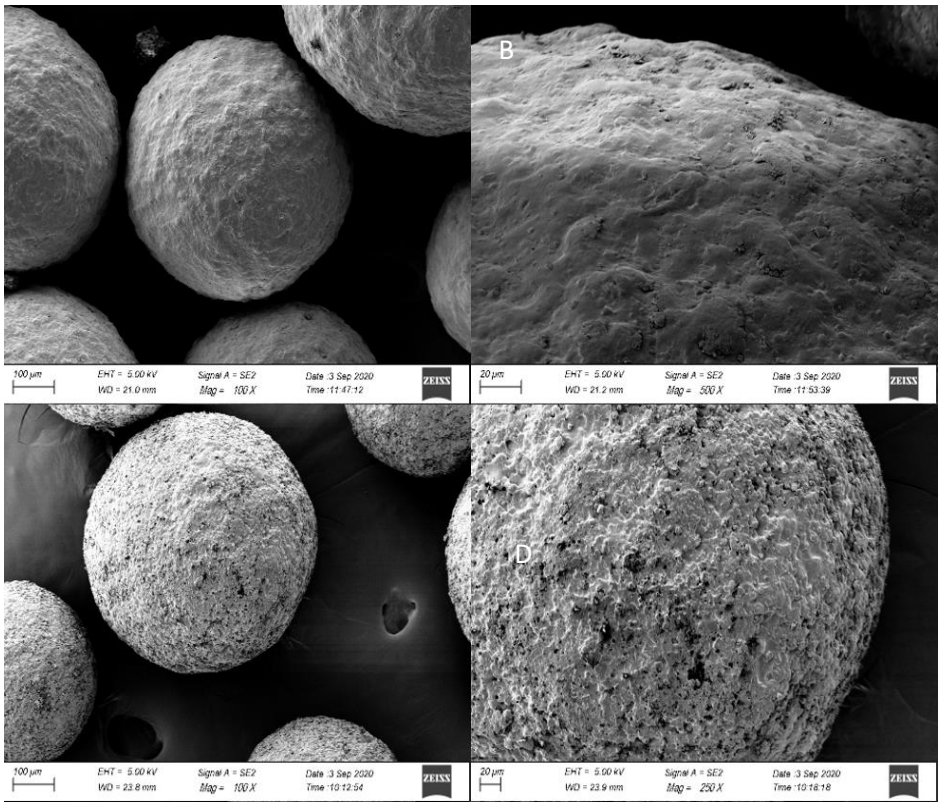

Figure 7. SEM images taken at different magnifications of unloaded beads (IR120) coated using the Wurster process and Kollicoat® SR 30 D as the coating dispersion. A) 100x (Kollicoat® SR 30 D diluted with acetone), B) 500x (Kollicoat® SR 30 D diluted with acetone), C) 100x (Kollicoat® SR 30 D diluted with H_20) and D) 250x (Kollicoat® SR 30 D diluted with H_20).

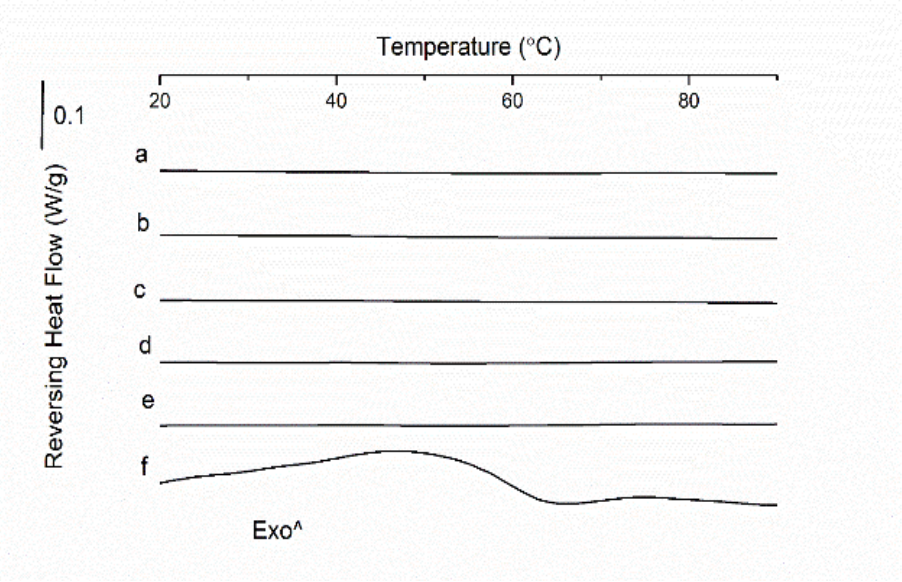

Figure 8. DSC thermograms of "blank" beads (IR120) spray-coated using different concentrations of Kollicoat® SR 30D as part of an aqueous liquid spray feed using the Wurster process. a) 2%, b) 1% w/v, c) 0.5% w/v, d) 0.25% w/v, e) 0.125% w/v and f) Kollicoat® SR 30 D.

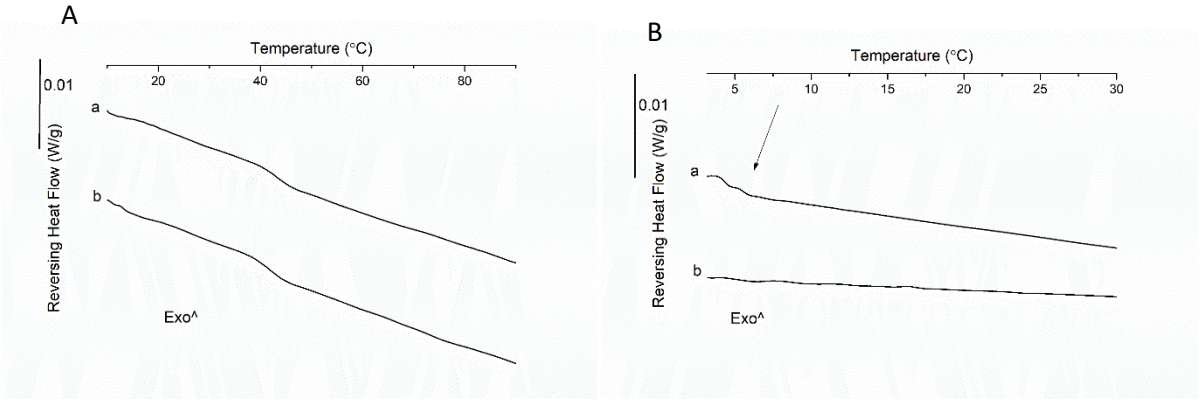

Figure 9. DSC thermograms of drug-loaded beads (IR120) spray-coated with A) Kollicoat® SR 30 D as part of a liquid spray feed diluted with acetone to produce two different concentrations a) 0.125% w/v and b) 0.25% w/v. B) Eudragit® NM 30 D as part of a liquid spray feed diluted with acetone to produce two different concentrations a) 0.125% w/v and b) 0.25% w/v.

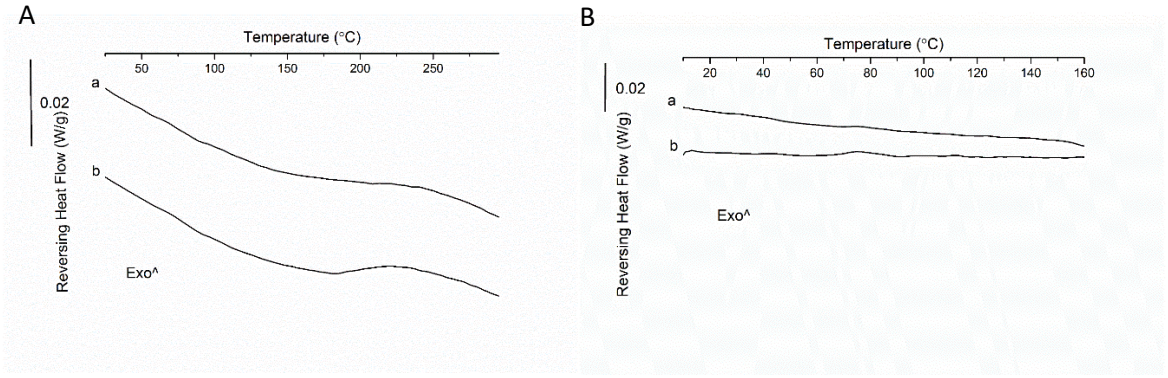

Figure 10. DSC thermograms of A) drug-loaded beads (IR120) spray-coated with a) IPA and b) acetone and B) drug-loaded beads spray-coated using 1% w/v coating solution of a) Eudragit® L100 and b) Eudragit® S100 in acetone.

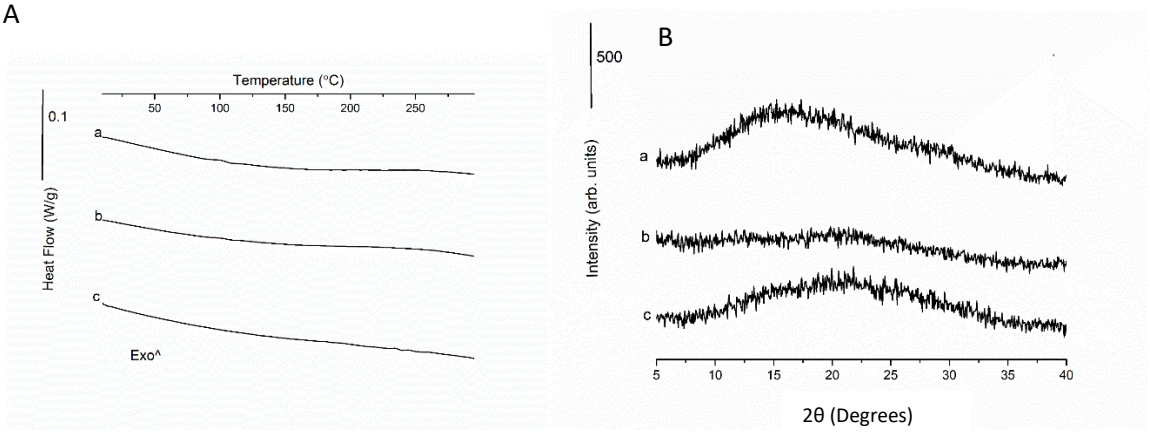

Figure 11. A) DSC thermograms and B) pXRD diffractograms of drug-resin complexes (IR120) coated with different concentrations of Eudragit® L100 in solution using the Wurster process. a) 1% w/v, b) 1.25% w/v and c) 2.5% w/v.

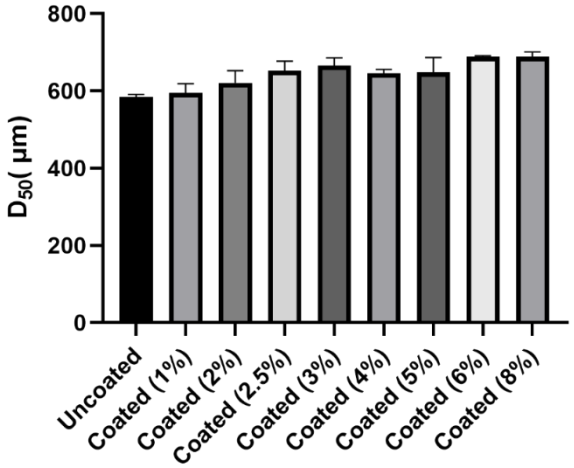

Figure 12. Comparison of d_{50} values for "blank" beads (IR120) coated with different concentrations (% w/v) of Eudragit® RS in the coating solution using the Wurster process.

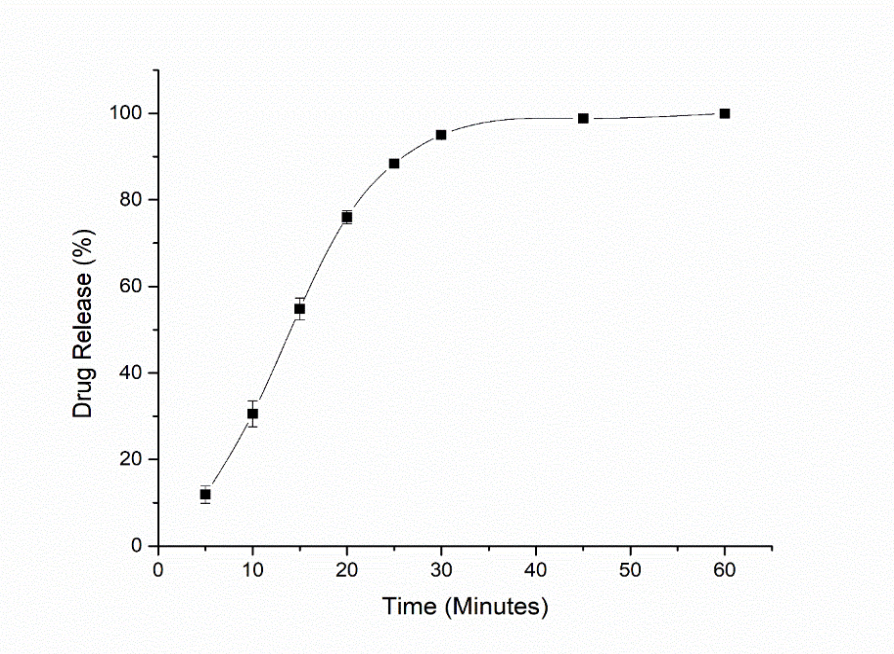

Figure 13. Drug release profile of Zanaflex® 2 mg tablets in 0.1 M HCl at 37 °C.

Table 1. Calculated drug loadings (% w/w) of the DRCs (IR120) Wurster coated using different concentrations (% w/v) of either Eudragit® RS or Eudragit® RL in the feed solution after recovery from the dissolution vessel post-drug release testing.

	Drug content of recovered coated complexes post-dissolution	
Polymer concentration (% w/v)	Eudragit® RS	Eudragit® RL
0.25	4.0 ± 0.2	-
0.50	22.0 ± 0.5	7.2 ± 0.3
0.75	38.0 ± 0.9	10.0 ± 0.6
1.00	55.0 ± 0.9	11.0 ± 0.6
1.25	70.0 ± 0.3	12.0 ± 0.5
2.50	94.0 ± 0.2	13.0 ± 0.6
3.75	95.9 ± 0.2	20.0± 0.9
5.00	93.5 ± 0.2	21.0 ± 0.9
7.50	93.9 ± 0.2	22.0 ± 0.9

Table 2. Comparison of correlation coefficients (r^2) for the model used to fit the dissolution data produced using the coated DRCs (9 concentrations (% w/v) of Eudragit® RS and Eudragit® RL).

Model		
Concentration of polymer in feed solution (% w/v)	r^2 value (RS)	r^2 value (RL)
0.25	0.9803	0.9026
0.50	0.9776	0.9568
0.75	0.9675	0.9518
1.00	0.9906	0.9477
1.25	0.9806	0.9700
2.50	0.9861	0.9673
3.75	0.9854	0.9669
5.00	0.9861	0.9717
7.50	0.9839	0.9718

A

B

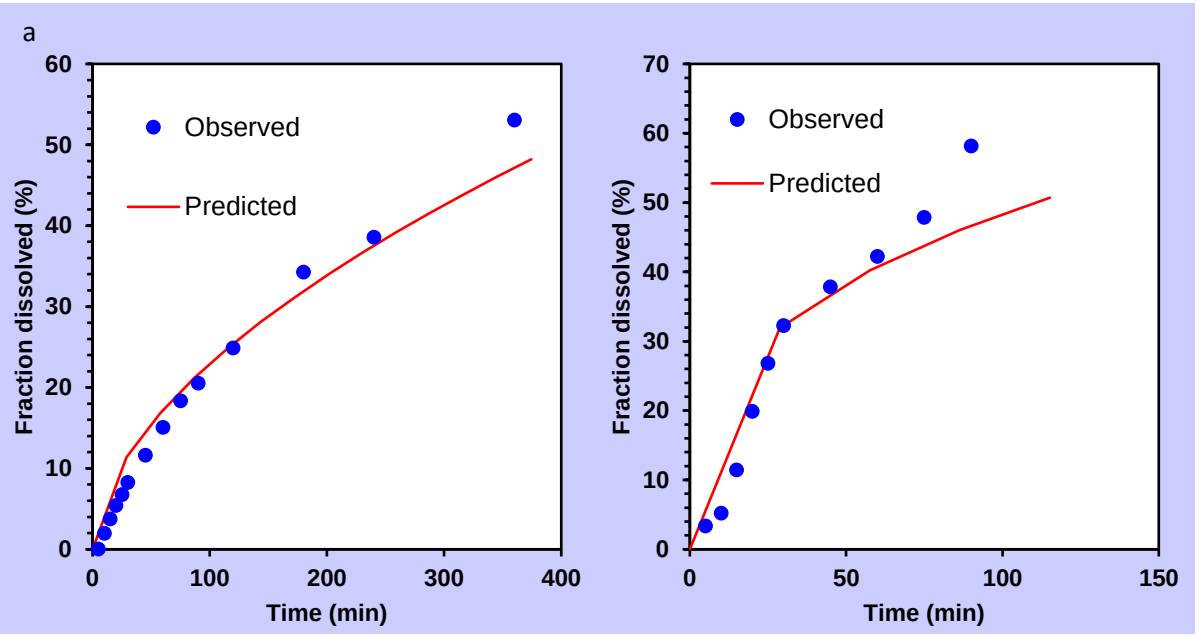

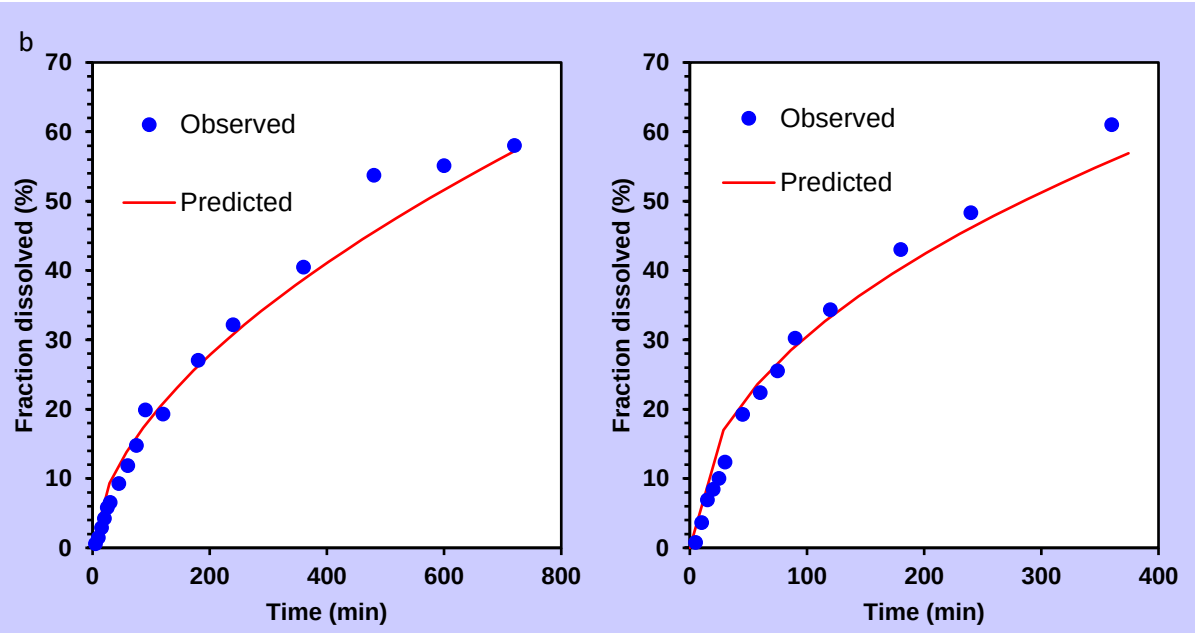
b
Fraction dissolved (%)
Time (min)
Observed
Predicted
0
10
20
30
40
50
60
70
0
200
400
600
800
Fraction dissolved (%)
Time (min)
Observed
Predicted
0
10
20
30
40
50
60
70
0
100
200
300
400

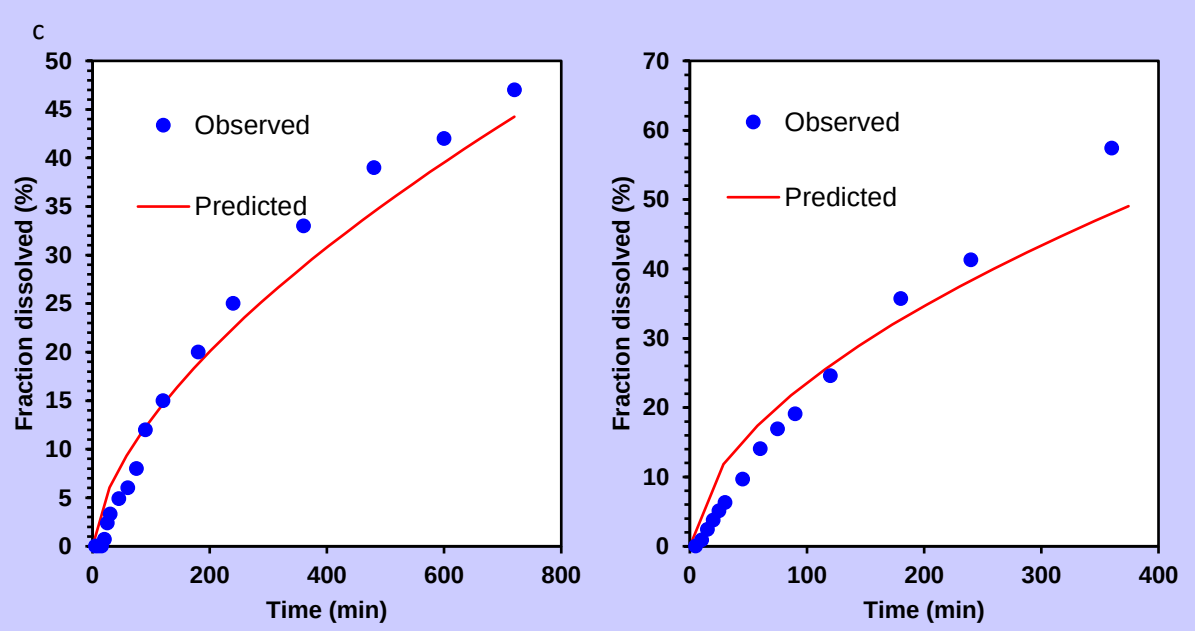
c
Fraction dissolved (%)
Time (min)
Observed
Predicted
0
5
10
15
20
25
30
35
40
45
50
0
200
400
600
800
Fraction dissolved (%)
Time (min)
Observed
Predicted
0
10
20
30
40
50
60
70
0
100
200
300
400

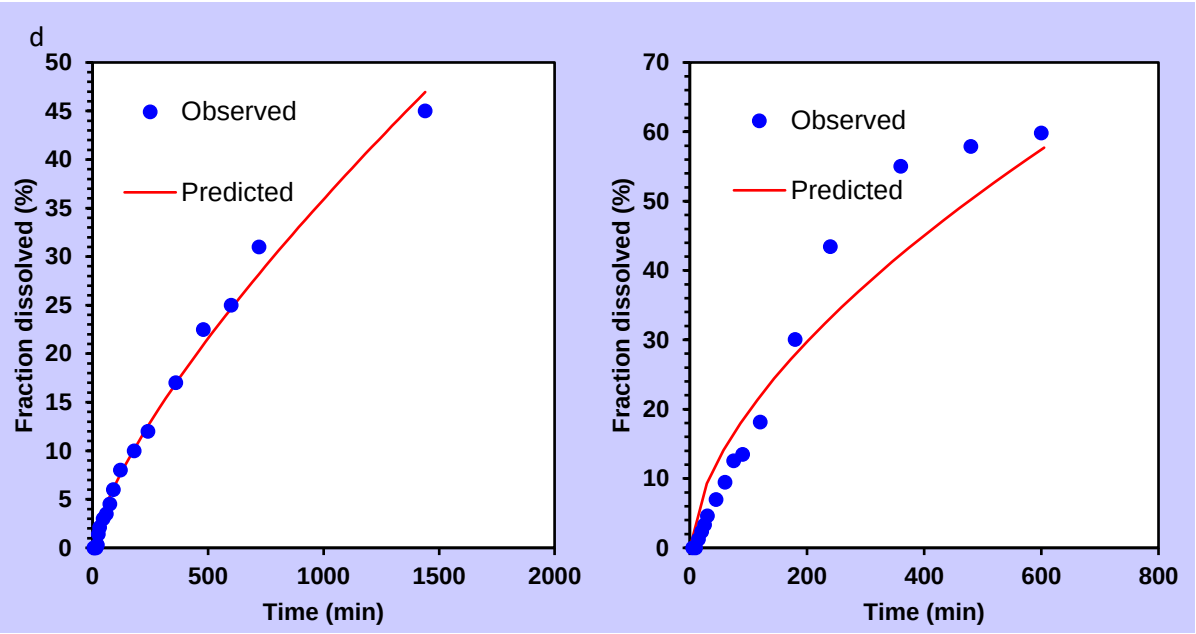
d
Observed
Predicted
Fraction dissolved (%)
Time (min)
0
5
10
15
20
25
30
35
40
45
50
500
1000
1500
2000
Observed
Predicted
Fraction dissolved (%)
Time (min)
0
10
20
30
40
50
60
70
200
400
600
800

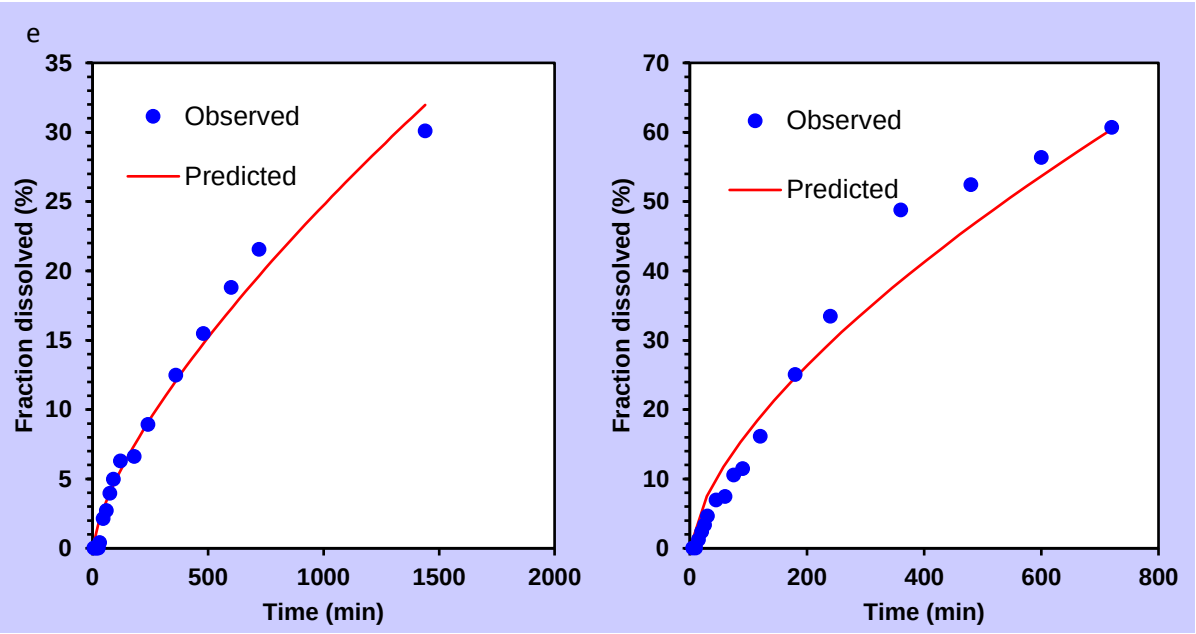
e
Observed
Predicted
Fraction dissolved (%)
Time (min)
0
5
10
15
20
25
30
35
500
1000
1500
2000
Observed
Predicted
Fraction dissolved (%)
Time (min)
0
10
20
30
40
50
60
70
200
400
600
800

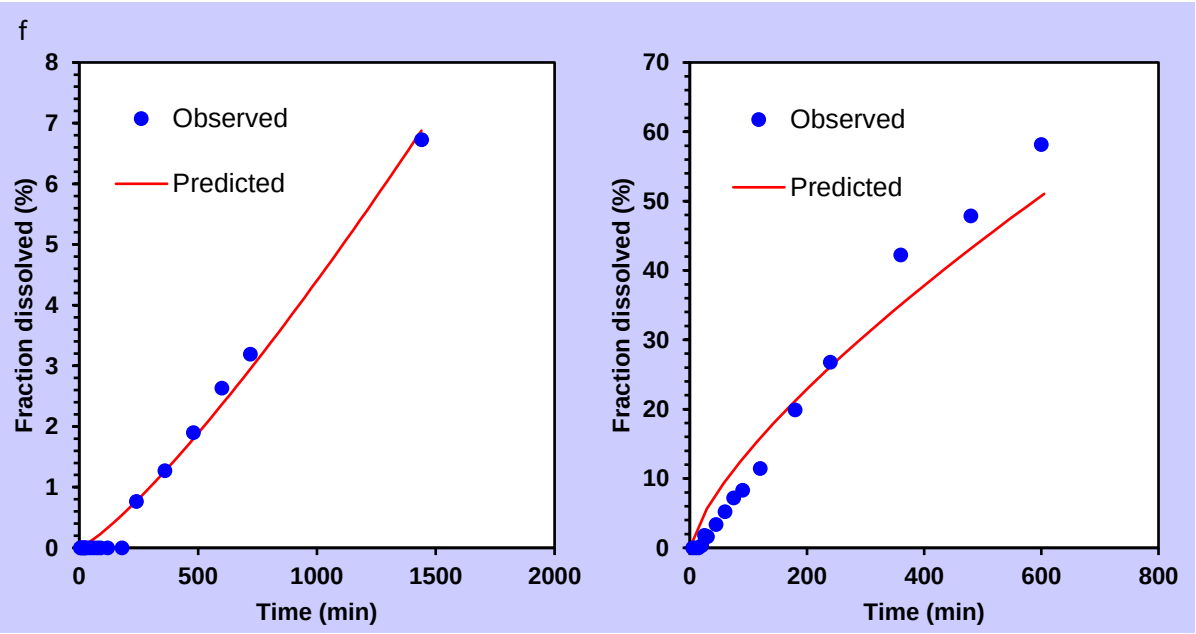
f
Observed
Predicted
Fraction dissolved (%)
Time (min)
0
1
2
3
4
5
6
7
8
0
500
1000
1500
2000
Observed
Predicted
Fraction dissolved (%)
Time (min)
0
10
20
30
40
50
60
70
0
200
400
600
800

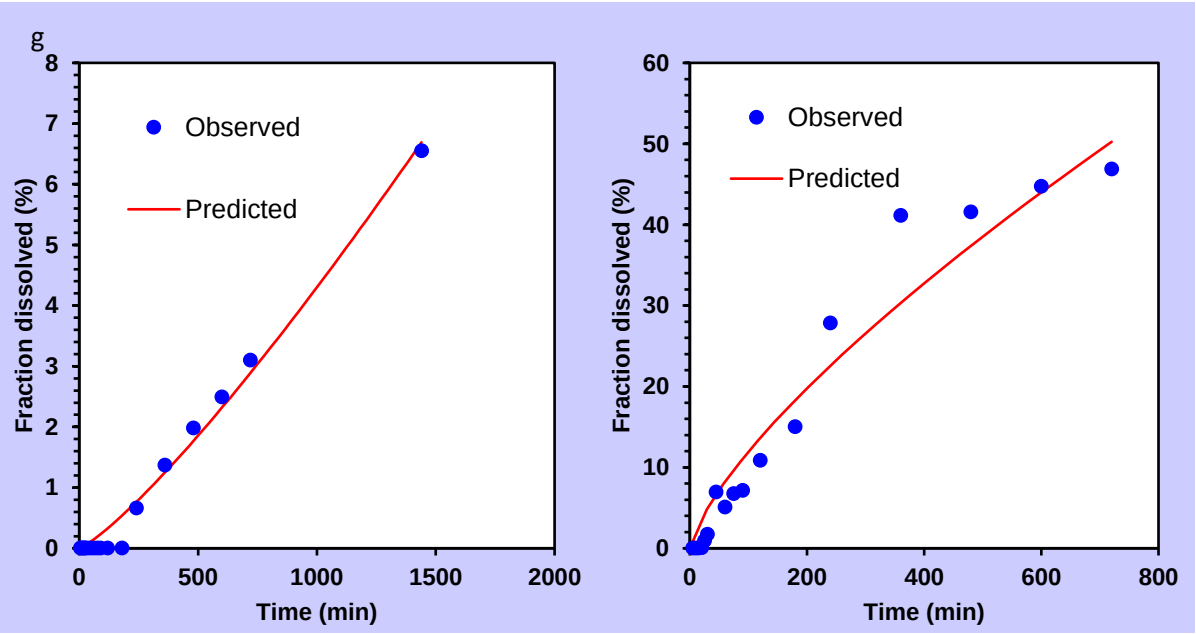
g
Observed
Predicted
Fraction dissolved (%)
Time (min)
0
1
2
3
4
5
6
7
8
0
500
1000
1500
2000
Observed
Predicted
Fraction dissolved (%)
Time (min)
0
10
20
30
40
50
60
0
200
400
600
800

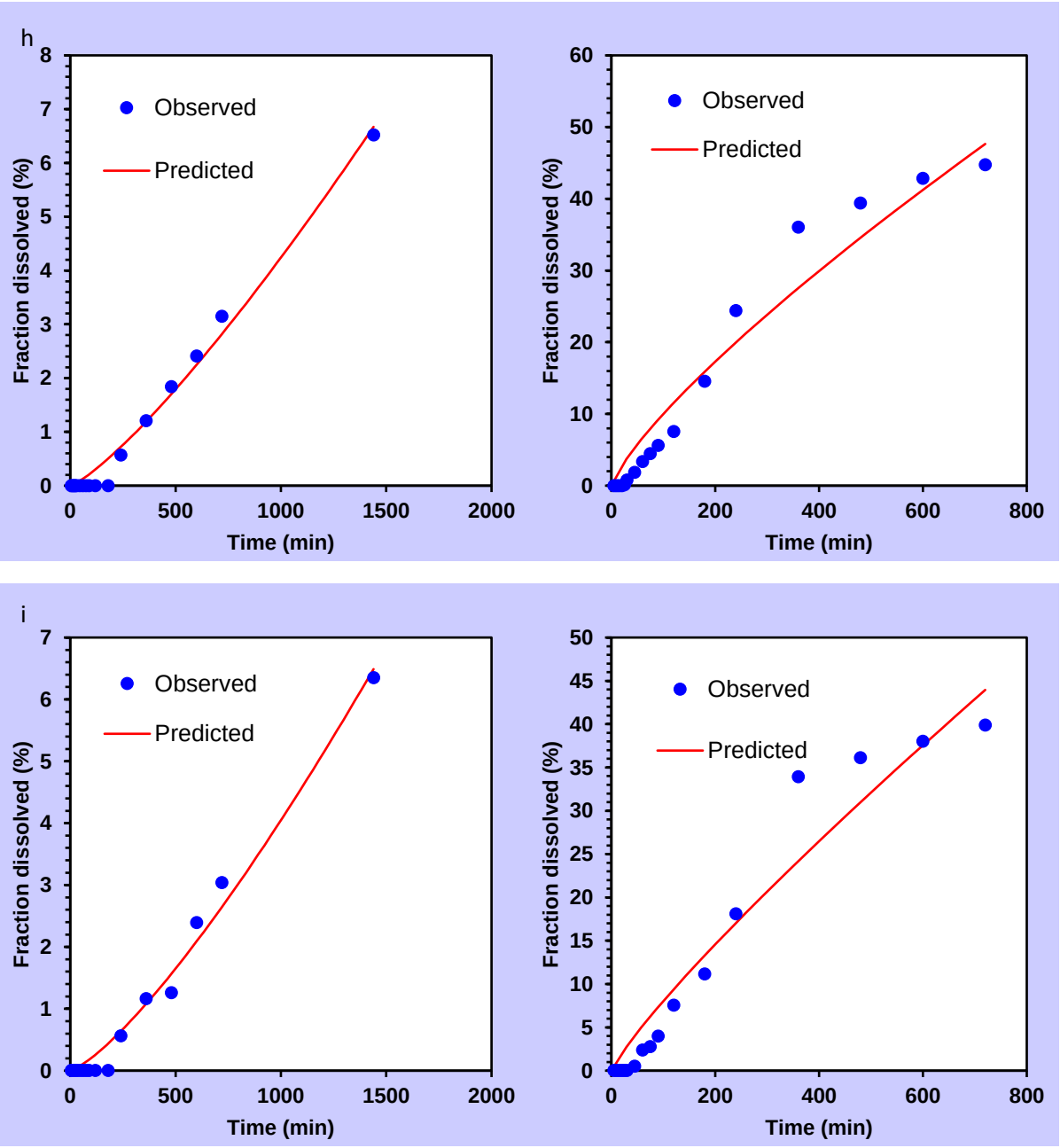

Figure 14. Plots of the drug release profiles of the Wurster coated systems produced using different concentrations of A) Eudragit® RS and B) Eudragit® RL. The data was modelled using the Korsmeyer-Peppas equation using the DDSolver software. a) 0.25%, b) 0.5%, c) 0.75%, d) 1%, e) 1.25%, f) 2.5%, g) 3.75%, h) 5% and i) 7.5%.

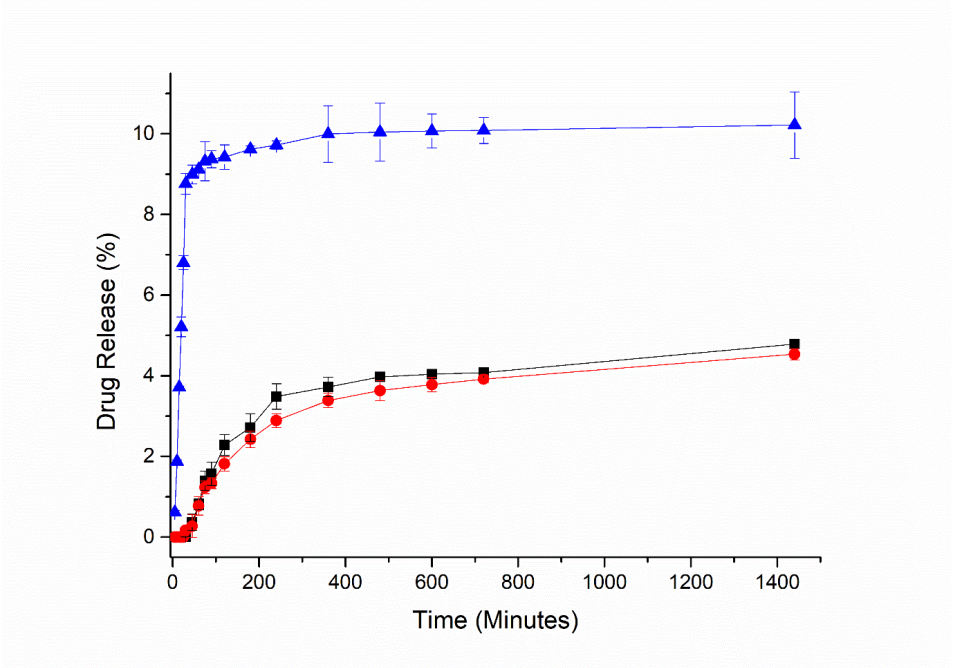

Figure 15. Drug release profiles (in DI H_20 at 37 °C) of uncoated and Wurster coated drug-loaded beads (IR120) with either the Eudragit® RL or Eudragit® RS grade. 0.25% w/v Eudragit® RS (Black square), 0.5% w/v Eudragit® RL (Red circle) and uncoated (Blue triangle). All coating concentrations refer to the concentration of polymer/plasticiser in the coating solution used to Wurster coat the DRCs.

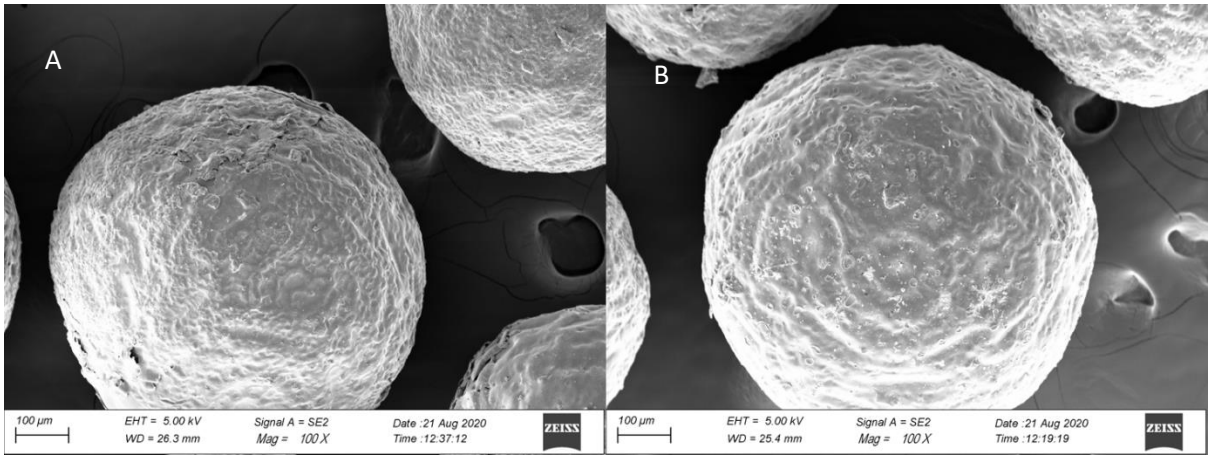

Figure 16. SEM images of Wurster coated DRCs (IR120) with A) Eudragit® RL and B) Eudragit® RS grade after being subject to a 24 hour drug release test in DI H_20.

Figure 17. Images of failed Wurster coating runs using "blank" beads (IR120) and dibutyl sebacate (DBS) and triacetin (TCT) as plasticisers.

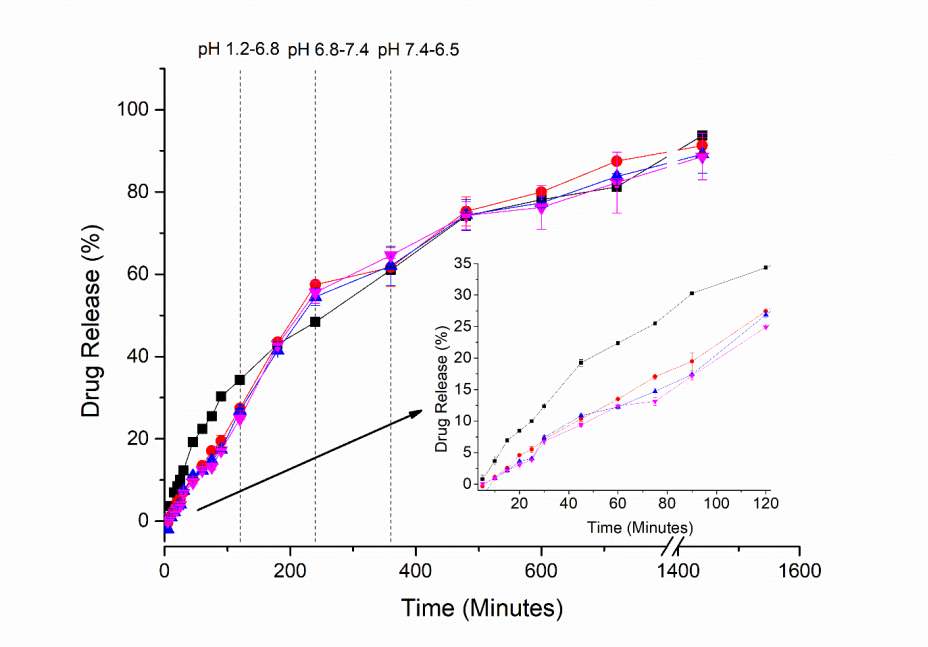

Figure 18. Drug release profiles of drug-loaded beads (IR120) coated with different Eudragit® RL (0.5% w/v) and triethyl citrate (TEC) (0.25% w/v) which have been subsequently cured for either 0 hours, 12 hours or 24 hours. The DRC coated using solely a 0.5% w/v Eudragit® RL concentration in the coating solution has been included for comparative purposes and is denoted by the "100% RL term". 100% Eudragit® RL (Black square), uncured (Red circle), cured (12 hours) (Blue triangle), and cured (24 hours)(Inverted magenta triangle).

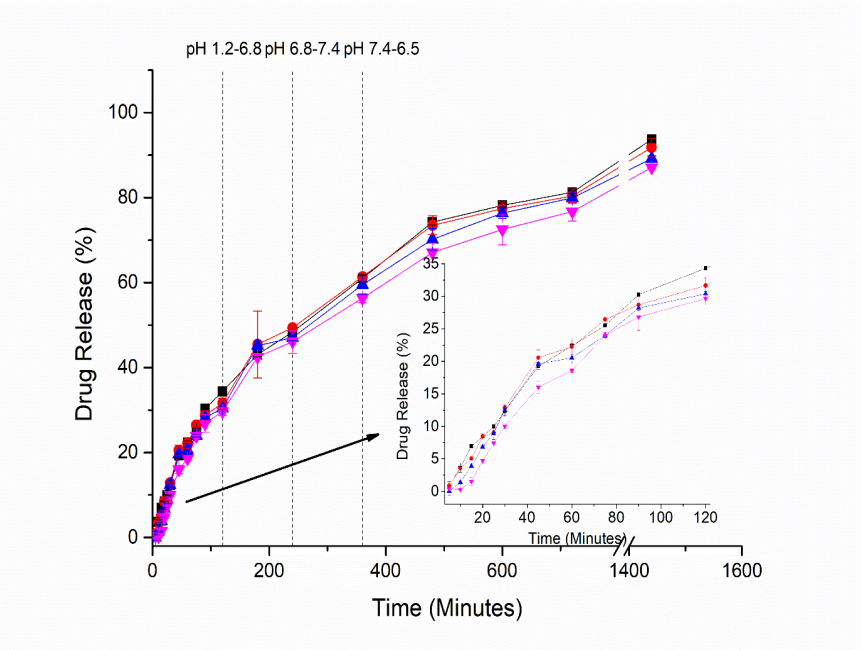

Figure 19. Drug release profiles of drug-loaded beads (IR120) coated with different Eudragit® RL (0.5% w/v) and TEC (0.5% w/v) which have been subsequently cured for either 0 hours, 12 hours or 24 hours. The DRC coated using solely a 0.5% w/v Eudragit® RL concentration in the coating solution has been included for comparative purposes and is denoted by the "100% RL term". 100% Eudragit® RL (Black square), uncured (Red circle), cured (12 hours) (Blue triangle), and cured (24 hours)(Inverted magenta triangle). All coating concentrations refer to the concentration of polymer/plasticiser in the coating solution used to Wurster coat the DRCs.

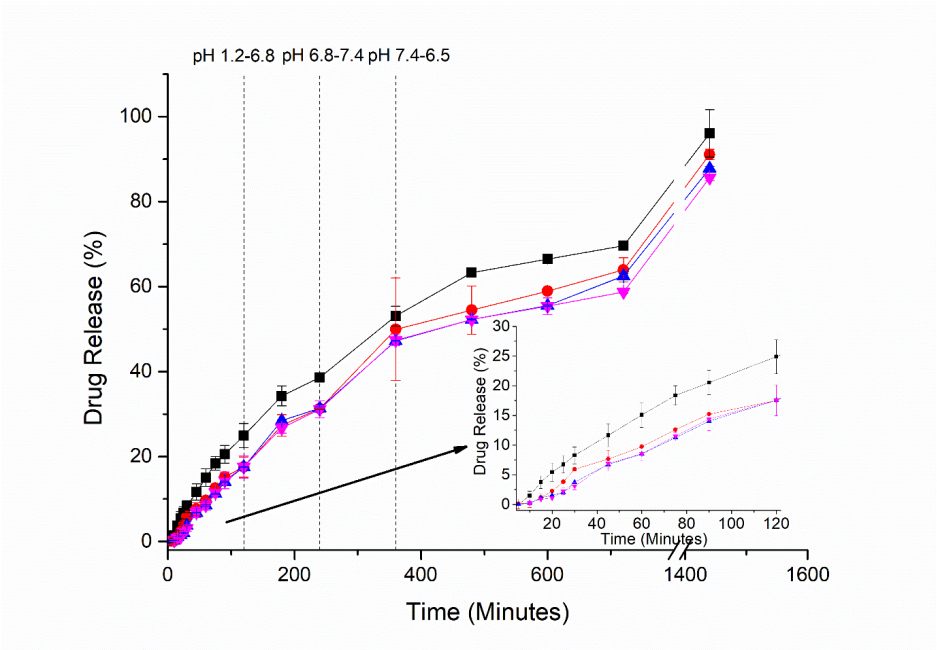

Figure 20. Drug release profiles of drug-loaded beads (IR120) coated with different Eudragit® RS (0.25% w/v) and TEC (0.25% w/v) which have been subsequently cured for either 0 hours, 12 hours or 24 hours. The DRC coated using solely a 0.25% w/v Eudragit® RS concentration in the coating solution has been included for comparative purposes and is denoted by the "100% RS term". 100% Eudragit® RS (Black square), uncured (Red circle), cured (12 hours) (Blue triangle), and cured (24 hours)(Inverted

magenta triangle). All coating concentrations refer to the concentration of polymer/plasticiser in the coating solution used to Wurster coat the DRCs.

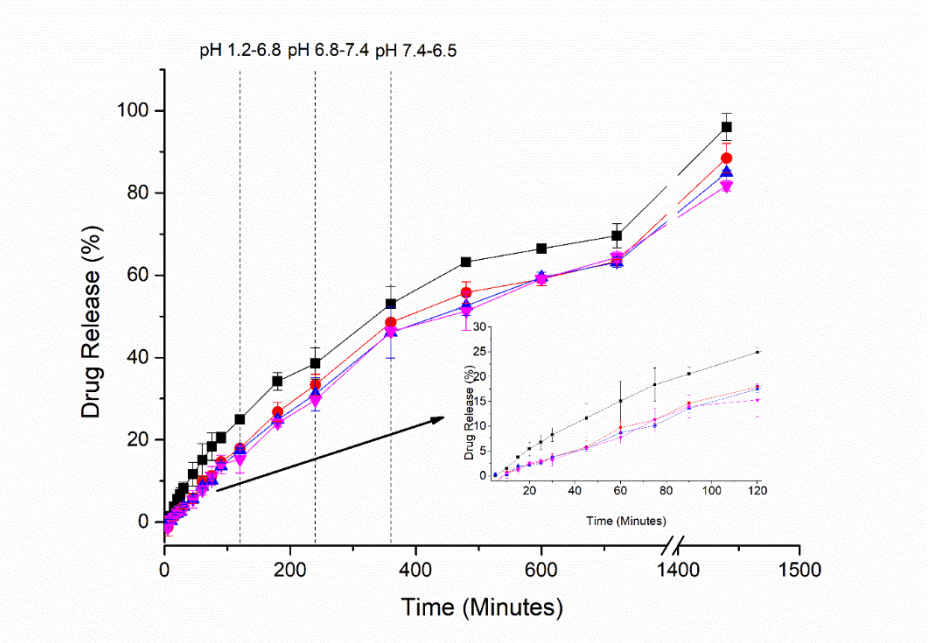

Figure 21. Drug release of drug-loaded beads (IR120) Wurster coated with Eudragit® RS (0.25% w/v) and TEC (0.5% w/v) which have been subsequently cured for either 0 hours, 12 hours or 24 hours. The DRC coated using solely a 0.25% w/v Eudragit® RS concentration in the coating solution has been included for comparative purposes and is denoted by the "100% RS term". 100% Eudragit® RS (Black square), uncured (Red circle), cured (12 hours) (Blue triangle), and cured (24 hours)(Inverted magenta triangle). All coating concentrations refer to the concentration of polymer/plasticiser in the coating solution.

A

B

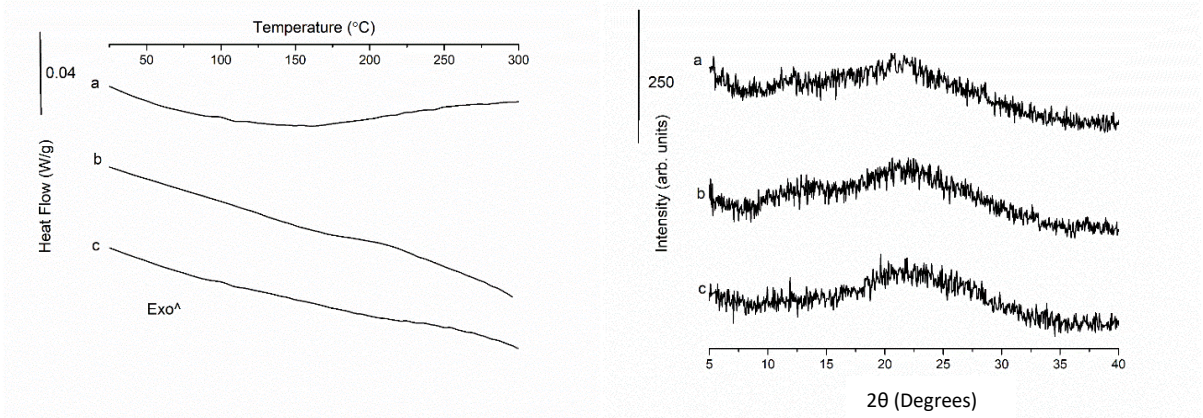

Figure 22. A) DSC thermograms and B) pXRD diffractograms of DRCs (IR120) Wurster coated with the Eudragit® RS grade (0.25% w/v) and different concentrations of TEC. a) Eudragit® RS and TEC (0.125% w/v), b) Eudragit® RS and TEC (0.25% w/v) and c) Eudragit® RS and TEC (0.5% w/v). All coating concentrations refer to the concentration of polymer/plasticiser in the coating solution.

A

B

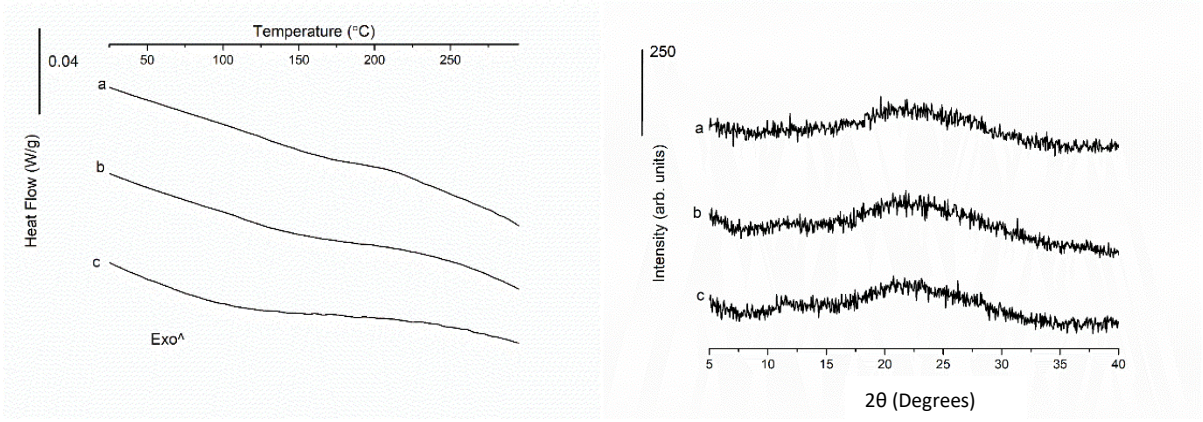

Figure 23. A) DSC thermograms and B) pXRD diffractograms of DRCs (IR120) Wurster coated with the Eudragit® RL grade (0.5% w/v) and different concentrations of TEC. a) Eudragit® RL and TEC (0.125% w/v), b) Eudragit® RL and TEC (0.25% w/v) and c) Eudragit® RL and TEC (0.5% w/v). All coating concentrations refer to the concentration of polymer/plasticiser in the coating solution.

A

B

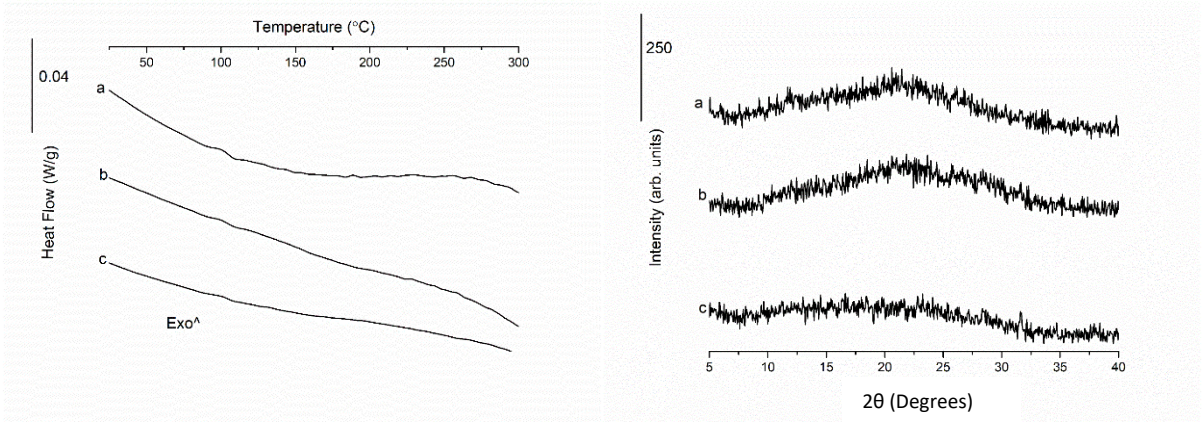

Figure 24. A) DSC thermograms and B) pXRD diffractograms of DRCs (IR120) Wurster coated with different ratios (w/w) of Eudragit® RS and Eudragit® RL in solution (total polymeric concentration in feed solution is 1% w/v). a) 10:90, b) 25:75 and c) 50:50.

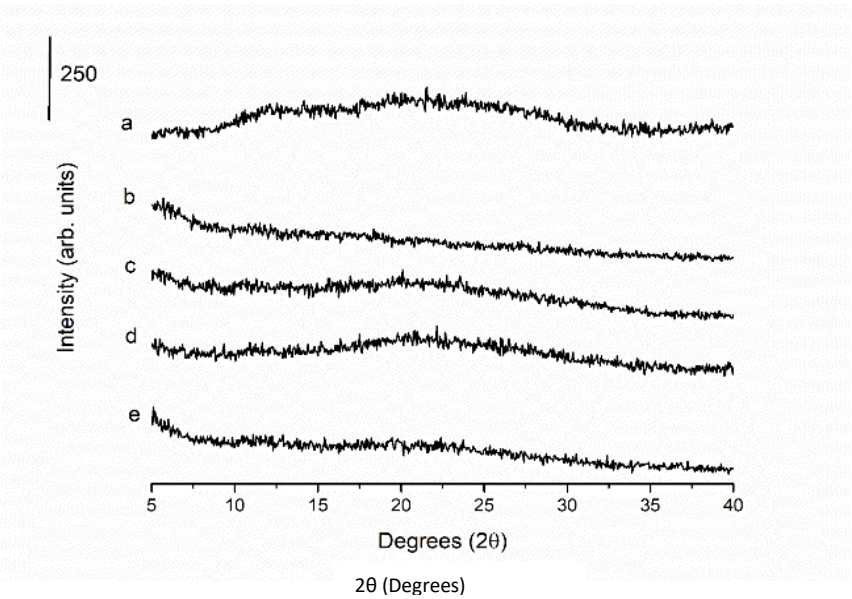

Figure 25. pXRD diffractograms of selected DRCs (IR120) (uncoated and Wurster coated) post-DVS analysis. a) uncoated DRC, b) coated DRC (0.25% w/v Eudragit® RS), c) coated DRC (0.5% w/v Eudragit® RL), d) coated DRC (0.25% w/v Eudragit® RS and 0.125% w/v TEC) and e) coated DRC (0.5% w/v Eudragit® RL and 0.125% w/v TEC). All coating concentrations refer to the concentration of polymer/plasticiser in the coating solution.

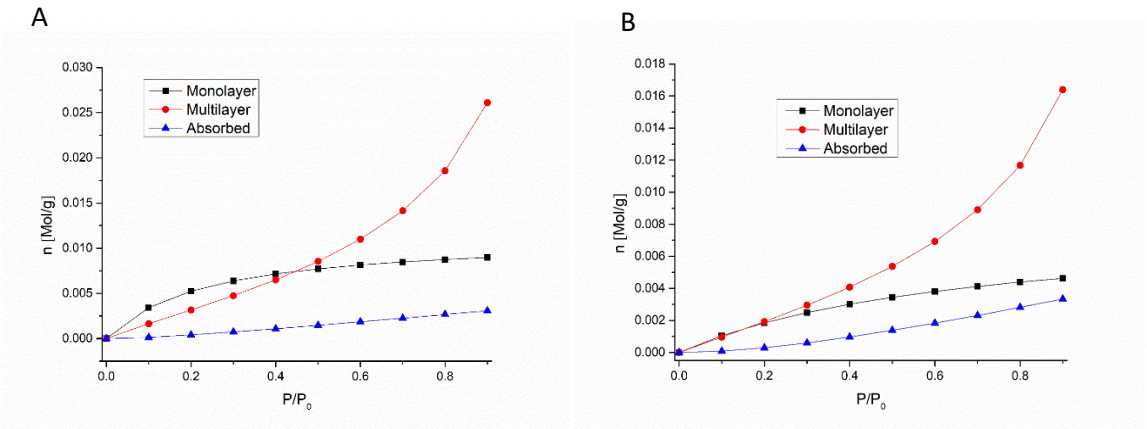

Figure 26. Moisture distribution patterns for A) Resin raw material (IR120) and B) Uncoated DRC (IR120)

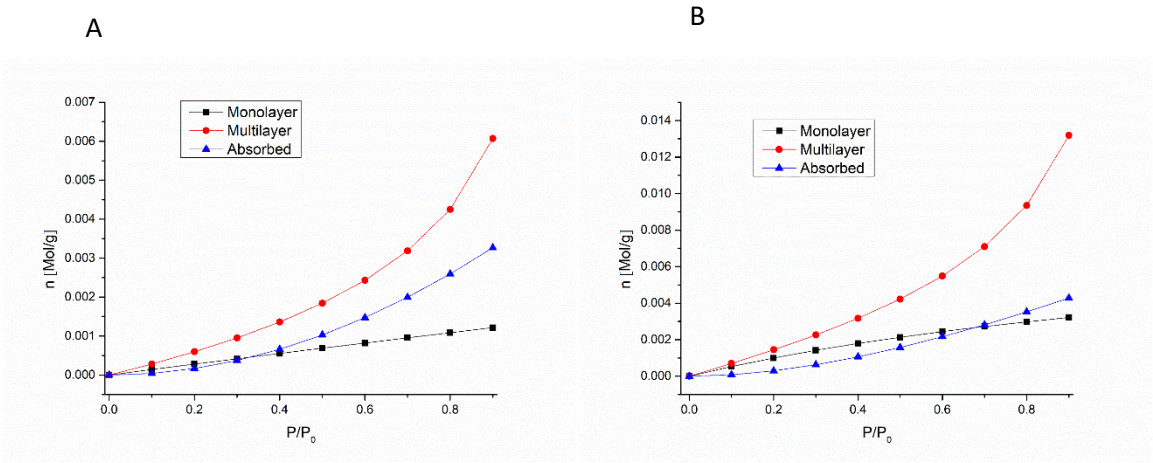

Figure 27. Moisture distribution patterns for Wurster coated DRCs (IR120) produced using A) Eudragit® RL (0.5% w/v) and B) Eudragit® RL (0.5% w/v) and TEC (0.125% w/v). All coating concentrations refer to the concentration of polymer/plasticiser in the coating solution.

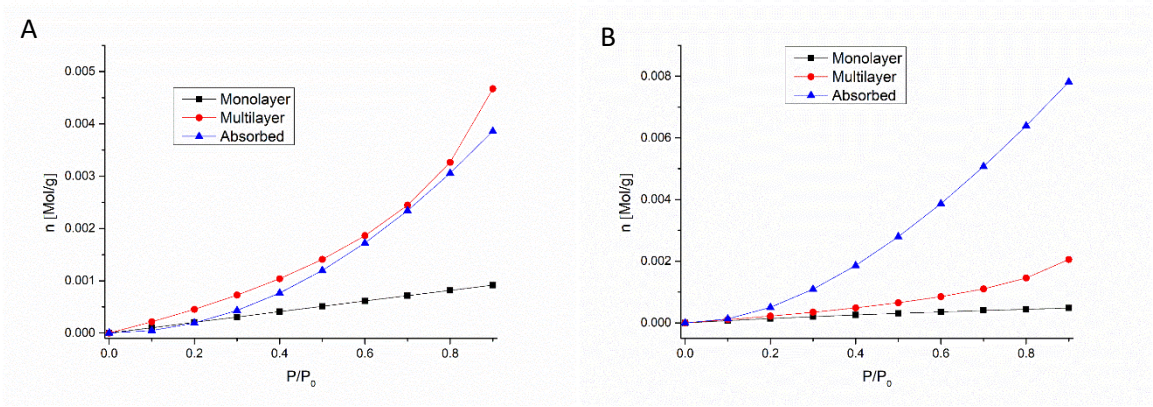

Figure 28. Moisture distribution patterns for Wurster coated DRCs (IR120) produced using A) Eudragit® RS (0.25% w/v) and B) Eudragit® RS (0.25% w/v) and TEC (0.125% w/v). All coating concentrations refer to the concentration of polymer/plasticiser in the coating solution.

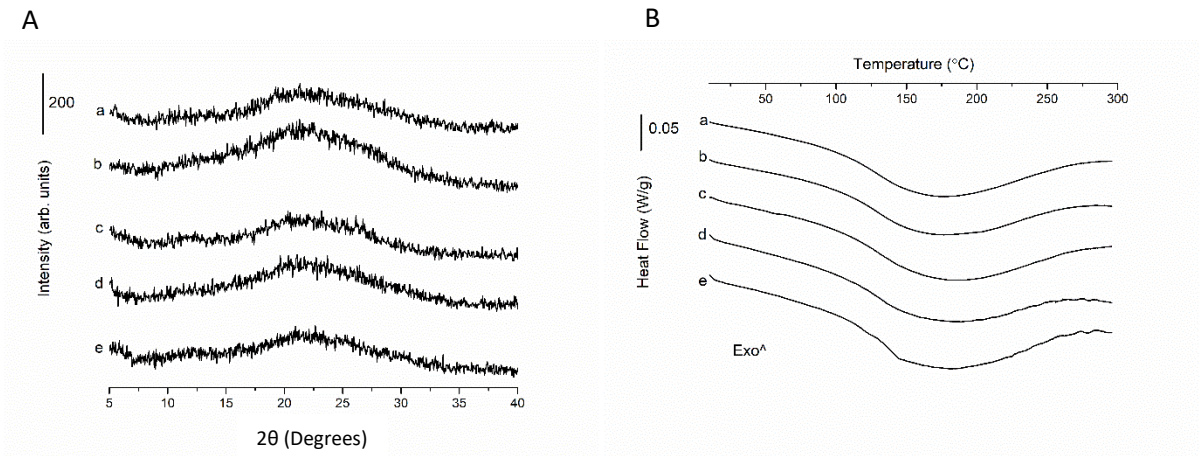

Figure 29. A) DSC thermograms and B) pXRD diffractograms of DRCs (IR120) stored at 25 °C and 60% RH for 2 months that were Wurster coated using a) Eudragit® RS (0.25% w/v) and TEC (0.125% w/v), b) Eudragit® RL (0.5% w/v) and TEC (0.125% w/v), c) Eudragit® RS (0.25% w/v), d) Eudragit® RL (0.5%

w/v) and e) uncoated. All coating concentrations refer to the concentration of polymer/plasticiser in the coating solution.

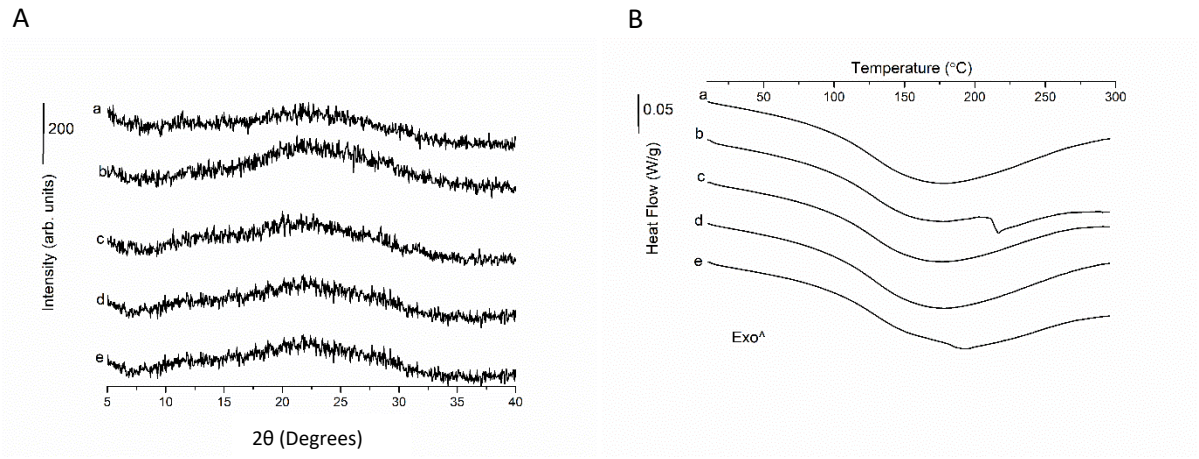

Figure 30. A) DSC thermograms and B) pXRD diffractograms of complexes (IR120) stored at 25 °C and <10%. RH for 2 months that were Wurster coated using a) Eudragit® RS (0.25% w/v) and TEC (0.125% w/v), b) Eudragit® RL (0.5% w/v) and TEC (0.125% w/v), c) Eudragit® RS (0.25% w/v), d) Eudragit® RL (0.5% w/v) and e) uncoated. All coating concentrations refer to the concentration of polymer/plasticiser in the coating solution.

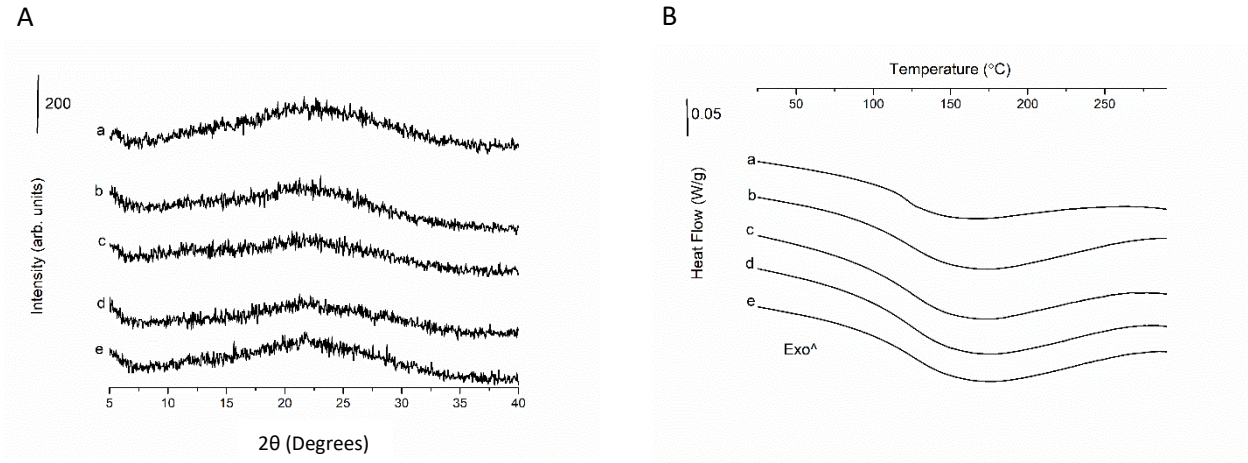

Figure 31. A) DSC thermograms and B) pXRD diffractograms of complexes (IR120), stored at 25 °C and 60%. RH for 3 months that were Wurster coated using a) Eudragit® RS (0.25% w/v) and TEC (0.125% w/v), b) Eudragit® RL (0.5% w/v) and TEC (0.125% w/v), c) Eudragit® RS (0.25% w/v), d) Eudragit® RL (0.5% w/v) and e) uncoated. All coating concentrations refer to the concentration of polymer/plasticiser in the coating solution.

A

B

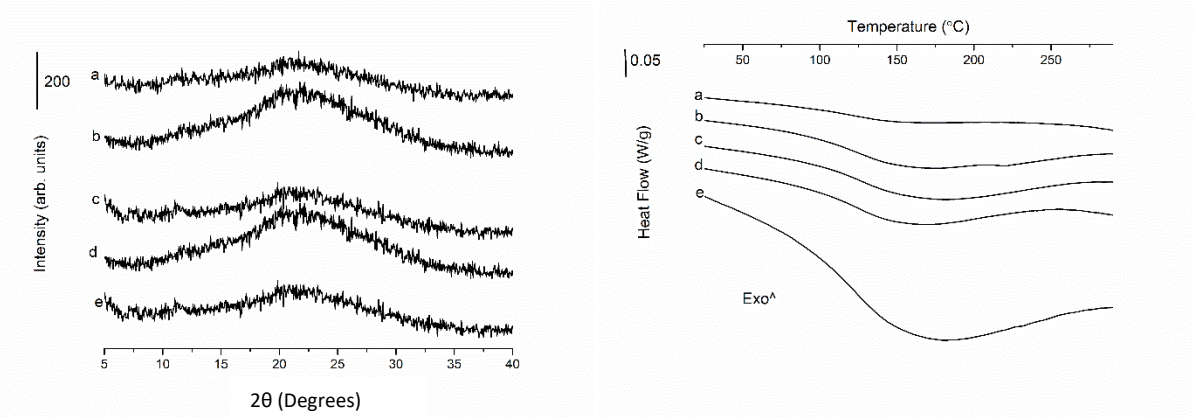

Figure 32. A) DSC thermograms and B) pXRD diffractograms of DRCs (IR120) stored at 25 °C and <10%. RH for 3 months that were Wurster coated using a) Eudragit® RS (0.25% w/v) and TEC (0.125% w/v), b) Eudragit® RL (0.5% w/v) and TEC (0.125% w/v), c) Eudragit® RS (0.25% w/v), d) Eudragit® RL (0.5% w/v) and e) uncoated. All coating concentrations refer to the concentration of polymer/plasticiser in the coating solution.

Table 3. List of calculated drug contents for DRCs (IR120)(coated and uncoated) placed on stability at both conditions (25°C, <10% RH and 25°C and 60% RH) for 3 months. All concentrations refer to the concentration of polymer/plasticiser in the coating solution.

Sample	Drug content of samples stored at 25 °C and <10% RH	Drug content of samples stored at 25 °C and 60% RH
Uncoated	99.90 ± 0.03 %	99.87 ± 0.04 %
Coated (0.25% w/v Eudragit® RS)	99.93 ± 0.05 %	99.51 ± 0.25 %
Coated (0.5% w/v Eudragit® RL)	99.84 ± 0.09 %	99.76 ± 0.21 %
Coated (0.25% w/v Eudragit® RS and 0.125% w/v TEC)	99.87 ± 0.04 %	99.85 ± 0.11 %
Coated (0.5% w/v Eudragit® RL and 0.125% w/v TEC)	99.59 ± 0.23 %	99.84 ± 0.20 %

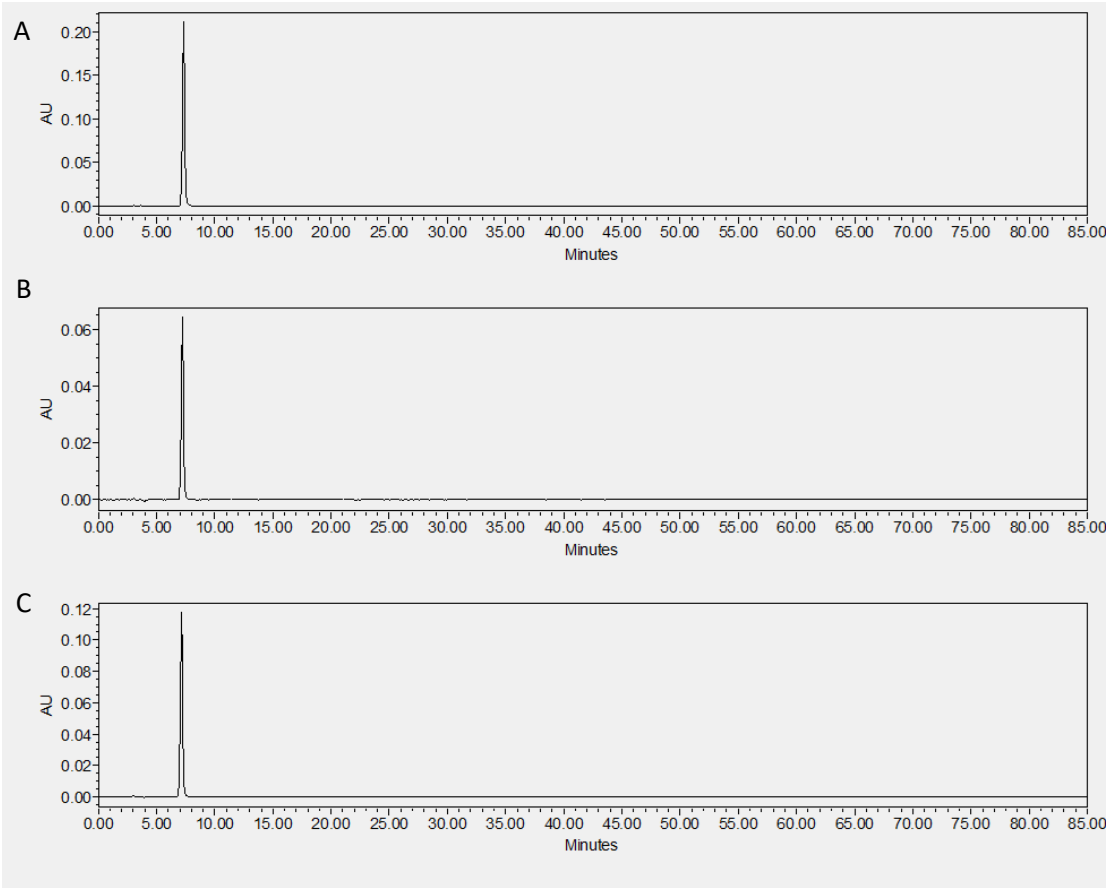

Figure 33. HPLC chromatograms of A) uncoated DRCs (IR120), B) DRCs coated using a 0.25% w/v Eudragit® RS coating solution and C) DRCs coated using a 0.5% w/v Eudragit® RL coating solution. All coating concentrations refer to the concentration of polymer/plasticiser in the coating solution.

Appendix 4

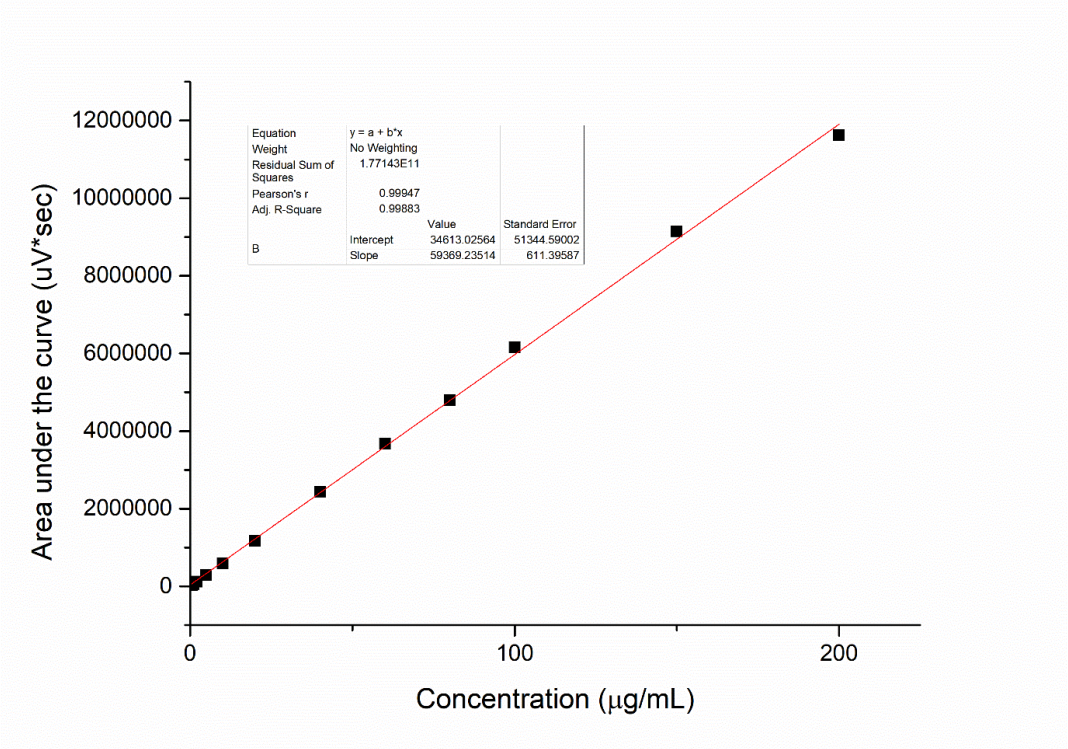

Figure 1. Calibration curve for MTZ.

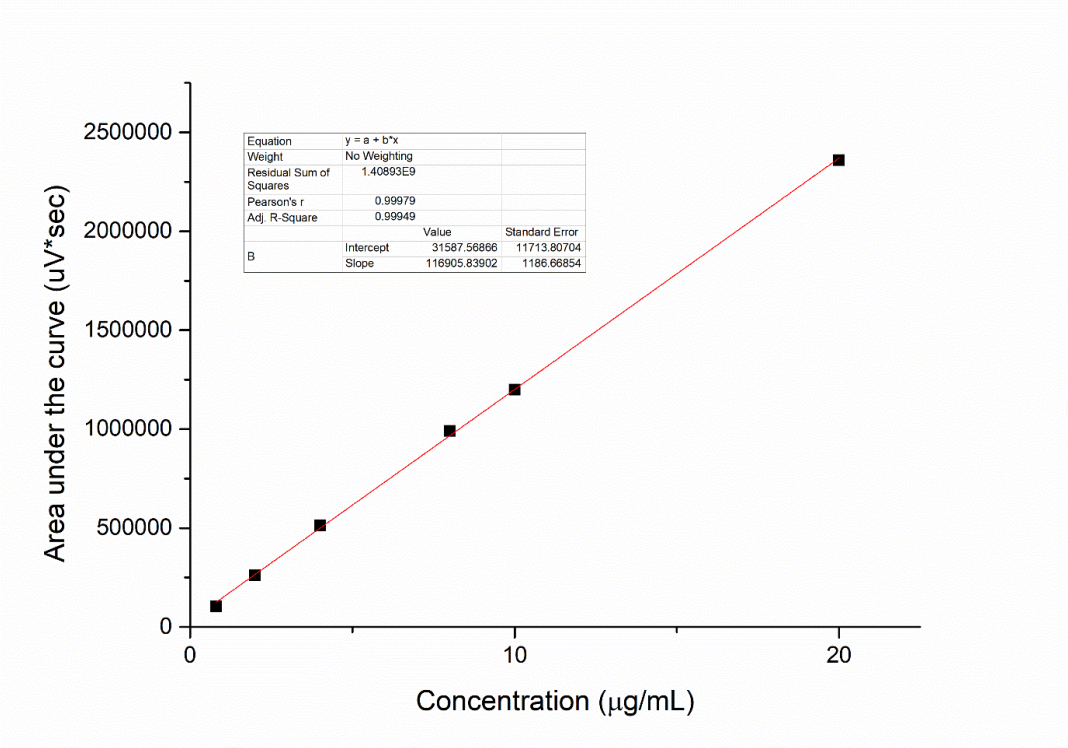

Figure 2. Calibration curve for TZD HCl.

References

1. Masaoka Y, Tanaka Y, Kataoka M, Sakuma S, Yamashita S. Site of drug absorption after oral administration: Assessment of membrane permeability and luminal concentration of drugs in each segment of gastrointestinal tract. Eur J Pharm Sci. 2006;29(3–4):240–50.

2. Zhang GGZ, Law D, Schmitt EA, Qiu Y. Phase transformation considerations during process development and manufacture of solid oral dosage forms. Adv Drug Deliv Rev. 2004;56(3):371–90.

3. Li S, He H, Parthiban LJ, Yin H, Serajuddin ATM. IV-IVC considerations in the development of immediate-release oral dosage form. J Pharm Sci. 2005;94(7):1396–417.

4. Boyd BJ, Bergström CAS, Vinarov Z, Kuentz M, Brouwers J, Augustijns P, Brandl M, Bernkop-Schnürch A, Shrestha N, Préat V, Müllertz A, Bauer-Brandl A, Jannin V. Successful oral delivery of poorly water-soluble drugs both depends on the intraluminal behavior of drugs and of appropriate advanced drug delivery systems. Eur J Pharm Sci. 2019;137.

5. Ali J, Zgair A, Hameed GS, Garnett MC, Roberts CJ, Burley JC, Gershkovich P. Application of biorelevant saliva-based dissolution for optimisation of orally disintegrating formulations of felodipine. Int J Pharm. 2019;555(1):228–36.

6. Sharma S, Lewis S. Taste masking technologies: A review. Int J Pharm Pharm Sci. 2010;2(2):6–13.

7. Zajicek A, Fossler MJ, Barrett JS, Worthington JH, Ternik R, Charkoftaki G, Lum S, Breitkreutz J, Baltezor M, Macheras P, Khan M, Agharkar S, MacLaren DD. A report from the pediatric formulations task force: Perspectives on the state of child-friendly oral dosage forms. AAPS J. 2013;15(4):1072–81.

8. Batchelor HK, Marriott JF. Formulations for children: Problems and solutions. Br J Clin Pharmacol. 2015;79(3):405–18.

9. Grimsrud KN, Sherwin CMT, Constance JE, Tak C, Zuppa AF, Spigarelli MG, Mihalopoulos NL. Special population considerations and regulatory affairs for clinical research. Clin Res Regul Aff. 2015;32(2):47–56.

10. Breitkreutz J, Boos J. Paediatric and geriatric drug delivery. Expert Opin Drug Deliv. 2007;4(1):37–45.

11. Purohit VS. Biopharmaceutic planning in pediatric drug development. AAPS J.

2012;14(3):519–22.

12. Trofimiuk M, Wasilewska K, Winnicka K. How to Modify Drug Release in Paediatric Dosage Forms? Novel Technologies and Modern Approaches with Regard to Children's Population. Int J Mol Sci. 2019;20(13).

13. Rose K, Walson PD. Do Paediatric Investigation Plans (PIPs) Advance Paediatric Healthcare? Pediatr Drugs. 2017;19(6):515–22.

14. Alyami H, Koner J, Huynh C, Terry D, Mohammed AR. Current opinions and recommendations of paediatric healthcare professionals – The importance of tablets: Emerging orally disintegrating versus traditional tablets. PLoS One. 2018;13(2).

15. Beckett VL, Tyson LD, Carroll D, Gooding NM, Kelsall AW. Accurately administering oral medication to children isn't child's play. Arch Dis Child [Internet]. 2012 Sep 30;97(9):838–41. Available from: https://adc.bmj.com/lookup/doi/10.1136/archdischild-2012-301850

16. Ryu GS, Lee YJ. Analysis of Liquid Medication Dose Errors Made by Patients and Caregivers Using Alternative Measuring Devices. J Manag Care Pharm [Internet]. 2012 Jul;18(6):439–45. Available from: http://www.jmcp.org/doi/10.18553/jmcp.2012.18.6.439

17. Dimatteo MR, Giordani PJ, Lepper HS, Croghan TW. Patient adherence and medical treatment outcomes A meta-analysis. Med Care. 2002;40(9):794–811.

18. Kozarewicz P. Regulatory perspectives on acceptability testing of dosage forms in children. Int J Pharm. 2014;469(2):245–8.

19. Walsh J, Cram A, Woertz K, Breitkreutz J, Winzenburg G, Turner R, Tuleu C. Playing hide and seek with poorly tasting paediatric medicines: Do not forget the excipients. Adv Drug Deliv Rev. 2014;73(6):14–33.

20. Strolin M, Whomsley R, Baltes EL. Differences in absorption, distribution, metabolism and excretion of xenobiotics between the paediatric and adult populations. Expert Opin Drug Metab Toxicol. 2005;3(10):447–71.

21. Kearns GL, Abdel-Rahman SM, Alander SW, Blowey DL, Leeder JS, Kauffman RE. Developmental pharmacology - Drug disposition, action, and therapy in infants and children. N Engl J Med. 2003;349(12):1157–67.

22. Rautamo M, Kvarnström K, Sivén M, Airaksinen M, Lahdenne P, Sandler N. A focus group study about oral drug administration practices at hospital wards—aspects to consider in drug

development of age-appropriate formulations for children. Pharmaceutics. 2020;12(2).

23. Cram A, Breitkreutz J, Desset-Brèthes S, Nunn T, Tuleu C. Challenges of developing palatable oral paediatric formulations. Int J Pharm. 2009;365(1–2):1–3.

24. Rocchi F, Tomasi P. The development of medicines for children. Pharmacol Res. 2011;64(3):169–75.

25. Marsot A, Boulamery A, Bruguerolle B, Simon N. Population pharmacokinetic analysis during the first 2 years of life: An overview. Clin Pharmacokinet. 2012;64(3):169–75.

26. Barker CIS, Germovsek E, Hoare RL, Lestner JM, Lewis J, Standing JF. Pharmacokinetic/pharmacodynamic modelling approaches in paediatric infectious diseases and immunology. Adv Drug Deliv Rev. 2014;73(6):127–39.

27. Walsh J, Ranmal SR, Ernest TB, Liu F. Patient acceptability, safety and access: A balancing act for selecting age-appropriate oral dosage forms for paediatric and geriatric populations. Int J Pharm. 2018;536(2):547–62.

28. Ivanovska V, Rademaker CMA, Van Dijk L, Mantel-Teeuwisse AK. Pediatric drug formulations: A review of challenges and progress. Pediatrics. 2014;134(2):361–72.

29. Batchelor HK, Kendall R, Desset-Brethes S, Alex R, Ernest TB. Application of in vitro biopharmaceutical methods in development of immediate release oral dosage forms intended for paediatric patients. Eur J Pharm Biopharm. 2013;85(3b):833–42.

30. Husain NR, Davies JG, Tomlin S. Supply of unlicensed medicines to children: Semi-structured interviews with carers. BMJ Paediatr Open. 2017;1(1).

31. Visser JC, Woerdenbag HJ, Hanff LM, Frijlink HW. Personalized Medicine in Pediatrics: The Clinical Potential of Orodispersible Films. AAPS PharmSciTech. 2017;18(2):267–72.

32. Bjerknes K, Bøyum S, Kristensen S, Brustugun J, Wang S. Manipulating tablets and capsules given to hospitalised children in Norway is common practice. Acta Paediatr Int J Paediatr. 2017;106(3):503–8.

33. Richey RH, Shah UU, Peak M, Craig J, Ford JL, Barker CE, Nunn AJ, Turner MA. Manipulation of drugs to achieve the required dose is intrinsic to paediatric practice but is not supported by guidelines or evidence. BMC Pediatr. 2013;13(1).

34. Ernest TB, Elder DP, Martini LG, Roberts M, Ford JL. Developing paediatric medicines: identifying the needs and recognizing the challenges. J Pharm Pharmacol. 2007;59(8):1043–

55.

35. Garcia-Palop B, Movilla Polanco E, Cañete Ramirez C, Cabañas Poy MJ. Harmful excipients in medicines for neonates in Spain. Int J Clin Pharm. 2016;38(2):238–42.

36. Valeur KS, Hertel SA, Lundstrøm KE, Holst H. The Cumulative Daily Tolerance Levels of Potentially Toxic Excipients Ethanol and Propylene Glycol Are Commonly Exceeded in Neonates and Infants. Basic Clin Pharmacol Toxicol. 2018;122(5):523–30.

37. Ferro A. Paediatric prescribing: Why children are not small adults. Br J Clin Pharmacol. 2015;79(3):351–3.

38. Salunke S, Liu F, Batchelor H, Walsh J, Turner R, Ju TR, Tuleu C. European Paediatric Formulation Initiative (EuPFI)—Formulating Ideas for Better Medicines for Children. AAPS PharmSciTech. 2017;18(2):257–62.

39. Medicines for Children [Internet]. European Commission. 2021 [cited 2021 Aug 4]. Available from: https://ec.europa.eu/health/human-use/paediatric-medicines_en

40. Ecker A, Mariz S, Naumann-Winter F, Norga K, Barisic I, Girard T, Tomasi P, Mentzer D, Sepodes B. Comparative analysis of the scope of European Union paediatric investigation plans with corresponding orphan designations. Arch Dis Child. 2018;103(5):427–30.

41. Mistry P, Batchelor H. Evidence of acceptability of oral paediatric medicines: a review. J Pharm Pharmacol. 2017;69(4):361–76.

42. Jasińska-Stroschein M, Kurczewska U, Orszulak-Michalak D. Statistical Considerations Concerning Dissimilar Regulatory Requirements for Dissolution Similarity Assessment. The Example of Immediate-Release Dosage Forms. J Pharm Sci. 2017;106(5):1275–84.

43. Center for Drug Evaluation and Research. Guidance for Industry SUPAC-MR: Modified Release Solid Oral Dosage Forms Scale-Up and Postapproval Changes: Chemistry, Manufacturing, and Controls; In Vitro Dissolution Testing and In Vivo Bioequivalence Documentation. Maryland; 1997.

44. Committee for Medicinal Products for Human Use (CHMP). Guideline on quality of oral modified release products. London; 2014.

45. Markl D, Zeitler JA. A Review of Disintegration Mechanisms and Measurement Techniques. Pharm Res. 2017;34(5):890–917.

46. Rouge N, Buri P, Doelker E. Drug absorption sites in the gastrointestinal tract and dosage

forms for site-specific delivery. Int J Pharm. 1996;136(1–2):117–39.

47. Martinez MN, Lindquist D, Modric S. Terminology challenges: Defining modified release dosage forms in veterinary medicine. J Pharm Sci. 2010;99(8):3281–90.

48. Chen ML, Shah VP, Ganes D, Midha KK, Caro J, Nambiar P, et al. Challenges and opportunities in establishing scientific and regulatory standards for determining therapeutic equivalence of modified-release products: Workshop summary report. Clin Ther. 2010;32(10):1704–12.

49. Lee PI, Li JX. Evolution of oral controlled release dosage forms. In: Wen H, Park K, editors. Oral Controlled Release Formulation Design and Drug Delivery: Theory to Practice. 1st ed. John Wiley and Sons Inc.; 2010. p. 21–31.

50. Chen Z, Zhu Q, Qi J, Lu Y, Wu W. Sustained and controlled release of herbal medicines: The concept of synchronized release. Int J Pharm. 2019;560(4):116–25.

51. Tanaka N, Imai K, Okimoto K, Ueda S, Tokunaga Y, Ohike A, Ibuki R, Higaki K, Kimura T. Development of novel sustained-release system, disintegration-controlled matrix tablet (DCMT) with solid dispersion granules of nilvadipine. J Control Release. 2005;108(2–3):386–95.

52. Abdul S, Chandewar A, Jaiswal SB. A flexible technology for modified-release drugs: Multiple-unit pellet system (MUPS). J Control Release. 2010;147(1):2–16.

53. Sigfridsson K, Arvidsson T, Xue A, Wagner DJ, Zhang G, Strimfors M. A candidate drug administered subcutaneously to rodents as drug particles showing hepatic recirculation which influenced the sustained release process. Int J Pharm. 2020;581(5).

54. Varum FJO, Merchant HA, Basit AW. Oral modified-release formulations in motion: The relationship between gastrointestinal transit and drug absorption. Int J Pharm. 2010;395(1–2):26–36.

55. Aulton ME. Modified-release peroral dosage forms. In: Aulton ME, editor. Aulton's Pharmaceutics. 3rd ed. Churchill Livingstone; 2007. p. 483–99.

56. Yun YH, Lee BK, Park K. Controlled Drug Delivery: Historical perspective for the next generation. J Control Release. 2015;219(12):2–7.

57. Skelly JP, Amidon GL, Barr WH, Benet LZ, Carter JE, Robinson JR, Shah VP, Yacobi A. In vitro and in vivo testing and correlation for oral controlled/ modified release dosage forms. J Control Release. 1990;14(1):95–106.

58. Layek B, Mandal S. Natural polysaccharides for controlled delivery of oral therapeutics: a recent update. Carbohydr Polym. 2020;230(2).

59. Koziolek M, Grimm M, Schneider F, Jedamzik P, Sager M, Kühn JP, Siegmund W, Weitschies W. Navigating the human gastrointestinal tract for oral drug delivery: Uncharted waters and new frontiers. Adv Drug Deliv Rev. 2016;101(6):75–88.

60. McConnell EL, Fadda HM, Basit AW. Gut instincts: Explorations in intestinal physiology and drug delivery. Int J Pharm. 2008;364(2):213–26.

61. Park K. Drug delivery of the future: Chasing the invisible gorilla. J Control Release. 2016;240:2–8.

62. Helfand WH, Cowen DL. Evolution of pharmaceutical oral dosage forms. Pharm Hist. 1983;25(1):7–18.

63. Park K. Controlled drug delivery systems: Past forward and future back. J Control Release. 2014;190(9):3–8.

64. Dragstedt CA. Oral medication with preparations for prolonged action. J Am Med Assoc. 1958;168(12):1652–5.

65. Lazarus J, Cooper J. Oral Prolonged Action Medicaments: Their Pharmaceutical Control and Therapeutic Aspects. J Pharm Pharmacol. 1959;11(1):257–90.

66. Yu J, Zhang Y, Yan J, Kahkoska AR, Gu Z. Advances in bioresponsive closed-loop drug delivery systems. Int J Pharm. 2018;544(2):350–7.

67. Acharya G, Park K. Mechanisms of controlled drug release from drug-eluting stents. Adv Drug Deliv Rev. 2006;58(3):387–401.

68. Sinko PJ. Drug release and dissolution. In: Singh Y, Sinko PJ, editors. Martin's Physical Pharmacy and Pharmaceutical Sciences. 6th ed. Lippincott Williams & Wilkins; 2011. p. 300–17.

69. Colombo P, Sonvico F, Colombo G, Bettini R. Novel platforms for oral drug delivery. Pharm Res. 2009;26(3):601–11.

70. Lee PI, Li JX. Evolution of oral controlled release dosage forms. Oral Control Release Formul Des Drug Deliv Theory to Pract. 2010;21–31.

71. Chaibva FA, Khamanga SMM, Walker RB. Swelling, erosion and drug release characteristics of

salbutamol sulfate from hydroxypropyl methylcellulose-based matrix tablets. Drug Dev Ind Pharm [Internet]. 2010 Dec 9;36(12):1497–510. Available from: http://www.tandfonline.com/doi/full/10.3109/03639045.2010.488648

72. Barmpalexis P, Kachrimanis K, Malamataris S. Statistical moments in modelling of swelling, erosion and drug release of hydrophilic matrix-tablets. Int J Pharm [Internet]. 2018 Apr;540(1–2):1–10. Available from: https://linkinghub.elsevier.com/retrieve/pii/S0378517318300723

73. Timmins P, Desai D, Chen W, Wray P, Brown J, Hanley S. Advances in mechanistic understanding of release rate control mechanisms of extended-release hydrophilic matrix tablets. Ther Deliv [Internet]. 2016 Aug;7(8):553–72. Available from: https://www.future-science.com/doi/10.4155/tde-2016-0026

74. Rosen H, Abribat T. The rise and rise of drug delivery. Nat Rev Drug Discov. 2005;4(5):381–5.

75. Malaterre V, Ogorka J, Loggia N, Gurny R. Oral osmotically driven systems: 30 years of development and clinical use. Eur J Pharm Biopharm. 2009;73(3):311–23.

76. Wen H, Park K. Introduction and overview of oral controlled release formulation design. In: Wen H, Park K, editors. Oral Controlled Release Formulation Design and Drug Delivery: Theory to Practice. 1st ed. Wiley; 2020. p. 6.

77. De Robertis S, Bonferoni MC, Elviri L, Sandri G, Caramella C, Bettini R. Advances in oral controlled drug delivery: the role of drug–polymer and interpolymer non-covalent interactions. Expert Opin Drug Deliv. 2015;12(3):441–53.

78. Jain KK. Drug Delivery Systems - An Overview. In: Jain KK, editor. Methods in Molecular Biology. 3rd ed. Humana Press; 2008. p. 1–54.

79. Vasiliu S, Bunia I, Racovita S, Neagu V. Adsorption of cefotaxime sodium salt on polymer coated ion exchange resin microparticles: Kinetics, equilibrium and thermodynamic studies. Carbohydr Polym. 2011;85(2):376–87.

80. Anand V, Kandarapu R, Garg S. Ion-exchange resins: carrying drug delivery forward. Drug Discov Today. 2001;6(17):905–14.

81. Belakhov V V., Momot NN. Regeneration of FAF and AV-17I anion exchange resins after absorption purification of alpha-amylase from Bacillus subtilis. Pharm Chem J. 1983;17(5):369–71.

82. Tawakkul MA, Shah RB, Zidan A, Sayeed VA, Khan MA. Complexation of risperidone with a taste-masking resin: Novel application of near infra-red and chemical imaging to evaluate complexes. Pharm Dev Technol. 2009;14(4):409–21.

83. Rajesh AM, Popat KM. Taste masking of ofloxacin and formation of interpenetrating polymer network beads for sustained release. J Pharm Anal. 2017;7(4):244–51.

84. Akkaramongkolporn P, Ngawhirunpat T, Opanasopit P. Preparation and evaluation of differently sulfonated styrene-divinylbenzene cross-linked copolymer cationic exchange resins as novel carriers for drug delivery. AAPS PharmSciTech. 2009;10(2):641–8.

85. Wrong O, Harland C. Sevelamer and Other Anion-Exchange Resins in the Prevention and Treatment of Hyperphosphataemia in Chronic Renal Failure. Nephron Physiol. 2007;107(1):17–33.

86. Nishida S, Horinouchi A, Higashimura Y, Akahori R, Matsumoto K. Cholestyramine, a Bile Acid Sequestrant, Increases Cecal Short Chain Fatty Acids and Intestinal Immunoglobulin A in Mice. Biol Pharm Bull. 2020;43(3):565–8.

87. Sterns RH, Rojas M, Bernstein P, Chennupati S. Ion-exchange resins for the treatment of hyperkalemia: Are they safe and effective? J Am Soc Nephrol. 2010;21(5):733–5.

88. Burke GM, Mendes RW, Jambhekar SS. Investigation of the applicability of ion exchange resins as a sustained release drug delivery system forpropranolol hydrochloride. Drug Dev Ind Pharm. 1986;12(5):713–32.

89. Irwin WJ, Belaid KA, Alpar HO. Drug-delivery by ion-exchange. Part IV: Coated resinate complexes of ester pro-drugs of propranolol. Drug Dev Ind Pharm. 1988;14(10):1307–25.

90. Sprockel OL, Prapaitrakul W. Effect of eluant properties on drug release from cellulose acetate butyrate-coated drug resin complexes. Int J Pharm. 1988;48(1–3):217–22.

91. Motycka S, Nairn JG. Influence of wax coatings on release rate of anions from ion-exchange resin beads. J Pharm Sci. 1978;67(4):500–3.

92. Motycka S, Newth CJL, Nairn JG. Preparation and evaluation of microencapsulated and coated ion-exchange resin beads containing theophylline. J Pharm Sci. 1985;74(6):643–6.

93. Adelli GR, Balguri SP, Bhagav P, Raman V, Majumdar S. Diclofenac sodium ion exchange resin complex loaded melt cast films for sustained release ocular delivery. Drug Deliv. 2017;24(1):370–9.

94. Kim J Il, Cho SM, Cui JH, Cao QR, Oh E, Lee BJ. In vitro and in vivo correlation of disintegration and bitter taste masking using orally disintegrating tablet containing ion exchange resin-drug complex. Int J Pharm. 2013;455(1–2):31–9.

95. Guo X, Chang RK, Hussain MA. Ion-exchange resins as drug delivery carriers. J Pharm Sci. 2009;98(11):3886–902.

96. Sriwongjanya M, Bodmeier R. Effect of ion exchange resins on the drug release from matrix tablets. Eur J Pharm Biopharm. 1998;46(3):321–7.

97. Shamma RN, Basalious EB, Shoukri RA. Development and optimization of a multiple-unit controlled release formulation of a freely water soluble drug for once-daily administration. Int J Pharm. 2011;405(1–2):102–12.

98. Chen Y, Burton MA, Codde JP, Napoli S, Martins IJ, Gray BN. Evaluation of Ion-exchange Microspheres as Carriers for the Anticancer Drug Doxorubicin: In-vitro Studies. J Pharm Pharmacol. 1992;44(3):211–5.

99. Patra S, Samantaray R, Pattnaik S, Barik BB. Taste masking of Etoricoxib by using ion-exchange resin. Pharm Dev Technol. 2010;15(5):511–7.

100. Jain AK, Sahu PK, Mohan P, Jain SJ. Ion Exchange Resins- Pharmaceutical and Clinical Applications. Asian J Biomater Res. 2016;2(2):51–61.

101. Singh I, Rehni AK, Kalra R, Joshi G, Kumar M, Aboul-Enein HY. Ion exchange resins: Drug delivery and therapeutic applications. Fabad J Pharm Sci. 2007;32(2):91–100.

102. Gupta S, Benien P, Sahoo PK. Ion Exchange Resins Transforming Drug Delivery Systems. Curr Drug Deliv. 2010;7(3):252–62.

103. Mehta K, Tu Y-H. Modified Release Formulations Containing Drug-Ion Exchange Resin Complexes. United States of America; US 9,675,703 B2, 2017.

104. Rohm and Haas. Amberlite IRP64-Pharmaceutical Grade Cation Exchange Resin (Polacrilex Resin) [Internet]. Technical Data Sheet. 2016 [cited 2020 Apr 1]. Available from: https://nshosting.dow.com/doc-archive/business/process_chemicals/amberlite_and_duolite_pharmaceutical_grade_resins/amberlite_irp64/tds/amberlite_irp64.pdf

105. Rohm and Haas. Amberlite IRP88-Pharmaceutical Grade Cation Exchange Resin (Polacrillin Potassium NF) [Internet]. Technical Data Sheet. 2006. Available from:

https://nshosting.dow.com/doc-archive/business/process_chemicals/amberlite_and_duolite_pharmaceutical_grade_resins/amberlite_irp88/tds/amberlite_irp88.pdf

106. Yamamoto Y, Kumagai H, Haneda M, Vertzoni M, Ouwerkerk N, Murayama D, Katakawa Y, Motonaga K, Reppas C, Tajiri T. The mechanism of solifenacin release from a pH-responsive ion-complex oral suspension in the fasted upper gastrointestinal lumen. Eur J Pharm Sci. 2020;142(1).

107. Sun C, Liu H, Zhao X, He H, Pan W. In vitro and in vivo evaluation of a novel diltiazem hydrochloride polydispersity sustained-release system. Drug Dev Ind Pharm. 2013;39(1):62–6.

108. Rohm and Haas. Amberlite IRP69-Pharmaceutical Grade Cation Exchange Resin (Sodium Polystyrene Sulfonate USP) [Internet]. Technical Data Sheet. 2016 [cited 2020 Apr 1]. Available from: https://nshosting.dow.com/doc-archive/business/process_chemicals/amberlite_and_duolite_pharmaceutical_grade_resins/amberlite_irp69/tds/amberlite_irp69.pdf

109. Pongjanyakul T, Prakongpan S, Rungsardthong U, Chancham P, Priprem A. Characteristics and in vitro release of dextromethorphan resinates. Powder Technol. 2005;152(1–3):100–6.

110. Jeong SH, Park K. Drug loading and release properties of ion-exchange resin complexes as a drug delivery matrix. Int J Pharm. 2008;361(1–2):26–32.

111. Jeong SH, Park K. Development of sustained release fast-disintegrating tablets using various polymer-coated ion-exchange resin complexes. Int J Pharm. 2008;353(1–2):195–204.

112. Boyd GE, Adamson AW, Myers LS. The Exchange Adsorption of Ions from Aqueous Solutions by Organic Zeolites. II. Kinetics 1. J Am Chem Soc. 1947;69(11):2836–48.

113. Plaizier-Vercammen JA. Investigation of the bioavailability of codeine from a cation ion-exchange sulfonic acid. 1. Effect of parameters. Int J Pharm. 1992;85(1–3):45–50.

114. Reichenberg D. Properties of Ion-Exchange Resins in Relation to their Structure. III. Kinetics of Exchange. J Am Chem Soc. 1953;75(3):589–97.

115. Al-Jubouri SM, Holmes SM. Hierarchically porous zeolite X composites for manganese ion-exchange and solidification: Equilibrium isotherms, kinetic and thermodynamic studies. Chem Eng J. 2017;

116. Zeng HX, Wang M, Jia F, Lin SJ, Cheng G, Pan WS. Preparation and in vitro release of dual-drug resinate complexes containing codeine and chlorpheniramine. Drug Dev Ind Pharm. 2011;37(2):201–7.

117. Junyaprasert VB, Manwiwattanakul G. Release profile comparison and stability of diltiazem-resin microcapsules in sustained release suspensions. Int J Pharm. 2008;352(1–2):81–91.

118. Shang R, Liu C, Quan P, Zhao H, Fang L. Effect of drug-ion exchange resin complex in betahistine hydrochloride orodispersible film on sustained release, taste masking and hygroscopicity reduction. Int J Pharm. 2018;545(1–2):163–9.

119. Tan DCT, Ong JJ, Gokhale R, Heng PWS. Hot melt extrusion of ion-exchange resin for taste masking. Int J Pharm. 2018;547(1–2):385–94.

120. Albertini B, Passerini N, González-Rodríguez ML, Cavallari C, Cini M, Rodriguez L. Wet granulation as innovative and fast method to prepare controlled release granules based on an ion-exchange resin. J Pharm Sci. 2008;97(3):1313–24.

121. Shah RB, Tawakkul MA, Sayeed VA, Khan MA. Complexation between risperidone and amberlite resin by various methods of preparation and binding study. Drug Dev Ind Pharm. 2009;35(12):1409–18.

122. Zhang ZY, Ping QN, Xiao B. Microencapsulation and characterization of tramadol-resin complexes. J Control Release. 2000;66(2–3):107–13.

123. Chaudhry NC, Saunders L. Sustained Release of Drugs From Ion Exchange Resins. J Pharm Pharmacol. 1956;8(1):975–86.

124. Elder DP. Products of Chemistry Pharmaceutical Applications of Ion-Exchange Resins. J Chem Educ. 2005;82(4):575–87.

125. Patel HH, Maniar M, Ren C, Dave RH. Determination of Degradation Kinetics and Effect of Anion Exchange Resin on Dissolution of Novel Anticancer Drug Rigosertib in Acidic Conditions. AAPS PharmSciTech. 2018;19(1):93–100.

126. Dashevskiy A, Mohylyuk V, Ahmed AR, Kolter K, Guth F, Bodmeier R. Micropellets coated with Kollicoat® Smartseal 30D for taste masking in liquid oral dosage forms. Drug Dev Ind Pharm. 2017;43(9):1548–56.

127. Cuña M, Vila Jato JL, Torres D. Controlled-release liquid suspensions based on ion-exchange particles entrapped within acrylic microcapsules. Int J Pharm. 2000;199(2):151–8.

128. Kasashima Y, Uchida S, Yoshihara K, Yasuji T, Sako K, Namiki N. Oral sustained-release suspension based on a lauryl sulfate salt/complex. Int J Pharm. 2016;515(1–2):677–83.

129. Zeng HX, Cheng G, Pan WS, Zhong GP, Huang M. Preparation of codeine-resinate and chlorpheniramine-resinate sustained-release suspension and its pharmacokinetic evaluation in beagle dogs. Drug Dev Ind Pharm. 2007;33(6):649–65.

130. Fundueanu G, Constantin M, Esposito E, Cortesi R, Nastruzzi C, Menegatti E. Cellulose acetate butyrate microcapsules containing dextran ion-exchange resins as self-propelled drug release system. Biomaterials. 2005;26(20):4337–47.

131. Ichikawa H, Fujioka K, Adeyeye MC, Fukumori Y. Use of ion-exchange resins to prepare 100 µm-sized microcapsules with prolonged drug-release by the Wurster process. Int J Pharm. 2001;216(1–2):67–76.

132. Torres D, García-Encina G, Seijo B, Vila Jato JL. Formulation and in vitro evaluation of HPMCP-microencapsulated drug-resin complexes for sustained release of diclofenac. Int J Pharm. 1995;121(2):239–43.

133. Sriwongjanya M, Bodmeier R. Entrapment of drug-loaded ion-exchange particles within polymeric microparticles. Int J Pharm. 1997;158(1):29–38.

134. Torres D, Boado L, Blanco D, Vila-Jato JL. Comparison between aqueous and non-aqueous solvent evaporation methods for microencapsulation of drug-resin complexes. Int J Pharm. 1998;173(1–2):171–82.

135. Torres D, Seijo B, García-Encina G, Alonso MJ, Vila-Jato JL. Microencapsulation of ion-exchange resins by interfacial nylon polymerization. Int J Pharm. 1990;59(1):9–17.

136. Huang RG, Schwartz JB, Ofner CM. Microencapsulation of chlorpheniramine maleate-resin particles with crosslinked chitosan for sustained release. Pharm Dev Technol. 1999;4(1):107–15.

137. Rajesh AM, Popat KM. In vivo and in vitro taste masking of ofloxacin and sustained release by forming interpenetrating polymer network beads. Pharm Dev Technol. 2017;22(1):26–34.

138. Mehta K, Tu Y-H. Modified release formulations containing drug-ion exchange resin complexes. United States of America; US 9,675,703 B2, 2016.

139. McMahen R, Tengler M, Sloane M, Lockhart D. Methods of formulating and designing liquid drug suspensions containing ion exchange resin particles. United States of America; US

8,512,759 B1, 2013.

140. Leonard SG, Cooper D. Oral liquid compositions containing paroxetin resinate. United Kingdom; 5,811,436, 1998.

141. Borodkin S, Sundberg DP. Polycarboxylic acid ion-exchange resin adsorbates for taste coverage in chewable tablets. J Pharm Sci. 1971;60(10):1523–7.

142. Borodkin S, Yunker MH. Interaction of amine drugs with a polycarboxylic acid ion-exchange resin. J Pharm Sci. 1970;59(4):481–6.

143. Bhise K, Shaikh S, Bora D. Taste mask, design and evaluation of an oral formulation using ion exchange resin as drug carrier. AAPS PharmSciTech. 2008;9(2):557–62.

144. Wei Y, Li C, Zhu Q, Zhang X, Guan J, Mao S. Comparison of thermosensitive in situ gels and drug-resin complex for ocular drug delivery: In vitro drug release and in vivo tissue distribution. Int J Pharm. 2020;578(3).

145. Raghunathan Y, Amsel L, Hinsvark O, Bryant W. Sustained-release drug delivery system I: Coated ion-exchange resin system for phenylpropanolamine and other drugs. J Pharm Sci. 1981;70(4):379–84.

146. Jeong SH, Park K. Simple preparation of coated resin complexes and their incorporation into fast-disintegrating tablets. Arch Pharm Res. 2010;33(1):115–23.

147. Atyabi F, Sharma HL, Mohammad HAH, Fell JT. Controlled drug release from coated floating ion exchange resin beads. J Control Release. 1996;42(1):25–8.

148. McDonagh AF, Tajber L. The control of paracetamol particle size and surface morphology through crystallisation in a spray dryer. Adv Powder Technol. 2020;31(1):287–99.

149. Singh A, Van den Mooter G. Spray drying formulation of amorphous solid dispersions. Adv Drug Deliv Rev. 2016;100(5):27–50.

150. Friesen DT, Shanker R, Crew M, Smithey DT, Curatolo WJ, Nightingale JAS. Hydroxypropyl methylcellulose acetate succinate-based spray-dried dispersions: An overview. Mol Pharm. 2008;5(6):1003–19.

151. Paudel A, Worku ZA, Meeus J, Guns S, Van den Mooter G. Manufacturing of solid dispersions of poorly water soluble drugs by spray drying: Formulation and process considerations. Int J Pharm. 2013;453(1):253–84.

152. Van Duong T, Van den Mooter G. The role of the carrier in the formulation of pharmaceutical solid dispersions. Part II: amorphous carriers. Expert Opin Drug Deliv. 2016;13(12):1681–94.

153. Paluch KJ, Tajber L, Corrigan OI, Healy AM. Impact of process variables on the micromeritic and physicochemical properties of spray-dried porous microparticles, part I: Introduction of a new morphology classification system. J Pharm Pharmacol. 2012;64(11):1570–82.

154. Vehring R. Pharmaceutical particle engineering via spray drying. Pharm Res. 2008;25(11):999–1022.

155. Grohganz H, Priemel PA, Löbmann K, Nielsen LH, Laitinen R, Mullertz A, Van Den Mooter G, Rades T. Refining stability and dissolution rate of amorphous drug formulations. Expert Opin Drug Deliv. 2014;11(6):977–89.

156. Davis MT, Potter CB, Mohammadpour M, Albadarin AB, Walker GM. Design of spray dried ternary solid dispersions comprising itraconazole, soluplus and HPMCP: Effect of constituent compositions. Int J Pharm. 2017;519(1–2):365–72.

157. McDonagh AF, Tajber L. Crystallo-co-spray drying as a new approach to manufacturing of drug/excipient agglomerates: Impact of processing on the properties of paracetamol and lactose mixtures. Int J Pharm. 2020;577(3).

158. Mendonsa N, Almutairy B, Kallakunta VR, Sarabu S, Thipsay P, Bandari S, Repka MA. Manufacturing strategies to develop amorphous solid dispersions: An overview. J Drug Deliv Sci Technol. 2020;55(12).

159. Gonnissen Y, Remon JP, Vervaet C. Effect of maltodextrin and superdisintegrant in directly compressible powder mixtures prepared via co-spray drying. Eur J Pharm Biopharm. 2008;68(2):277–82.

160. Vasconcelos T, Marques S, das Neves J, Sarmento B. Amorphous solid dispersions: Rational selection of a manufacturing process. Adv Drug Deliv Rev. 2016;100(5):85–101.

161. Thybo P, Pedersen BL, Hovgaard L, Holm R, Müllertz A. Characterization and physical stability of spray dried solid dispersions of probucol and PVP-K30. Pharm Dev Technol. 2008;13(5):375–86.

162. Davis M, Walker G. Recent strategies in spray drying for the enhanced bioavailability of poorly water-soluble drugs. J Control Release. 2018;269(7):110–27.

163. Legako J, Dunford NT. Effect of spray nozzle design on fish oil-whey protein microcapsule

properties. J Food Sci. 2010;75(6):394–400.

164. Ichikawa H, Fukumori Y, Moji Adeyeye C. Design of prolonged-release microcapsules containing diclofenac sodium for oral suspensions and their preparation by the Wurster process. Int J Pharm. 1997;156(1):39–48.

165. Howick K, Alam R, Chruscicka B, Kandil D, Fitzpatrick D, Ryan AM, Cryan JF, Schellekens H, Griffin BT. Sustained-release multiparticulates for oral delivery of a novel peptidic ghrelin agonist: Formulation design and in vitro characterization. Int J Pharm. 2018;536(1):63–72.

166. Shao ZJ, Morales L, Diaz S, Muhammad NA. Drug release from kollicoat SR 30D-coated nonpareil beads: Evaluation of coating level, plasticizer type, and curing condition. AAPS PharmSciTech. 2002;3(2):15.

167. Melegari C, Bertoni S, Genovesi A, Hughes K, Rajabi-Siahboomi AR, Passerini N, Albertini B. Ethylcellulose film coating of guaifenesin-loaded pellets: A comprehensive evaluation of the manufacturing process to prevent drug migration. Eur J Pharm Biopharm. 2016;100:15–26.

168. Foroughi-Dahr M, Sotudeh-Gharebagh R, Mostoufi N. Effect of operation conditions on coating of pharmaceutical pellets with a film of HPMC/PEG in a Wurster coater. Powder Technol. 2019;354:804–14.

169. Dreu R, Luštrik M, Perpar M, Žun I, Srčič S. Fluid-bed coater modifications and study of their influence on the coating process of pellets. Drug Dev Ind Pharm. 2012;38(4):501–11.

170. Knop K, Kleinebudde P. PAT-tools for process control in pharmaceutical film coating applications. Int J Pharm. 2013;457(2):527–36.

171. Luštrik M, Dreu R, Šibanc R, Srčič S. Comparative study of the uniformity of coating thickness of pellets coated with a conventional Wurster chamber and a swirl generator-equipped Wurster chamber. Pharm Dev Technol. 2012;17(3):268–76.

172. Foroughi-Dahr M, Sotudeh-Gharebagh R, Mostoufi N. Development of a PAT tool for monitoring the Wurster coater performance. Int J Pharm. 2019;561(4):171–86.

173. Ronchi F, Sereno A, Paide M, Sacré P, Guillaume G, Stéphenne V, Goole J, Amighi K. Development and evaluation of an omeprazole-based delayed-release liquid oral dosage form. Int J Pharm. 2019;567(8).

174. Teunou E, Poncelet D. Batch and continuous fluid bed coating - Review and state of the art [Internet]. Vol. 53, Journal of Food Engineering. 2002. p. 325–40. Available from:

www.elsevier.com/locate/jfoodeng

175. Albanez R, Nitz M, Taranto OP. Enteric coating process of diclofenac sodium pellets in a fluid bed coater with a wurster insert: Influence of process variables on coating performance and release profile. Adv Powder Technol. 2013;24(3):659–66.

176. Jiang Z, Rieck C, Bück A, Tsotsas E. Modeling of inter- and intra-particle coating uniformity in a Wurster fluidized bed by a coupled CFD-DEM-Monte Carlo approach. Chem Eng Sci. 2020;211(1).

177. Fukumori Y, Ichikawa H, Yamaoka Y, Akaho E, Takeuchi Y, Fukuda T, Kanamori R, Osako Y. Microgranulation and encapsulation of pulverized pharmaceutical powders with ethyl cellulose by the Wurster process. Chem Pharm Bull. 1991;39(7):1806–12.

178. Mohylyuk V, Patel K, Scott N, Richardson C, Murnane D, Liu F. Wurster Fluidised Bed Coating of Microparticles: Towards Scalable Production of Oral Sustained-Release Liquid Medicines for Patients with Swallowing Difficulties. AAPS PharmSciTech. 2020;21(1).

179. Tang ESK, Wang L, Liew C V., Chan LW, Heng PWS. Drying efficiency and particle movement in coating-Impact on particle agglomeration and yield. Int J Pharm. 2008;350(1–2):172–80.

180. Goole J, Deleuze P, Vanderbist F, Amighi K. New levodopa sustained-release floating minitablets coated with insoluble acrylic polymer. Eur J Pharm Biopharm. 2008;68(2):310–8.

181. Semdé R, Amighi K, Devleeschouwer MJ, Moës AJ. Studies of pectin HM/Eudragit® RL/Eudragit® NE film-coating formulations intended for colonic drug delivery. Int J Pharm. 2000;197(1–2):181–92.

182. Marucci M, Andersson H, Hjärtstam J, Stevenson G, Baderstedt J, Stading M, Larsson A, Von Corswant C. New insights on how to adjust the release profile from coated pellets by varying the molecular weight of ethyl cellulose in the coating film. Int J Pharm. 2013;458(1):218–23.

183. Speer I, Lenhart V, Preis M, Breitkreutz J. Prolonged release from orodispersible films by incorporation of diclofenac-loaded micropellets. Int J Pharm. 2019;554(1):149–60.

184. Lorck CA, Grunenberg PC, Jünger H, Laicher A. Influence pellets of process parameters on sustained-release theophylline coated with aqueous polymer dispersions and organic solvent-based polymer solutions. Eur J Pharm Biopharm. 1997;43(2):149–57.

185. Kramar A, Turk S, Vrečer F. Statistical optimisation of diclofenac sustained release pellets coated with polymethacrylic films. Int J Pharm. 2003;256(1–2):43–52.

186. Abbaspour MR, Sadeghi F, Afrasiabi Garekani H. Design and study of ibuprofen disintegrating sustained-release tablets comprising coated pellets. Eur J Pharm Biopharm. 2008;68(3):747–59.

187. Buhler V. Kollicoat Grades-Functional Polymers for the Pharmaceutical Industry. BASF; 2007. 104 p.

188. Kaur S, Sivasankaran S, Wambolt E, Jonnalagadda S. Determinants of zero-order release kinetics from acetaminophen-layered Suglet® pellets, Wurster-coated with plasticized Aquacoat® ECD (ethyl cellulose dispersion). Int J Pharm. 2020;573(1).

189. Hamed E, Sakr A. Effect of Curing Conditions and Plasticizer Level on the Release of Highly Lipophilic Drug from Coated Multiparticulate Drug Delivery System. Pharm Dev Technol. 2003;8(4):397–407.

190. Muschert S, Siepmann F, Cuppok Y, Leclercq B, Carlin B, Siepmann J. Improved long term stability of aqueous ethylcellulose film coatings: Importance of the type of drug and starter core. Int J Pharm. 2009;368(1–2):138–45.

191. Kucera SA, Felton LA, McGinity JW. Physical aging in pharmaceutical polymers and the effect on solid oral dosage form stability. Int J Pharm. 2013;457(2):428–36.

192. Yang QW, Flament MP, Siepmann F, Busignies V, Leclerc B, Herry C, Tchoreloff P, Siepmann J. Curing of aqueous polymeric film coatings: Importance of the coating level and type of plasticizer. Eur J Pharm Biopharm. 2010;74(2):362–70.

193. Pearnchob N, Bodmeier R. Dry polymer powder coating and comparison with conventional liquid-based coatings for Eudragit® RS, ethylcellulose and shellac. Eur J Pharm Biopharm. 2003;56(3):363–9.

194. Dashevsky A, Wagner K, Kolter K, Bodmeier R. Physicochemical and release properties of pellets coated with Kollicoat® SR 30 D, a new aqueous polyvinyl acetate dispersion for extended release. Int J Pharm. 2005;290(1–2):15–23.

195. Bordaweka MS, Zia H, Quadir A. Evaluation of polyvinyl acetate dispersion as a sustained release polymer for tablets. Drug Deliv J Deliv Target Ther Agents. 2006;13(2):121–31.

196. Wesseling M, Bodmeier R. Drug release from beads coated with an aqueous colloidal ethylcellulose dispersion, Aquacoat®, or an organic ethylcellulose solution. Eur J Pharm Biopharm. 1999;47(1):33–8.

197. Abbaspour MR, Sadeghi F, Afrasiabi Garekani H. Thermal treating as a tool to produce plastic pellets based on Eudragit RS PO and RL PO aimed for tableting. Eur J Pharm Biopharm. 2007;67(1):260–7.

198. Khatri P, Desai D, Shelke N, Minko T. Role of plasticizer in membrane coated extended release oral drug delivery system. J Drug Deliv Sci Technol. 2018;44(12):231–43.

199. Bodmeier R, Paeratakul O. The distribution of plasticizers between aqueous and polymer phases in aqueous colloidal polymer dispersions. Int J Pharm. 1994;103(1):47–54.

200. Chaudhary RS, Patel T, Kumar JR, Chan M. Effect of substitution of plasticizer dibutyl phthalate with dibutyl sebacate on Eudragit ® RS30D drug release rate control. Pharm Dev Technol. 2019;24(3):276–82.

201. Wesseling M, Kuppler F, Bodmeier R. Tackiness of acrylic and cellulosic polymer films used in the coating of solid dosage forms. Eur J Pharm Biopharm. 1999;47(1):73–8.

202. Heng PWS, Wan LSC, Tan YTF. Relationship between aggregation of HPMC coated spheroids and tackiness/viscosity/additives of the coating formulations. Int J Pharm. 1996;138(1):57–66.

203. Shanmugam S. Granulation techniques and technologies: recent progresses. BioImpacts [Internet]. 2017 Aug 15;5(1):55–63. Available from: http://bi.tbzmed.ac.ir/Abstract/BI_2365_20141208084816

204. Burggraeve A, Monteyne T, Vervaet C, Remon JP, Beer T De. Process analytical tools for monitoring, understanding, and control of pharmaceutical fluidized bed granulation: A review. Eur J Pharm Biopharm [Internet]. 2013 Jan;83(1):2–15. Available from: https://linkinghub.elsevier.com/retrieve/pii/S0939641112003049

205. Iveson SM, Litster JD, Hapgood K, Ennis BJ. Nucleation, growth and breakage phenomena in agitated wet granulation processes: a review. Powder Technol [Internet]. 2001 Jun;117(1–2):3–39. Available from: https://linkinghub.elsevier.com/retrieve/pii/S0032591001003138

206. Parikh DM, Mogavero M. Batch Fluid Bed Granulation. In: Handbook of Pharmaceutical Granulation Technology [Internet]. CRC Press; 2016. p. 220–76. Available from: https://www.taylorfrancis.com/books/9781616310035/chapters/10.3109/9781616310035-13

207. Sivaraman A, Banga A. Quality by design approaches for topical dermatological dosage forms. Res Reports Transdermal Drug Deliv. 2015;

208. Pallagi E, Ambrus R, Szabó-Révész P, Csóka I. Adaptation of the quality by design concept in early pharmaceutical development of an intranasal nanosized formulation. Int J Pharm [Internet]. 2015 Aug;491(1–2):384–92. Available from: https://linkinghub.elsevier.com/retrieve/pii/S0378517315005384

209. Ali R, Mehta P, Kyriaki Monou P, Arshad MS, Panteris E, Rasekh M, Singh N, Qutachi O, Wilson P, Tzetzis D, Chang M-W, Fatouros DG, Ahmad Z. Electrospinning/electrospraying coatings for metal microneedles: A design of experiments (DOE) and quality by design (QbD) approach. Eur J Pharm Biopharm [Internet]. 2020 Nov;156:20–39. Available from: https://linkinghub.elsevier.com/retrieve/pii/S0939641120302678

210. Yu LX. Pharmaceutical quality by design: Product and process development, understanding, and control. Pharmaceutical Research. 2008.

211. Politis SN, Colombo P, Colombo G, Rekkas DM. Design of experiments (DoE) in pharmaceutical development. Drug Development and Industrial Pharmacy. 2017.

212. Lee SH, Heng D, Ng WK, Chan HK, Tan RBH. Nano spray drying: A novel method for preparing protein nanoparticles for protein therapy. Int J Pharm. 2011;

213. Villar AMS, Naveros BC, Campmany ACC, Trenchs MA, Rocabert CB, Bellowa LH. Design and optimization of self-nanoemulsifying drug delivery systems (SNEDDS) for enhanced dissolution of gemfibrozil. Int J Pharm. 2012;

214. Cahyadi C, Koh JJS, Loh ZH, Chan LW, Heng PWS. A feasibility study on pellet coating using a high-speed quasi-continuous coater. AAPS PharmSciTech. 2012;

215. Singh B, Kumar R, Ahuja N. Optimizing Drug Delivery Systems Using Systematic "Design of Experiments." Part I: Fundamental Aspects. Crit Rev Ther Drug Carrier Syst [Internet]. 2005;22(1):27–105. Available from: http://www.dl.begellhouse.com/journals/3667c4ae6e8fd136,40286fbf130b38e6,2195fce72d663157.html

216. Adeleke OA, Tsai P-C, Karry KM, Monama NO, Michniak-Kohn BB. Isoniazid-loaded orodispersible strips: Methodical design, optimization and in vitro-in silico characterization. Int J Pharm [Internet]. 2018 Aug;547(1–2):347–59. Available from: https://linkinghub.elsevier.com/retrieve/pii/S0378517318303958

217. Arpagaus C, Collenberg A, Rütti D, Assadpour E, Jafari SM. Nano spray drying for encapsulation of pharmaceuticals. Int J Pharm [Internet]. 2018 Jul;546(1–2):194–214.

Available from: https://linkinghub.elsevier.com/retrieve/pii/S0378517318303454

218. Özakın AN, Kaya F. Experimental thermodynamic analysis of air-based PVT system using fins in different materials: Optimization of control parameters by Taguchi method and ANOVA. Sol Energy. 2020;

219. Kacker RN, Lagergren ES, Filliben JJ. Taguchi's orthogonal arrays are classical designs of experiments. J Res Natl Inst Stand Technol [Internet]. 1991 Sep;96(5):577. Available from: https://nvlpubs.nist.gov/nistpubs/jres/096/jresv96n5p577_A1b.pdf

220. Verma U, Mujumdar A, Naik J. Preparation of Efavirenz resinate by spray drying using response surface methodology and its physicochemical characterization for taste masking. Dry Technol. 2020;38(5–6):793–805.

221. Lopes-de-Campos D, Nunes C, Sarmento B, Jakobtorweihen S, Reis S. Metronidazole within phosphatidylcholine lipid membranes: New insights to improve the design of imidazole derivatives. Eur J Pharm Biopharm. 2018;129(8):204–14.

222. Houghton GW, Smith J, Thorne PS, Templeton R. The pharmacokinetics of oral and intravenous metronidazole in man. J Antimicrob Chemother. 1979;9(5):621–3.

223. Houghton G, Thorne P, Smith J, Templeton R, Collier J. Comparison of the pharmacokinetics of metronidazole in healthy female volunteers following either a single oral or intravenous dose. Br J Clin Pharmacol. 1979;10(4):337–41.

224. Sanofi-aventis Canada Inc. Product Monograph: Flagyl (Metronidazole) 10% w/w Cream [Internet]. 2018 [cited 2020 Apr 1]. Available from: http://products.sanofi.ca/en/flagyl.pdf

225. Medicines.ie. Flagyl 400mg Tablets [Internet]. Summary of Product Characteristics (SPC). 2018 [cited 2020 Mar 25]. Available from: https://www.medicines.ie/medicines/flagyl-400mg-tablets-32157/smpc

226. U.S. Food & Drug Administration. Drugs@FDA: FDA-Approved Drugs [Internet]. Drug Databases. [cited 2020 Mar 25]. Available from: https://www.accessdata.fda.gov/scripts/cder/daf/index.cfm?event=overview.process&ApplNo=018353

227. Committee for Orphan Medicinal Products. Public summary of opinion on orphan designation-Metronidazole for the treatment of pouchitis. London; 2011.

228. Van Den Mooter G, Rutgeerts P. Formulations of Metronidazole for the Treatment of

Pouchitis. Belgium; W0 2013/186191 A1, 2013.

229. Medicines.ie. Flagyl-S 200mg/5ml Oral Suspension [Internet]. Summary of Product Characteristics (SPC). 2019 [cited 2020 Mar 22]. Available from: https://www.medicines.ie/medicines/flagyl-s-200mg-5ml-oral-suspension-32159/patient-info

230. Mathew M, Gupta V Das, Bethea C. Stability of metronidazole in solutions and suspensions. J Clin Pharm Ther. 1994;19(1):27–9.

231. Bempong DK, Manning RG, Mirza T, Bhattacharyya L. A stability-indicating HPLC assay for metronidazole benzoate. J Pharm Biomed Anal. 2005;38(4):776–80.

232. Guarini Jr BJ, Doran J, Radovic Z, Sullivan K. Oral Formulations of Metronidazole and Methods of Treating an Infection Using Same. United States of America; WO 2019/140516, 2019.

233. Appili Therapeutics. Appili Receives Orphan Drug Designation from FDA for ATI-1501 [Internet]. business wire. 2016 [cited 2020 May 1]. Available from: https://www.businesswire.com/news/home/20160412005836/en/Appili-Receives-Orphan-Drug-Designation-FDA-ATI-1501

234. Hutchinson DR. Modified Release Tizanidine: A Review. J Int Med Res. 1989;17(6):565–73.

235. Wagstaff AJ, Bryson HM. Tizanidine. A review of its pharmacology, clinical efficacy and tolerability in the management of spasticity associated with cerebral and spinal disorders. Drugs. 1997;53(3):435–52.

236. Lataste X, Emre M, Davis C, Groves L. Comparative profile of tizanidine in the management of spasticity. Neurology. 1994;11(9):53–9.

237. Ono H, Matsumoto K, Kato K, Kato F, Miyamoto M, Mori T, Nakamura T, Oka J, Fukuda H. Effects of tizanidine, a centrally acting muscle relaxant, on motor systems. Gen Pharmacol. 1986;17(2):137–42.

238. Wallace JD. Summary of combined clinical analysis of controlled clinical trials with tizanidine. Neurology. 1994;44(11):60–8.

239. The Health Products Regulatory Agency (HPRA). Zanaflex 2mg tablets [Internet]. Summary of Product Characteristics (SPC). 2019 [cited 2020 Mar 25]. Available from: https://www.hpra.ie/img/uploaded/swedocuments/Licence_PA0749-054-001_19112019125824.pdf

240. Henney HR, Shah J. Relative bioavailability of tizanidine 4-mg capsule and tablet formulations

after a standardized high-fat meal: A single-dose, randomized, open-label, crossover study in healthy subjects. Clin Ther. 2007;29(4):661–9.

241. Bhakay A, Rahman M, Dave R, Bilgili E. Bioavailability Enhancement of Poorly Water-Soluble Drugs via Nanocomposites: Formulation–Processing Aspects and Challenges. Pharmaceutics. 2018;10(3):86.

242. Müller RH, Jacobs C, Kayser O. Nanosuspensions as particulate drug formulations in therapy: Rationale for development and what we can expect for the future. Adv Drug Deliv Rev. 2001;47(1):3–19.

243. Pendekal MS, Tegginamat PT. Formulation and evaluation of a bioadhesive patch for buccal delivery of tizanidine. Acta Pharm Sin B. 2012;2(3):318–24.

244. Shah J, Wesnes KA, Kovelesky RA, Henney HR. Effects of food on the single-dose pharmacokinetics/pharmacodynamics of tizanidine capsules and tablets in healthy volunteers. Clin Ther. 2006;28(9):1308–17.

245. Sun Pharma Advanced Research Company. Investor Update on R&D Pipeline [Internet]. 2015 [cited 2020 Apr 28]. Available from: https://www.sparc.life/sites/default/files/2018-09/SPARC-Investors-Presentation-10-Jun-2015.pdf

246. Corrigan OI. The biopharmaceutic drug classification and drugs administered in extended release (ER) formulations. Adv Exp Med Biol. 1997;423:111–28.

247. El-Mahrouk GM, El-Gazayerly ON, Aboelwafa AA, Taha MS. Chitosan lactate wafer as a platform for the buccal delivery of tizanidine HCl: In vitro and in vivo performance. Int J Pharm. 2014;467(1–2):100–12.

248. Ilhan D, Aktas T, Mollaoglu F, Kanik B, Oner L. Sustained Release Formulation Comprising Tizanidine. Turkey; WO 2017/222488 A1, 2019.

249. Dharmadhikari NB. Oral composition of tizanidine. India; WO 2017/037742 Al, 2017.

250. Dos Santos L, Heineck I. Drug utilization study in pediatric prescriptions of a university hospital in southern Brazil: Off-label, unlicensed and high-alert medications. Farm Hosp. 2012;

251. Tilton AH. Management of Spasticity in Children with Cerebral Palsy. Seminars in Pediatric Neurology. 2004.

252. McManus M. Medical Management of Spasticity in Children with Cerebral Palsy. In: Miller F,

Bachrach S, Lennon N, O'Neil M, editors. Cerebral Palsy. Springer; 2019.

253. Henney HR, Chez M. Pediatric Safety of Tizanidine. Pediatr Drugs [Internet]. 2009 Dec;11(6):397–406. Available from: http://link.springer.com/10.2165/11316090-000000000-00000

254. Palazón García R, Benavente Valdepeñas A, Arroyo Riaño O. Protocol for tizanidine use in infantile cerebral palsy. An Pediatr (Barcelona, Spain). 2008;

255. Abdel Azim AM, El-Ashmoony M, Swealem AM, Shoukry RA. Transdermal films containing tizanidine: In vitro and in vivo evaluation. J Drug Deliv Sci Technol. 2014;24(1):92–9.

256. Patel D, Naik S, Misra A. Improved transnasal transport and brain uptake of tizanidine HCl-loaded thiolated chitosan nanoparticles for alleviation of pain. J Pharm Sci. 2012;101(2):690–706.

257. Mutalik S, Parekh HS, Davies NM, Udupa N. A combined approach of chemical enhancers and sonophoresis for the transdermal delivery of tizanidine hydrochloride. Drug Deliv. 2009;16(2):82–91.

258. Khalil RM, Abdelbary A, Arini SK El, Basha M, El-Hashemy HA, Farouk F. Development of tizanidine loaded aspasomes as transdermal delivery system: ex-vivo and in-vivo evaluation. J Liposome Res. 2019;(11):1–11.

259. Mylan Pharmaceuticals ULC. Product Monograph: Mylan-Tizanidine (Tizanidine Hydrochloride Tablets) 4 mg [Internet]. 2010 [cited 2020 Mar 25]. Available from: https://s3-us-west-2.amazonaws.com/drugbank/cite_this/attachments/files/000/004/471/original/Canadian_monograph__Tizanidine.pdf?1556041234

260. Pellegrini C, Stark P. Method of Reducing Somnolence in Patients Treated with Tizanidine. United States of America; US 2014/0341985A1, 2014.

261. Mehta K, Tu Y-H. Clonidine Formulation. United States of America; US 8,623,409 B1, 2014.

262. Tizanidine hydrochloride monograph [Internet]. British Pharmacopoeia. 2021 [cited 2021 Jun 21]. Available from: https://www.pharmacopoeia.com/bp-2021/monographs/tizanidine-hydrochloride.html?date=2021-04-01&text=tizanidine

263. Lloyd De D. Preparation of pH Buffer Solutions [Internet]. 2021. [cited 2021 Jul 13]. Available from: http://delloyd.50megs.com/moreinfo/buffers2.html

264. Sigma Aldrich. Buffer Reference Table [Internet]. 2021 [cited 2020 Jul 13]. Available from:

https://www.sigmaaldrich.com/IE/en/technical-documents/protocol/protein-biology/protein-concentration-and-buffer-exchange/buffer-reference-center

265. Zhong T, Ruan J, Liu C, Quan P, Fang L. Development of Tizanidine Drug-in-Adhesive Patch: Molecular Mechanism of Permeation Enhancer on Regulating Miscibility and Drug Release by Affecting the Status of Ion-Pair in Polymer Matrix. J Pharm Sci. 2020;

266. Serrano DR, Persoons T, D'Arcy DM, Galiana C, Dea-Ayuela MA, Healy AM. Modelling and shadowgraph imaging of cocrystal dissolution and assessment of in vitro antimicrobial activity for sulfadimidine/4-aminosalicylic acid cocrystals. Eur J Pharm Sci [Internet]. 2016 Jun;89:125–36. Available from: https://linkinghub.elsevier.com/retrieve/pii/S0928098716301361

267. Evans DF, Pye G, Bramley R, Clark AG, Dyson TJ, Hardcastle JD. Measurement of gastrointestinal pH profiles in normal ambulant human subjects. Gut [Internet]. 1988 Aug 1;29(8):1035–41. Available from: https://gut.bmj.com/lookup/doi/10.1136/gut.29.8.1035

268. Andrews GP, Li S, Almajaan A, Yu T, Martini L, Healy A, Jones DS. Fixed Dose Combination Formulations: Multilayered Platforms Designed for the Management of Cardiovascular Disease. Mol Pharm. 2019;

269. Zhang Y, Huo M, Zhou J, Zou A, Li W, Yao C, Xie S. DDSolver: An add-in program for modeling and comparison of drug dissolution profiles. AAPS J. 2010;

270. Siepmann J, Siepmann F. Mathematical modeling of drug delivery. Vol. 364, International Journal of Pharmaceutics. 2008. p. 328–43.

271. Ayyoubi S, Cerda JR, Fernández-García R, Knief P, Lalatsa A, Healy AM, Serrano DR. 3D printed spherical mini-tablets: Geometry versus composition effects in controlling dissolution from personalised solid dosage forms. Int J Pharm [Internet]. 2021 Mar;597:120336. Available from: https://linkinghub.elsevier.com/retrieve/pii/S037851732100140X

272. Tizanidine Tablets monograph [Internet]. United States Pharmacopeia. 2021 [cited 2021 Jun 11]. Available from: https://online.uspnf.com/uspnf/document/1_GUID-51C3E693-9D76-4603-A77C-511E1BACBE62_1_en-US?source=Search Results&highlight=tizanidine

273. Khan NI. Oral controlled release dosage forms (reconstitutable powder) by ion exchange resins. Freie Universitat Berlin; 2019.

274. Bianco S, Tewes F, Tajber L, Caron V, Corrigan OI, Healy AM. Bulk, surface properties and water uptake mechanisms of salt/acid amorphous composite systems. Int J Pharm. 2013;

275. Bravo-Osuna I, Ferrero C, Jiménez-Castellanos MR. Water sorption–desorption behaviour of methyl methacrylate–starch copolymers: effect of hydrophobic graft and drying method. Eur J Pharm Biopharm [Internet]. 2005 Apr;59(3):537–48. Available from: https://linkinghub.elsevier.com/retrieve/pii/S0939641104002784

276. Tewes F, Tajber L, Corrigan OI, Ehrhardt C, Healy AM. Development and characterisation of soluble polymeric particles for pulmonary peptide delivery. Eur J Pharm Sci. 2010;

277. Amaro MI, Tewes F, Gobbo O, Tajber L, Corrigan OI, Ehrhardt C, Healy AM. Formulation, stability and pharmacokinetics of sugar-based salmon calcitonin-loaded nanoporous/nanoparticulate microparticles (NPMPs) for inhalation. Int J Pharm. 2015;

278. Qin F, Zeng L, Zhu Y, Cao J, Wang X, Liu W. Preparation and evaluation of a timolol maleate drug-resin ophthalmic suspension as a sustained-release formulation in vitro and in vivo. Drug Dev Ind Pharm. 2016;42(4):535–45.

279. Deng Y, Wang T, Li J, Sun W, He H, Gou J, Wang Y, Yin T, Zhang Y, Tang X. Studies on the in vitro ion exchange kinetics and thermodynamics and in vivo pharmacokinetics of the carbinoxamine-resin complex. Int J Pharm [Internet]. 2020 Oct;588:119779. Available from: https://linkinghub.elsevier.com/retrieve/pii/S0378517320307638

280. Hughes L. No Title. Pharmaceutical Technology Europe. 2005;38–42.

281. Miyazaki S, Kawasaki N, Kubo W, Endo K, Attwood D. Comparison of in situ gelling formulations for the oral delivery of cimetidine. Int J Pharm. 2001;220(1–2):161–8.

282. Lamp KC, Freeman CD, Klutman NE, Lacy MK. Pharmacokinetics and Pharmacodynamics of the Nitroimidazole Antimicrobials. Clin Pharmacokinet [Internet]. 1999;36(5):353–73. Available from: http://link.springer.com/10.2165/00003088-199936050-00004

283. Bundsaard H, Andersen FM. Inclusion complexation of rnetronidazole benzoate with cyclodextrin and its depression of anhydrate-hydrate transition in aqueous suspensions. Int J Pharm. 1984;19:189–97.

284. Aleanizy FS, Alqahtani F, Al Gohary O, El Tahir E, Al Shalabi R. Determination and characterization of metronidazole-kaolin interaction. Saudi Pharm J. 2015;

285. Li S, Culkin A, Jones DS, Andrews GP. Development of Polycaprolactone-Based metronidazole matrices for intravaginal extended drug delivery using a mechanochemically prepared therapeutic deep eutectic system. Int J Pharm. 2021;

286. El-Mahrouk GM, El-Gazayerly ON, Aboelwafa AA, Taha MS. Chitosan lactate wafer as a platform for the buccal delivery of tizanidine HCl: In vitro and in vivo performance. Int J Pharm. 2014;

287. Liu F, Ranmal S, Batchelor HK, Orlu-Gul M, Ernest TB, Thomas IW, Flanagan T, Tuleu C. Patient-Centered Pharmaceutical Design to Improve Acceptability of Medicines: Similarities and Differences in Paediatric and Geriatric Populations. Drugs [Internet]. 2014 Oct 2;74(16):1871–89. Available from: http://link.springer.com/10.1007/s40265-014-0297-2

288. Lopez FL, Ernest TB, Tuleu C, Gul MO. Formulation approaches to pediatric oral drug delivery: Benefits and limitations of current platforms. Vol. 12, Expert Opinion on Drug Delivery. 2015. p. 1727–40.

289. Wu Y, Fassihi R. Stability of metronidazole, tetracycline HCl and famotidine alone and in combination. Int J Pharm. 2005 Feb 16;290(1–2):1–13.

290. Carrales-Alvarado DH, Ocampo-Pérez R, Leyva-Ramos R, Rivera-Utrilla J. Removal of the antibiotic metronidazole by adsorption on various carbon materials from aqueous phase. J Colloid Interface Sci. 2014;

291. Erah PO, Goddard AF, Barrett DA, Shaw PN, Spiller RC. The stability of amoxycillin, clarithromycin and metronidazole in gastric juice: Relevance to the treatment of Helicobacter pylori infection. J Antimicrob Chemother. 1997;39(1):5–12.

292. Hills AG. pH and the Henderson-Hasselbalch equation. Am J Med [Internet]. 1973 Aug;55(2):131–3. Available from: https://linkinghub.elsevier.com/retrieve/pii/0002934373901605

293. Cheng YH, Watts P, Hinchcliffe M, Hotchkiss R, Nankervis R, Faraj NF, Smith A, Davis SS, Illum L. Development of a novel nasal nicotine formulation comprising an optimal pulsatile and sustained plasma nicotine profile for smoking cessation. J Control Release. 2002;79(1–3):243–54.

294. Conaghey OM, Corish J, Corrigan OI. The release of nicotine from a hydrogel containing ion exchange resins. Int J Pharm. 1998;170(2):215–24.

295. Michael Rajesh A, Bhatt SA, Brahmbhatt H, Anand PS, Popat KM. Taste masking of ciprofloxacin by ion-exchange resin and sustain release at gastric-intestinal through interpenetrating polymer network. Asian J Pharm Sci. 2014;10(4):331–40.

296. Sharma M, Soni R. Improved therapeutic potential of tapentadol employing cationic

exchange resins as carriers in neuropathic pain: evidence from pharmacokinetic and pharmacodynamics study. Sci Rep [Internet]. 2018 Dec 12;8(1):2812. Available from: http://www.nature.com/articles/s41598-018-21214-2

297. Alayoubi A, Daihom B, Adhikari H, Mishra S, Helms R, Almoazen H. Development of a taste-masked oral suspension of clindamycin HCl using ion exchange resin Amberlite IRP 69 for use in pediatrics. Drug Dev Ind Pharm [Internet]. 2016 Oct 2;42(10):1579–89. Available from: http://www.tandfonline.com/doi/full/10.3109/03639045.2016.1160102

298. S. S, E. K, D. V, P.J. C, P. SS, P. S, L. R, R. R, C.K. AK. Physiochemical characterization of taste masking levetiracetam ion exchange resinates in the solid state and formulation of stable liquid suspension for pediatric use. Beni-Suef Univ J Basic Appl Sci. 2016;5(2):126–33.

299. Chikukwa MTR, Wesoly M, Korzeniowska AB, Ciosek-Skibinska P, Walker RB, Khamanga SMM. Assessment of taste masking of captopril by ion-exchange resins using electronic gustatory system. Pharm Dev Technol [Internet]. 2020 Mar 15;25(3):281–9. Available from: https://www.tandfonline.com/doi/full/10.1080/10837450.2019.1687520

300. Vuorio M, Manzanares JA, Murtomäki L, Hirvonen J, Kankkunen T, Kontturi K. Ion-exchange fibers and drugs: A transient study. J Control Release. 2003;

301. Rohm and Haas. Amberlite IRP69 Pharmaceutical Grade Cation Exchange Resin (Sodium Polystyrene Sulfonate USP) Technical Data Sheet. :1–5. Available from: http://www.dow.com/assets/attachments/business/process_chemicals/amberlite_and_duolite_pharmaceutical_grade_resins/amberlite_irp69/tds/amberlite_irp69.pdf

302. Chen L, Yang G, Zhang J. A study on the exchange kinetics of ion-exchange fiber. React Funct Polym. 1996;

303. Chiang PC, Shi Y, Cui Y. Temperature dependence of the complexation mechanism of celecoxib and hydroxyl-β-cyclodextrin in aqueous solution. Pharmaceutics. 2014;

304. Plaizier-Vercammen JA. Investigation of the bioavailability of codeine from a cation-exchange sulphonic acid 2. Evaluation of release kinetics of codeine from the resinate and uptake of Na+ from the solution. Int J Pharm. 1992;87(1–3):31–6.

305. Akkaramongkolporn P, Ngawhirunpat T, Nunthanid J, Opanasopit P. Effect of a pharmaceutical cationic exchange resin on the properties of controlled release diphenhydramine hydrochloride matrices using methocel K4M or ethocel 7cP as matrix formers. AAPS PharmSciTech. 2008;9(3):899–908.

306. Zaman M, Hanif M, Khan MA. Arabinoxylan-Based Mucoadhesive Oral Films of Tizanidine HCL Designed and Optimized Using Central Composite Rotatable Design. Polym Plast Technol Eng [Internet]. 2018 Mar 24;57(5):471–83. Available from: https://www.tandfonline.com/doi/full/10.1080/03602559.2017.1324575

307. AKKARAMONGKOLPORN P, YONEMOCHI E, TERADA K. Molecular State of Chlorpheniramine in Resinates. Chem Pharm Bull [Internet]. 2000;48(2):231–4. Available from: http://www.jstage.jst.go.jp/article/cpb1958/48/2/48_2_231/_article

308. Jagdale S, Brahmane S, Chabukswar A. Optimization of Microemulgel for Tizanidine Hydrochloride. Antiinflamm Antiallergy Agents Med Chem [Internet]. 2020 Jun 8;19(2):158–79. Available from: https://www.eurekaselect.com/170571/article

309. Cheng YH, Watts P, Hinchcliffe M, Hotchkiss R, Nankervis R, Faraj NF, Smith A, Davis SS, Illum L. Development of a novel nasal nicotine formulation comprising an optimal pulsatile and sustained plasma nicotine profile for smoking cessation. J Control Release. 2002;

310. Mehta K, Tu Y-H. Modified release formulations containing drug-ion exchange resin complexes. United States; US8747902B2, 2007.

311. Matsuzuru H, Wadachi Y. Influence of differences in resin-matrix structure on ion-exchange adsorption of trace amounts of Ag(I), Co(II) and Cr(III). J Nucl Sci Technol. 1975;

312. Takemura S, Watanabe H, Nishihara T, Okamoto A, Tanabe K. Monitoring intracellular metal ion complexation with an acetylene-tagged ligand by Raman spectroscopy. RSC Adv. 2020;

313. Han X, Zhang S, Chai Z, Dong Y, He W, Yin L, Yang L, Qin C. In vitro and in vivo evaluation of the taste-masking efficiency of Amberlite IRP88 as drug carries in chewable tablets. J Drug Deliv Sci Technol. 2019 Feb 1;49:547–55.

314. Siddiqui A, Shah RB, Khan MA. Oseltamivir phosphate-amberliteTM IRP 64 ionic complex for taste masking: Preparation and chemometric evaluation. J Pharm Sci. 2013;

315. Tajber L, Corrigan OI, Healy AM. Spray drying of budesonide, formoterol fumarate and their composites—II. Statistical factorial design and in vitro deposition properties. Int J Pharm [Internet]. 2009 Feb;367(1–2):86–96. Available from: https://linkinghub.elsevier.com/retrieve/pii/S0378517308006625

316. Yu LX, Amidon G, Khan MA, Hoag SW, Polli J, Raju GK, Woodcock J. Understanding pharmaceutical quality by design. AAPS Journal. 2014.

317. Kaur A, Bhoop BS, Chhibber S, Sharma G, Gondil VS, Katare OP. Supramolecular nano-engineered lipidic carriers based on diflunisal-phospholipid complex for transdermal delivery: QbD based optimization, characterization and preclinical investigations for management of rheumatoid arthritis. Int J Pharm. 2017;

318. Wu T, Wang G, Shi C, Li J, Zhao N, Dong Z, Pan W, Zhang X. Development and evaluation of orally disintegrating tablets containing the mosapride resin complex. Acta Pharm. 2018;68(2):159–70.

319. Akkaramongkolporn P, Wongsermsin K, Opanasopit P, Ngawhirunpat T. Comparison between the effect of strongly and weakly cationic exchange resins on matrix physical properties and the controlled release of diphenhydramine hydrochloride from matrices. AAPS PharmSciTech. 2010;11(3):1104–14.

320. Shukla D, Chakraborty S, Singh S, Mishra B. Fabrication and Evaluation of Taste Masked Resinate of Risperidone and Its Orally Disintegrating Tablets. Chem Pharm Bull [Internet]. 2009;57(4):337–45. Available from: http://www.jstage.jst.go.jp/article/cpb/57/4/57_4_337/_article

321. Gupta D, Bhatia D, Dave V, Sutariya V, Varghese Gupta S. Salts of Therapeutic Agents: Chemical, Physicochemical, and Biological Considerations. Molecules [Internet]. 2018 Jul 14;23(7):1719. Available from: http://www.mdpi.com/1420-3049/23/7/1719

322. Agarwal R, Mittal R, Singh A. Studies of Ion-Exchange Resin Complex of Chloroquine Phosphate. Drug Dev Ind Pharm [Internet]. 2000 Jan 6;26(7):773–6. Available from: http://www.tandfonline.com/doi/full/10.1081/DDC-100101297

323. Kril MB, Fung H -L. Influence of hydrophobicity on the ion exchange selectivity coefficients for aromatic amines. J Pharm Sci. 1990;

324. Bele MH, Derle D V. Effect of polacrilin potassium as disintegrant on bioavailability of diclofenac potassium in tablets: A technical note. AAPS PharmSciTech. 2012;13(3):756–9.

325. Waterman KC, Gerst P, MacDonald BC. Relative humidity hysteresis in solid-state chemical reactivity: A pharmaceutical case study. J Pharm Sci. 2012;

326. Poozesh S, Bilgili E. Scale-up of pharmaceutical spray drying using scale-up rules: A review. International Journal of Pharmaceutics. 2019.

327. Sundheim BR, Waxman MH, Gregor HP. Studies on ion exchange resins. VII. Water vapor sorption by cross-linked polystyrenesulfonic acid resins. J Phys Chem. 1953;

328. Thielmann F. Hysteresis Effects in Vapour Sorption [Internet]. DVS Application Note 37. 2004 [cited 2021 Jul 1]. p. 2–3. Available from: https://surfacemeasurementsystems.com/wp-content/uploads/2015/08/App37-Hysteresis-Effects.pdf

329. Driemeier C, Mendes FM, Oliveira MM. Dynamic vapor sorption and thermoporometry to probe water in celluloses. Cellulose [Internet]. 2012 Aug 25;19(4):1051–63. Available from: http://link.springer.com/10.1007/s10570-012-9727-z

330. Box G, Meyer RD. SOME NEW IDEAS IN THE ANALYSIS OF SCREENING DESIGNS. J Res Natl Bur Stand (United States). 1985;

331. Huntington DH. The Influence of the Spray Drying Process on Product Properties. Dry Technol [Internet]. 2004 Jun;22(6):1261–87. Available from: http://www.tandfonline.com/doi/abs/10.1081/DRT-120038730

332. Maghsoodloo S, Ozdemir G, Jordan V, Huang CH. Strengths and limitations of taguchi's contributions to quality, manufacturing, and process engineering. J Manuf Syst. 2004;

333. Wilkinson L. Revising the Pareto Chart. Am Stat. 2006;

334. Macfhionnghaile P, Hu Y, Gniado K, Curran S, Mcardle P, Erxleben A. Effects of Ball-Milling and Cryomilling on Sulfamerazine Polymorphs: A Quantitative Study. J Pharm Sci [Internet]. 2014 Jun;103(6):1766–78. Available from: https://linkinghub.elsevier.com/retrieve/pii/S0022354915305670

335. Sheokand S, Modi SR, Bansal AK. Dynamic vapor sorption as a tool for characterization and quantification of amorphous content in predominantly crystalline materials. Journal of Pharmaceutical Sciences. 2014.

336. Price R, Young PM. Visualization of the Crystallization of Lactose from the Amorphous State. J Pharm Sci. 2004;

337. Caron V, Hu Y, Tajber L, Erxleben A, Corrigan OI, McArdle P, Healy AM. Amorphous Solid Dispersions of Sulfonamide/Soluplus® and Sulfonamide/PVP Prepared by Ball Milling. AAPS PharmSciTech. 2013;14(1):464–74.

338. Wong SN, Chan SWS, Peng X, Xuan B, Lee HW, Tong HHY, Chow SF. Effects of the glass-forming ability and annealing conditions on cocrystallization behaviors via rapid solvent removal: A case study of voriconazole. Pharmaceutics. 2020;

339. Todaro V, Worku ZA, Cabral LM, Healy AM. In Situ Cocrystallization of Dapsone and Caffeine

during Fluidized Bed Granulation Processing. AAPS PharmSciTech. 2019 Jan 1;20(1).

340. Zhang R, Hoffmann T, Tsotsas E. Novel technique for coating of fine particles using fluidized bed and aerosol atomizer. Processes. 2020;

341. Wan LSC, Heng PWS, Ling BL. Effect of polyvinylpyrrolidone solutions containing dissolved drug on characteristics of lactose fluidized bed granules. Int J Pharm. 1996;

342. Link KC, Schlünder EU. Fluidized bed spray granulation Investigation of the coating process on a single sphere. Chem Eng Process Process Intensif. 1997;

343. Hoashi Y, Tozuka Y, Takeuchi H. Solventless dry powder coating for sustained drug release using mechanochemical treatment based on the tri-component system of acetaminophen, carnauba wax and glidant. Drug Dev Ind Pharm [Internet]. 2013 Feb 12;39(2):259–65. Available from: http://www.tandfonline.com/doi/full/10.3109/03639045.2012.673625

344. Seong HJ, Berhane NH, Haghighi K, Park K. Drug release properties of polymer coated ion-exchange resin complexes: Experimental and theoretical evaluation. J Pharm Sci. 2007;96(3):618–32.

345. Bordaweka MS, Zia H, Quadir A. Evaluation of polyvinyl acetate dispersion as a sustained release polymer for tablets. Drug Deliv J Deliv Target Ther Agents. 2006;

346. Shi H, Mohanty R, Chakravarty S, Cabiscol R, Morgeneyer M, Zetzener H, Ooi JY, Kwade A, Luding S, Magnanimo V. Effect of Particle Size and Cohesion on Powder Yielding and Flow. KONA Powder Part J [Internet]. 2018;35:226–50. Available from: https://www.jstage.jst.go.jp/article/kona/35/0/35_2018014/_article

347. Tsavalas JG, Sundberg DC. Hydroplasticization of polymers: Model predictions and application to emulsion polymers. Langmuir. 2010;

348. Leung CY, Trementozzi AN, Lin Y, Xu J, Irdam E, MacPhee JM, He M, Karki SB, Boulas P, Zawaneh PN. Enteric coating of micron-size drug particles through a Würster fluid-bed process. Powder Technol. 2017;

349. Bando H, McGinity JW. Relationship between drug dissolution and leaching of plasticizer for pellets coated with an aqueous Eudragit® S100:L100 dispersion. Int J Pharm [Internet]. 2006 Oct;323(1–2):11–7. Available from: https://linkinghub.elsevier.com/retrieve/pii/S0378517306004273

350. Patra CN, Priya R, Swain S, Kumar Jena G, Panigrahi KC, Ghose D. Pharmaceutical significance

of Eudragit: A review. Futur J Pharm Sci. 2017;

351. Mehta K, Tu Y-H. Clonidine Formulation. United States of America; US 8,623,409, 2014.

352. Khan MZI, Štedul HP, Kurjaković N. A pH-dependent colon-targeted oral drug delivery system using methacrylic acid copolymers. II. Manipulation of drug release using Eudragit® L100 and Eudragit S100 combinations. Drug Dev Ind Pharm. 2000;

353. Ronchi F, Sereno A, Paide M, Hennia I, Sacré P, Guillaume G, Stéphenne V, Goole J, Amighi K. Development and evaluation of budesonide-based modified-release liquid oral dosage forms. J Drug Deliv Sci Technol. 2019 Dec 1;54.

354. Abbaspour MR, Sadeghi F, Garekani HA. Preparation and characterization of ibuprofen pellets based on Eudragit RS PO and RL PO or their combination. Int J Pharm. 2005;303(1–2):88–94.

355. Kaur G, Grewal J, Jyoti K, Jain UK, Chandra R, Madan J. Oral controlled and sustained drug delivery systems: Concepts, advances, preclinical, and clinical status. In: Drug Targeting and Stimuli Sensitive Drug Delivery Systems. 2018.

356. Ehlers H, Larjo J, Antikainen O, Räikkönen H, Heinämäki J, Yliruusi J. In situ droplet size and speed determination in a fluid-bed granulator. Int J Pharm. 2010;

357. Sprockel OL, Price JC. Evaluation of sustained release aqueous suspensions containing microencapsulated drug-resin complexes. Drug Dev Ind Pharm [Internet]. 1989 Jan 20;15(8):1275–87. Available from: http://www.tandfonline.com/doi/full/10.3109/03639048909043677

358. Hegazy N, Demirel M, Yazan Y. Preparation and in vitro evaluation of pyridostigmine bromide microparticles. Int J Pharm. 2002;

359. Dave VS, Fahmy RM, Bensley D, Hoag SW. Eudragit® RS PO/RL PO as rate-controlling matrix-formers via roller compaction: Influence of formulation and process variables on functional attributes of granules and tablets. Drug Dev Ind Pharm. 2012;

360. Thakral S, Thakral NK, Majumdar DK. Eudragit®: A technology evaluation. Expert Opinion on Drug Delivery. 2013.

361. Pongjanyakul T. Effect of sampling procedures of release testing on drug release and scale-up production feasibility of multiple-unit dextromethorphan resinate tablets: A technical note. AAPS PharmSciTech [Internet]. 2007 Oct;8(4):298–304. Available from: http://link.springer.com/10.1208/pt0804117

362. Mathematical models of drug release. In: Strategies to Modify the Drug Release from Pharmaceutical Systems [Internet]. Elsevier; 2015. p. 63–86. Available from: https://linkinghub.elsevier.com/retrieve/pii/B9780081000922000059

363. Llabot JM, Manzo RH, Allemandi DA. Drug release from carbomer:carbomer sodium salt matrices with potential use as mucoadhesive drug delivery system. Int J Pharm. 2004;

364. Wiranidchapong C, Tucker IG, Rades T, Kulvanich P. Miscibility and interactions between 17β-estradiol and Eudragit® RS in solid dispersion. J Pharm Sci [Internet]. 2008 Nov;97(11):4879–88. Available from: https://linkinghub.elsevier.com/retrieve/pii/S0022354916327769

365. Jeong SH, Park K. Drug loading and release properties of ion-exchange resin complexes as a drug delivery matrix. Int J Pharm [Internet]. 2008 Sep;361(1–2):26–32. Available from: https://linkinghub.elsevier.com/retrieve/pii/S0378517308003608

366. Quinten T, Andrews GP, De Beer T, Saerens L, Bouquet W, Jones DS, Hornsby P, Remon JP, Vervaet C. Preparation and Evaluation of Sustained-Release Matrix Tablets Based on Metoprolol and an Acrylic Carrier Using Injection Moulding. AAPS PharmSciTech [Internet]. 2012 Dec 11;13(4):1197–211. Available from: http://link.springer.com/10.1208/s12249-012-9848-6

367. Wulff R, Leopold CS. Coatings of Eudragit® RL and L-55 Blends: Investigations on the Drug Release Mechanism. AAPS PharmSciTech [Internet]. 2016 Apr 12;17(2):493–503. Available from: http://link.springer.com/10.1208/s12249-015-0377-y

368. Qu Y, Lai W-L, Xin Y-R, Zhu F-Q, Zhu Y, Wang L, Ding Y, Xu Y, Liu H-F. Development, Optimization, and Evaluation In Vitro/In Vivo of Oral Liquid System for Synchronized Sustained Release of Levodopa/Benserazide. AAPS PharmSciTech [Internet]. 2019 Nov 16;20(8):312. Available from: http://link.springer.com/10.1208/s12249-019-1511-z

369. Bodmeier R, Paeratakul O. Process and formulation variables affecting the drug release from chlorpheniramine maleate-loaded beads coated with commercial and self-prepared aqueous ethyl cellulose pseudolatexes. Int J Pharm [Internet]. 1991 Mar;70(1–2):59–68. Available from: https://linkinghub.elsevier.com/retrieve/pii/037851739190164J

370. Nikowitz K, Pintye-Hódi K, Regdon G. Study of the recrystallization in coated pellets – Effect of coating on API crystallinity. Eur J Pharm Sci [Internet]. 2013 Feb;48(3):563–71. Available from: https://linkinghub.elsevier.com/retrieve/pii/S0928098712004927

371. Li G, Han D, Guan T, Zhao X, He H, Tang X. Isosorbide-5-mononitrate (5-ISMN) sustained-

release pellets prepared by double layer coating for reducing 5-ISMN migration and sublimation. Int J Pharm [Internet]. 2010 Nov;400(1–2):138–44. Available from: https://linkinghub.elsevier.com/retrieve/pii/S0378517310006769

372. Siepmann J, Siepmann F, Paeratakul O, Bodmeier R. Aqueous Polymeric Coatings for Pharmaceutical Dosage Forms [Internet]. Felton LA, editor. Aqueous Polymeric Coatings for Pharmaceutical Dosage Forms: Fourth Edition. CRC Press; 2016. Available from: https://www.taylorfrancis.com/books/9781498732093

373. Agrawal AM, Manek R V., Kolling WM, Neau SH. Water distribution studies within microcrystalline cellulose and chitosan using differential scanning calorimetry and dynamic vapor sorption analysis. J Pharm Sci. 2004;

374. Agrawal AM, Manek R V., Kolling WM, Neau SH. Studies on the interaction of water with ethylcellulose: Effect of polymer particle size. AAPS PharmSciTech. 2003;

375. No Title [Internet]. TA Instruments Thermal Analysis Brochure. 2009 [cited 2021 Jun 30]. p. 5. Available from: http://www.tainstruments.com/pdf/2009 DSC Brochure.pdf

376. Kulthe V V., Chaudhari PD. Drug resinates an attractive approach of solubility enhancement of atorvastatin calcium. Indian J Pharm Sci [Internet]. 2013 Sep;75(5):523–32. Available from: http://www.ncbi.nlm.nih.gov/pubmed/24403652

377. Aman RM okhta., Meshali MM ohame., Abdelghani GM ahmou. Ion-exchange complex of famotidine: sustained release and taste masking approach of stable liquid dosage form. Drug Discov Ther [Internet]. 2014;8(6):268–75. Available from: https://www.jstage.jst.go.jp/article/ddt/8/6/8_2014.01043/_article

378. Kouchak M, Ramezani Z, Bagheri F. Preparation and Evaluation of Taste Masking Iron Suspension: Taking Advantage of Weak Cationic Exchange Resin. AAPS PharmSciTech. 2018;19(2):719–29.

379. Kadam A, Sakarkar D, Kawtikwar P. Development and evaluation of oral controlled release chlorpheniramine-ion exchange resinate suspension. Indian J Pharm Sci [Internet]. 2008;70(4):531. Available from: http://www.ijpsonline.com/text.asp?2008/70/4/531/44613

380. Mehta R, Martin L, Cunnigham C, Rane M, Rajabi-Siahboomi A. Investigation of Ion Exchange Resin Concentration, Particle Size and Process Temperature for Dextromethorphan HBr Complexation. AAPS; 2017. p. 1–4.

381. Neumann P. Certain 4-Substituted Amino-2,1,3-Benzothiadiozoles. United States; 3843668,

1974.

382. Leng D, Thanki K, Foged C, Yang M. Formulating Inhalable Dry Powders Using Two-Fluid and Three-Fluid Nozzle Spray Drying. Pharm Res. 2018;35(12):247.

383. Oth MP, Moës AJ. Sustained release solid dispersions of indomethacin with Eudragit RS and RL. Int J Pharm. 1989;55(2–3):157–64.